DEPARTMENT OF TRANSPORTATION

BMP For Issues with Asphalt Centerline Joint and Intelligent Compaction for Local Agencies

Syed W. Haider, Principal Investigator
Civil and Environmental Engineering Department
Michigan State University

November 2023

Research Project
Final Report 2023-35

LRRB
LOCAL ROAD RESEARCH BOARD

To request this document in an alternative format, such as braille or large print, call 651-366-4718 or 1-800-657-3774 (Greater Minnesota) or email your request to ADArequest.dot@state.mn.us. Please request at least one week in advance.

Technical Report Documentation Page

1. Report No.	2.	3. Recipients Accession No.
MN 2023-35		

4. Title and Subtitle	5. Report Date
BMP For Issues with Asphalt Centerline Joint and Intelligent Compaction for Local Agencies	November 2023
	6.

7. Author(s)	8. Performing Organization Report No.
Syed W. Haider, Hamad B. Muslim, Lev Khazanovich, Muhammed E. Kutay, Bora Cetin	

9. Performing Organization Name and Address	10. Project/Task/Work Unit No.
Civil and Environmental Engineering Department Michigan State University 3546 Engineering Building East Lansing, MI 48824	11. Contract (C) or Grant (G) No. (c) 1036336 (wo) 2

12. Sponsoring Organization Name and Address	13. Type of Report and Period Covered
Minnesota Department of Transportation Office of Research & Innovation 395 John Ireland Boulevard, MS 330 St. Paul, Minnesota 55155-1899	Final Report
	14. Sponsoring Agency Code

15. Supplementary Notes

http://mdl.mndot.gov/

16. Abstract (Limit: 250 words)

It is well-known that longitudinal joint construction quality is critical to flexible pavement life. The maintenance activities caused by longitudinal joint deterioration's direct or indirect effects and raveling problems along the centerline paving joint of asphalt roadways have become challenging for many highway agencies. A poorly constructed joint can lead to premature deterioration of an otherwise sound pavement. Thus, improving the joint's construction can improve density and decrease permeability. It is probably the single most crucial remedy to enhance pavement performance. A density profiling system (DPS) provides continuous, instead of limited, coverage provided by conventional joint quality evaluation methods. Statistical, probabilistic, and percent-within-limits (PWL) analysis of DPS data suggests avoiding the construction of an unconfined joint. Tapered joints, confined butt joints employing the Maryland method or otherwise, echelon paved, and unconfined butt joints with cut back can produce adequate compaction at the joint.

17. Document Analysis/Descriptors	18. Availability Statement
Asphalt pavements, Compaction, Air voids, Density, Longitudinal joints	No restrictions. Document available from: National Technical Information Services, Alexandria, Virginia 22312

19. Security Class (this report)	20. Security Class (this page)	21. No. of Pages	22. Price
Unclassified	Unclassified	312	

BMP for Issues with Asphalt Centerline Joint and Intelligent Compaction for Local Agencies

Final Report

Prepared by:

Syed Waqar Haider, Ph.D., P.E.
Hamad Bin Muslim,
M. Emin Kutay, Ph.D., P.E.
Bora Cetin, Ph.D.
Department of Civil and Environmental Engineering
Michigan State University

Lev Khazanovich, Ph.D.
Department of Civil Engineering
University of Pittsburgh

November 2023

Published by:

Minnesota Department of Transportation
Office of Research & Innovation
395 John Ireland Boulevard, MS 330
St. Paul, Minnesota 55155-1899

Acknowledgements

The authors would like to thank Minnesota's Local Roads Research Board (LRRB) and the Minnesota Department of Transportation (MnDOT) for funding this project and, specifically, the members of the Technical Assistance Panel (Andrew Giesen, Anthony Pirkl, Rod Rue, Carter Schulze, Dan Swanson), Marcus Bekle, David Glyer, Naomi Eckerd and Kyle Puent. The team also appreciates the assistance provided by MnRoad in data collection on Minnesota projects, especially Kyle Hough and Mercedes Maupin. The authors also appreciate Fawaz Kaseer and Ethan Akerly from the Michigan Department of Transportation (MDOT) for data collection for Michigan projects. Their input was invaluable to the researchers and helped improve the quality of this report.

Table of Contents

List of Figures

List of Tables

List of Abbreviations

AQL	Acceptable quality level
G_{mb}	Bulk specific gravity
G_{sb}	Bulk specific gravity of the stone
R^2	Coefficient of determination
CI	Confidence interval
CFS	Construction Field Services
DPS	Density Profiling system
G_{se}	Effective specific gravity of the stone
FHWA	Federal Highway Administration
GPR	Ground penetrating radar
HDPE	High-density polyethylene
HD	Hoegh-Dai
HMA	Hot-mix asphalt
LJQI	Longitudinal joint quality index
MOT	Maintaining of traffic
Gmm	Maximum specific gravity of the mix
MI	Michigan
MDOT	Michigan Department of Transportation
MN	Minnesota
MnDOT	Minnesota Department of Transportation
MASW	multi-channel analysis of surface waves
NMAS	Nominal maximum aggregate size
NDT	Non-destructive testing
ODOT	Ohio Department of Transportation
Pb	Percent binder
PWL	Percent within limit
PG	Performance grade
PFWD	Portable falling weight deflectometer
PCC	Portland cement concrete
QA	Quality assurance
QC	Quality control
RQL	Rejectable quality level
RDM	Rolling density meter
RMSE	Root mean squared error
SSD	Saturated surface dry
SSC	Scaled sensitivity coefficients
SP	Special provision
SHAs	State Highway Agencies
SE	Standard error
SMA	Stone matrix asphalt
TMD	Theoretical maximum density
VIF	Variance inflation factor
VRAM	Void-reducing asphalt membrane
VFA	Voids filled with asphalt
VMA	Voids in mineral aggregates

Executive Summary

From a construction standpoint, asphalt pavements minimize disruptions in traffic flow as these can be paved and opened to traffic quickly. Generally, asphalt pavement construction occurs by paving one lane at a time while traffic flow is maintained in the adjacent lane. Consequently, it requires a longitudinal joint between the lanes. It is well-known that the quality of longitudinal joint construction is critical to the life of flexible pavements. A poorly constructed weak joint can prematurely deteriorate an otherwise sound pavement (1). The maintenance activities caused by a longitudinal joint deterioration's direct or indirect effects have become challenging for many highway agencies. The issue has been thoroughly evaluated to find methods to improve the quality of joints since the 1960s (2). Several studies estimated that a 1% decrease in air void content in the compacted asphalt mat could enhance a pavement's service life by approximately 10% (3-7). Thus, compaction is the most critical construction-related factor directly related to the in-place density and air void content and can provide long-term serviceability (8).

The main objective of this study is to identify the best approach to enhance the performance of longitudinal joints for future projects and recognize how to fix failed centerline joints cost-effectively. The research does not aim to do additional investigations on longitudinal joint construction or to evaluate the density and its relationship to permeability and oxidation. Instead, this study focuses on taking advantage of past research information and searching for consensus to recommend best practices for constructing and specifying longitudinal joints in flexible pavements. The study documents the best practices based on literature and a survey of pavement agencies in Minnesota and Michigan. In addition, it evaluates and compares longitudinal joint quality achieved by constructing different types of joints using in-field dielectric measurements from the Density Profiling System (DPS).

Literature shows that most longitudinal joints constructed are butt joints. However, a few states use tapered joints, with a vertical notch used in Michigan. While building a hot mix asphalt (HMA) in multiple layers, staggering the longitudinal joints with a minimum of a 6-in (150-mm) offset is good practice. Moreover, a successful longitudinal joint requires a perfectly straight edge (or smooth edge when following a curved alignment), aiding the compaction of adjacent lanes. In addition, the rolling of the longitudinal joint significantly affects the achieved joint density. Vibratory rolling of an unconfined edge of a joint with a 6 in (150 mm) overhang aids in avoiding stress crack formation due to the roller's edge. The hot pinch and the hot overlap methods are used for rolling a confined joint. Since both ways require vibratory rolling, the hot pinch method is better because it pushes the hot material into the joint and aids compaction.

Furthermore, using tack, joint adhesive, or longitudinal joint seals improves the joint's bond and decreases its permeability. The literature also suggests overlapping the cold joint edge with the hot asphalt material by 1 ± 0.5 in (25 ± 12.5 mm) while paving the adjacent lane helps construct a durable joint. The overlapped material should be at least 0.25 in (6.25 mm) higher than the adjoining mat to allow for compaction.

Echelon paving is considered the best technique to avoid joint construction altogether. In addition, using a safety edge and matching lanes daily, where possible, eliminates the construction of a cold unconfined joint. In addition, cutting and removing the high air void material from an unconfined edge before laying the adjacent lane is believed to produce adequate compaction at the joint. The Michigan Department of Transportation (MDOT) allows a credit of up to 4 in (100 mm) of removal at a joint before the adjacent lane is paved, allowing the contractor to mill back 4 in (100 mm) without deducting this quantity. Most agencies do not monitor joint density as it requires additional resources and time. The destructive nature of pavement coring, the most commonly used option among agencies that evaluate joint quality, is another reason for not monitoring the joint density. Most agencies use a simple average approach to determine joint density based on limited pavement cores. However, using percent-within-limit (PWL) to calculate the joint quality measure is better. The lower PWL specification limit would typically represent 90% acceptable values with only 10% unsatisfactory results for a 100% payment to the contractor. In contrast, a simple average would have 50% values below the specified density limit.

The DPS data collection effort under this research involved in-place dielectric data measurements at two project sites in Minnesota and six in Michigan: 16 pavement sections. Joint dielectric data was collected at different project sites constructed with different types of longitudinal joints about 500 ft (152 m) behind the finish roller. Each data collection commenced with the air and metal plate calibration of the DPS sensors, followed by sensor validation using the high-density polyethylene (HDPE) block and conducting the Swerve test to ensure that the sensor median dielectric values were within 0.08 of each other (9). DPS air void vs. dielectric relationship was calibrated using pucks prepared in the laboratory from loose HMA mix collected from these projects and validated using field cores. The joint dielectric values measured at a 6 in (150 mm) offset from the joint were compared with the mat values measured at least 3.5 ft (1 m) into the pavement lane. The comparison showed that out of all the joint types studied in this research, the unconfined joint dielectric values were lower throughout the length of the project sections. However, the data displayed a higher variability for all the projects.

For an in-depth analysis, the data from each section were discretized into smaller subsections of 25, 50, 100, and 200 ft (7.6, 15.2, 30.5, and 61 m). The mean dielectric values from each subsection were compared statistically using paired *t*-tests to quantify the differences in dielectric values between a joint and its corresponding mat. The paired *t*-tests tested the null hypothesis that the mean dielectric difference between the mat and the joint was equal to 0.2 ($\mu_{difference} = 0.2$); it is greater than 0.2 ($\mu_{difference} > 0.2$) as the alternate hypothesis. Similarly, paired *t*-tests were conducted with a null hypothesis of air void difference lesser than 2% while their difference was greater than 2% as the alternate hypothesis. A dielectric difference greater than 0.2 corresponded to a joint air void content difference of more than 2% compared to the mat. The results showed that constructing an unconfined joint can result in 45 to 100% subsections within a project having greater than 0.2 dielectric and 2% air void differences between the joint and the corresponding mat. Thus, constructing an unconfined joint should be avoided where possible. All the other joint types (i.e., confined and unconfined tapered joint, confined butt joint constructed employing Maryland method or otherwise, echelon constructed joint, and unconfined joint with cut back) showed no differences between mat and joint that are greater than 0.2 dielectrics or greater than 2% air voids.

A probabilistic approach was used in addition to the paired *t*-test to compare different longitudinal joint types. The dielectric values for each type of joint and its corresponding mat from each project were divided into six groups. The conditional probabilities for each dielectric and air void category were determined for the mat and the joint. For a mat dielectric reference range of 5.2 – 5.4, irrespective of the project for an unconfined joint, there was a 95% chance that the joint dielectrics would be less than 5, i.e., greater than 8% air voids given the reference dielectric range for the mat (5.2 – 5.4). Also, there was nearly a 70% chance that the joint would have the same dielectric range as the mat's reference range for echelon, taper confined, and tapered unconfined joints. For the same joint types, there was about a 20% chance that the joint dielectrics would be a category low (i.e., 5 – 5.2), while there was about a 10% chance of the joint dielectric being a category higher (5.4 – 5.6). A confined joint 50% of the time will produce a joint with dielectrics like the reference, while 40% of the time, the joint dielectric will be a category higher (5.4 – 5.6) than the reference range. An unconfined joint constructed by cutting back a portion of the HMA before laying the adjacent lane may have a 50% chance of producing joint dielectric like the mat reference range. A similar comparison can be accomplished using a different mat dielectric reference range. Similar results were observed using a mat air void reference range of 6.2 to 4.7% (corresponding to the dielectric range of 5.2 – 5.4). Like the statistical results, the probabilistic results implied that an unconfined joint should be avoided when possible. An unconfined joint with cutback material can be a better alternative.

This study also determined one-sided PWL for the mat and joint dielectric values and their difference by subsections (of variable lengths). Using an upper specification limit of 0.2 dielectric difference (mat–joint) for calculating PWL for each subsection, the data analyses showed that 70 to 100% of the subsections for an unconfined joint had PWL lower than the rejection quality limit (RQL) of 60%. Similar results were observed from PWL analyses using an upper specification limit of 2% air voids difference between the joint and its corresponding mat. Overall, the statistical and probabilistic approach results agreed with the summary PWL results using either dielectrics or air voids data in comparing different joint types and suggested avoiding the construction of an unconfined joint when possible.

The paired *t*-test approach identifies differences in joint types based on the subsection's mean mat and joint dielectric values. However, it does not consider the mat and joint dielectric values, which results in a mean difference of 0.2 or higher. The approach treats the 0.2 dielectric difference equally, irrespective of the individual mat and joint dielectric values. A subsection with a significant difference (> 0.2 dielectrics) can occur even if the joint and mat have acceptable compaction. Thus, considering such a section with a significant dielectric difference in the paired *t*-test approach is unreasonable for the contractor. Therefore, it is crucial to consider the individual mean mat and joint dielectric values of the subsections. This study proposes a new index that determines the percentage of stations with problematic compaction using dielectric data to evaluate the joint quality while correcting for a good mat density. The new index involves calculating the dielectric difference between the mat and the joint while considering the mat dielectric value of the station. The proposed index showed that only 40 to 70% of stations had acceptable joint compaction for the projects using an unconfined joint. All the other projects, irrespective of the longitudinal joint types, result in almost 100% acceptable compaction at the joints.

Chapter 1: Introduction

1.1 Research Objective

It is well-known that the quality of longitudinal joint construction is critical to the life of flexible pavements. The maintenance activities caused by longitudinal joint deterioration's direct or indirect effects have become challenging for many highway agencies. A 2009 Federal Highway Administration (FHWA) survey of its divisional offices found that about 50% of its engineers were unhappy with the performance of longitudinal joints. Local agencies report problems with deterioration (raveling) along the centerline paving joint of asphalt roadways. Several questions are raised to understand this widespread problem, including whether the source of the issue is related to material, specifications, constructional quality, method, or a combination of these issues.

Consequently, academia, highway agencies, and industry have made numerous research efforts in the last 30 years. Besides, training on the placement and compaction of HMA pavements is available within the industry. Despite all these efforts, longitudinal joint deterioration is still one of the prime causes of premature failure of flexible pavements. Improving longitudinal joint construction can improve density and decrease permeability. It is probably the single most crucial remedy to enhance pavement performance.

1.2 Research Problem and Historical Background

From a construction standpoint, asphalt pavements minimize disruptions in traffic flow by their ability to be paved and opened to traffic quickly. Generally, asphalt pavement construction occurs while traffic flow is maintained in an adjacent lane, and such an operation results in paving one lane at a time. Consequently, a longitudinal joint is required between the lanes. As in all engineering materials, the weakest links considered are the joints, and the same is true for asphalt pavements. A poorly constructed weak joint can prematurely deteriorate an otherwise sound pavement (1). The issue has been thoroughly evaluated to find methods to improve the quality of joints since the 1960s (2).

Foster et al. pointed out that a low-density zone in the joint area of the pavements leads to long-term performance issues of flexible pavements (10). This is a direct consequence of paving a single lane at a time. Once the first lane is paved, the mat is compacted with an unconfined edge. The unsupported condition at the edge results in lateral sloughing of the fresh asphalt material during compaction, resulting in a lower density. Additionally, the material along the edge of the mat tends to cool more quickly than the material within the mat. Thus, the cooler material at the edge inhibits proper compaction and decreases density. Although the cold edge of the first paved mat presents a confined edge for compaction of hot asphalt material of the second lane, it may lead to an uneven surface along with a bonding problem between the edges, hindering the achievement of a monolithic mat (11).

According to Estakhri et al., the structural support and temperature differences while paving and compacting the two adjacent lanes result in lower density, higher permeability, higher segregation, and

lower adhesion at the joint (1). Insufficient asphalt material at the joint while compacting is also anticipated to have a lower longitudinal joint density (12). The low-density weak bonded centerline joint within the pavement eventually cracks, leading to water and moisture infiltration, and such ingress of water results in debonding due to stripping. Also, the infiltrated water can undergo freeze-thaw cycles, especially in colder regions, and increase the chances of joint failure and pavement raveling near the joint (13). Several studies estimated that a 1% decrease in air void content in the compacted asphalt mat could enhance a pavement's service life by approximately 10% (3-7). Thus, compaction is the most crucial construction-related factor directly related to the in-place density and air void content and can provide long-term serviceability (8).

1.3 Scope

This study's main focus was identifying the best approach to enhance the performance of longitudinal joints for future projects and recognizing how to cost-effectively fix the failed centerline joints. This research did not aim to do additional investigations on longitudinal joint construction or to evaluate the density and its relationship to permeability and oxidation. The research team took advantage of past research information and searched for consensus to recommend constructing and specifying longitudinal joints in flexible pavements. The best practices were documented based on literature and recent experiences. This research also aimed to evaluate density/air void measurements using the Density Profiling System (DPS) to assess longitudinal joint quality by local road agencies. This was achieved by performing a pilot study to demonstrate the technology's use and identify specific needs for its implementation at the local level in the future.

1.4 Summary of Research and Methodology

The research methodology adopted to conduct this study addressed the following main elements:

- Review existing literature and longitudinal joint construction practices, comparison of methods, and issues.
- Identify the best practices for construction, materials, non-destructive testing (NDT), and repair.
- A pilot study to demonstrate the use of DPS.
- Final recommendations.

The research methodology primarily involved conducting a detailed literature review of the existing practices and comparing various approaches for longitudinal joint construction and identification of issues. The research team conducted a review on three main areas (a) construction practices, (b) evaluation of the longitudinal joint quality, and (c) repair and remedial measures. Subsequently, the team identified the best practices for joint construction, materials, design, NDT for quality evaluation, and repair of deteriorated joints. A pilot study measured joint quality for city and county roads using traditional pavement cores and DPS. The team compared the results from both types of testing in the pilot study to demonstrate their effectiveness in identifying joint quality. Based on the literature review and pilot study findings, the team made final recommendations to improve longitudinal joint quality and

construction practices. This study's expected outcomes included identifying best practices, construction specifications, and quality control/assurance for longitudinal joints in flexible pavements.

1.5 Research Tasks

The research was conducted in five (5) tasks, briefly discussed below, to accomplish the above objectives.

1.5.1 Task 1: Initial Memorandum on Expected Research Benefits and Potential Implementation Steps

During the proposal phase and the development of the work plan, key benefits were selected to clearly define the benefits the state will receive from the results and conclusions of this research. This task will initially assess research benefits, a proposed methodology, and potential implementation steps.

1.5.2 Task 2: Review of Existing Practices and Literature, Comparison of Practices and Issues

This task primarily involves conducting a detailed literature review of the existing practices to construct longitudinal joints, comparing various approaches, and identifying issues. The literature review involves three main areas (a) construction practices, (b) evaluation of the longitudinal joint quality, and (c) repair and remedial measures.

1.5.3 Task 3: Identify the Best Practices for Construction, Materials, NDT, and Repair

Based on Task 2, the research team will identify the best practices for construction, materials, joint evaluation, and repair of longitudinal joints. The best practices will be aimed at addressing the following broad areas related to longitudinal joints in flexible pavements: (a) HMA selection and design considerations, (b) pre-construction planning, (c) specifications, (d) construction best practices, and (e) repair of longitudinal joints.

1.5.4 Task 4: Study to Investigate the Use of DPS

In this task, the team coordinated with the Minnesota Department of Transportation (MnDOT) and the Michigan Department of Transportation (MDOT) to identify potential projects where different longitudinal joints were being constructed in the summer of 2022. The data collection at these potential projects involved measuring density/air voids in the laboratory destructively (i.e., using cores) and non-destructively using DPS. The data were analyzed to obtain correlations between field-measured air voids by the above two methods for joint quality evaluations. This task focused on local agencies (cities and counties) to (a) demonstrate how this technology was being used and (b) identify what specific needs counties and towns will have to implement the technology in the future.

1.5.5 Task 5: Final Recommendations

The research team prepared final recommendations based on the results and findings of Tasks 2 to 4. These recommendations were based on this study's practical and implementable outcomes. The findings aimed to answer (a) best practices for constructing longitudinal joints and how to repair existing failed centerline construction joints, (b) the evaluation of joint quality during construction, (c) the use of DPS for joint evaluation and its comparison with traditional procedures, and (d) construction specifications for the potential use of DPS in quality assurance.

1.6 Outline of the Report

The report contains six (6) chapters. Chapter 1 outlines the project abstract and objectives, summarizes the research methodology, and briefly explains the research tasks. Chapter 2 documents the literature review regarding construction practices, quality evaluation, and repair and remedial measures for asphalt pavement longitudinal joints. The chapter also summarizes the survey results for longitudinal joint construction practices in Minnesota and Michigan. Chapter 3 discusses the data collected at different projects. Chapter 4 details the analysis methods for data analysis and presents the results for different longitudinal joint types. Chapter 5 contains the significant findings, potential benefits, and DPS implementation strategy. Chapter 6 presents project recommendations. Appendix A includes the pavement cores and pucks dielectric and air voids data used in this study, while Appendix B contains the DPS data analyses plots for all the project sections.

Chapter 2: Literature and the State-Of-Practice Review

The following sections document the existing practices and aspects of the longitudinal joint:

- Type of joints
- Joint geometry
- Rolling methods
- Construction techniques
- Comparisons of various practices
- Joint quality evaluation
- Repair and maintenance practices
- Practices in various states

2.1 Type of Longitudinal Joints

The literature documents several methods to construct longitudinal joints in asphalt pavements. Based on the laying conditions of HMA layers, the resulting longitudinal joint can be of the following three broad types (10, 11, 14, 15):

2.1.1 Hot Joints

A hot joint is when the adjacent lanes are paved in the echelon technique (i.e., two pavers are spaced, so the first lane does not cool significantly before laying the second lane side by side). Thus, it results in a joint that appears almost seamless and produces the highest density compared to the other types.

2.1.2 Semi-hot Joints

A semi-hot or warm joint is produced when the asphalt paver is only allowed to a certain distance before moving back to pave the adjacent lane (i.e., the two lanes are paved within a short time). Consequently, HMA in the first lane cools down to about 120 to 140 °F (49 to 60 °C) before being placed in the adjoining lane, whose material is still hot.

2.1.3 Cold Joints

Cold joint results from a paving operation in which the first lane is paved one day, followed by the second lane paving conducted the next day. Thus, the HMA edge from the first day is cooled overnight when the second lane is placed. Generally, a cold joint will also be created if the temperature of the first lane is below 120 °F (49 °C).

2.2 Longitudinal Joint Geometry

Typically, two different geometries are used while constructing a longitudinal joint, as described below:

2.2.1 Butt Joint

The vertical or butt joint is the most commonly used conventional joint type in asphalt pavement construction. The butt joint "butts" the hot material from the second pass (i.e., the second lane being laid) to the cold material's edge from the first pass (i.e., lane laid earlier or a night before), thus having a vertical interface between the two lanes (12). If constructed with due consideration to its construction details, a butt joint can perform well. However, improper construction can lead to poor performance of the butt joints (14).

2.2.2 Wedge Joint

The tapered or wedge joint is a sloped edge joint that tapers continuously to the surface. However, continuous tapering is problematic, particularly when a large nominal maximum aggregate size is used (14). Thus, a notched wedge joint was introduced and first used in Michigan in the mid-1980s (13). Also, the wedge's slope and the notch's size and location can be variable. The joint's wedge is believed to significantly reduce the chances of transverse migration of the hot asphalt material during compaction. The edge of a wedge joint presents a sloped interface that is overlapped by the hot asphalt material. Since the sloped surface of the wedge joint is usually a thin asphalt layer, its temperature rises while being laid over by hot lane's asphalt material that can develop a better aggregate interlock at the joint during compaction and improve density (16).

2.3 Rolling Methods

Constructing a longitudinal joint requires compaction using a steel drum and pneumatic tire rollers using different methods/patterns. These methods affect the joint's density differently, hence the performance. A brief description of such methods is presented in this section.

2.3.1 Hot Overlap

In this method, the compaction at the joint takes place from the hot side. Most of the breakdown steel drum roller is on the hot lane while overlapping 6 in (150 mm) onto the cold lane, as illustrated in Figure 2.1. The compaction is usually accomplished using the roller in vibratory mode.

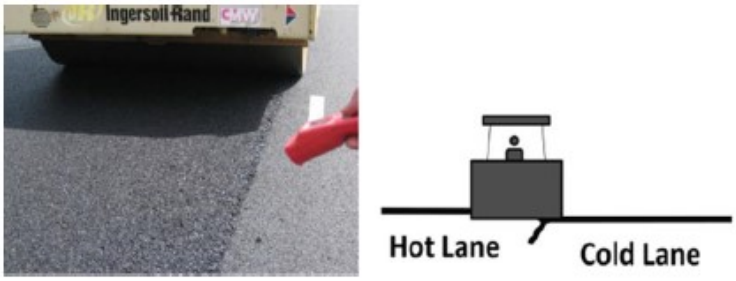

Figure 2.1 Hot overlap method (*16*)

2.3.2 Hot Pinch

The hot pinch method differs from the hot overlap method in that the drum of the breakdown roller completely sits on the hot side, keeping the drum's edge at least 6 in (150 mm) away from the joint (Figure 2.2). Rolling with the vibratory mode is believed to push the hot asphalt material toward the joint and help enhance the achieved density using the hot pinch method. The hot pinch method should be used while compacting tender mixes or thick lifts since such conditions can force the asphalt material toward the joint (15). Pushing the asphalt material towards the joint can form a slight hump over the joint, usually after the first pass. Such a hump of material can help attain an even uniform surface at the joint with improved density (17). Literature shows that using a pneumatic tire roller is beneficial during compaction instead of the steel roller. A pneumatic tire roller can knead the low-density areas near the joint, helping improve joint density, which is not achievable using the steel drum roller due to the bridging effect (16).

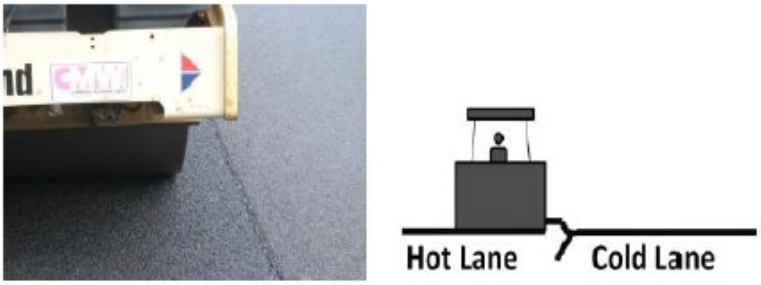

Figure 2.2 Hot pinch method (*16*)

2.3.3 Cold Roll

In the cold roll method, the compaction is accomplished while most of the roller's drum is on the cold side and overlaps the hot side by 6 to 12 in (150 to 300 mm) (see Figure 2.3. The roller should be used in static mode to avoid cracking on the cold side. Timing is critical while using this method. Since compaction of the mat commences from the cold side, the hot side loses heat by the time the roller can cover the complete width of the hot side. Such cooling hinders the compaction of the hot asphalt mat. A pneumatic tire roller is not well suited while using this rolling method and compacting the mat at the

free edge of the cold side of the joint as it will transversely move the hot material away from the joint (*16*). The use of a steel drum roller is suggested instead.

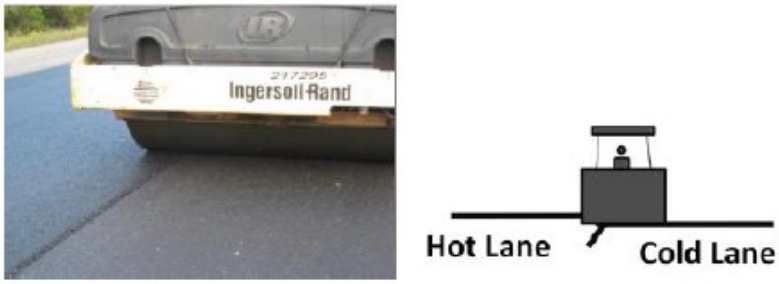

Figure 2.3 Cold roll method (*16*)

2.3.4 The Maryland Method

The "Maryland Method" refers to a method-based specification used for rolling and compaction of confined joints. The method involves the following three steps:

1. The existing adjoining mat's edge (constructed previously) is overlapped by 1 to 1.5 in (25 to 38.1 mm) with the hot asphalt material while paving. Any HMA material exceeding 1.5 in (38.1 mm) should be bumped back. Ensuring a true straight edge while paving (the previously constructed lane) is essential for achieving a better density at the joint.
2. The hot asphalt material is locked and consolidated by compacting it, keeping the roller 6 to 12 in (150 to 300 mm) away from the longitudinal joint. This helps in pushing additional hot asphalt material into the joint.
3. Finally, employing the maximum vibratory force of the roller, the overlapped and the pushed hot HMA material is compacted into the confined space, resulting in optimum joint density. The appearance of a thin white line on the top of the longitudinal joint indicates the successful application and completion of the Maryland Method (see Figure 2.4). A video clip showing the use of the Maryland Method for the construction of confined longitudinal joints can be found at https://mdasphalt.org/2019/best-practices-maryland-method-longitudinal-joint-compaction/.

Figure 2.4 Appearance of a thin white line over the confined joint using the Maryland method at the Manning Trail project, MN

2.4 Construction Techniques

Different techniques are used to construct longitudinal joints in asphalt pavements. Each of these techniques is believed to impact the quality and performance of the joint. This section presents a brief description of the different longitudinal joint construction techniques.

2.4.1 Tandem or Echelon Paving

Echelon paving is a construction technique that can construct multiple adjacent lanes simultaneously using at least two pavers, one following the other at a short distance. Tandem paving is similar to echelon paving; the only difference is the spacing between the pavers that are further apart than the echelon paving setup. These paving techniques ensure the construction of a hot joint, achieving a seamless mat.

2.4.2 Sequential Mill and Fill Technique

This technique is used for a mill & fill project, where one lane is milled & filled at a time rather than milling all lanes simultaneously, followed by asphalt laying lane-wise. In the sequential mill and fill technique, thoroughly cleaning the milled surface and the confined edge is required before laying fresh asphalt material. This technique provides a confined edge for the hot lane to be laid and compacted, thus helping achieve better density.

2.4.3 Wedge Construction Technique

The free edge of the longitudinal joint is constructed with a wedge shape. The wedge construction requires a special plate attached to the paver's screed that shapes the edge at the unconfined edge like the one shown in Figure 2.5. The wedge joint can be constructed with or without the notch at the top.

The compaction of the wedge is achieved using truck tires, a steel side roller wheel, a rubber side roller wheel, or a tag-along roller attached to the compactor (18, 19). Varying degrees of sloped surfaces with slopes of 3:1, 6:1, or 12:1 can be constructed using the different wedge compaction techniques.

Figure 2.5 Schematic drawing of a notched wedge joint (*17*)

2.4.4 Edge Restraint Technique

Like the wedge construction, this technique uses an additional fixture attached to the compacting roller, as seen in Figure 2.6, that pinches the unconfined edge of the first laid lane towards the roller simultaneously. Such a practice provides lateral resistance to the hot material's movement away from the joint (15, 20, 21). The joint's edge constructed using the edge restraint technique is steeper than the one constructed with a wedge technique.

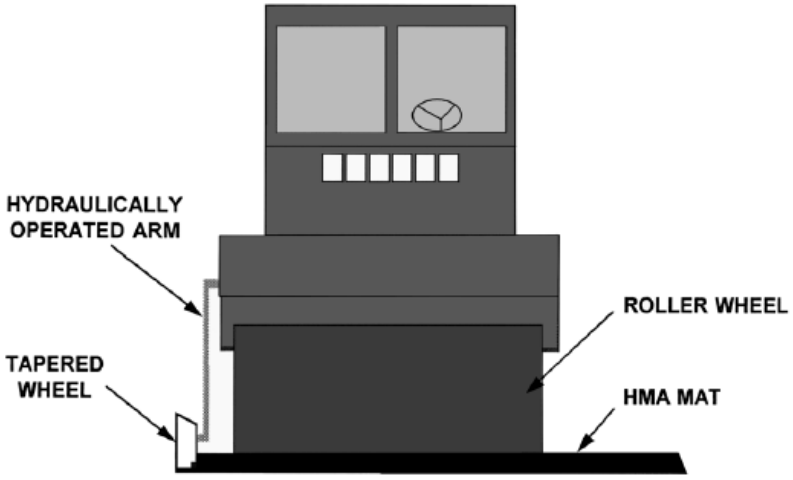

Figure 2.6 Schematic of an edge restraining device (*21*)

2.4.5 Joint Maker Technique

This technique also restraints the unsupported edge of the mat using an inclined rounded-edge metal mass attached to the side of the paver screed (Figure 2.7). The device helps pre-compaction the asphalt material before being fed into the screed for subsequent laying. The excess material is racked back into the joint by a kicker plate attached to the end of the paver's screed and helps produce a more vertical face at the edge and a smooth joint (16). The joint maker can also be combined with a notched wedge technique to construct a longitudinal joint.

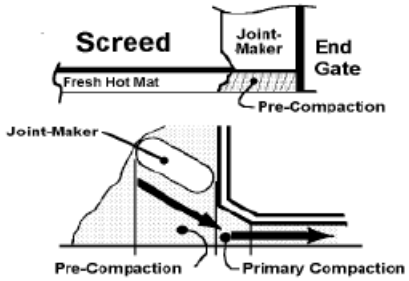

Figure 2.7 Longitudinal joint construction with a joint maker (*22*)

2.4.6 Cutting Wheel Technique

A cutting wheel with a diameter of 10 in (250 mm) is used to cut the unconfined edge [usually 2 to 6 in (50 to 150 mm)] of the freshly laid asphalt while still in a plastic state (15, 16). The cutting wheel is generally attached to a roller or other plant equipment (Figure 2.8). Since the low-density edge material is removed by cutting away from the cold lane, a high-density, smooth, and cleaner confined edge is provided to the adjacent lane whose construction will follow.

Figure 2.8 Cutting wheel attached to grader (2)

2.4.7 Joint Adhesives and Sealants

Several products have been used to seal the longitudinal joints to inhibit water and air access into the joint. Joint adhesives and sealers are believed to enhance the bonding between the lanes and seal the pavement's surface, respectively. Thus, the chances of the lanes separating at the joint are minimized, and the joint's integrity is preserved. Commonly, the sealants are applied (on top of the joint) after construction and are intended to reduce permeability (Figure 2.9). The adhesives can be applied on the edge of a cold lane before laying and compacting the hot asphalt material for the adjacent lane. It can also be applied over the joint after compacting both sides. The adhesives can also be applied to the underlying layer before laying either of the asphalt layers, expecting the heat from the hot material to transport the adhesive into the joint and theoretically reducing the number of interconnected voids (16).

Figure 2.9 Application of joint adhesive and sealants (*16*)

Void-reducing asphalt membranes (VRAM) have also been used to construct longitudinal joints. It can be applied to the surface at the joint location before laying asphalt material for either lane. The idea behind its use is that it heats once hot asphalt material is laid over it, migrates up, and fills 50 to 70% of the joint's air voids rendering it impermeable (23).

2.4.8 Infrared Joint Heaters

The density differential occurring at the joint and adjacent areas is the primary cause of the problems that arise once hot asphalt material is laid against an already cold edge of the earlier lane. A hot joint can be obtained if the cold edge is warmed up and the hot lane is laid. The infrared joint heaters use the same premise, where the cold edge of the lane laid earlier can be pre-heated just before laying the adjacent hot lane. Thus, like echelon paving, the obtained hot joint will ensure better adhesion between the two lanes and improved compaction ability. The concept of a joint heater has existed for over 30 years. Modern joint heaters employ propane-powered, highly efficient infrared technology mounted on a trailer that can travel immediately ahead of the paver and heat the joint area relatively quickly. In most cases, it can travel at speeds similar to the paver as these can raise the pavement temperature to 200 to 250 °F (93 to 121 °C) (16).

2.4.9 Warm Mix Asphalt (WMA)

The use of WMA has proved to be beneficial in achieving higher-density longitudinal joints in Canada. The ease of compaction of the WMA asphalt is believed to enhance its ability to achieve denser joints. Also, the reduced temperature difference between the hot asphalt material being laid coupled with the ability of the cold edge material to absorb heat, becoming slightly workable, are considered to help achieve tighter joints with improved density and enhanced adhesion between the joint interfaces (24, 25).

2.5 Comparison of Practices

Table 2.1 presents the benefits and drawbacks of all the longitudinal joint construction types, methods, and techniques explained earlier.

Table 2.1 Comparing benefits and drawbacks of different longitudinal joint construction methods.

Construction method	Benefits	Drawbacks
Butt joint	• Commonly used joints; can perform well if constructed properly (11)	• Present safety issues if traffic is maintained during the construction of thick lifts (20) • Edge drop-off requires pulling up the adjacent lane, thus impacting productivity • Water ingresses the pavement easily if the joint separates, especially if underlying layer joints are not staggered (14) • Prone to raveling (19)
Tapered or notched wedge joint/ wedge construction	• Creates a small ramp for traffic avoiding edge drop-off issues improving productivity, i.e., the adjacent lane does not require pulling up within a short time window (13, 14) • Reduces permeability and enhances density by restraining the mat's edge, providing confinement (1, 2, 13, 15, 16, 19, 22, 26)	• Without the notch, crushing of aggregates under roller load can cause raveling problems along the joint (27) • Compaction of the wedge requires special attention, especially for thick lifts with larger NMAS and coarse gradation (13, 14) • Notch and taper dimensions are required to be appropriate for the NMAS and layer thickness (14) • Not suitable for thin overlay projects (2)
Hot overlap rolling method	• An efficient rolling method as the majority of the roller sits over the hot asphalt material (17) • Minimizes vertical differential between lanes; recommended for achieving adequate bond (15, 16, 28)	• It may cause the hot asphalt material to move laterally away from the joint (2, 17)
Hot pinch rolling method	• Preferred for tender mixes or relatively thick mixes as pushes material toward the joint (15, 17) • Results in improved joint performance (16, 29)	• The formation of a hump can hinder proper compaction of the neighboring material due to the bridging effect (16) • Development of secondary cracks along the pinch line (2, 16)

Table 2.1 Comparing benefits and drawbacks of different longitudinal joint construction methods. (continued…)

Cold roll method	• Provides good initial compaction and reduces vertical differential at the joint (16) • Experience has proved that this method produces joints with minimal cracking and better performance (16, 30)	• Placing most of the roller over the compacted mat wastes compaction energy; static mode rolling provides less compaction (16) • The hot asphalt material of the second lane mat loses heat while the joint is being compacted, hindering its compaction (15, 16, 21)
Tandem or echelon paving technique	• Provides good performance avoiding cold joints (14) • Provided excellent joint quality; eliminating the need for joint maintenance (31) • Saves time (17) • Produces joint density close to the mat's density at the center (32)	• Used under no traffic (for echelon paving) or traffic control at the site (for tandem paving); requires at least two pavers with crew thus increasing the cost; needs a high-capacity plant (14)
Sequential mill and fill technique	• Improves joint density by providing a confined edge to the hot asphalt being laid (29) • Eliminates common uneven surface issues at the joint; does not require any special equipment (17)	• Delays the project; milling needs to wait for the paving operation, thus increasing cost (14, 32) • Milling operation might damage the new mix in the adjacent lane; which can cause "new" mix wastage (14) • Thorough cleaning of the milled surface before paving is difficult, especially at night (32)
Edge restraint technique	• Helps increase density at the joint (14, 15, 22) • Reduces permeability (22) • Produces a fairly uniform edge (19)	• Quality depends on the operator's skill (14, 15, 21, 22, 33) • Difficult for the operator to see, and maintain position; requires removal of excess material from the adjacent lane (19)
Joint maker technique	• Claimed to improve joint density and aggregate interlock at the joint, if used properly	• No significant improvement in the joint density has been observed using a joint maker (15, 22, 34)
Cutting wheel technique	• Removes the low-density material from the joint (14, 19)	• Wastes new mix material; requires equipment and manpower for cutting and cleaning; quality is operator's skill dependent (14, 15) (19)

Table 2.1 Comparing benefits and drawbacks of different longitudinal joint construction methods. (continued…)

Joint adhesives	• Reduces permeability (22) • Can improve adhesion at the interface with no negative impacts on performance (14)	• Have not always demonstrated better performance (i.e., reduced permeability) (14) • Require equipment and manpower; Increase costs (14) (22)
Joint sealants	• Can improve permeability around the joint; no additional equipment is required; no negative impact on performance (14)	• Have not always demonstrated better performance (i.e., reduced permeability) (14) • Increase costs (14)
Void-reducing asphalt membrane (VRAM)	• Dries quickly after application (15 to 30 minutes) and can be driven over by the construction traffic; reduces permeability and air voids; can improve cracking resistance as well (23)	• Increased initial material cost; however, the gained benefits can offset this drawback (23)
Infrared joint heaters	• Avoids cold joints; increases adhesion at the joint's interface (14) • Most effective to mitigate joint cracking by enhancing compaction, increasing density, and decreasing permeability (16, 35, 36) • Produce better IDT strength, and reduce cracking and segregation (22, 36, 37)	• Require extra equipment and fuel; increases the length of the paving train; interferes with paving operations; presents safety issues; can scorch mix (14, 22) • Efficiency might decrease along with scorching of the top layer if used on thicker lifts (17) • High wind conditions may impede its efficacy of raising the joint's temperature (31)
Warm mix asphalt (WMA)	• Reduces temperature differential between the joints; reduced temperature results in lower asphalt aging; the versatility of use in various climates; fewer fumes, and less energy consumption in various processes; hence environmental-friendly; reduces joint permeability (24, 25)	

2.6 Joint Quality Evaluation

As mentioned earlier, the longitudinal joints have been considered one of the root causes of the deterioration of flexible pavement since the 1960s when they were highlighted as "low-density

zones"(10). Several studies concluded that a well-constructed longitudinal joint should have 1- to 2% lower density than the mat; 5 to 10% lower if poorly constructed (1, 10, 15, 22, 38). A study in Washington state estimated the effect of air voids on the overall service life of HMA pavements—a reduction of 17 to 36% is expected in the service life of the pavement if the mat density reduces from 92% (8% air voids) to 88 and 90% (10 to 12% air voids) (see Figure 2.10) (5). Seed et al. concluded that a 1% decrease in air voids of a flexible pavement improves its fatigue performance by 8 to 43%; and rutting resistance by 7 to 66% (39). Thus, the longitudinal joint quality is usually determined by estimating its density. The NCAT study presented the joint density and performance data generated by various joint construction techniques. The study reports the following general findings (7, 21, 38, 40, 41):

- "The performance of the longitudinal joint appears to be influenced by the overall density achieved at the longitudinal joint.
- The joint density should be within 2% of the mat density.
- Use cores to measure joint density. The nuclear gauge is impractical."

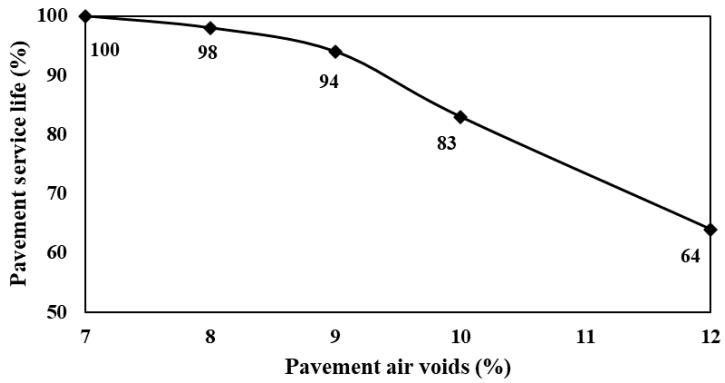

Figure 2.10 Effect of in-place density on service life (5)

2.6.1 Density Measurement

The longitudinal joint density specifications in various State Highway Agencies (SHAs) are tabulated in Table 3.1. Several methods are used to measure the mat's density and longitudinal joints. Determining the density in the laboratory using cores from the pavement is one of the commonly used methods. Some agencies also use nuclear and non-nuclear density gauges.

2.6.1.1 Pavement Coring

Laboratory-derived density measured using cores cut from the pavement is generally believed to be the most accurate (41). There is no particular recommendation for the most appropriate method of determining density from pavement cores in the laboratory (16). Several procedures are used, such as the Saturated Surface Dry (SSD), vacuum sealing, parafilm, CoreReader, dimensional analysis, and X-ray tomography methods. However, determination using AASHTO T166 (i.e., bulk specific gravity (G_{mb}) of compacted asphalt mixtures using SSD specimens) is common. The use of cores for density

determination is widespread among SHAs. According to an NCAT report, 38 SHAs use pavement cores to determine the achieved in-field compaction (*3*). However, assessing the pavement compaction using cores has particular merits and demerits (42, 43):

MERITS

- Most common
- Easy to obtain cores and test
- Useful for post-construction analysis
- Often used as primary components of quality assurance (QA)

DEMERITS

- Destructive in nature
- Expensive
- Time-consuming
- Provides limited coverage, i.e., increases chances of missing localized problem areas
- Unable to provide real-time feedback about the compaction during construction
- Results have a longer turnaround time (1 to 2 days)
- If the longitudinal joint is cored with the core barrel centered over the joint line, the retrieved core will have a larger portion of the cold lane i.e., the lane laid first, especially in the case of a wedge joint (44).

2.6.1.2 Nuclear and Non-Nuclear Density Gauges

The nuclear and non-nuclear gauges were developed as a non-destructive alternative to the pavement coring for density determination. The nuclear density gauge measures HMA density by releasing gamma rays into the pavement and receiving the scattered rays back. The scattering or absorption of the gamma rays depends on the amount of HMA material instead of air voids volumetrically (45). The non-nuclear gauges work by sending an electric field into the pavement; the response is affected by the dielectric constant of the components in the pavement multiplied by their volumes (46, 47). The merits and demerits of the nuclear and the non-nuclear gauges include:

MERITS

- Many measurements can be taken quickly
- Non-destructive

DEMERITS

- Seating is a problem over the joint, especially at the crown of the joint (16). The density gauges are known to underestimate density (41), thus, these devices are used to measure joint density by placing them very close to the joint but not over it.

- The nuclear gauge requires special handling, training, and certification due to the presence of radioactive material.
- Provides limited coverage, i.e., increases chances of missing localized problem areas
- Require calibration

2.6.2 Non-destructive Methods

In Ontario, Canada, deflections measured using a Portable Falling Weight Deflectometer (PFWD) and multi-channel analysis of surface waves (MASW) have been used to evaluate the longitudinal joint quality non-destructively through the elastic modulus estimations (48). The propagation of the waves in a medium is affected by the material properties, such as stiffness and density. Thus, a measurement of wave characteristics can be used to estimate the change in material condition across a joint. The MASW method uses ultrasonic transducers to measure the surface waves traveling through the pavement and estimate the elastic modulus of different layers. The PFWD and MASW methods were applied on both sides of the joints to assess their quality. More minor changes in deflections across the joint were observed using the PFWD data; they cannot be attributed to the joint quality, as pavement sublayers also contribute to the measured deflections. MASW measurements showed promising results for joint evaluations; however, further work was suggested.

2.6.3 Ground Penetrating Radar (GPR)

A Ground Penetrating Radar (GPR) is a device that uses electromagnetic waves to explore the subsurface. GPR has been commonly used to detect free water (49). Using GPR estimation of dielectric properties of pavement materials, layer thicknesses, and evaluation of the HMA layer's density has been accomplished (50-55). It can also help estimate in-field HMA density variability using variations in dielectric properties (56). Traditionally, to determine the HMA layer dielectric properties using GPR, measurements of the round trip travel time from the reflection at a depth of the HMA layer or the surface reflection must be conducted. The issue with the travel time methodology is that it requires prior knowledge of the HMA thickness, which is often unknown or can present significant variability. In addition, the construction of HMA layers in several lifts or the presence of an overlay over an existing HMA layer can add an extra challenge to analyzing the travel time from various lifts and different layers.

To compute the bulk dielectric constant (e_r) of the HMA, the AC surface reflection method relates the amplitude (A_0) of the GPR signal reflection from air to the HMA surface to the incident amplitude (A_i) (characterized by the reflection from a metal plate) as shown in Figure 2.11. The dielectric constant of the surface is calculated using the equation (1) (57). For sufficiently thick layers, i.e., a thickness of more than 1.2 in (30 mm), the measurement of HMA surface reflection is related only to the properties of the upper layer. This represents a significant advantage of this method as it can better characterize the layer of interest. The bulk dielectric response of an HMA mixture (i.e., the effective dielectric constant) depends on the mixture components' dielectric response, affected by their dielectric constant and volume fractions in the mixture (58). Although the aggregate types and their volumetric proportions significantly impact the HMA's bulk dielectric properties, the air volume is the primary variation in the

dielectric constant if the mix contains uniform aggregates and their proportions. This phenomenon offers an opportunity to use GPR technology to estimate the HMA compaction uniformity in the mat and the longitudinal joint.

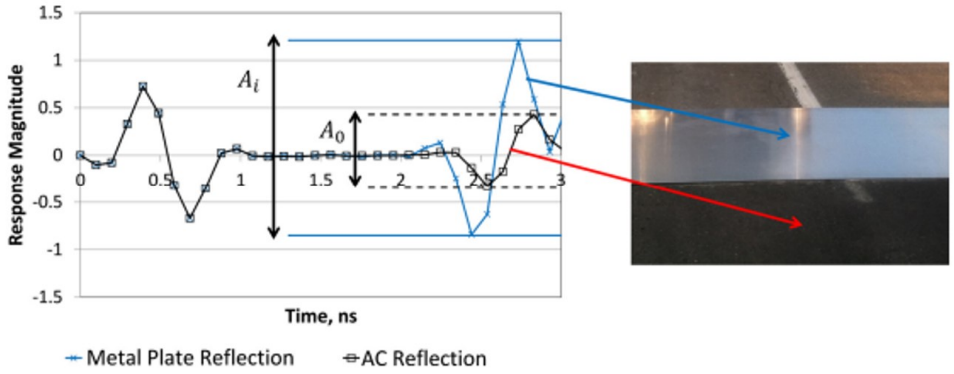

Figure 2.11 GPR reflection signals

$$e_r = \left(\frac{1 + \left(\frac{A_0}{A_i}\right)}{1 - \left(\frac{A_0}{A_i}\right)} \right)^2 \quad (1)$$

However, measurements of the dielectric constant obtained from coring for each new HMA mix are necessary because the dielectric properties of the HMA mix will vary in different projects based on the dielectric properties of the various mix components. A rolling density meter (RDM – Figure 2.12), GPR-based equipment known as the density profiling system (DPS), evolved from recent research conducted under the National Academies of Science sponsored second Strategic Highway Research Program (SHRP2) (42, 59). The system utilizes specially-designed GPR sensors, whose collected data helps determine the dielectric constant of the HMA layer in flexible pavement. All the data collected by the GPR sensors is analyzed and processed in a concentrator box. The DPS onboard computer reports the dielectric constant values of the HMA surface in real-time. The obtained HMA dielectric values can be correlated with the newly constructed pavement's air void percentage and density.

Several field studies in Minnesota demonstrated the device's high accuracy (42, 60, 61). One of Minnesota's field trials identified low joint compaction as a critical issue (42). When there is access to a fully-formed longitudinal joint, conducting a DPS pass with the closest to the joint sensor positioned 6 in (150 mm) from the joint on its unconfined side is recommended. The measured dielectric properties can be compared with the mat's dielectric properties away from the joint. A lower dielectric constant at the joint would indicate higher air void content. A similar dielectric content would indicate similar levels of compaction. The dielectric constants measured by DPS can be correlated with the percent air voids and density using the lab-measured air void content from the cores or Superpave gyratory compactor (SGC) specimens (62).

Figure 2.12 Three-sensor Density Profiling System (*courtesy of MnDOT*)

Figure 2.13 displays the variation of the DPS-measured dielectric constants for the inner and outer lanes along with the confined and unconfined sides of the joint at different stations of a 1,000-ft stretch section of HWY 52 near Zumbrota, Minnesota. The compaction levels for the inner and outer lanes appear very similar and uniform across the different stations. However, the unconfined side of the joint has lower dielectric values (i.e., higher air void content) compared to the confined side of the joint. The figure also shows that the dielectric values for the joint's confined side are lower than for the unconfined side in some areas. Such results indicated inconsistency in the joint compaction for the section and were used to provide real-time feedback to the crew. The low dielectric values indicated poor compaction occurred at locations where the roller pattern would reset. Thus, paving was modified, and the issue was resolved (42).

The long-term performance of flexible pavements is highly affected by the general compaction quality of the mat and the longitudinal joint in particular. However, the traditional compaction evaluation methods (i.e., coring or nuclear gauges) to provide quick and continuous data collection, desired for minimum traffic delays on major highways, make DPS an attractive alternative. The DPS data collection is fast and continuous, ensures greater coverage, and can provide real-time results during compaction. Figure 2.14 shows a DPS survey in which areas with higher dielectric constant locations indicate satisfactory compaction levels, while areas with lower dielectric values indicate deficient compaction. The data provides real-time compaction mapping to contractors and inspectors. Therefore, DPS can be an efficient and reliable quality control (QC) tool that can help achieve optimum compaction, thereby improving the as-built density and, eventually, the performance of flexible pavements.

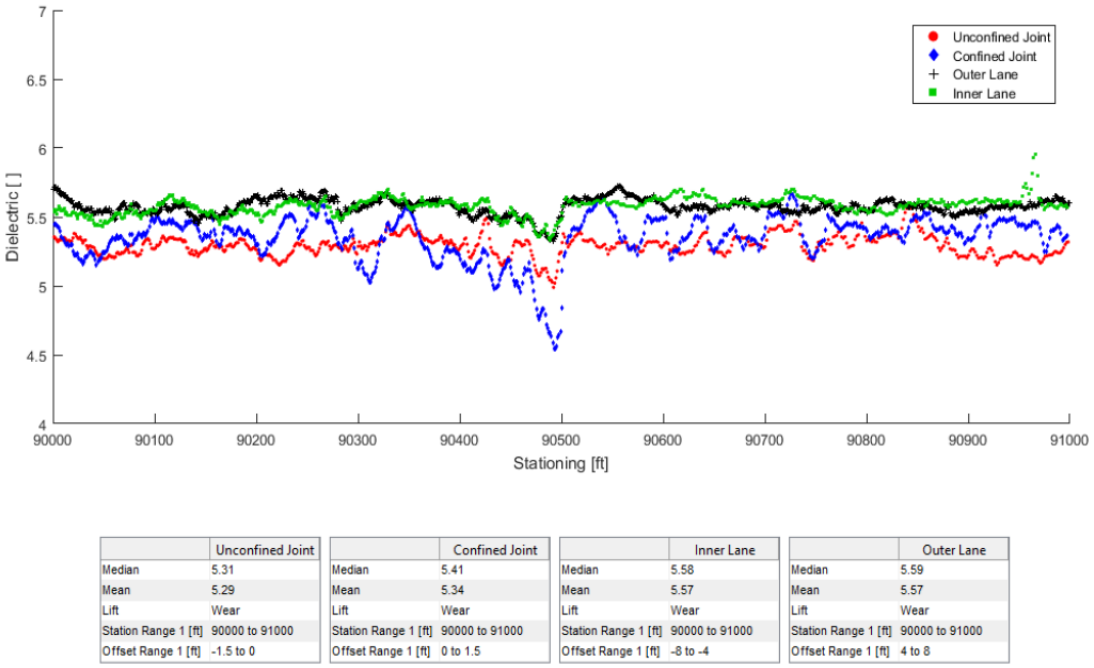

	Unconfined Joint
Median	5.31
Mean	5.29
Lift	Wear
Station Range 1 [ft]	90000 to 91000
Offset Range 1 [ft]	-1.5 to 0

	Confined Joint
Median	5.41
Mean	5.34
Lift	Wear
Station Range 1 [ft]	90000 to 91000
Offset Range 1 [ft]	0 to 1.5

	Inner Lane
Median	5.58
Mean	5.57
Lift	Wear
Station Range 1 [ft]	90000 to 91000
Offset Range 1 [ft]	-8 to -4

	Outer Lane
Median	5.59
Mean	5.57
Lift	Wear
Station Range 1 [ft]	90000 to 91000
Offset Range 1 [ft]	4 to 8

Figure 2.13 Variation in measured HMA dielectric values using DPS (*42*)

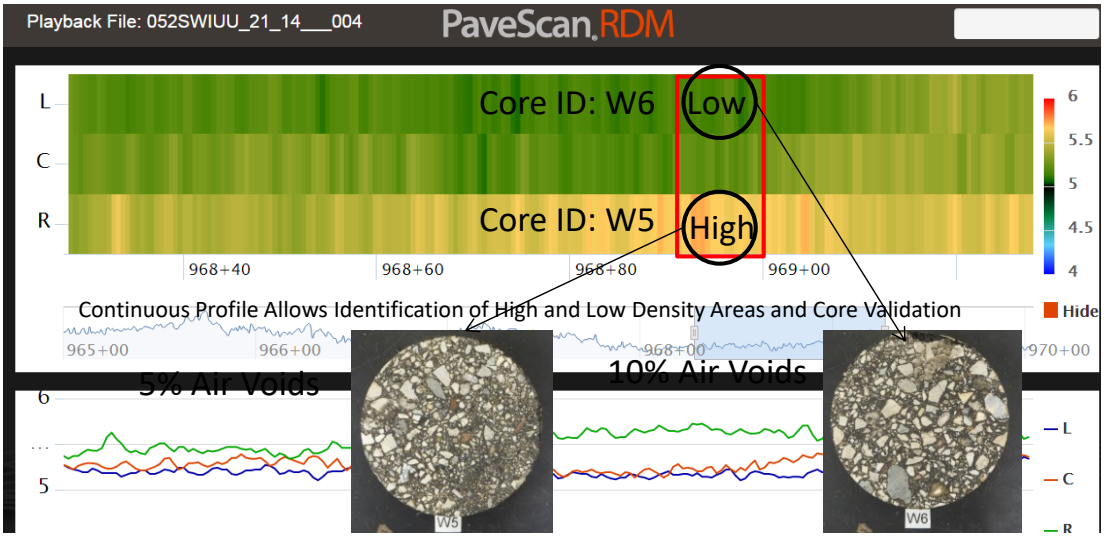

Figure 2.14 Real-time data visualization and comparison with cores (*42*)

2.7 Repair and Maintenance

After the appearance of deterioration on the longitudinal joints, immediate repair is warranted. The repair timing is critical as it influences whether to implement a preventive treatment (i.e., less expensive) or reactive (i.e., most expensive alternatives). A brief description of the different longitudinal joint distress repair techniques is presented.

2.7.1 Slot Paving

The slot paving involves milling a narrow pavement width around a distressed and deteriorated longitudinal joint, cleaning the slotted area, applying tack to the sides and bottom of the excavated area, and then repaving with HMA. Ohio Department of Transportation (ODOT) has successfully used this longitudinal joint repair technique to repair medium and high-severity joint distresses (see Figure 2.15). The width of slots varies; slot widths from 4 to 12 ft require a standard paver for laying the HMA material, while a "berm" box attachment mounted on the side of a paver is used to fill smaller slot widths. According to an ODOT supervisor, a successful slot construction requires that each inch of slot depth is accompanied by at least one foot of slot width. The estimated treatment life for slot paving is 4.3 years (63). However, slot paving results in two joints instead of a single one to maintain, and also, the joints get closer to the wheel path.

Figure 2.15 Slot paving in Ohio (*63*)

2.7.2 Spray Injection

The spray injection technique substitutes the traditional pothole patching process. It involves cleaning the pothole using air to remove debris or water, applying emulsified asphalt, mixing the aggregate chips with emulsified asphalt, and filling the repair area with the aggregate-asphalt blend using compressed air. After applying an aggregate layer over the repaired joint, the pavement is opened to traffic with or without compaction. ODOT uses the semi-automated spray injection process to repair longitudinal joints (Figure 2.16). Spray injection is considered a corrective repair; however, it can work as a preventive maintenance treatment if used on time. Present ODOT practices estimate a service life expectancy of 2.2 years for a spray injection, a suitable treatment for medium to high-severity distress levels on joints (63).

2.7.3 Crack Sealing

Crack sealing is a commonly used treatment that fills the distressed longitudinal joint and prevents the ingress of moisture, debris, and air into the crack. It involves the injection of bituminous materials into the crack to impede the rate of moisture infiltration into it (Figure 2.17). According to ODOT practices, it is the most cost-effective treatment for low to medium-level distressed longitudinal joints with 4.5 years of expected service life (63). It is also used as a preventive maintenance treatment in longitudinal joint

repair practices by the Minnesota Department of Transportation (MnDOT). It can perform satisfactorily for three years if applied at the right time (64, 65).

Figure 2.16 Spray injection in Ohio (*63*)

Figure 2.17 Crack sealing in Ohio (*63*)

2.7.4 Overbanding

It is a joint seal treatment applied to the joint after construction, mainly if the joint density is not up to the specification and applied in early pavement life (Figure 2.18). It is quick, requires minimal traffic disruptions, and is a cost-effective treatment. Caution should be exercised in deciding to use the overbanding treatment for cracks, especially on curves, as these may cause slipping problems for motorcycle traffic (64).

2.7.5 Additional Repair/Maintenance Options

MnDOT has also used chip seals, fog seals, and sealants as preventive maintenance treatments over the longitudinal joints to prevent severe deterioration. Fog seal application includes diluted emulsions and rejuvenators applied not more than two feet wide over the joints (65). Fog seals were found to effectively seal the joints reducing permeability without any aesthetic issues (66). Sealants were found to reduce the ingress of water infiltrating into the joint; however, they could not help limit the deterioration of areas near the joint with a lower density. Medium to high severity levels of distress over

the joints present safety issues; cold mix patching, micro surface, and mastic treatments have also been used (65).

Figure 2.18 Overbanding in Michigan (*67*)

The literature review suggests that crack sealing and micro surfacing should be used for longitudinal joint maintenance and repair until they cannot be used further due to the crack conditions. These are cost-effective alternatives compared to the other options, as shown in Table 2.2. Spray injection treatment should be used if the joint deterioration is medium to severe level. Slot paving should be the last resort since it is the most expensive alternative and forms two joints instead of a single one closer to the wheel path.

Table 2.2 Longitudinal joint repair techniques cost comparisons (*63*)

Treatment	Life (years)	Cost (per mile)	Cost (per mile per year)
Crack sealing	4.5	$3,362	$747
Spray injection	2.2	$12,763	$5,801
Slot paving	4.3	$104,644	$24,336

2.8 Statewide Practices for Longitudinal Joint Construction

Table 2.3 summarizes the longitudinal joint construction, specification, and/or repair practices used by different states in the US and Canada.

Table 2.3 Longitudinal joint construction, evaluation, specification, and repair practices (11, 23, 63, 68-70).

State	Longitudinal joint practices
Minnesota	• **Construction**: Joints are constructed at the centerline or lane lines of the pavement; no joint be located in the wheel path; a 6 in (150 mm) offset is required in joints of the overlying layer; over concrete pavements, HMA longitudinal joint be aligned over the concrete longitudinal joint; tack coat is required except when a joint adhesive is used; uses Maryland joint method that requires a 1 to 1.5 in (25 to 38.1 mm) overlap over the adjacent lane which is 0.25 in (6.35 mm) thick • **Density measurements**: Cores are taken from both sides of the joints with the outer edge of the core 6 in (150 mm) away from the joint, a companion core 12 in (300 mm) apart longitudinally from the first core is always taken along with two pavement cores from the mat, 2 ft (0.6 m) right and left of the joint for density measurements • **Specifications**: Wear course joints require 89.5% minimum density along a confined edge, and 88.1% at the unconfined edge; lower layers require 90.5% density at a confined while 89.1% density at the unconfined edge; Incentive and disincentive payments system is in place for longitudinal joints • **Repair**: Use chip seals, fog seals, and sealants as preventive maintenance treatments; treat medium to high-severity distressed joints with micro-surfacing, cold mix patching, and mastic treatments
Ohio	• **Construction**: Uses butt or notched wedge joint (commonly used); requires tack coating the edges before paving; 3 in (76.2 mm) or lesser joint offset; 0.5 in (12.5 mm) minimum overlap of the joint edges is required. • **Density measurements**: Use 6 in (150 mm) diameter cores for density measurements taken within 48 hours of the joint construction; joint core location depends on the type of joint; cores are centered on the visible seam for butt joints but taken 1 in (25 mm) towards the wedge from the visible seam for a notched wedge joint • **Specifications**: An incentive and disincentive payments system is in place for longitudinal joints using percent within tolerance (PWT) determined by the department • **Repair**: Uses crack sealing followed by spray injection for joint PM and repair; uses slot paving as a last resort.

Table 2.3 Longitudinal joint construction, evaluation, specification, and repair practices. (continued…)

Illinois	• **Construction**: Joints are constructed at the centerline or lane lines of the pavement; stage construction requires a 3 in (75 mm) offset of the joint from the preceding layer's joint; a notched wedge joint is required for greater than 2 in (50 mm) lifts; requires a 1 in (25 mm) deep or up to 1.5 in (38.1 mm) (for thicker lifts) vertical notch at top and bottom of the paving lift with 9 to 12 in (228.6 to 300 mm) of width between the notches; notch wedge joints requires a tack coat; Use 18 in (457.2 mm) wide [0.19 in (4.76 mm) thick for the top course] longitudinal joint sealant (LJS) centered under all the joints with or without a tack coat to reduce air voids; rolling is required to start at the lower elevation edge of the pavement, moving towards the other end overlapping the previous trip; unconfined edges should not be overlapped however if allowed, pneumatic tire roller should be used to roll the edge; rolling at a confined edge requires using hot pinch method for the first pass (i.e., keeping away not more than 6-inches from the joint) while using hot overlap rolling [overlapping cold side not more than 12 in (300 mm)] on the second pass beyond which the rolling should continue from the lower elevation edge towards the other side ensuring some overlap on each roller trip • **Density measurements**: No density measurement within 12 in (300 mm) of the LJS applied joint between adjacent lanes; requires 92.5% and 90.5% density at the confined and unconfined edges for SP mixes, respectively. The SMA mixes require 93.5% and 91.5% density at the confined and the unconfined edge, respectively; joint density testing is required at a distance equal to the lift thickness or a minimum of 4 in (100 mm) from each of the pavement edges. • **Repair**: Uses micro surfacing for joint repairs; two-layered if the joint is severely distressed; 18 in (457 mm) centered over the joint
Connecticut	• **Construction**: Uses notched wedge joint for lifts thickness between 1.5 to 3 in (38 to 75 mm) with a 0.5 to 1.5 in (12.5 to 25 mm) notch at top and bottom; wedge slope varies between 8:1 and 12:1, contractor option; tack coat applied on the cold face; wedge compaction is required by specifications; butt joint is used for lift thickness less than 1.5 in (38.1 mm) or greater than 3 in (75 mm); when notched wedge cannot be used due to site restrictions, a butt joint with hot poured rubberized asphalt treatment is constructed • **Density measurements**: Cores from a notched wedge joint should be taken such that the core's center is 5 in (127 mm) from the visible joint on the hot side of the mat; the edge of the cores taken from a butt joint should be within 1 in (25 mm) of the joint and taken from the hot side; 4 or 6 in (100 or 150 mm) cores are used • **Specifications**: An incentive/disincentive system is in place with a minimum of 91% of TMD required for full payment; remove and replace if the density is 86.9% or less
Indiana	• **Construction**: Advocates notched wedge joint with a 0.5 in (12.5 mm) notch and 12 in (300 mm) taper but joint construction details are left at the contractor's discretion; requires locating joint on lane lines with a 6 in (150 mm) offset in joint in the underlying layers; use joint adhesive on unconfined edges of the surface course and top of the intermediate layer; applying 12 in (300 mm) emulsified asphalt (fog seal) on either side of the joint only on the top layer • **Density measurements**: Uses density for joint evaluation using cores from random locations taken not less than 6 in (150 mm) and 3 in (75 mm) from the unconfined and the confined edges, respectively. • **Specifications**: The lower specification limit for joint density is 91% of the percent G_{mm}.

Table 2.3 Longitudinal joint construction, evaluation, specification, and repair practices. (continued…)

Washington	• **Construction**: Uses notched wedge joints; requires sealing material application on the vertical butt joint before paving the second lane; uses half-inch NMAS in a 1.8 in (45.7 mm) thick layer.
Rhode Island	• **Construction**: Uses sealants over joints and edges of newly placed pavements; requires staggering of joints in successive layers by 6 in (150 mm) allows hot asphalt material to be raked onto the joint but not broadcasted back over the hot mat
New York	• **Construction**: Uses either a butt or wedge joint (optional); joint over 100 ft (30.5 m) that is to cool overnight before laying subsequent lane next day is to be a tapered wedge joint; Butt joint construction requires 2 to 3 in (50 to 75 mm) of HMA material overlap over the cold edge; Notched wedge will have a half-inch notch on top, wedge slope not greater than 1:8 inches, and requires 1 to 1.5 in (25 to 38.1 mm) overlap of hot asphalt over the cold edge of the joint; allows hot asphalt material to be raked onto either (butt or notched) joint but not broadcasted back over the hot mat • **Specifications**: No joint density specification; however, cores used for acceptance are not allowed within 23 in (584 mm) of any edge
Missouri	• **Construction**: All top surface joints are constructed at the lane lines of the pavement, with no pavement markings over the joint; overlying layers have a 6 in (150 mm) stagger in the joint location; the engineer may require a light coating of bituminous material over the exposed edges before paving hot material • **Specifications**: For confined edges, density specification of the mat will be used (i.e., 92% for SP and 94% for SMA mixes), while the minimum density within 6 in (150 mm) of the joint should not be less than 2% of the minimum required mat density at the unconfined edge (i.e., 90% for SP and 92% for SMA mixes)
Michigan	• **Construction**: Categorizes longitudinal joints into two types. A Type 1 joint will abut new HMA pavement; when butt joint is used, the adjacent lane is laid on the same day; a notched wedge joint can also be used [with a 0.5 to 1 in (12.5 to 25 mm) notch on the top and tapered at a slope not greater than 1:12); the tapered portion extending beyond the lane width; A Type 2 joint is when a mat is abutting an existing pavement (HMA, PCC) or curb and gutter; type 2 joints are subject to matt density specification; All joints should coincide with painted lane lines; require tack coats, type 2 joints require double coat over the vertical face; unconfined edge on butt joint is rolled keeping roller 3 to 6 in (75 to 150 mm) away from the joint in the first pass followed by roller overhanging 3 to 6 in (75 to 150 mm) over the joint in the second pass; while rolling a confined edge, use hot pinch method keeping roller 6 to 8 in (150 to 200 mm) from the joint on the first pass while using the hot overlap method [overlapping cold side by 6 to 8 in (150 to 200 mm)] on the second roller pass; when using wedge joints, adjacent lanes are required to be laid within 24 hours • **Density measurements**: Joint density is measured using cores 6 in (150 mm) in diameter taken at the center of the joint; if different mixes are used on either side of the joint, take the core 4 in (100 mm) off-center on the cold side • **Specifications**: Average joint density based on five consecutive joint core less than 89% require the contractor to stop asphalt laying and make the necessary adjustments to improve the density; joint density less than 88% require saw or route and sealing of the joint; joint density less than 86% requires to remove and replacement of the entire lane 6 in (150 mm) past the joint; Incentive and disincentive payments system is in place for longitudinal joints

Table 2.3 Longitudinal joint construction, evaluation, specification, and repair practices. (continued…)

Wisconsin	• **Construction**: Joints are constructed at the centerline or lane lines of the pavement; uses wedge joint on all unconfined edges with 0.5 to 1 in (12.5 to 25 mm) notch on top after compaction and tapers 12:1 that is extended beyond the lane width; the wedge of all layers is required to overlap and slope in the same direction directly; wedge construction requires a strike-off device, a roller having the same width as the wedge is required to compact the initial portion of the wedge to almost the final density level; tack application to the wedge is required; confined edges require cutting back to achieve a full depth butt joint; clean and paint the joint with a hot asphaltic, cutback, or emulsified asphalt • **Specification**: Has a special provision for reheating HMA joints when abutting cold edges; reheats an 8 in (200 mm) wide strip of the cold edge to a temperature within 60 °F of the temperature of the hot material at the time of paving
Maine	• **Construction**: Require all cold edges to be coated with emulsified asphalt along with a 3 in (75 mm) coating on the overlaid pavement; require butt joint waived off for echelon paving only • **Density measurements**: Joint density is not monitored; cores for the mat density testing are not allowed within 9 in (228.6 mm) of the joint
Vermont	• **Construction**: Require pavers to be equipped with a wedge or notched wedge forming devices and joint heaters; use wedge joints with a wedge slope of 1:3; cold wedge joints are required to be heated to 95 °C before placing the hot asphalt material of the adjacent lane; require joint compaction first, then compacting from the outer edge towards the center • **Density measurements**: No joint density specification and disallows coring for the mat density testing within 6 in (150 mm) of the joint
Massachusetts	• **Construction**: Require all joints to be treated with a hot pour rubberized asphalt before laying hot asphalt material; joint treatment is waived off if echelon paving is being used and the material temperature is not below 95 °C on the first laid edge before paving with hot material; joint reheating is not allowed • **Density measurements**: No joint density specification is used, cores from the mat for density measurements are not allowed within 12 in (300 mm) of an unconfined edge or joint
New Hampshire	• **Construction**: Requires 1 to 2 in (25 to 50 mm) overlap of hot asphalt material over the cold side; compaction starts with rolling using the hot pinch method [i.e., roller kept 6 in (150 mm) away from joint] followed by rolling with the hot overlap method (6-inch overlap on the cold side); no specific joint density specification, no cores allowed within 1 ft (0.3 m) of edge or joint
California	• **Construction**: All top surface joints are constructed at lane lines of the pavement; joints in lower layers are staggered by 6 in; lifts thicker than 1.8 in (45 mm) require a notched wedge joint with 0.75 in (19 mm) vertical notches at the top and bottom and a 1 ft (0.3 m) wedge in their middle; laying hot HMA against existing pavement require saw cutting and removal of the edge material; tack coat is required at all surfaces • **Density measurements**: Uses calibrated density gauges for testing random locations 6 in (150 mm) from the upper vertical notch after laying the adjacent lane before opening to traffic. Also, uses 4 or 6 in (100 or 150 mm) diameter cores taken 6 in (150 mm) from the upper vertical notch, after placement of the adjacent lane and before opening to traffic for every 3000 ft (914 m) at engineer-selected locations.

	• **Specifications**: Both confined and unconfined edge or mat require a minimum 91% relative density measured through density gauge and core testing; disincentivize contractors for densities below 91% and above 97% of the TMD

Table 2.3 Longitudinal joint construction, evaluation, specification, and repair practices. (continued…)

Pennsylvania	• **Construction**: Used a method specification (Maryland method) and joint type left at the contractor's discretion • **Density measurements**: Now uses a minimum density specification based on 6 in (150 mm) cores centered over the joint for a butt-type joint and centered over the wedge for a wedge joint • **Specifications**: Joint density below 88% requires corrective action; an incentive/disincentive system is in place based on the joint's density • **Repair**: Corrective action includes overbanding the joint with PG-graded asphalt; a 4 in (100 mm) wide band is used centered over the visible joint on surface courses and newly constructed joints where mats on either side of the joint were placed as part of the contract only
Maryland	• **Construction**: Uses exclusively butt joints employing a method specification for the longitudinal joints construction that clearly defines the placement and rolling procedures.
Colorado	• **Construction**: The type of joint (butt or wedge) is left at the contractor's discretion for lifts greater than 1 in (25 mm), while any wedge configuration can be used to meet the safety requirement that disallows an edge drop-off greater than 1 in (25 mm) for the traffic; the majority wedges have 3:1 slope with a notch at the top only; a butt joint is used for lifts thinner than 1 in (25 mm) • **Density measurements**: Uses 6 in (150 mm) cores centered within ± 1 in (± 25 mm) of the visible joint; density calculations are based on $G_{mm,}$ which is the average of both sides of the joint. • **Specifications**: Uses Percent-within-limits (PWL) based on an 88% lower limit; with ≥ 80% PWL = 100% payment; specification is applied to joints in all lifts; requires one core on joint per sublot for QA, while QC requires 2 cores per 2500 linear feet
Texas	• **Construction**: The type of joint (butt or wedge) is left to the decision of the Districts or contractor's discretion; the butt joint is used for thinner lifts while the wedge joint is employed for constructing thicker lift HMA layers; rolling patterns involve overlapping the unconfined edges by 6 in (150 mm) during the first roller pass; tack is applied over the entire wedge; uses a rubber tire roller for intermediate rolling on most of the dense-graded jobs • **Density measurements**: Uses minimum joint density relative to the mat's density measured by a density gauge; one measurement is taken next to the core locations extracted from the mat; a second reading is taken 8 in (200 mm) off the joint; uses cores if the specified joint density is not met • **Specifications**: Any joint density not lower than 3 pcf from the corresponding mat density taken at the same station is acceptable; for an unacceptable joint density, it is calculated using cores and correlated with mat cores; joint density fails if the correlated density is less than 90% of the TMD; no bonus/penalty system is used
North Dakota	• **Repair**: No ideal joint distress solution; uses small equipment to place a microsurface seal over the distressing joint

Table 2.3 Longitudinal joint construction, evaluation, specification, and repair practices. (continued…)

West Virginia	• **Repair**: Uses micro surfacing centered 18 to 24 in (457 to 610 mm) on the joint
Tennessee	• **Repair**: Uses slot paving for joint repairs
British Columbia	• **Repair**: Uses spray injection treatment to repair small potholes, greater than 1 in (25 mm) wide cracks, and longitudinal joints
Alberta	• **Repair**: Uses spray injection as a deteriorated joint repair treatment

2.9 Longitudinal Joint Construction Survey

An online survey was conducted to identify the best longitudinal joint construction practices, material usage, testing, and repair techniques. Several responses received from different Michigan and Minnesota transportation agencies are summarized in this section. The agency and contractor surveys are attached as an appendix to this report. Figure 2.19 shows the distribution of the responses received from different road agencies. The majority (i.e., 39) of the responses received pertain to either city or county transportation agencies of the State of Minnesota. In contrast, six responses were received from the Michigan Department of Transportation (MDOT), representing the State practices. Responses to each question of the agency survey are summarized with additional information (if any).

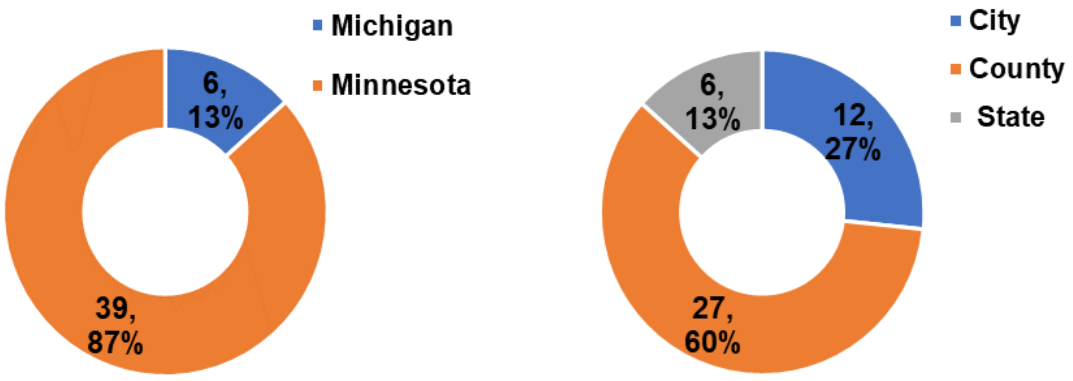

Figure 2.19 Representation of different agencies in the survey data

Question #1: Does the agency specify the type of longitudinal joint for flexible pavement construction? If YES, please specify the type and configuration below:

Figure 2.20 summarizes the responses to survey question #1. Nine (20%) of the total 45 responded that their agency specifies the type of longitudinal joint to be constructed. The following additional information was provided by the individuals who responded in the affirmative to the question:

- Construct the longitudinal joints between strips and parallel to the edge of the through lanes. Construct the longitudinal joints between passes in each lift on top of the previous joint in multiple lift construction. Construct the longitudinal joints to match the plan through lane configuration. As approved by the Engineer, the contractor will align longitudinal joints in multiple lift construction over Portland cement concrete pavements directly over the concrete pavement longitudinal joints.
- Maryland Joint
- Safety Edge
- Spell out echelon or joint density requirements
- Staggered
- Tapered, butt, and feathered joints are specified in the MDOT and echelon paving. These are also listed in the MDOT 2020 Standard Specifications for Construction but are not specified as the only options, so others could potentially be used. From our observations, most joints are being built as butt joints.
- Type 1 (MDOT): A joint that will abut new HMA pavement; when butt joint is used, the adjacent lane is laid on the same day; in lieu notched wedge joint can be used, with a 0.5- to 1-inch notch on the top and tapered at a slope not greater than 1:12, the tapered portion extending beyond the lane width.
- Vertical or tapered

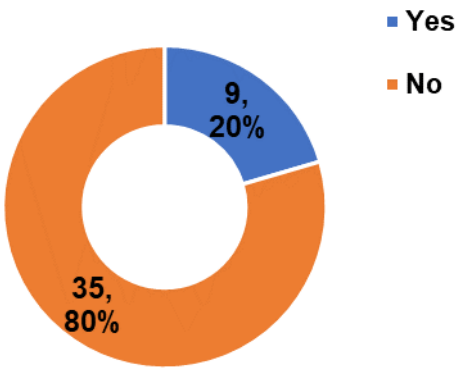

Figure 2.20 Response to survey question #1

Summary comment: The responses show that most agencies do not specify the type of longitudinal joint to be constructed. Most longitudinal joints constructed are butt joints. However, tapered joints with a vertical notch are also used in Michigan. The responses show split opinions regarding staggering the joint in multiple lifts.

Question #2: Does your agency specify a method to roll the unsupported edge while constructing a longitudinal joint for a flexible pavement? If YES, what is the specified method for rolling the unsupported edge?

Figure 2.21 displays the summary of the responses to the question. Nine (22%) of the total 41 responses to the question specify a method for rolling the unsupported edge when constructing a longitudinal joint. In response to the specified method, 67% specify overhanging the joint edge by at least 6 in (150 mm) while rolling it for the first time. The use of a joint maker is also mentioned (1 response) while constructing an unsupported edge. Additional comments received with the responses are as under:

- Stay back on the first pass and overlap on the second pass.
- Close up the Longitudinal joint at the end of the day if possible.

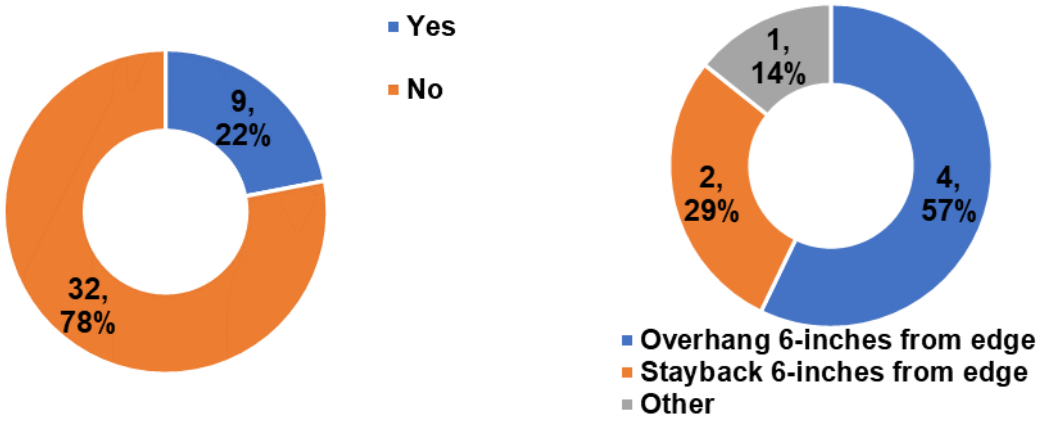

Figure 2.21 Response to survey question #2

Summary comment: A majority of the agencies do not specify the method to roll the unsupported edge of the longitudinal joint. However, overhanging the edge by 6 in (150 mm) while rolling for the first time is a common practice. The use of a joint maker essentially supports the edge; hence, its use can be a good construction practice if available.

Question #3: Does your agency use an infrared joint heater on the longitudinal joint to heat HMA on the cold side?

The survey responses show that none of the agencies require the use of infrared joint heaters. All the responses received for this question were against using infrared heaters (36 replies). The reasons/comments specified by the respondents for not using the infrared joint heaters in the survey are as under:

- Cost, time, and benefit
- Did not improve joint
- Do not like to heat the joint as it can burn off asphalt content, SP specifies no artificial heat
- I did not know it was an option

- Not a common practice in the Twin City metro area
- Not that I am aware of
- Not worth the expense
- St. Louis County matches paving lanes daily
- To date, we have not done this but are interested in advancing our specs to improve joint density
- We have never seen one of these in use locally
- We have not had longitudinal joint issues
- We just do standard paving per MnDOT specifications
- We overlap the joints and thus have not had a problem with the joints

Summary comment: The use of infrared heaters is not common, and the same is evident from the survey results. Also, the observations show that agencies do not favor their use due to the additional costs and time requirements, while some have concerns regarding its performance and benefits.

Question #4: Does your agency specify a method to roll the material while compacting a confined edge, i.e., when laying the adjacent lane after the first lane has been compacted earlier? If YES, what is your agency's specified method to roll the material while compacting a confined joint?

Figure 2.22 shows that only 27% (10 responses) of the agencies specify the method to roll a confined edge, i.e., laying the adjacent lane after the first lane is laid. In contrast, most agencies leave it at the contractor's discretion. The responses are equally split on the method. Half of the responders use the hot overlap method; the compaction takes place from the hot side, overlapping the cold side by 6 in (150 mm). The other half of the responders suggest the hot pinch method in which the roller stays 6 in (150 mm) behind the joint for the first pass and overlaps it by 6 in (150 mm) in the second pass.

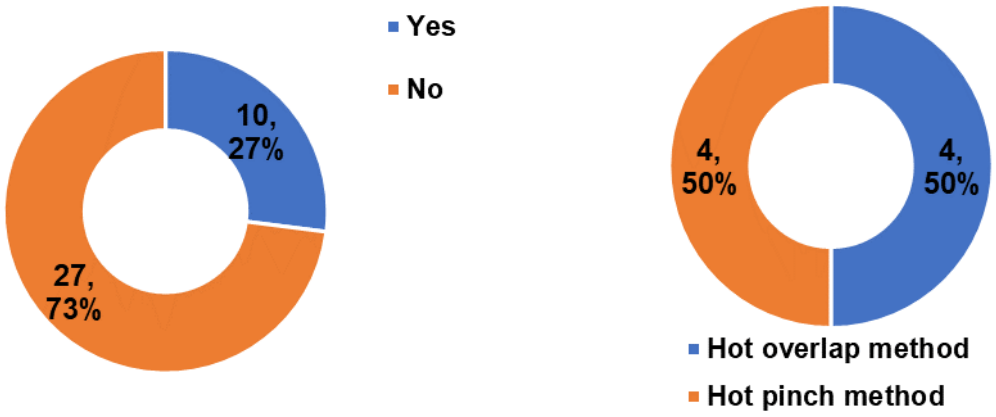

Figure 2.22 Response to survey question #4

Summary comment: As earlier, most agencies do not specify any method to roll the supported edge of the longitudinal joint. However, of those who specify, half of the responding agencies specify using the hot overlap method, while the other half require using the hot pinch method. Since both methods require a roller in a vibratory mode, the hot pinch method may be better as it pushes the hot material

into the joint. This lateral material movement makes a small hump near the joint that is compacted back into the joint. Thus, the joint is not starved of material.

Question #5: Does your agency require the joints to be staggered while laying multiple lifts? If YES, the joints are staggered by how many inches at the least?

Figure 2.23 displays that most (59%) of the agencies require longitudinal joints to be staggered while laying multiple asphalt concrete lifts. The offset between the joints ranges from 2 to 12 in (50 to 300 mm), with 6 in (150 mm) being the most common offset in use. An additional comment from a respondent (from MDOT) is as under:

> *This is not required but is often performed. It is something that needs to be addressed in the design along with the Maintaining of Traffic (MOT) or sometimes in construction and does not work in all situations. Typically we have seen the base and leveling stacked with the top course offset. If the contractor is not able to pave the adjoining mat or offset 12 in (300 mm) minimum, the requirement for longitudinal joint density through coring is removed. Of all the issues we need to work through, one of the more common is poor density due to the poor condition of the existing joint below the roadway (i.e., basically, unsuitable material is present at the centerline due to poor joint construction and creates difficulty for an overlay). Echelon paving is also popular and is determined during design with the locations of joints strategically placed.*

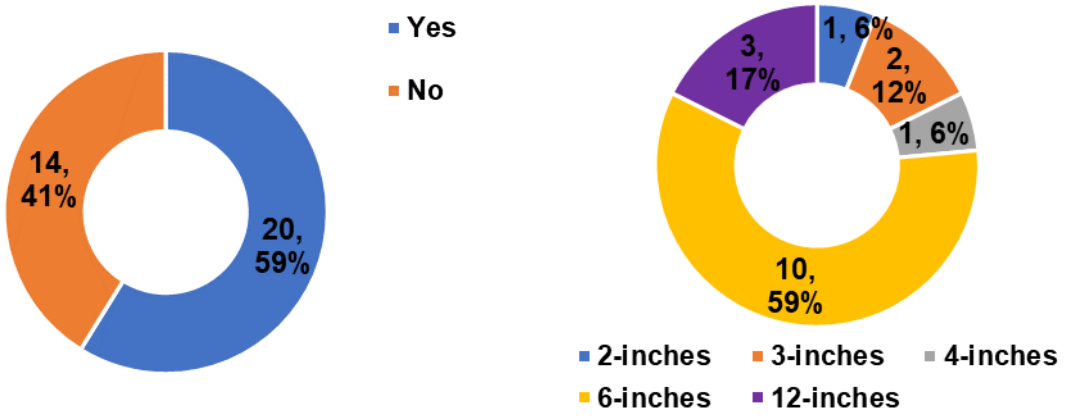

Figure 2.23 Response to survey question #5

Summary comment: It is a good practice to stagger the longitudinal joint while laying multiple lifts. By staggering, one avoids the placement of the weak areas (joints) at the same location throughout the depth of the asphalt concrete layers. It also helps reduce water ingress into the pavement, especially if the longitudinal joint in the top layer separates/opens. The survey responses show that a 6 in (150 mm) offset between joints of multiple lifts is the most common.

Question #6: Does your agency require contractors to seal the longitudinal joints (referred to as "overbanding")? If YES, specify the preferred width and the material.

Most agencies do not require sealing the longitudinal joints, as shown in Figure 2.24. However, only 6% (2 responses) of the agencies require joint sealing. A 0.13 in (3.2 mm) thick, 0.5 in (12.5 mm) overlap on the top and 2 in (50 mm) overlap on the bottom is required with joint adhesive mastic material. Additional comments from respondents who answered with a "No" to this question are as under:

- We have tried applying proprietary material below the joint.
- Not unless core results necessitate corrective action. We require a bond coat on the cold side of the joint but not a surface seal after placing the second pass.
- Sometimes.
- We just follow MnDOT Standard Specification. So, my no answer is for requirements beyond the standard specifications.
- We require a sprayed bond coat on the face of adjacent longitudinal joints

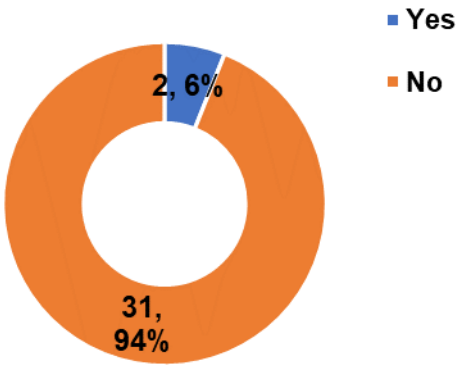

Figure 2.24 Response to survey question #6

Summary comment: The responses show that joint sealing is not usually required on the surface; however, a bond/tack coat or some proprietary material is needed on the face of the longitudinal joint or below the joint. Overbanding is only done over joints that require some corrective action, not as a routine practice for new joints.

Question #7: Does your agency have any specifications for monitoring the longitudinal joint quality? If YES, please specify. Give reasons if NO.

Figure 2.25 summarizes the responses to this question; only 24% (8 responses) of the respondent agencies have some specifications to determine the longitudinal joint quality. The specifications mentioned in the survey responses are:

- 12SP-501Y-04 (MDOT's Special Provision for Acceptance of Longitudinal Joint Density in Hot-Mix Asphalt Pavements
- We require longitudinal joint cores (density)

Most agencies replied negatively to the question, with some giving the following reasons for their replies.

- We do not see a need
- Just use standard MnDOT specifications
- Most of our paving activities are on low-volume, low-speed residential streets. We specify echelon paving on our collector street system to achieve one longitudinal joint at the centerline
- We apply crack seals every five years but do not monitor other than monitoring overall PQI
- We have specified longitudinal joint density in the past. We did not see a benefit from the extra testing as our contractors use the same means and methods, no matter the specifications.

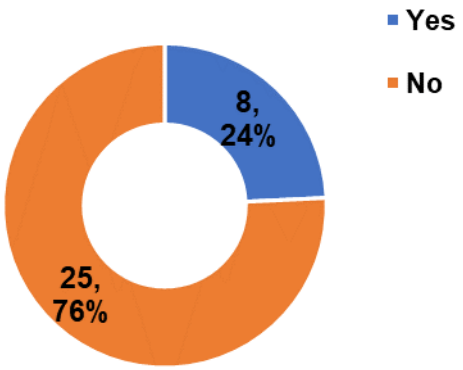

Figure 2.25 Response to survey question #7

Summary comment: The responses reveal that the longitudinal joint quality is monitored via a Special Provision in Michigan that specifies density requirements for different joint types. However, the majority of the local agencies from Minnesota do not specify/measure the joint quality except one that requires joint density measurements using cores.

Question #8: In your opinion, which type of specification offers the best chance for long-term joint performance?

The responses to this survey question suggest that there is no single choice between the type of joint specification that can result in long-term performance. Figure 2.26 shows a nearly equal split between method-based and minimum-density requirement specifications. Two respondents think using both can result in a good-performing longitudinal joint. The recommended practical minimum density specified by the respondents is between 92% to 95% (based on five responses). Additional comments received in response to the question are as under:

- Both are likely important. The method is easier to observe, track, and document in the field and can cover the entire project. A minimum percent density can be used to verify the method, but it is only a spot check of a couple of feet in miles of paving

- Echelon paving
- Changing material specifications to increase asphalt cement in the pavement would be better
- This is subjective, but we think the coring is a better option overall. The method-based could work, but the responsibility remains with construction to monitor, and this is not always possible, especially with relatively new inspectors. Coring is a defined procedure that needs to be followed versus something the inspector is expected to watch. We think coring has encouraged good practices by contractors who seem to carry through even in situations where we don't core
- Warranty
- We do not have a problem (Clearwater County, MN)
- We have not experienced significant longitudinal joint issues (Pope County, MN)

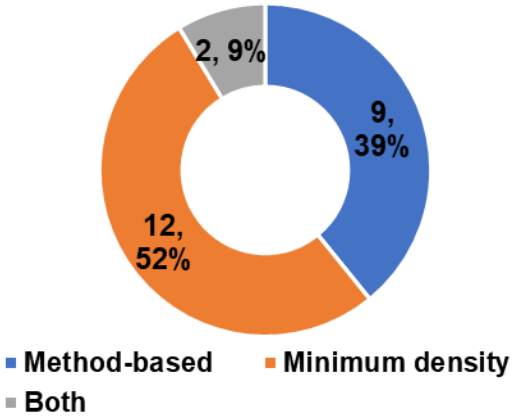

Figure 2.26 Response to survey question #8

Summary comment: The responses suggest that having a minimum density requirement for the joints can help improve their performance by sensitizing the contractors. Although near equal votes are in favor of the method-based specifications as well. However, the comments show concern about the inspector's responsibility and experience while using a method-based specification. Using both the method-based specifications and minimum density requirements seems to be a better option. However, using cores for density verification has drawbacks, such as limited coverage and the possibility of the cored area not being a true sample of the complete pavement. Thus, specifying a method with a minimum density requirement along with using a Density Profiling System (DPS) to get full coverage of the in-place density is needed and logical.

Question #9: Does your agency monitor the longitudinal joint density for Quality Assurance (QA)? If YES, how does your agency monitor the longitudinal joint density for QA? If you use cores, please specify the diameter.

About 33% (11 responses) of respondents monitor the longitudinal joint density for QA purposes (see Figure 2.27). Eight of the 11 use cores only; one uses a density gauge, while two use both.

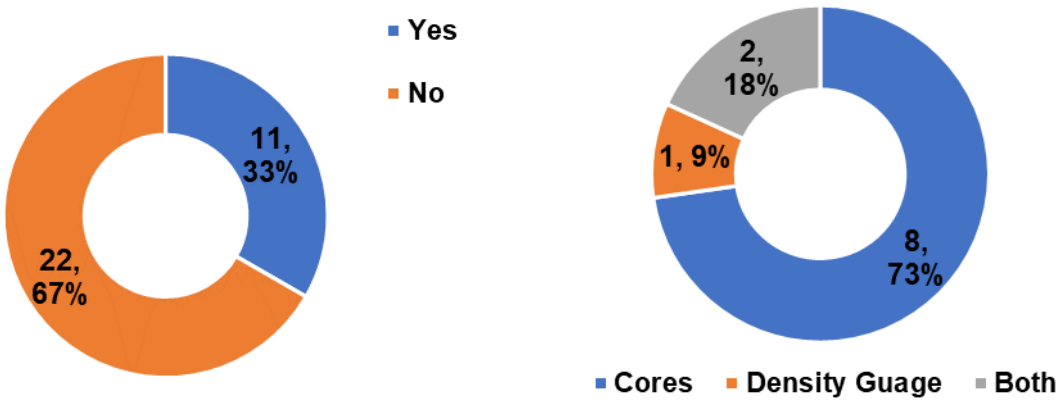

Figure 2.27 Response to survey question # 9

Summary comment: Most agencies do not monitor the joint density, which is a weak link even on well-constructed and good-performing pavements. The reason may be additional resources required (such as equipment and workforce) and time. Another reason for not monitoring the joint density can be the destructive nature of pavement coring, which is the most widely used option, as evident from Figure 2.27. Thus, using portable equipment such as DPS can help reduce the need for coring and offset its adverse effects on the pavements in the long run.

Question #10: If you use cores for QA, please specify the core diameter, core location (i.e., on joint center, offset, and side of the joint), number of cores, and coring frequency (cores per mile/lot/sublot, etc.).

Figure 2.28 shows that most of the joint cores collected for QA purposes are 6 in (150 mm) in diameter taken on the joint's center, mainly if the same asphalt mix is used on both sides of the joint. However, some do collect cores at an offset [6 in (150 mm)] from the joint on the cold side of the joint. Cores are also taken at an offset if similar asphalt mixes are not used on either side of the joint. However, coring on the center of the joint has a challenge, as mentioned by a respondent:

> *Ideally, the center but offset to the cold side if different mixes. We used to core on the center and average the determined G_{mm} values, but this proved difficult to ensure the core was exactly centered (i.e., 50/50 on either side of the joint).*

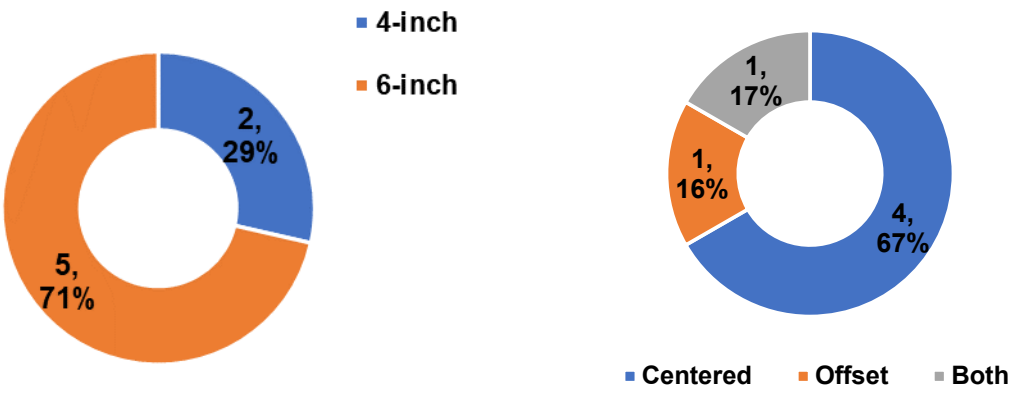

Figure 2.28 Response to survey question #10

One core every 2000 ft was a common reply (3 responses) to the question regarding the number of joint cores required and their frequency. The summary of responses is given below:

- One joint core per 2000 ft with a payment based on five cores averaged together. The coring frequency is reduced for smaller projects, with a minimum of three cores required for joint acceptance
- 4 joint cores per lot (1 response)

Question #11: Does your agency use a required joint density specification different from the mat density specification? If YES, please specify.

Figure 2.29 shows that most agencies do not use different specifications for the longitudinal joint and mat densities. The affirmative responses are mainly from MDOT which has a Special Provision for the acceptance of longitudinal joints different from the mat density requirements.

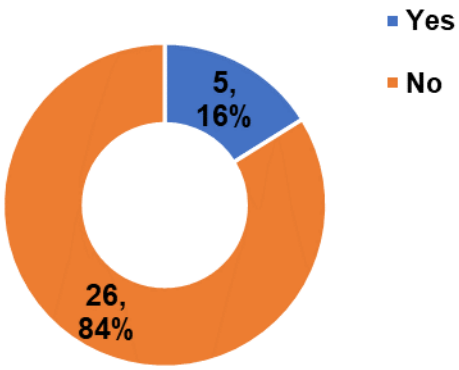

Figure 2.29 Response to survey question #11

Question #12: How is the quality measure calculated for the longitudinal joints?

Figure 2.30 shows that the longitudinal joint quality measure is calculated using a simple average of the core densities in most cases. Percent-within-limits (PWL) is also used. The respondents with "Other" replied with the following comments:

- Use a random number procedure that involves a random identification of a core location per 2000 ft (subsection of the constructed joint) and uses an average of 5 cores (MDOT)
- We do not calculate, and it is covered during construction operations
- We do not calculate and have no problem (3 responses)

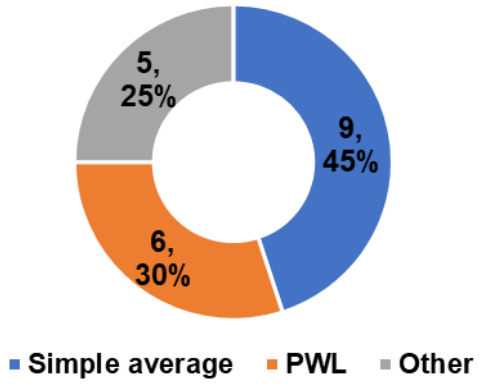

Figure 2.30 Response to survey question #12

Summary comment: The simple average is quite common; however, half of the joint cores would have a density less than the specified. The lower PWL specification limit would typically represent 90% acceptable values with only 10% defective results for a 100% payment to the contractor. Thus, using a simple average rather than the PWL is not a good measure to gauge the quality of the joints.

Question #13: How does your agency deal with poor quality, i.e., when the QA criterion is not met just after constructing the longitudinal joint?

Figure 2.31 shows that the contractor is currently penalized if the joint quality does not meet specifications right after the construction in most cases. The following comments further elaborate on this option:

- Greater than 90.5% joint density will result in an incentive. Joint sealers are placed if the density is below 88%. However, if the density is below 86%, the corrective plan includes removing and replacing the full lane for the top course and 15 in (381 mm) on each side of the joint for base/leveling courses. Density below 89% requires changes in the mix design to improve the in-place density (MDOT).
- Penalize below 85 to 87% joint density (depending on the asphalt mixture air void content and confined vs. unconfined edge) (MnDOT).

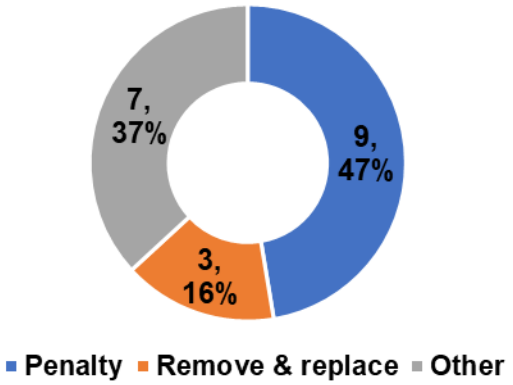

Figure 2.31 Response to survey question #13

The remove and replace is exercised when the joint density is below 86% as per the MDOT's SP for the longitudinal joint acceptance specifications. The City of Duluth, MN, exercises the remove and replace option by visually inspecting the pavement and does not decide based on density measurements. The responses for the "Other" option include the following comments:

- Depending on the severity, the contractor is either penalized or asked to remove and replace the pavement (2 responses)
- We don't have specific criteria. If the quality is poor upon placement, we may have the contractor use infrared heaters or mill and repave
- Never had an issue (4 responses)

Question #14: How does your agency maintain a poor-performing longitudinal joint while the pavement is in service?

Figure 2.32 shows that joint sealing is the most popular option for maintaining a poor-performing longitudinal joint. Additional comments for the question are as under:

- Skin patching for sealing the joint.
- We have seen both joint sealing and slot paving used, but not sure how this is monitored from a pavement management perspective. I could come up with a warranty inspection; otherwise, it is probably a maintenance issue.

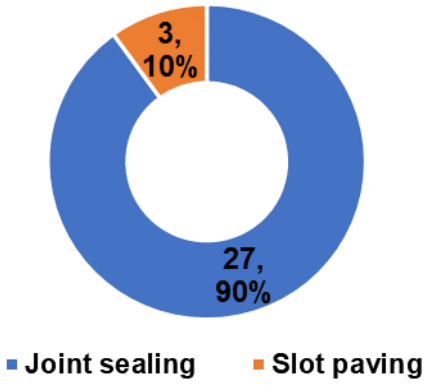

Figure 2.32 Response to survey question #14

Summary comment: Joint sealing is a common and economical treatment to maintain low to medium-level distressed longitudinal joints (*63*). At the same time, slot paving is used for maintaining joints with medium to severe level distress with the drawback of converting a single joint into two closer to the wheel paths.

Question #15: In your opinion, does an asphalt mixture type and binder content help in a better longitudinal joint construction/performance? If YES, which mix type [0.37 in (9.5 mm) NMAS or 0.5 in (12 mm) NMAS] and what binder content (>6% or <6%)?

Most respondents think that asphalt mixture type and binder content play a role in better construction and performance of the longitudinal joint (see Figure 2.33). A minority believe that lift thickness is more critical instead. Additional comments received for the question are as under:

- It is probably more of a means and methods issue, but a material that can more readily be compacted would help. There are many factors to consider.
- The use of oil is much better for long-term performance.
- We have not noticed any difference between mix types or binder contents.
- Our mixes use higher asphalt film thickness (AFT) specifications.
- 0.37 in (9.5 mm) NMAS mixes seal joints better than ones with larger aggregates.
- The contractor's means and methods are the most important rather than asphalt mix type or binder content.

The replies also reveal that 0.37 in (9.5 mm) NMAS asphalt mixtures are better than the 0.50 in (12.5 mm) mixes for the better construction and performance of longitudinal joints. Regarding binder content, the responses do not reveal a clear distinction between mixes with greater and less than 6% binders. Additional comments regarding the mix type and binder content (other than the ones specified) that can improve joint construction and performance received in the survey are as under:

- Appropriate lift thickness for the NMAS is most critical to getting appropriate density.
- The contractor constructed it correctly and rolled it properly

- Use oil
- We use SPWEA330B mix with 9.0 microns AFT.

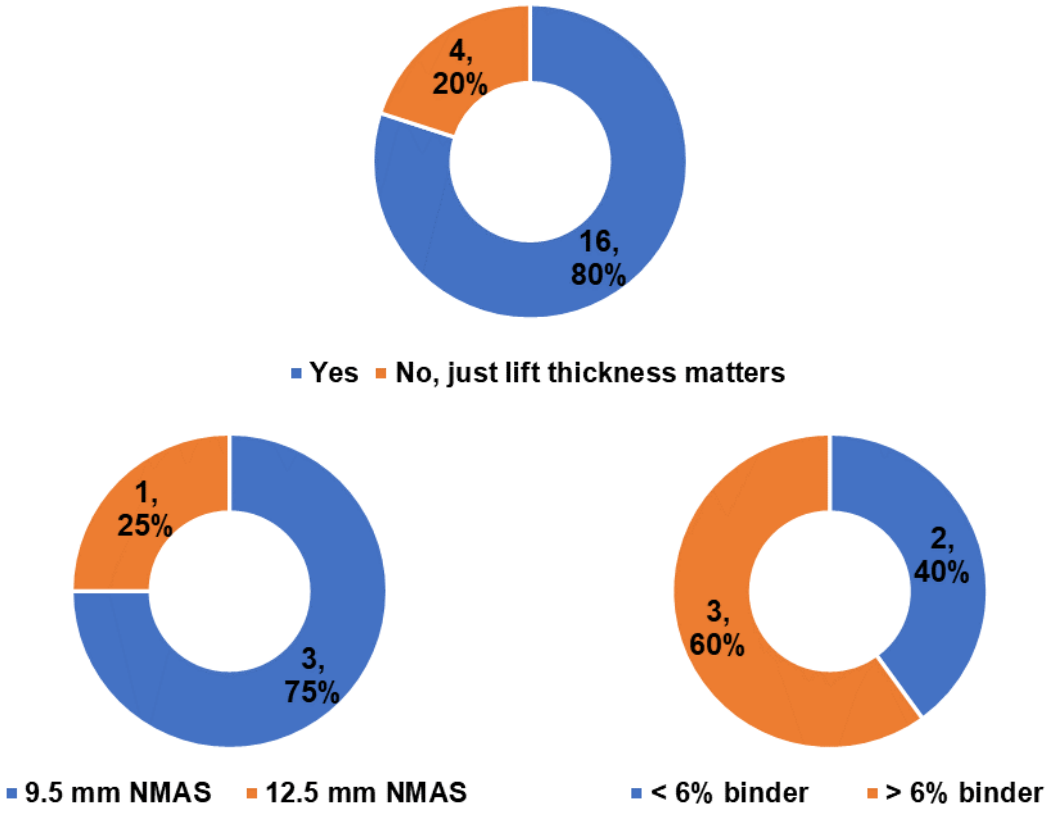

Figure 2.33 Response to survey question #15

Question #16: Any other useful and practical "TIP(s)" that you think can help improve the longitudinal joint construction and performance?

The following responses were received in reply to this question:

- J-band, a void-reducing asphalt membrane (VRAM), along the longitudinal joint, can help prevent water intrusion and wash away the subbase layer fines. J-band has had great success recently as an innovative product. MDOT always uses echelon paving practices where and when applicable to eliminate as many longitudinal joints as possible and pave two lanes simultaneously.
- Some contractors put much more effort and care into providing a quality product.
- The MDOT allows a credit of up to 4 in (100 mm) of removal at a joint before paving the second half of the joint. This allows the contractor to mill back 4 in (100 mm) of the mix without deducting this quantity. Often contractors will mill back more to remove additional material at their expense.
- The use of oil and crack sealing the joint when needed/cracked.

- Specify application of tack coat at the joint face, modify specification on paving methods, wider paving, and dual crews running side by side can improve joint construction quality.
- Echelon paving, when possible, eliminates the cold joints and produces the best-performing longitudinal joints.
- I think the cold joint is the biggest reason we see longitudinal joint failure, so echelon paving is the best way to avoid this issue.
- We have low-volume roads, and our pavement is mostly deteriorated by weather and not by traffic loading. Therefore, an open centerline joint is a minor issue, and higher oil contents would help there as well as with a longer performance lifespan.
- St. Louis County incorporates a bituminous safety edge and matches lanes daily; therefore, never paving a cold joint.
- Include incentive/disincentive specifications for longitudinal joints.

2.10 Summary of Best Longitudinal Joint Construction Practices

The survey shows that most agencies in Michigan and Minnesota do not specify the type of longitudinal joint to be constructed. Literature shows that most longitudinal joints constructed are butt joints. However, tapered joints are used in some states, with a vertical notch used in Michigan. Staggering the longitudinal joints in multiple HMA lifts is a good practice and is followed by most agencies using a minimum of 6 in (150 mm) offset. By staggering, one avoids placing the weak areas (joints) at the same location throughout the depth of the asphalt concrete layers. It also helps reduce water ingress into the pavement, especially if the longitudinal joint in the top layer separates/opens. Literature also shows that a successful longitudinal joint requires a perfectly straight or smooth edge following a curved alignment. A straight or smooth edge aids in better joint compaction once the adjacent lanes are being constructed.

Rolling of the longitudinal joint significantly affects the achieved joint density. Survey shows that many agencies do not specify the method for rolling an unsupported/unconfined joint; overhanging the joint's edge by a minimum of 6 in (150 mm) while rolling it for the first time from the hot side is common. Literature shows that vibratory rolling of an unconfined edge of a joint with a 6 in (160 mm) overhang aids in avoiding stress crack formation due to the roller's edge. However, the roller should not overhang too far off the edge as it may break down the joint's edge. Regarding rolling a confined joint, the survey results showed the use of either method, the hot pinch, and the hot overlap methods. Since both methods require vibratory rolling, the hot pinch method should be used for rolling the confined edge for the first time. It is because the hot pinch method pushes the hot material into the joint and thus may be better. This lateral material movement makes a small hump near the joint that is compacted back into the joint, ensuring that the joint is not starved of hot material. If insufficient hot asphalt material is paved near the cold joint, the hot overlap method will not produce a good compacted joint due to roller bridging over the hot material.

Literature suggests overlapping the cold joint edge with the hot asphalt material by 1 ± 0.5 in (25 ± 12.5 mm) while paving the adjacent lane is very important in the construction of a durable joint. The overlapped material should be at least 0.25 in (6.25 mm) higher than the adjacent mat to allow for

compaction. In addition to overlapping, it is important to apply tack to the full width of the lane as well as the existing face of the joint. Some agencies use either a joint adhesive in place of tack or a longitudinal joint seal (such as VRAM) to improve the joint's bond and decrease its permeability. An advantage of using such material below an asphalt lift is that it melts and migrates up into the lift after being heated by the overlaid hot asphalt. The migration fills the excess air voids associated with unconfined edge construction.

Concerning the longitudinal joint construction technique, paving in the echelon is considered the best to avoid the construction of a joint altogether. In addition, using a safety edge and matching lanes daily, where possible, eliminates the construction of a cold joint. Allowance for cutting and removal of newly paved HMA material from an unconfined edge before laying the adjacent lane is believed to produce adequate compaction at the joint. As indicated in the survey responses, the MDOT allows a credit of up to 4 in (100 mm) of removal at a joint before the adjacent lane is paved. Thus, allowing the contractor to mill back 4 in (100 mm) without deducting this quantity. Removal of the high air void material from an unconfined edge is believed to produce a better longitudinal joint.

According to the survey, most agencies do not monitor the joint density, which is a weak link even on well-constructed and good-performing pavements. The reason may be additional resources required (such as equipment and workforce) and time. Another reason for not monitoring the joint density can be the destructive nature of pavement coring, which is the most widely used option among agencies that monitor joint quality. While PWL is used to calculate the quality measure, most agencies use a simple average. Using the simple average means half of the joint cores would have a density less than the specified. This is different from the PWL. The lower PWL specification limit would typically represent 90% acceptable values with only 10% defective results for a 100% payment to the contractor. Thus, using a simple average rather than the PWL is not a good measure to gauge the quality of the joints.

Chapter 3: DPS Data Collection

Task 4 of the project included a study to investigate the use of DPS for constructing and evaluating the asphalt centerline longitudinal joints. The research team coordinated with the MnDOT and MDOT and collected DPS data on several projects constructed in the summer of 2022. The data collection effort included two locations in Minnesota and six in Michigan. Table 3.1 summarizes the DPS data collected along with the number of joint and mat cores and loose material samples. This chapter briefly explains the data collection effort undertaken at each project site. Each data collection started with the air and metal plate calibration of the DPS sensors, followed by sensor validation using the high-density polyethylene (HDPE) block and conducting the Swerve test to ensure that the sensor median dielectric values are within 0.08 of each other (9).

Table 3.1 Summary of DPS testing, material samples, and cores

Project	State	Location	Longitudinal joint type	Material samples and cores		
				Joint cores	Mat cores	Loose mix
Xerxes Rd	MN	City of Bloomington	Unconfined and a confined butt joint	10	10	5 buckets
Manning Trail	MN	Washington County	Echelon paved and confined (Maryland method) joint	-	-	3 buckets
M-89	MI	Fennville	Confined butt joint (Sequential mill & fill)	5	10	6 buckets
M-28	MI	Munising	Unconfined and confined Tapered joint	5	5	3 buckets
US-23	MI	Standish	Unconfined and confined butt joint (SMA mix)	9	5	3 buckets
M-25	MI	Port Austin	Confined butt joint (Sequential mill & fill)	10	14	6 buckets
US-31	MI	Holland	Echelon paved	-	10	3 buckets
I-496	MI	East Lansing	Unconfined butt joint (Cut back)	5	5	3 buckets

3.1 Xerxes Road – City of Bloomington, MN

The paving operation on the Xerxes Road project included laying a 2 in (50 mm) thick asphaltic concrete overlay over 20 ft (6 m) lanes (one in each direction) on two consecutive days. The DPS data were collected in two project sections, each on a separate paving day. The first section involved DPS testing on a 1000 ft pavement between the 84th and 90th streets (Station 29+91 to 39+91) on the first day. Dielectric values were measured using DPS in both lanes on the unconfined joint after the 1st lane was

laid (as seen in Figure 3.1) and the confined joint following the construction of the adjoining lane. As recommended, the DPS measurements were taken with the sensor at a minimum 6 in (150 mm) offset from the joint, as seen in Figure 3.1 (9). Figure 3.2 displays a schematic drawing of the data collection sequence. After the left lane was paved, the dielectric measurements commenced about 500 ft (152 m) behind the finish roller on the unconfined joint. Ten core locations identified by the DPS were marked (5 each on the mat and the unconfined joint). Similar DPS data were collected on the confined side of the joint once the adjoining lane was constructed later in the day. Core locations were marked on the confined joint and the mat using the DPS core location identification feature. The marked cores were retrieved a day after the paving job was finished. The second section on the Xerxes Road involved DPS data collection on a 500 ft (152 m) length of the project on the 2nd day of paving between the 98th and 102nd streets on the unconfined joint only due to the limited DPS equipment availability that day. No pavement cores were collected on the second day. A total of 5 loose HMA mix buckets were collected from the project site on either paving day.

Figure 3.1 DPS data collection on the unconfined joint with a 6 in (150 mm) offset – Xerxes Road #1, MN

3.2 Manning Trail – Washington County, MN

The Manning Trail project involved the construction of a 2 in (50 mm) thick HMA wearing course on a 12 ft (4 m) lane with an extended 8 ft (2 m) shoulder in the echelon with a confined joint at the center line abutting the lane constructed a day prior. DPS measurements were taken on the confined joint and the echelon joint with a 6 in (150 mm) offset inward on two separate 1000 ft (304 m) long sections between stations 411+75 to 401+75 and 391+75 to 381+75 paved on the same day. Figure 3.3 displays the schematic of the data collection procedure followed at the Manning Trail project, while Figure 3.4 shows

the data collection pictorially. The confined joint on this project was constructed using the Maryland Method. Only HMA loose mix samples were collected from this project site.

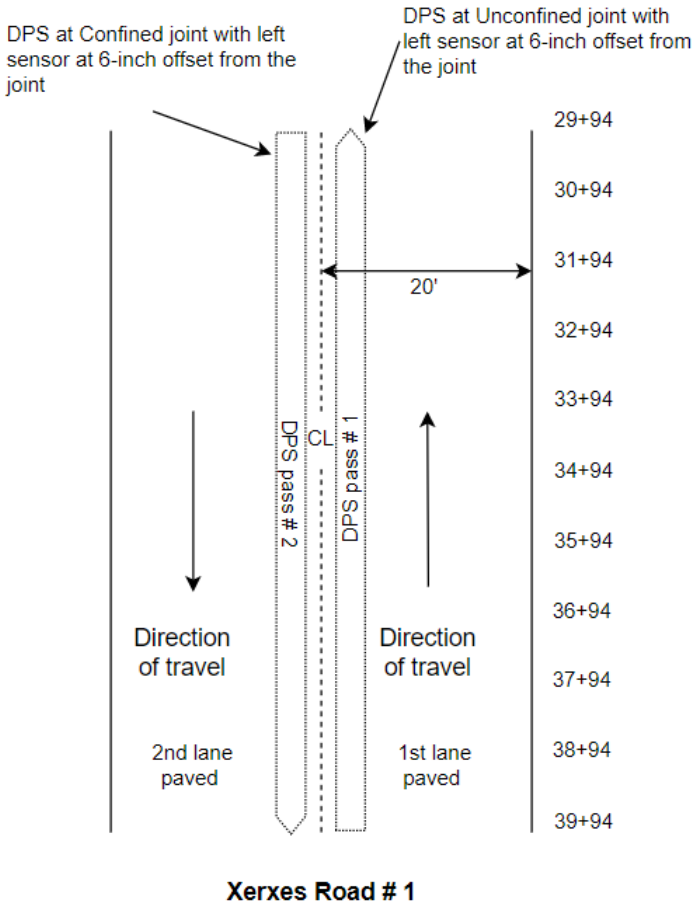

Figure 3.2 DPS data collection on the confined and unconfined joint – Xerxes Road #1, MN

3.3 M-89 Project (Station 391+75 to 381+75) – Fennville, MI

The construction work on M-89 involved cold milling and 1.5 in (38.1 mm) thick HMA resurfacing accomplished on two consecutive days. Each 11 ft (3.4 m) lane was milled and resurfaced before milling the other lane, thus, constructing a confined butt joint each time. DPS data were collected on a 1000 ft (304 m) long section between stations 391+75 to 381+75 with a 6 in (150 mm) offset from the joint at one lane only, as shown in Figure 3.5, on the second day of paving. Five mat cores and loose mix samples were collected on the first paving day, while on the second day of asphalt paving, ten cores were collected (5 each) from the pavement mat and the confined joint along with loose HMA mix samples.

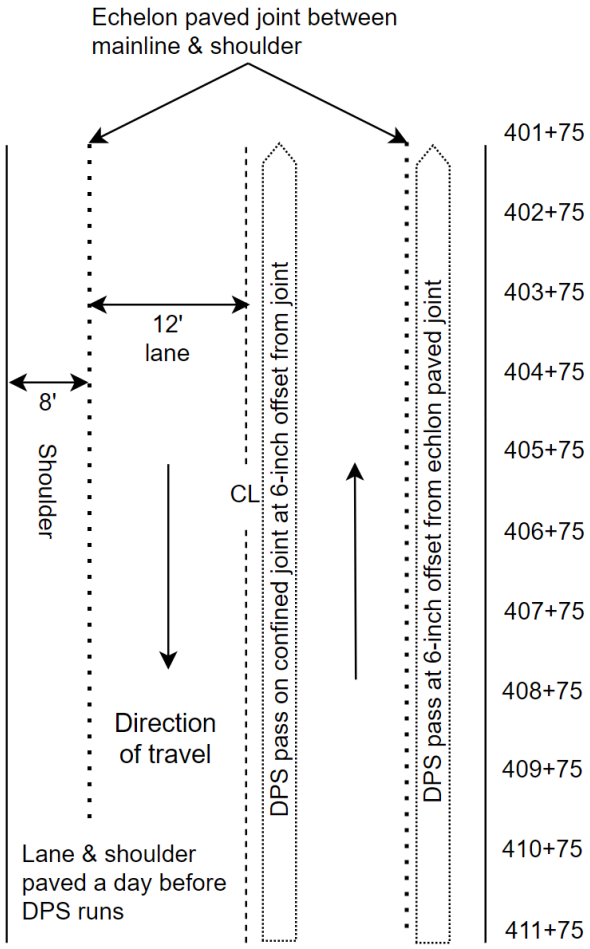

Figure 3.3 DPS data collection on the confined and echelon-paved joints – Manning Trail #1

3.4 M-28 Project – Munising, MI

The M-28 project involved the construction of a 1.5 in (38.1 mm) thick HMA layer in both directions using a Tapered centerline joint. The DPS data were collected at two 1000 ft (304 m) and 860 ft (262 m) sections in one direction on an unconfined joint on the first day of construction, while two 1000 ft (304 m) sections on the confined joint on the second day of construction. All measurements were taken at a 6 in (150 mm) offset from the centerline joint, as shown in Figure 3.6. The measurements were taken between stations 4089+00 to 4079+00 (1st section) and 4039+00 to 4029+00 (2nd section). The sequence of data collection is similar to Figure 3.2, with a taper joint instead of a butt joint at the centerline. A total of 5 cores were collected from each day of paving. Three joint and two mat cores and loose HMA mix samples were collected on the first day, while two joint and three mat cores were retrieved from the pavement on the second day.

Figure 3.4 DPS data collection on the cold confined, and hot echelon paved joints – Manning Trail, MN

Figure 3.5 DPS data collection on confined butt joint - M-89 project, MI

(a) Data collection on unconfined taper joint – Day 1

(b) DPS data collection on confined taper joint – Day 2

Figure 3.6 DPS data collection on the M-28 project, MI

3.5 US-23 Project (Station 1350+00 to 1340+00) – STANDISH, MI

Construction on US-23 involved laying a 1.5 in (38.1 mm) thick HMA surface layer using a stone matrix asphalt (SMA) mix, laying each lane on two consecutive days. The DPS data were collected on a 1000 ft (304 m) section between stations 1350+00 to 1340+00 over the unconfined joint on the first day of paving, followed by data collection within the same stations but over a 465 ft (142 m) section over the confined joint on the second day. The data collection sequence is like the one shown earlier in Figure 3.2. The DPS measurements were taken at a 6 in (150 mm) offset from the longitudinal centerline joint. A total of 14 pavement cores were collected on this project; three joint and two mat cores on the first day, while two joint and three mat cores were retrieved from the pavement on the second day. An additional four joint cores were collected but outside the mentioned stations. Loose HMA material samples were also collected from the project site.

3.6 M-25 Project (Station 343+00 to 353+00) – Port Austin, MI

The M-25 project was a cold-milling and one-course 1.5 in (38.1 mm) thick HMA resurfacing job. Like the M-89 project, one lane was milled and resurfaced before milling and re-constructing the other lane. Thus, a confined butt joint was constructed every time. DPS data were collected on both sides of the confined joint with a 6 in (150 mm) offset from the joint. The construction of the two lanes spanned over two days, constructing one lane a day. Thus, the DPS data was collected on 1000 ft (304 m) sections of the project between stations 343+00 to 353+00, with HMA produced on two different days. The data collection sequence is similar to the one shown in Figure 3.2, with the only difference of having a confined joint between the lanes. A total of 10 joint cores (5 from each day), 14 mat cores (7 from each day), and 6 loose mix buckets (3 from each day) were collected from this project.

3.7 US-31 Project (Station 774+07 to 773+07) – Holland, MI

The US-31 project involved the construction of a 2.25 in (57 mm) HMA surface layer over two lanes constructed in the echelon. The DPS data were collected on the centerline echelon constructed joint on a 1000 t (304 m) section between stations 774+07 to 773+07 with a 6 in (150 mm) offset from the joint. The data collection scheme was similar to the one shown for the echelon joint in Figure 3.3. Ten mat cores (no joint cores) and three loose HMA mix buckets were collected from this project.

3.8 I-496 Project (Station 440+00 to 330+00) – East Lansing, MI

The construction of I-496 involved laying a 2 in (50 mm) thick HMA surface course over two 12 ft (4 m) lanes. The DPS data were collected on a 1000-foot section between stations 440+00 to 330+00 on the unconfined joint with a 6 in (150 mm) offset from the final centerline joint of one of the two lanes. The contractor was paving more than 12 ft (4 m) and was cutting back the additional HMA material laid at the joint, as shown in Figure 3.7.

Figure 3.7 Paving operation on I-496, East Lansing, MI

Chapter 4: METHODS AND DATA ANALYSIS

4.1 DPS Calibration

4.1.1 Modified MnDOT Model (Non-linear)

As described in the PaveScan® Mix Design Module Manual, the DPS puck calibration requires a minimum of six pucks with a 6 in (150 mm) diameter and 3.5 to 4.5 in (89 to 114 mm) thickness. At least two pucks shall be within the air void range of 4-5%, two within 7-9%, and two within 11-14%. The dielectric measurements of the pucks are recommended before bulking them for air void determination. 4 in (100 mm) thick pucks were prepared from loose HMA material for all projects using a gyratory compactor targeting each of the three air void ranges mentioned earlier. The dielectric values of the pucks were determined at the MDOT Construction Field Services (CFS) building using the DPS equipment (Figure 4.1).

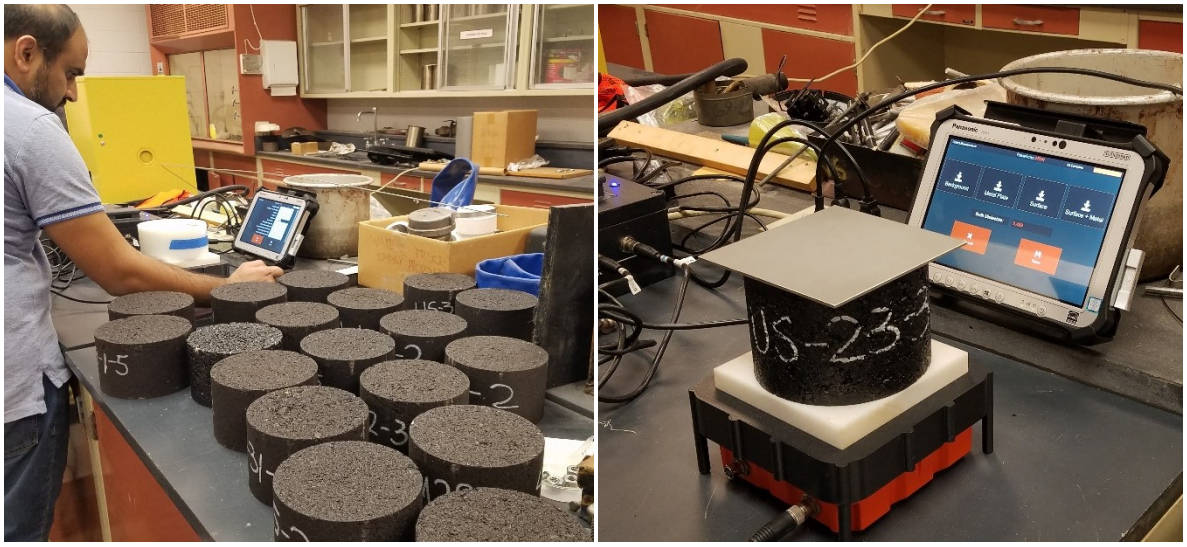

Figure 4.1 Puck dielectric measurements in progress

Table 4.1 contains the HMA mix details of all the materials tested at each project. Since the wearing course layers are tested, all the MN mixes have a nominal maximum aggregate size (NMAS) of 0.5 in (12.5 mm), while the MI mixes are all 0.36 in (9 mm) NMAS. The HMA layer thickness is 1.5 in (38.1 mm) for most projects, with the thickest HMA lift of 2.25 in (57 mm) at US-31. The air voids of the pucks were determined using the saturated surface dried method (AASHTO T 166). In contrast, the AASHTO T331 method was used for pucks that absorbed more than 2% of water by volume, as determined by AASHTO T 166 (71, 72). The traditional empirically fitted exponential and the Hoegh-Dai (HD) models that relate the dielectric of the HMA pavements to its air void content were limited to reasonably estimating the air voids within the 5 to 10% and 4 to 12%, respectively, while failing at the extremes (73). The MnDOT

model overcomes the limitations of the exponential and HD models and can correctly convert the measured dielectric data into in-place air voids, especially at the extremes (73). Thus, the MnDOT model [equation (2)] was adopted to calibrate the relationship between air void and dielectric values.

$$AV = \frac{0.20}{\left(1 + \left(\frac{e}{c}\right)^{b}\right)^{g}} + \frac{0.0008}{(e-1)} \quad (2)$$

where;

AV = air voids (x100, %),
e = dielectric value,
c,b,g = regression parameters.

Table 4.1 HMA mix details

Project	Layer thickness (inch)	NMAS (mm)	Percent binder	G_{mm} (kg/m^3)	G_{sb} (kg/m^3)	G_{se} (kg/m^3)	P #4 (%)	P #200 (%)	Percent binder
Xerxes Rd	2.0	12.5	5.00	2512	2678	2719	62	3.4	5.00
Manning Trail	2.0	12.5	5.50	2525	2715	2758	68	4.0	5.50
M-89	1.5	9.0	6.03	2495	2709	2748	71.8	4.6	6.03
M-28	1.5	9.0	6.22	2467	2683	2719	79.8	6.4	6.22
US-23	1.5	9.0	6.77	2462	2717	2741	39.7	8.0	6.77
M-25	1.5	9.0	6.42	2452	2643	2709	82.1	5.9	6.42
US-31	2.25	9.0	5.55	2494	2686	2722	69.5	4.9	5.55
I-496	2.0	9.0	6.60	2466	2657	2736	78.7	5.1	6.60

Parameter estimation is needed whenever a model is fitted to data to explain a phenomenon, and it is usually considered the same as curve-fitting or optimization. However, both are distinctly different. While the optimization only focuses on minimizing the sum-of-squares or any other criterion considering the parameters as unimportant, parameter estimation also considers the parameters' errors (74). According to Beck and Arnold, parameter estimation is “a discipline that provides tools for the efficient use of data in the estimation of constants that appear in mathematical models and for aiding in modeling phenomena” (75).

Microsoft Excel’s Solver® routine is generally used to estimate the parameters of a nonlinear model but without computing the parameter errors, thus making it acceptable only for curve-fitting (74). However, according to Geeraerd et al., Solver® can accomplish parameter estimation if the sensitivity matrix is formulated and matrix multiplication is employed to compute the parameter errors (76). As per Dolan, the sensitivity matrix or Jacobian is a matrix of the first derivatives of the model for each parameter and has the dimensions of n-by-p, where n and p are the numbers of data points and parameters, respectively (77). Thus, it is essential to know if any or all the parameters in a model are accurate and whether they are estimable, i.e., if they are statistically significant, they do not contain zero in the

parameter confidence interval (CI). Hence, reporting the CI of any estimated parameter is equally important as the parameter errors.

The parameter identifiability depends on the scaled sensitivity coefficients (SSC) and the objective function minimization (74). The SSC can help determine whether a parameter is estimable and informs about its accuracy in terms of relative error. The i_{th} sensitivity coefficient of a model, $\eta(x,\beta)$, where x is an independent variable, and β represents the parameter vector, is given by $X_i = \partial \eta / \partial \beta_i$ and indicates the magnitude of change of the response resulting from perturbations in the parameter (75). An initial parameter value is required if the model is nonlinear in that parameter, i.e., $\partial \eta / \partial \beta_i = f(\beta_i)$, and requires an iterative solution using any nonlinear regression algorithm (75). The parameter's SSC is the product of its sensitivity coefficient and the parameter itself $X'_i = \beta_i (\partial \eta / \partial \beta_i)$, which has the same units as the model η and can be directly compared to it. The SSCs for the parameters are desired to be large compared to the model η and uncorrelated with each other (74). The larger the SSC is for a parameter, the greater its effect on the model and the easier it will be to estimate. However, suppose any of the SSCs are correlated, i.e., in that case, one is a linear function of the other; those parameters will not be estimable separately as the model η will respond to either of them identically.

Figure 4.2 shows the SSC for the three parameters of the model shown in equation (2) compared to the response, air voids in percentage units. It is worth noting that estimating and plotting the SSCs is a forward problem and only requires initial parameter guesses rather than data. The total span of the model, i.e., the dependent variable (air voids), is from 0 to 20%. It can be observed that the SSC for parameter c is large compared to the model; hence, parameter c will have the least error. However, parameters c and g peak at the same dielectric value (the independent variable), showing a correlation between the two parameters. Thus, parameters c and g are expected to be insignificant, with a larger parameter error in g than in c if both these parameters are estimated simultaneously. The parameter b is expected to have the least error since it is large compared to the independent variable and is not correlated with any parameter.

Table 4.2 shows the three parameters' ordinary least squares (OLS) estimates, CI, and relative errors. As shown by the SSCs, the parameters c and g are insignificant as the CI for these parameters includes zero. Also, the relative error in parameter g is the highest, second highest for parameter c, and least for parameter b. Based on these results, the research team modified the MnDOT model by removing parameter g. The SSC plot in Figure 3(a) suggests that parameters c and b are no longer correlated and that parameter c can be estimated with the least error. Table 4.3 shows both parameters' OLS estimates, CI, and relative errors. Since the parameters were uncorrelated, their CI is significant, i.e., it doesn't contain zero. Parameter c is the most accurate, with only a 0.37% relative error, while parameter b has a 6% error. The model root means squared error (RMSE) is only about 1%, while the model's coefficient of determination (R^2) is about 84%.

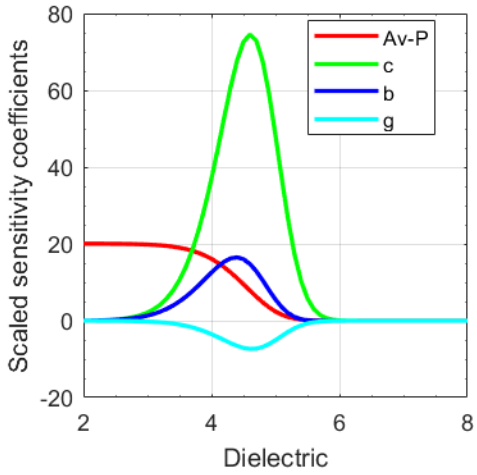

Figure 4.2 Scaled sensitivity coefficients with initial parameter guesses

Table 4.2 Ordinary least squares parameter estimates, CI, and relative errors

Parameter	*c*	*b*	*g*
Initial guess	5.61	10.74	8.35
Final OLS estimates	6.95	7.05	9.67
Parameter CI	-10.43 to 24.33	2.15 to 11.95	-137.74 to 157.08
Relative parameter error, %	125.08	34.78	762.64

A resampling technique, bootstrapping, was used to enhance confidence in the estimated parameters of the modified model. Bootstrap resamples the data with replacement using random numbers from a uniform distribution without making assumptions about the data distribution or the true values of the parameters. It differs from the Monte Carlo method, which generates synthetic data based on the model function and estimated parameters by making assumptions about the distributions and the true parameters. The advantage of using the resampling method includes quantifying the variability in terms of the CI of the parameters and the associated model predictions.

Two ways to accomplish bootstrapping are based on (a) data and (b) residuals. Bootstrapping the data involves randomly choosing *n* (the number of data points in the original dataset) pairs of the original data, with replacement, based on *n* random numbers from a uniform distribution with the possibility of repeats of the data pairs. Residual bootstrapping randomly chooses *n* pairs of the original residuals, with replacement, based on *n* random numbers from a uniform distribution with the possibility of repeats of the residuals and adds them to the predicted data to obtain a new data set with *n* pairs. The latter is preferred while dealing with fewer data points, and the SSCs are large only within a small range of the independent variable. Table 4.3 also displays the bootstrap CI of the parameters from both the bootstrap methods and the associated model RMSE resulting from parameter estimation from 1000 bootstrapped samples.

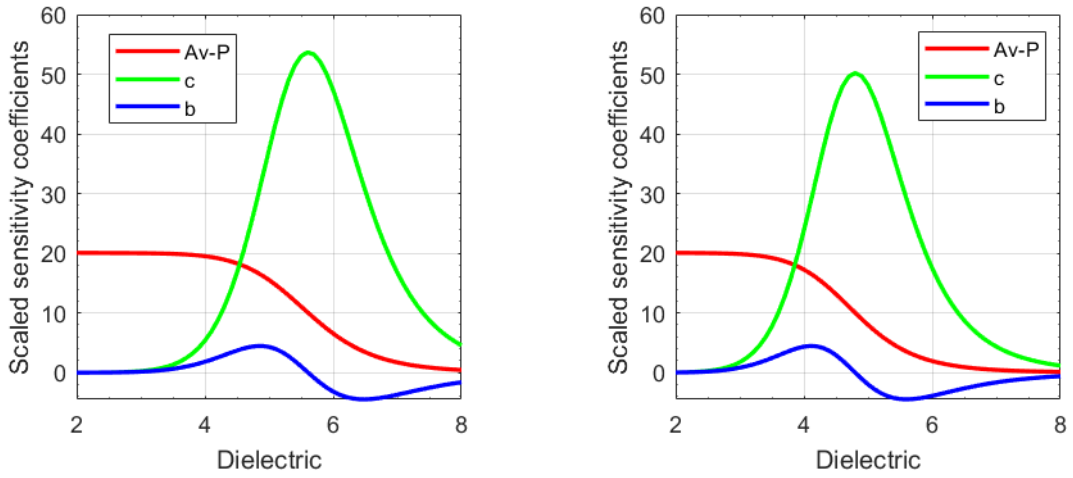

(a) With initial parameter guesses (b) With final parameter estimates

Figure 4.3 Scaled sensitivity coefficients for the modified MnDOT model

Table 4.3 OLS and bootstrap estimates, CI, and relative errors – modified MnDOT model

Parameter	*c*	*b*
Initial guess	5.61	10.74
Ordinary least square estimation results		
Final OLS estimates	4.7995	10.0454
Parameter CI (OLS)	4.76 to 4.83	8.83 to 11.26
Standard error	0.02	0.61
Relative error, %	0.37	6.04
Model R^2, %	83.51	
Model RMSE, %	1.12	
Bootstrap estimation results		
Bootstrapped CI (residuals)	4.76 to 4.8313	8.87 to 11.29
Bootstrapped RMSE, % (residuals)	1.01	
Bootstrapped CI (data)	4.76 to 4.84	8.86 to 11.28
Bootstrapped RMSE, % (data)	1.21	

Figure 4.4 displays the residual analysis plots for the model. The standard statistical assumptions should hold to have meaningful conclusions from the model. The errors are assumed to be: (a) additive, (b) have a zero mean with a (c) constant variance, (d) should be uncorrelated, and (e) normally distributed (5). Figure 4.4(a) shows that the residuals meet assumptions *a* through *d* as the residuals do not display any trend (e.g., fanning out), have a mean of zero, and their values have a constant variance (i.e., ± 3 about the zero). Figure 4.4(b) also shows that the residuals are normally distributed with a zero mean. Figure 4.4(c) and Figure 4.4(d) show the confidence and prediction bands estimated using the OLS and bootstrap methods. In contrast, Figure 4.4(e) and Figure 4.4(f) display the distribution of the bootstrap estimated parameters. The estimated parameters are normally distributed with mean values like the

OLS estimates. Equation (3) shows the final calibrated model used in the analyses with one fewer parameter (parameter *g* excluded).

$$AV = \frac{0.20}{1 + \left(\frac{e}{4.80}\right)^{10.04}} + \frac{0.0008}{(e-1)} \quad (3)$$

Figure 4.5 displays the model verification using the dielectric and air void measurements from the collected field cores after calibration. It is observed that the core air voids are within the prediction band of the model. Thus, the plot infers that the model calibrated using all the data combined can be used for the relative comparison between a joint and its respective mat and the relative comparison among the different joint types. It should be noted that separate calibration of the DPS data is recommended for each mix. However, since the objective of this project was to compare the different longitudinal joint geometries and construction techniques, a combined calibration of the model was undertaken using Puck dielectric and air voids from all the projects. Using one calibrated model will eliminate the separate model variability effects on the comparison and make the relative comparisons of the different joints straightforward. While the MnDOT model was chosen for the analyses in this project, additional models were fitted to the data incorporating volumetric parameters to cater to the recommended mix-specific calibration requirement. Additionally, linear relationships were explored since the air voids and dielectric relationship is linear within the expected air void range between 3 to 15% (see Figure 4.4).

4.1.2 Exponential Model (Non-linear)

The conventional exponential model has been commonly used to relate asphalt air voids to their dielectric values. As mentioned earlier, the conventional exponential model shown in equation (4) below has a limitation in predicting the air voids at the extremes but still can be used for the regular air voids range observed in the field. where;

AV = air voids (x100, %),
e = dielectric value,
A, B = regression parameters.

displays the model's parameters along with other details while equation (5) shows the final calibrated model. Figure 4.6 displays a reasonable fit of the model to the data with low bias and SE.

$$AV = A * exp(-B^{*}e) \quad (4)$$

where;

AV = air voids (x100, %),
e = dielectric value,

A, *B* = regression parameters.

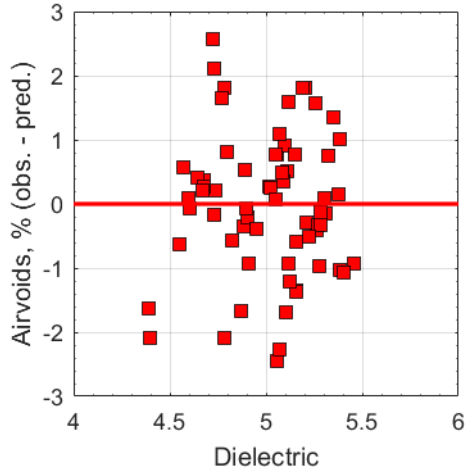

(a) Residual plot

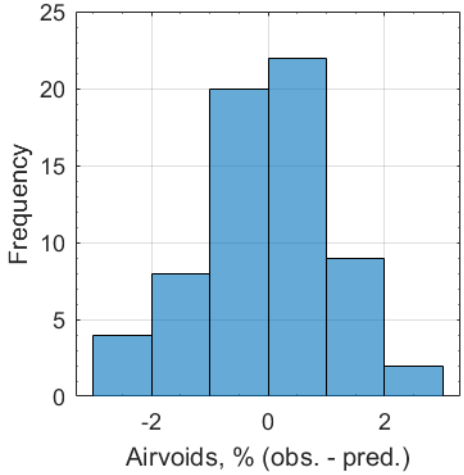

(b) Residual histogram

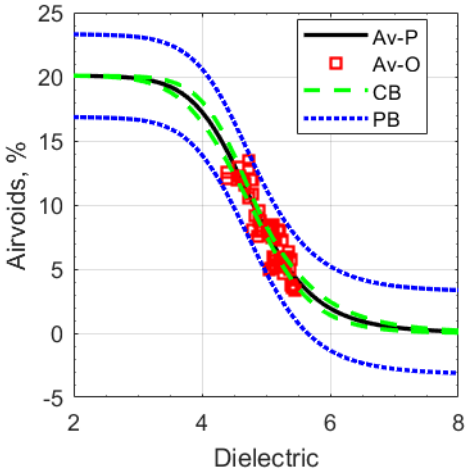

(c) OLS confidence and prediction bands

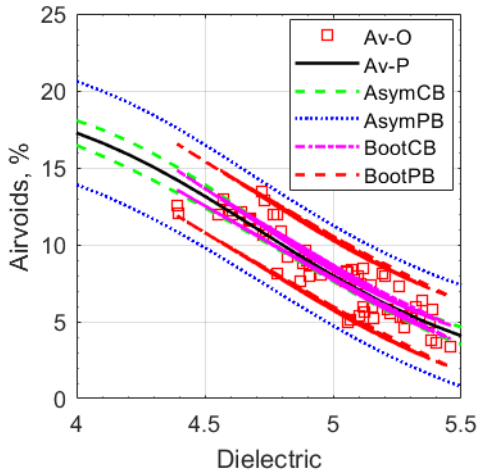

(d) Bootstrap confidence and prediction bands

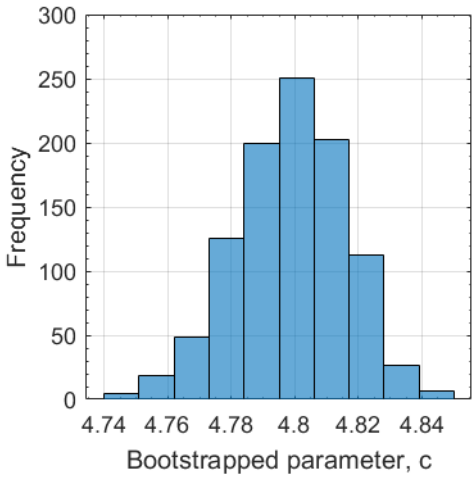

(e) Estimate distribution, parameter *c*

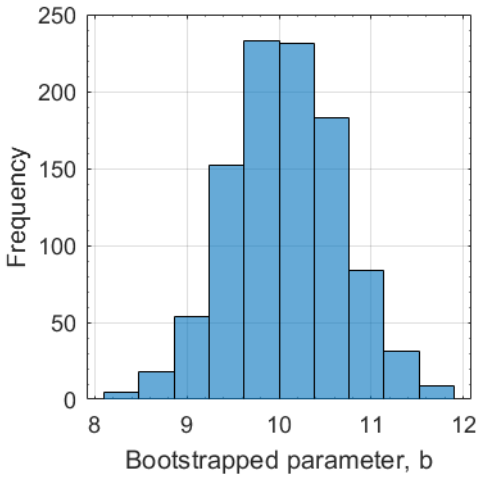

(f) Estimate distribution, parameter *b*

Figure 4.4 Residual analysis, confidence and prediction bands, and bootstrap estimated parameter distribution

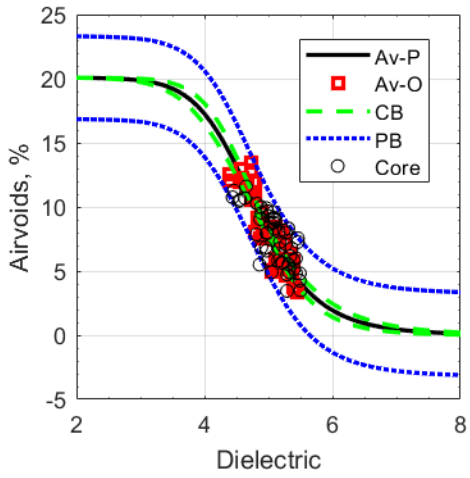

Figure 4.5 Model validation using pavement cores

Table 4.4 Parameter Estimates, CI, and RMSE for the conventional non-linear exponential model

Parameter	*A*	*B*
Initial guess	1	1
Final estimates	15.45	-1.06
Parameter CI	8.35 to 28.54	-1.18 to -0.93
Standard error	4.89	0.07
Model RMSE, %	1.21	

$$AV = 15.45 * exp(-1.06 * e) \quad (5)$$

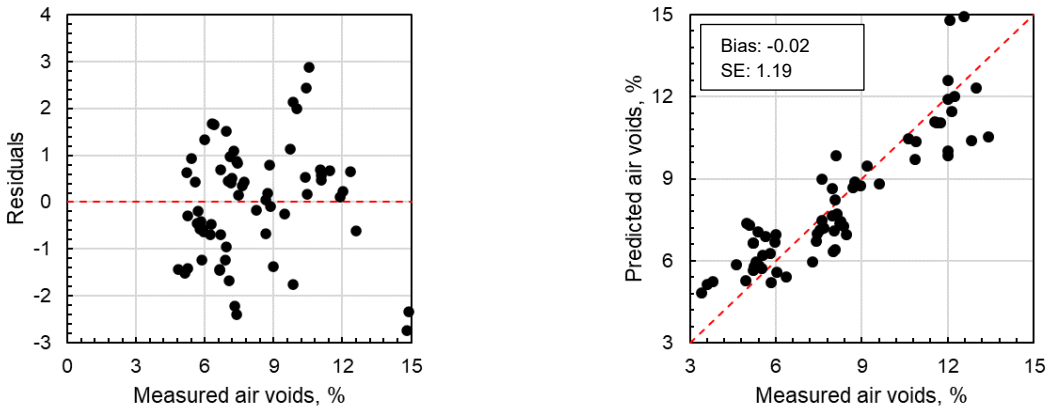

(a) Residual plot **(b) Measured vs. predicted air voids**

Figure 4.6 Conventional non-linear exponential model's residual plot and its performance

4.1.3 Correlation Analysis

To investigate the air voids vs. dielectric relationship, a correlation analysis was undertaken between different asphalt mix volumetric parameters and the asphalt dielectric values. Correlation analysis is a statistical method that helps determine the strength and direction of a linear relationship between variables. In other words, it can identify the effect of a variable on the target metric. Figure 4.7 shows a correlation analysis between the measured dielectric values with the bulk specific gravity of the mix (G_{mb}), the maximum specific gravity of the mix (G_{mm}), voids in the mineral aggregates (VMA), voids filled with asphalt (VFA), the bulk specific gravity of the stone (G_{sb}), the effective specific gravity of the stone (G_{se}), and percent binder content (P_b). In the color map, red indicates a positive, while blue indicates a negative correlation. It is observed that G_{mb} (0.82) and VFA (0.90) are positively correlated, while VMA (-0.77) has a negative correlation with the asphalt dielectric values. Thus, these parameters should be excluded from any relationship relating to air voids and dielectric values to avoid multicollinearity issues. While G_{sb} and G_{se} do not correlate with the dielectric values, their correlation with G_{mm} displayed high variance inflation factor (VIF) values in the regression analysis. Thus, these factors were omitted from the linear relationship. Finally, P_b was not used in the relationship as it also shows a negative correlation (-0.87) with the Gmm parameter.

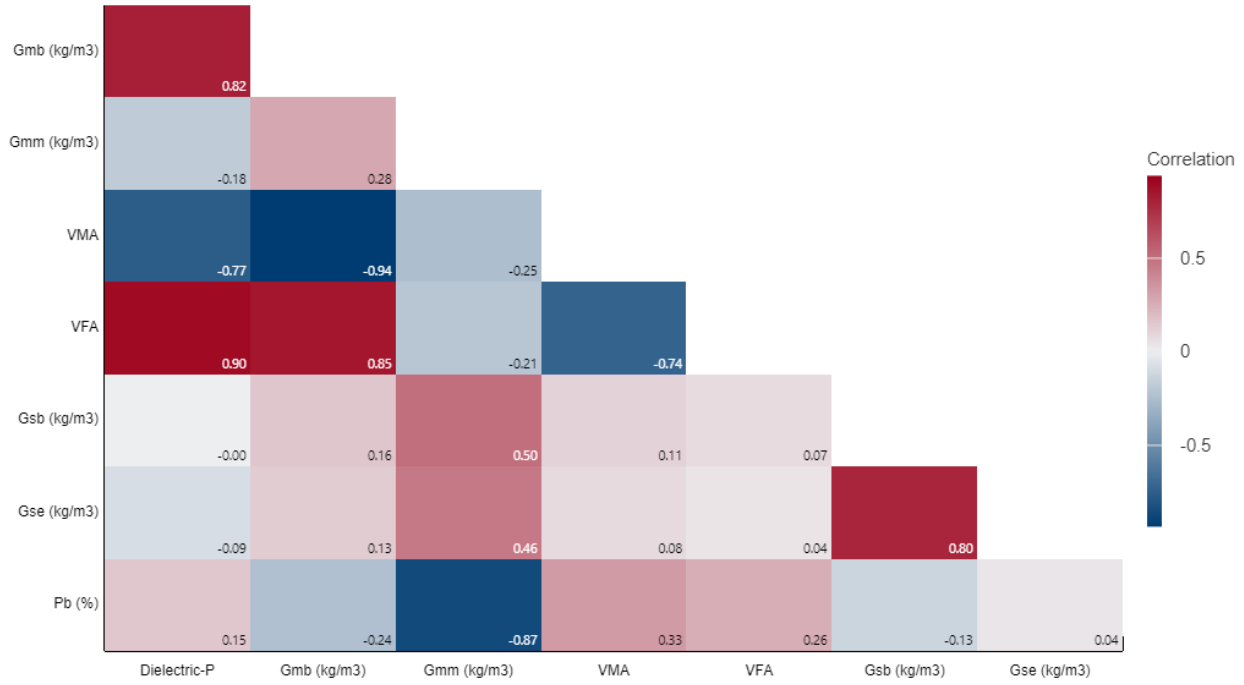

Figure 4.7 Correlation analysis

4.1.4 Linear Regression Model

Considering the correlation analysis results, measured air voids were linearly regressed against the measured dielectric values and the G_{mm} of the asphalt mixes. The G_{mm} values were standardized by

subtracting its mean from the individual values and dividing it by the standard deviation. Table 4.5 displays the estimated coefficients with standard errors and 95% confidence intervals. Using an error rate of 5% (α = 0.05), the table shows that both the regressors (i.e., dielectric values and the standardized G_{mm}) have a significant effect on the achieved air voids (*p*-value < 0.05) with the model showing an R-square of 85%. Figure 4.8(a) displays the residual plot for the linear regression analysis. The residuals do not display any pattern and have a constant variance around zero, indicating their normal distribution. Figure 4.8(b) compares the predicted air voids with the measured values. The linear regression model displays a negligible bias (5.06E-16) and low SE (1.05). Equation (6) shows the linear regression model:

$$AV = 0.5669 - 0.09706\, e - 0.00366\, (\frac{G_{mm_i} - G_{mm_{mean}}}{G_{mm_{std}}}) \quad (6)$$

where;

AV = air voids (x 100, %),
e = dielectric value,
G_{mm_i} = G_{mm} of the asphalt mix,
$G_{mm_{mean}}$ = Mean of G_{mm},
$G_{mm_{Std}}$ = Standard deviation of G_{mm}.

Table 4.5 Estimated coefficients and RMSE for the linear regression model

Term	Coefficient	SE Coefficient	95% CI	*t*-value	*p*-value	VIF
Constant	0.5669	0.0258	(0.52, 0.62)	21.96	0.000	
Dielectric value	-0.09706	0.00515	(-0.11, -0.09)	-18.86	0.000	1.03
Standardized G_{mm}	-0.00366	0.00137	(-0.006, -0.0009)	-2.68	0.009	1.03
Model RMSE, %	1.21					

Note: SE = standard error; CI = confidence interval; VIF = variance inflation factor

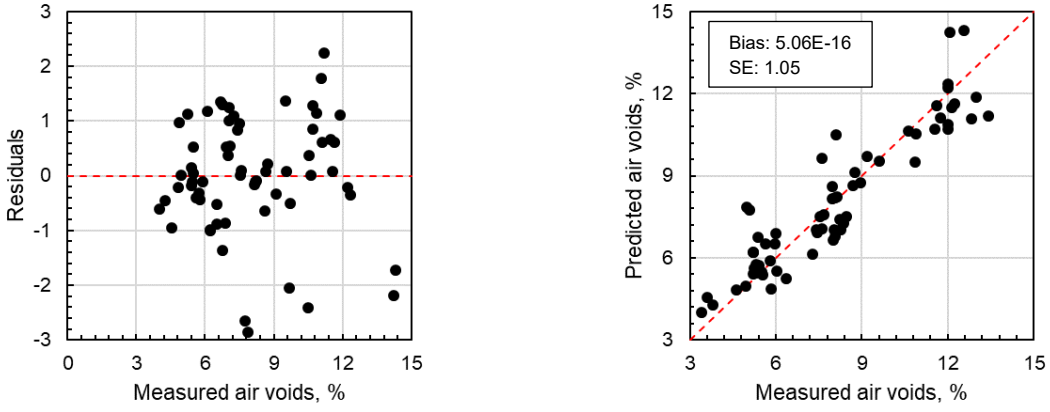

(a) Residual plot **(b) Measured vs. predicted air voids**

Figure 4.8 Linear regression model's residual plot and its performance

4.1.5 Additional Non-Linear Regression Model

Using the asphalt dielectrics and G_{mm} values as independent variables, an additional non-linear regression model is presented, which is an extension of the model presented earlier in equation (3). The main difference between the two models is the additional term incorporating the (standardized) G_{mm} value into the model. Equation (7) shows the additional non-linear model, while Table 4.6 shows the estimated parameters, their CI, SE, and the model RMSE. Figure 4.9 shows the residual plot for the model. The residuals do not display any trend and have almost constant variance. Figure 4.9(b) shows that the model's performance adequately predicts the air voids. Although the linear model presented earlier had a smaller bias and SE, the non-linear model in equation (7) has a smaller RMSE than the linear one.

$$AV = \frac{0.20}{1 + \left(\frac{e}{4.80}\right)^{10.27}} + \frac{0.0008}{(e-1)} - 0.0032\left(\frac{G_{mm_i} - G_{mm_{mean}}}{G_{mm_{std}}}\right) \quad (7)$$

where;

AV = air voids (x100, %),
e = dielectric value,
G_{mm_i} = G_{mm} of the asphalt mix,
$G_{mm_{mean}}$ = Mean of G_{mm},
$G_{mm_{Std}}$ = Standard deviation of G_{mm}.

Table 4.6 Parameter Estimates, CI, and RMSE for the additional non-linear regression model

Parameter	*Theta 1*	*Theta 2*	*Theta 3*
Initial guess	4	10	1
Final estimates	4.80	10.27	-0.0032
Parameter CI	4.76 to 4.83	9.08 to 11.50	-0.0059 to -0.0004
Standard error	0.016	0.596	0.001
Model RMSE, %	1.08		

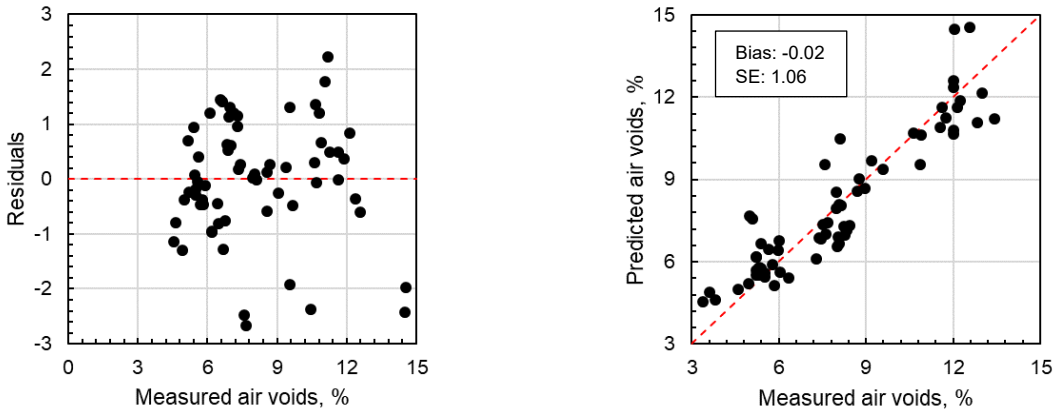

(a) Residual plot

(b) Measured vs. predicted air voids

Figure 4.9 Additional non-linear regression model's residual plot and its performance

4.2 DPS Data Analysis

This section presents examples of data analyses conducted using the collected dielectric data at different projects.

4.2.1 Xerxes Road #1 (Station 29+91 to 39+91) – City of Bloomington, MN

The dielectric values measured on the unconfined joint [i.e., at 6 in (150 mm) offset] are lower throughout the 1000 ft (304 m) section than those measured 3.5 ft (1 m) into the asphalt mat, as seen in Figure 4.10(a). On the other hand, Figure 4.10(b) shows that the dielectric values from the confined joint are very close to those measured on the mat. The trend observed is as expected because an edge confined by a previously constructed lane aids in paving and compacting the longitudinal joint while laying the adjoining lane. Although Figure 4.10 confirms that the unconfined joint has a lower dielectric than the mat compared to the confined one, data variability is high. Thus, an in-depth analysis is required to understand the differences between both joints.

According to the model shown in equation (3), a dielectric of 5.0 corresponds to an air void content of 8%, set as an upper limit for the expected air void content in the HMA mat for this study. Likewise, 10% air void content at the joint was set as the limit keeping in view the commonly used criterion for joint density acceptance, i.e., acceptable joint density should be a maximum of 2% less than the mat density. A dielectric value of 4.81 corresponds to 10% air voids. Thus, according to the model, a dielectric difference of about 0.2 between the mat and the joint (mat minus joint) corresponds to a joint air void content difference of more than 2% compared to the mat. Figure 4.11 illustrates the distribution of the dielectric values of the mat, the corresponding joint, and their difference. It is observed that mat dielectric values are higher than the unconfined joint with only a fraction of overlapping values. More than half of the mat dielectric values differ from the unconfined joint dielectrics by a value greater than 0.2. However, the mat and confined joint dielectric values are very similar, with only a fraction of their

differences greater than 0.2. This shows that constructing a confined joint will produce more compaction than an unconfined joint.

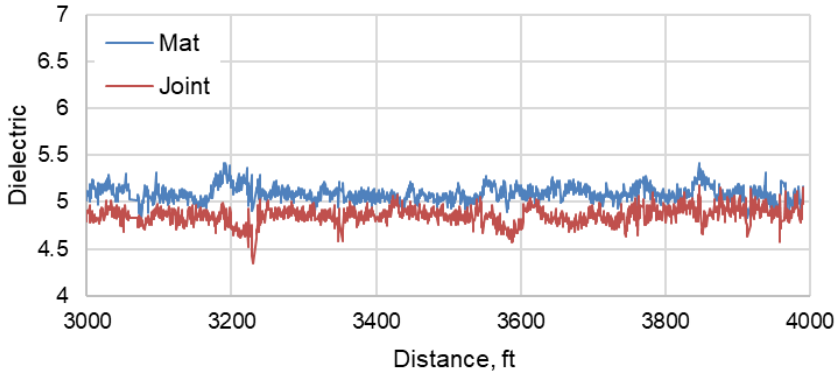

(a) Unconfined joint

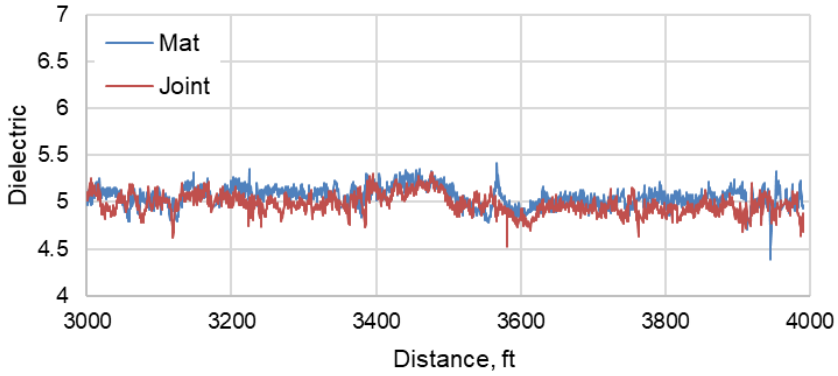

(b) Confined joint

Figure 4.10 Dielectric values comparison between confined and unconfined joints – Xerxes Road #1

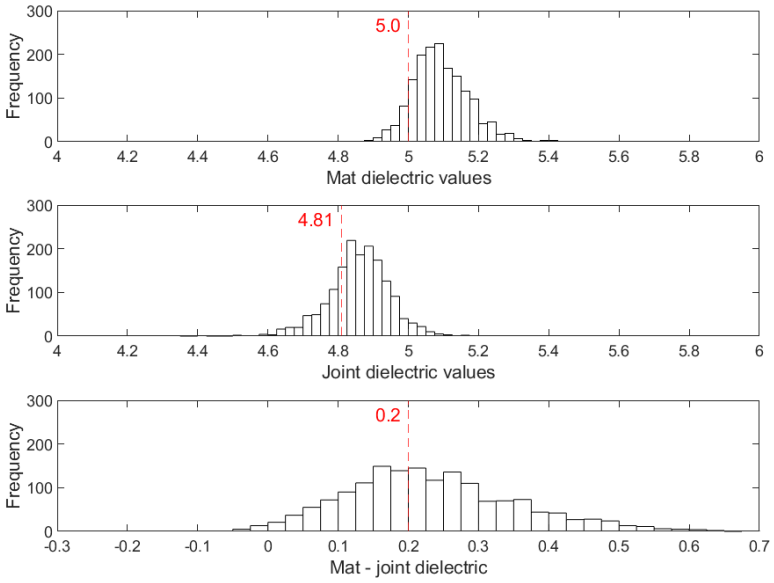

(a) Unconfined joint

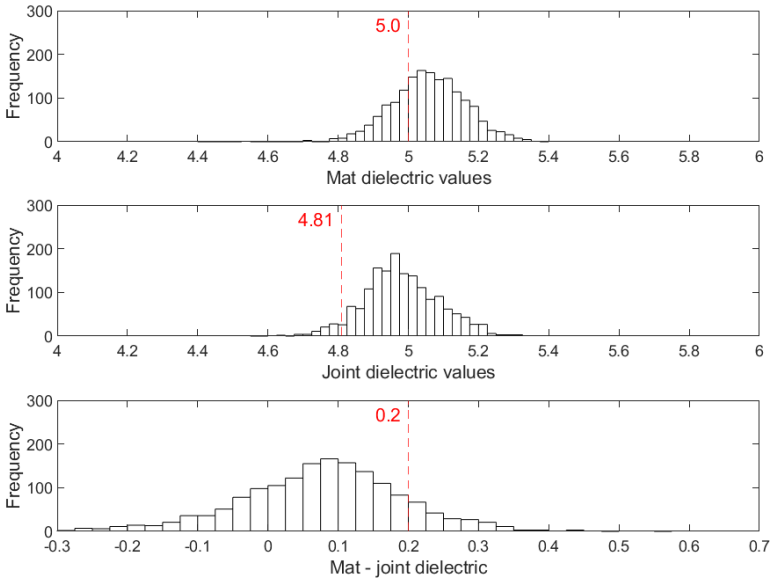

(b) Confined joint

Figure 4.11 Distributions of the dielectric values and their differences between confined and unconfined joints – Xerxes Road #1

4.2.2 Xerxes Road #2 (Station 20+89 to 25+89) – City of Bloomington, MN

Figure 4.12 shows the dielectric values of the mat and the unconfined joint for the 500 ft (152 m) section of the Xerxes Road #2 project. No DPS measurements were taken on the confined joint for this project. The plot shows that the unconfined joint dielectrics are lower than the mat. Looking at the distributions of the dielectric values of the mat and the joint and their difference, Figure 4.13 shows no overlapping of

the dielectric values between the mat and the unconfined joint. In contrast, almost all the dielectric differences are larger than 0.2, indicating an air void difference of over 2% between mat and joint.

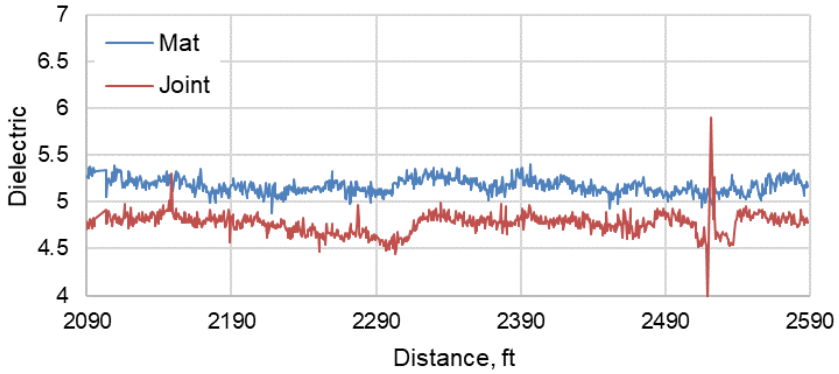

Figure 4.12 Mat and unconfined joint dielectric values – Xerxes Road #2

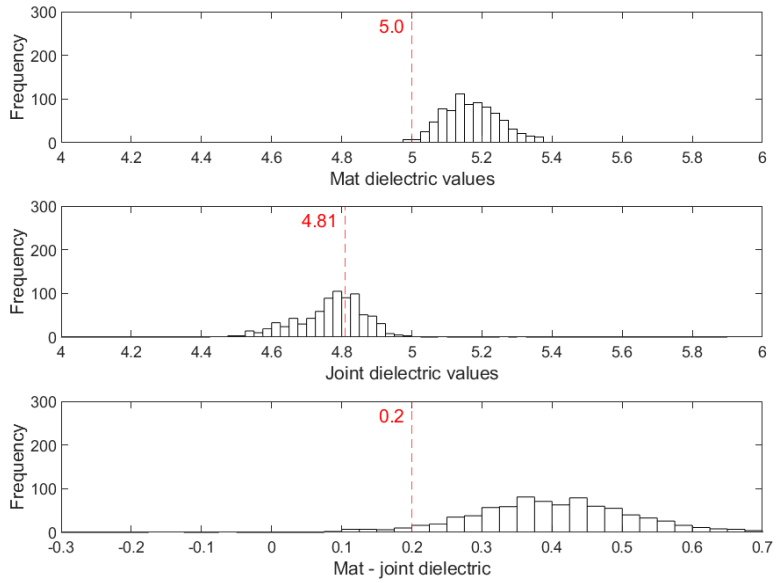

Figure 4.13 Distributions of the dielectric values and their differences on the unconfined joint – Xerxes Road #2

4.3 Statistical Analysis

Although Figure 4.10 through Figure 4.13 display the difference in compaction between the unconfined and confined joints, these figures show the overall dielectric data that is highly variable. Thus, for in-depth data analysis, the data from the 1000 ft (304 m) section were discretized into smaller subsections of 25, 50, 100, and 200 ft (7.6, 15.2, 30.5, and 61 m). The purpose of discretization into different lengths was to determine a subsection length that can better explain the variability of the dielectric data and help differentiate areas with similar and dissimilar compaction. The mean dielectric values from each subsection were compared statistically using paired *t*-tests to quantify the differences in dielectric values between a joint and its corresponding mat. The paired *t*-tests tested the null hypothesis that the

mean dielectric difference between the mat and the joint is equal to 0.2 (μ_difference = 0.2); it is greater than 0.2 (μ_difference > 0.2) as the alternate hypothesis. As stated earlier, a dielectric difference greater than 0.2 corresponds to a joint air void content difference of more than 2% compared to the mat.

Table 4.7 summarizes the *t*-test results for the unconfined and confined joints of the Xerxes Road #1 project discretized into 40 subsections of 25 ft (7.6 m) each. Out of the 40 *t*-tests [one for each 25 ft (7.6 m) subsection along the 1000 ft (304 m) length], 50% of the tests show that there is a significant difference (***p*-value < *α***) between the dielectric values of the unconfined joint and its corresponding mat using a Type 1 error rate of 5% (α = 0.05). However, the dielectric values along the 1000 ft (304 m) section of the confined joint did not show any significant differences compared to the corresponding mat values (i.e., ***p*-value > *α***). This finding implies that constructing a confined joint will result in joint density similar to the mat density and shall be recommended when possible.

Similar data analyses have been conducted for all projects, and Appendix B contains all the plots for the different projects. Table 4.8 summarizes the paired *t*-test results for the longitudinal joint types by subsection lengths. The approach demonstrates that the unconfined joint can result in more subsections where the mat and joint dielectric values will differ by more than 0.2, resulting in an air void difference greater than 2%. All the other joint types do not display dielectric differences greater than 0.2. The table also compares different subsection lengths to demonstrate their suitability for investigating the dielectric differences between the mat and the joint. The data for the unconfined joint of the Xerxes Road #1 (XX1) project shows that using a longer subsection length of 200 ft (61 m) displays that 80% of the subsections of the 1000 ft (304 m) section have a dielectric difference of greater than 0.2. For the 100, 50, and 25 ft (30.5, 15.2, and 7.6 m) subsections, 70%, 55%, and 50% subsections have significant differences greater than 0.2, respectively. The results imply that using a longer subsection can result in rejecting a constructed pavement based on the compaction differences between the mat and the longitudinal joint. In contrast, the compaction is acceptable in specific lengths. That also means using longer subsection length may not identify compaction issues locally.

Table 4.9 shows the summarized paired *t*-test results conducted over air voids for the different longitudinal joint types using different subsection lengths of all the projects. The results are very similar to those shown in Table 4.8. The slight differences observed between the summary results from the two tables are due to the variability of the model affecting the predicted air voids.

Table 4.7 Summary of *t*-tests – Xerxes Road #1

Subsection	Unconfined joint				Confined joint			
	N	Mean difference	Std.	*p*-value	N	Mean difference	Std.	*p*-value
1	43	0.26	0.09	**0.000**	43	-0.01	0.10	1.000
2	42	0.25	0.08	**0.000**	42	0.18	0.07	0.967
3	30	0.28	0.07	**0.000**	41	-0.06	0.12	1.000
4	35	0.24	0.11	**0.027**	42	0.06	0.14	1.000
5	42	0.19	0.09	0.794	42	0.01	0.08	1.000
6	41	0.24	0.08	**0.002**	41	0.04	0.14	1.000
7	42	0.16	0.07	1.000	42	0.05	0.10	1.000
8	42	0.35	0.13	**0.000**	29	0.01	0.08	1.000
9	41	0.47	0.08	**0.000**	41	0.12	0.08	1.000
10	36	0.44	0.12	**0.000**	42	0.14	0.11	1.000
11	42	0.22	0.08	**0.038**	42	0.15	0.07	1.000
12	41	0.19	0.06	0.890	41	0.15	0.08	1.000
13	42	0.20	0.08	0.388	42	0.12	0.07	1.000
14	42	0.24	0.07	**0.000**	42	0.11	0.08	1.000
15	35	0.25	0.12	**0.014**	32	0.12	0.09	1.000
16	42	0.19	0.07	0.724	42	0.07	0.17	1.000
17	42	0.21	0.07	0.315	42	0.03	0.10	1.000
18	41	0.10	0.06	1.000	41	0.09	0.08	1.000
19	42	0.20	0.07	0.481	42	0.09	0.08	1.000
20	42	0.17	0.07	0.999	42	0.02	0.06	1.000
21	41	0.21	0.07	0.092	41	0.10	0.07	1.000
22	42	0.18	0.08	0.958	42	-0.02	0.10	1.000
23	42	0.30	0.13	**0.000**	42	-0.06	0.15	1.000
24	41	0.37	0.09	**0.000**	41	0.13	0.14	0.999
25	42	0.26	0.14	**0.005**	42	0.10	0.08	1.000
26	42	0.19	0.09	0.765	42	0.09	0.07	1.000
27	41	0.31	0.10	**0.000**	41	0.04	0.07	1.000
28	42	0.36	0.07	**0.000**	42	0.08	0.07	1.000
29	42	0.20	0.09	0.413	42	0.07	0.07	1.000
30	41	0.26	0.08	**0.000**	41	0.07	0.11	1.000
31	41	0.26	0.09	**0.000**	39	0.05	0.17	1.000
32	37	0.26	0.11	**0.002**	37	0.13	0.07	1.000
33	41	0.16	0.07	0.999	41	0.11	0.09	1.000
34	42	0.14	0.09	1.000	42	0.12	0.07	1.000
35	42	0.37	0.11	**0.000**	42	0.10	0.08	1.000
36	41	0.14	0.08	1.000	41	0.10	0.06	1.000
37	38	0.16	0.08	0.999	38	0.20	0.13	0.420
38	40	0.17	0.10	0.973	39	0.04	0.12	1.000
39	35	0.15	0.13	0.982	33	0.04	0.23	1.000
40	42	0.11	0.07	1.000	42	0.10	0.14	1.000
Summary	20/40 *100 = 5**0%**				0/40 * 100 = **0%**			

Note: ***p*-value less than 0.05** (α = 0.05) suggests that the mean dielectric difference between the mat and the joint is greater than 0.2 which corresponds to 2% or higher joint air voids as compared to the mat.

Table 4.8 Summary results of *t*-tests over dielectric values

Project & joint type	25 ft	50 ft	100 ft	200 ft
XX1-UnconJt	20/40[#] (50*)	11/20 (55)	7/10 (70)	4/5 (80)
XX2-UnconJt	20/20 (100)	10/10 (100)	5/5 (100)	-
US23-UnconJt	24/40 (60)	12/20 (60)	7/10 (70)	4/5 (80)
I496-UnconJt-Cutback	0/40 (0)	0/20 (0)	0/10 (0)	0/5 (0)
M28-UnconJt-Taper-1	0/40 (0)	0/20 (0)	0/10 (0)	0/5 (0)
M28-UnconJt-Taper-2	0/36 (0)	0/18 (0)	0/9 (0)	0/5 (0)
XX1-ConJt	0/40 (0)	0/20 (0)	0/10 (0)	0/5 (0)
M89-ConJt	0/40 (0)	0/20 (0)	0/10 (0)	0/5 (0)
M25-ConJt-1	9/40 (22.5)	3/20 (15)	1/10 (10)	0/5 (0)
M25-ConJt-2	0/40 (0)	0/20 (0)	0/10 (0)	0/5 (0)
US23-ConJt	1/19 (5)	0/10 (0)	0/5 (0)	-
MT1-ConJt-Maryland method	0/40 (0)	0/20 (0)	0/10 (0)	0/5 (0)
MT2-ConJt-Maryland method	0/40 (0)	0/20 (0)	0/10 (0)	0/5 (0)
M28-ConJt-Taper-1	6/40 (15)	3/20 (15)	2/10 (20)	0/5 (0)
M28-ConJt-Taper-2	0/40 (0)	0/20 (0)	0/10 (0)	0/5 (0)
MT1-EchJt-1	6/40 (15)	2/20 (10)	2/10 (20)	0/5 (0)
MT1-EchJt-2	9/40 (22.5)	6/20 (30)	3/10 (30)	1/5 (20)
US31-EchJt	13/40 (32.5)	5/20 (25)	3/10 (30)	2/5 (40)

Notes: [#]Fraction showing the sections that have greater than 0.2 difference between the mat and the joint over the total subsections. *Percentage of sections that have greater than 0.2 difference between the mat and the joint.

Table 4.9 Summary results of *t*-tests over air voids

Project & joint type	25 ft	50 ft	100 ft	200 ft
XX1-UnconJt-1	19/40 (47.5)	10/20 (50)	7/10 (70)	4/5 (80)
XX1-UnconJt-2	20/20 (100)	10/10 (100)	5/5 (100)	-
US23-UnconJt	25/40 (62.5)	13/20 (65)	8/10 (80)	4/5 (80)
I496-UnconJt-Cutback	0/40 (0)	0/20 (0)	0/10 (0)	0/5 (0)
M28-UnconJt-Taper-1	0/40 (0)	0/20 (0)	0/10 (0)	0/5 (0)
M28-UnconJt-Taper-2	0/36 (0)	0/18 (0)	0/9 (0)	0/5 (0)
XX1-ConJt	0/40 (0)	0/20 (0)	0/10 (0)	0/5 (0)
M89-ConJt	0/40 (0)	0/20 (0)	0/10 (0)	0/5 (0)
M25-ConJt-1	1/40 (2.5)	0/20 (0)	0/10 (0)	0/5 (0)
M25-ConJt-2	0/40 (0)	0/20 (0)	0/10 (0)	0/5 (0)
US23-ConJt	1/19 (5)	0/10 (0)	0/5 (0)	-
MT1-ConJt-Marryland method	0/40 (0)	0/20 (0)	0/10 (0)	0/5 (0)
MT2-ConJt-Maryland method)	0/40 (0)	0/20 (0)	0/10 (0)	0/5 (0)
M28-ConJt-Taper-1	3/40 (7.5)	2/20 (10)	0/10 (0)	0/5 (0)
M28-ConJt-Taper-2	0/40 (0)	0/20 (0)	0/10 (0)	0/5 (0)
MT1-EchJt-1	2/40 (5)	2/20 (10)	0/10 (0)	0/5 (0)
MT1-EchJt-2	1/40 (2.5)	2/20 (10)	1/10 (10)	1/5 (20)
US31-EchJt	0/40 (0)	0/20 (0)	0/10 (0)	0/5 (0)

Notes: [#]Fraction showing the sections that have greater than 2% air void difference between the mat and the joint over the total subsections. *Percentage of sections that have greater than 2% air void difference between the mat and the joint.

4.4 Probabilistic Analysis for Joint Types Comparison

A probabilistic approach was used in addition to the paired *t*-test to compare different longitudinal joint types. The dielectric values for each type of joint and its corresponding mat from each project were divided into six groups, as displayed in Table 4.10, along with their corresponding air voids. The conditional probabilities for each dielectric and air void category were determined for the mat and the joint based on equation (8). Table 4.11 through Table 4.14 display the conditional probabilities for the different dielectric and air void categories of the mat and joint for the unconfined and confined joints of the Xerxes Road #1 project. Table 9 shows that if the mat dielectric values are between < 5, 5 – 5.2, or 5.2 – 5.4, the unconfined joint will have a 99%, 95%, or 92% chance of having dielectric < 5. Table 4.12 shows similar results for air void-based probabilities using the calibrated model presented earlier in equation (3). For a confined joint, there is a 59% chance of the joint dielectric being < 5, while there is a 39% chance of being between 5 – 5.2, given that the mat has dielectric values between 5 – 5.2, as shown in Table 4.13. Table 4.14 shows a similar comparison of the probabilities resulting from the air voids. Similar project-wise probability matrices were developed for all the longitudinal joint types.

$$P(\text{joint}/\text{mat}) = \frac{P(\text{joint}) \times P(\text{mat})}{P(\text{mat})} = \frac{P(\text{joint}) \cap P(\text{mat})}{P(\text{mat})} \quad (8)$$

Table 4.10 Categories for probabilistic analysis

Category	Dielectric ranges	Corresponding air void ranges
1	< 5	> 8
2	≥ 5 & < 5.2	≤ 8 & > 6.2
3	≥ 5.2 & < 5.4	≤ 6.2 & > 4.7
4	≥ 5.4 & < 5.6	≤ 4.7 & > 3.5
5	≥ 5.6 & < 5.8	≤ 3.5 & > 2.6
6	> 5.8	≤ 2.6

Table 4.11 Conditional probabilities for the unconfined joint using dielectrics – Xerxes Road #1

Joint \ Mat	< 5	≥ 5 & < 5.2	≥ 5.2 & < 5.4	≥ 5.4 & < 5.6	≥ 5.6 & < 5.8	≥ 5.8
< 5	99%	95%	92%	67%	-	-
≥ 5 & < 5.2	1%	5%	8%	33%	-	-
≥ 5.2 & < 5.4	-	-	-	-	-	-
≥ 5.4 & < 5.6	-	-	-	-	-	-
≥ 5.6 & < 5.8	-	-	-	-	-	-
≥ 5.8	-	-	-	-	-	-

Note: Cells with a dash (-) mean no data was available in that category.

Table 4.12 Conditional probabilities for the unconfined joint using air voids – Xerxes Road #1

Joint \ Mat	> 8	≤ 8 & > 6.2	≤ 6.2 & > 4.7	≤ 4.7 & > 3.5	≤ 3.5 & > 2.6	≤ 2.6
> 8	99%	95%	92%	67%	-	-
≤ 8 & > 6.2	1%	5%	8%	33%	-	-
≤ 6.2 & > 4.7	-	-	-	-	-	-
≤ 4.7 & > 3.5	-	-	-	-	-	-
≤ 3.5 & > 2.6	-	-	-	-	-	-
≤ 2.6	-	-	-	-	-	-

Note: Cells with a dash (-) mean no data was available in that category.

Table 4.13 Conditional probabilities for the confined joint using dielectrics – Xerxes Road #1

Joint \ Mat	< 5	≥ 5 & < 5.2	≥ 5.2 & < 5.4	≥ 5.4 & < 5.6	≥ 5.6 & < 5.8	≥ 5.8
< 5	74%	59%	14%	-	-	-
≥ 5 & < 5.2	26%	39%	70%	-	-	-
≥ 5.2 & < 5.4	-	2%	16%	-	-	-
≥ 5.4 & < 5.6	-	-	-	-	-	-
≥ 5.6 & < 5.8	-	-	-	-	-	-
≥ 5.8	-	-	-	-	-	-

Note: Cells with a dash (-) mean no data was available in that category.

Table 4.14 Conditional probabilities for the confined joint using air voids – Xerxes Road #1

Joint \ Mat	> 8	≤ 8 & > 6.2	≤ 6.2 & > 4.7	≤ 4.7 & > 3.5	≤ 3.5 & > 2.6	≤ 2.6
> 8	74%	59%	14%	-	-	-
≤ 8 & > 6.2	26%	39%	70%	-	-	-
≤ 6.2 & > 4.7	-	2%	16%	-	-	-
≤ 4.7 & > 3.5	-	-	-	-	-	-
≤ 3.5 & > 2.6	-	-	-	-	-	-
≤ 2.6	-	-	-	-	-	-

Note: Cells with a dash (-) mean no data was available in that category.

Figure 4.14 summarizes the conditional probabilities for a mat dielectric reference range of 5.2 – 5.4, combining probabilities from different projects for each longitudinal joint type. This dielectric range corresponds to an air void range of 6.2% to 4.7%. The figure shows that irrespective of the project for an unconfined joint, there is a 95% chance that the joint dielectrics will be less than 5, i.e., greater than 8% air voids given the reference dielectric range for the mat (5.2 – 5.4). Also, there is about a 70% chance that the joint will have the same dielectric range as the reference range for the mat for echelon, taper confined, and tapered unconfined joints. For the same joint types, there is about a 20% chance that the joint dielectrics will be a category low (i.e., 5 – 5.2), while there is about a 10% chance of the joint

dielectric being a category higher (5.4 – 5.6). A confined joint will 50% times produce a joint with dielectrics like the reference, while there is a 40% chance of the joint dielectric being a category higher (5.4 – 5.6) than the reference range. An unconfined joint constructed by cutting back a portion of the HMA before laying the adjacent lane has a 50% chance of producing joint dielectric like the mat reference range. A similar comparison can be accomplished using a different mat dielectric reference range. Using mat air void reference range of 6.2% to 4.7% resulted in similar results as shown in Figure 4.14 (see Appendix B). The results from the probabilistic approach shown in Figure 4.14 are similar to the ones reported earlier in the report for the *t*-test approach (see Table 4.8). This also implies that an unconfined joint should be avoided when possible. An unconfined joint with cutback material can be a better choice. It should be noted that these conclusions are based on data collected for this study.

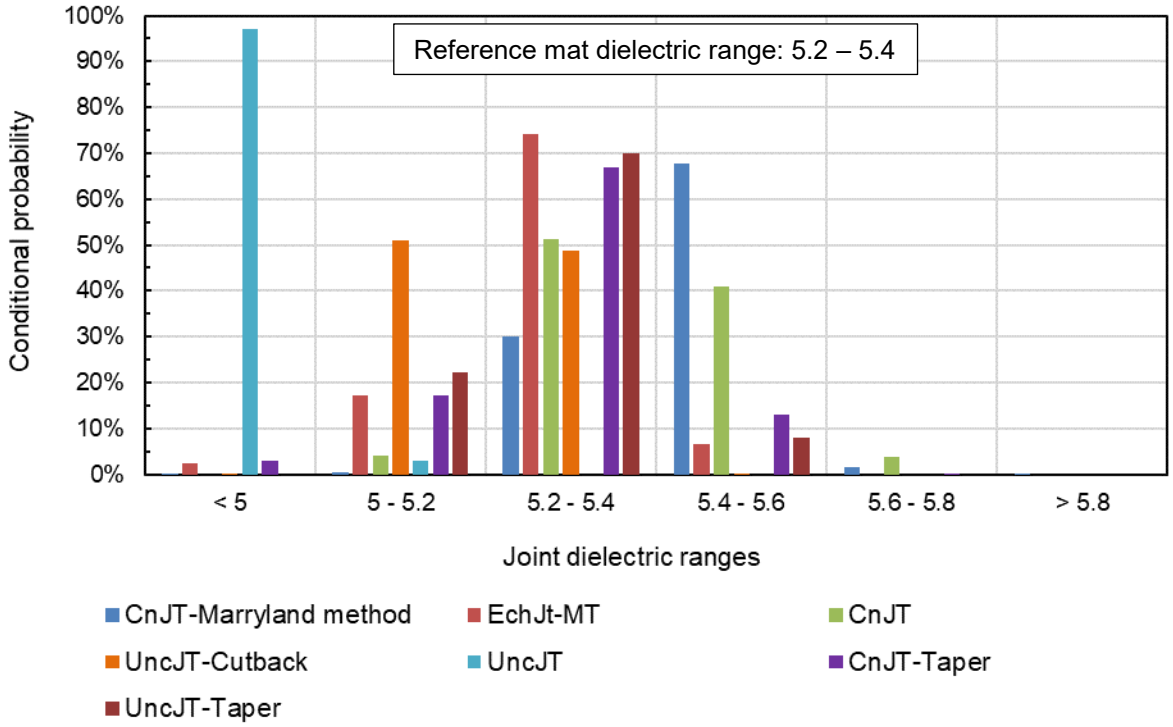

Figure 4.14 Conditional probabilities for different dielectric categories by joint type for reference mat dielectric range of 5.2 – 5.4.

4.5 Longitudinal Joint Quality Control and Assurance – Using PWL

Percent within limits (PWL) is a quality measure preferred by most agencies due to its ability to measure the population average and data variability statistically efficiently. It is defined as the percentage of the population (or lot) falling above the single lower specification limit, below a single upper specification limit, or between the lower and the upper limits. This study determined one-sided PWL for the mat and joint dielectric values and their difference by subsections (of variable lengths). Lower specification limits

of 5 and 4.81 dielectric values were used to calculate individual mat and joint PWL for every subsection, respectively. As mentioned earlier, the dielectric values of 5 and 4.81 correspond to 8% and 10% air voids per the calibrated model in equation (3). This research used an upper specification limit of 0.2 dielectric difference (mat–joint) for calculating PWL for each subsection. Figure 4.15 shows the dielectric-based PWL calculated for every 25 ft (7.6 m) subsection of the unconfined joint and its corresponding mat for the Xerxes Road #1 project. The rejectable quality level (RQL) and acceptable quality level (AQL) of 60% and 90%, respectively, are used for reference. In addition, this study uses an acceptance limit of 60%. It can be observed that the individual mat and joint PWL are within the acceptance levels for most of the subsections. However, the figure shows that 29 subsections out of the total 40 (72.5%) have unacceptable PWL (using the dielectric difference of 0.2 as the upper specification limit) in contrast to the paired *t*-test approach results showing that 50% of the subsections had a dielectric difference of greater than 0.2 between the mat and the joint. This is because the paired *t*-test considers statistical significance between the mean difference, while PWL shows the probability of dielectric difference less than 0.2.

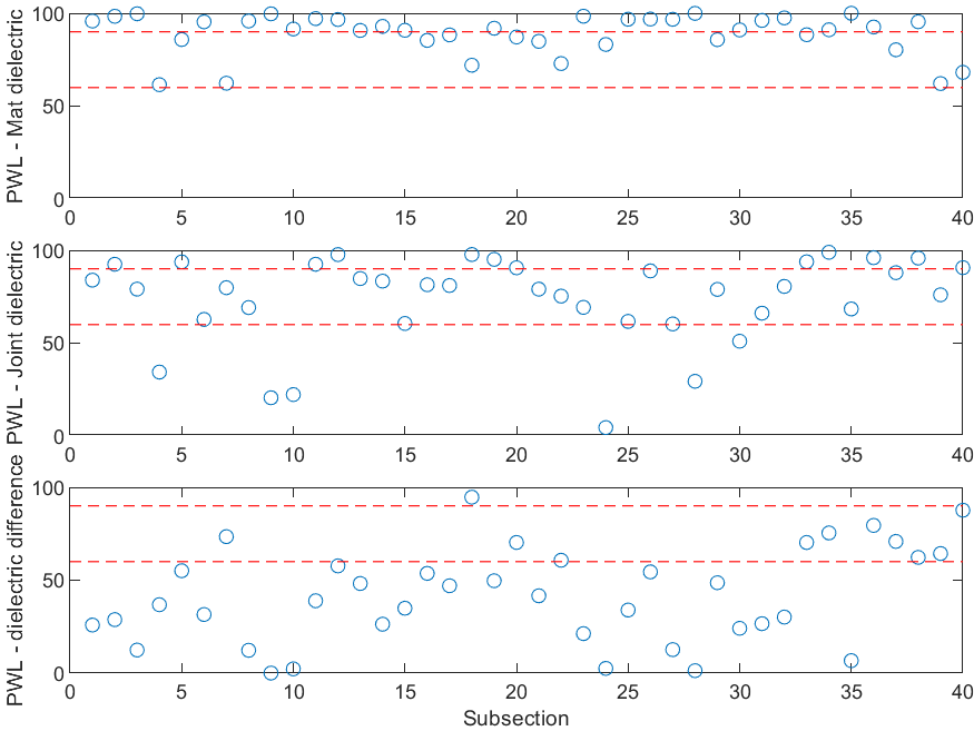

Figure 4.15 Dielectric-based PWL for the unconfined joint – Xerxes Road #1 project

The box plots show (see Figure 4.16) that most mat dielectrics are above the lower specified limit (dielectric of 5). The variations in the PWL values are due to the slight variability of the dielectric data within each subsection. The figure also shows that the joint dielectrics are lower than the mat's dielectrics, with higher variation between them within each subsection. The PWL for subsections 4, 9, 10, 24, 28, and 30 are lower than the acceptance limit of 60%. The dielectrics for these sections show that most of the data lie below the lower specified limit of 4.81 for the joint.

On the contrary, the mat and the confined joint dielectrics have higher variations; most joint dielectrics are higher than 4.81, resulting in higher PWL values (see Figure 4.17 and Figure 4.18). At the same time, the mat has subsections where the dielectrics are lower than the threshold value of 5, resulting in lower PWL values for the mat. PWL based on the dielectric difference (mat – joint) at the confined joint is within the specified quality levels (i.e., AQL and RQL) for almost the whole 1000 ft (304 m) section.

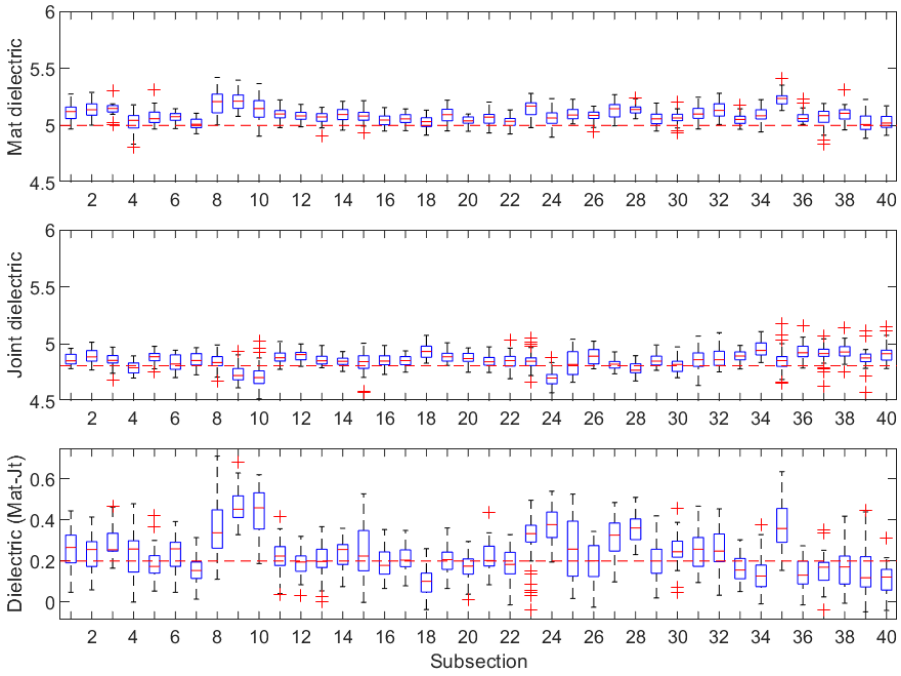

Figure 4.16 Dielectric-based box plots for the unconfined joint – Xerxes Road #1 project

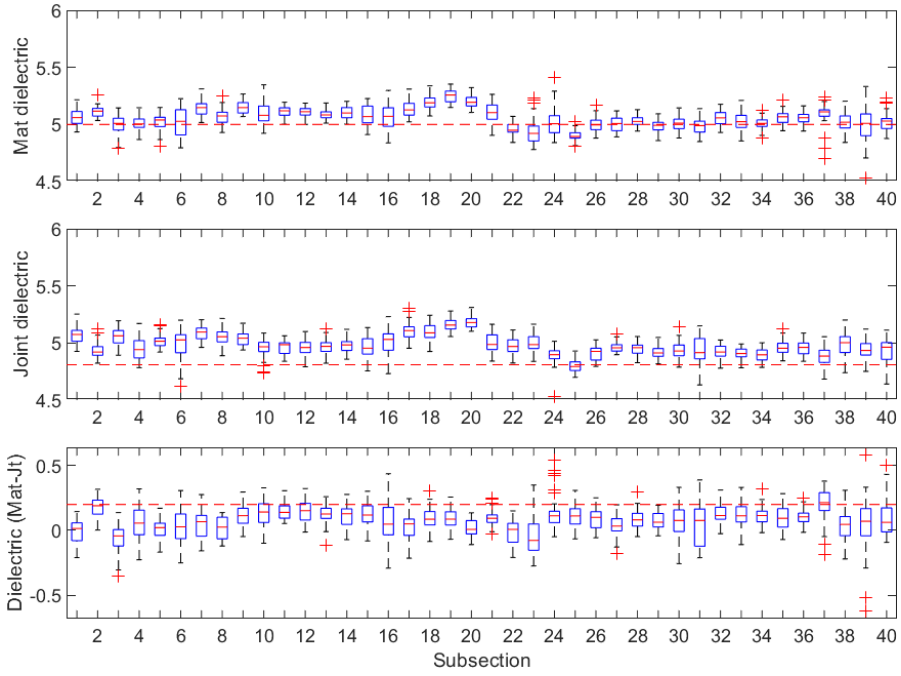

Figure 4.17 Dielectric-based box plots for the confined joint – Xerxes Road #1 project

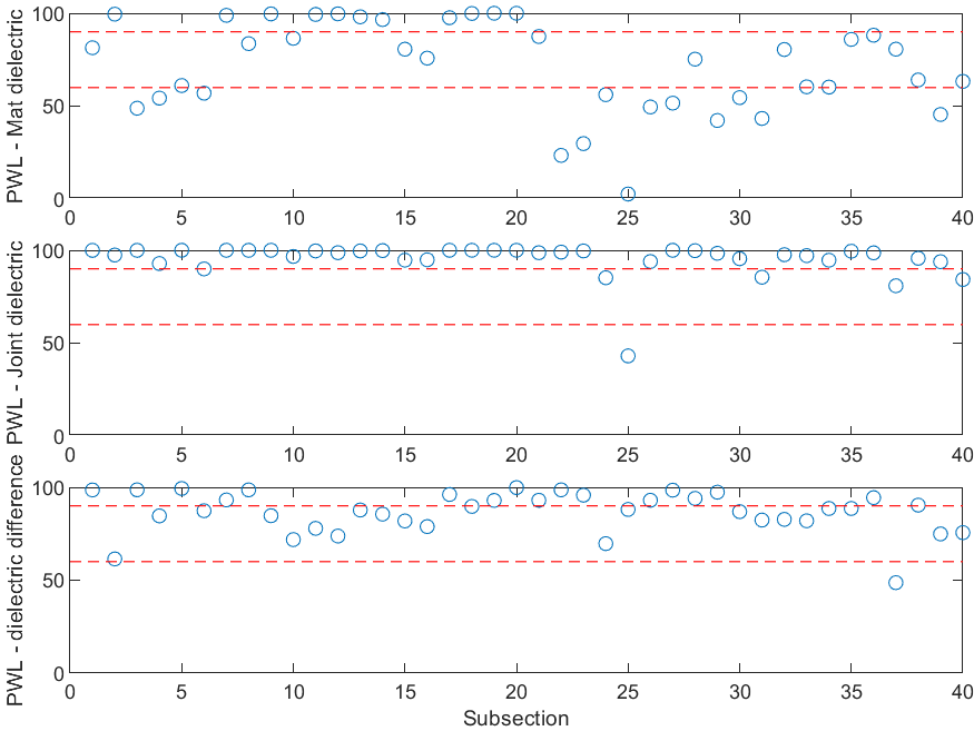

Figure 4.18 Dielectric-based PWL for the confined joint – Xerxes Road #1 project

Table 4.15 summarizes the results for PWL determined using dielectric data for the different longitudinal joint types (see Appendix B for plots). PWL values determined using air voids were also determined for all the projects (see Appendix B), and results are summarized in Table 4.16. Table 4.15 shows the number of sections with PWL values lesser than the RQL of 60% and their percentage (in brackets) to the total sections for each subsection length. The table confirms the statistical and probabilistic dielectric data analyses showing that constructing an unconfined joint would result in inadequate compaction. Observing the unconfined joint from the Xerxes Road#1 (XX1-UnconJt) project, the table shows that about 72% of the sections have PWL values lower than the 60% RQL values, indicating a low probability of the dielectric difference less than 0.2. In other words, 72% of the subsections have a higher chance of having a dielectric difference greater than 0.2.

In contrast, Table 4.8 showed (based on *t*-tests) that 50% of the sections have a mean dielectric difference greater than 0.2. Although table 4.15 shows a higher percentage of subsections having PWL lower than the RQL value for the echelon joint, Table 4.16 illustrates that the echelon joint has air voids similar to the mat with no considerable PWL values below the RQL. Paired *t*-tests displayed similar differences in results for the echelon joints that can be attributed to the air void vs. dielectric calibration model's variability. Overall, the statistical and probabilistic approach results agree with the summary PWL results using either dielectrics or air voids data in comparing different joint types.

Table 4.15 Summary PWL results for dielectric values

Project & joint type	25 ft	50 ft	100 ft	200 ft
XX1-UnconJt	29/40[#] (72.5*)	15/20 (75)	8/10 (80)	5/5 (100)
XX2-UnconJt	20/20 (100)	10/10 (100)	5/5 (100)	No data
US23-UnconJt	29/40 (72.5)	15/20 (75)	8/10 (80)	4/5 (80)
I496-UnconJt-Cutback	4/40 (10)	1/20 (5)	0/10 (0)	0/5 (0)
M28-UnconJt-Taper-1	0/40 (0)	0/20 (0)	0/10 (0)	0/5 (0)
M28-UnconJt-Taper-2	0/36 (0)	0/18 (0)	0/9 (0)	0/5 (0)
XX1-ConJt	1/40 (2.5)	0/20 (0)	0/10 (0)	0/5 (0)
M89-ConJt	1/40 (2.5)	0/20 (0)	0/10 (0)	0/5 (0)
M25-ConJt-1	12/40 (30)	4/20 (20)	3/10 (30)	1/5 (20)
M25-ConJt-2	0/40 (0)	0/20 (0)	0/10 (0)	0/5 (0)
US23-ConJt	1/19 (5)	0/10 (0)	0/5 (0)	No data
MT1-ConJt-Maryland method	0/40 (0)	0/20 (0)	0/10 (0)	0/5 (0)
MT2-ConJt-Maryland method	0/40 (0)	0/20 (0)	0/10 (0)	0/5 (0)
M28-ConJt-Taper-1	9/40 (22.5)	4/20 (20)	2/10 (20)	0/5 (0)
M28-ConJt-Taper-2	0/40 (0)	0/20 (0)	0/10 (0)	0/5 (0)
MT1-EchJt-1	11/40 (27.5)	5/20 (25)	3/10 (30)	2/5 (40)
MT1-EchJt-2	18/40 (55)	9/20 (45)	4/10 (40)	2/5 (40)
US31-EchJt	19/40 (47.5)	9/20 (45)	5/10 (50)	2/5 (40)

Notes: [#]Fraction showing the sections that have PWL lower than the RQL (60%) over the total subsections. *Percentage of sections with PWL lower than the acceptance limit.

Table 4.16 Summary PWL results for air voids

Project & joint type	25 ft	50 ft	100 ft	200 ft
XX1-UnconJt-1	28/40 (70)	5/20 (75)	8/10 (80)	4/5 (80)
XX1-UnconJt-2	20/20 (100)	10/10 (100)	5/5 (100)	No data
US23-UnconJt	29/40 (72.5)	15/20 (75)	8/10 (80)	4/5 (80)
I496-UnconJt-Cutback	0/40 (0)	0/20 (0)	0/10 (0)	0/5 (0)
M28-UnconJt-Taper-1	0/40 (0)	0/20 (0)	0/10 (0)	0/5 (0)
M28-UnconJt-Taper-2	0/36 (0)	0/18 (0)	0/9 (0)	0/5 (0)
XX1-ConJt	1/40 (2.5)	0/20 (0)	0/10 (0)	0/5 (0)
M89-ConJt	0/40 (0)	0/20 (0)	0/10 (0)	0/5 (0)
M25-ConJt-1	2/40 (5)	1/20 (5)	0/10 (0)	0/5 (0)
M25-ConJt-2	0/40 (0)	0/20 (0)	0/10 (0)	0/5 (0)
US23-ConJt	1/19 (5)	0/10 (0)	0/5 (0)	No data
MT1-ConJt-Marryland method	0/40 (0)	0/20 (0)	0/10 (0)	0/5 (0)
MT2-ConJt-Maryland method	0/40 (0)	0/20 (0)	0/10 (0)	0/5 (0)
M28-ConJt-Taper-1	3/40 (7.5)	2/20 (10)	2/10 (20)	0/5 (0)
M28-ConJt-Taper-2	0/40 (0)	0/20 (0)	0/10 (0)	0/5 (0)
MT1-EchJt-1	4/40 (10)	2/20 (10)	1/10 (10)	0/5 (0)
MT1-EchJt-2	4/40 (10)	2/20 (10)	1/10 (10)	1/5 (20)
US31-EchJt	0/40 (0)	0/20 (0)	0/10 (0)	0/5 (0)

Notes: #Fraction showing the sections that have PWL lower than the RQL (60%) over the total subsections. *Percentage of sections with PWL lower than the acceptance limit.

4.6 Longitudinal Joint Quality Index (LJQI)

The paired *t*-test approach can identify differences in joint types based on the subsection's mean mat and joint dielectric values. However, it does not consider the mat and joint dielectric values, which resulted in a mean difference of 0.2 or higher. The approach treats the 0.2 dielectric difference equally, irrespective of the individual mat and joint dielectric values. A subsection with a significant difference (> 0.2 dielectrics) can occur even if the joint and mat have acceptable compaction. Thus, considering such a section with a significant dielectric difference in the paired *t*-test approach is unreasonable to the contractor. Therefore, it is crucial to consider the individual mean mat and joint dielectric values of the subsections.

Figure 4.19 displays the mean dielectric differences with their 95% CI for all the 25 ft (7.6 m) subsections for the unconfined joint of the Xerxes Road #1 project. The figure shows that half of the mean values and their corresponding CI are greater than the threshold dielectric value of 0.2 for the unconfined joint. However, most of the mean joint dielectrics are greater than 4.81—corresponding to 10% air voids. Only subsections 9, 10, and 24 have mean joint dielectric values less than 4.81. On the contrary, subsections 8 and 35 have a mean joint dielectric value greater than 4.81. Still, since the mat's compaction at these subsections is better than any other subsection within the length of the project, their mean differences are the highest. Such situations imply a correction strategy that does not penalize the contractor for a higher degree of compaction achieved at the mat relative to an acceptable one at the joint. A similar plot shown in Figure 4.20 displays the mean mat and joint dielectric values and their differences with 95% CI for the confined joint of the project. All the differences are lower than 0.2, showing the mat and joint have similar compaction.

This study proposes a new index, i.e., longitudinal joint quality index (LJQI), that determines the percentage of stations with acceptable compaction by subtracting the proportion of stations with problematic areas. The scale ranges from 0 to 100 using dielectric data to evaluate the joint quality while correcting for the mat density. The proposed LJQI requires minimum specified mat and joint dielectric values and a specified acceptable dielectric difference between them (mat – joint). The index involves calculating the dielectric difference between the mat and the joint while considering the mat dielectric value of the station. Suppose the mat dielectric value is greater than the minimum specified value. In that case, the difference between the mat and the joint is calculated by subtracting the joint dielectric from the minimum specified mat dielectric value. This correction will cater to the adequate compaction at the mat, which may result in a difference greater than 0.2, causing a penalty to the contractor even with acceptable joint compaction. In addition, the proposed LJQI also checks the joint dielectric values against the specified value individually and rejects the station's compaction if the condition is met. The LJQI calculation procedure is as follows:

1. Establish an acceptable value for the dielectric in the control population (e.g., mat or the confined side of the joint, etc.), $\varepsilon_{mat,min}$.

2. Establish an acceptable difference in the dielectric values between the corresponding mat and the joint), $\Delta\varepsilon_{crit}$
3. Establish a minimum acceptable level of dielectric for the joint, $\varepsilon_{joint,min}$
4. Compute the number of stations for each of the two criteria described below. Each criterion determines the number of stations with an unacceptable value for the dielectric:

$$\varepsilon_{joint} < \varepsilon_{joint,min} \text{ OR } \min(\varepsilon_{mat,}\, \varepsilon_{mat,min}) - \varepsilon_{joint} > \Delta\varepsilon_{crit}$$

where:

ε_{joint} = dielectric at the joint.
$\varepsilon_{joint,min}$ = minimum specified joint dielectric.
ε_{mat} = dielectric of the control population (e.g., mat).
$\varepsilon_{mat,min}$ = minimum specified dielectric of the control population (e.g., mat).
$\Delta\varepsilon_{crit}$ = minimum specified dielectric difference between the mat (i.e., control population) and the joint (mat – joint)

5. Determine the total percentage of stations with unacceptable dielectric values meeting any of the two criteria in Step 4 above.
6. Calculate the LJQI by subtracting the determined percentage (in Step 5 above) from 100% to get the percentage of stations with acceptable compaction.

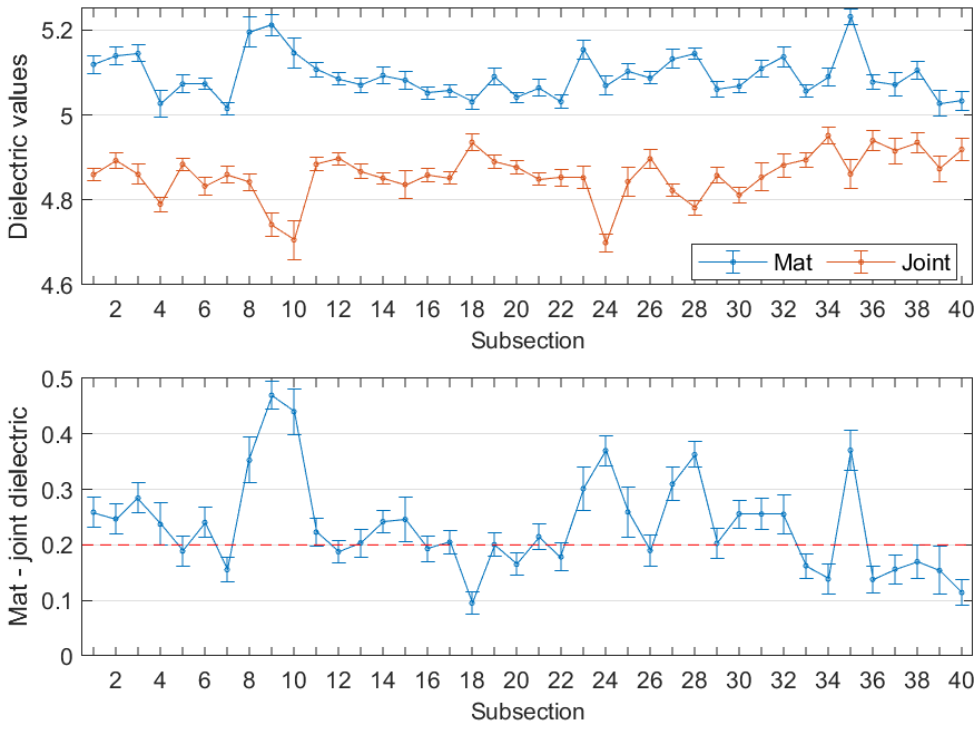

Figure 4.19 Mean mat and joint dielectric values and their difference with 95% CI for the unconfined joint for each 25 feet subsection – Xerxes Road #1

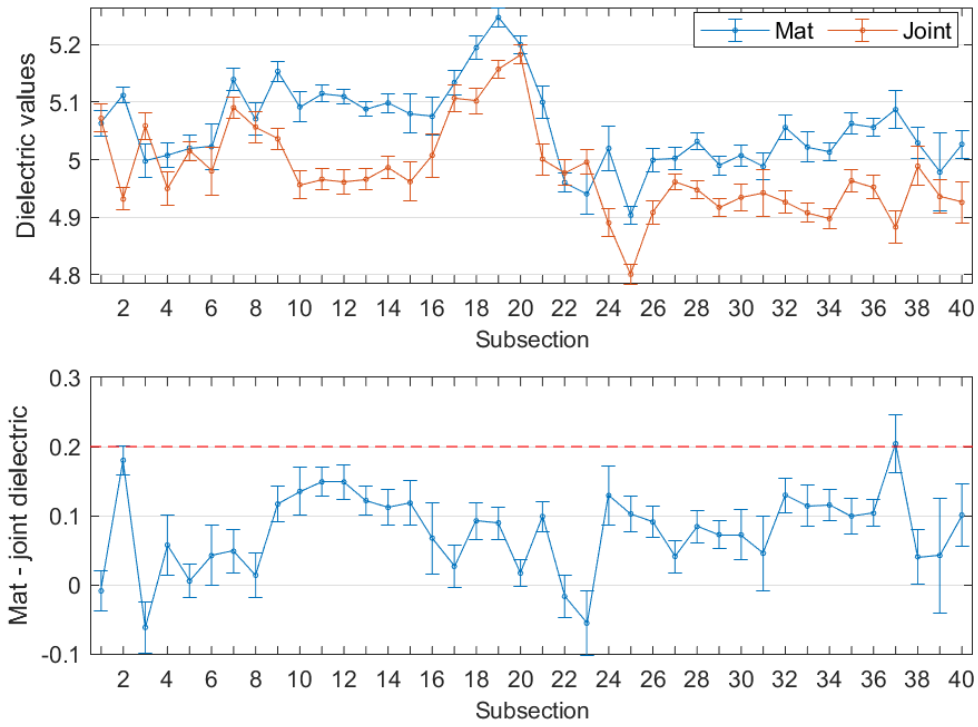

Figure 4.20 Mean mat and joint dielectric values and their difference with 95% CI for the confined joint for each 25 feet subsection – Xerxes Road #1

The first criterion in Step 4 ($\varepsilon_{joint} < \varepsilon_{joint,min}$) checks the joint's compaction (i.e., joint dielectric) against the minimum specified value for the joint. If the joint dielectric is less than the minimum specified, that station is considered unacceptable due to inadequate compaction. The second criterion in Step 4 evaluates the difference between the mat (i.e., control population) and the joint dielectric value for every station while correcting for the mat dielectric value as described earlier. If any of the two criteria are met at a station, that station has unacceptable compaction. In this study, $\varepsilon_{mat,min}$ is specified as 5, corresponding to 8% air voids in the mat. $\Delta\varepsilon_{crit}$ is specified at 0.2, a dielectric difference between the mat and the joint that corresponds to greater than 2% air voids, while $\varepsilon_{joint,min}$ is specified as 4.81, which corresponds to 10% air voids at the joint using the calibrated model. These specified limits can be altered based on individual calibration curves for different HMA mixes or the expertise of the agencies.

Table 4.17 demonstrates the effect of both criteria in determining the stations with unacceptable compaction. The 1st row of the table shows the baseline criteria defined in this study. With the specified mat dielectric of 5 (8% air voids) and joint dielectric of 4.8 (10% air voids), none of the three criteria is met, and hence the station is not considered unacceptable. Consider a station with more than 10% air voids at the joint but adequate mat compaction; such a station will be considered unacceptable (see rows 2nd and 3rd). Similarly, stations with inadequate joint compaction but an acceptable relative difference between the mat and joint dielectric (see rows 4th and 5th) will also be considered unacceptable. Finally, the proposed index will not consider a station unacceptable if the mat and joint

have adequate compaction individually, but the dielectric difference is greater than the specified limit due to excellent mat compaction (see 6th and 7th row). Thus, the proposed index can correct for excellent mat compaction and consider individual joint compaction to determine stations with compaction issues.

Table 4.17 Demonstrating the three criteria for determining the LJQI

Row no.	Mat air voids	Joint air voids	Mat dielectric	Joint dielectric	Criterion 1 (joint)	Criterion 2 (difference)	Unacceptable
1	8	10	5	4.8	N	N	N
2	8	10.5	5	4.75	Y	Y	Y
3	7	11	5.10	4.7	Y	Y	Y
4	10	11	4.8	4.7	Y	N	Y
5	8.9	11	4.9	4.7	Y	N	Y
6	4	9	5.5	4.89	N	N	N
7	7	10	5.10	4.8	N	N	N

Figure 4.21 shows the application of the proposed index for the individual project sections (not subsections). The figure shows that only 79%, 42%, and 27% of stations have acceptable joint compaction using an unconfined joint at Xerxes Road #1, Xerxes Road #2, and US-23 projects, respectively. The unconfined joint at the I-496 project resulted in 100% acceptable compaction throughout the section, where the contractor cut back the newly compacted unconfined edge of the joint before paving the adjacent lane. The confined joints constructed at US-23 and Xerxes Road #1 projects have about 100% acceptable compaction at the joint. Similarly, confined joints constructed using the Maryland method (Manning Trail projects #1 and #2) also have 100% acceptable compaction throughout the section. Projects with joints constructed using echelon paving (Manning Trail projects #1 and #2), sequential mill and fill technique to construct confined joints (M-25 and M-89 projects), and joints with tapered geometry (M-28 project) also resulted in 100% acceptable compaction at the joints. Although applied to whole sections, the proposed index can be applied to the subsections within each project as well.

Figure 4.22 displays the sensitivity of the proposed index for different pairs of the maximum specified air voids of the joint and the mat with a minimum specified air void difference of 2% ($\Delta\varepsilon_{crit} = 0.2$) for all the projects sections (not subsections). The right-most joint and mat air voids pair (10% joint and 8% mat) shows the same percent acceptable values as in Figure 4.21. As the specified mat and joint air voids are reduced, the percent acceptable (i.e., LJQI) value reduces for all the projects except the US-31, where the echelon joint is used. While the unconfined joints of the Xerxes Road #2 and US-23 projects show LJQI values less than 60% for all the pairs of the mat and the joint air voids, the LJQI value for the unconfined joint at Xerxes Road #1 drops below 60% as soon as the minimum specified mat and joint air voids is reduced to 7.5% and 9.5%, respectively. The unconfined joint (constructed using cutting back technique) at the I-496 project and the confined joint at the US-23 project result in LJQI lower than 60% if the specified air void values are significantly reduced to 4% for the mat and 6% for the joint. The LJQI

value for the confined joint at Xerxes Road #1 project falls below 60% if the minimum specified air void levels are changed to 6% (mat) and 8% (joint). For the confined joint constructed using the Maryland method (Manning Trail projects #1 and #2), sequential mill and fill technique (M-25 and M-89 projects), and joints with tapered geometry (M-28 project) result in LJQI of 76% for all the pairs of mat and joint air voids. The same is the case for the echelon joint at the US-31 project. However, the LJQI value for the echelon joints at the Manning Trail project drops below 60% if the specified air voids are below 4% (mat) and 6% (joint). Based on the sensitivity, this study suggests a minimum LJQI value of 60% for accepting a centerline longitudinal joint without penalty. However, the acceptable index level can be determined per the agency's requirements.

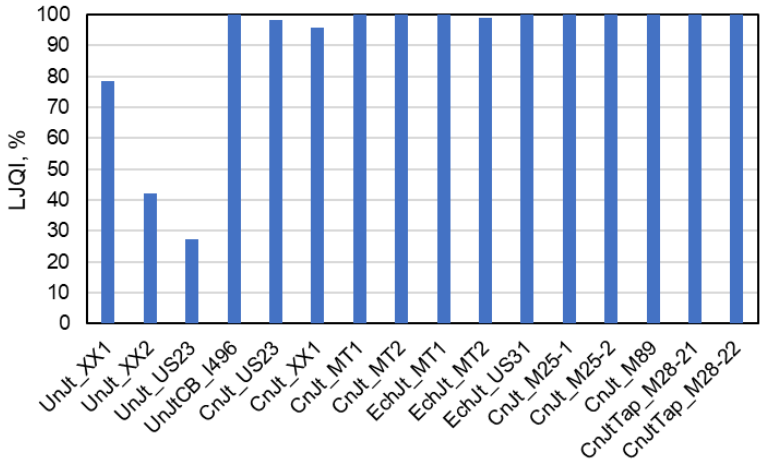

Figure 4.21 Application of the new index for longitudinal joint quality evaluation

Figure 4.23 displays the effect of correcting for the exceptional mat compaction (using criteria 2) on the PWL based on the dielectric difference for every 25 ft (7.6 m) subsection of the unconfined joint. The figure shows that correcting for the mat's compaction, six out of the 40 subsections have PWL below the acceptance limit (60%), while only 11 subsections passed before correction. Although the strategy has corrected the PWL values, it should be noted that most subsections are below the AQL of 90%, displaying an unsatisfactory quality and warranting a financial penalty to the contractor. This implies that constructing an unconfined joint should be avoided even if correction is applied for excellent mat density and PWL is based on the relative joint and corresponding mat difference. Table 4.18 confirms the same, where the unconfined joints still display significant differences in relative compaction and a higher percentage of subsections with a greater probability of a relative dielectric difference of more than 0.2.

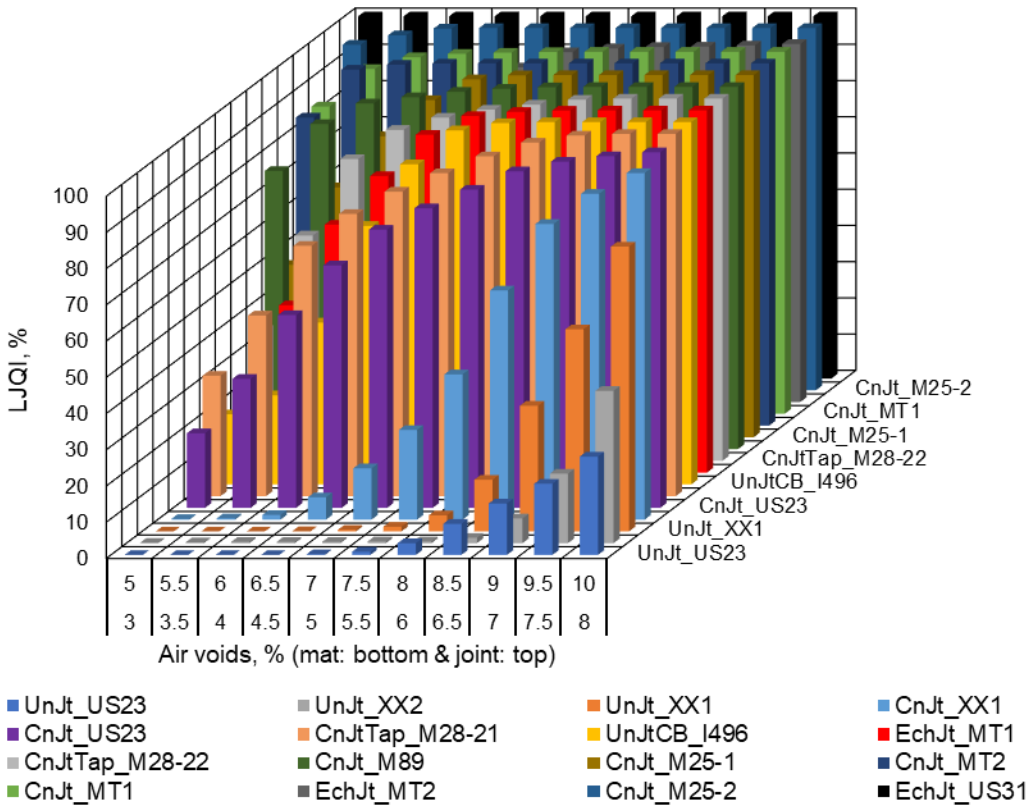

Figure 4.22 Sensitivity of the new index for longitudinal joint quality evaluation

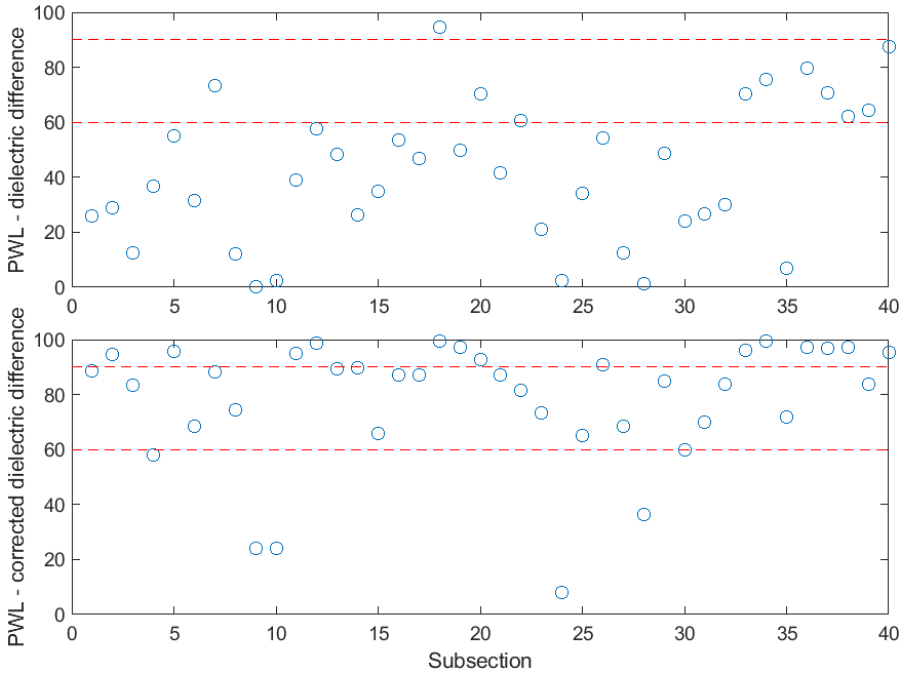

Figure 4.23 PWL based on dielectric difference before and after correction for the unconfined joint – Xerxes Road #1 project

Table 4.18 Summary PWL results for dielectric values after correction

Project & joint type	25 ft	50 ft	100 ft	200 ft
XX1-UnconJt-1	5/40 (12.5)	3/20 (15)	2/10 (20)	0/5 (0)
XX1-UnconJt-2	15/20 (75)	7/10 (70)	4/5 (80)	No data
US23-UnconJt	27/40 (67.5)	15/20 (75)	7/10 (70)	4/5 (80)
I496-UnconJt-Cutback	0/40 (0)	0/20 (0)	0/10 (0)	0/5 (0)
M28-UnconJt-Taper-1	0/40 (0)	0/20 (0)	0/10 (0)	0/5 (0)
M28-UnconJt-Taper-2	0/35 (0)	0/18 (0)	0/9 (0)	0/5 (0)
XX1-ConJt	0/40 (0)	0/20 (0)	0/10 (0)	0/5 (0)
M89-ConJt	0/40 (0)	0/20 (0)	0/10 (0)	0/5 (0)
M25-ConJt-1	0/40 (0)	1/20 (5)	0/10 (0)	0/5 (0)
M25-ConJt-2	0/40 (0)	0/20 (0)	0/10 (0)	0/5 (0)
US23-ConJt	0/19 (0)	0/10 (0)	0/5 (0)	No data
MT1-ConJt-Marryland method	0/40 (0)	0/20 (0)	0/10 (0)	0/5 (0)
MT2-ConJt-Maryland method	0/40 (0)	0/20 (0)	0/10 (0)	0/5 (0)
M28-ConJt-Taper-1	0/40 (0)	0/20 (0)	0/10 (0)	0/5 (0)
M28-ConJt-Taper-2	0/40 (0)	0/20 (0)	0/10 (0)	0/5 (0)
MT1-EchJt-1	0/40 (0)	0/20 (0)	1/10 (10)	0/5 (0)
MT1-EchJt-2	0/40 (0)	0/20 (0)	0/10 (0)	1/5 (20)
US31-EchJt	0/40 (0)	0/20 (0)	0/10 (0)	0/5 (0)

Notes: #Fraction showing the sections that have PWL lower than the RQL (60%) over the total subsections. *Percentage of sections with PWL lower than the acceptance limit.

Chapter 5: Conclusions and Recommendations

5.1 Major Research Findings and Advantages

This research enhances the current understanding of best practices for longitudinal joint construction, quality evaluations, and repair and maintenance. The results from this research helped advance the construction of long-lasting longitudinal joints, improved construction specifications and methodologies, provided guidance regarding selecting appropriate joint types, enhanced understanding of the joint's performance, and facilitated the improvement of construction specification for longitudinal joints. Considering the mentioned benefits, the essential findings and advantages of the study can be summarized as follows:

- An unconfined joint can produce poor compaction if a butt joint is constructed.
- Utmost effort should be made to avoid constructing an unconfined joint. Avoiding unconfined joint construction becomes difficult when building a new asphalt pavement. However, it can be avoided by using a taper joint or by providing a provision in the contract for cutting back the edge material by at least 6 in (150 mm) but still paid for by the agency. In addition, using an edge restraint technique (such as a safety edge, taper forming attachment, etc.) can also help offset the issues related to unconfined joint construction.
- Both the butt and the taper joint geometry can produce good compaction at the joint.
- The study results propose using the sequential mill and fill technique where appropriate.
- Echelon paving displayed the best compaction results by altogether avoiding the construction of a longitudinal centerline joint.
- A hot overlap method is proposed for rolling an unconfined joint as part of a new asphalt pavement construction. At the same time, this study suggests using the Maryland Method for rolling all confined joints.
- Based on the DPS's continuous coverage capability, its use is recommended for evaluating the joint quality instead of cores that provide limited coverage. The ability of the DPS to evaluate in-field compaction just about 500 ft (152 m) behind the finished roller makes it an excellent tool for QA of the longitudinal joints. It can also highlight compaction issues during construction which, once related to the field operations, can be used to alter them, resulting in better compaction at the joint.
- A dielectric difference of 0.2 between the joint and its corresponding mat (mat minus joint) is proposed as a reasonable measure to evaluate joint compaction. The agency can determine the minimum specified mat and joint dielectric values by calibrating the air void and dielectric relationship for the asphalt mix.
- The proposed index can determine the acceptability of a longitudinal joint, correcting for the level of compaction achieved at the mat. An LJQI of 60% is proposed to accept a joint without penalty to the contractor.

5.2 Research Implementation Benefits

The implementation benefits of this research include:

5.2.1 Construction, Operations, Maintenance, and Lifecycle Savings

Consider a scenario that involves implementing the proposed approach from this study for constructing the centerline longitudinal joint between two lanes of a 10 mi (16 km) long asphalt pavement. The proposed joint is compared to a joint made using conventional practices based on Table 2.2 for cost comparisons and longitudinal joint repair techniques. Table 5.1 shows the estimated potential savings in 10 years resulting from achieving a better density at the longitudinal joint. The saving estimations assume that the pavement remains in service for 10 years without exhibiting other distress. However, the treatments in the table only apply to joints with medium to severe deterioration. A poorly compacted joint would quickly deteriorate from low to high levels even if maintained using low-cost preventive treatments like chip seals, fog seals, or sealants. In addition to cost savings from using the proposed approach for joint construction, adopting DPS for the evaluation of longitudinal joints would save costs incurred on core extraction, core testing, and related workforce costs.

Table 5.1 Estimated longitudinal joint repair cost savings

Treatment	Life (years)	Cost (per mile)	Cost (for 10 miles)	Number of repair cycles within 10 years	Total cost
Crack sealing	4.5	$3,362	$33,362	2.22	$74,064
Spray injection	2.2	$12,763	$127,630	4.50	$574,335
Slot paving	4.3	$104,644	$1,046,440	2.33	$2,438,205

5.2.2 Reduced Road User Costs and Risks

Table 5.1 refers to cost savings related to the treatments only. However, implementing the research findings from this study will reduce the maintenance and repair cycles. The reduced maintenance and repair cycles would save vehicle operating costs (VOC), user delays, and workforce/labor costs. Thus, the lifecycle costs of flexible pavements would also be reduced further. In addition, better-performing longitudinal joints with reduced maintenance activities will curb traffic congestion and improve the local road infrastructure's level of service (LOS). It will also improve road safety for motorists and motorcyclists.

5.2.3 Environmental Benefits

Improved longitudinal joint performance would eventually lead to longer-lasting pavement infrastructure. Reduced pavement maintenance, repair, and reconstruction activities would reduce the need for construction materials, benefiting the environment. Improved LOS of the infrastructure will reduce traffic congestion, leading to low fuel consumption. In addition, fuel will be conserved due to lesser construction activities. Adopting the non-destructive DPS technology for joint quality evaluation will help reduce or eliminate the need for coring and reduce asphaltic waste.

5.2.4 Technological Benefits

As mentioned above, cores have limited coverage, while the ground penetration radar (GPR) based DPS ensures continuous coverage of the longitudinal joint throughout its length. Thus, adopting DPS benefits technological innovations will improve the QA process for longitudinal joints.

5.3 Recommendations

Based on the work accomplished in this study, the research recommends:

5.3.1 Best Practices for Longitudinal Joint Construction and How to Repair Existing Failed Centerline Construction Joints

Although most agencies do not specify the type and technique of longitudinal joint construction, the following longitudinal joint construction methods are recommended:

- The sequential mill and fill technique can help produce longitudinal joints with better compaction, avoiding constructing an unconfined joint. However, such a technique can only be employed during mill and fill projects. The sequential mill and fill technique involves milling and filling one lane at a time rather than milling all lanes at once, followed by asphalt laying lane-wise (see Figure 5.1). Thus, using the sequential mill and fill technique eliminates the construction of an unconfined joint. In the sequential mill and fill technique, thoroughly cleaning the milled surface and the confined edge of the newly laid mat is required before laying fresh asphalt material.

Figure 5.1 Sequential mill and fill technique

- For constructing an unconfined joint for a new HMA pavement, as shown in Figure 3.1, using an edge restraint attachment (such as a safety edge or taper joint constructing attachment) can improve the joint's compaction. Figure 5.2 shows the construction of a tapered, unconfined longitudinal joint that resulted in similar compaction as the mat.

Figure 5.2 Using an attachment for constructing a tapered unconfined joint at the M-28 project, MI

- Another way to get better compaction at an unconfined joint is to specify a minimum of 6 in (150 mm) to be cut back by the contractor from the unconfined edge before laying the adjacent lane. Such practice does not require the use of any additional paver/roller attachments as described earlier. The data analyses conducted in this research showed that similar compaction was achieved at the mat and the joint constructed using this technique on the I-496 project in Michigan (see Figure 5.3).

Figure 5.3 Constructing an unconfined joint with cutting back technique at I-496 project, MI

- Echelon paving displayed the best compaction results and is recommended for use (where possible) while constructing a new asphalt pavement to avoid the construction of a centerline joint.
- Whatever technique is used, it is crucial to pave the joint's edge as straight as possible during construction. Figure 5.3 shows an example of asphalt material laid with the joint's edge paved perfectly straight. A straight edge aids in better joint compaction once the adjacent lanes are being constructed.
- The survey results and literature show that applying a bond/tack coat or some proprietary material on the vertical face and bottom of the adjacent joints benefits its quality and helps in sealing. Thus, this study recommends the application of a bond/tack coat for longitudinal joint construction.

The asphalt material's compaction requires the use of steel drum rollers and pneumatic tire rollers. Several rolling patterns are employed during the construction of the longitudinal joint; however, this study recommends the following:

- The hot pinch method is recommended while constructing a confined longitudinal joint. In this rolling method, the drum of the breakdown roller completely sits on the hot asphalt material (i.e., the hot side of the joint), keeping the drum's edge at least 6 inches away from the joint (see Figure 5.4). The roller is operated in vibratory mode and helps push hot asphalt material toward the joint.

Figure 5.4 Hot pinch rolling method used on the I-496 project, MI, for constructing the confined joint

- The Maryland method is recommended for rolling and compaction of all confined joints. As mentioned earlier, the method involves the following three steps:

    1. Overlap the existing adjoining mat's edge (constructed previously) by 1 to 1.5 in (25 to 38.1 mm) with the hot asphalt material while paving. Bump back any HMA material exceeding 1.5 in (38.1 mm).
    2. Compact the hot asphalt material by keeping the roller 6 to 12 in (150 to 300 mm) away from the longitudinal joint. Such compaction locks and consolidates the hot asphalt material and pushes additional material into the joint.
    3. Finally, compact the overlapped and the pushed hot HMA material into the confined space employing the maximum vibratory force of the roller resulting in optimum joint density. The appearance of a thin white line on the top of the longitudinal joint indicates the successful application and completion of the Maryland Method, as seen in Figure 5.5. A video clip showing the use of the Maryland Method for the construction of confined longitudinal joints can be found at https://mdasphalt.org/2019/best-practices-maryland-method-longitudinal-joint-compaction/.

Figure 5.5 Appearance of a thin white line over the confined joint using the Maryland method at the Manning Trail project, MN

- An unconfined longitudinal joint is recommended to be rolled with the drum overhanging at least 6 inches over the edge. The roller should be used in vibratory mode.

As far as the joint geometry is concerned, the results from this study suggest that any joint geometry, i.e., a butt joint or a tapered longitudinal joint, can result in better compaction if a traditional unconfined joint construction is avoided. The vertical or butt joint is the most used conventional joint type in asphalt pavement construction. The butt joint "butts" the hot material from the second pass (i.e., the second lane being laid) to the cold material's edge from the first pass (i.e., the lane laid earlier or a night before), thus having a vertical interface between the two lanes (see Figure 5.6). The tapered or wedge joint is simply a sloped edge joint that tapers down continuously to the surface. The tapered

joint investigated in this study has a notch at the top [generally 1 in (25 mm)] only and a 12:1 taper as shown in Figure 5.2 and schematically in Figure 5.6.

(a) Butt joint **(b) Tapered joint**

Figure 5.6 Schematic of butt and tapered joints.

The literature suggests that crack sealing and micro surfacing should be used for longitudinal joint maintenance and repair based on the crack condition. These are cost-effective alternatives compared to the other options, as shown in Table 5.2. Spray injection treatment should be used if the joint deterioration is medium to severe. Slot paving should be the last resort since it is the most expensive alternative. A brief description of each of these techniques is given below:

Table 5.2 Longitudinal joint repair techniques cost comparisons (63)

Treatment	Life (years)	Cost (per mile)	Cost (per mile per year)
Crack sealing	4.5	$3,362	$747
Spray injection	2.2	$12,763	$5,801
Slot paving	4.3	$104,644	$24,294

- **Crack sealing** is a commonly used treatment that fills the distressed longitudinal joint and prevents the ingress of moisture, debris, and air into the crack. It involves the injection of bituminous materials into the crack to impede the rate of moisture infiltration into it. It is one of the most cost-effective treatments for low- to medium-level distressed longitudinal joints. It is also used as a preventive maintenance technique by MnDOT.
- **Spray injection** is a suitable treatment for medium to high-severity distress levels on joints. It substitutes the traditional pothole patching process. It involves cleaning the pothole using air to remove debris or water, applying emulsified asphalt, mixing the aggregate chips with emulsified asphalt, and filling the repair area with the aggregate-asphalt blend using compressed air. Spray injection is considered a corrective repair; however, it can work as a preventive maintenance treatment if used timely.
- **Slot paving** has been successfully used as a longitudinal joint repair technique to repair medium and high-severity joint distresses. The slot paving involves milling a narrow pavement width around a distressed and deteriorated longitudinal joint, cleaning the slotted area, applying tack to the sides and bottom of the excavated area, and then repaving with HMA. The width of the slot varies, while a successful slot construction requires that each inch of slot depth is

accompanied by at least one foot of slot width. However, slot paving results in two joints instead of one to maintain, and the joints get closer to the wheel path.

5.3.2 Evaluation of Joint Quality During Construction

The survey results showed that most agencies do not monitor the joint quality (in terms of density), which is a weak link even on well-constructed and good-performing pavements. Additional resources and time may be required (such as equipment and workforce). Another reason for not monitoring the joint density can be the destructive nature of pavement coring, which is the most common option used by agencies that monitor density at the joints. Although simple, coring has limited coverage with a high chance of missing localized problematic areas. Quality acceptance programs rely on random coring measuring less than 1% of the total asphalt mixtures produced and laid (73). It also has a longer turnaround time for the results, not practical to provide real-time feedback about the compaction operation during construction. Thus, using portable equipment such as DPS can help reduce the need for coring and offset its adverse effects on pavements in the long run. Also, continuous coverage by the DPS gives the equivalent of about 100,000 cores per mile, aiding better monitoring and evaluation of the joint's quality (9).

The results from this study recommend using field-measured dielectric data using DPS to evaluate the joint's quality during construction. Using the DPS for joint quality evaluation during construction is explained as follows:

- Perform the air void and dielectric relationship calibration for the asphalt mix being laid. This study shows that after calibrating the mix's air void to its dielectric relationship, one can obtain a suitable mat dielectric value based on the calibration and minimum acceptable mat air voids.
- This study recommends using a relative mat and joint dielectric difference of 0.2 to monitor joint quality during construction using DPS. A dielectric difference greater than 0.2 would indicate compaction issues at the joint. However, the agency can use any other number for the dielectric difference between the mat and the joint.
- Using the calibrated model, any joint dielectric values lower than the decided mat value and having a relative dielectric difference between the mat and the joint (mat minus joint) higher than 0.2 dielectrics would indicate compaction issues at the joint.
- Determining a suitable minimum mat dielectric value will ensure that the contractor is not penalized by rejecting a joint with an acceptable density that could occur due to excellent mat compaction.
- Suppose a relative dielectric difference of greater than 0.2 is observed between the joint and the corresponding mat (using the specified mat dielectric value) during construction. In this case, the construction operation should be monitored for possible causes and corrected before further paving operations resume.

5.3.3 Use of DPS for Joint Evaluation and its Comparison with Traditional Procedures

As mentioned earlier, the DPS can provide continuous coverage of the asphalt pavement and better determine the density of the compacted mat and joints compared to the destructive and limited coverage by coring. Different approaches can be used to assess the quality of the joint in comparison with the mat using dielectric data collected by DPS:

- The DPS data can be divided into suitable section lengths, and statistical analysis (such as paired *t*-test) can determine the percentage of sections having compaction differences with greater than 2% air voids between the joint and the corresponding mat.
- The DPS data can be used to determine PWL for each subsection. Thus, DPS data enables PWL calculation for measurements taken every 6 in (150 mm) instead of its calculation based on two cores collected in one lot per day (or two lots if the daily asphalt material is more than 5000 tons).
- By employing the proposed index in this study, the percentage of acceptable compaction can be determined using the DPS data, which is not otherwise possible using limited cores. The proposed index also corrects for good mat density and will not reject a joint merely based on the difference between the joint and the mat.
- The DPS data is also capable of locally isolating areas with compaction issues. It is an important capability that cannot be achieved using cores. The contractor can be asked to repair or re-construct the isolated areas with higher air voids.
- Additionally, one can maintain localized areas with compaction issues more frequently than normal if their air voids are insufficient to warrant reconstruction (per specification).

In addition, monitoring the performance of the longitudinal joints evaluated in this study for the next five years will be beneficial to validate the findings from DPS testing.

5.3.4 Construction Specifications for the Potential Use of DPS in Quality Assurance

Testing with a DPS should be included in the construction specifications of the longitudinal joint in addition to the best practices mentioned earlier. The specifications for the use of DPS may consist of the following:

- The DPS testing should begin once a 500-ft (152 m) section is ready behind the finish roller.
- The DPS measurements should be taken with a side sensor at a 6-in (150-mm) offset from the joint. The center sensor should be positioned at a 2- or 2.5-ft (0.6- or 0.8-m) offset, while the other side's sensor be adjusted at a 3.5- or 4.5-ft (1.1- or 1.4-m) offset from the centerline joint to measure the mat dielectric values.
- Once a calibrated dielectric and air void relationship is obtained for the mix, the PWL can be obtained for the dielectric values and their corresponding air voids.

- The PWL would require a minimum acceptable dielectric value related to the maximum specified air voids for the mat and the joint; however, when payment is determined based on the quality delivered by the contractor, payment adjustment factors can be estimated using individual mat and joint PWL.
- The joint density can be evaluated using the proposed LJQI by determining the minimum acceptable dielectric values for the mat, joint, and their difference. This study suggests using minimum dielectric values of 5.0 and 4.8 for the mat and joint, respectively, along with a dielectric difference of 0.2. The LJQI should only be used as a pass/fail criterion for accepting a joint in cases where the air void vs. the dielectric relationship cannot be calibrated due to logistic/capacity issues.
- This study suggests a minimum LJQI value of 60% for accepting a centerline longitudinal joint without penalty. However, the acceptable index level can be determined per the agency's requirements.

References

1. Estakhri, C. K., Freeman, T. J., & Spiegelman, C. H. (2001). *Density evaluation of the longitudinal construction joint of hot-mix asphalt pavements* (No. FHWA/TX-01/1757-1). Texas Transportation Institute, Texas A & M University System, College Station, TX.

2. Buncher, M. S., & Rosenberger, C. (2012). *Best practices for constructing and specifying HMA longitudinal joints*. *Asphalt Institute: Lexington, KY, USA*.

3. Aschenbrener, T., Brown, E. R., Tran, N., & Blankenship, P. B. (2018). The FHWA's demonstration project for enhanced durability of asphalt pavements through increased in-place pavement density. *Transportation Research Record*, *2672*(26), 57-67.

4. Tran, N., Turner, P., & Shambley, J. (2016). Enhanced compaction to improve durability and extend pavement service life: A literature review. *National Center of Asphalt Technology at Auburn University, Auburn, AL.*

5. Linden, R. N., Mahoney, J. P., & Jackson, N. C. (1989) Effect of compaction on asphalt concrete performance. *Transportation Research Record*, 1217, 20-28.

6. Kim Willoughby, P. E., Olympia, W., Mahoney, J. P., & Walter, J. (2007). *An assessment of WSDOT's hot-mix asphalt quality control and assurance requirements*. Washington State Transportation Center (TRAC), University of Washington, Seattle, WA.

7. Sebaaly, P. E., & Barrantes, J. C. (2004). Development of a joint density specification: Phase I-literature review and test plan. *Nevada Dept. of Transportation, Carson City, NV.*

8. Hughes, C. S. (1989). *Compaction of asphalt pavement*. National Research Council, Transportation Research Board, Washington, DC.

9. Hoegh, K., Steiner, T., Zegeye Teshale, E., & Dai, S. (2020). Minnesota Department of Transportation case studies for coreless asphalt pavement compaction assessment. *Transportation Research Record*, *2674*(2), 291-301.

10. Foster, C.R., Hudson, S. B., & Nelson, R. S. (1964). Constructing longitudinal joints in hot mix asphalt pavements. *Highway Research Record*, *51,* 124-136.

11. McDaniel, R. S., Shah, A., & Olek, J. (2012). *Longitudinal joint specifications and performance* (FHWA-IN-JTRP-2012-29). Joint Transportation Research Program, Indiana Dept. of Transportation and Purdue University, West Lafayette, IN.

12. Zinke, S., Mahoney, J., Jackson, E., & Shaffer, G. (2008). *Comparison of the use of notched wedge joints vs. traditional butt joints in Connecticut* (No. CT-2249-F-08-4). Connecticut Transportation Institute, University of Connecticut, Storrs, CT.

13. Buchanan, M. S. (2000). Evaluation of notched-wedge longitudinal joint construction. *Transportation Research Record*, *1712*(1), 50-57.

14. McDaniel, R. S., Shah, A., & Olek, J. (2012). *Longitudinal joint specifications and performance* (Joint Transportation Research Program Publication No. FHWA/IN/JTRP-2012/29). Purdue University, West Lafayette, IN.

15. Kandhal, P. S., & Mallick, R. B. (1997). *Longitudinal joint construction techniques for asphalt pavements* (NCAT Report 97-4). National Center for Asphalt Technology, Auburn University, AL.

16. Williams, S. G. (2011). *HMA longitudinal joint evaluation and construction* (No. TRC-0801). University of Arkansas, Dept. of Civil Engineering, Fayetteville, AR.

17. Putman, B. J., & Kim, E. M. Y. (2018). *Best practices for longitudinal joint construction and compaction* (No. FHWA-SC-18-06). South Carolina Dept. of Transportation, Columbia, SC.

18. Burati Jr, J. L., & Elzoghbi, G. B. (1987). Study of joint densities in bituminous airport pavements. *Transportation Research Record*, 1126, 76-85.

19. Toepel, A. (2003). *Evaluation of techniques for asphaltic pavement longitudinal joint construction*. Wisconsin Department of Transportation, Division of Transportation, Madison, WI.

20. Crawford, C., & Scherocman, J. A. (1990). Hot mix asphalt joint construction (No. QIP 115). National Asphalt Pavement Association**.**

21. Kandhal, P. S., & Rao, S. S. (1994). *Evaluation of longitudinal joint construction techniques for asphalt pavements* (Michigan and Wisconsin projects-interim report, *NCAT Report*, pp. 94-1). *National Center of Asphalt Technology at Auburn University, Auburn, AL.*

22. Fleckenstein, L. J., Allen, D. L., & Schultz, D. B. (2002). *Compaction at the longitudinal construction joint in asphalt pavements* (Report No. KTC-02-10/SPR-208-00-1F). Kentucky Transportation Center, University of Kentucky, Lexington, KY**.**

23. Williams, R. C., Podolsky, J., & Kamau. J. (2020). *Use of J-band to improve the performance of the HMA longitudinal joint* (No. MN 2020-33). Minnesota Department of Transportation, Saint Paul, MN.

24. OHMPA. (2013). *The ABCs of longitudinal joints*. Ontario Hot Mix Producers Association, Ontario, Canada.

25. Uzarowski, L., Moore, G., Halloran, M., & Henderson, V. (2009). Construction of durable longitudinal joints—the courage to use innovations pays off. In 2009 Annual Conference and Exhibition of the Transportation Association of Canada -Transportation in a Climate of Change, Vancouver, British Columbia, October, 18-21.

26. Nener-Plante, D. (2012). *Longitudinal pavement joint performance: A field study of infrared heated and notched wedge joint construction* (No. 43076). Maine. Dept. of Transportation, Augusta, ME.

27. Mallick, R. B., Kandhal, P. S., Ahlrich, R., & Parker, S. (2007). *Project 04-05: Improved performance of longitudinal joints on asphalt airfield*, Airfield Asphalt Pavement Technology Program (AAPTP). Auburn University, Auburn, AL**.**

28. Transportation Research Board. (2006). *Factors affecting compaction of asphalt pavements* (Transportation Research Circular Number E-C105). Transportation Research Board, Washington, D.C.

29. Williams, R. C., Chen, C., Ahmed, T., & Lee, H. (2013). *Quality control/quality assurance testing for joint density and segregation of asphalt mixtures.* Iowa. Dept. of Transportation, Ames, IA.

30. Marquis, B. (2001). *Longitudinal joint study*/ Maine. Dept. of Transportation, Augusta, ME.

31. Uzarowski, L., Moore, G., Halloran, M., & Henderson, V. (2009). Construction of durable longitudinal joints—The courage to use innovations pays off. In 2009 Annual Conference and Exhibition of the Transportation Association of Canada -Transportation in a Climate of Change, Vancouver, British Columbia, October, 18-21.

32. Hand, A. J., Aschenbrener, T., & Buncher, M. (2020). *Tech brief: Improving longitudinal joint performance* (FHWA-HIF-21-023). Federal Highway Administration, Washington, DC.

33. Kassem, E., Masad, E., Chowdhury, A., & Claros, G. (2008). Influence of field compaction pattern on asphalt pavement uniformity (with discussion). *Journal of the Association of Asphalt Paving Technologists*, vol. 77, 257-298.

34. Marks, P. (2004). Longitudinal joint compaction–improving paved lanes. *RoadTalk, Ontario's Transportation Technology Transfer Digest*, *10*(2)

35. Baker, R. F., Croteau, J. R., Quinn, J. J., & Hellriegel, E. J. (1990). Longitudinal wedge joint study. *Transportation Research Record*, 1282, 18-26.

36. Huang, B., Shu, X., Chen, J., & Woods, M. (2010). Evaluation of longitudinal joint construction techniques for asphalt pavements in Tennessee. *Journal of Materials in Civil Engineering*, *22*(11)*,* 1112-1121.

37. Daniel, J. S. (2006). Use of an infrared joint heater to improve longitudinal joint performance in hot mix asphalt pavements. *Journal of Performance of Constructed Facilities*, *20*(2)*,* 167-175.

38. Kandhal, P. S., & Mallick, R. B. (1996). Study of longitudinal-joint construction techniques in hot-mix asphalt pavements. *Transportation Research Record*, *1543*(1)*,* 106-112.

39. Seeds, S. B., Hicks, G. R., Elkins, G. E., Zhou, H., & Scholz, T. V. (2002). *LTTP data analysis: Significance of 'as-constructed' AC air voids to pavement performance* (NCHRP Project 20-50(14)). *Applied Pavement Technology, Inc.,* Urbana, IL.

40. Kandhal, P. S., & Mallick, R. B. (1997). *Longitudinal joint construction techniques for asphalt pavements* (NCAT Report No. 97-4)*.* National Center for Asphalt Technology, Auburn University, AL.

41. Kandhal, P. S., Ramirez, T. L., & Ingram, P. M. (2002). Evaluation of eight longitudinal joint construction techniques for asphalt pavements in Pennsylvania. *Transportation Research Record*, *1813*(1)*,* 87-94.

42. Khazanovich, L., Hoegh, K. & Conway, R. (2017). Non-destructive evaluation of bituminous compaction uniformity using rolling density. *SHRP2 Solutions*.

43. Wilson, B., Sebesta, S., & Scullion, T. (2019). Evaluation of the rolling density meter for rapid continuous measurement of asphalt mixture density (No. FHWA/TX-17/0-6889-R1). Texas A&M Transportation Institute, Austin, TX.

44. Prowell, B. D. (2007). Practices and specifications for longitudinal joint — a national perspective. Presentation at the Greater Iowa Asphalt Conference.

45. Smith, B. C., & Diefenderfer, B. K. (2008). Comparison of nuclear and nonnuclear pavement density testing devices. *Transportation Research Record*, *2081*(1), 121-129.

46. TransTech System. (2002). *Model, P. Q. I., 301 operator's handbook*. TransTech Systems, Inc., Schenectady, NY.

47. Henault, J. W. (2001). Field evaluation of a non-nuclear density pavement quality indicator (No. FHWA-CT-RD-2227-F-01-3). *Connecticut. Dept. of Transportation, Newington, CT.*

48. du Tertre, A., Cascante, G., & Tighe, S. L. (2010). Combining portable falling weight deflectometer and surface wave measurements for evaluation of longitudinal joints in asphalt pavements. *Transportation Research Record*, *2152*(1)*,* 28-36.

49. Al-Qadi, I. L., Ghodgaonkar, D. K., Varada, V. K., & Varadan, V. V. (1991). Effect of moisture on asphaltic concrete at microwave frequencies. *IEEE Transactions on Geoscience and Remote Sensing*, *29*(5)*,* 710-717.

50. Al-Qadi, I. L., Lahouar, S., & Loulizi, A. (2001). In situ measurements of hot-mix asphalt dielectric properties. *NDT & e International*, *34*(6)*,* 427-434.

51. Al-Qadi, I. L., & Lahouar, S. (2005). Measuring layer thicknesses with GPR–theory to practice *Construction and Building Materials*, *19*(10)*,* 763-772.

52. Leng, Z., Al-Qadi, I. L., & Lahouar, S. (2011). Development and validation for in situ asphalt mixture density prediction models. *NDT & e International*, *44*(4)*,* 369-375.

53. Leng, Z. (2012). *Prediction of in-situ asphalt mixture density using ground penetrating radar: theoretical development and field verification.* University of Illinois at Urbana-Champaign, IL.

54. Shangguan, P., & Al-Qadi, I. L. (2014). Calibration of FDTD simulation of GPR signal for asphalt pavement compaction monitoring. *IEEE Transactions on Geoscience and Remote Sensing*, *53*(3)*,* 1538-1548.

55. Shangguan, P., & Al-Qadi, I. L. (2014). Content-based image retrieval approaches to interpret ground penetrating radar data. *Construction and Building Materials*, *69,* 10-17.

56. Scullion, T., & Chen, Y. (1999). Using ground-penetrating radar for real-time quality control measurements on new HMA surfaces. Texas Department of Transportation, Austin, TX.

57. Saarenketo, T., & Scullion, T. (2000). Road evaluation with ground penetrating radar. *Journal of Applied Geophysics*, *43*(2-4), 119-138.

58. Al-Qadi, I. L., Leng, Z., Lahouar, S., & Baek, J. (2010). In-place hot-mix asphalt density estimation using ground-penetrating radar. *Transportation Research Record*, *2152*(1)*,* 19-27.

59. Sebesta, S., Scullion, T., & Saarenketo, T. (2013). *Using infrared and high-speed ground-penetrating radar for uniformity measurements on new HMA layers*. Transportation Research Board, Washington, D.C.

60. Hoegh, K., Dai, S., Steiner, T., & Khazanovich, L. (2018). Enhanced model for continuous dielectric-based asphalt compaction evaluation. *Transportation Research Record*, *2672(26)*, 144-154.

61. Teshale, E. Z., Hoegh, K., Dai, S., Turgeon, C., & Giessel, R. (2020). Ground penetrating radar sensitivity to marginal changes in asphalt mixture composition. *Journal of Testing and Evaluation*, *48(3),* 2295-2310.

62. Hoegh, K., Roberts, R., Dai, S., & Zegeye Teshale, E. (2019). Toward core-free pavement compaction evaluation: An innovative method relating asphalt permittivity to density. *Geosciences*, *9*(7)*,* 280.

63. Duncan, G. M., Sibaja, L. V., Seeds, S. B., Peshkin, D. G., Sminchak, M., & Sophocleous, S. (2017). *Longitudinal joint repair best practices for the Ohio Department of Transportation* (No. FHWA/OH-2017-39). Ohio. Dept. of Transportation, Columbus, OH.

64. Johnson, A. M. (2000). *Best practices handbook on asphalt pavement maintenance*. University of Minnesota Center for Transportation Studies, Minneapolis, MN.

65. Watson, M. (2011). *Improving HMA longitudinal joints through construction preventive maintenance and repairs*. Minnesota Department of Transportation, Saint Paul, MN.

66. Watson, M. (2009). *Longitudinal joint fog seal test sections.* Minnesota Department of Transportation, Saint Paul, MN.

67. MDOT. (2020). *Capital preventive maintenance manual*. Michigan. Dept. of Transportation, Construction Field Services Division, Lansing**,** MI.

68. Zinke, S., & Mahoney, J. (2015). *Evaluation of longitudinal joint density specification on 2012 polymer-modified warm-mix asphalt projects in Connecticut* (No. CT-2280-F-14-6). Connecticut. Dept. of Transportation, Newington**,** CT.

69. NRRA Flexible Team. (2018). Longitudinal joint construction. *National Road Research Alliance*, (*19 pages).*

70. Buncher, M. S., & Rosenberger, C. (2012). *Best practices for constructing and specifying HMA longitudinal joints.* Asphalt Institute, Lexington, KY.

71. AASHTO. (2017). *Bulk specific gravity and density of compacted hot mix asphalt using automatic vacuum sealing method* (AASHTO T331). AASHTO, Washington, DC.

72. AASHTO. (2017). *Bulk specific gravity of compacted bituminous mixtures using saturated surface-dry specimens* (AASHTO T166). AASHTO, Washington, DC.

73. Steiner, T., Hoegh, K., Teshale, E. Z., & Dai, S. (2020). Method for assessment of modeling quality for asphalt dielectric constant to density calibration. *Journal of Transportation Engineering, Part B: Pavements*, *146(3),* 04020054.

74. Dolan, K. D., & Mishra, D. K. (2013). Parameter estimation in food science. *Annual Review of Food Science and Technology*, *4,* 401-422.

75. Beck, J. V., & Arnold, K. J. (1977). *Parameter estimation in engineering and science*. James Beck, New York, NY.

76. Geeraerd, A. H., Valdramidis, V. P., & Van Impe, J. F. (2005). GInaFiT, a freeware tool to assess non-log-linear microbial survivor curves. *International Journal of Food Microbiology*, *102(1),* 95-105.

77. Dolan, K. D. (2003). Estimation of kinetic parameters for nonisothermal food processes. *Journal of Food Science*, *68(3),* 728-741.

Appendix A
Core and Puck Dielectric and Air Voids Data

Table A-1 Puck and core dielectric and air voids data – M-89 project, MI

Puck			Cores		
Puck ID	Dielectric	Air voids, %	Core ID	Dielectric	Air voids, %
M89-1-1	4.676	11.7	M89C1	5.8	7.24
M89-1-2	4.736	10.9	M89C2	5.09	8.31
M89-1-3	5.059	8.2	M89C3	4.96	6.85
M89-1-4	5.262	5.3	M89C5	5.69	4.66
M89-1-5	5.097	8	M89C6	4.86	5.5
M89-2-1	5.213	5.8	M89C7	5.46	7.56
M89-2-2	4.728	10.6	M89C9	5.76	3.96
M89-2-3	5.107	7.5	M89C10	5.79	4.73
M89-2-4	5.382	3.8	M89C11	4.89	6.85
M89-2-5	5.073	8.4	M89C12	5.49	4.82
No data.			M89C13	5.32	4.91
			M89C14	5.49	4.25
			M89C15	4.97	6.59

Table A-2 Puck and core dielectric and air voids data – US-31 project, MI

Puck			Cores		
Puck ID	Dielectric	Air voids, %	Core ID	Dielectric	Air voids, %
US31-1	5.115	US31-1	5.115	US31-1	5.115
US31-2	4.884	US31-2	4.884	US31-2	4.884
US31-3	5.154	US31-3	5.154	US31-3	5.154
US31-4	4.823	US31-4	4.823	US31-4	4.823
US31-5	4.641	US31-5	4.641	US31-5	4.641
US31-6	4.551	US31-6	4.551	US31-6	4.551
No data.			US31C7	No data.	US31C7
			US31C8		US31C8
			US31C9		US31C9
			US31C10		US31C10

Table A-3 Puck and core dielectric and air voids data – M-25 project, MI

Puck			Cores		
Puck ID	Dielectric	Air voids, %	Core ID	Dielectric	Air voids, %
M25-1-1	5.378	5	M25C1	5.16	8.07
M25-1-2	5.202	8	M25C2	5.11	8.95
M25-1-3	4.784	12	M25C3	5.08	8.77
M25-1-4	5.116	8.5	M25C4	5.08	9.18
M25-1-5	5.321	6	M25C5	5.18	7.27
M25-2-1	5.349	6.4	M25C6	5.73	4.01
M25-2-2	5.258	7.3	M25C7	5.74	4.66
M25-2-3	5.386	5.8	M25C8	5.75	3.7
M25-2-4	4.769	12	M25C9	5.08	9.61
M25-2-5	5.19	8.1	M25C10	5.43	5.99
No data.			M25C11	4.82	10.26
			M25C12	4.81	7.85
			M25C13	5.36	6.76
			M25C14	5.27	7.07
			M25C15	5.34	6.15
			M25C16	5.39	5.9
			M25C17	5.31	8.33
			M25C18	5.91	4.76
			M25C19	5.31	5.53
			M25C20	5.21	5.67
			M25C21	5.99	4.72
			M25C22	5.91	4.19
			M25C23	4.98	9.67
			M25C24	5.09	9.06

Table A-4 Puck and core dielectric and air voids data – M-28 project, MI

Puck			Cores		
Puck ID	Dielectric	Air voids, %	Core ID	Dielectric	Air voids, %
M28-1-1	5.09	7.5	M28C1	4.87	9.05
M28-1-2	5.309	5.2	M28C2	4.97	9.91
M28-1-3	5.083	7.7	M28C3	4.99	9.31
M28-1-4	4.675	11.6	M28C4	5.69	4.59
M28-1-5	5.301	5.5	M28C5	5.4	5.16
M28-2-1	5.017	8.1	M28C6	4.89	9.53
M28-2-2	5.271	5.3	M28C7	5.79	5.19
M28-2-3	4.606	12	M28C8	5.03	8.67
M28-2-4	5.285	5.2	M28C9	5.77	5.2
M28-2-5	5.026	8	M28C10	5.17	6.76

Table A-5 Puck and core dielectric and air voids data – I-496 project, MI

Puck			Cores		
Puck ID	Dielectric	Air voids, %	Core ID	Dielectric	Air voids, %
I496-1	5.057	5	I496C1	4.95	3.32
I496-3	5.067	5.1	I496C2	5.43	4.82
I496-4	4.872	7.6	I496C3	5.5	3.49
I496-5	4.784	8.1	I496C4	5.01	2.89
I496-6	4.392	12.58	I496C5	5.29	3.45
I496-7	4.399	12.06	I496C6	5.29	4.73
No data.			I496C7	5.22	5.62
			I496C8	5.05	4.91
			I496C9	5.15	5.82
			I496C10	5	5.87

Table A-6 Puck and core dielectric and air voids data – US-23 project, MI

Puck			Cores		
Puck ID	Dielectric	Air voids, %	Core ID	Dielectric	Air voids, %
US23-1	5.149	7.4	US23C1	4.46	11.27
US23-2	4.891	9.6	US23C2	4.63	10.69
US23-3	5.459	3.4	US23C3	5.27	7.99
US23-4	5.404	3.6	US23C4	5.24	8.17
US23-5	5.283	5.4	US23C5	4.54	10.46
US23-6	4.733	12.84	US23C6	4.44	10.75
US23-7	4.721	13.42	US23C7	4.56	10.56
No data.			US23C8	4.65	11.6
			US23C9	5.29	6.55
			US23C10	4.61	2.33
			US23C11	4.69	3.55
			US23C12	4.88	9.99
			US23C13	4.98	8.01
			US23C14	4.97	7.94

Table A-7 Puck and core dielectric and air voids data – Manning Trail project, MN

Puck			Cores		
Puck ID	Dielectric	Air voids, %	Core ID	Dielectric	Air voids, %
MT-1	5.047	7.61	No data.		
MT-2	4.672	11.57			
MT-3	4.797	10.85			
MT-4	5.22	5.53			
MT-5	5.05	8.28			
MT-6	5.278	4.61			

Table A-8 Puck and core dielectric and air voids data – Xerxes Road #1 project, MN

Puck			Cores		
Puck ID	Dielectric	Air voids, %	Core ID	Dielectric	Air voids, %
XX1-1	4.908	7.97	XX1-J1	4.47	7.79
XX1-2	5.1	5.38	XX1-J2	4.59	8.23
XX1-3	4.906	8.71	XX1-J3	4.69	8.19
XX1-4	4.597	12.24	XX1-J4	4.71	9.04
XX1-5	5.156	5.21	XX1-J5	4.64	9.13
XX2-6	5.155	5.21	XX1-J6	4.54	7.99
XX2-7	4.572	12.98	XX1-J7	4.71	9.06
XX2-8	5.123	5.65	XX1-J9	4.74	8.26
XX2-9	4.953	8.07	XX1-J10	4.74	8.65
XX2-10	4.896	8.95	XX1-H1	5.55	8.5
No data.			XX1-H2	5.37	7
			XX1-M1	5.02	5.66
			XX1-L1	4.52	6.69
			XX1-L2	4.59	6.86
			XX1-H3	5.39	6.77
			XX1-H4	5.47	6.17
			XX1-M2	4.95	7.23
			XX1-L3	4.42	7.01

Appendix B
DPS Data Analysis Plots

Xerxes Road #1 Project

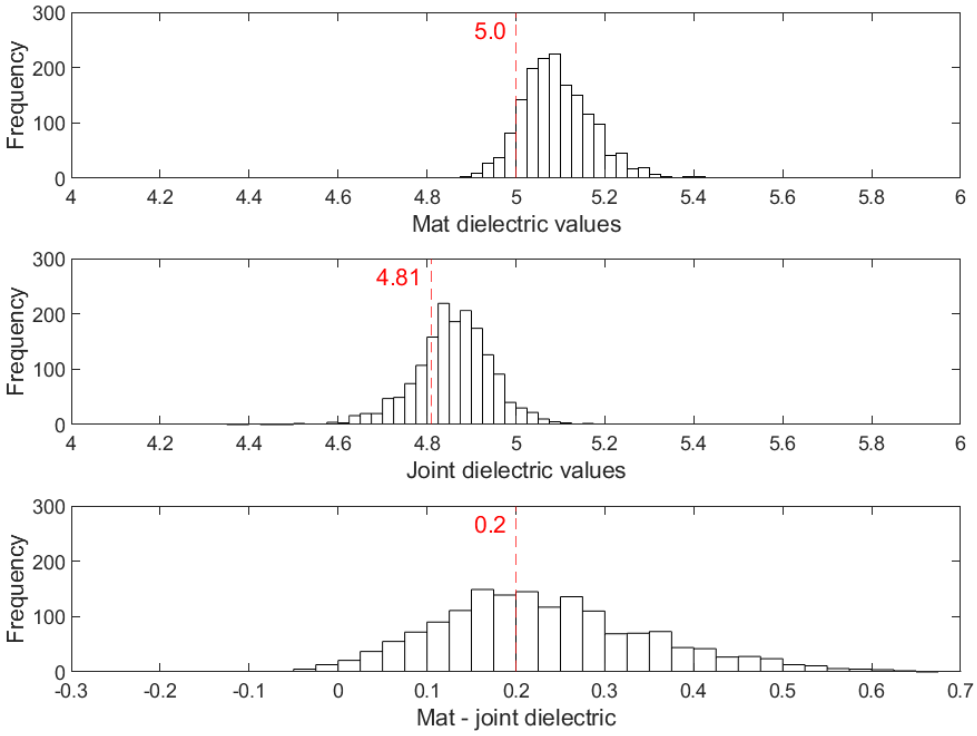

Figure B-1 Histogram of dielectric values for unconfined joint – Xerxes Road #1

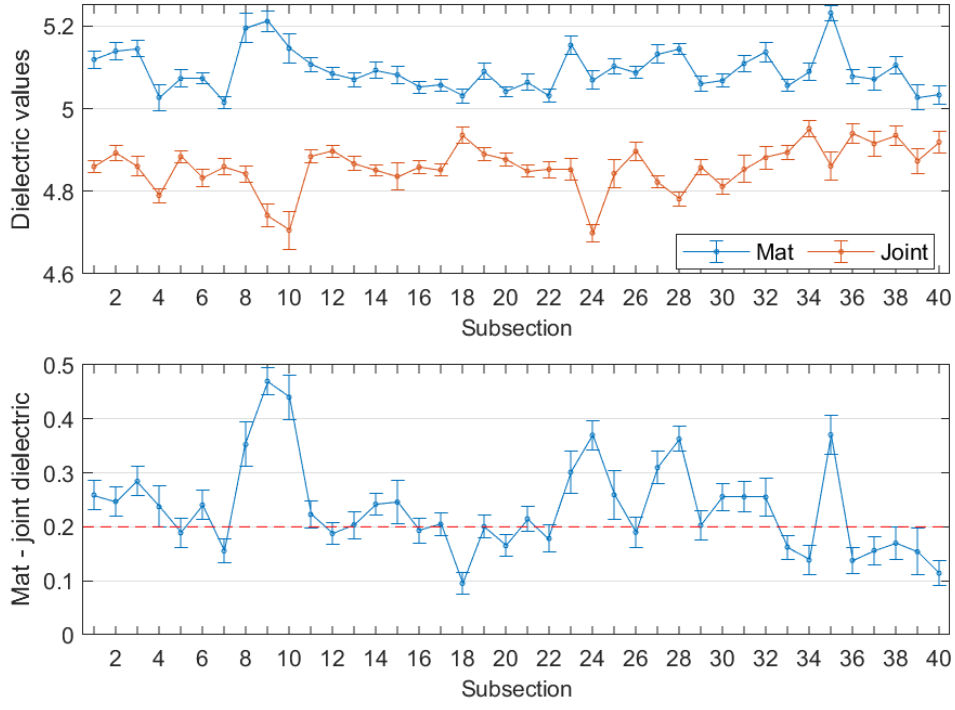

Figure B-2 Interval plot of dielectric values for unconfined joint (25 ft subsections) – Xerxes Road #1

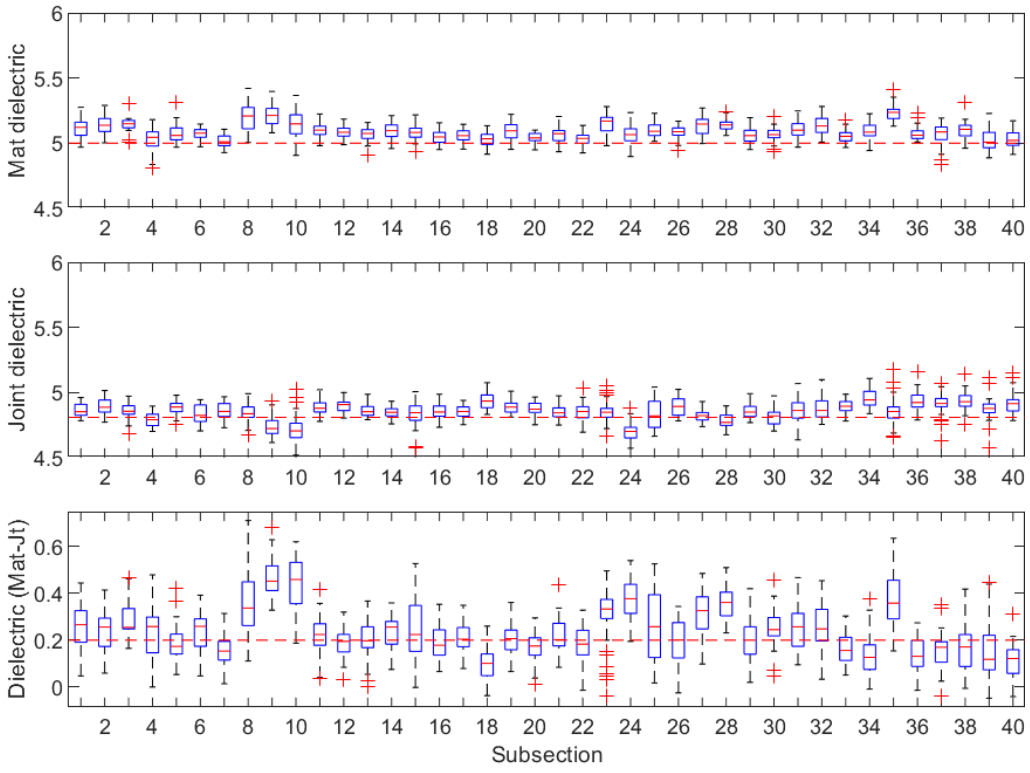

Figure B-3 Box plot of dielectric values for unconfined joint (25 ft subsections) – Xerxes Road #1

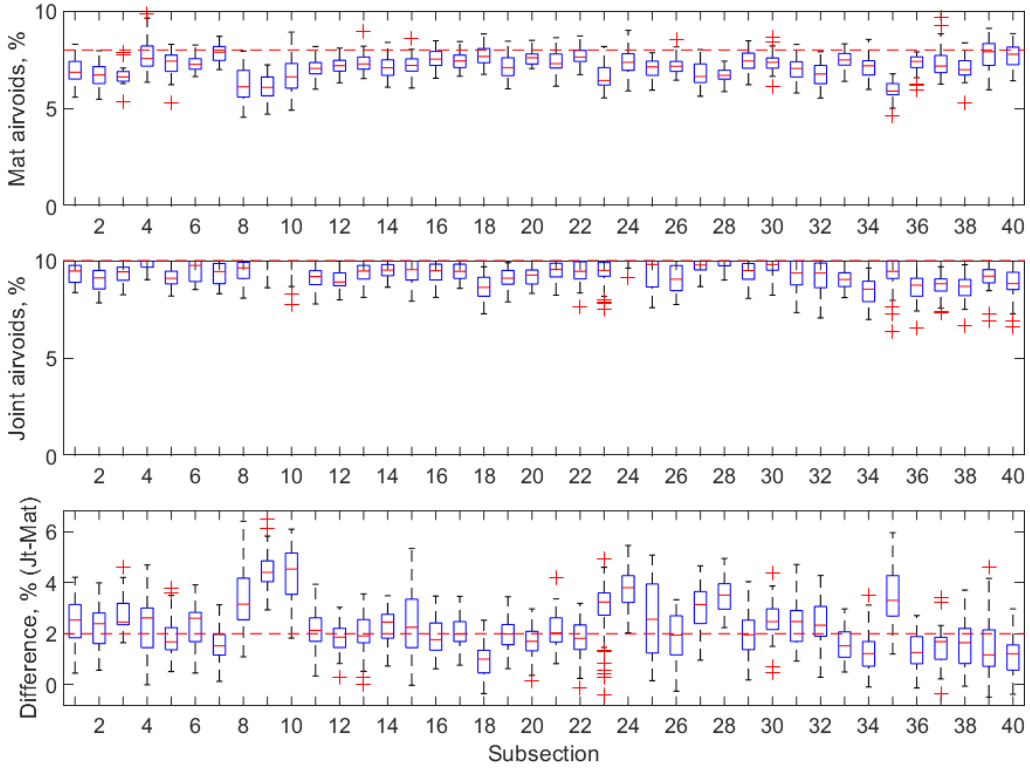

Figure B-4 Box plot of air voids for unconfined joint (25 ft subsections) – Xerxes Road #1

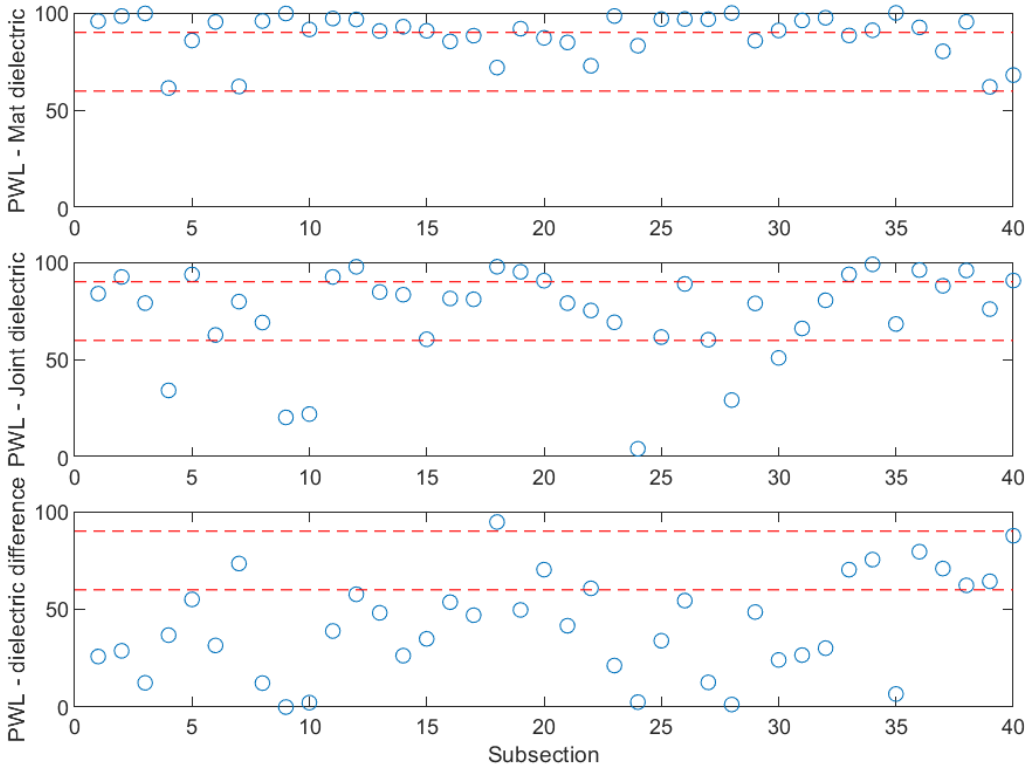

Figure B-5 PWL for dielectric values for unconfined joint (25 ft subsections) – Xerxes Road #1

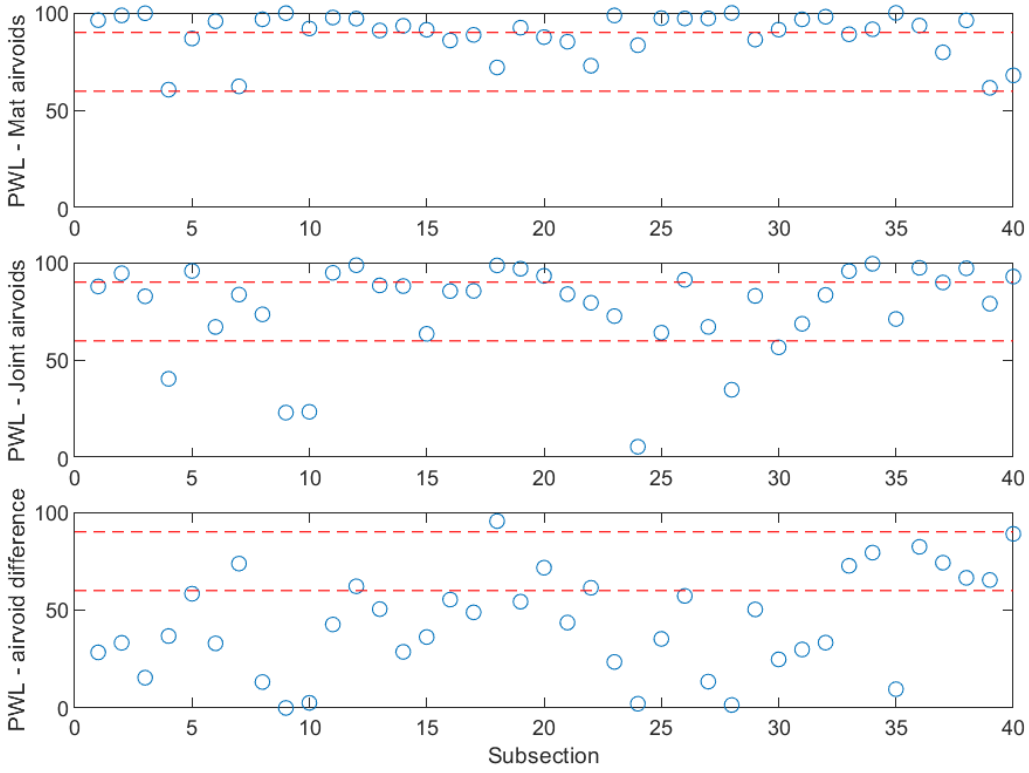

Figure B-6 PWL for air voids for unconfined joint (25 ft subsections) – Xerxes Road #1

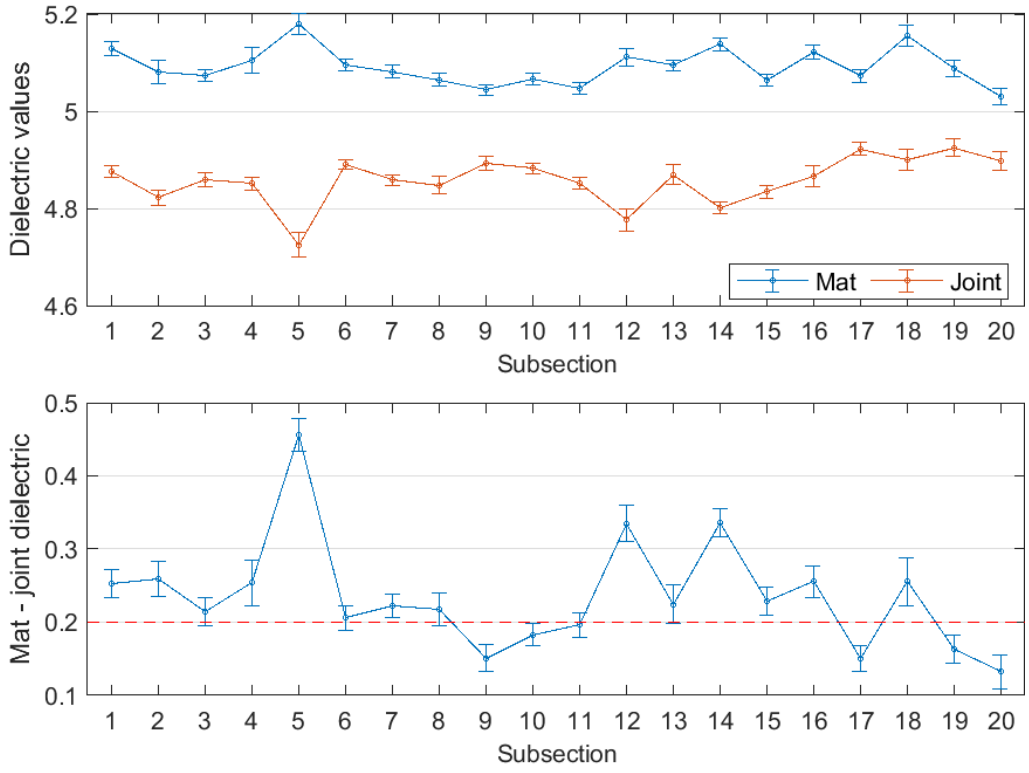

Figure B-7 Interval plot of dielectric values for unconfined joint (50 ft subsections) – Xerxes Road #1

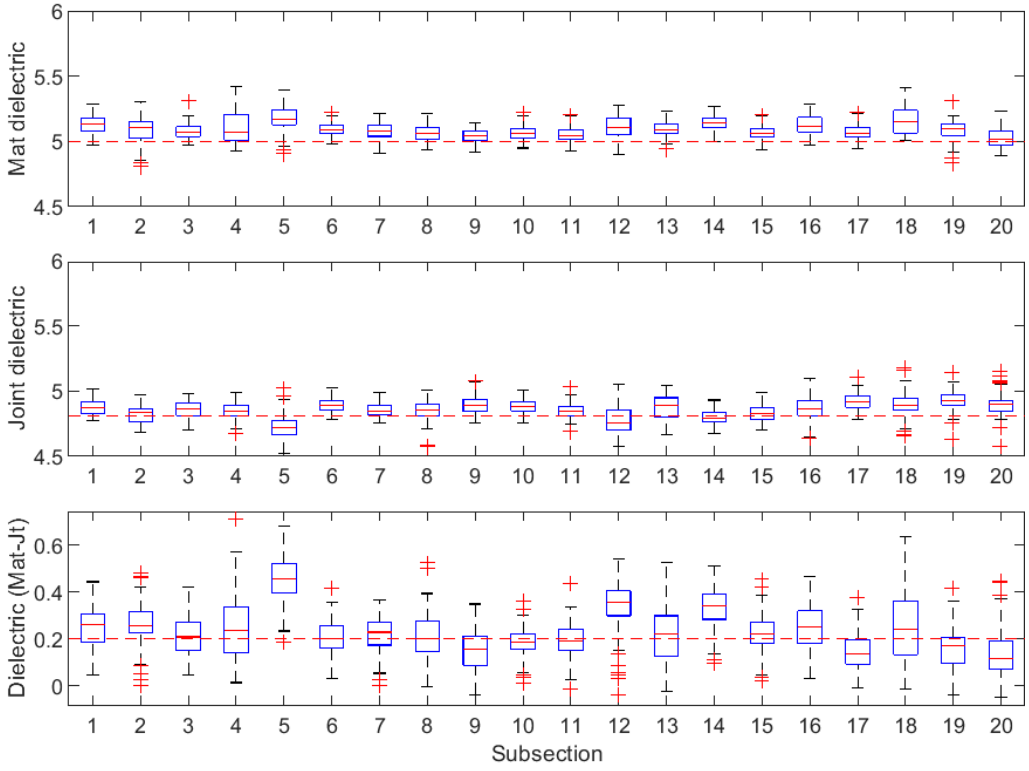

Figure B-8 Box plot of dielectric values for unconfined joint (50 ft subsections) – Xerxes Road #1

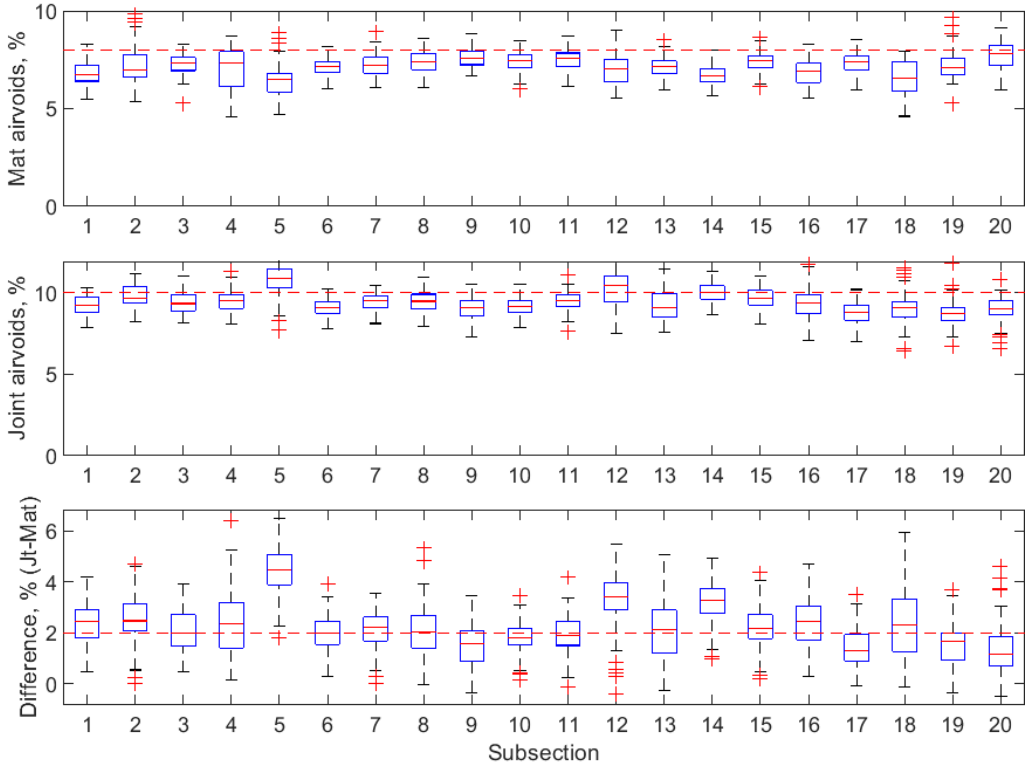

Figure B-9 Box plot of air voids for unconfined joint (50 ft subsections) – Xerxes Road #1

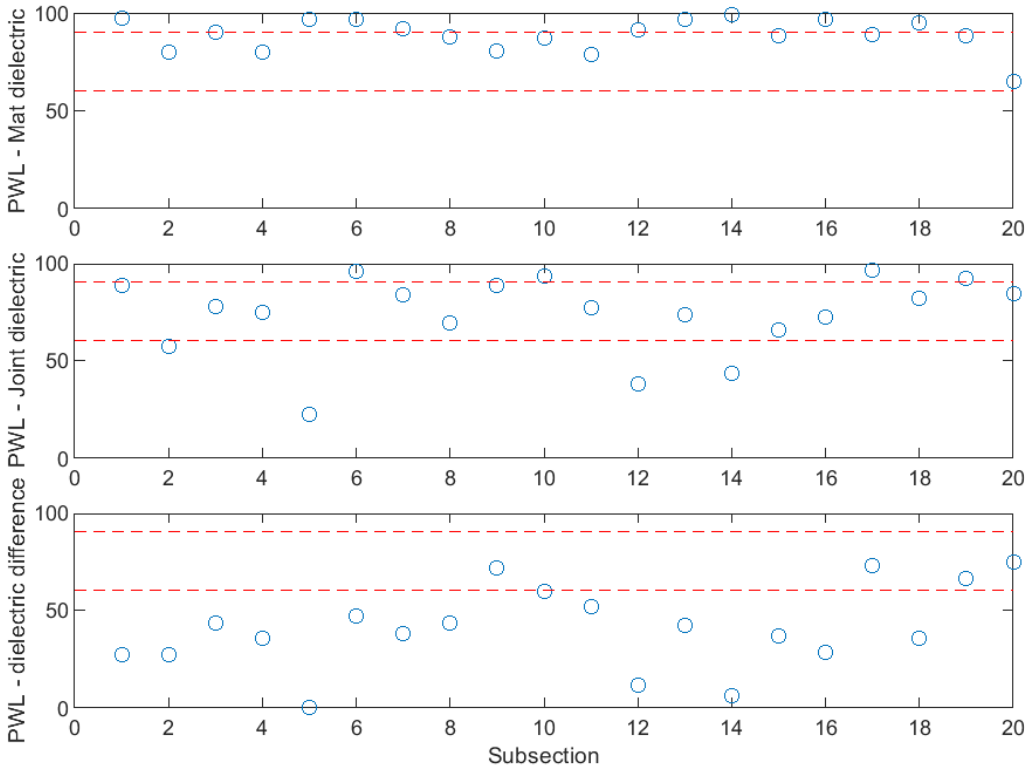

Figure B-10 PWL for dielectric values for unconfined joint (50 ft subsections) – Xerxes Road #1

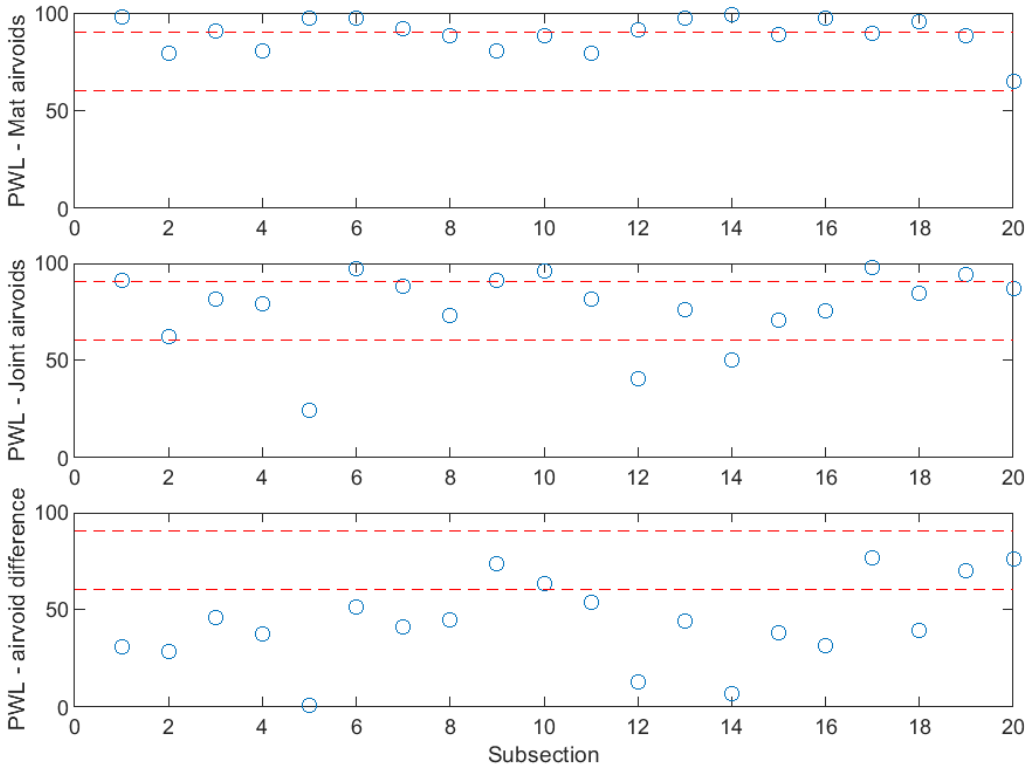

Figure B-11 PWL for air voids for unconfined joint (50 ft subsections) – Xerxes Road #1

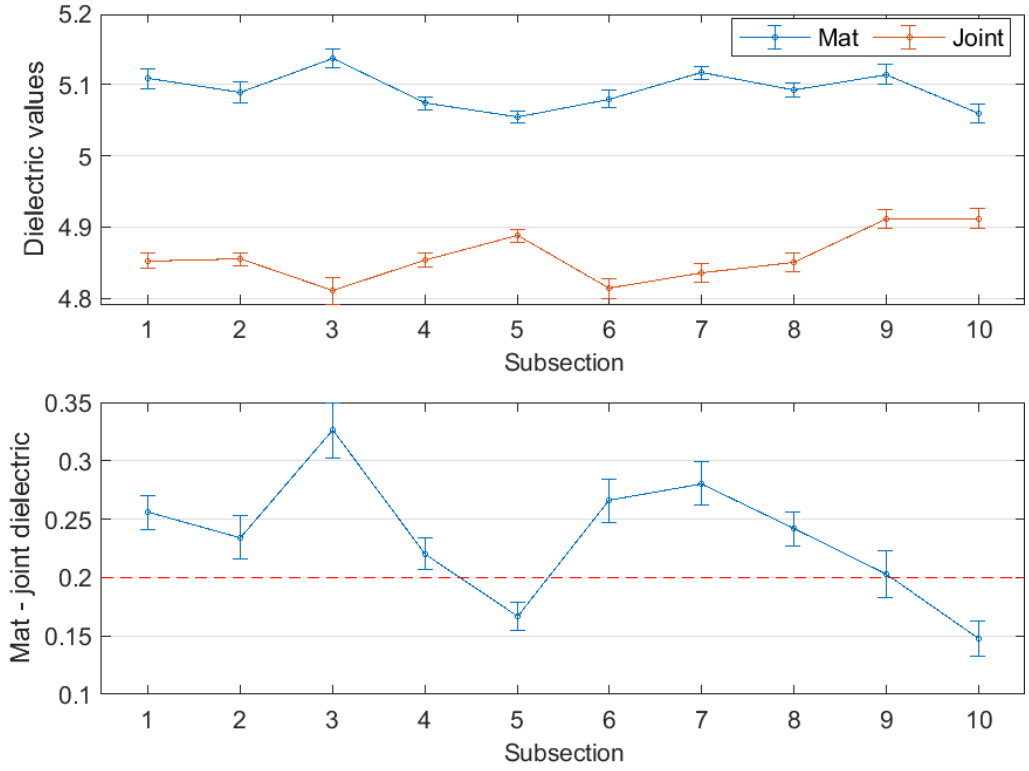

Figure B-12 Interval plot of dielectric values for unconfined joint (100 ft subsections) – Xerxes Road #1

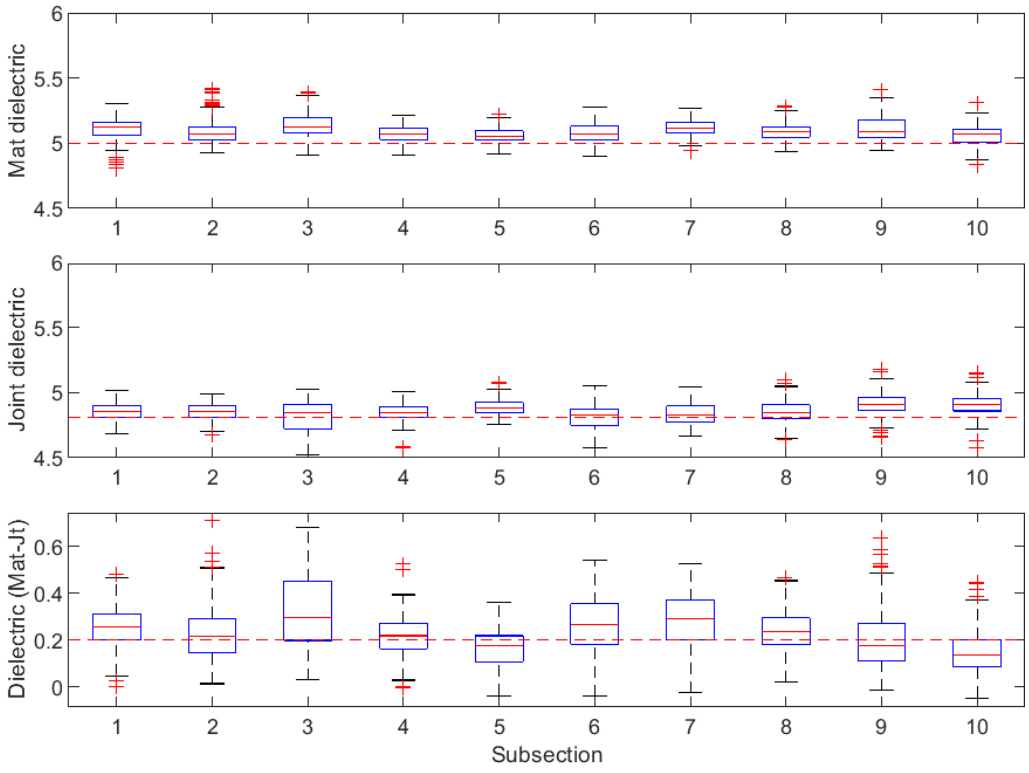

Figure B-13 Box plot of dielectric values for unconfined joint (100 ft subsections) – Xerxes Road #1

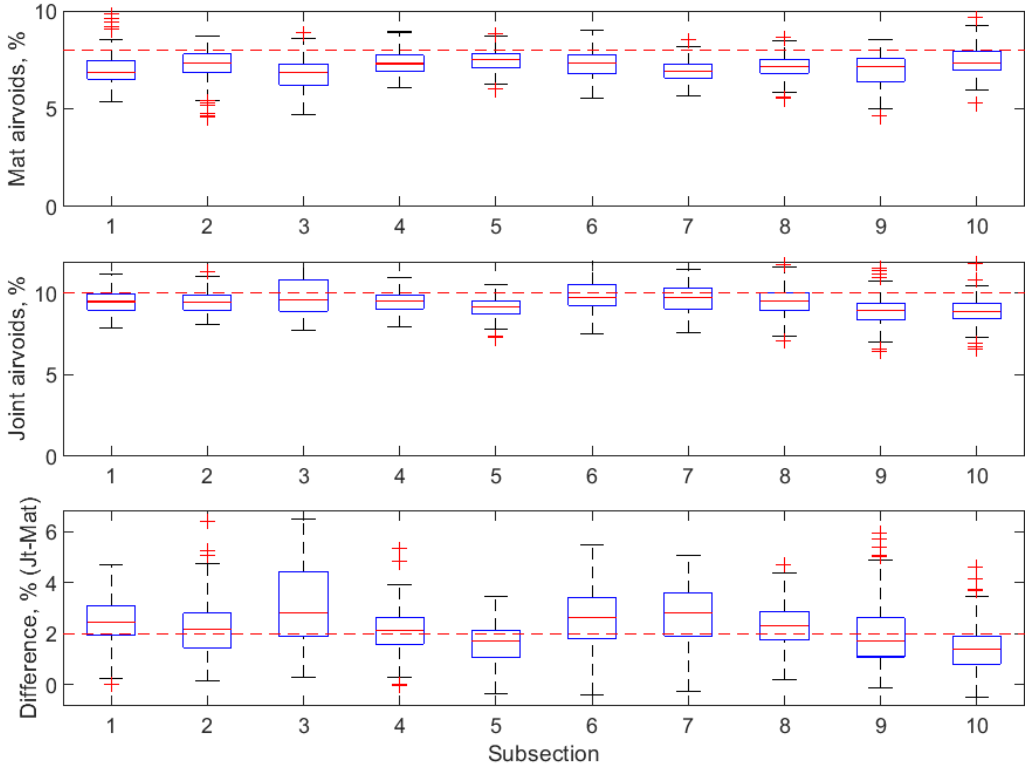

Figure B-14 Box plot of air voids for unconfined joint (100 ft subsections) – Xerxes Road #1

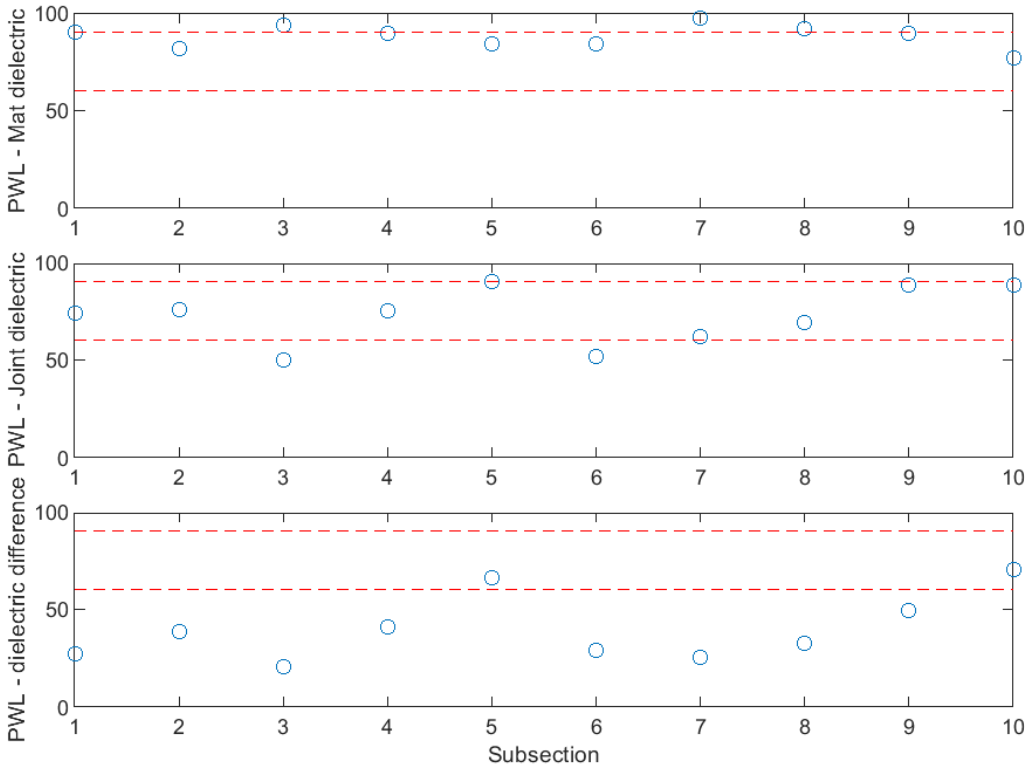

Figure B-15 PWL for dielectric values for unconfined joint (100 ft subsections) – Xerxes Road #1

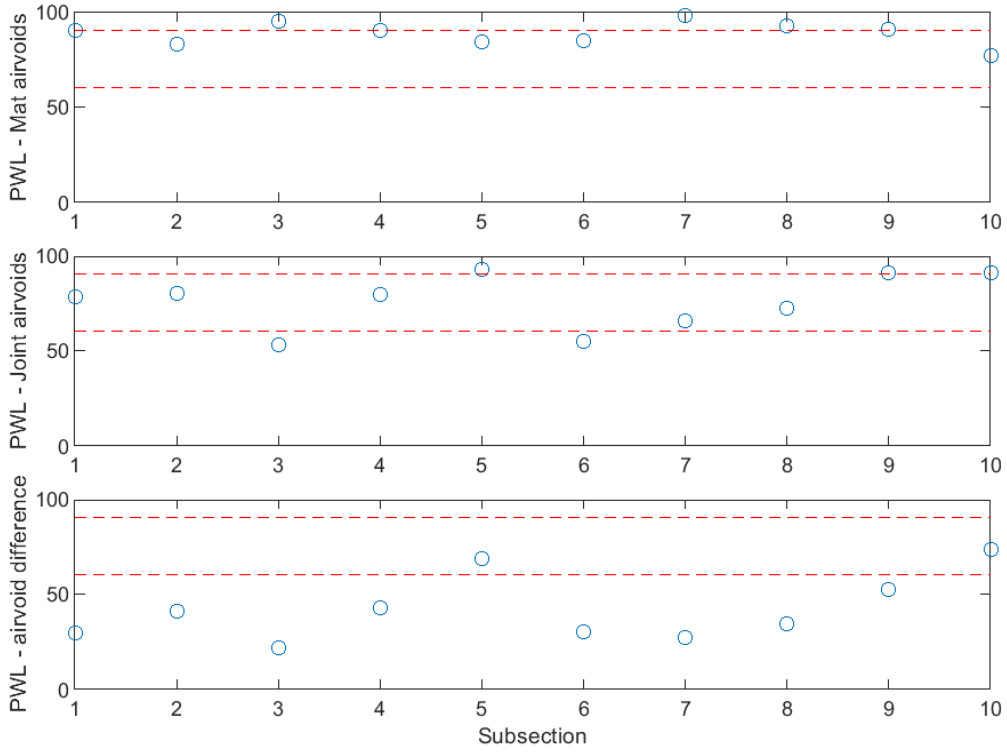

Figure B-16 PWL for air voids for unconfined joint (100 ft subsections) – Xerxes Road #1

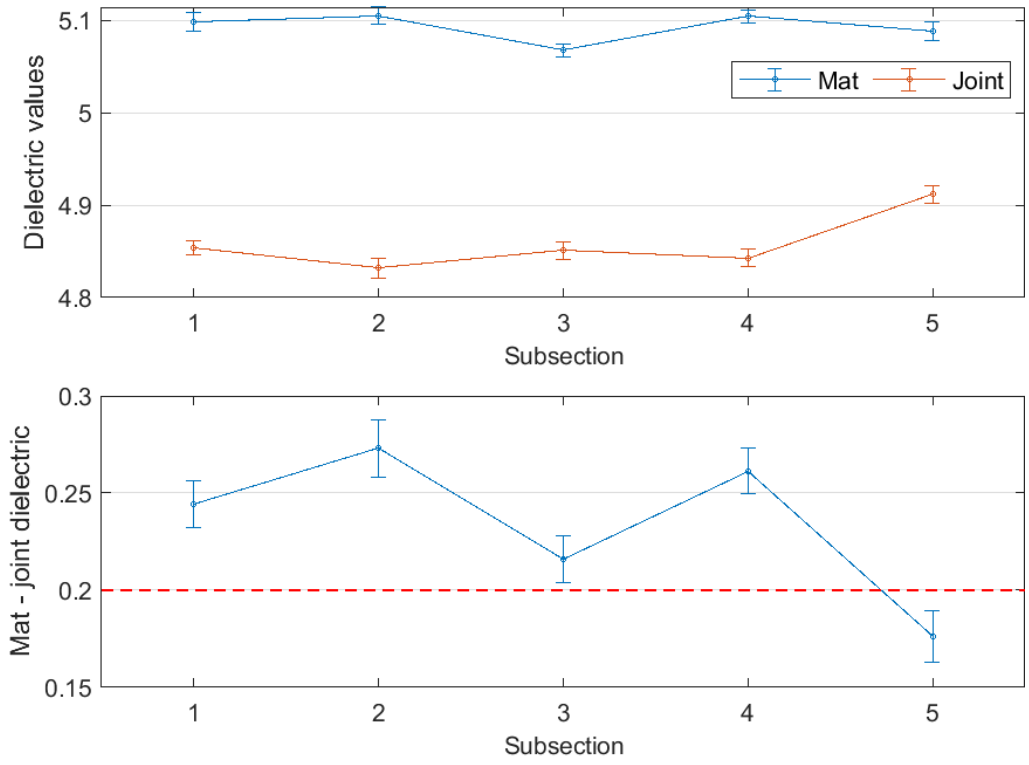

Figure B-17 Interval plot of dielectric values for unconfined joint (200 ft subsections) – Xerxes Road #1

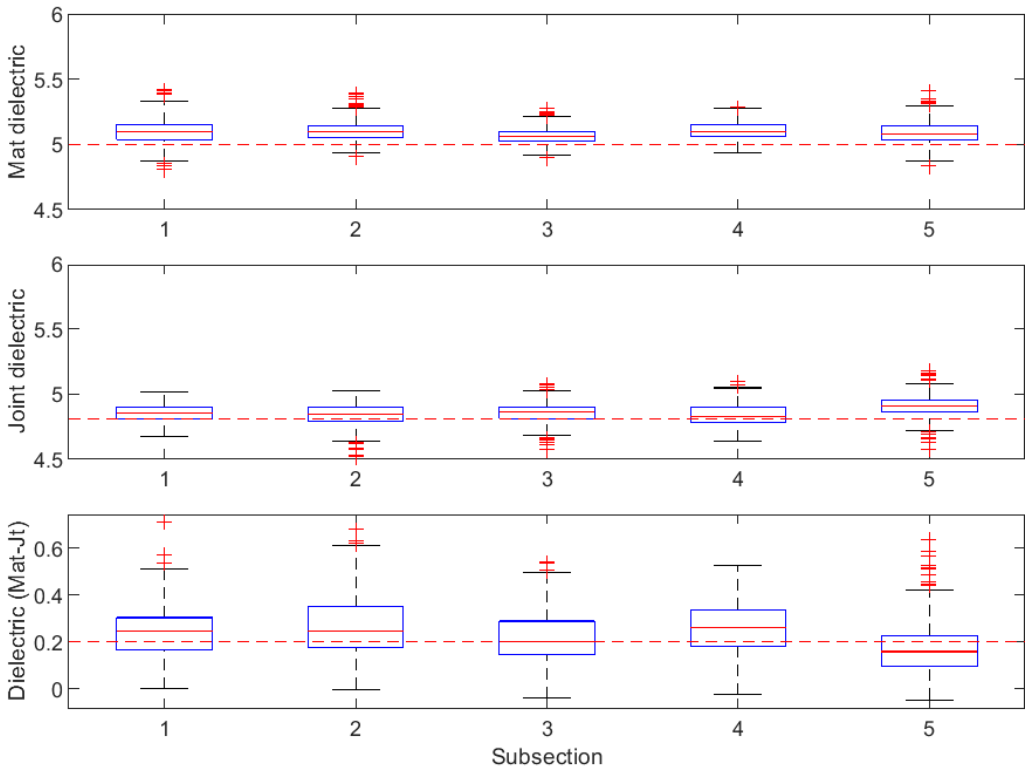

Figure B-18 Box plot of dielectric values for unconfined joint (200 ft subsections) – Xerxes Road #1

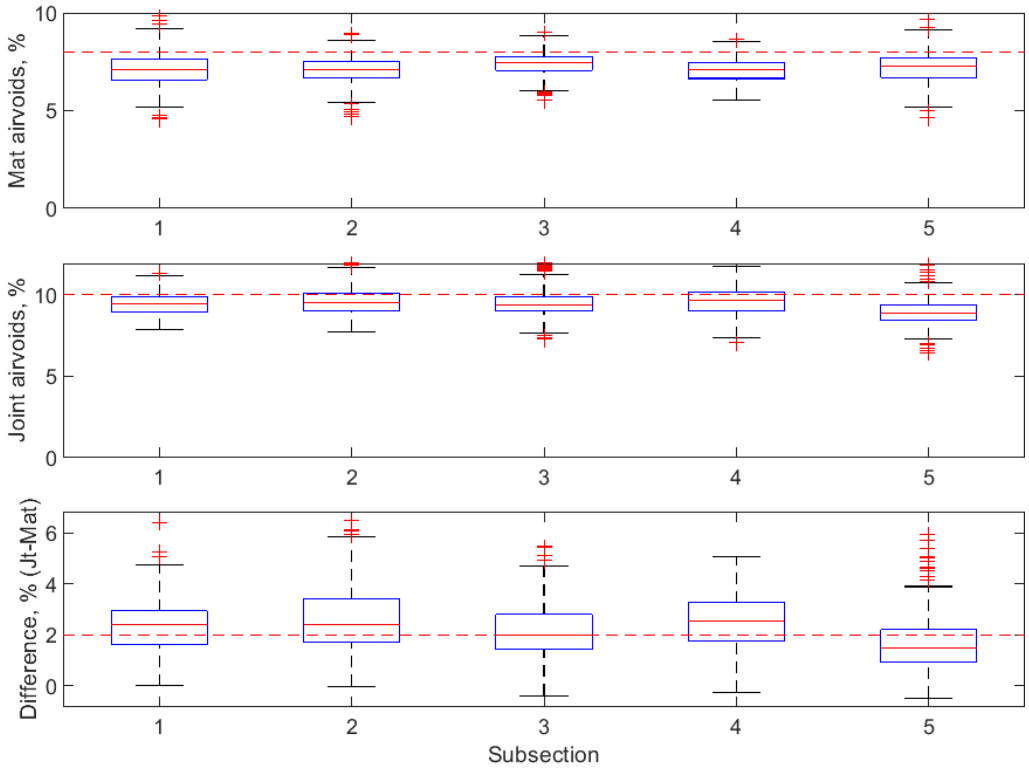

Figure B-19 Box plot of air voids for unconfined joint (200 ft subsections) – Xerxes Road #1

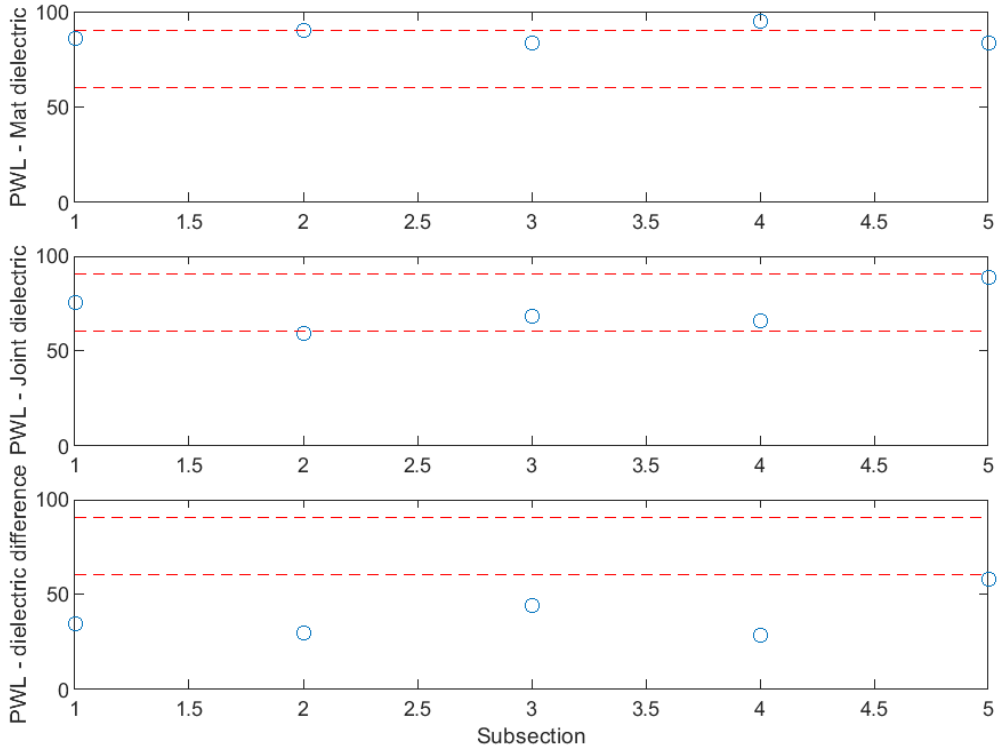

Figure B-20 PWL for dielectric values for unconfined joint (200 ft subsections) – Xerxes Road #1

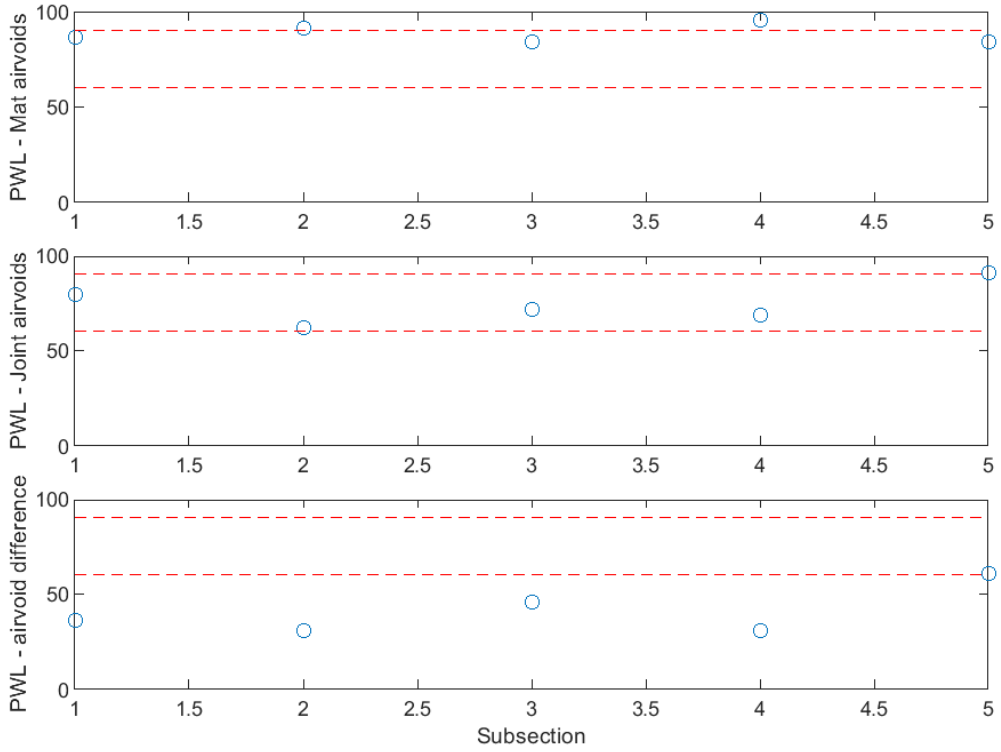

Figure B-21 PWL for air voids for unconfined joint (200 ft subsections) – Xerxes Road #1

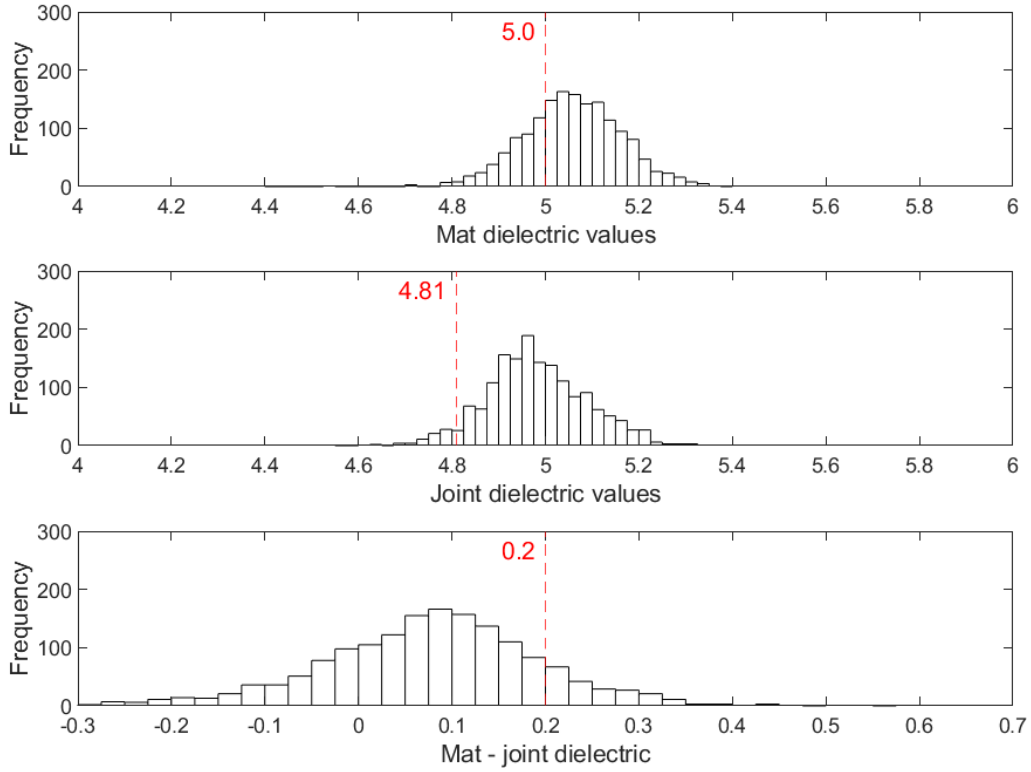

Figure B-22 Histogram of dielectric values for confined joint – Xerxes Road #1

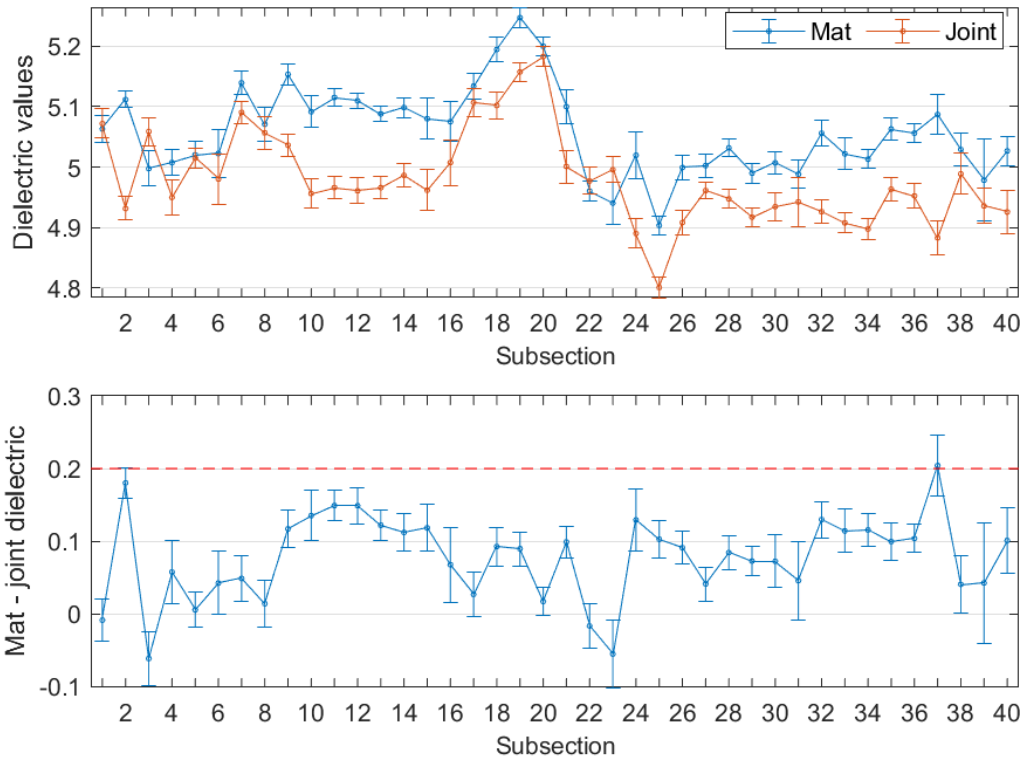

Figure B-23 Interval plot of dielectric values for confined joint (25 ft subsections) – Xerxes Road #1

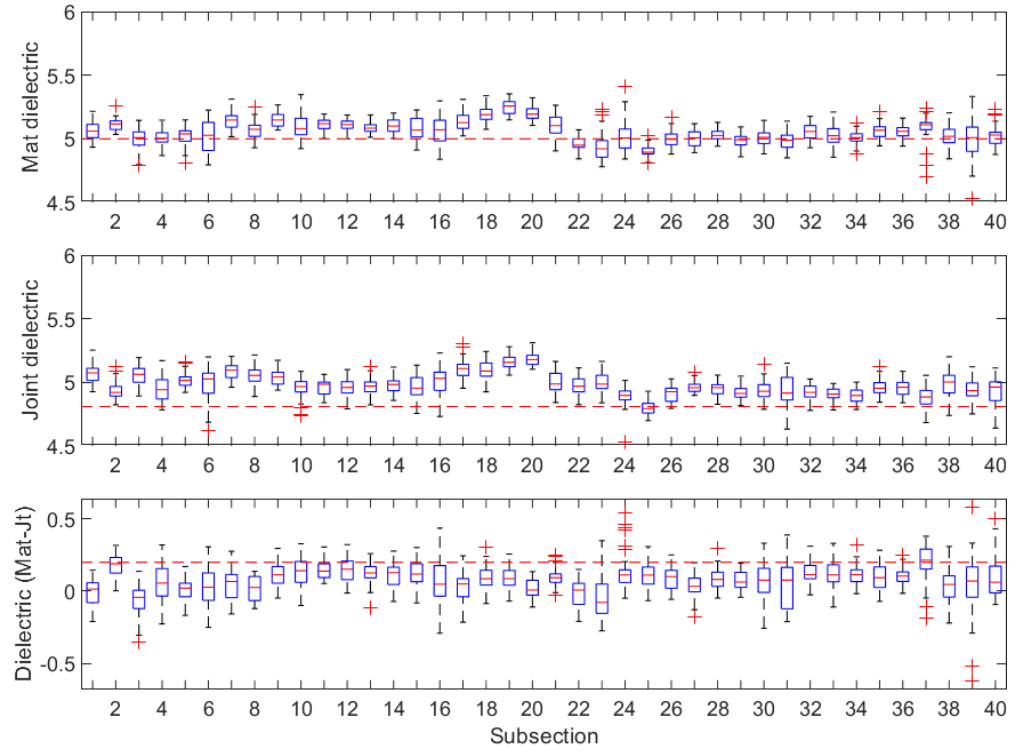

Figure B-24 Box plot of dielectric values for confined joint (25 ft subsections) – Xerxes Road #1

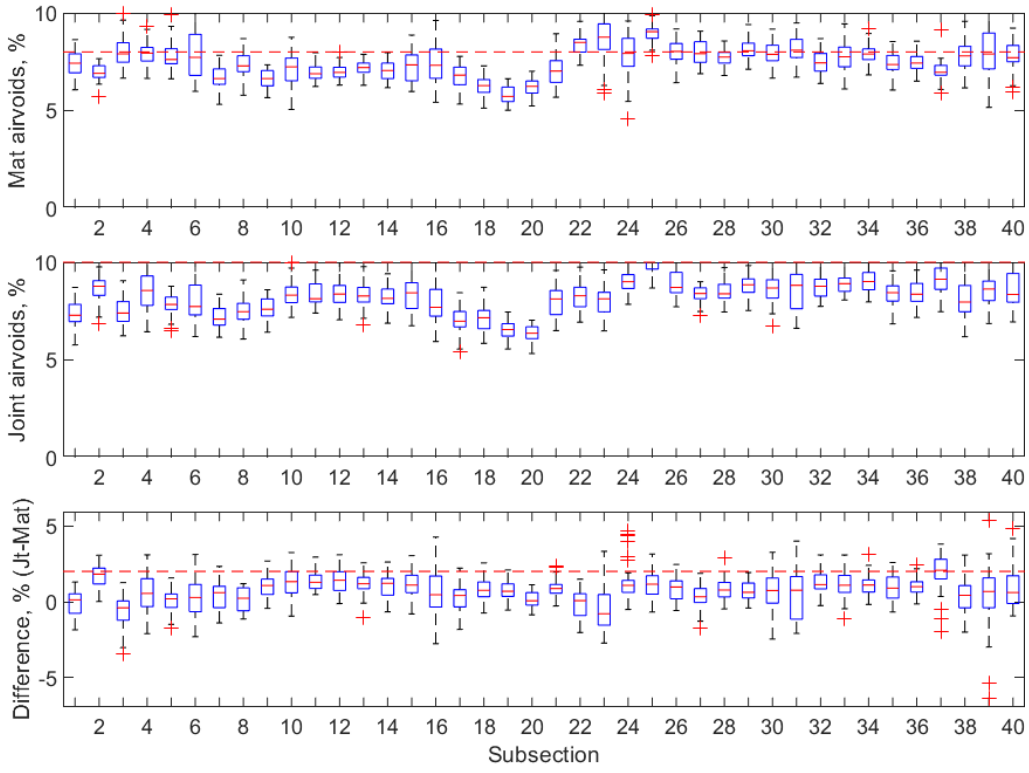

Figure B-25 Box plot of air voids for confined joint (25 ft subsections) – Xerxes Road #1

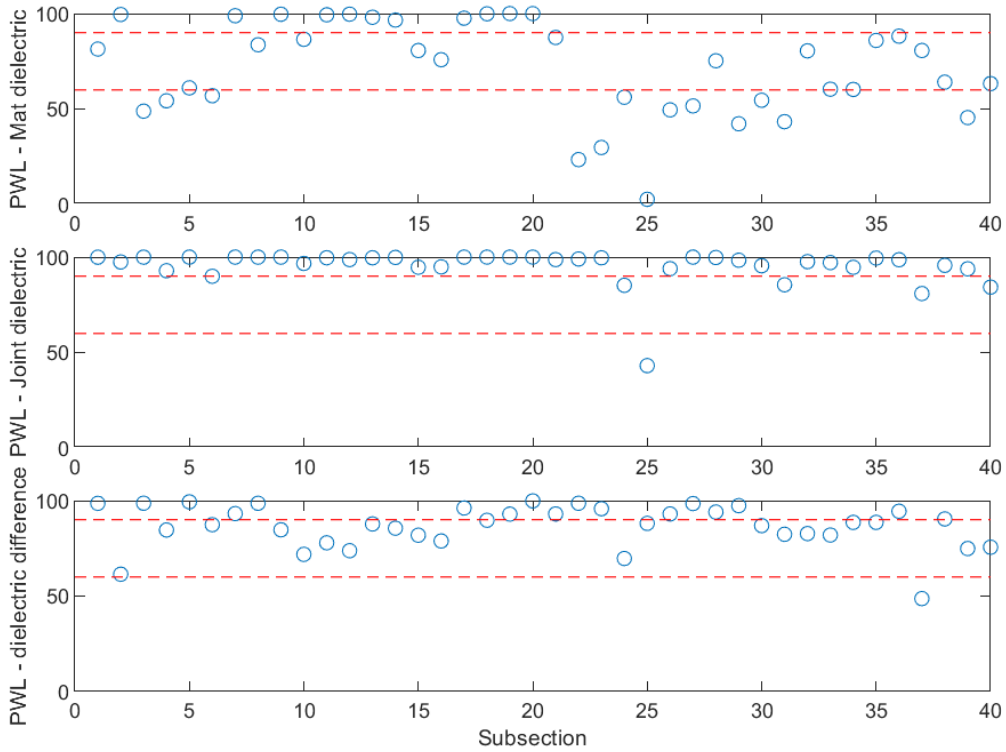

Figure B-26 PWL for dielectric values for confined joint (25 ft subsections) – Xerxes Road #1

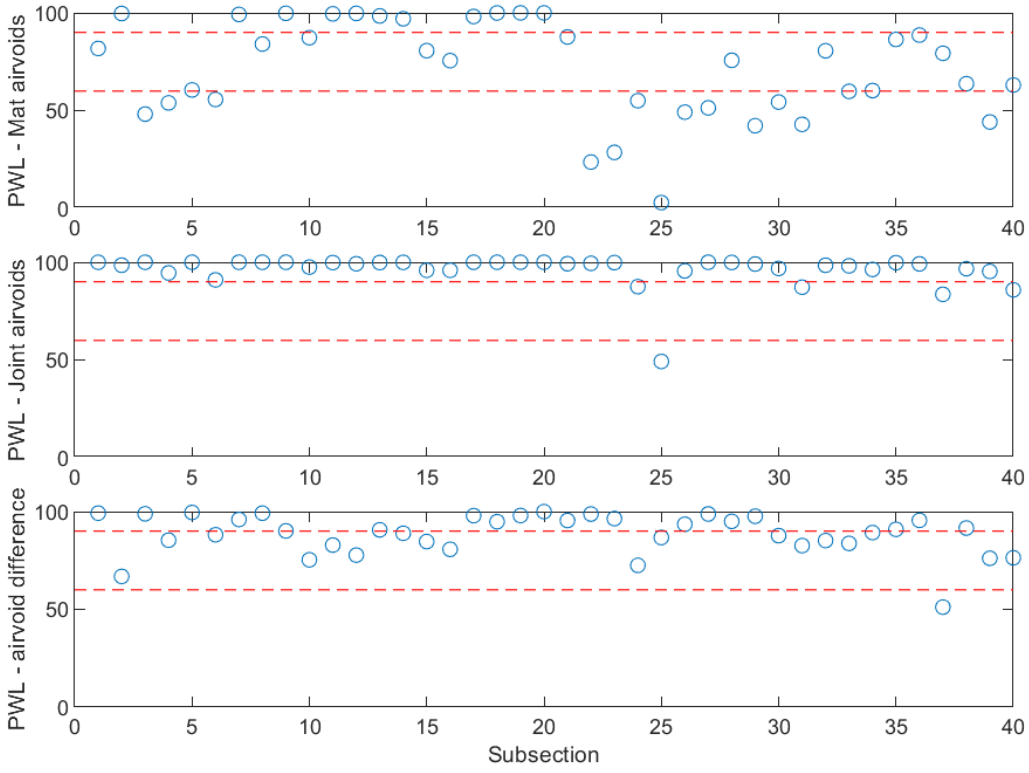

Figure B-27 PWL for air voids for confined joint (25 ft subsections) – Xerxes Road #1

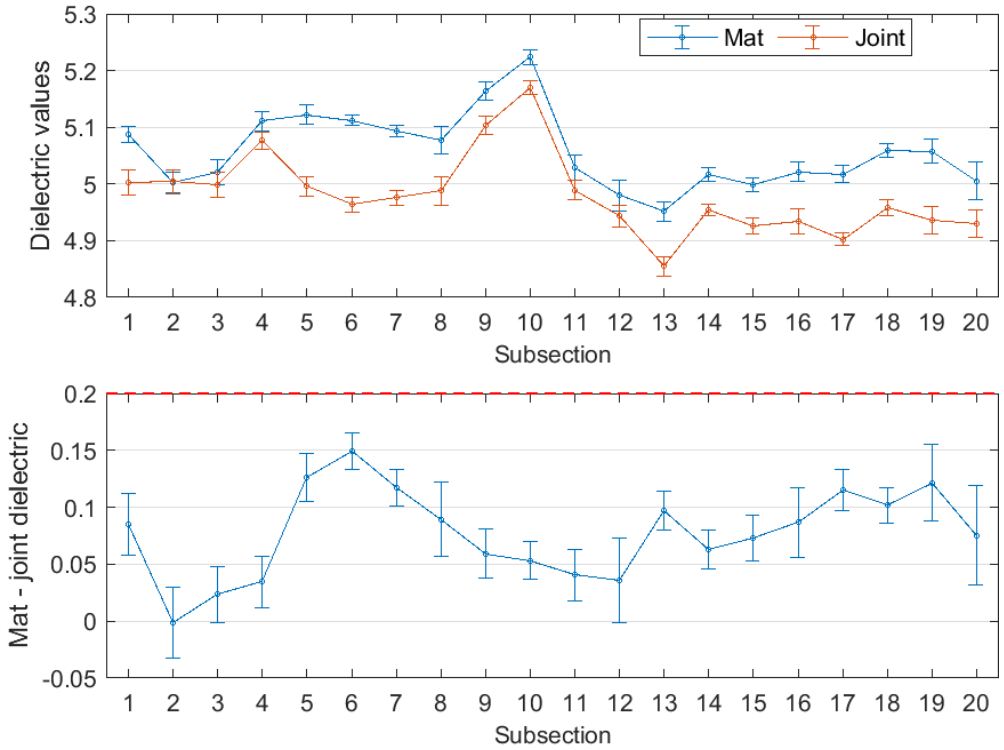

Figure B-28 Interval plot of dielectric values for confined joint (50 ft subsections) – Xerxes Road #1

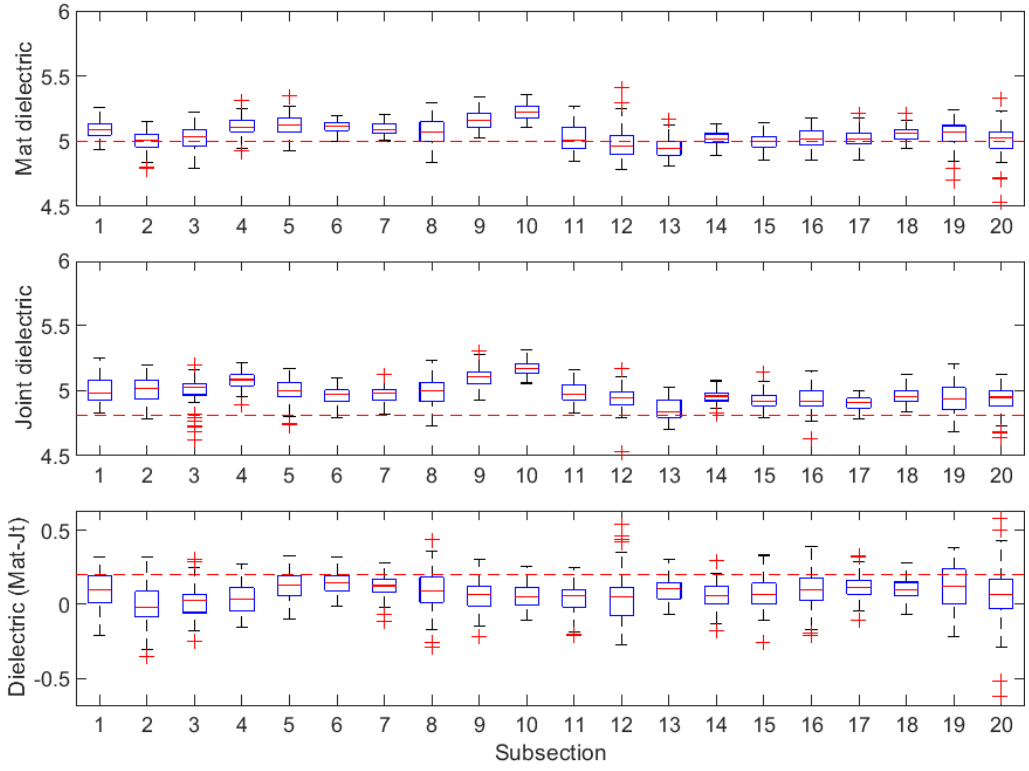

Figure B-29 Box plot of dielectric values for confined joint (50 ft subsections) – Xerxes Road #1

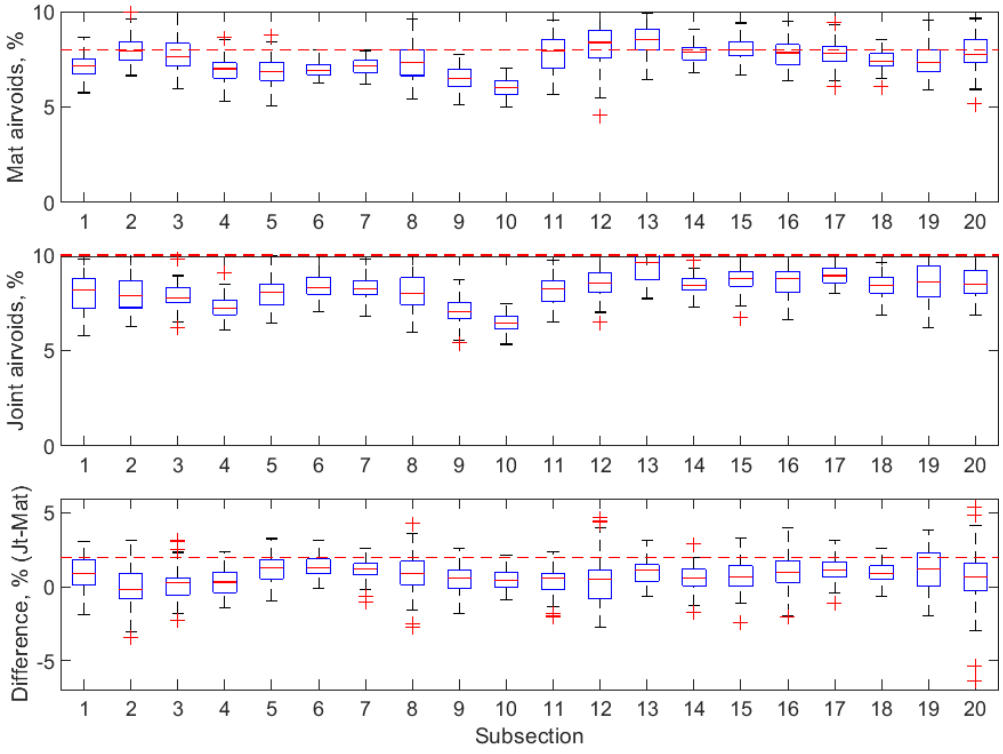

Figure B-30 Box plot of air voids for confined joint (50 ft subsections) – Xerxes Road #1

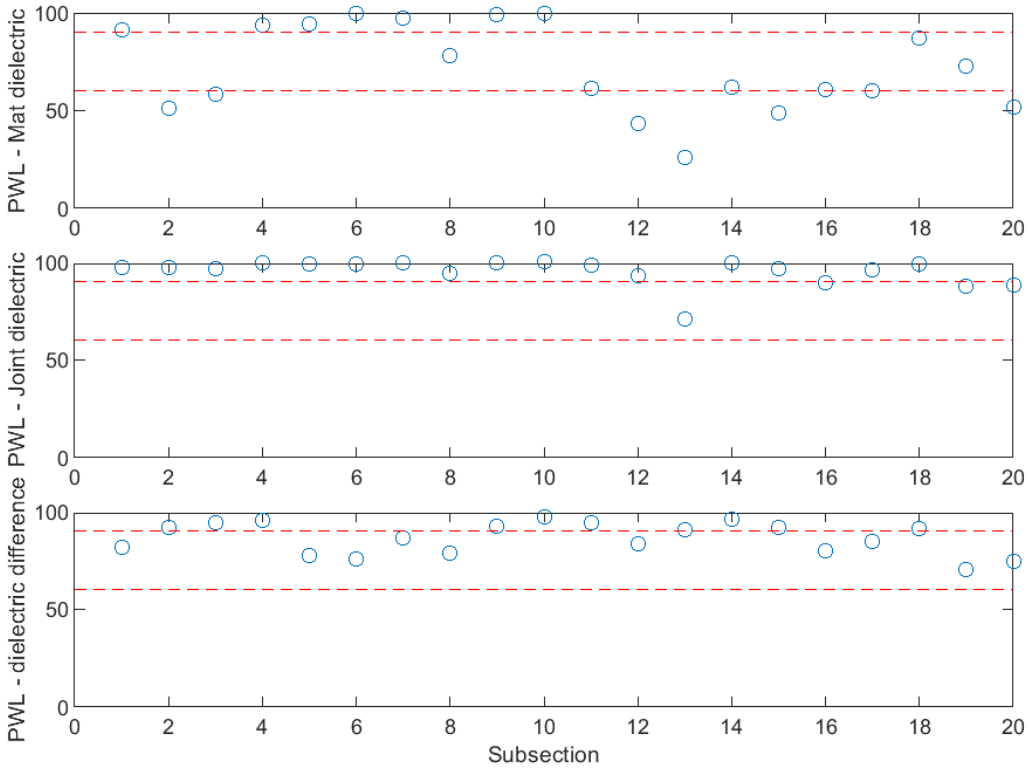

Figure B-31 PWL for dielectric values for confined joint (50 ft subsections) – Xerxes Road #1

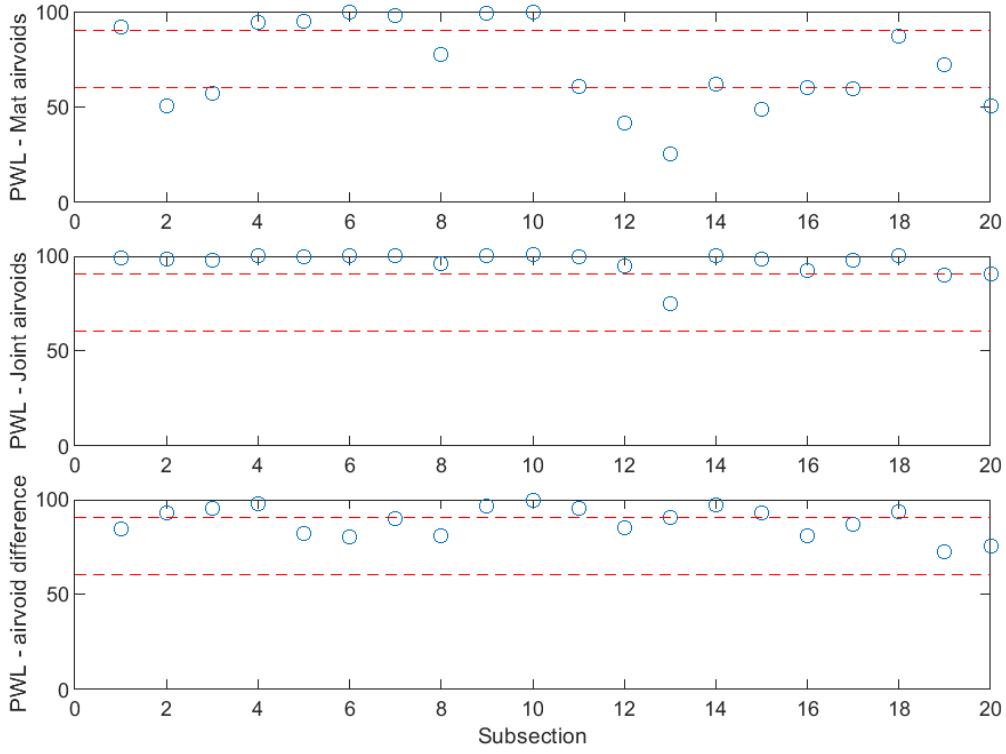

Figure B-32 PWL for dielectric values for confined joint (50 ft subsections) – Xerxes Road #1

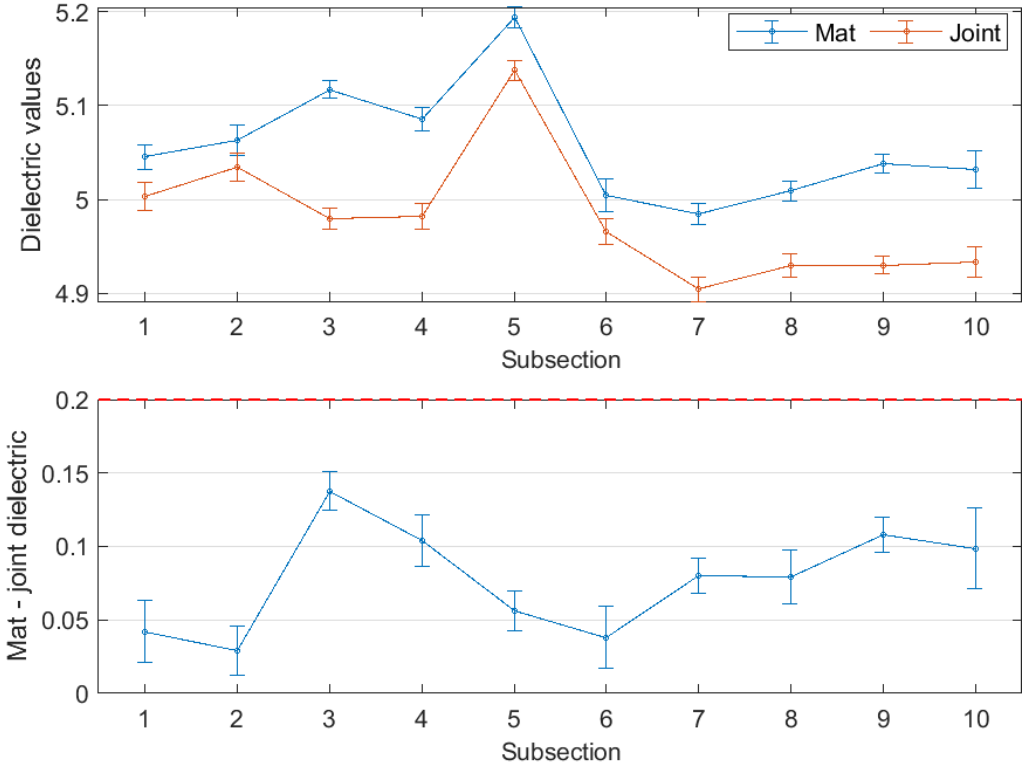

Figure B-33 Interval plot of dielectric values for confined joint (100 ft subsections) – Xerxes Road #1

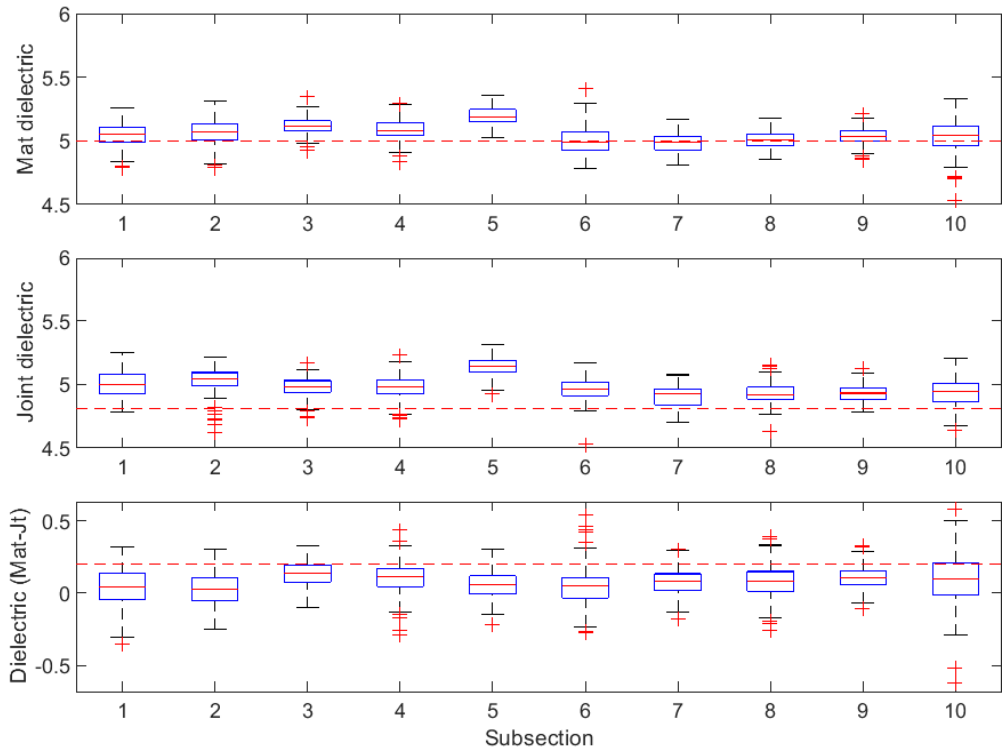

Figure B-34 Box plot of dielectric values for confined joint (100 ft subsections) – Xerxes Road #1

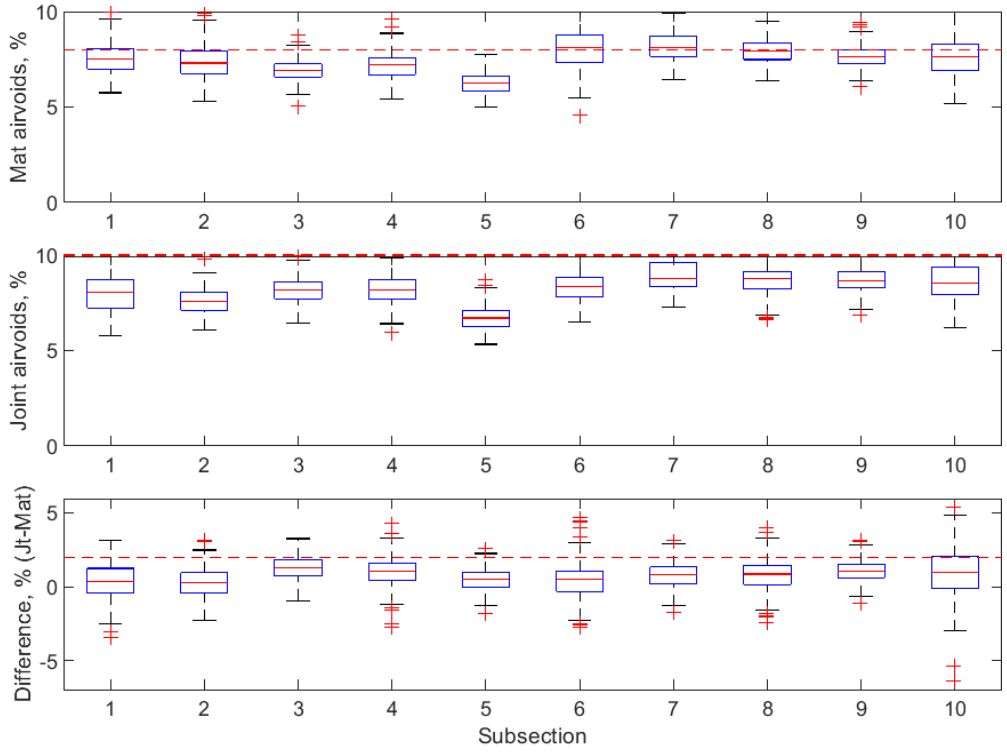

Figure B-35 Box plot of air voids for confined joint (100 ft subsections) – Xerxes Road #1

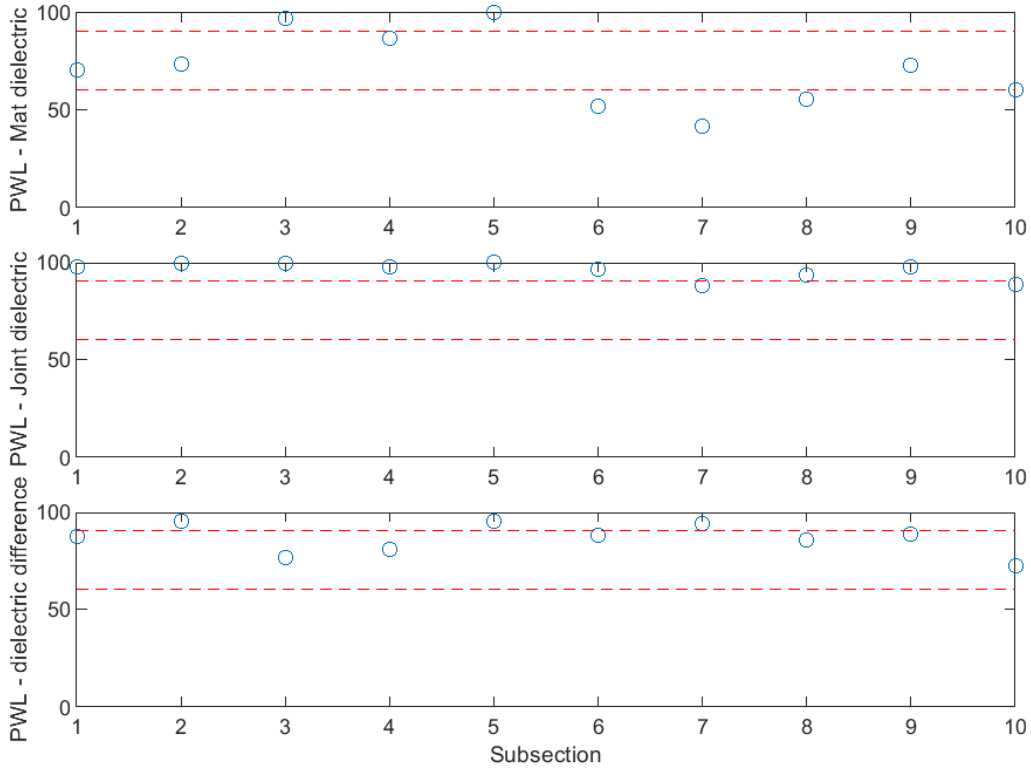

Figure B-36 PWL for dielectric values for confined joint (100 ft subsections) – Xerxes Road #1

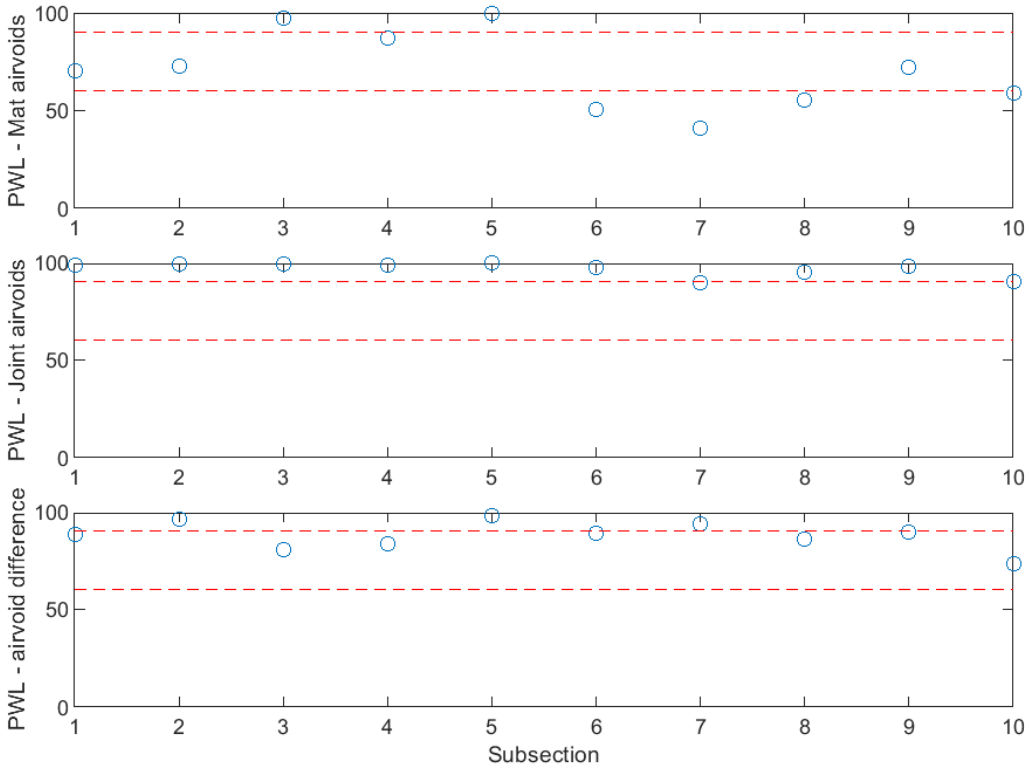

Figure B-37 PWL for dielectric values for confined joint (100 ft subsections) – Xerxes Road #1

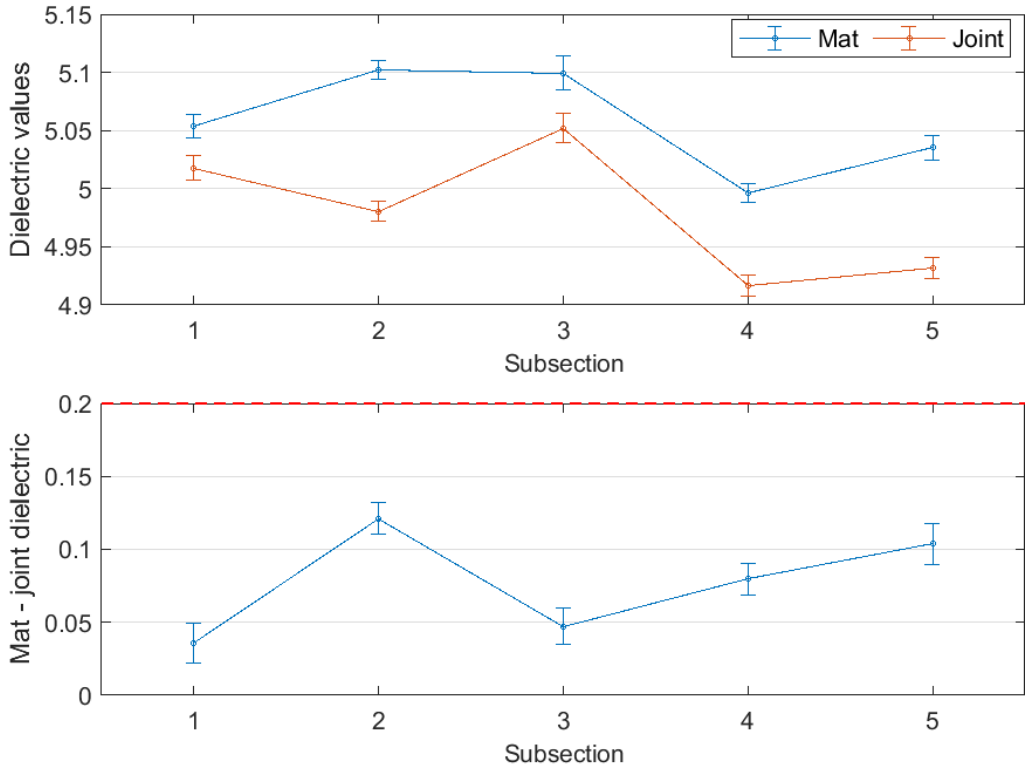

Figure B-38 Interval plot of dielectric values for confined joint (200 ft subsections) – Xerxes Road #1

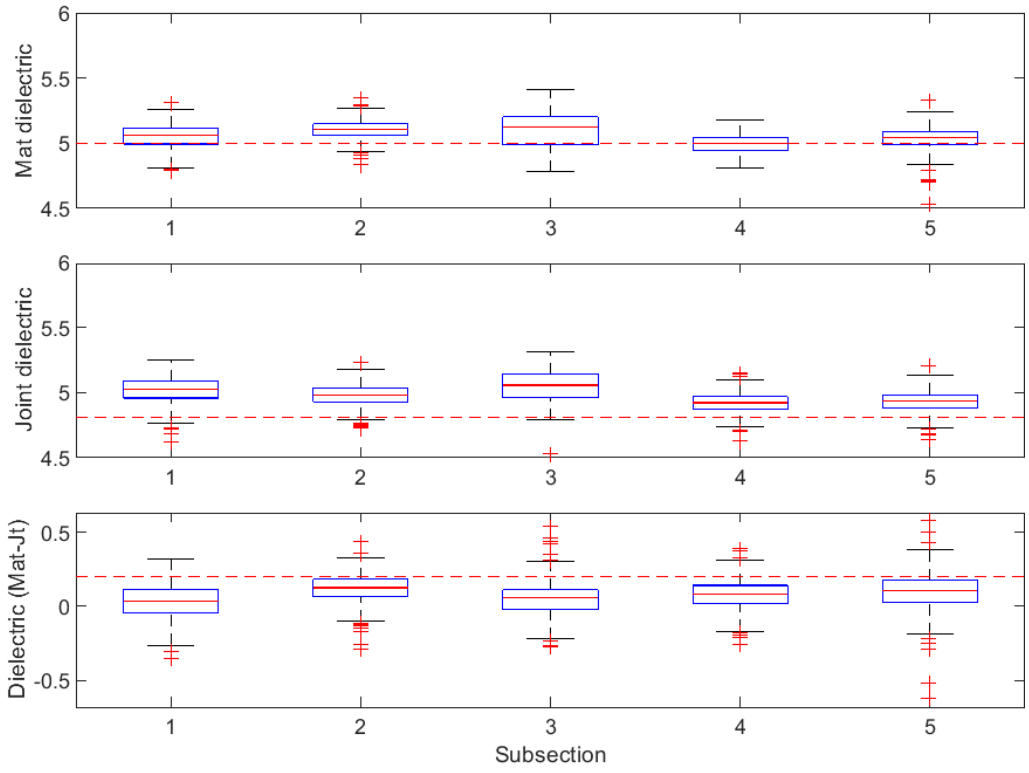

Figure B-39 Box plot of dielectric values for confined joint (200 ft subsections) – Xerxes Road #1

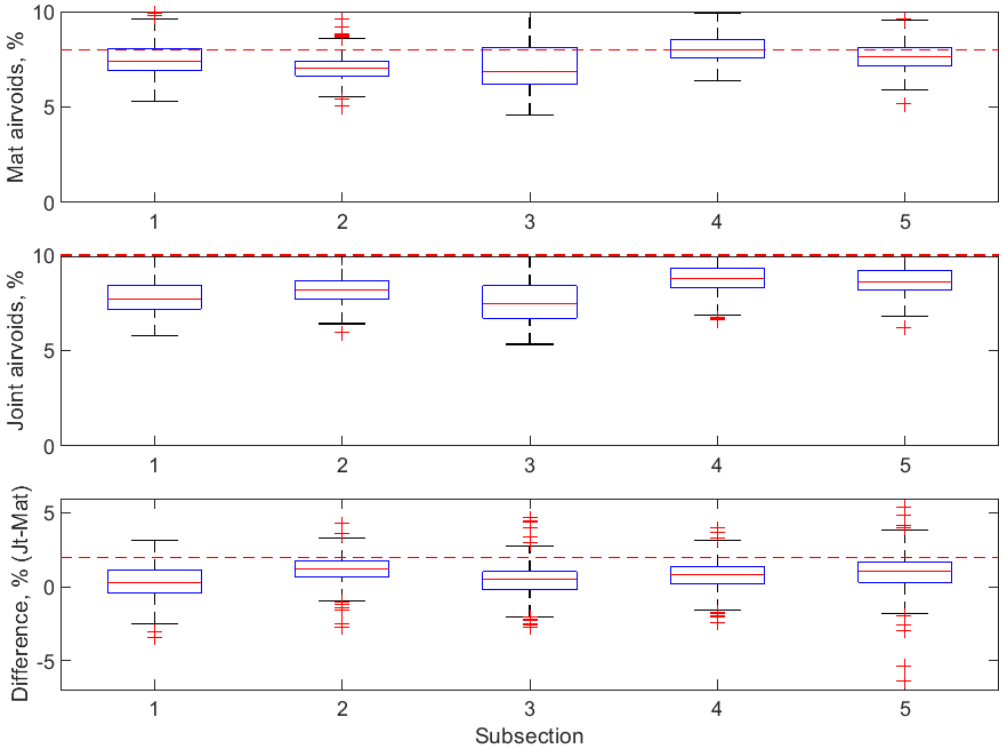

Figure B-40 Box plot of air voids for confined joint (200 ft subsections) – Xerxes Road #1

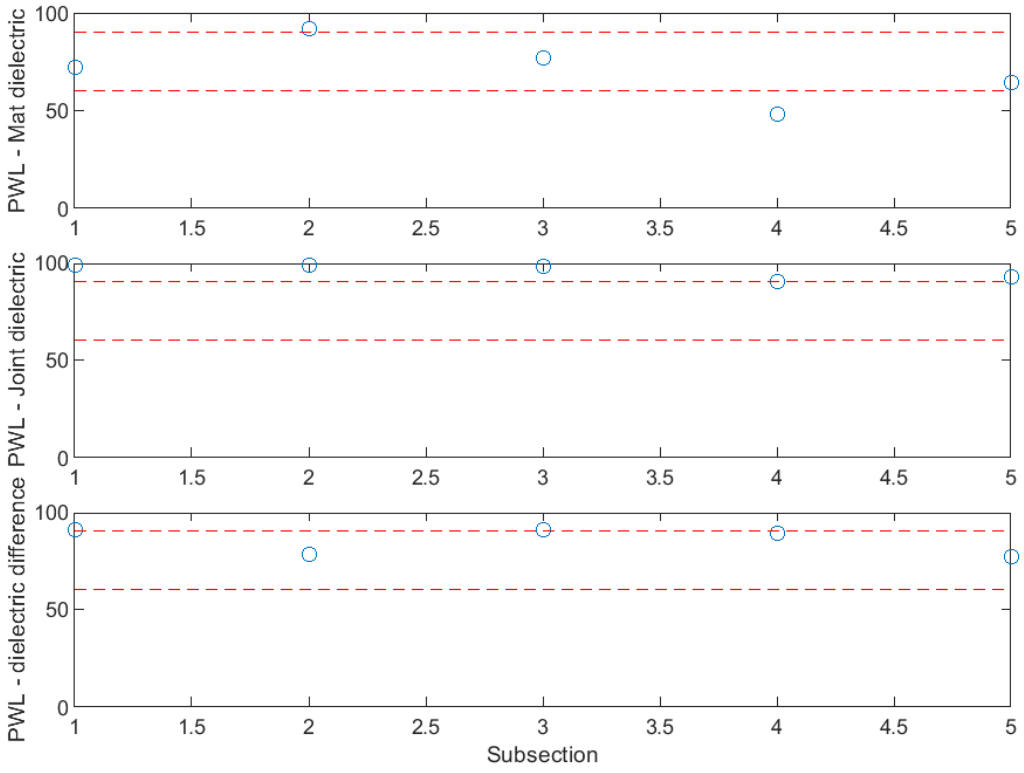

Figure B-41 PWL for dielectric values for confined joint (200 ft subsections) – Xerxes Road #1

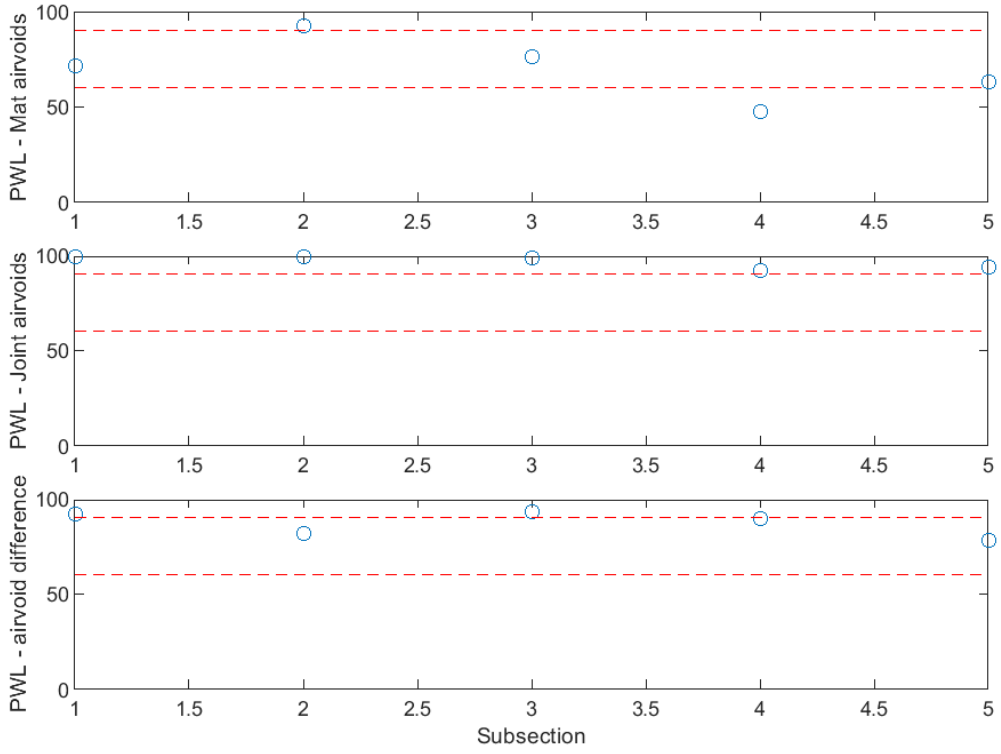

Figure B-42 PWL for dielectric values for confined joint (200 ft subsections) – Xerxes Road #1

Xerxes Road #2 Project

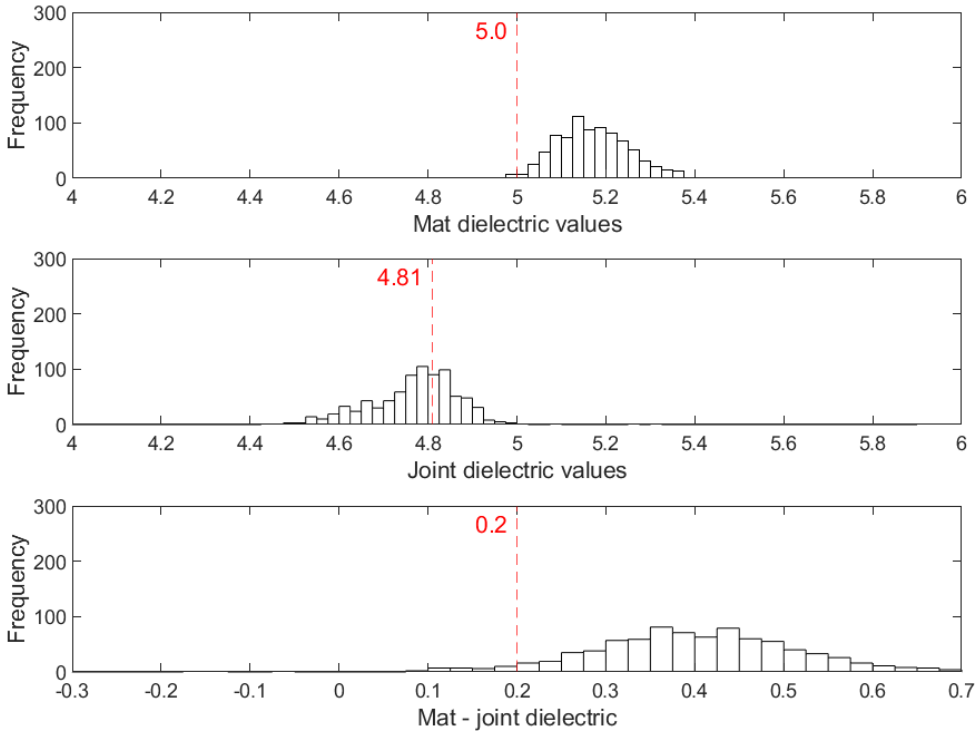

Figure B-43 Histogram of dielectric values for unconfined joint – Xerxes Road #2

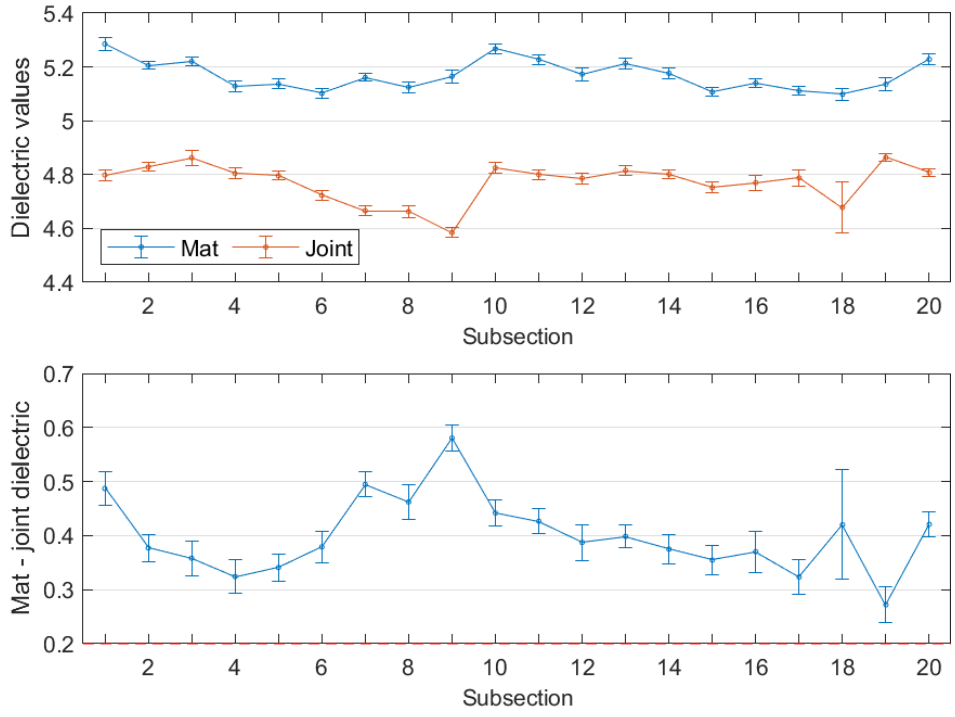

Figure B-44 Interval plot of dielectric values for unconfined joint (25 ft subsections) – Xerxes Road #2

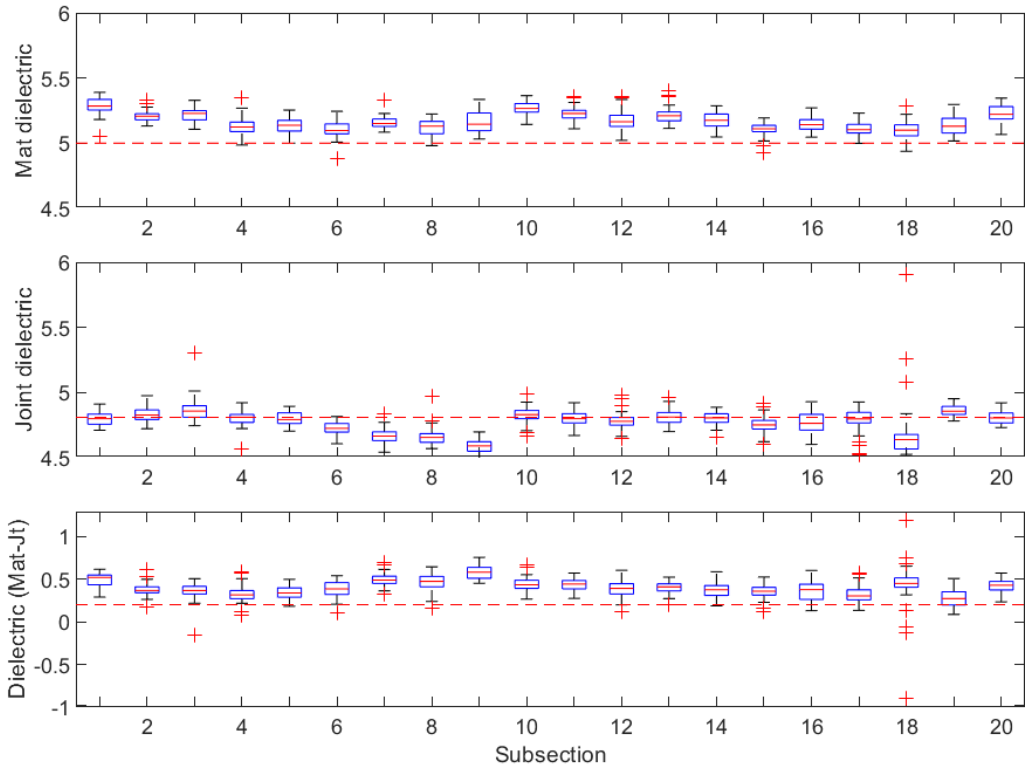

Figure B-45 Box plot of dielectric values for unconfined joint (25 ft subsections) – Xerxes Road #2

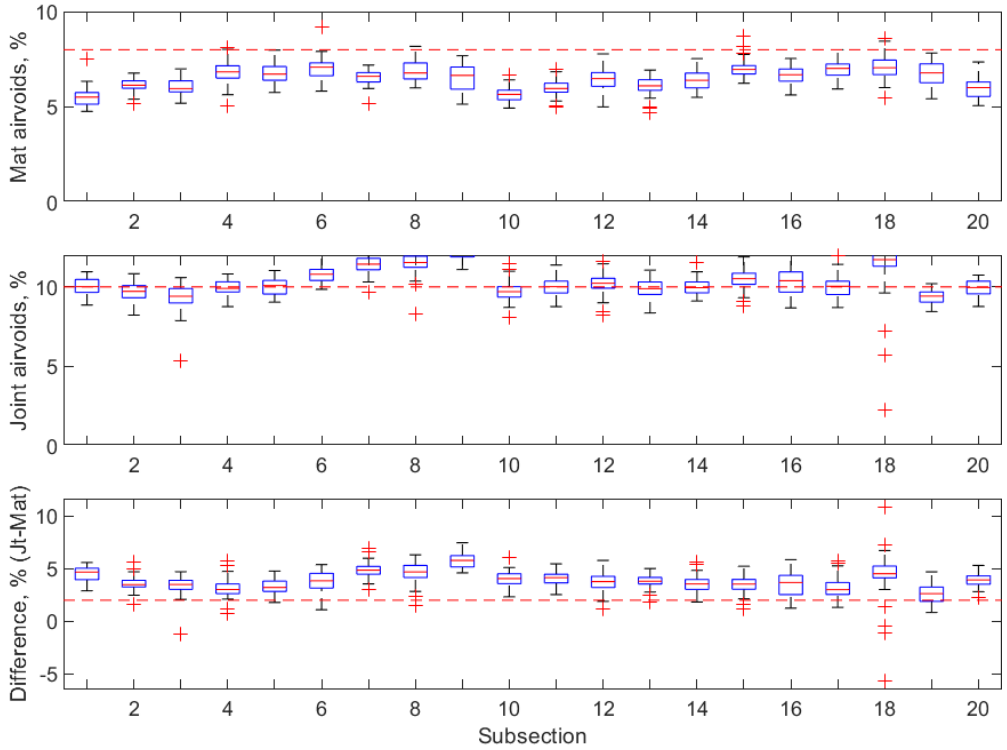

Figure B-46 Box plot of air voids for unconfined joint (25 ft subsections) – Xerxes Road #2

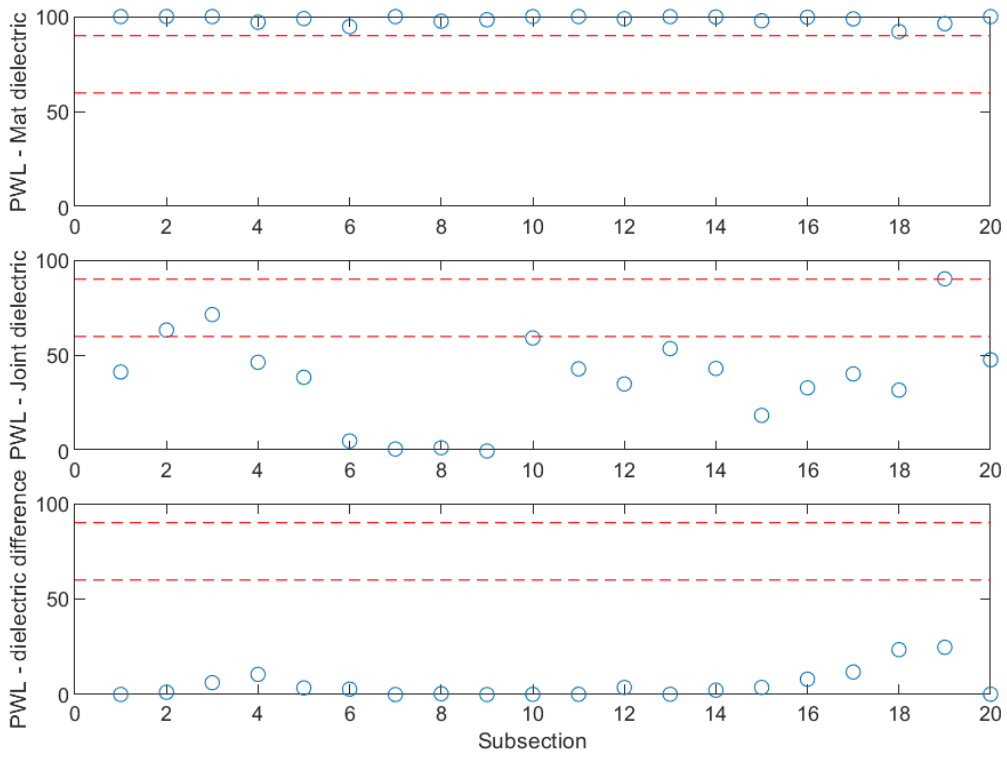

Figure B-47 PWL for dielectric values for unconfined joint (25 ft subsections) – Xerxes Road #2

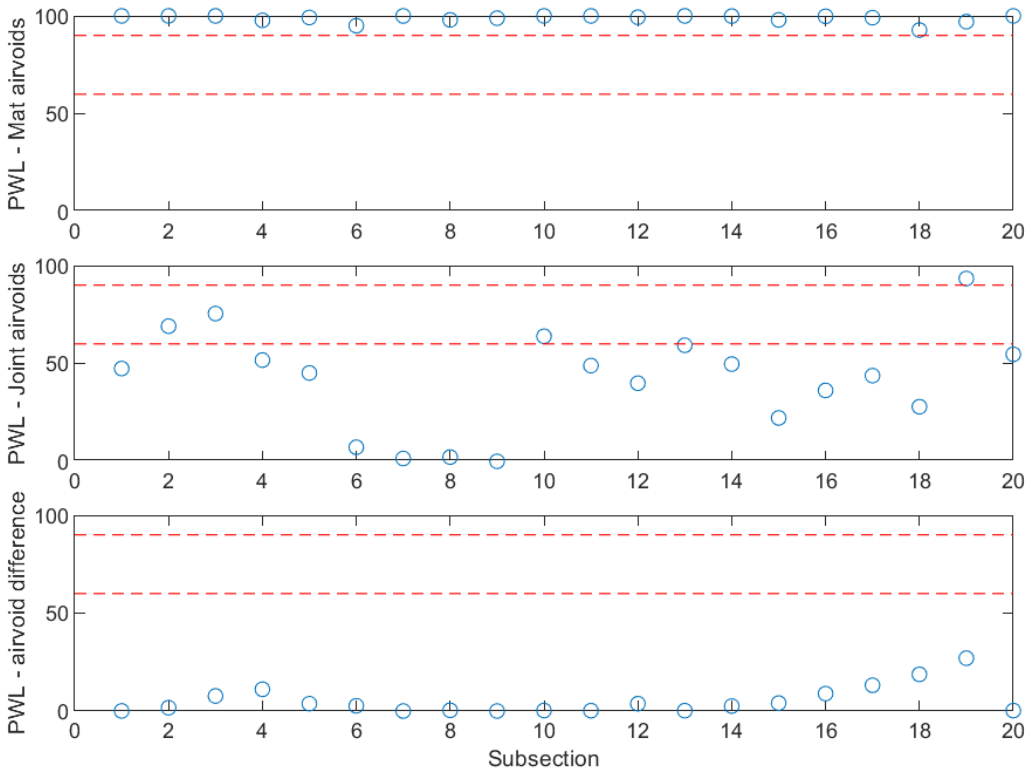

Figure B-48 PWL for air voids for unconfined joint (25 ft subsections) – Xerxes Road #2

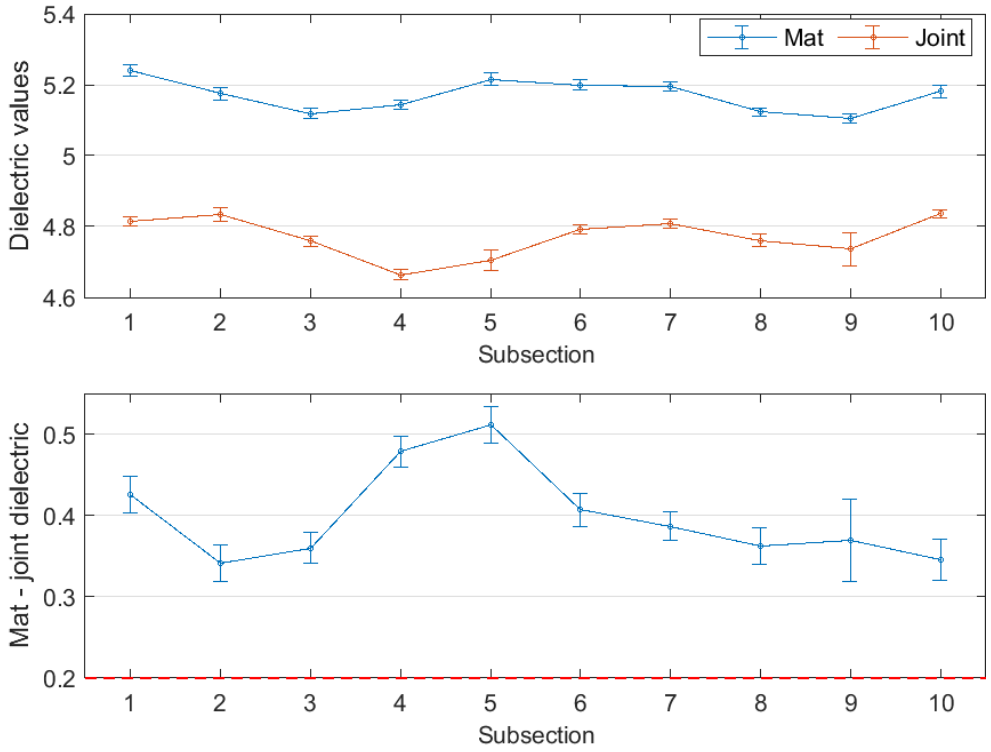

Figure B-49 Interval plot of dielectric values for unconfined joint (50 ft subsections) – Xerxes Road #2

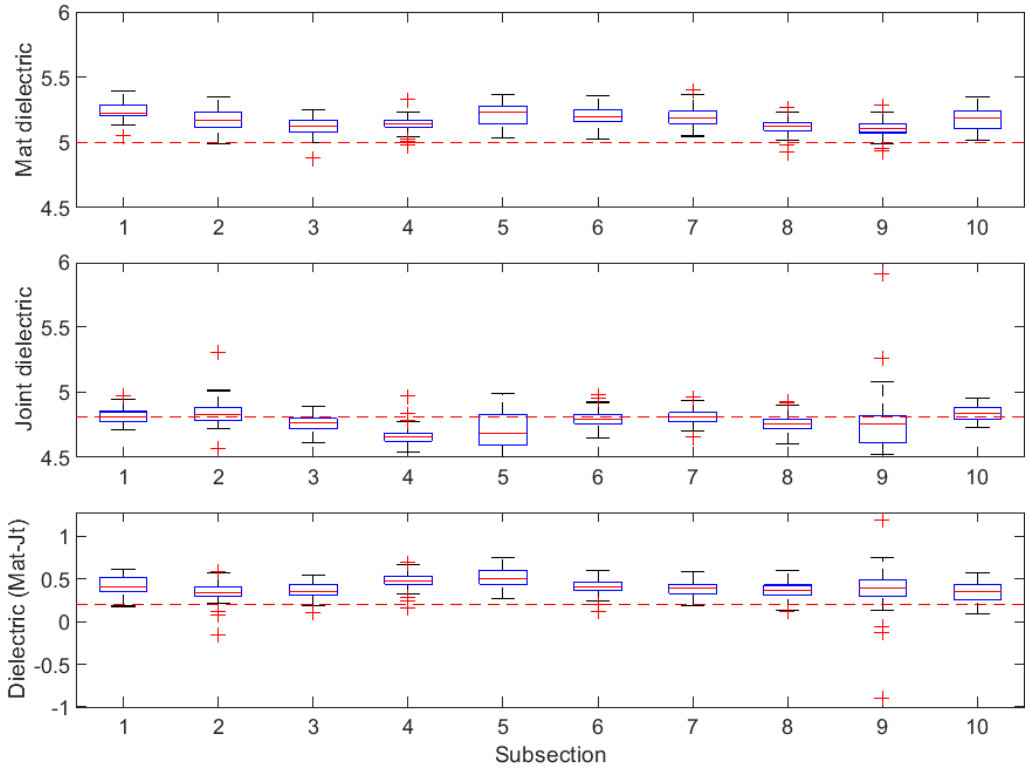

Figure B-50 Box plot of dielectric values for unconfined joint (50 ft subsections) – Xerxes Road #2

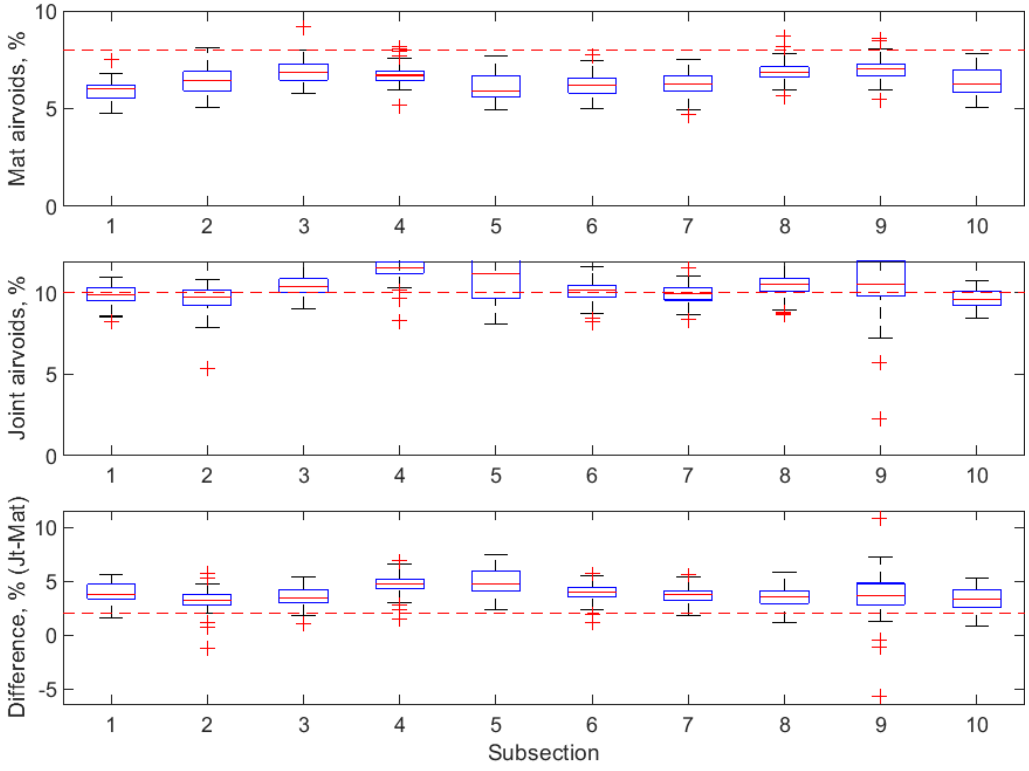

Figure B-51 Box plot of air voids for unconfined joint (50 ft subsections) – Xerxes Road #2

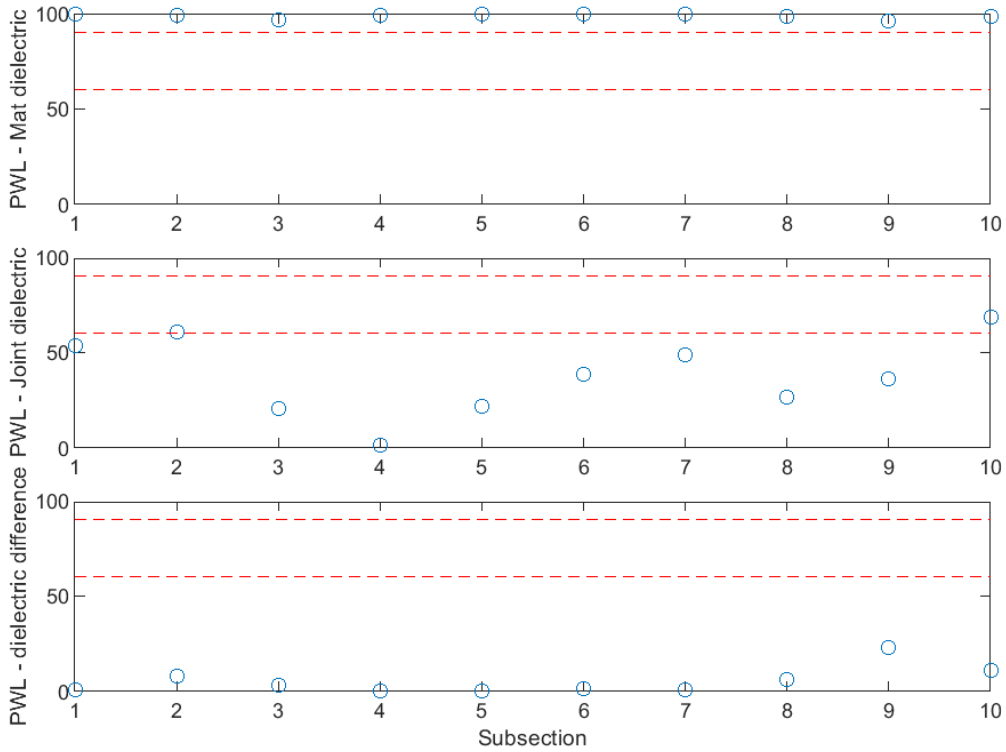

Figure B-52 PWL for dielectric values for unconfined joint (50 ft subsections) – Xerxes Road #2

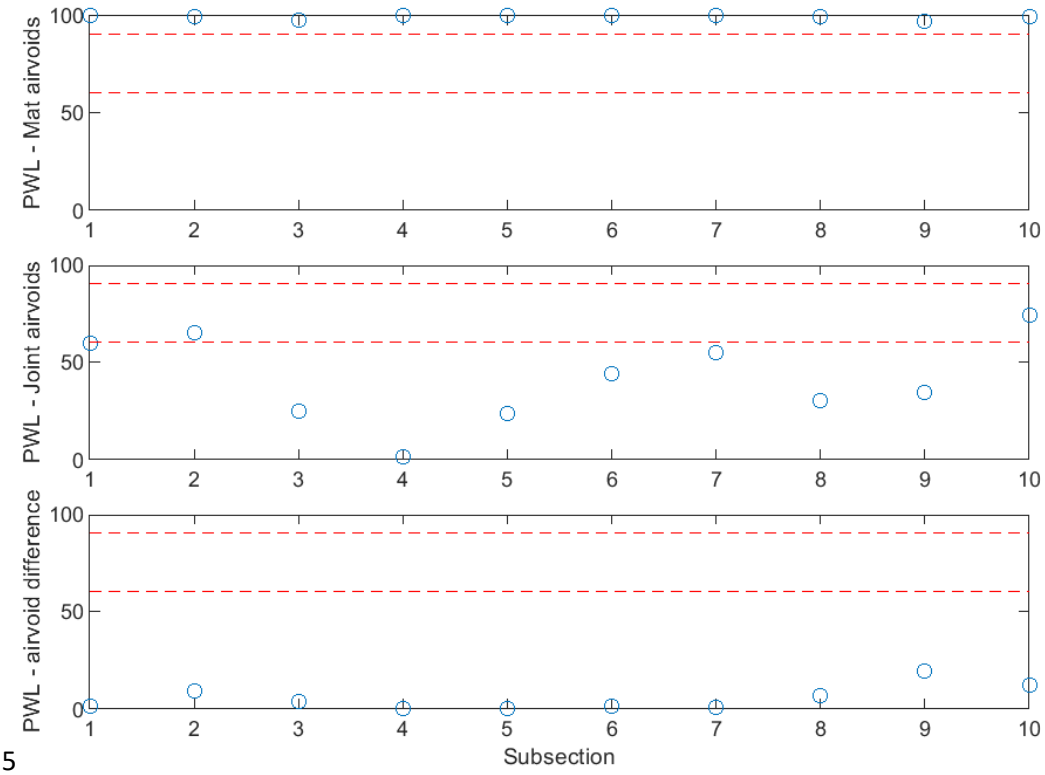

5

Figure B-53 PWL for air voids for unconfined joint (50 ft subsections) – Xerxes Road #2

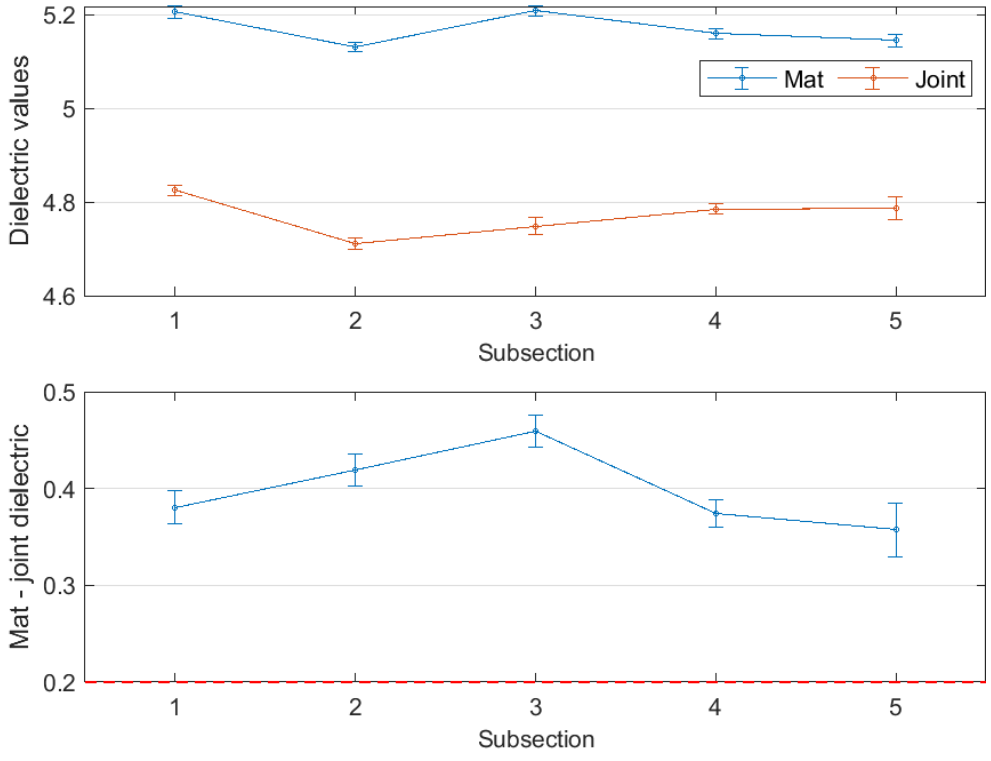

Figure B-54 Interval plot of dielectric values for unconfined joint (100 ft subsections) – Xerxes Road #2

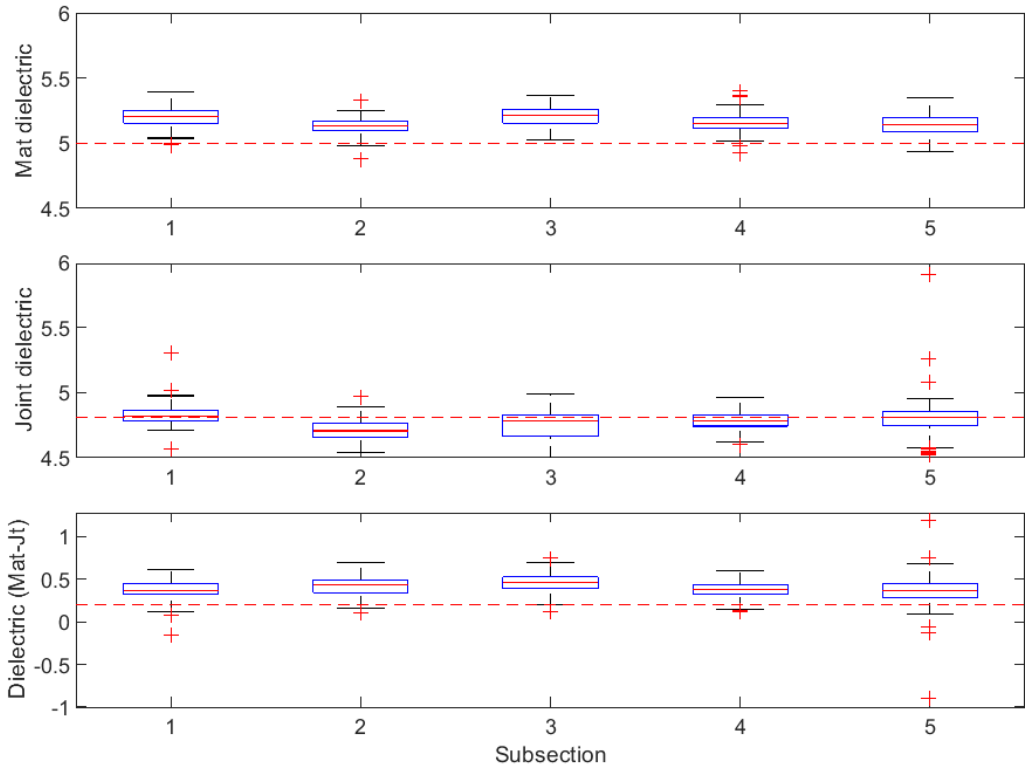

Figure B-55 Box plot of dielectric values for unconfined joint (100 ft subsections) – Xerxes Road #2

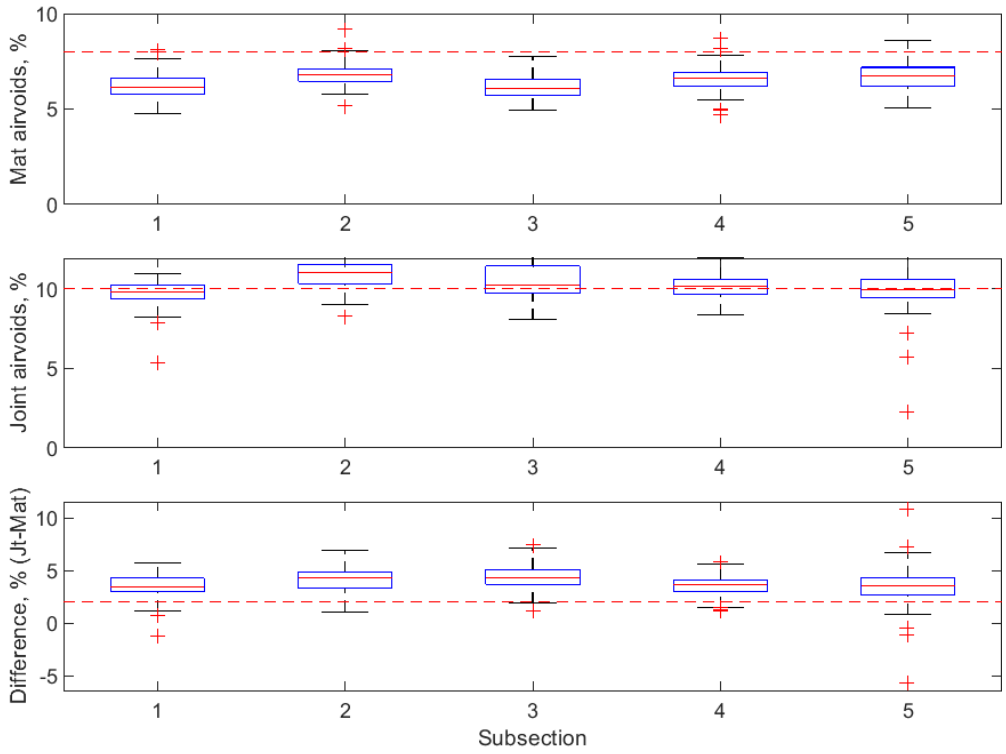

Figure B-56 Box plot of air voids for unconfined joint (100 ft subsections) – Xerxes Road #2

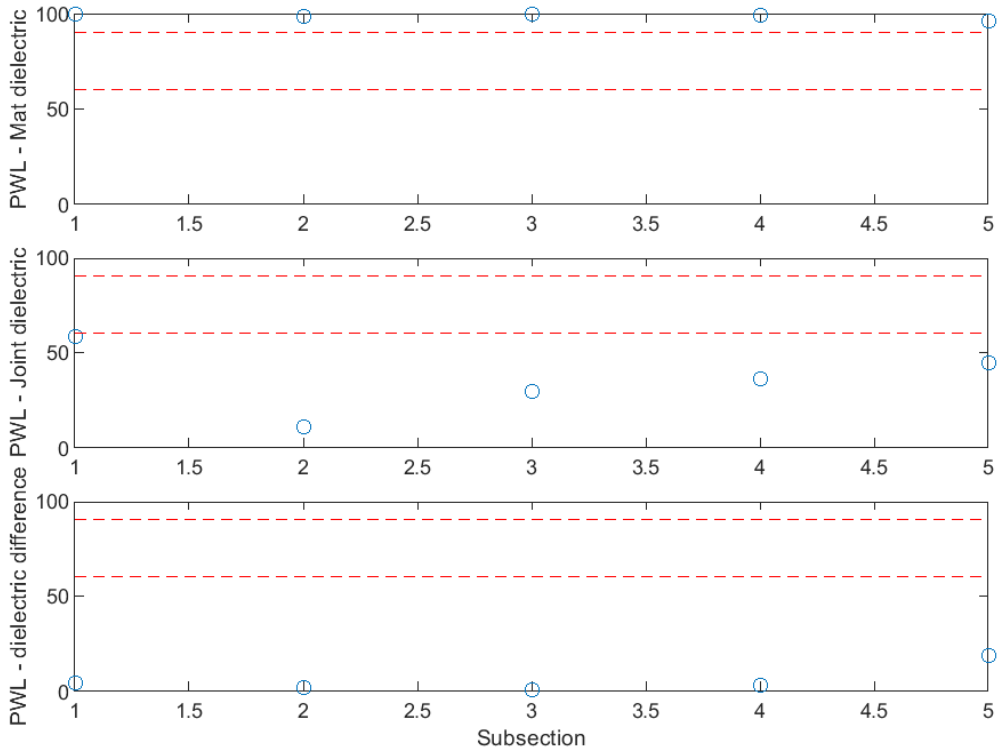

Figure B-57 PWL for dielectric values for unconfined joint (100 ft subsections) – Xerxes Road #2

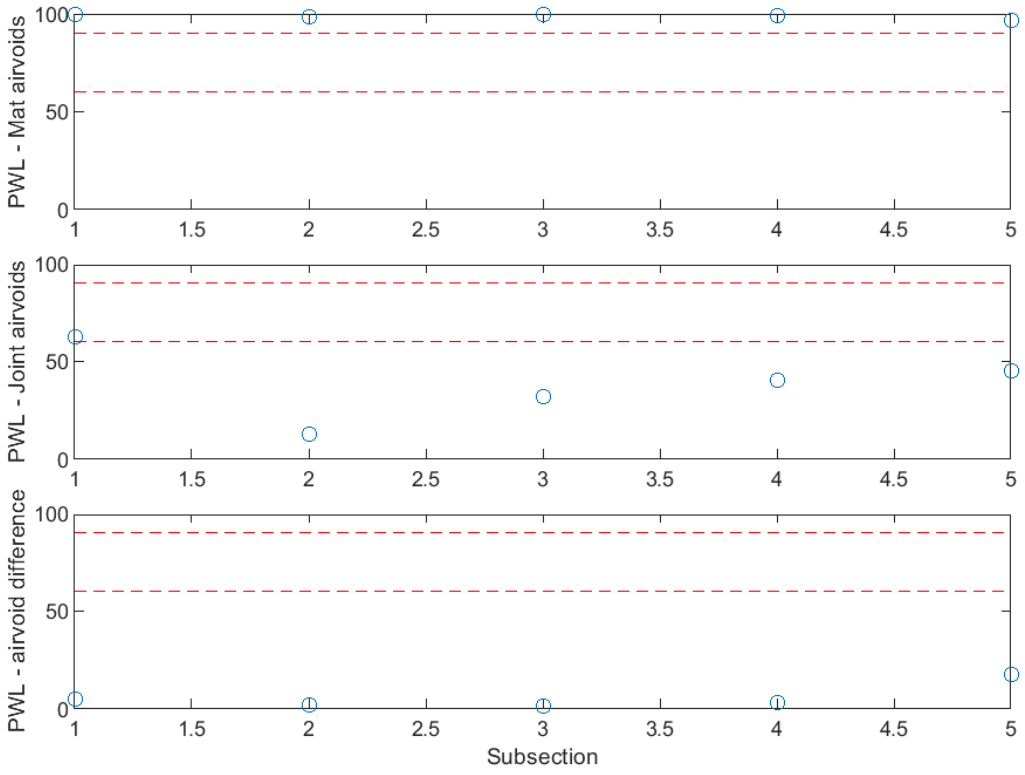

Figure B-58 PWL for air voids for unconfined joint (100 ft subsections) – Xerxes Road #2

Manning Trail #1 Project

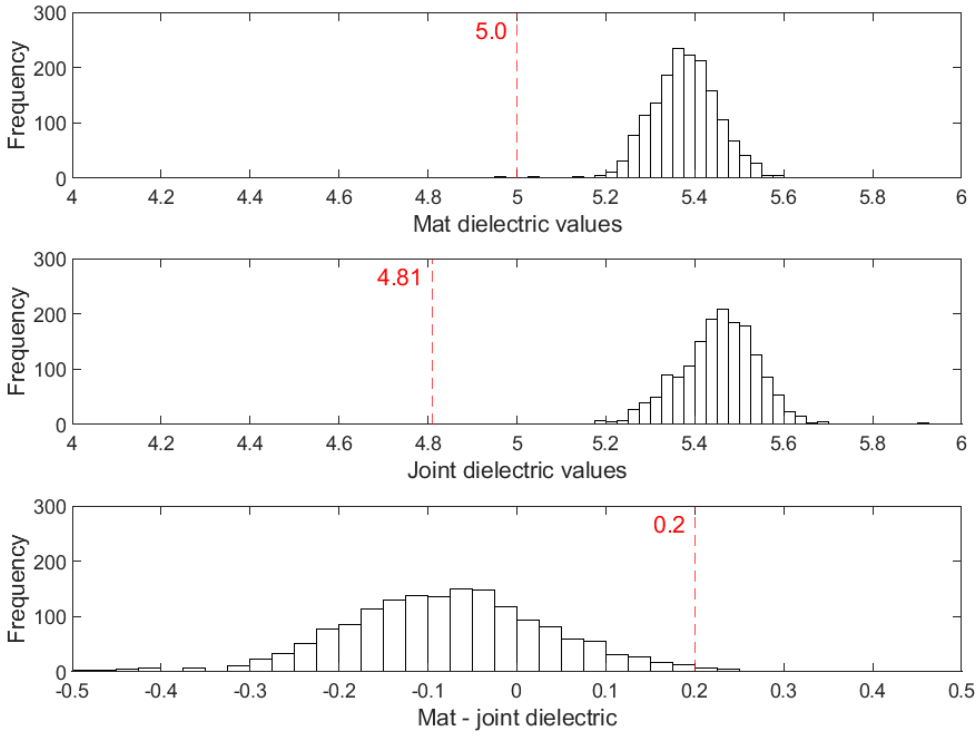

Figure B-59 Histogram of dielectric values for confined joint – Manning Trail #1

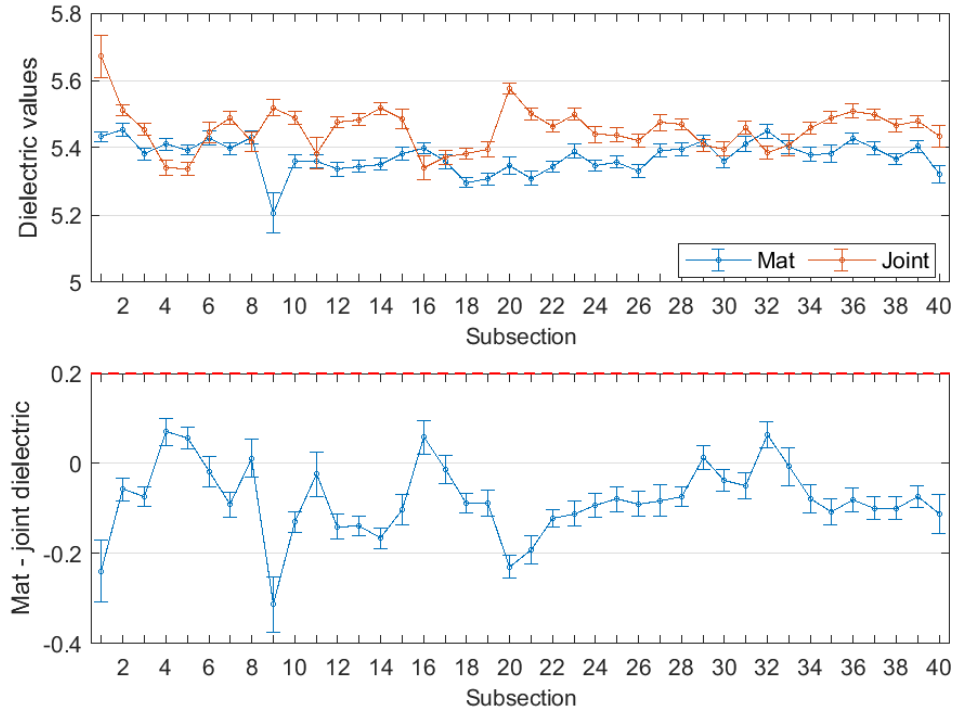

Figure B-60 Interval plot of dielectric values for confined joint (25 ft subsections) – Manning Trail #1

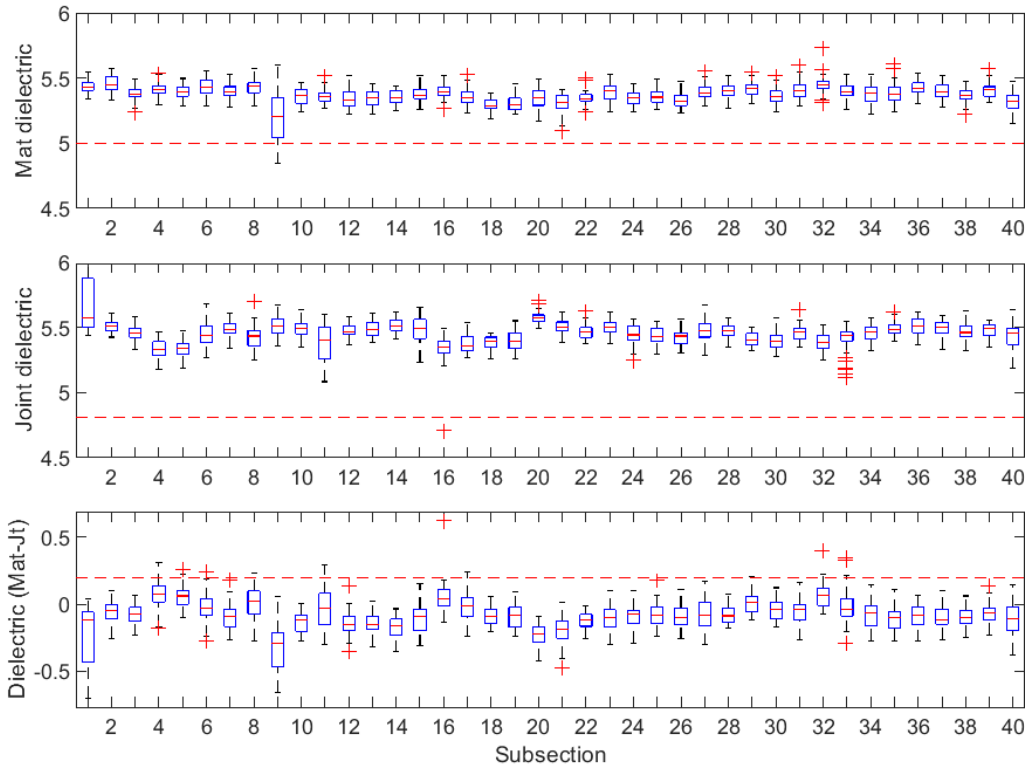

Figure B-61 Box plot of dielectric values for confined joint (25 ft subsections) – Manning Trail #1

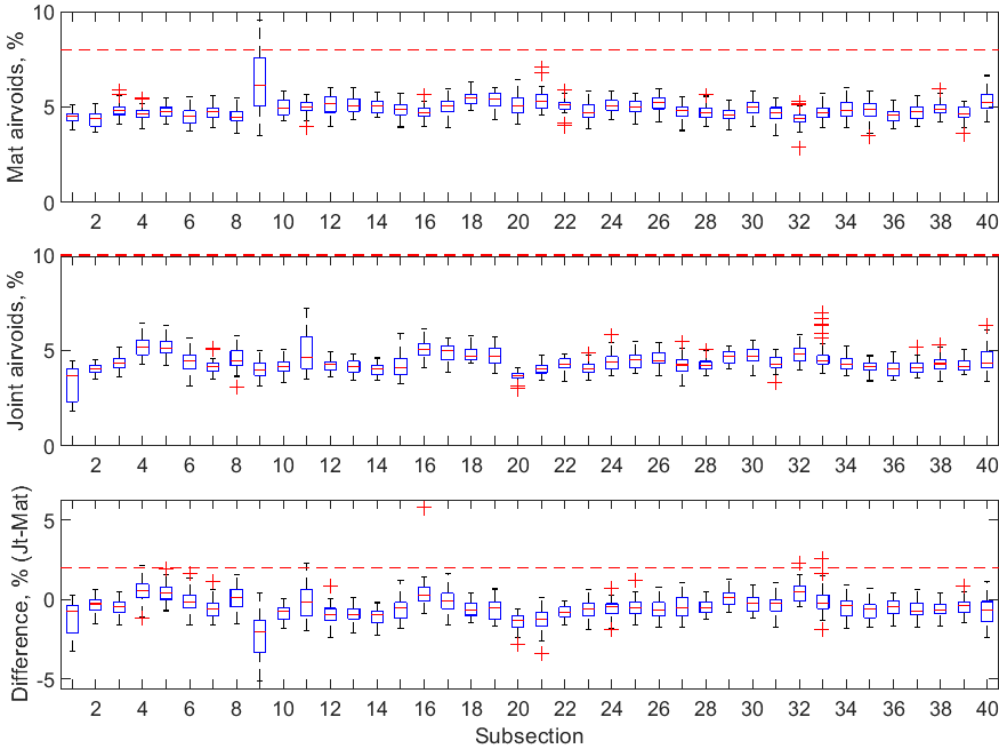

Figure B-62 Box plot of air voids for confined joint (25 ft subsections) – Manning Trail #1

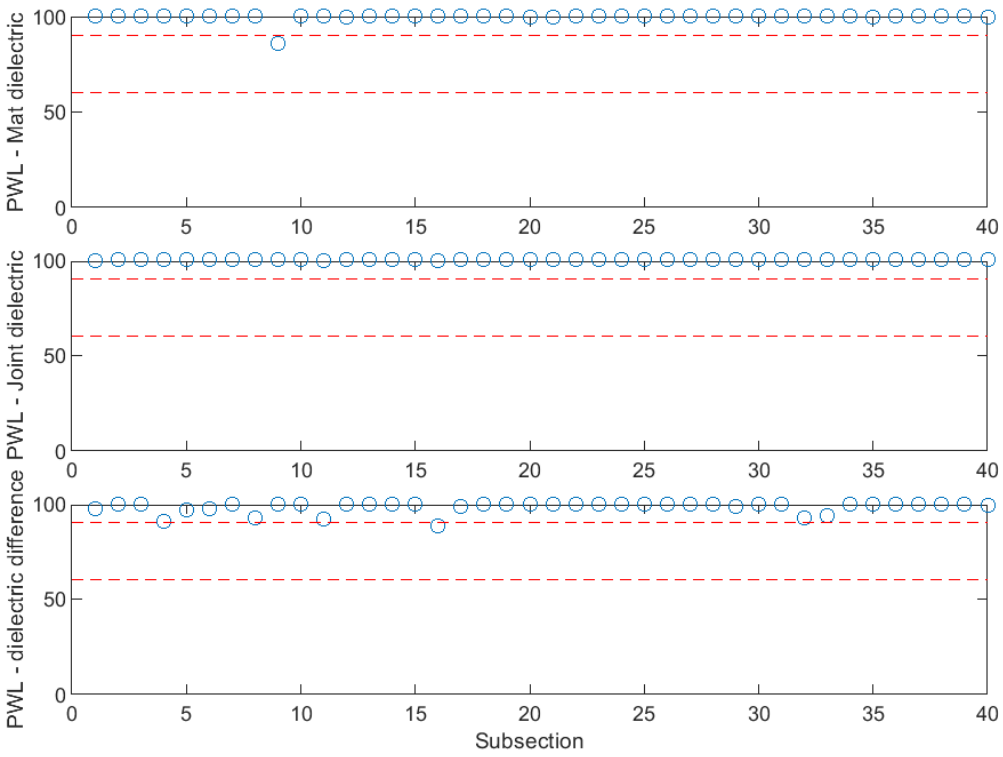

Figure B-63 PWL for dielectric values for confined joint (25 ft subsections) – Manning Trail #1

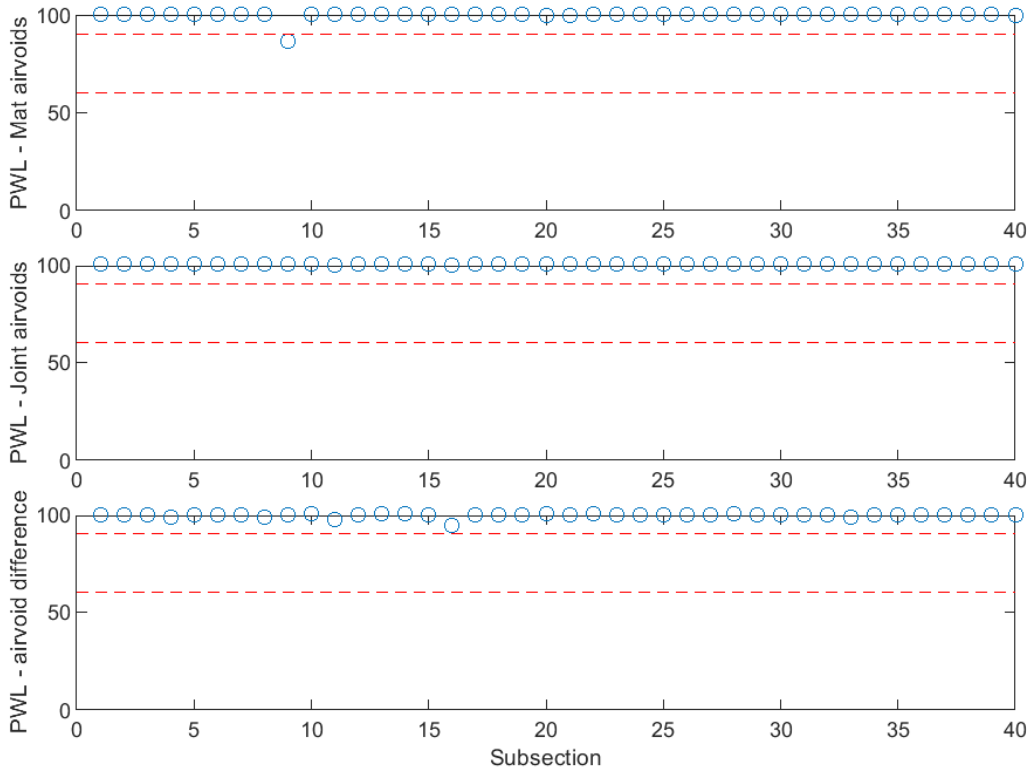

Figure B-64 PWL for air voids for confined joint (25 ft subsections) – Manning Trail #1

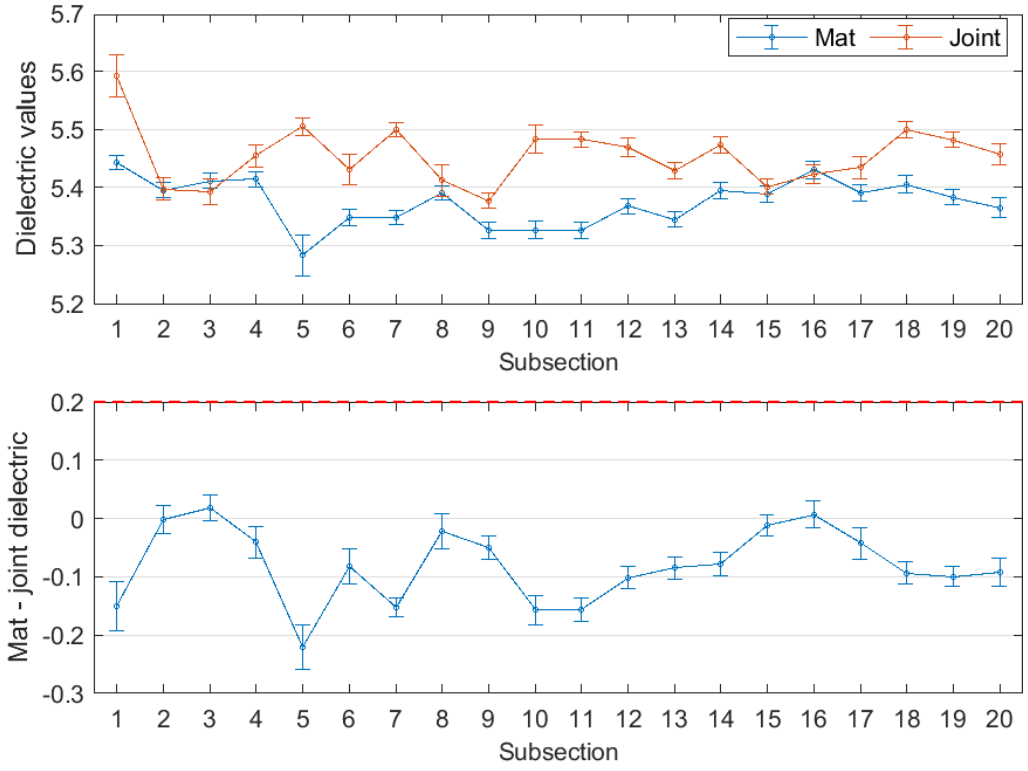

Figure B-65 Interval plot of dielectric values for confined joint (50 ft subsections) – Manning Trail #1

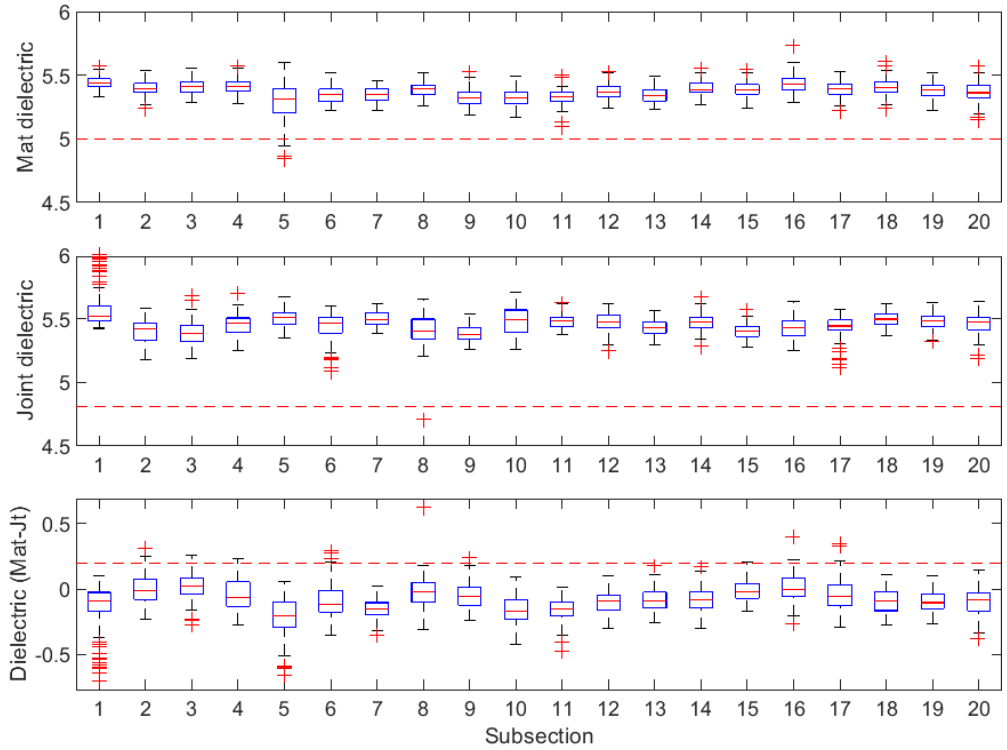

Figure B-66 Box plot of dielectric values for confined joint (50 ft subsections) – Manning Trail #1

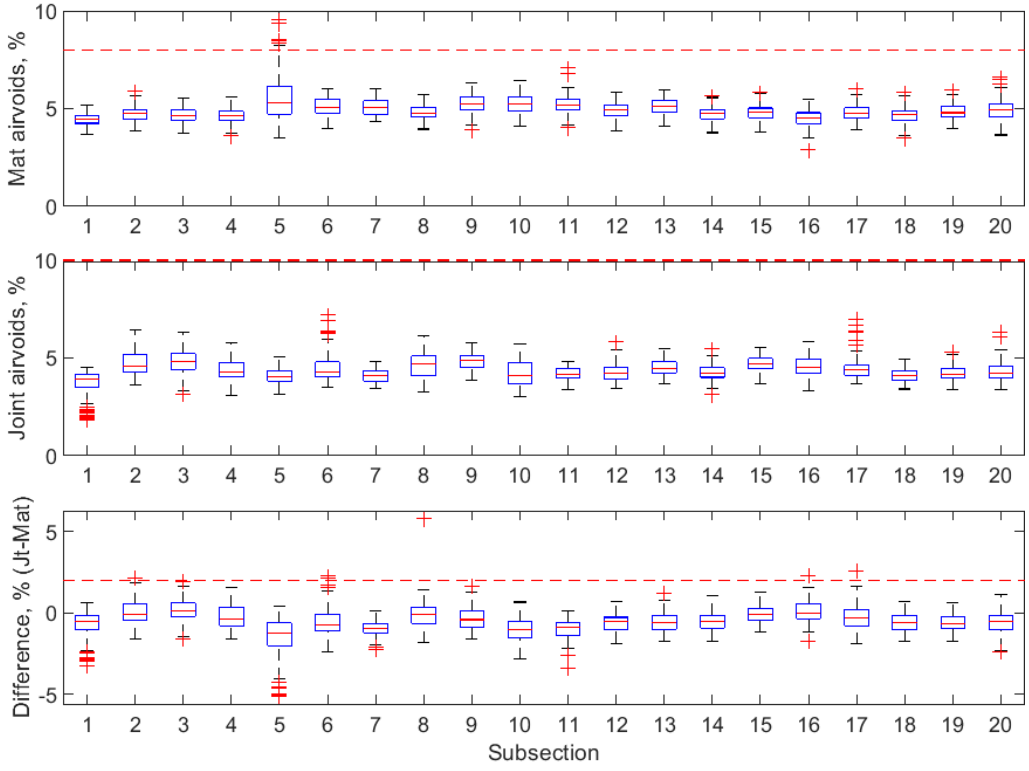

Figure B-67 Box plot of air voids for confined joint (50 ft subsections) – Manning Trail #1

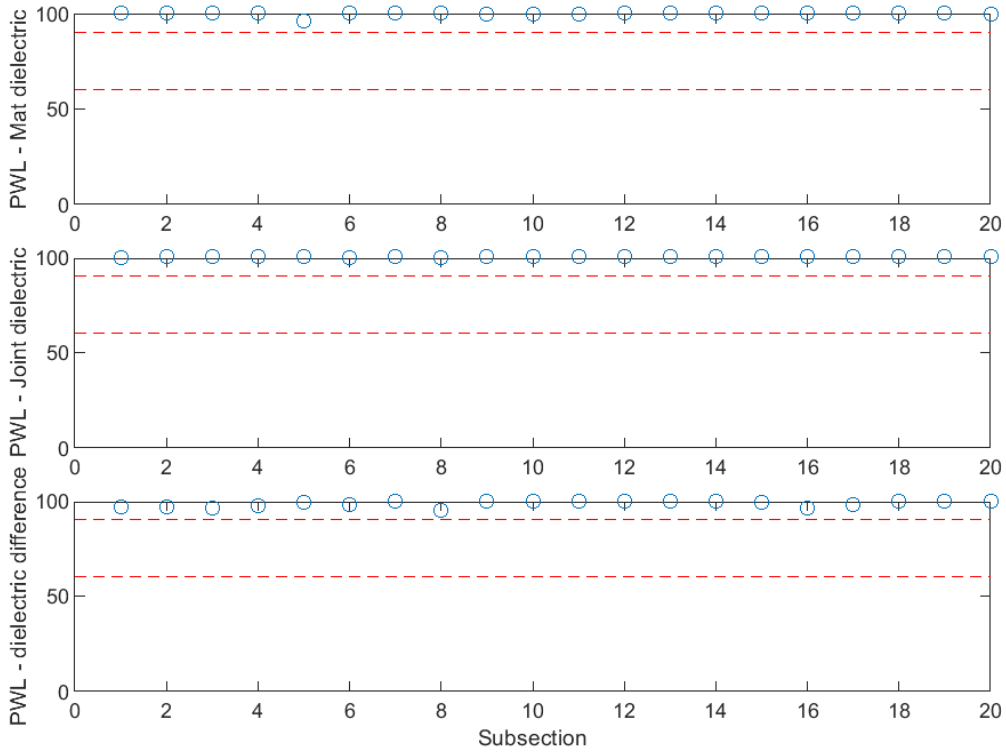

Figure B-68 PWL for dielectric values for confined joint (50 ft subsections) – Manning Trail #1

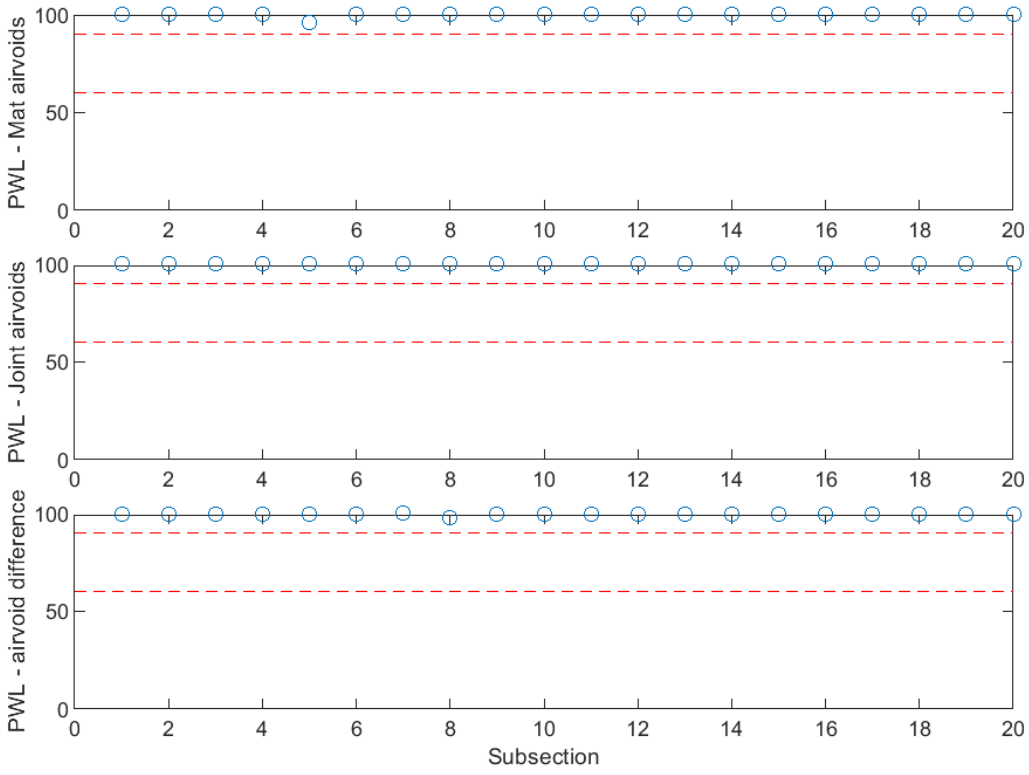

Figure B-69 PWL for air voids for confined joint (50 ft subsections) – Manning Trail #1

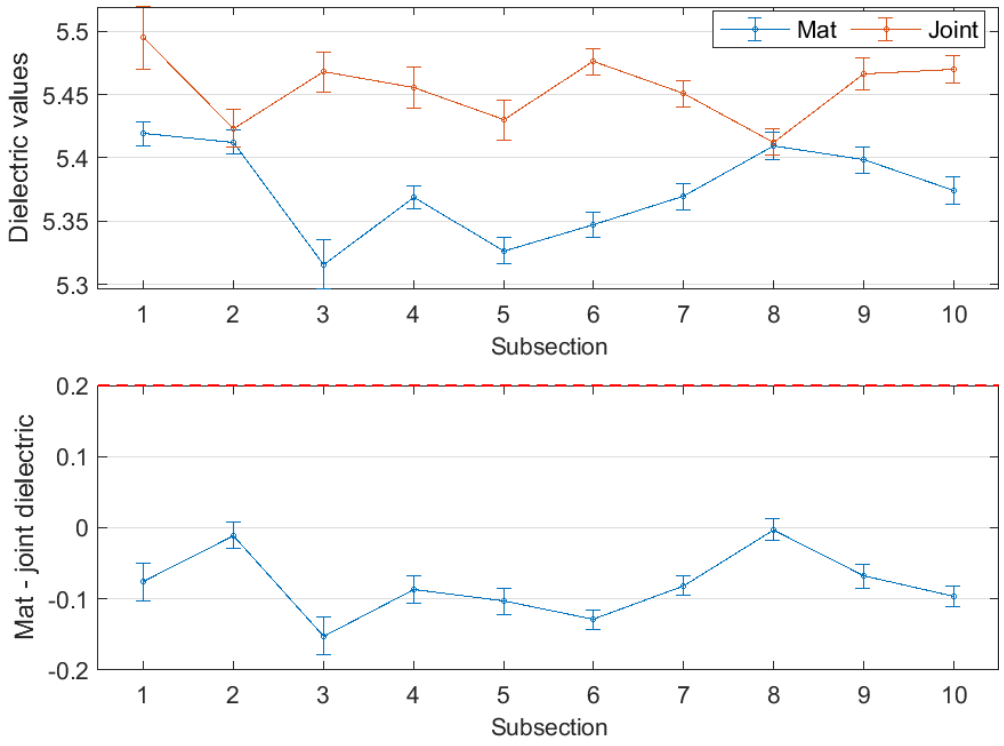

Figure B-70 Interval plot of dielectric values for confined joint (100 ft subsections) – Manning Trail #1

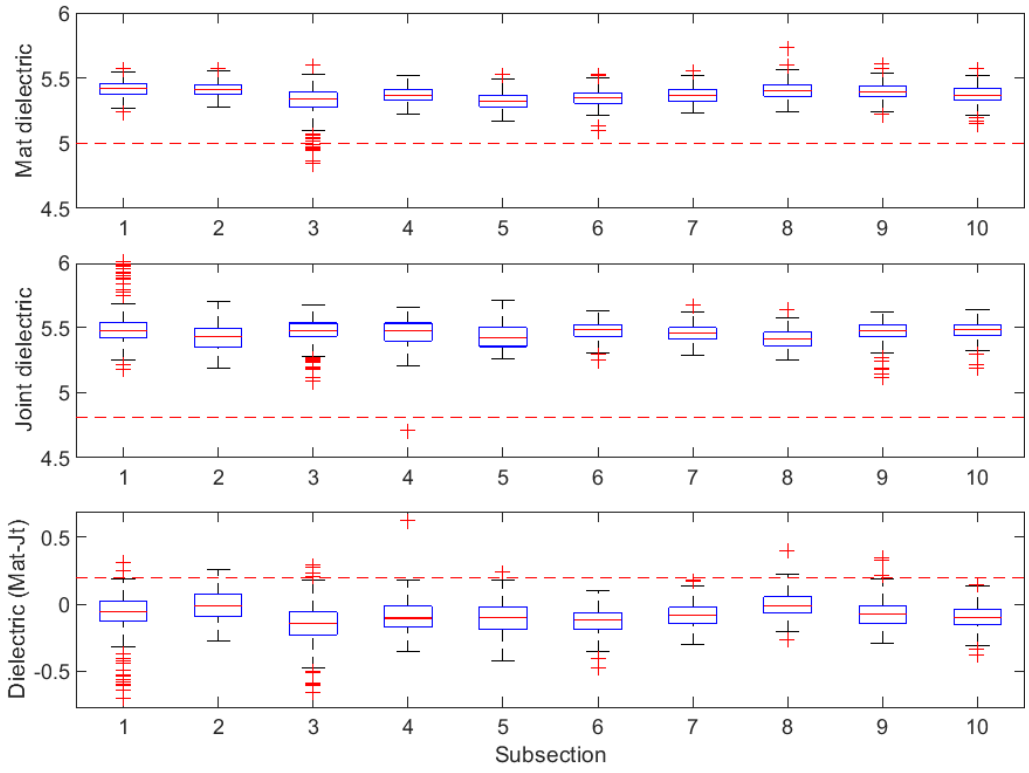

Figure B-71 Box plot of dielectric values for confined joint (100 ft subsections) – Manning Trail #1

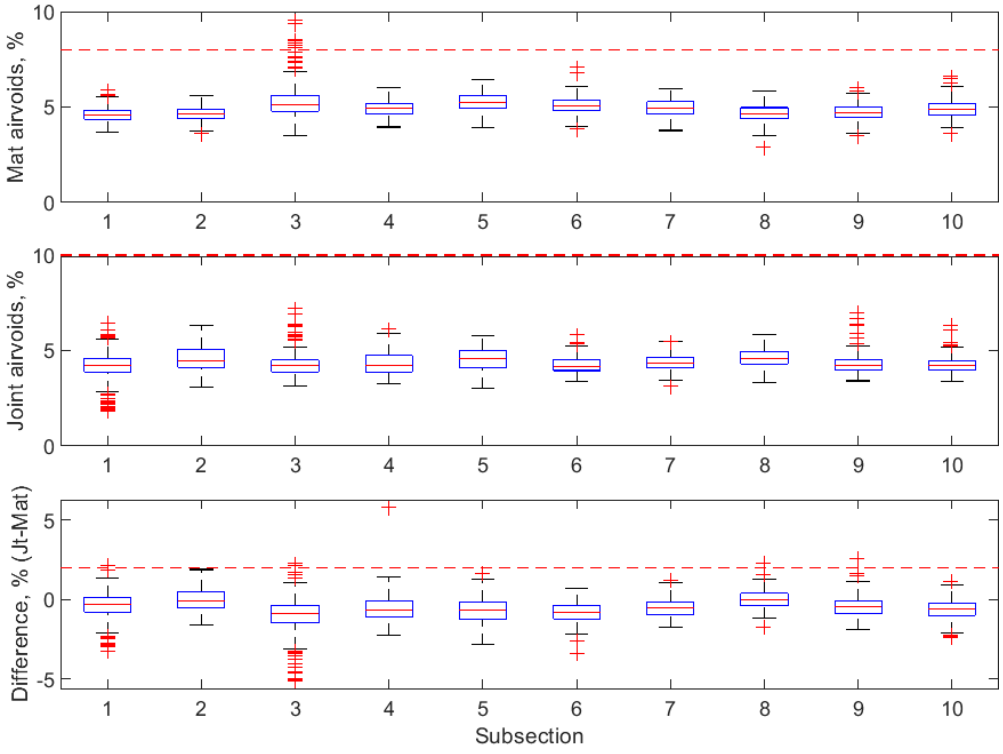

Figure B-72 Box plot of air voids for confined joint (100 ft subsections) – Manning Trail #1

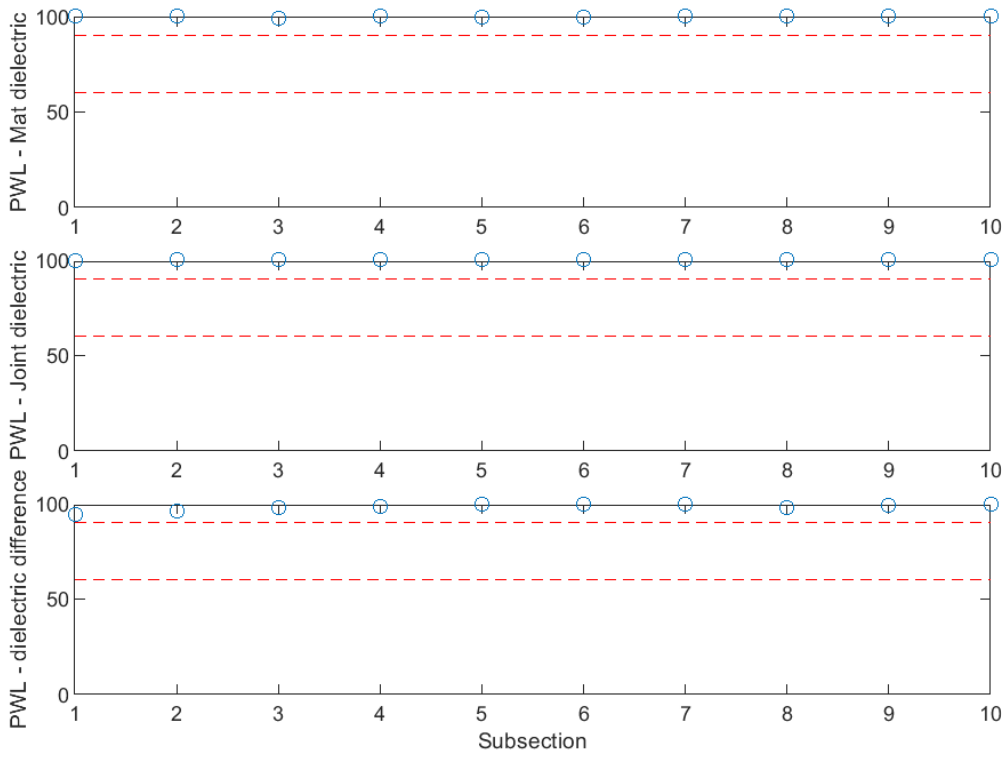

Figure B-73 PWL for dielectric values for confined joint (100 ft subsections) – Manning Trail #1

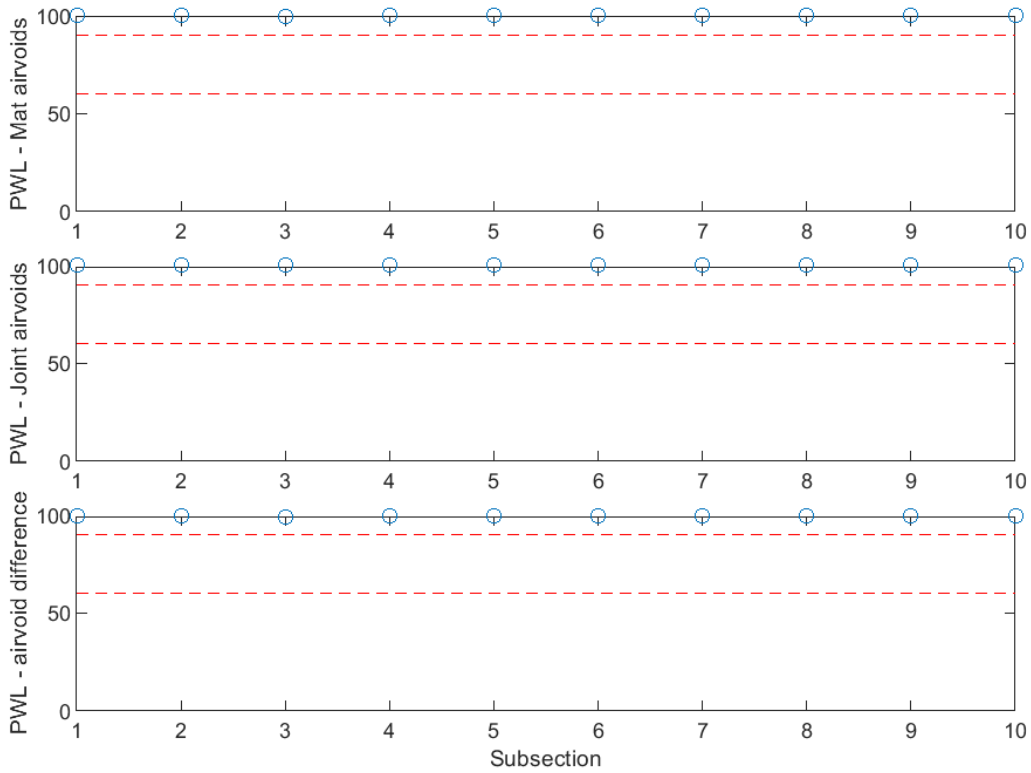

Figure B-74 PWL for air voids for confined joint (100 ft subsections) – Manning Trail #1

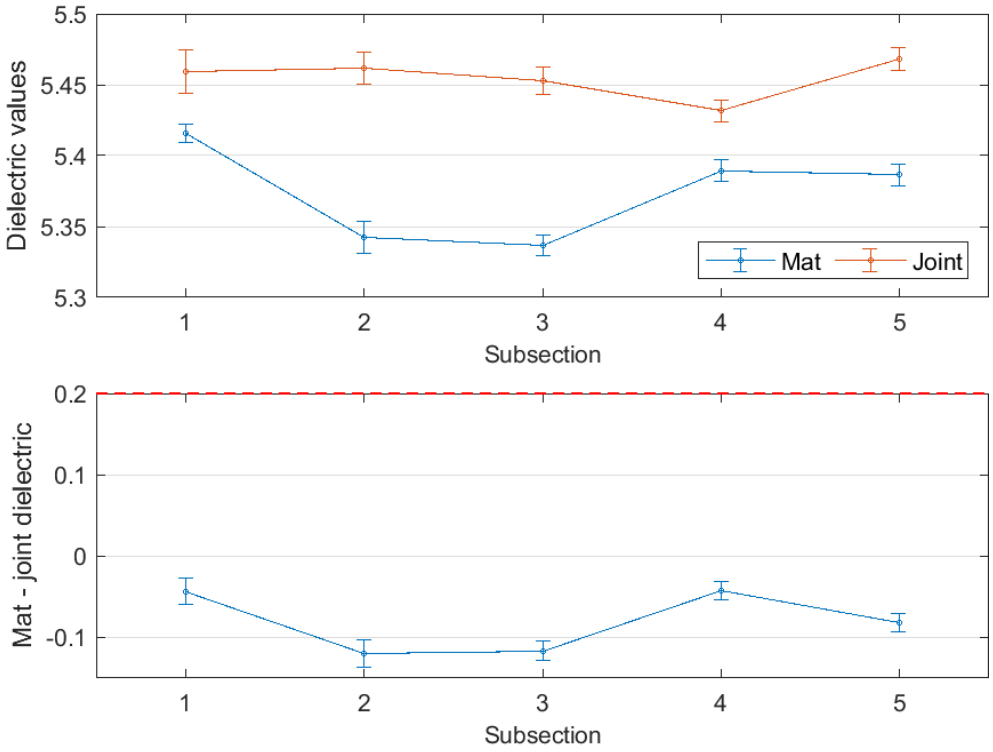

Figure B-75 Interval plot of dielectric values for confined joint (200 ft subsections) – Manning Trail #1

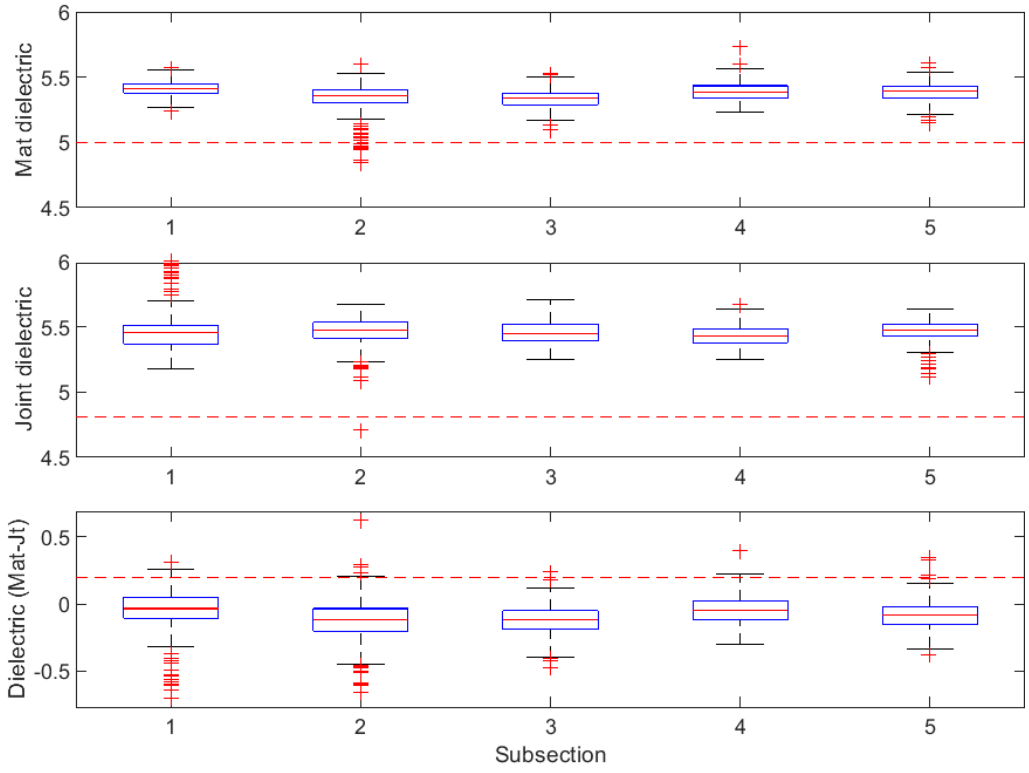

Figure B-76 Box plot of dielectric values for confined joint (200 ft subsections) – Manning Trail #1

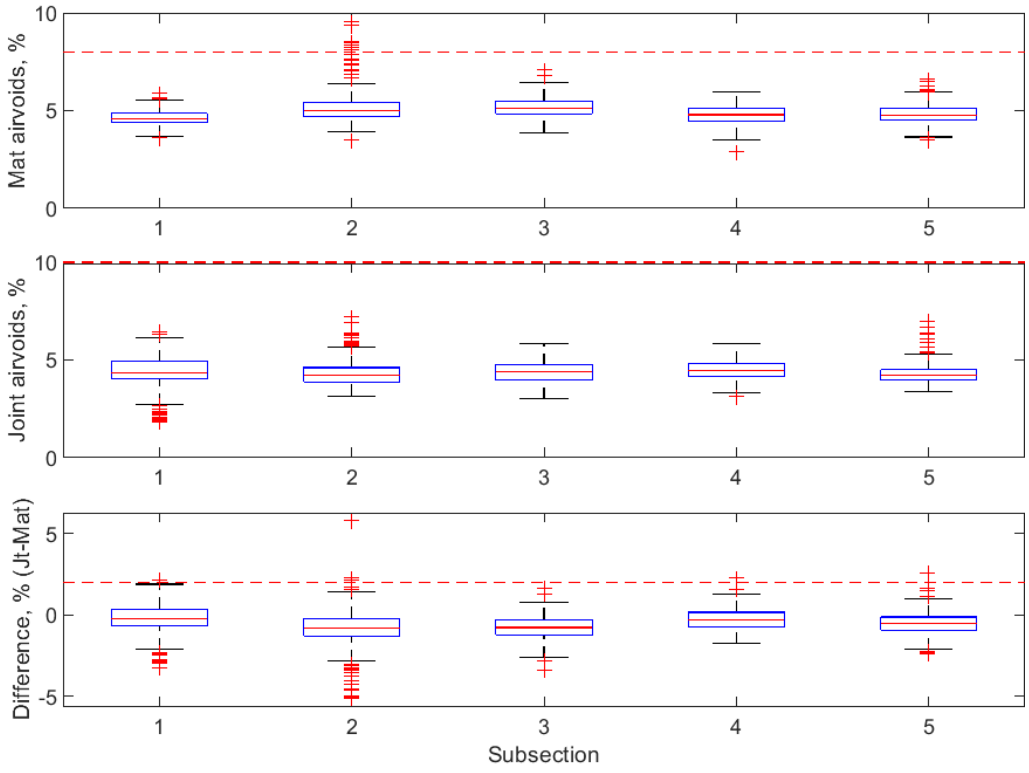

Figure B-77 Box plot of air voids for confined joint (200 ft subsections) – Manning Trail #1

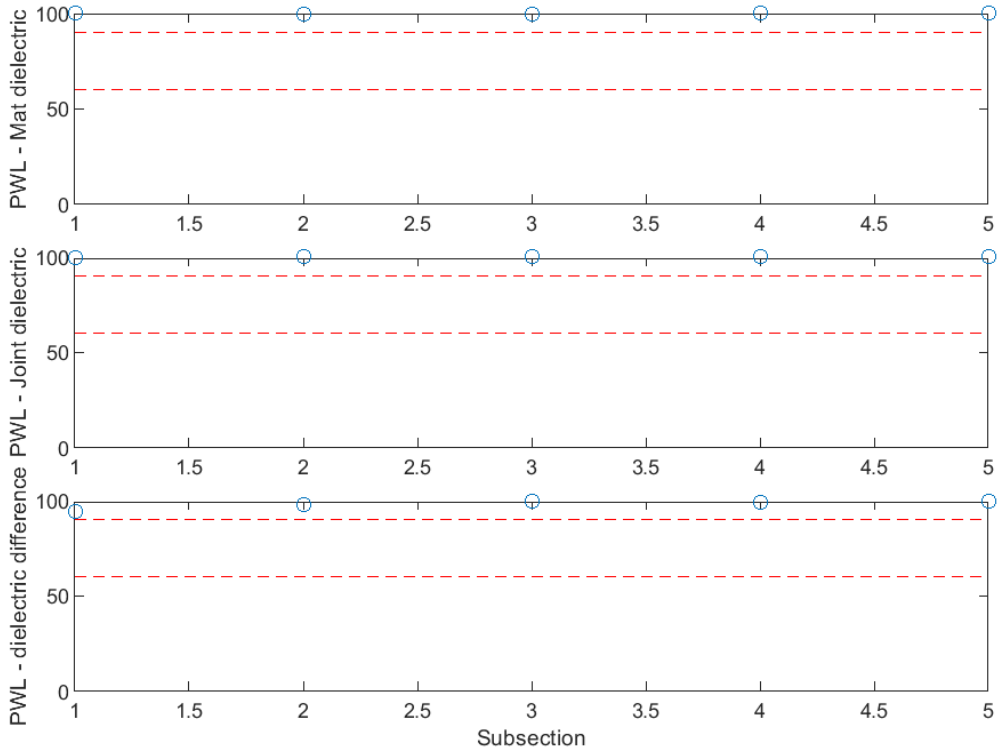

Figure B-78 PWL for dielectric values for confined joint (200 ft subsections) – Manning Trail #1

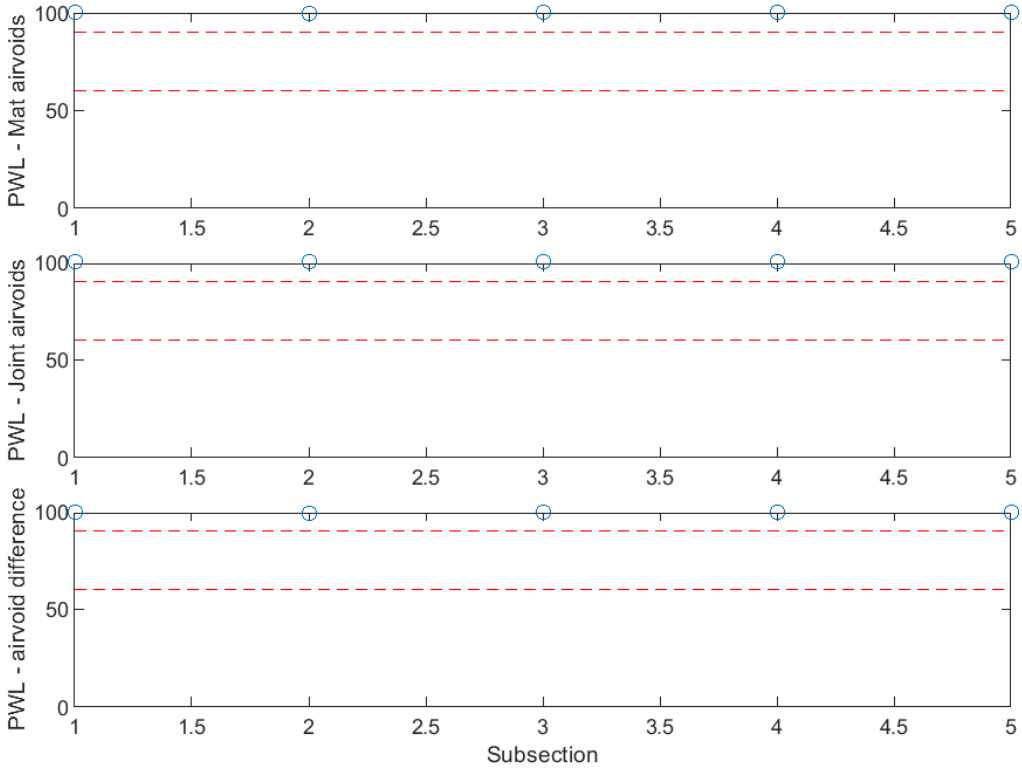

Figure B-79 PWL for air voids for confined joint (200 ft subsections) – Manning Trail #1

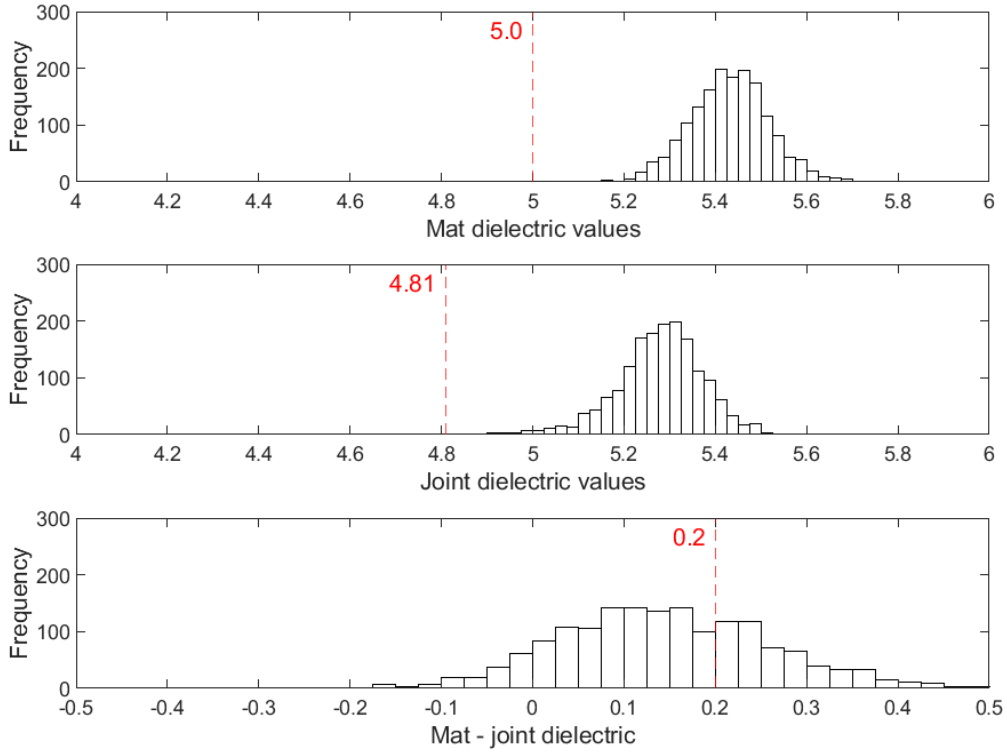

Figure B-80 Histogram of dielectric values for echelon joint – Manning Trail #1

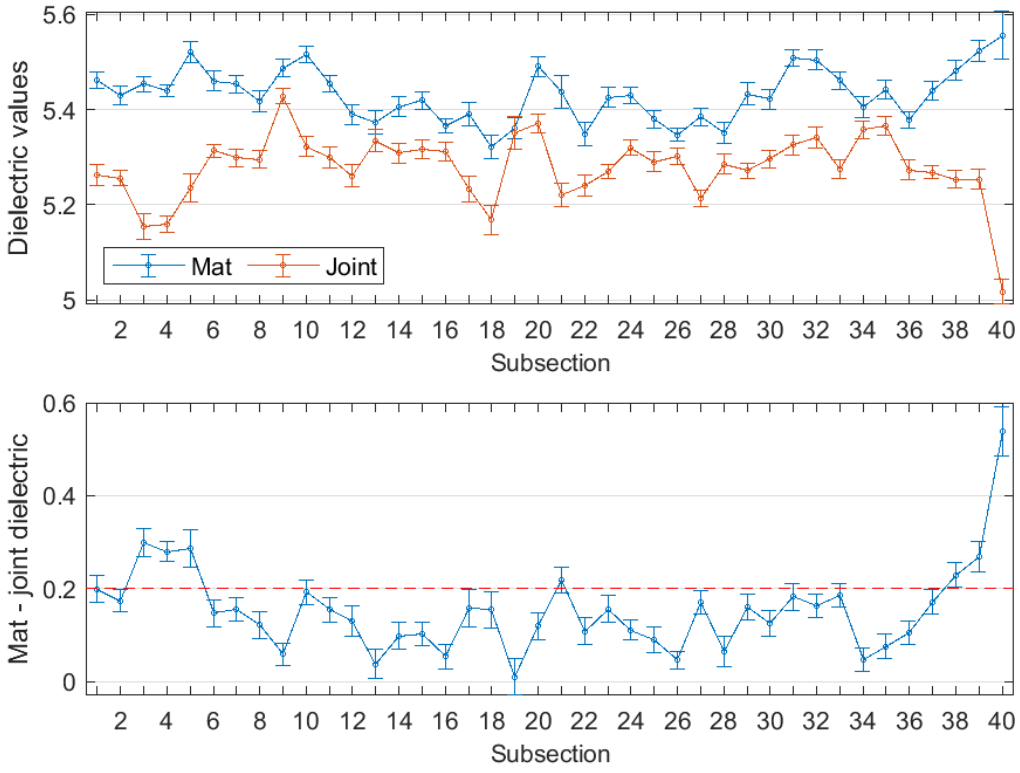

Figure B-81 Interval plot of dielectric values for echelon joint (25 ft subsections) – Manning Trail #1

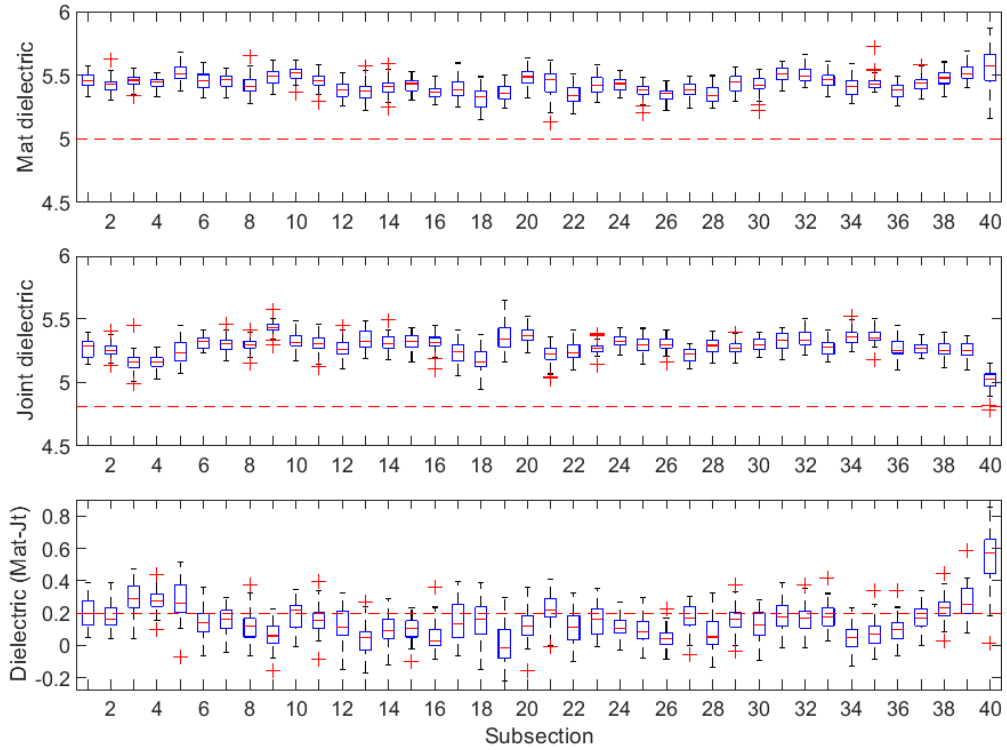

Figure B-82 Box plot of dielectric values for echelon joint (25 ft subsections) – Manning Trail #1

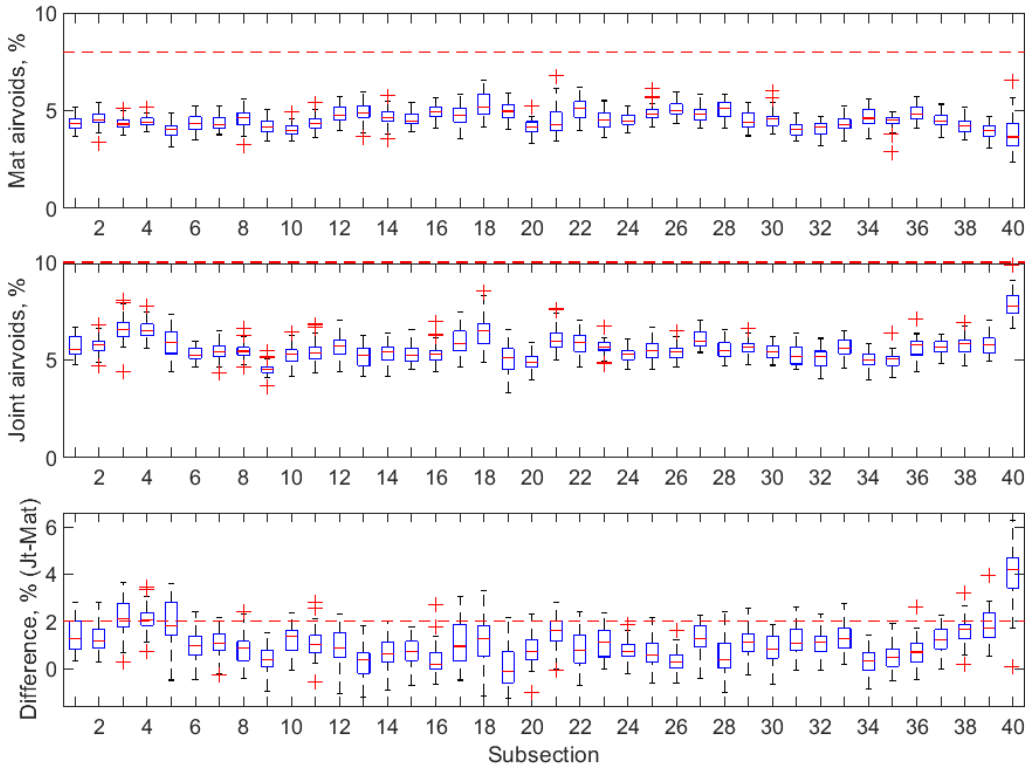

Figure B-83 Box plot of air voids for echelon joint (25 ft subsections) – Manning Trail #1

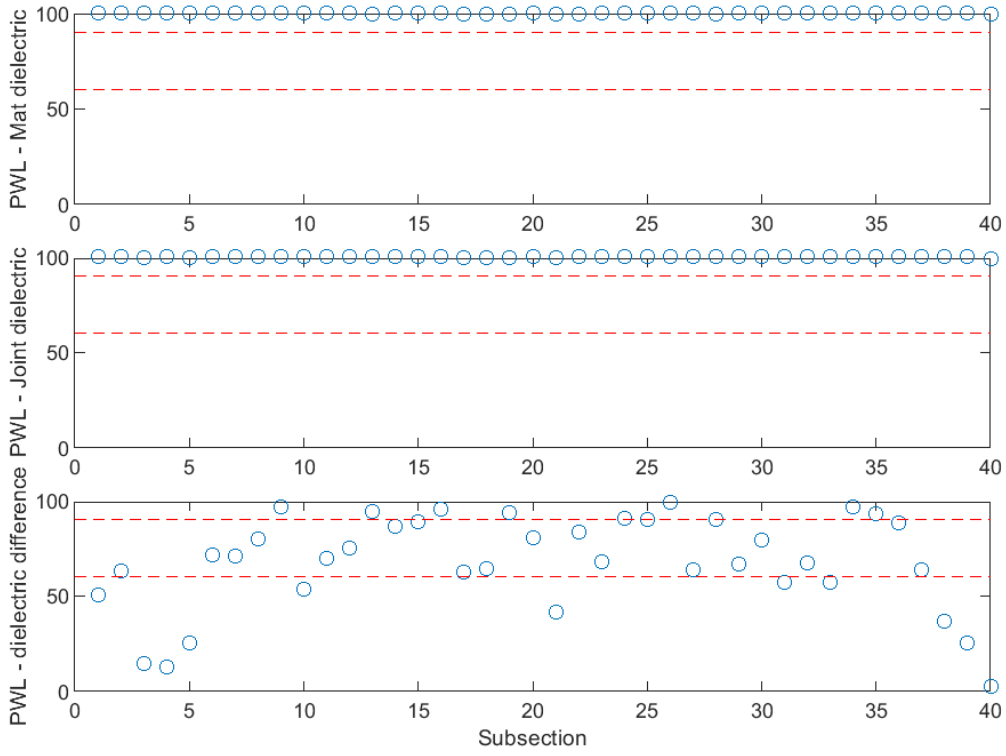

Figure B-84 PWL for dielectric values for echelon joint (25 ft subsections) – Manning Trail #1

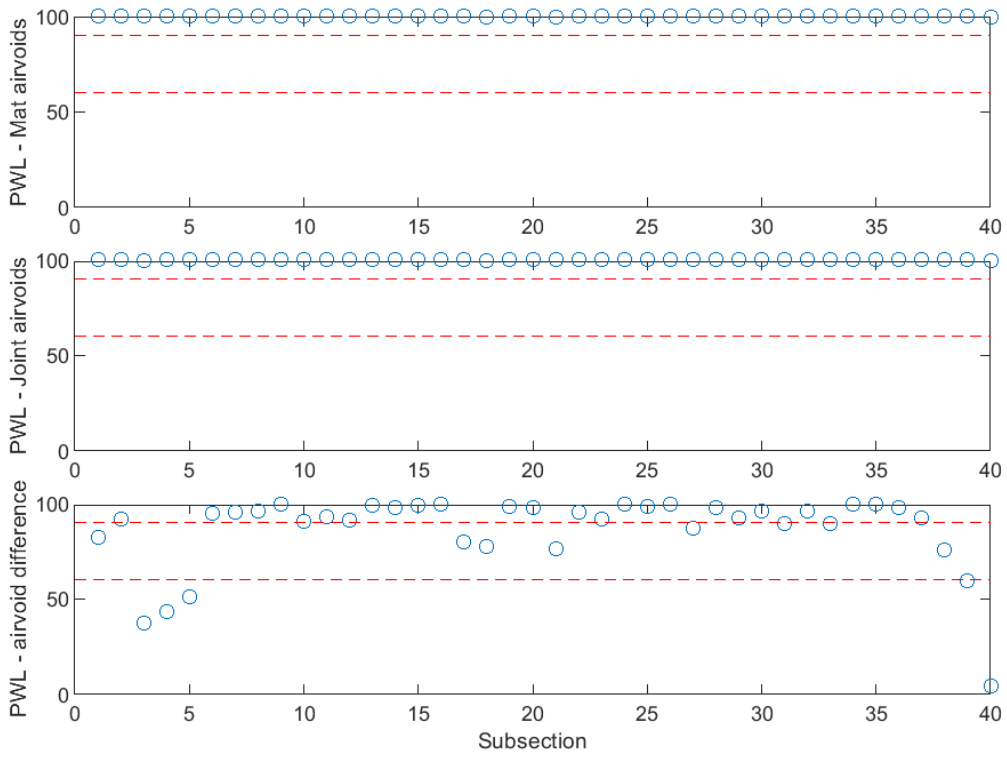

Figure B-85 PWL for air voids for echelon joint (25 ft subsections) – Manning Trail #1

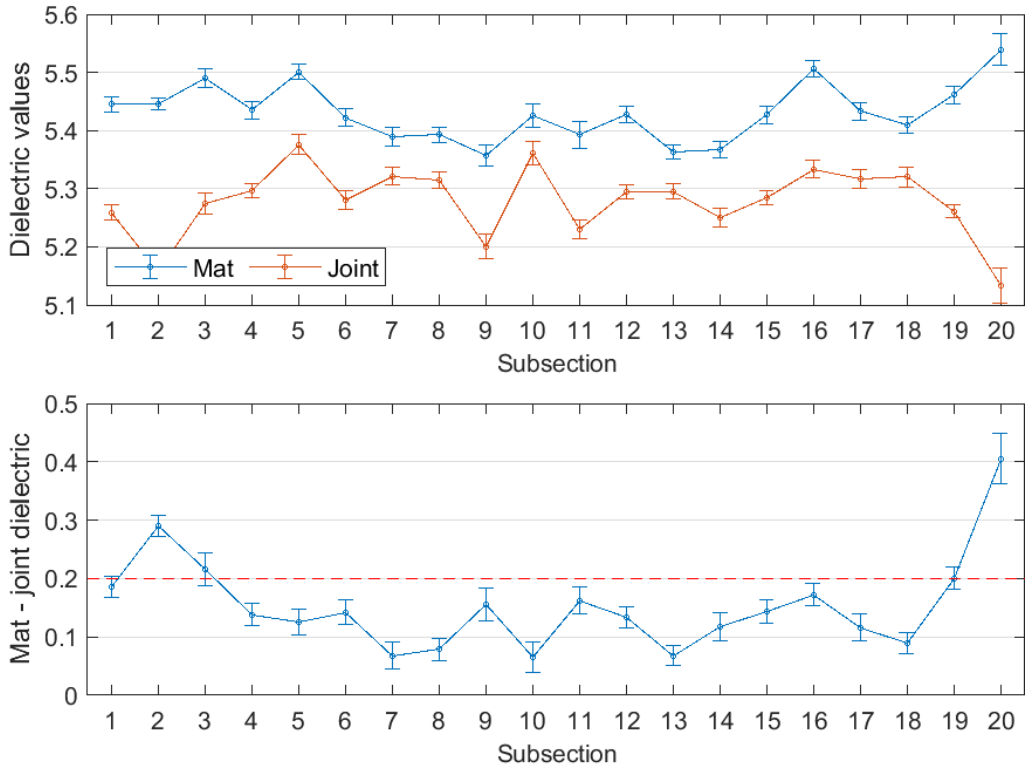

Figure B-86 Interval plot of dielectric values for echelon joint (50 ft subsections) – Manning Trail #1

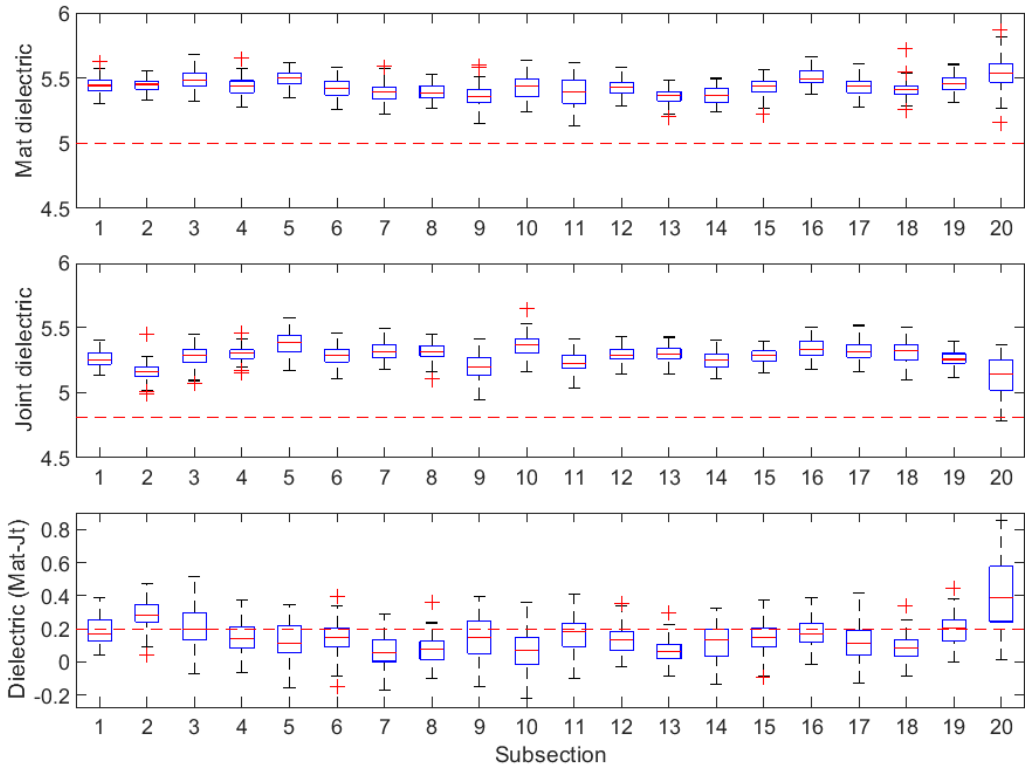

Figure B-87 Box plot of dielectric values for echelon joint (50 ft subsections) – Manning Trail #1

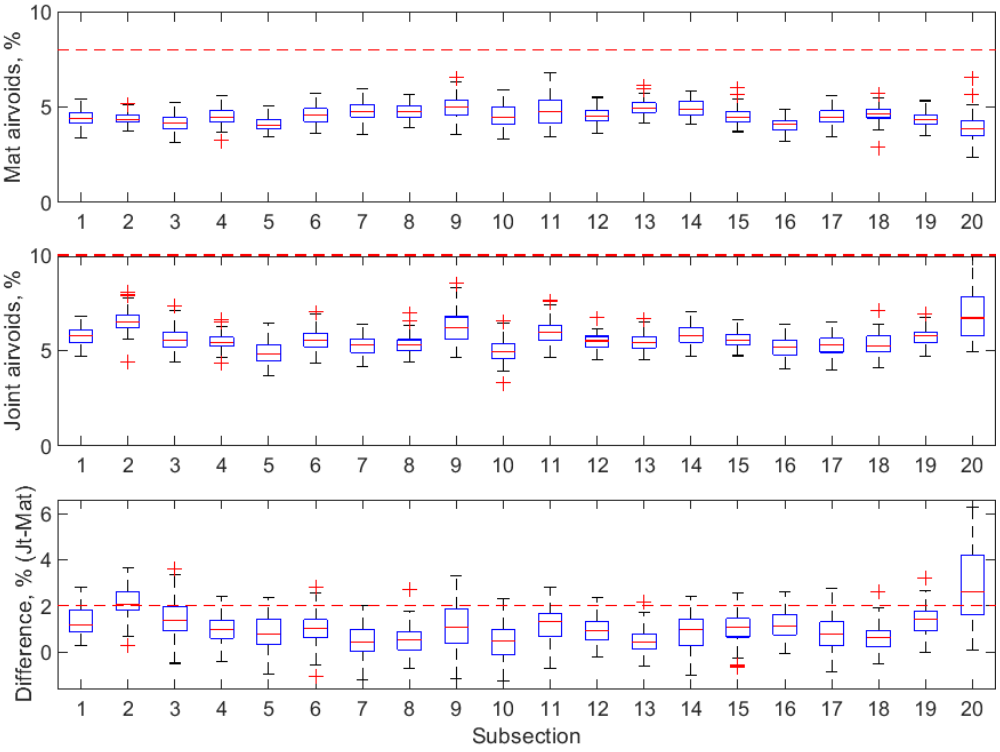

Figure B-88 Box plot of air voids for echelon joint (50 ft subsections) – Manning Trail #1

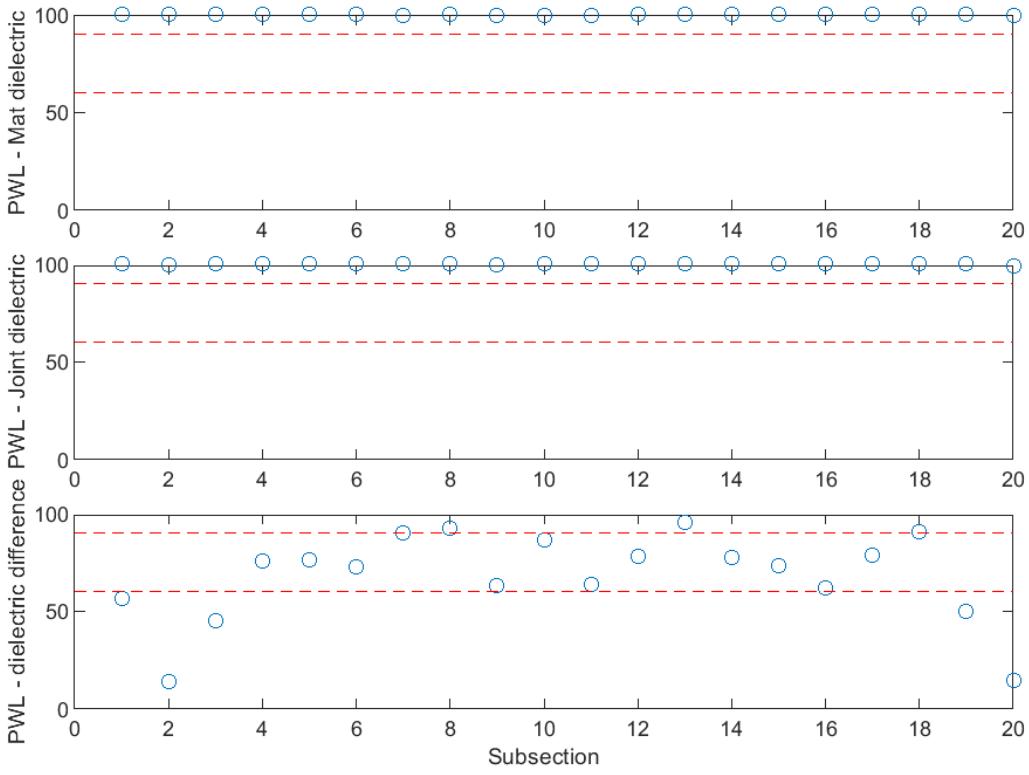

Figure B-89 PWL for dielectric values for echelon joint (50 ft subsections) – Manning Trail #1

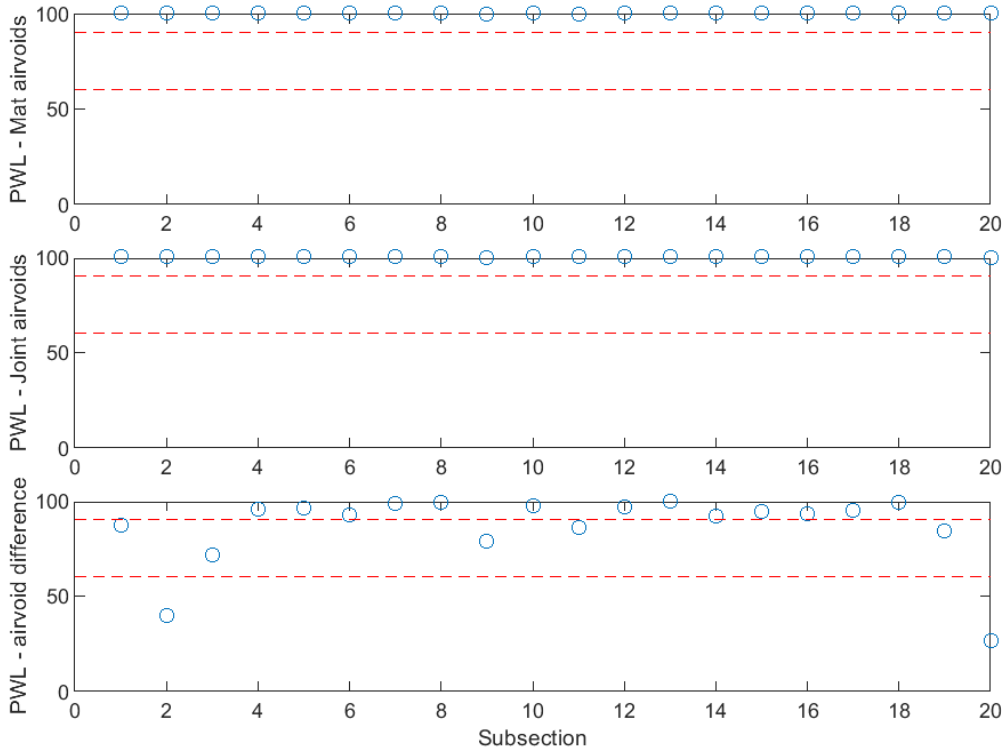

Figure B-90 PWL for air voids for echelon joint (50 ft subsections) – Manning Trail #1

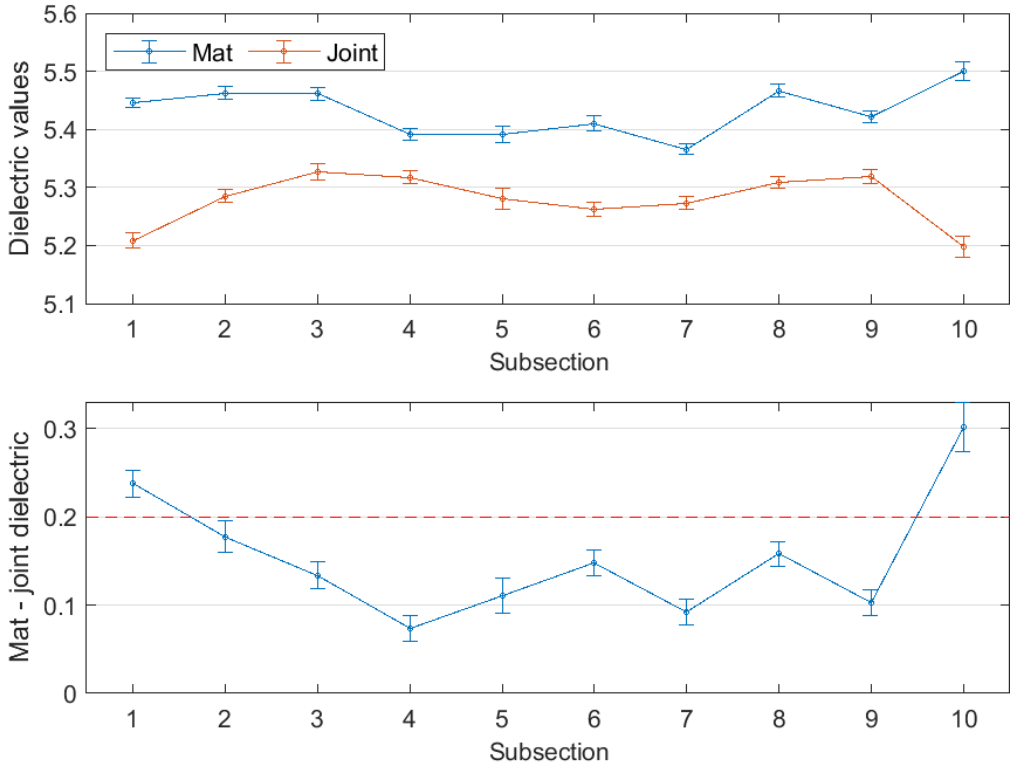

Figure B-91 Interval plot of dielectric values for echelon joint (100 ft subsections) – Manning Trail #1

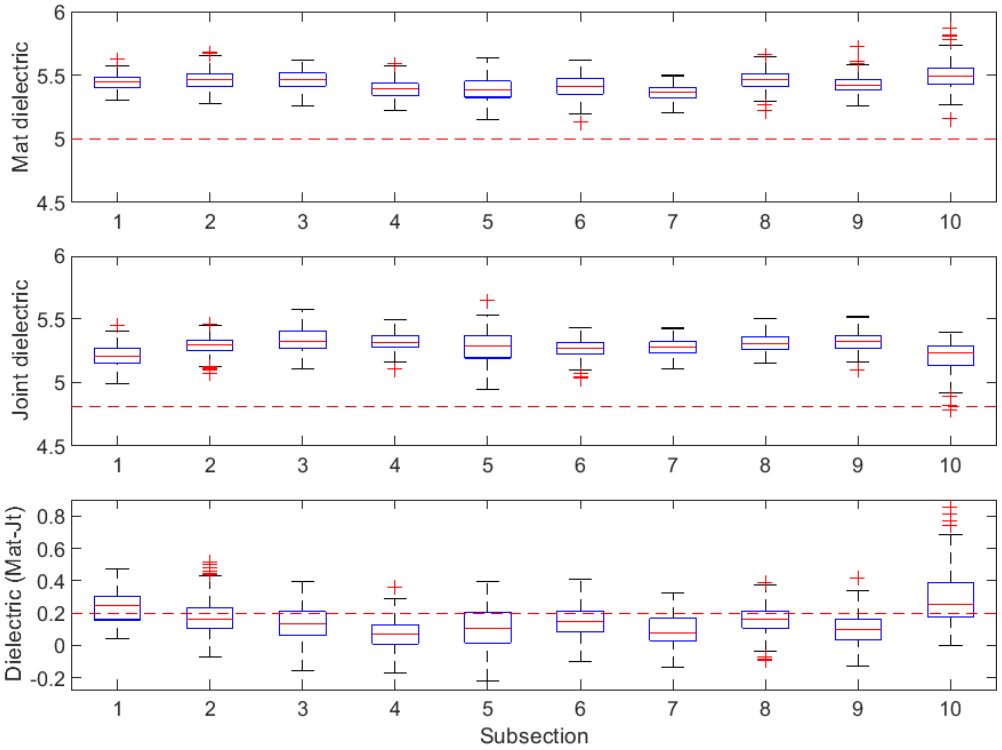

Figure B-92 Box plot of dielectric values for echelon joint (100 ft subsections) – Manning Trail #1

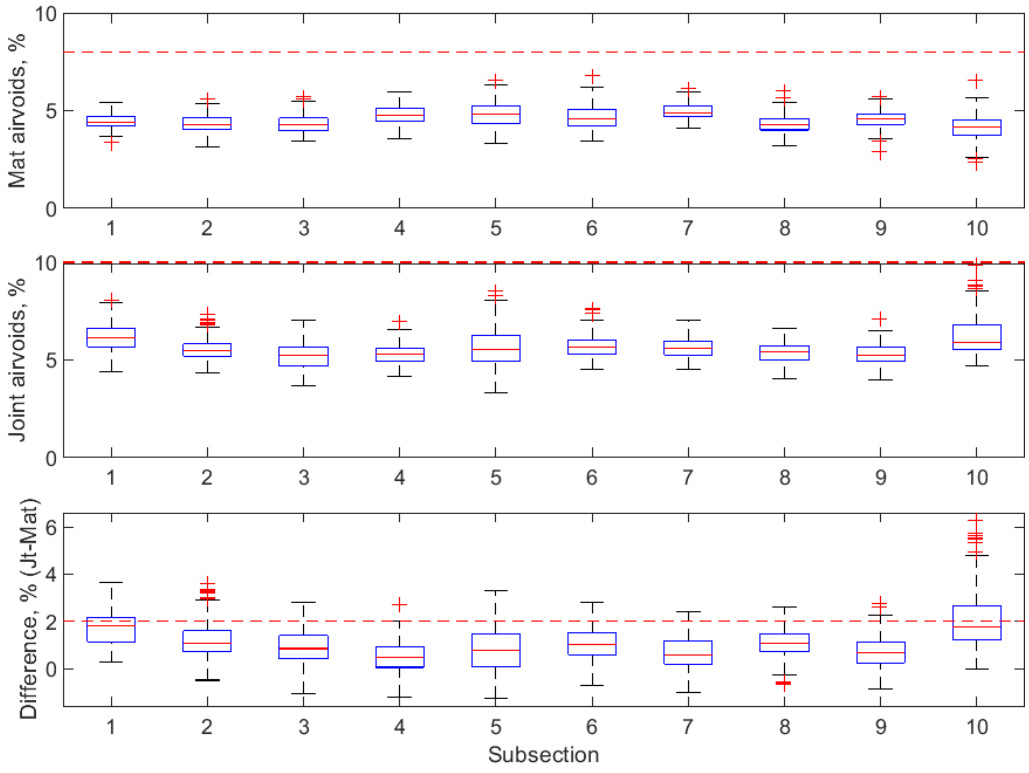

Figure B-93 Box plot of air voids for echelon joint (100 ft subsections) – Manning Trail #1

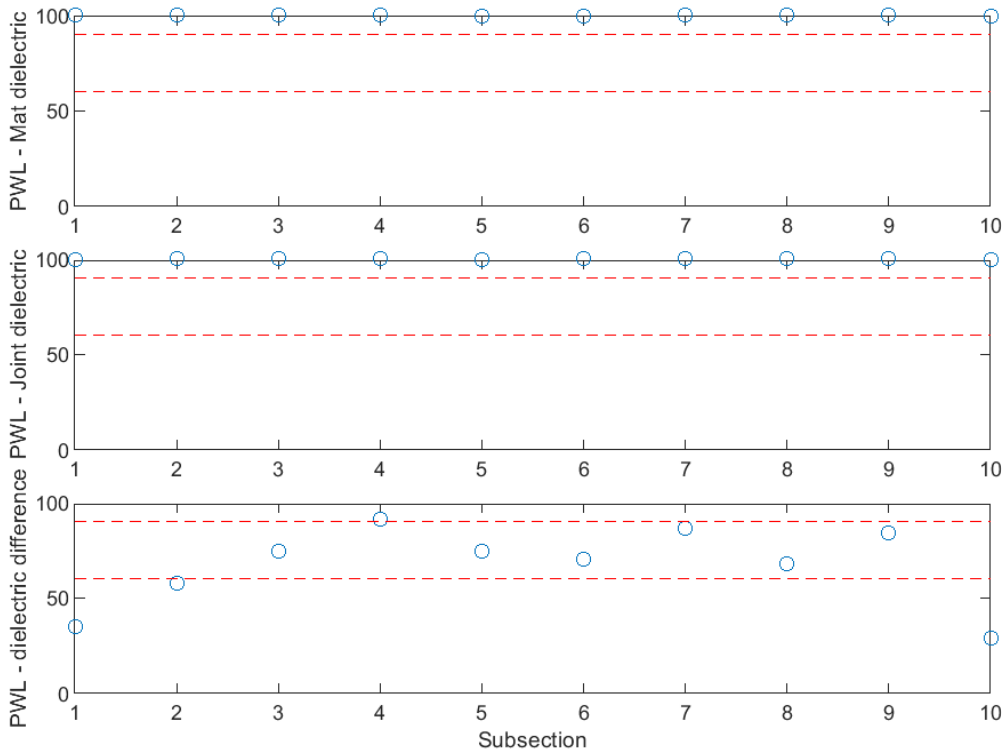

Figure B-94 PWL for dielectric values for echelon joint (100 ft subsections) – Manning Trail #1

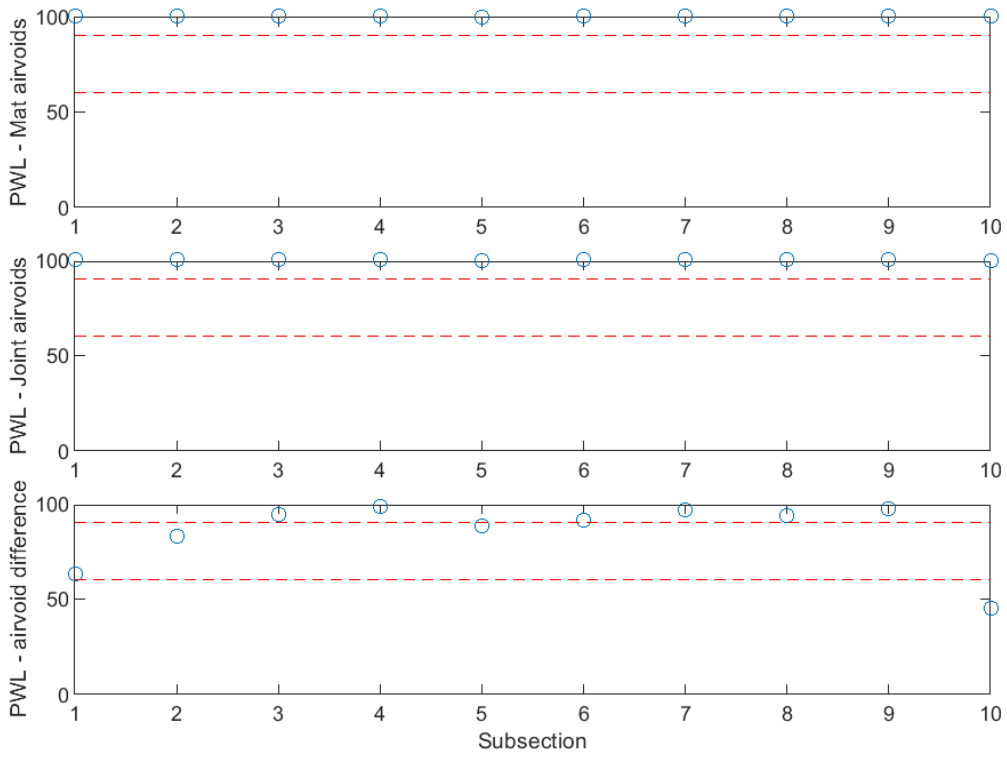

Figure B-95 PWL for air voids for echelon joint (100 ft subsections) – Manning Trail #1

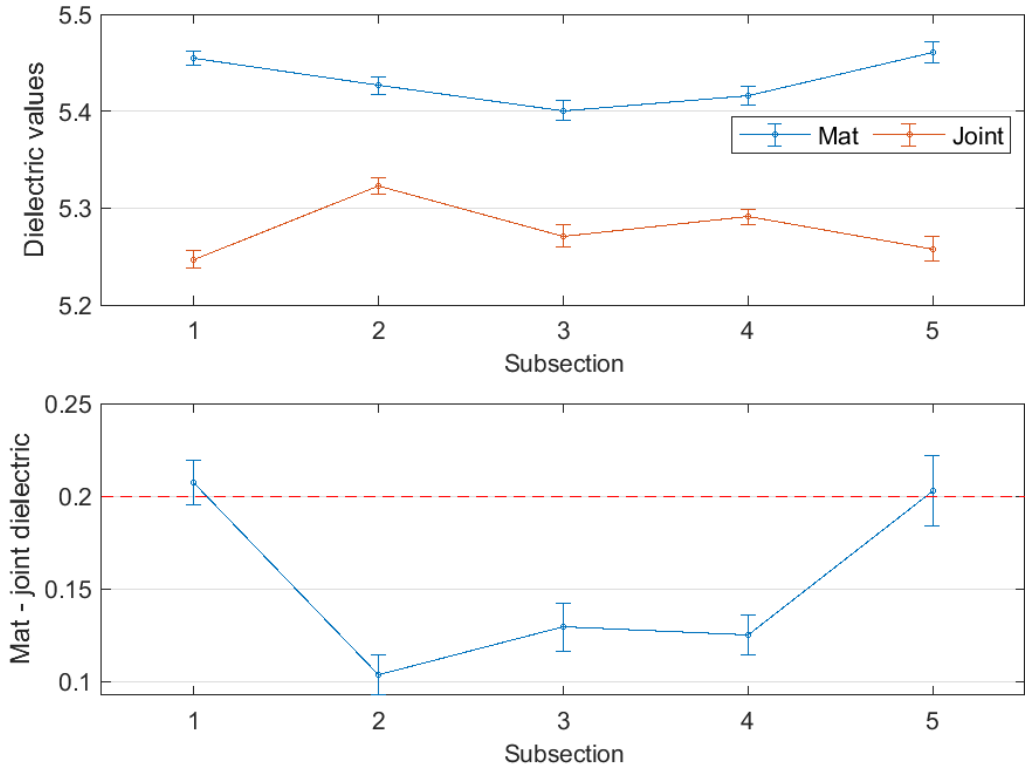

Figure B-96 Interval plot of dielectric values for echelon joint (200 ft subsections) – Manning Trail #1

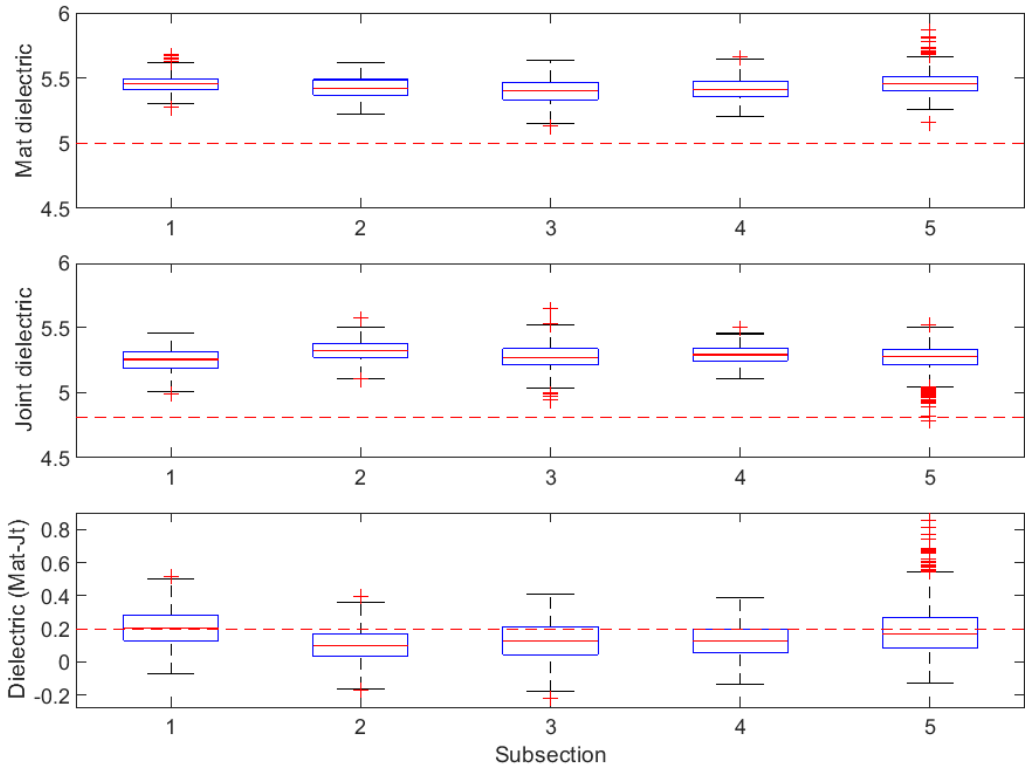

Figure B-97 Box plot of dielectric values for echelon joint (200 ft subsections) – Manning Trail #1

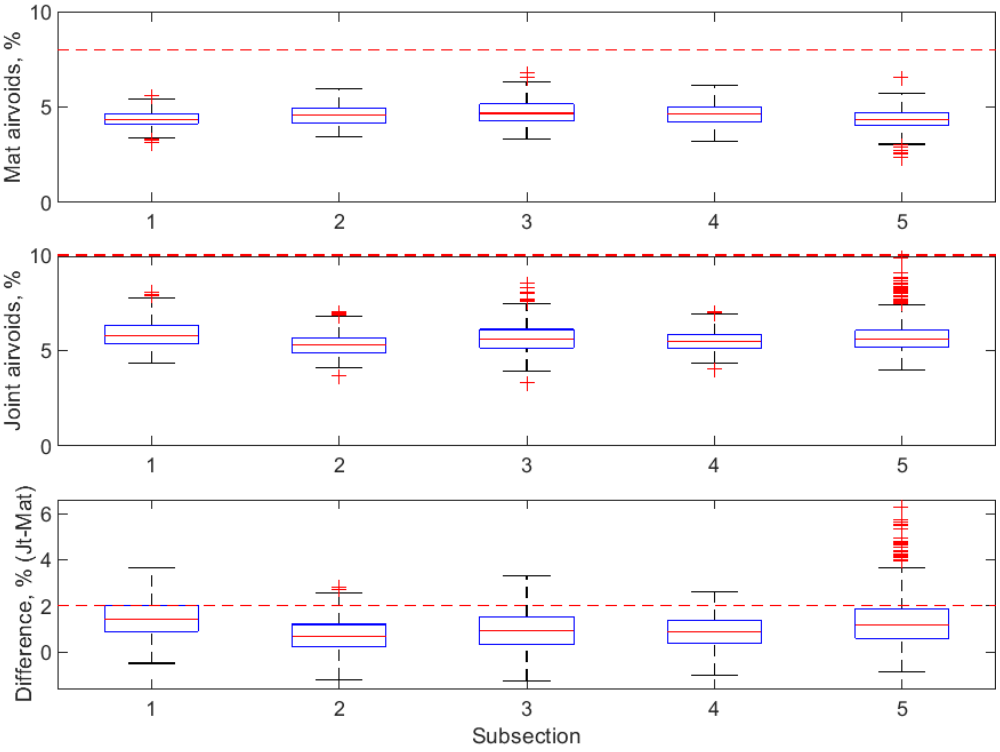

Figure B-98 Box plot of air voids for echelon joint (200 ft subsections) – Manning Trail #1

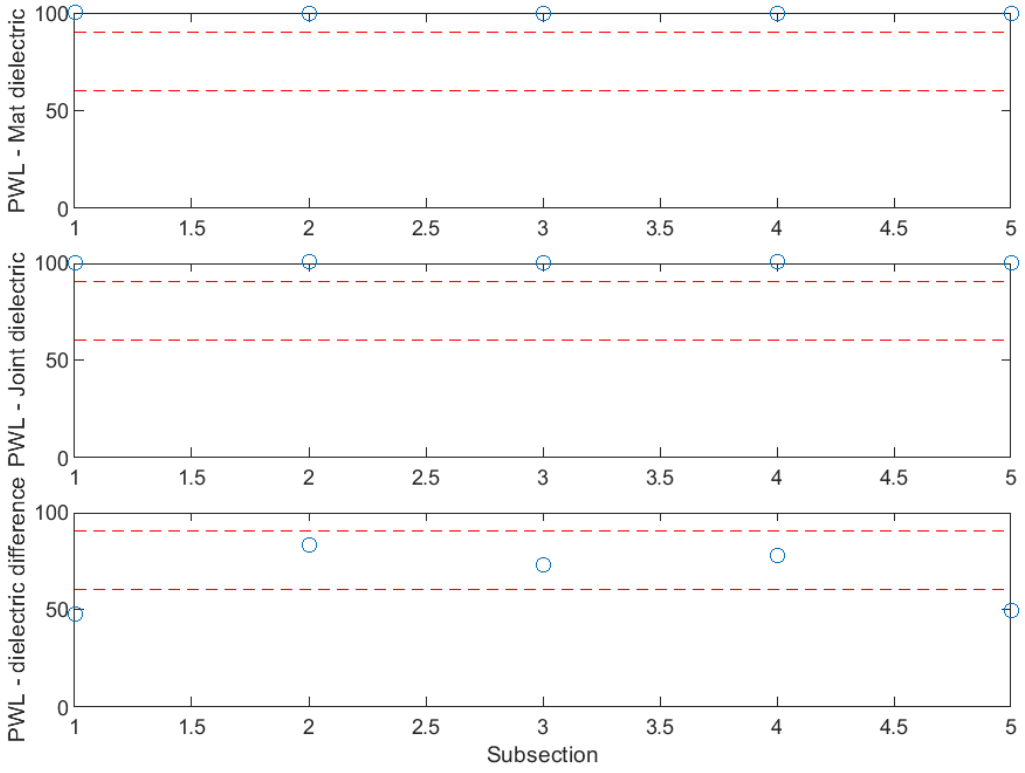

Figure B-99 PWL for dielectric values for echelon joint (200 ft subsections) – Manning Trail #1

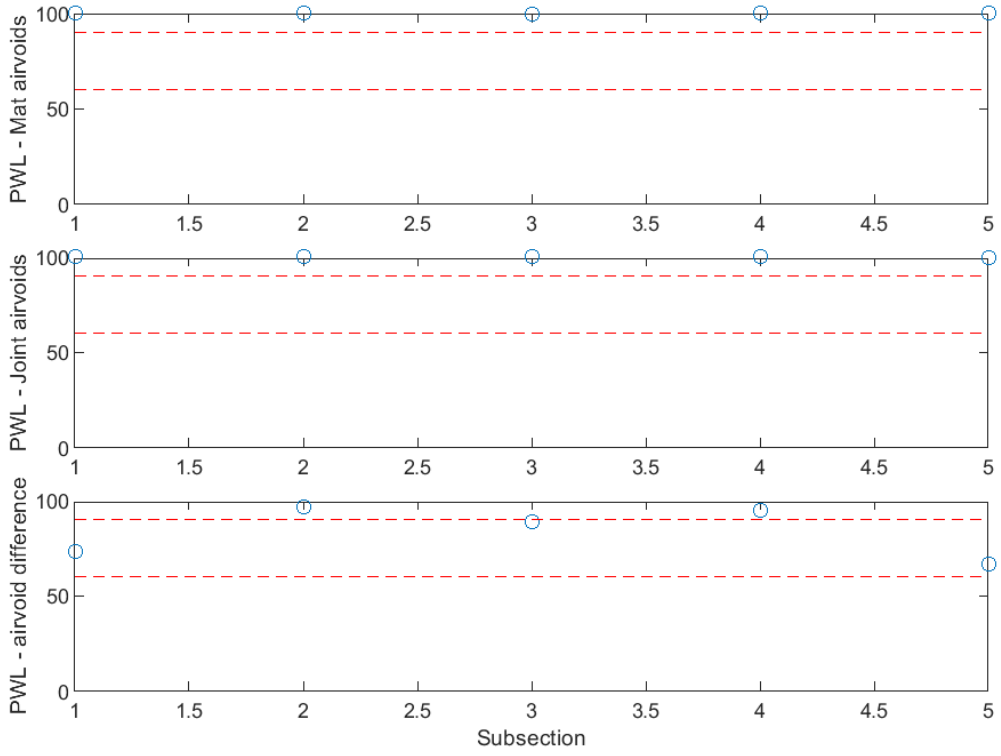

Figure B-100 PWL for air voids for echelon joint (200 ft subsections) – Manning Trail #1

Manning Trail #2 Project

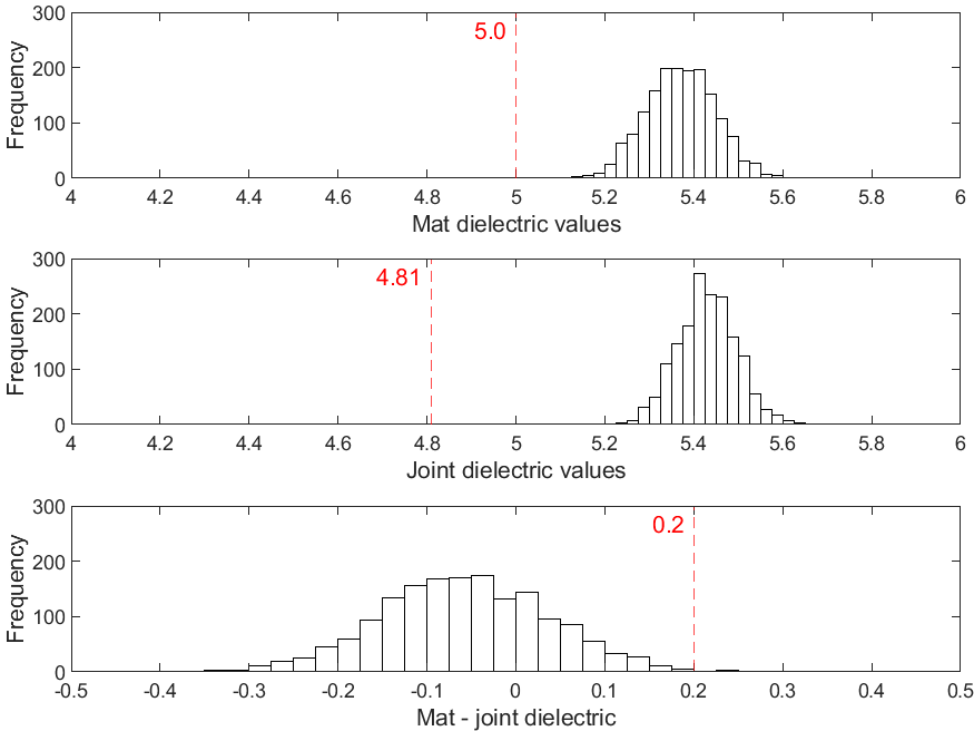

Figure B-101 Histogram of dielectric values for confined joint – Manning Trail #2

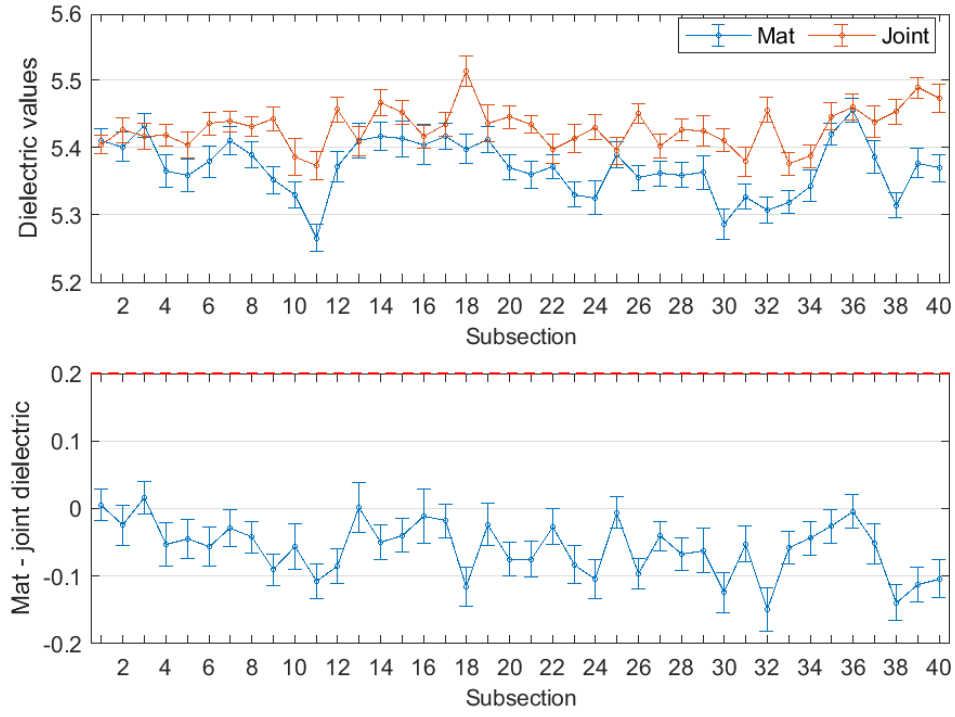

Figure B-102 Interval plot of dielectric values for confined joint (25 ft subsections) – Manning Trail #2

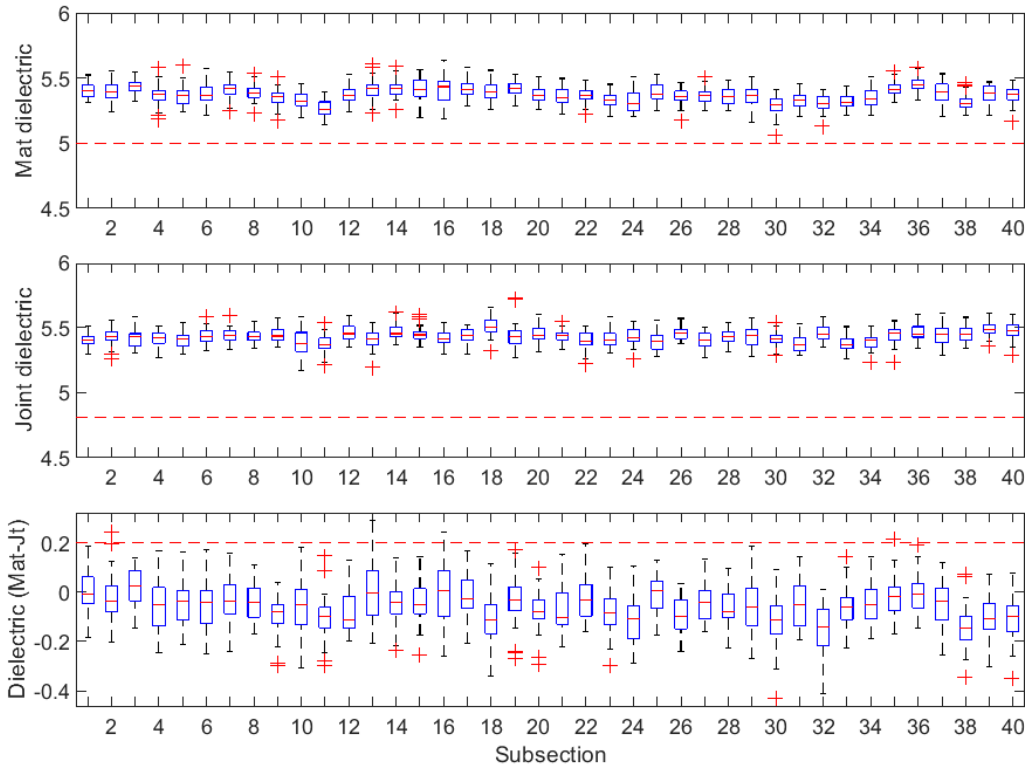

Figure B-103 Box plot of dielectric values for confined joint (25 ft subsections) – Manning Trail #2

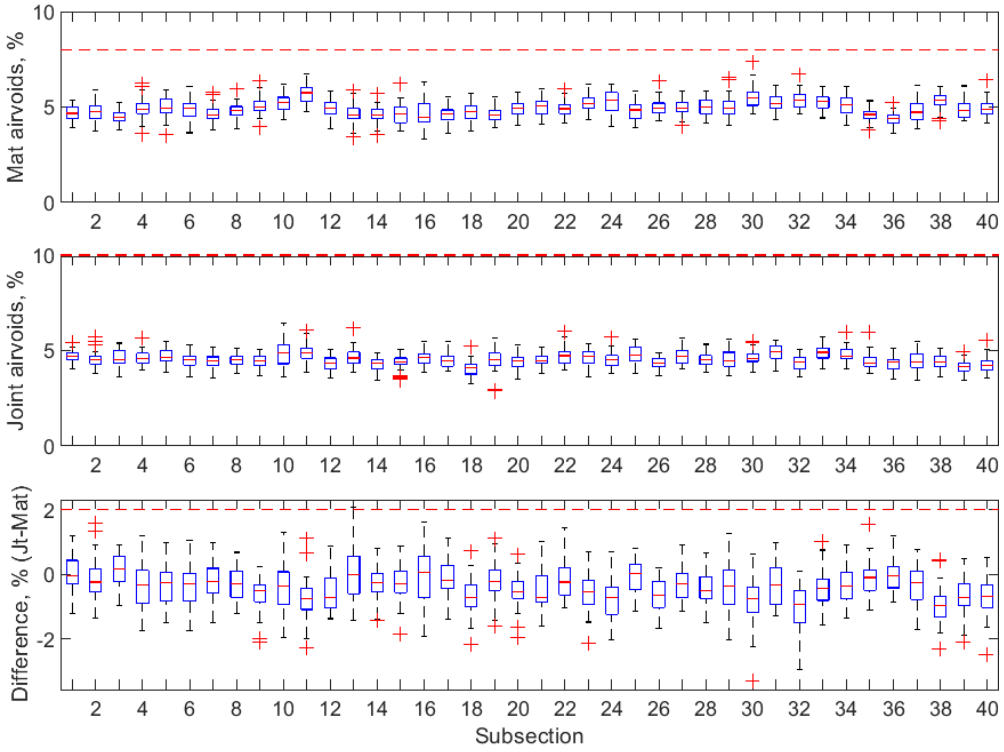

Figure B-104 Box plot of air voids for confined joint (25 ft subsections) – Manning Trail #2

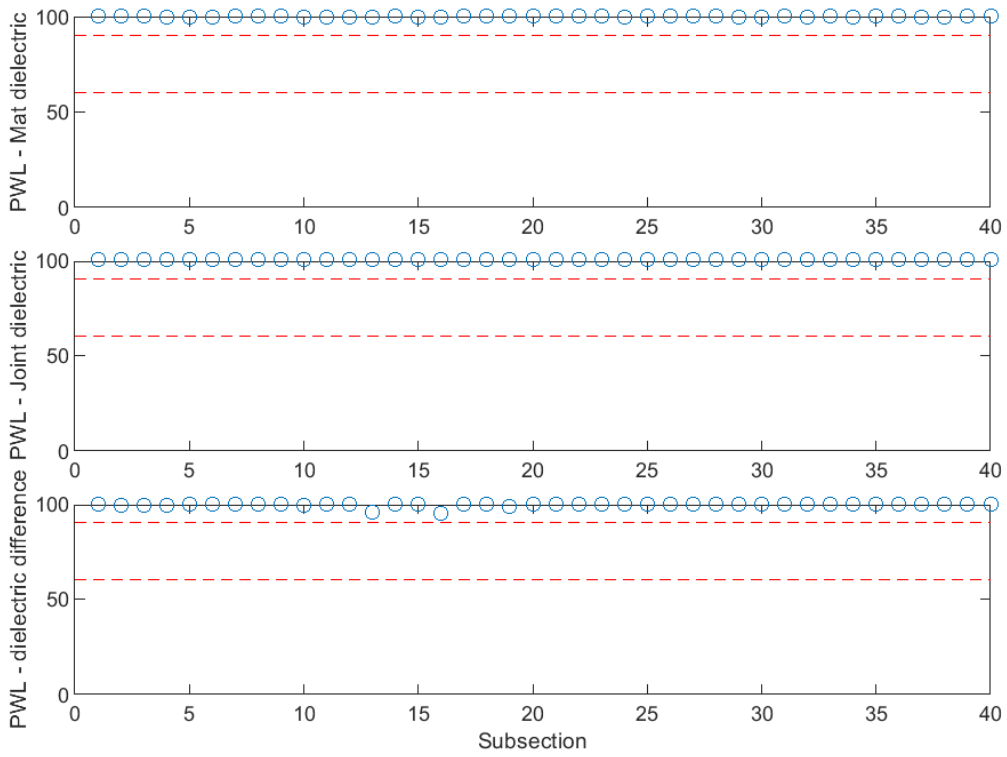

Figure B-105 PWL for dielectric values for confined joint (25 ft subsections) – Manning Trail #2

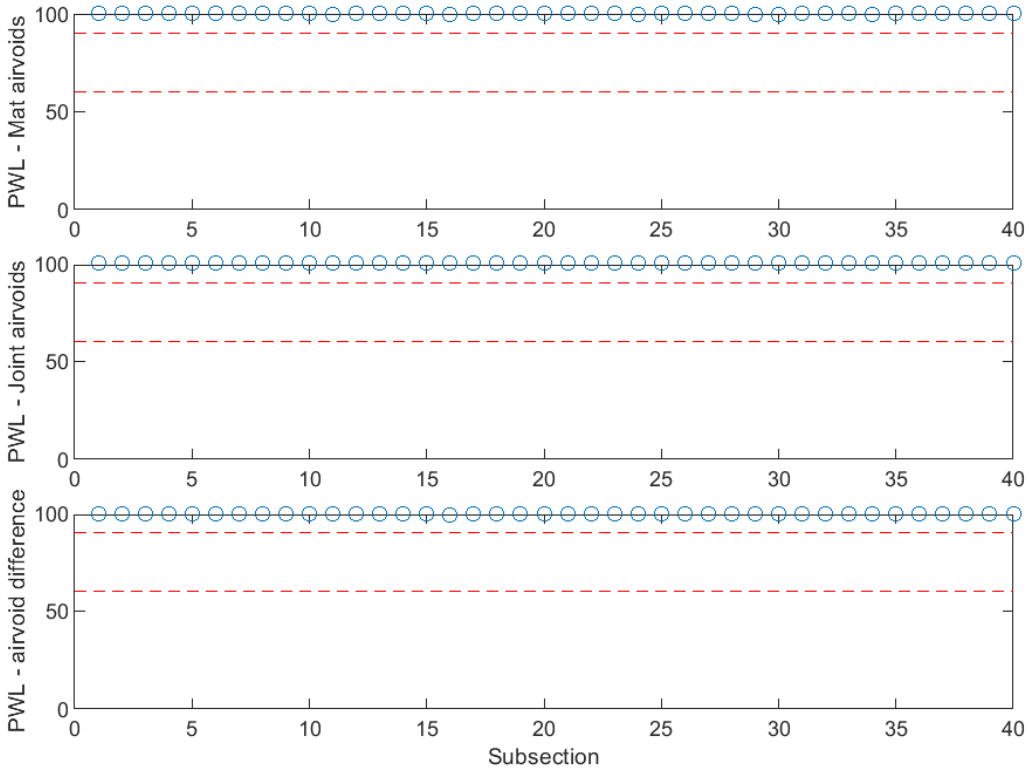

Figure B-106 PWL for air voids for confined joint (25 ft subsections) – Manning Trail #2

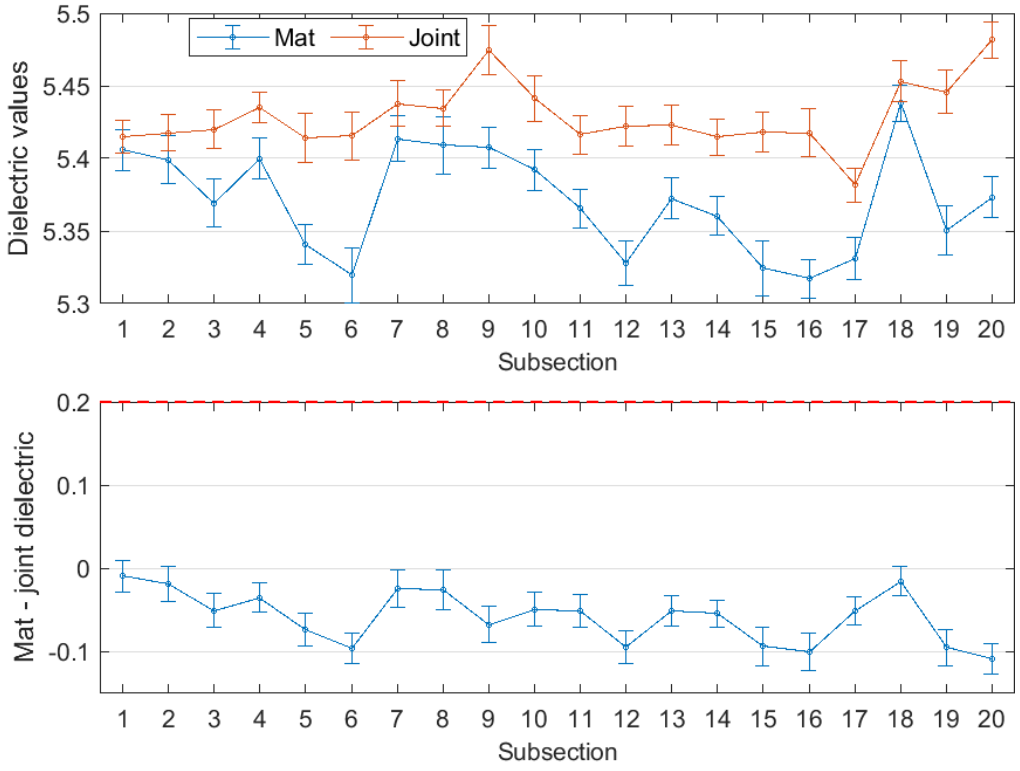

Figure B-107 Interval plot of dielectric values for confined joint (50 ft subsections) – Manning Trail #2

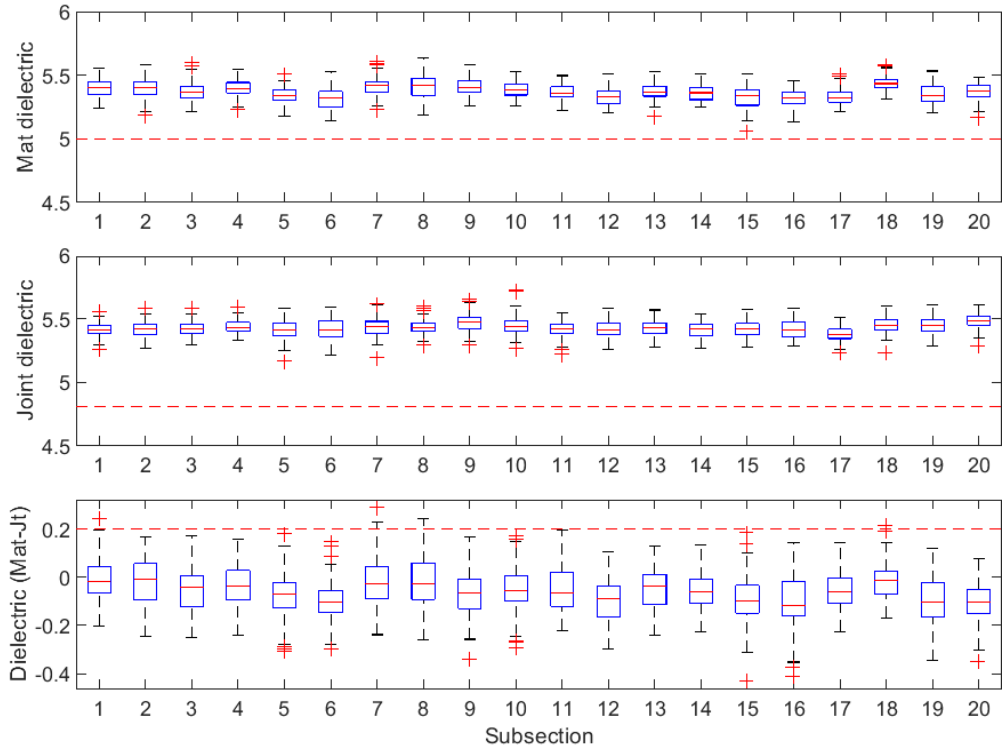

Figure B-108 Box plot of dielectric values for confined joint (50 ft subsections) – Manning Trail #2

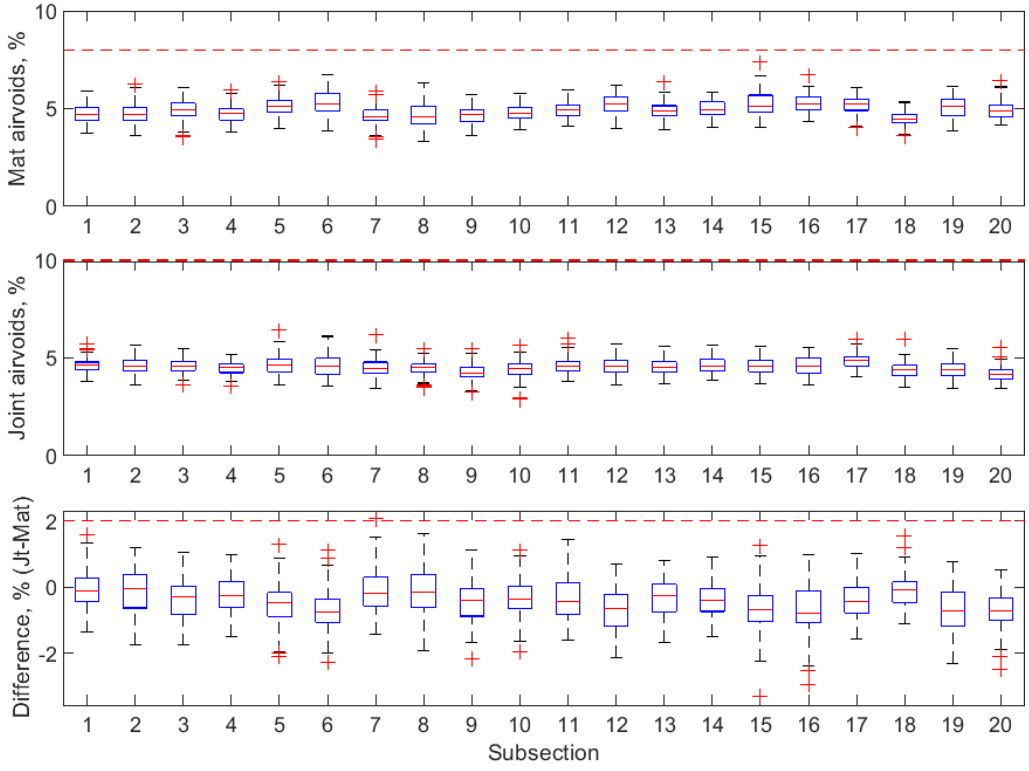

Figure B-109 Box plot of air voids for confined joint (50 ft subsections) – Manning Trail #2

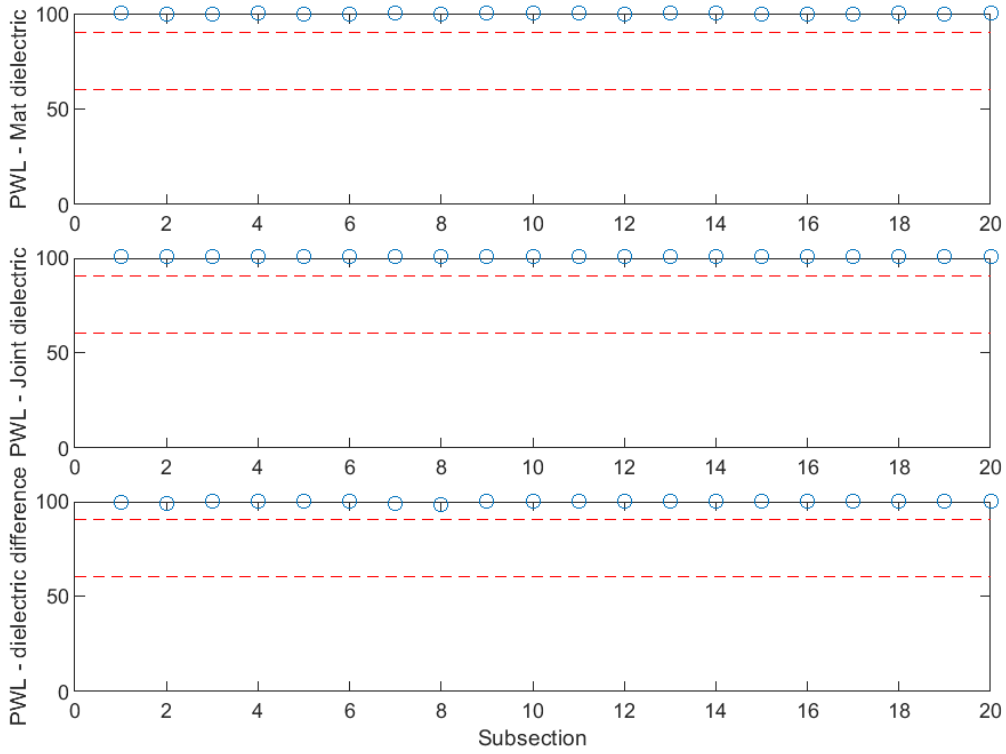

Figure B-110 PWL for dielectric values for confined joint (50 ft subsections) – Manning Trail #2

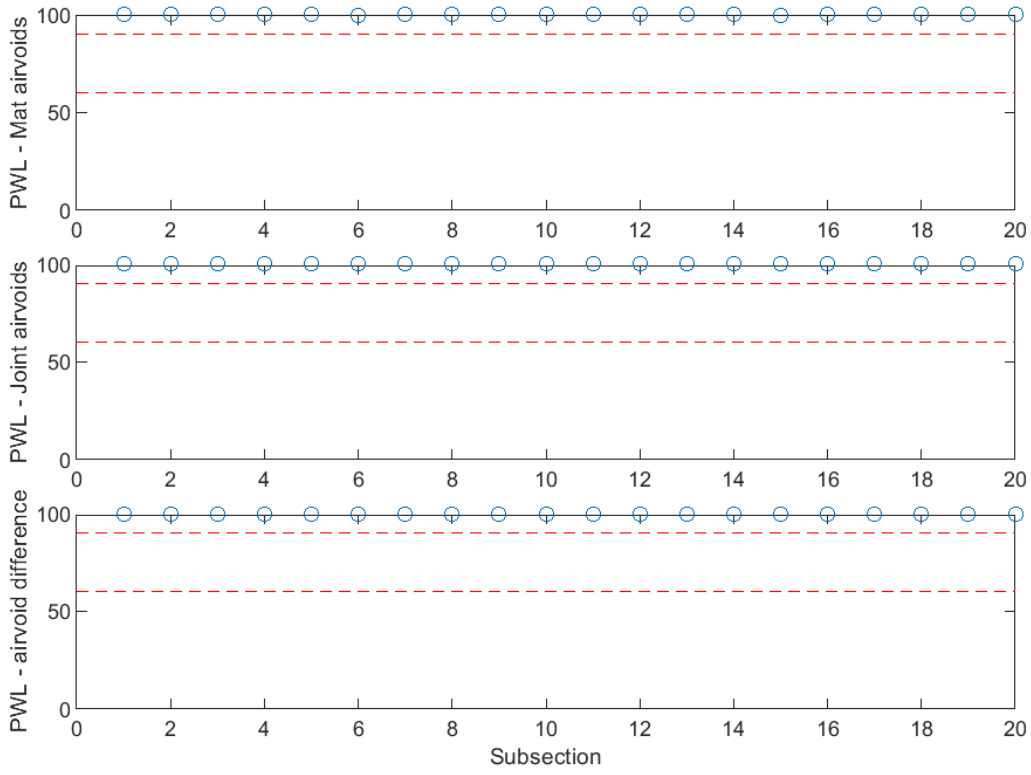

Figure B-111 PWL for air voids for confined joint (50 ft subsections) – Manning Trail #2

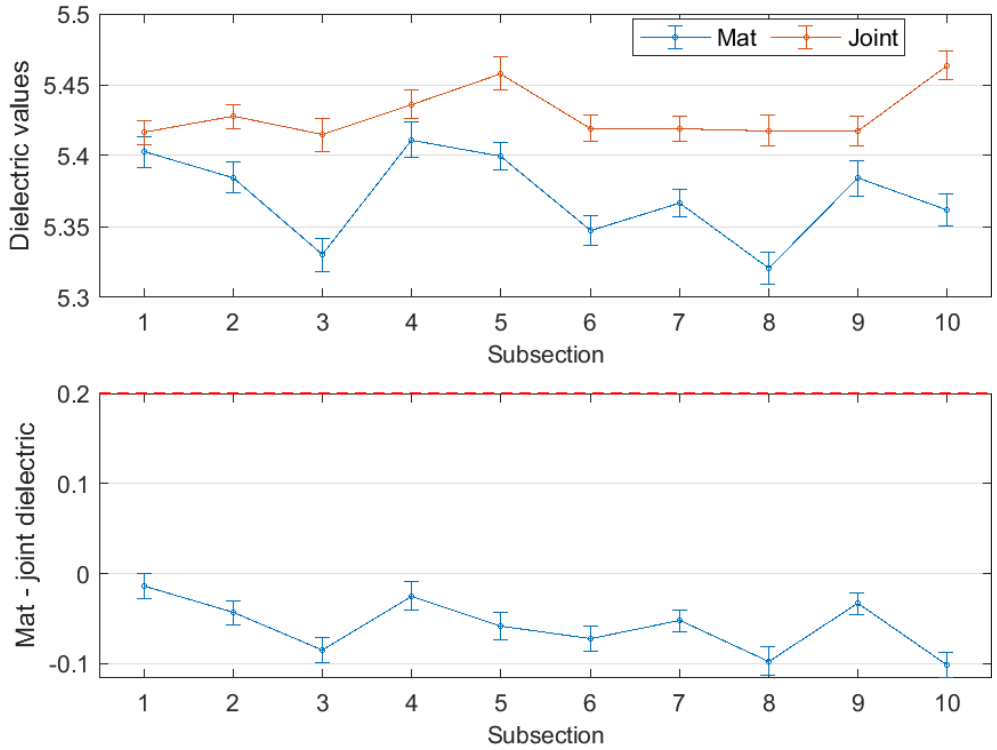

Figure B-112 Interval plot of dielectric values for confined joint (100 ft subsections) – Manning Trail #2

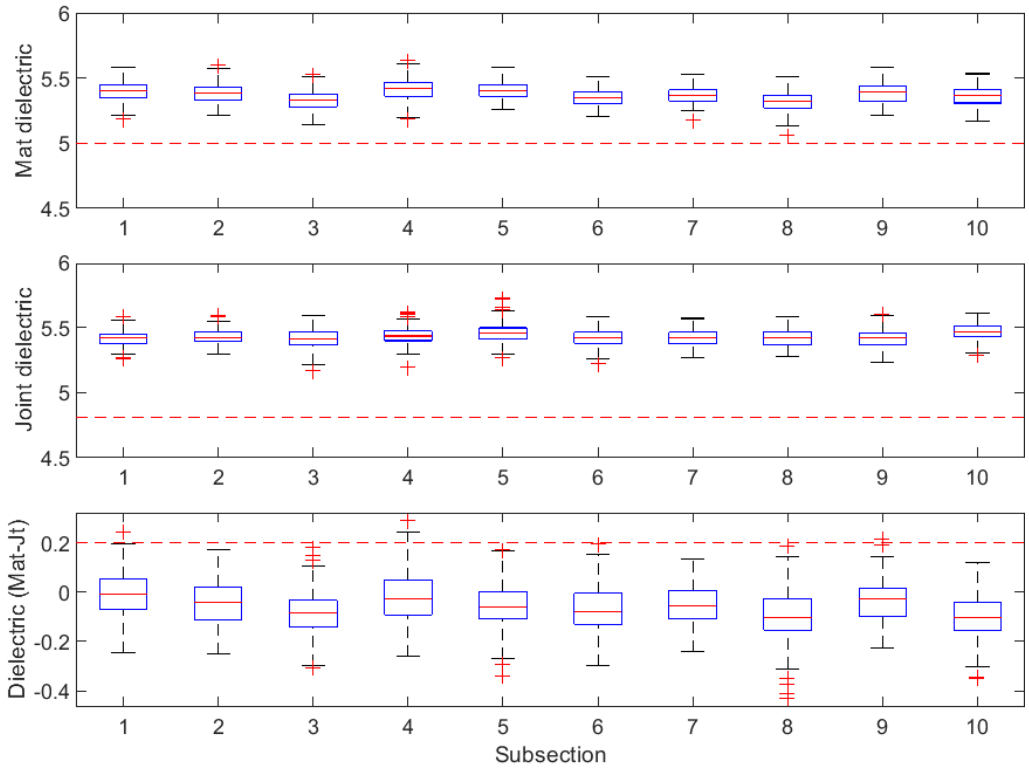

Figure B-113 Box plot of dielectric values for confined joint (100 ft subsections) – Manning Trail #2

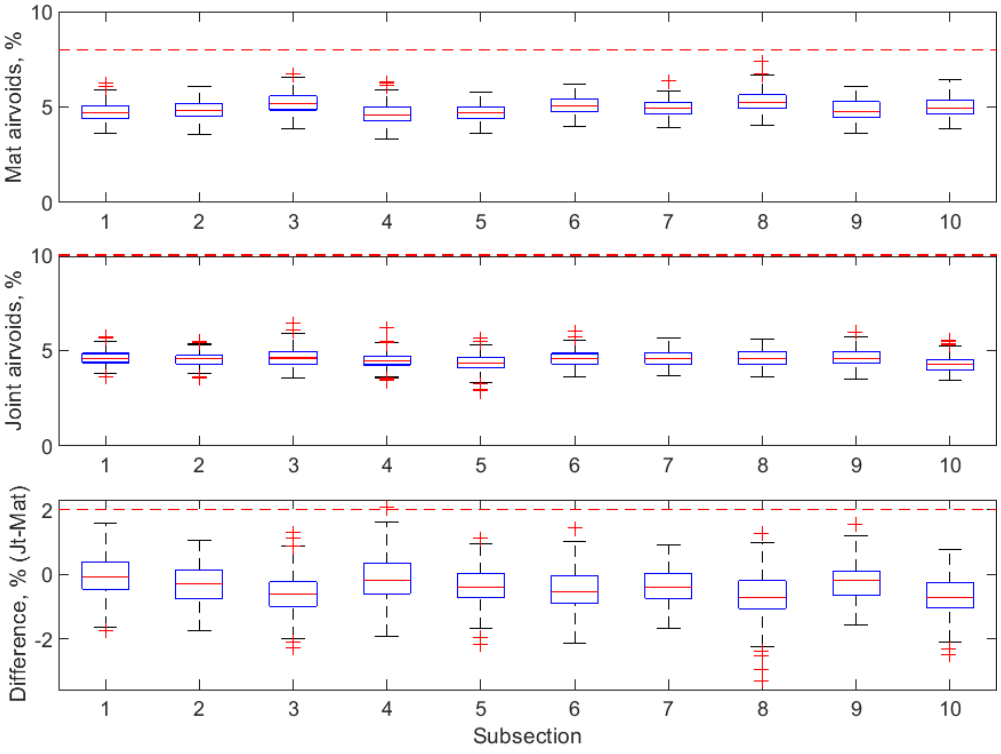

Figure B-114 Box plot of air voids for confined joint (100 ft subsections) – Manning Trail #2

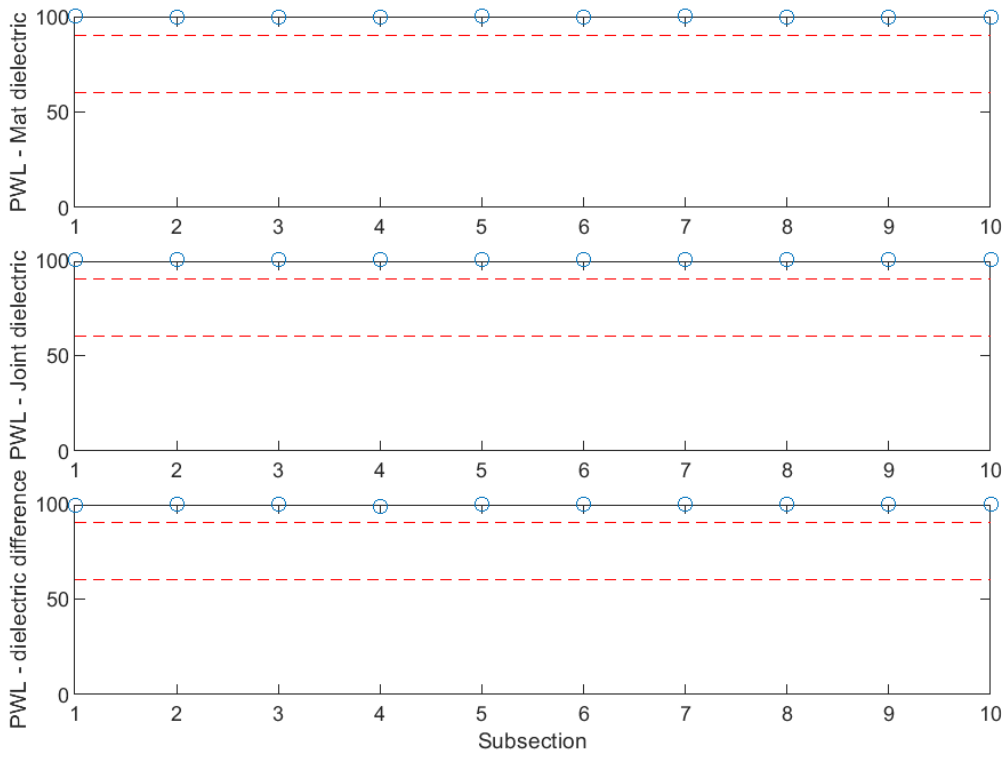

Figure B-115 PWL for dielectric values for confined joint (100 ft subsections) – Manning Trail #2

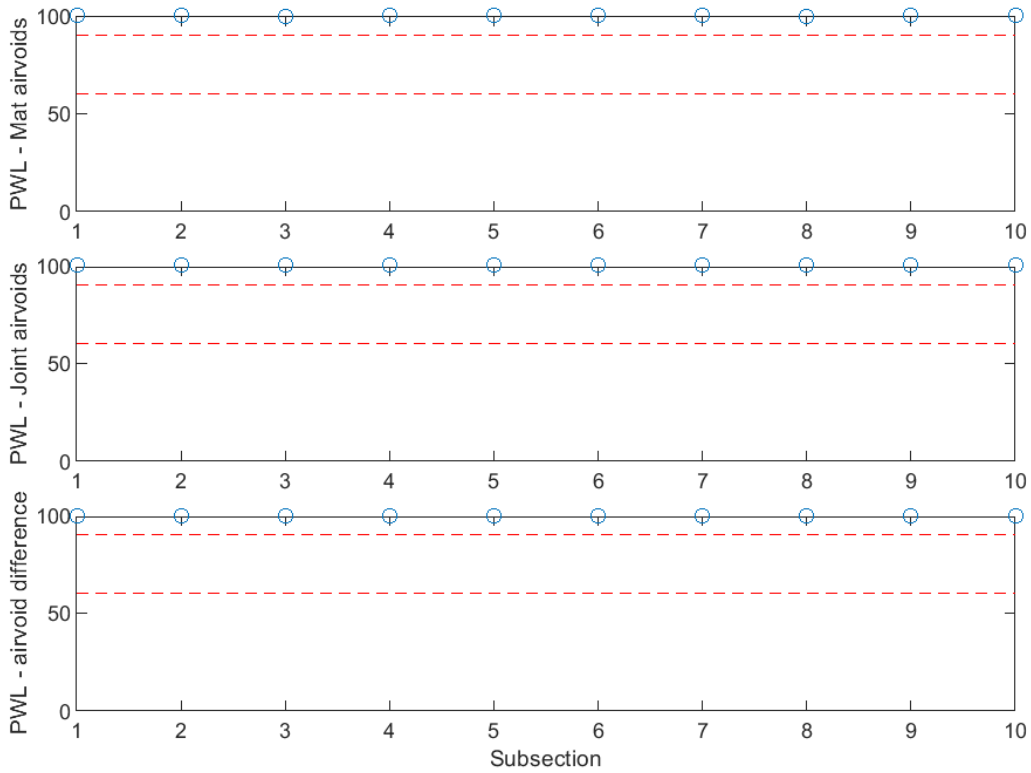

Figure B-116 PWL for air voids for confined joint (100 ft subsections) – Manning Trail #2

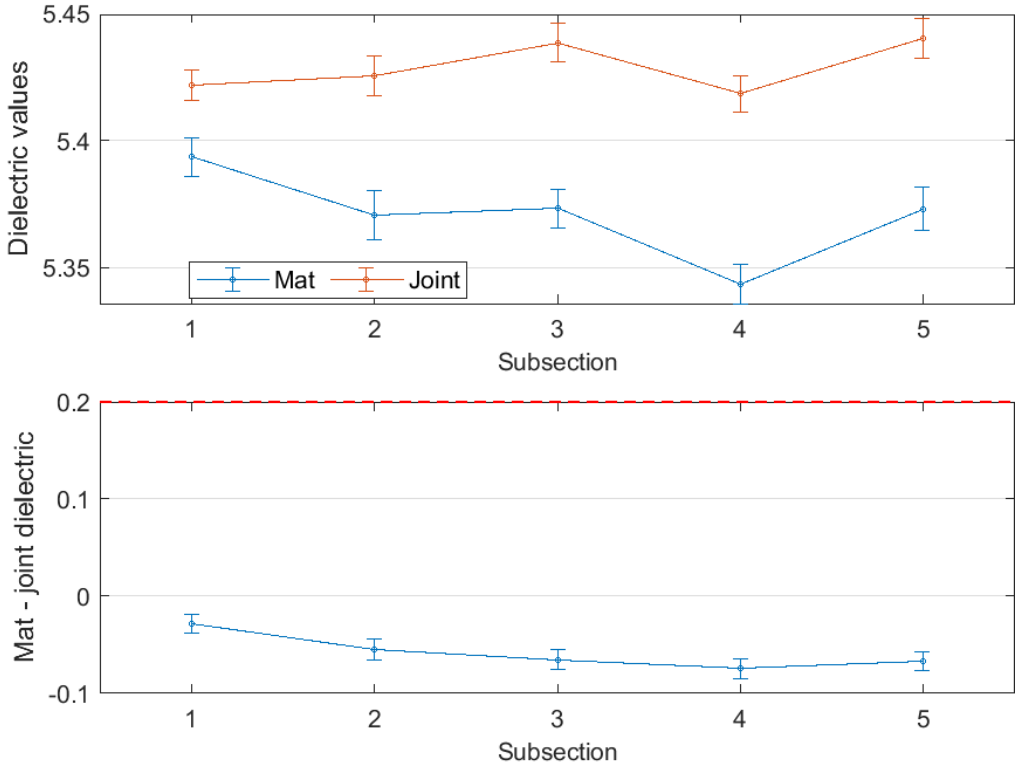

Figure B-117 Interval plot of dielectric values for confined joint (200 ft subsections) – Manning Trail #2

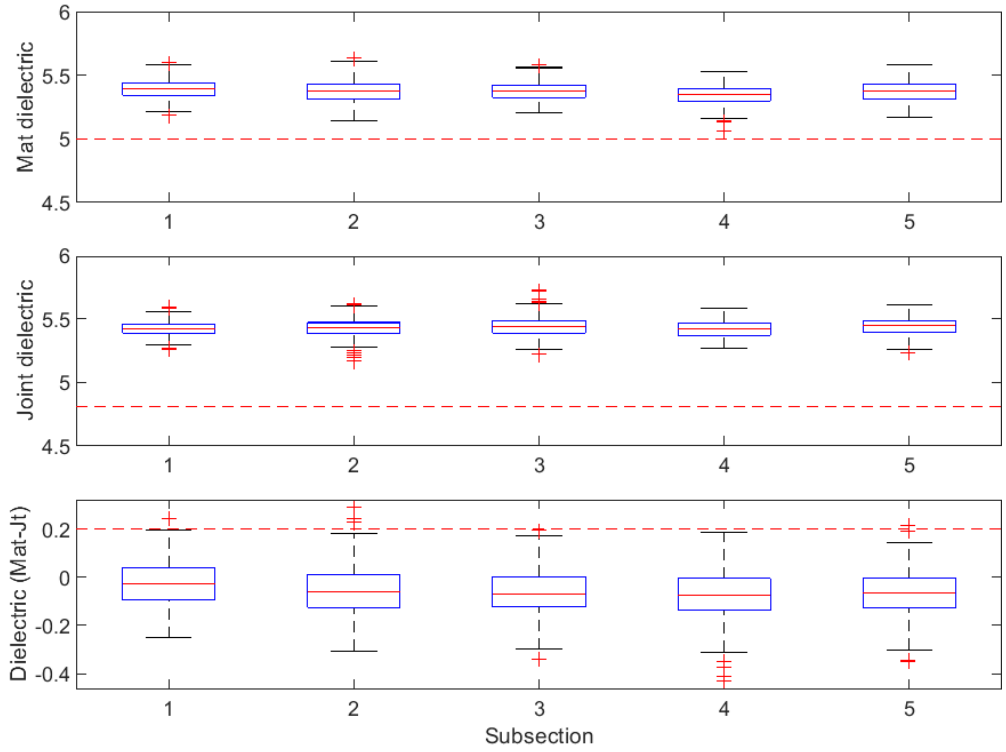

Figure B-118 Box plot of dielectric values for confined joint (200 ft subsections) – Manning Trail #2

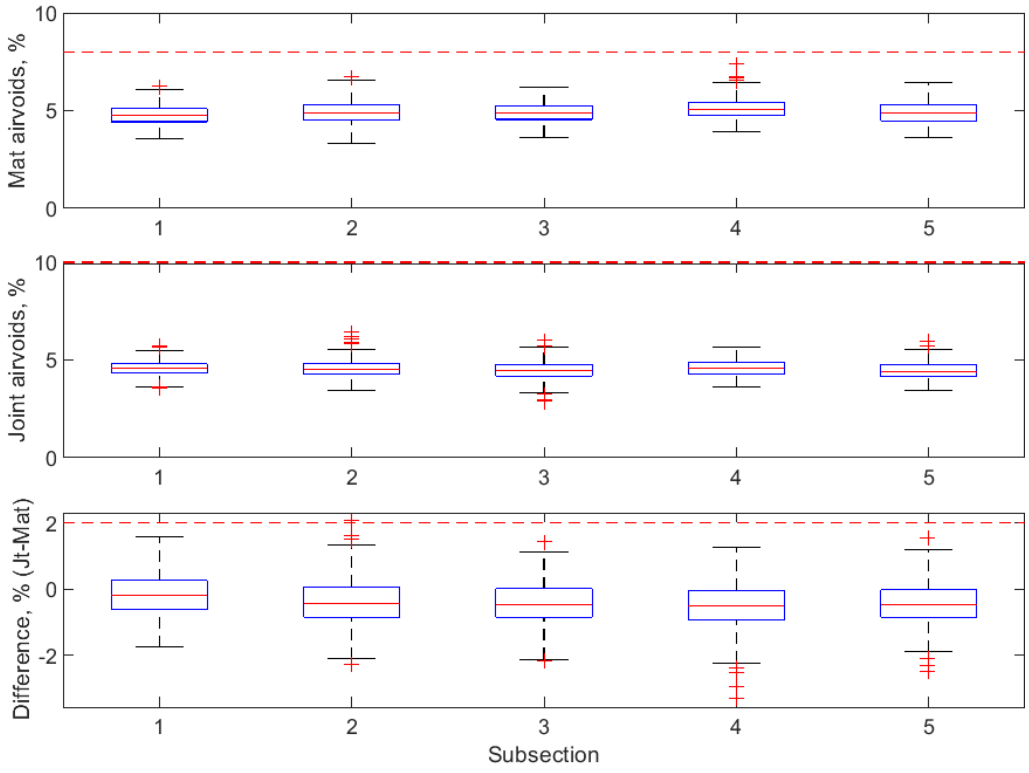

Figure B-119 Box plot of air voids for confined joint (200 ft subsections) – Manning Trail #2

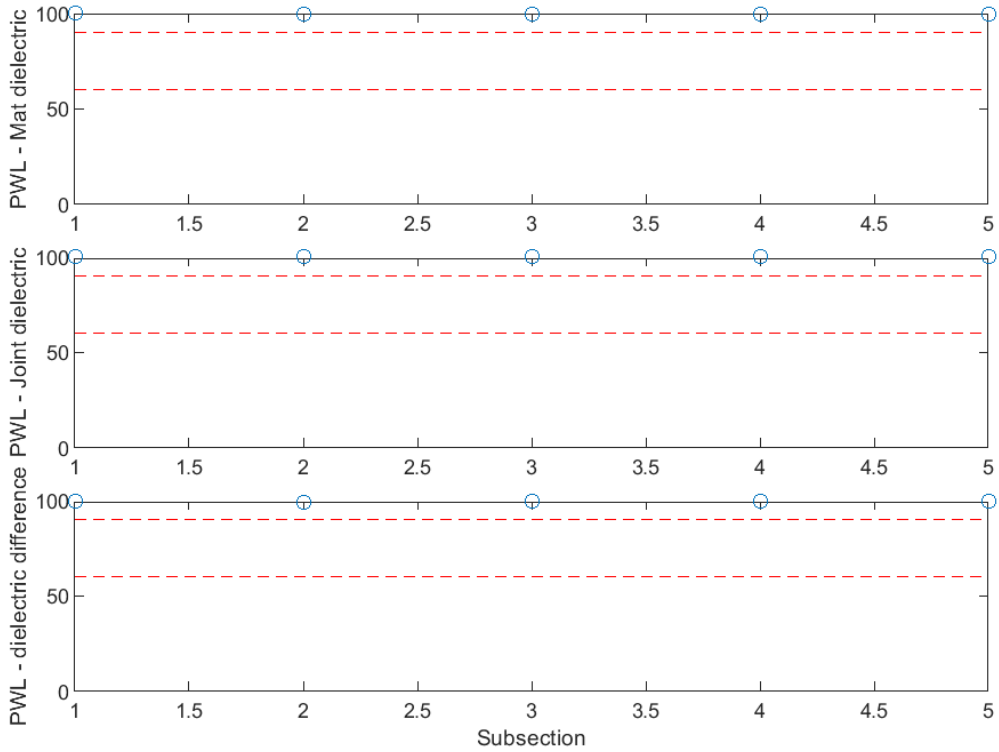

Figure B-120 PWL for dielectric values for confined joint (200 ft subsections) – Manning Trail #2

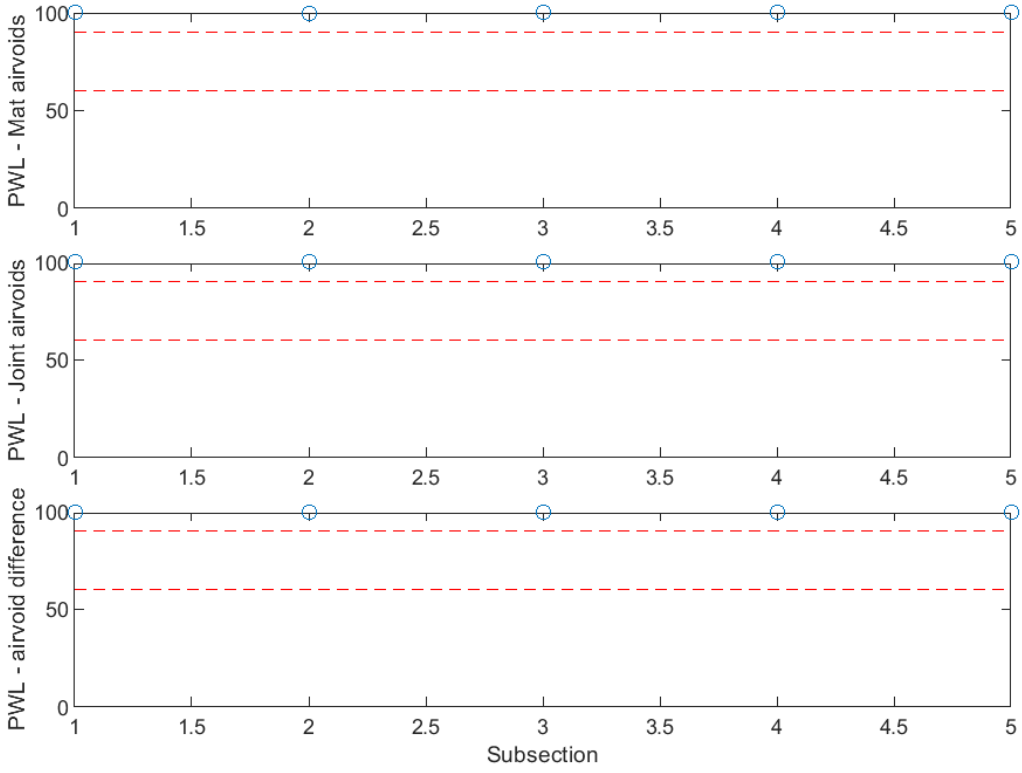

Figure B-121 PWL for air voids for confined joint (200 ft subsections) – Manning Trail #2

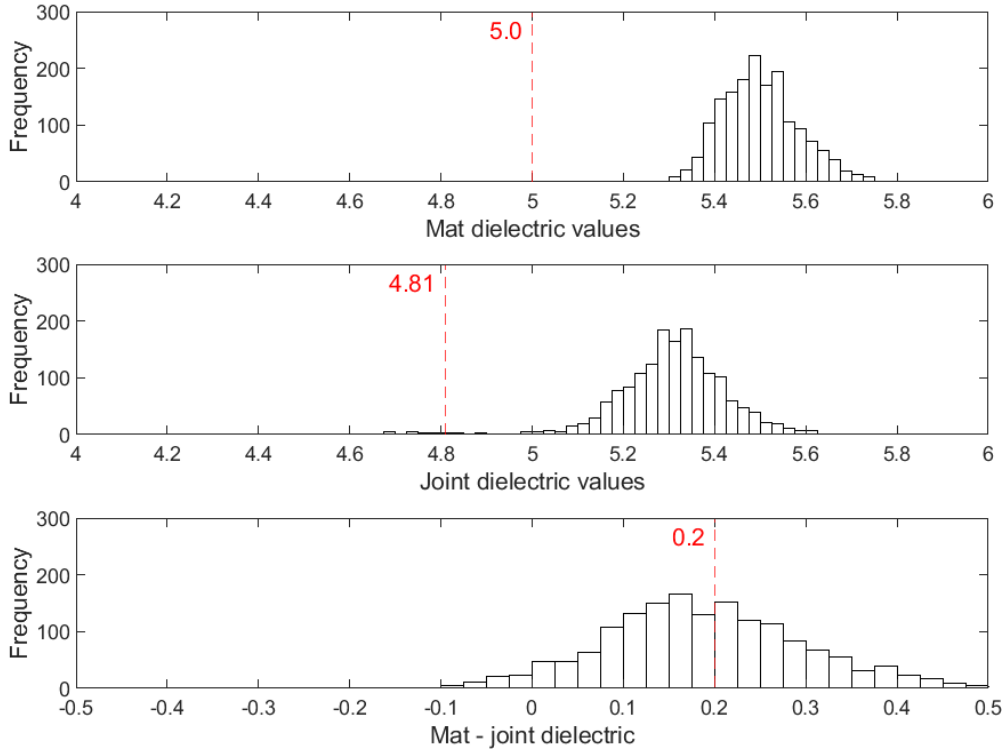

Figure B-122 Histogram of dielectric values for echelon joint – Manning Trail #2

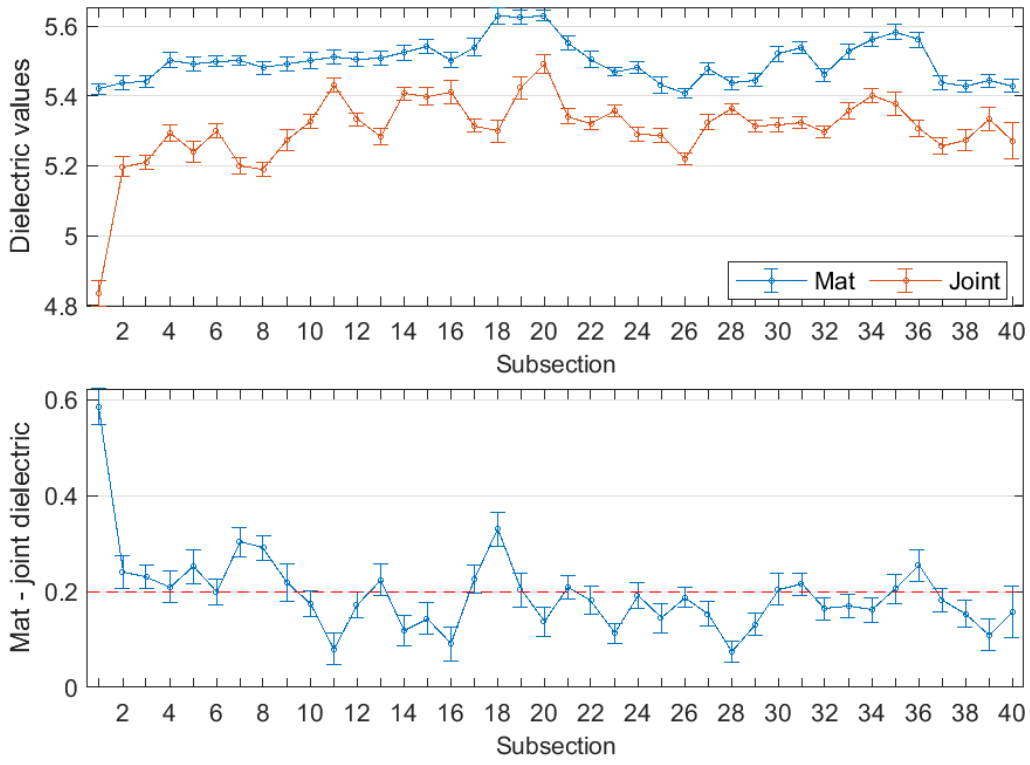

Figure B-123 Interval plot of dielectric values for echelon joint (25 ft subsections) – Manning Trail #2

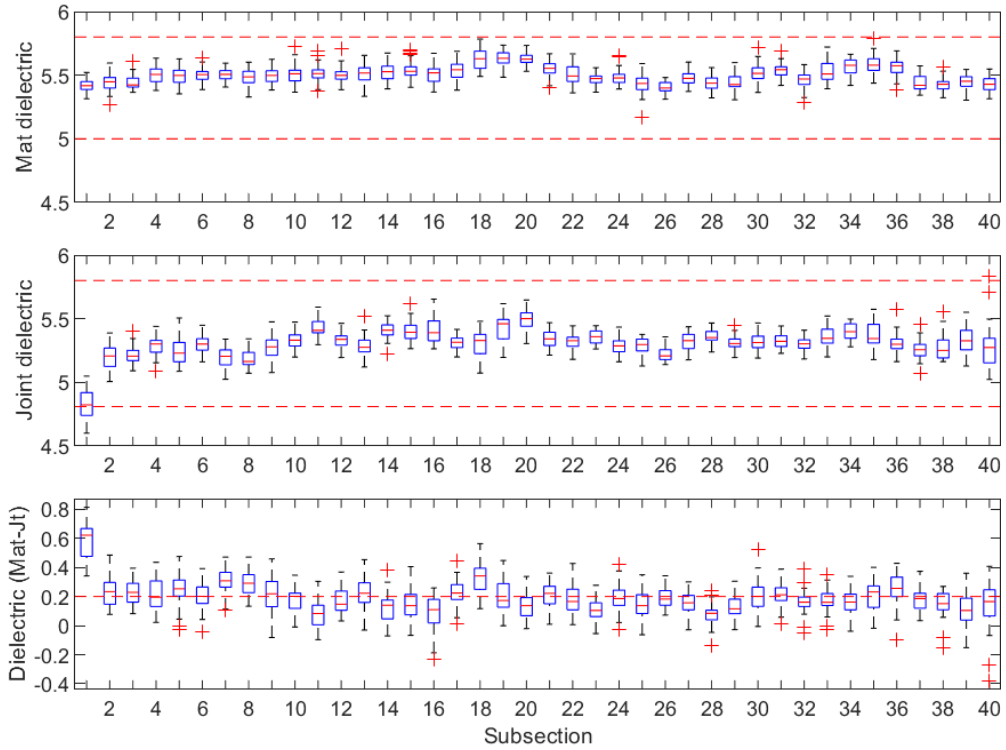

Figure B-124 Box plot of dielectric values for echelon joint (25 ft subsections) – Manning Trail #2

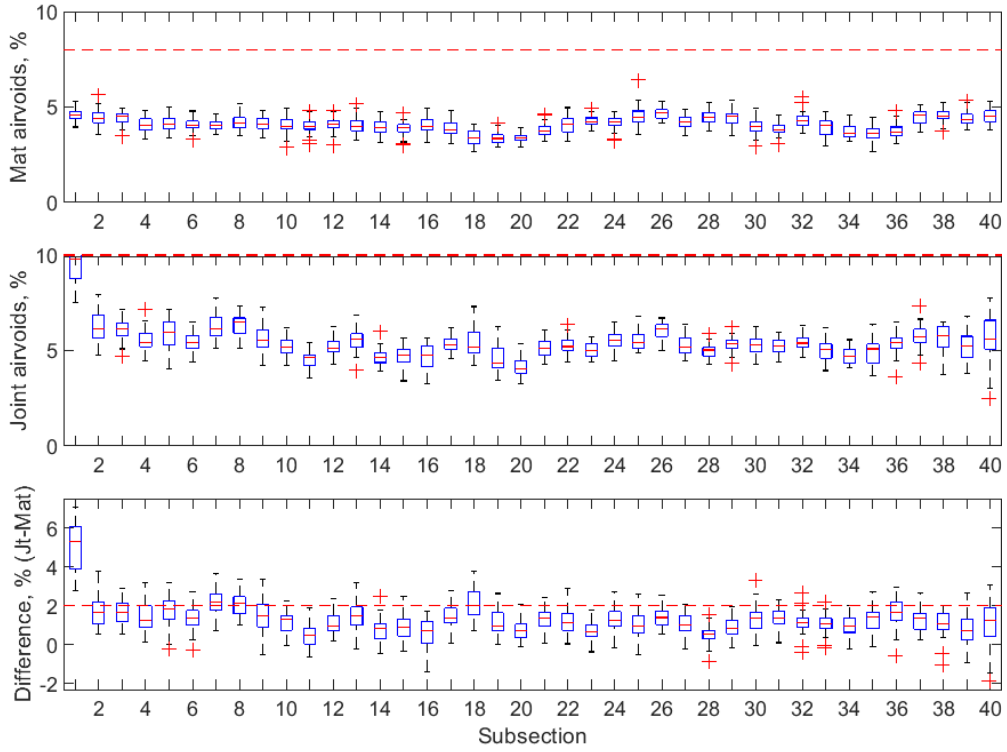

Figure B-125 Box plot of air voids for echelon joint (25 ft subsections) – Manning Trail #2

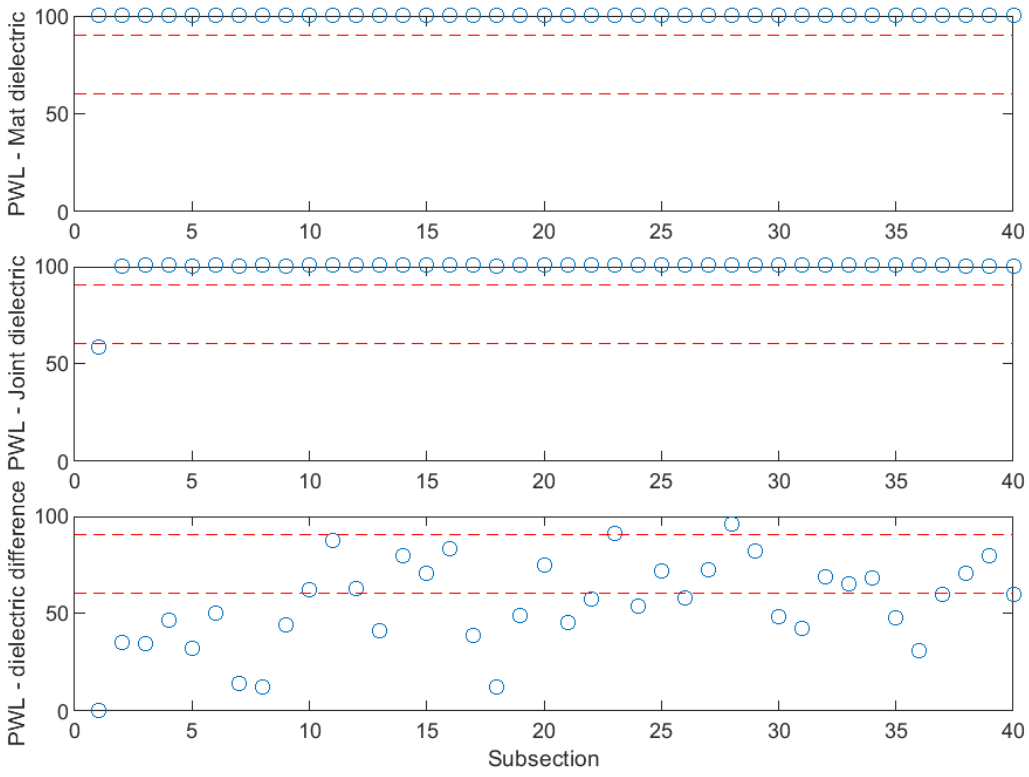

Figure B-126 PWL for dielectric values for echelon joint (25 ft subsections) – Manning Trail #2

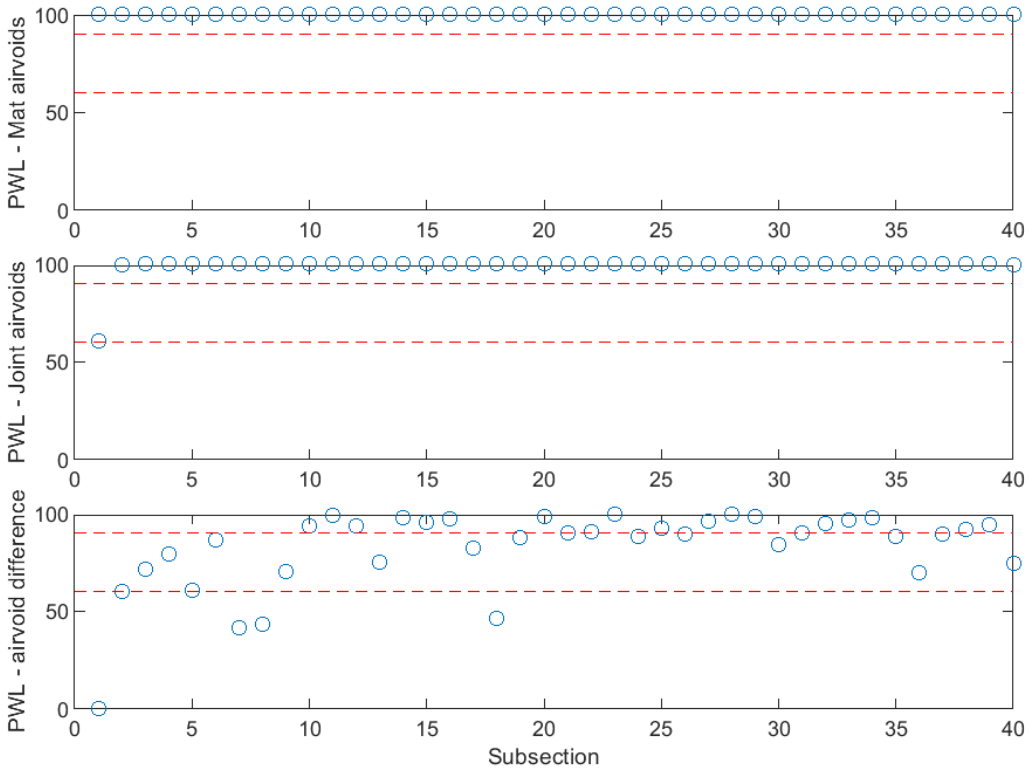

Figure B-127 PWL for air voids for echelon joint (25 ft subsections) – Manning Trail #2

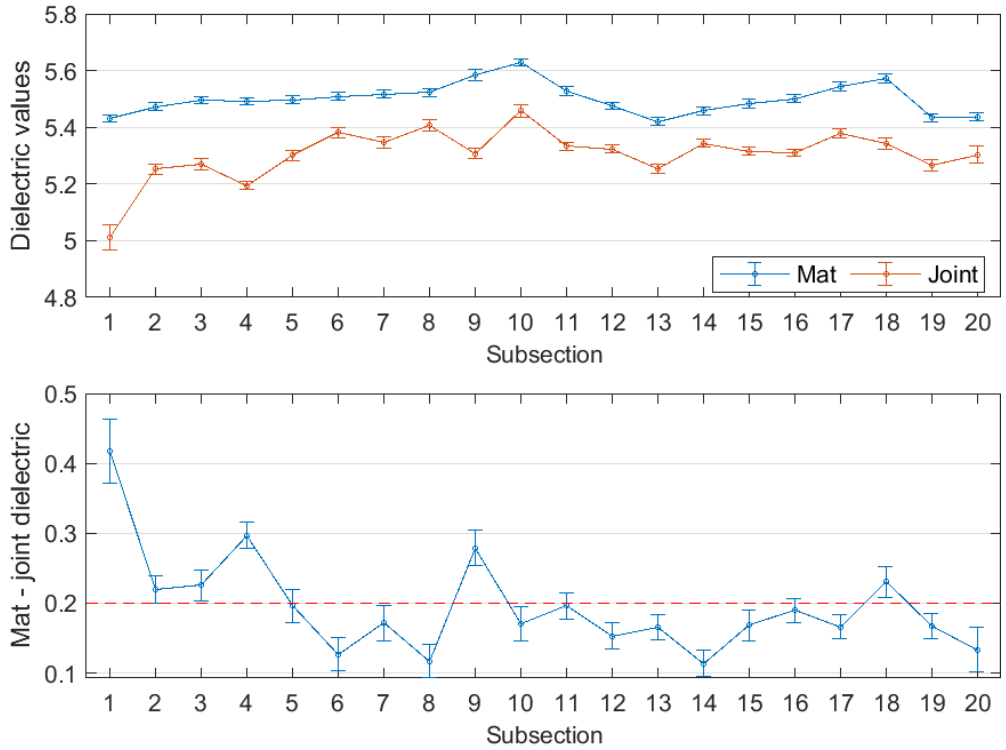

Figure B-128 Interval plot of dielectric values for echelon joint (50 ft subsections) – Manning Trail #2

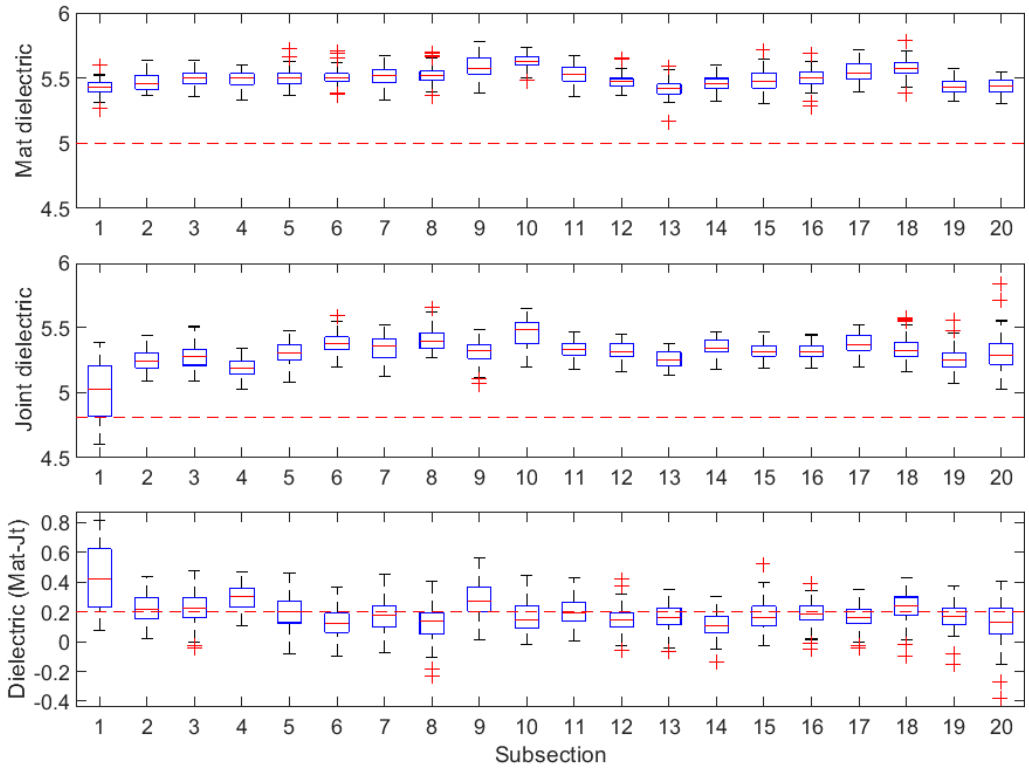

Figure B-129 Box plot of dielectric values for echelon joint (50 ft subsections) – Manning Trail #2

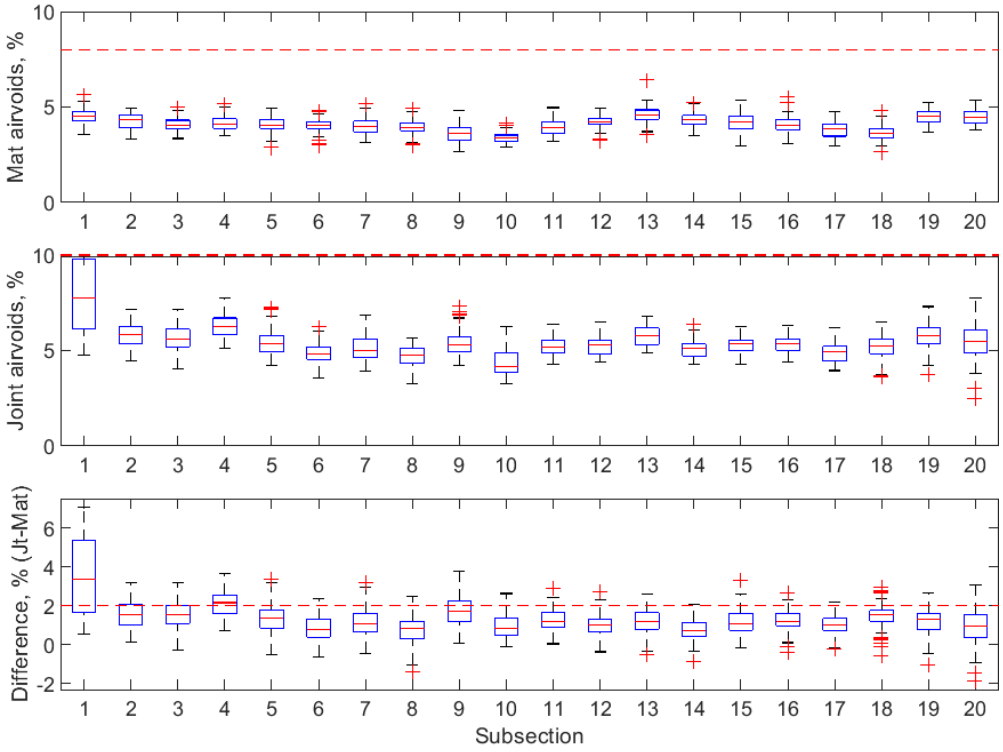

Figure B-130 Box plot of air voids for echelon joint (50 ft subsections) – Manning Trail #2

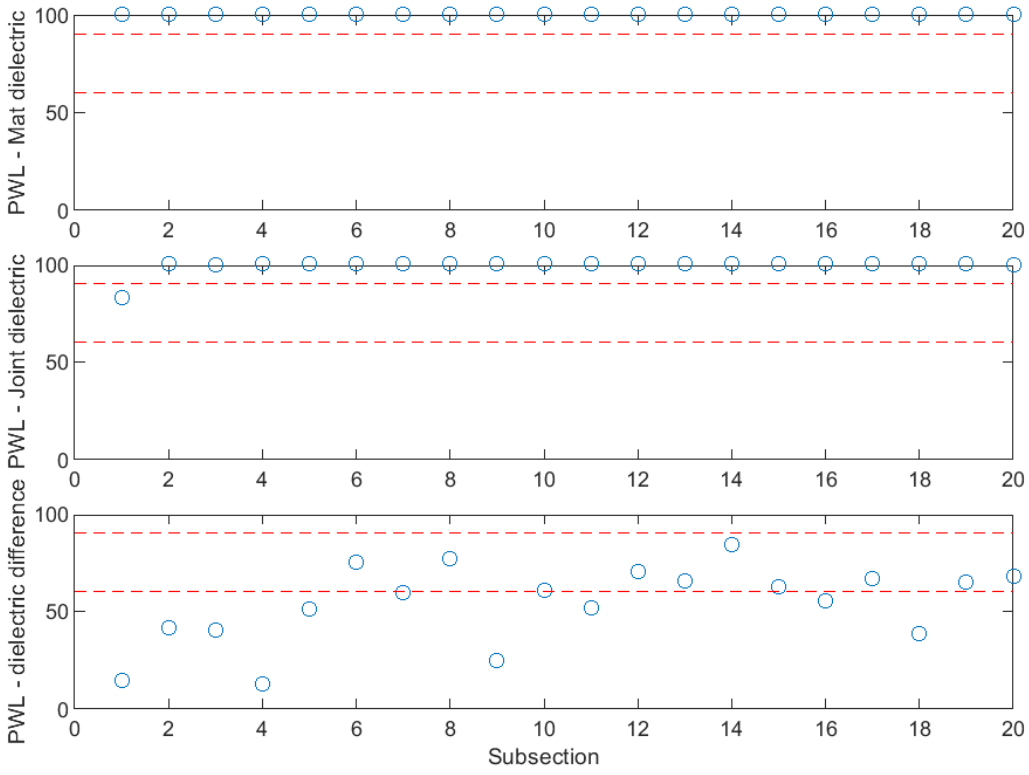

Figure B-131 PWL for dielectric values for echelon joint (50 ft subsections) – Manning Trail #2

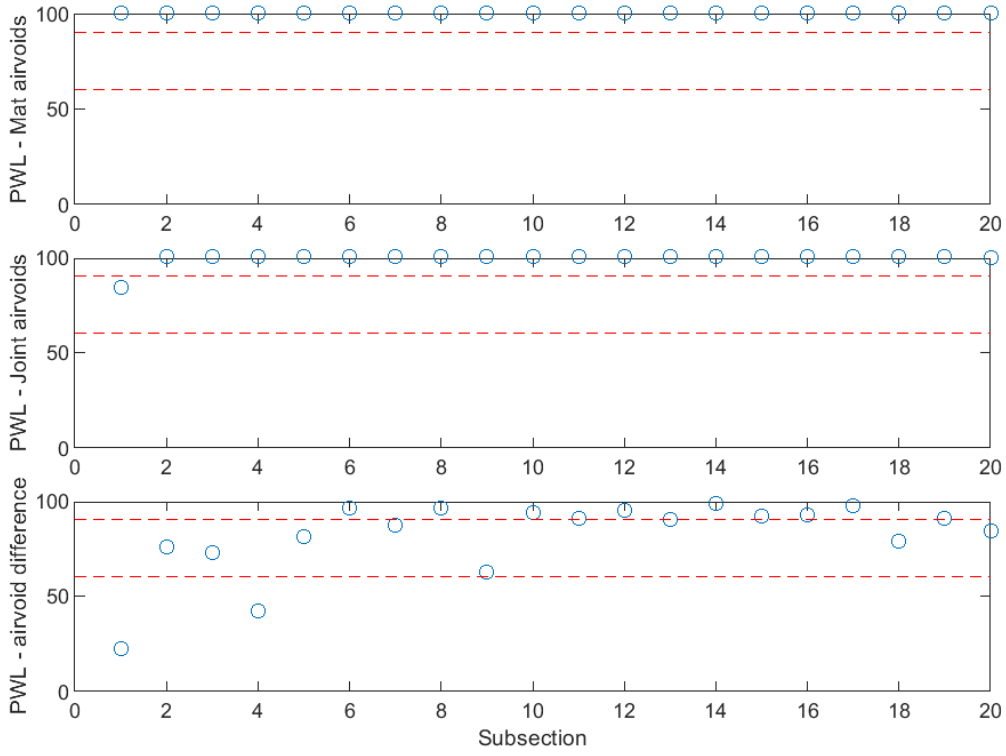

Figure B-132 PWL for air voids for echelon joint (50 ft subsections) – Manning Trail #2

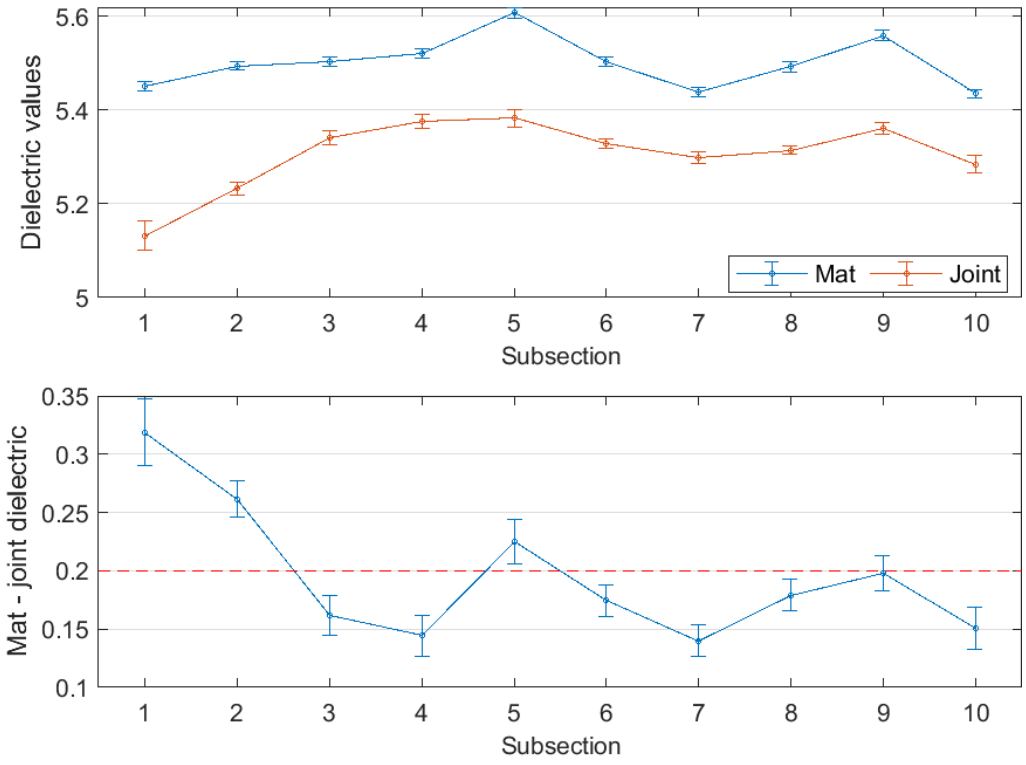

Figure B-133 Interval plot of dielectric values for echelon joint (100 ft subsections) – Manning Trail #2

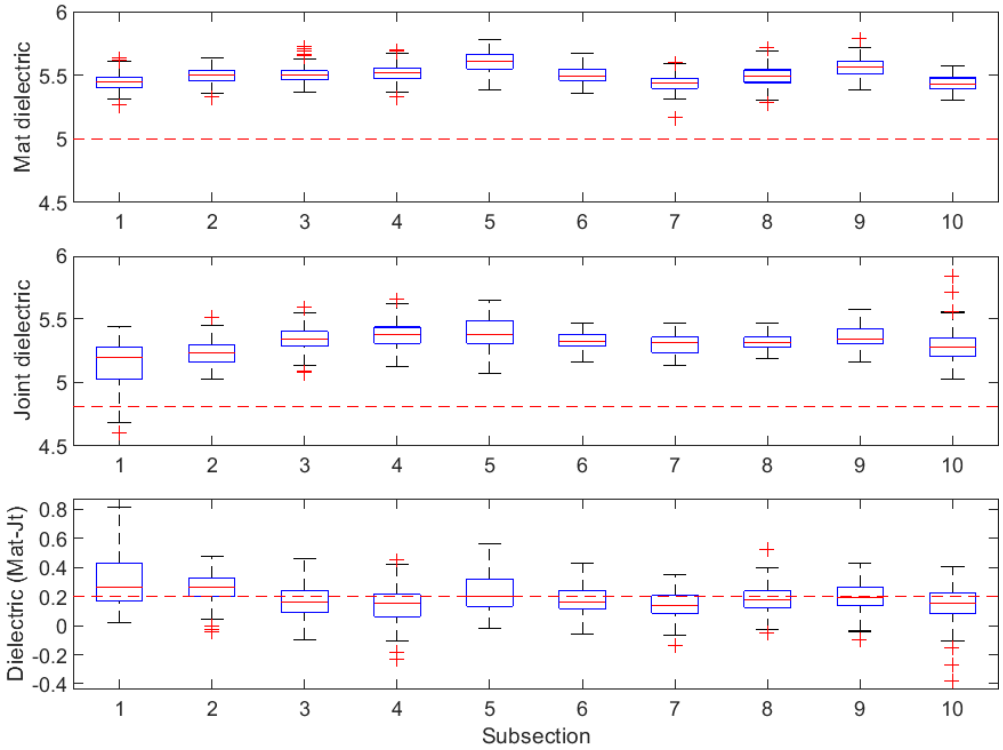

Figure B-134 Box plot of dielectric values for echelon joint (100 ft subsections) – Manning Trail #2

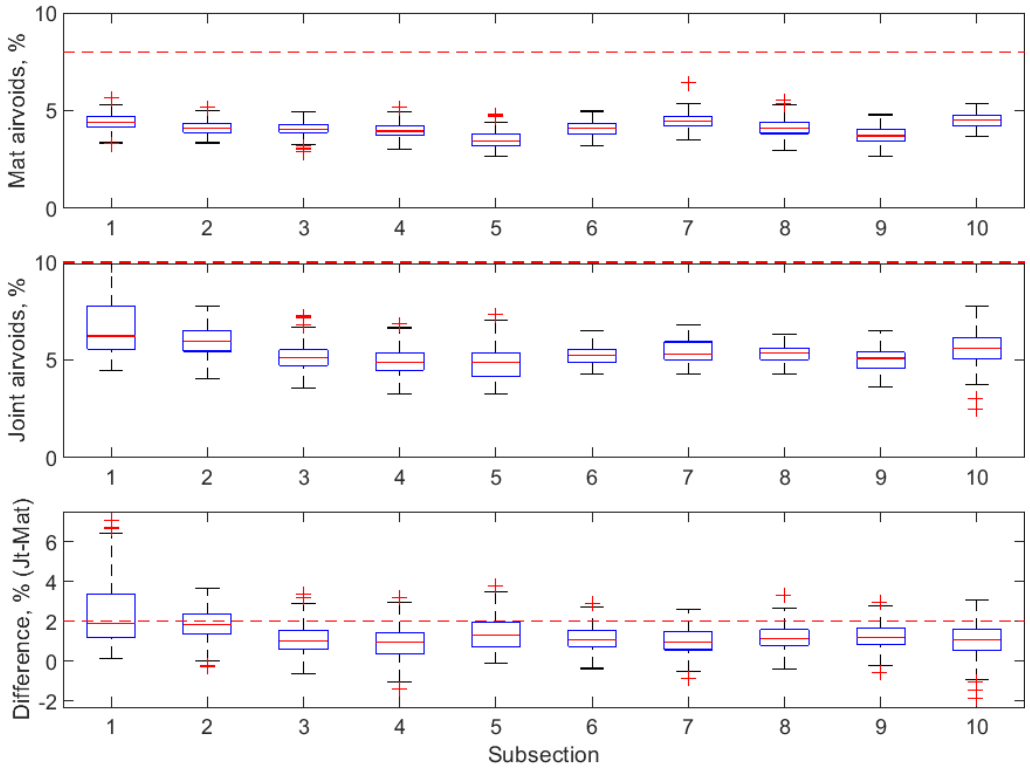

Figure B-135 Box plot of air voids for echelon joint (100 ft subsections) – Manning Trail #2

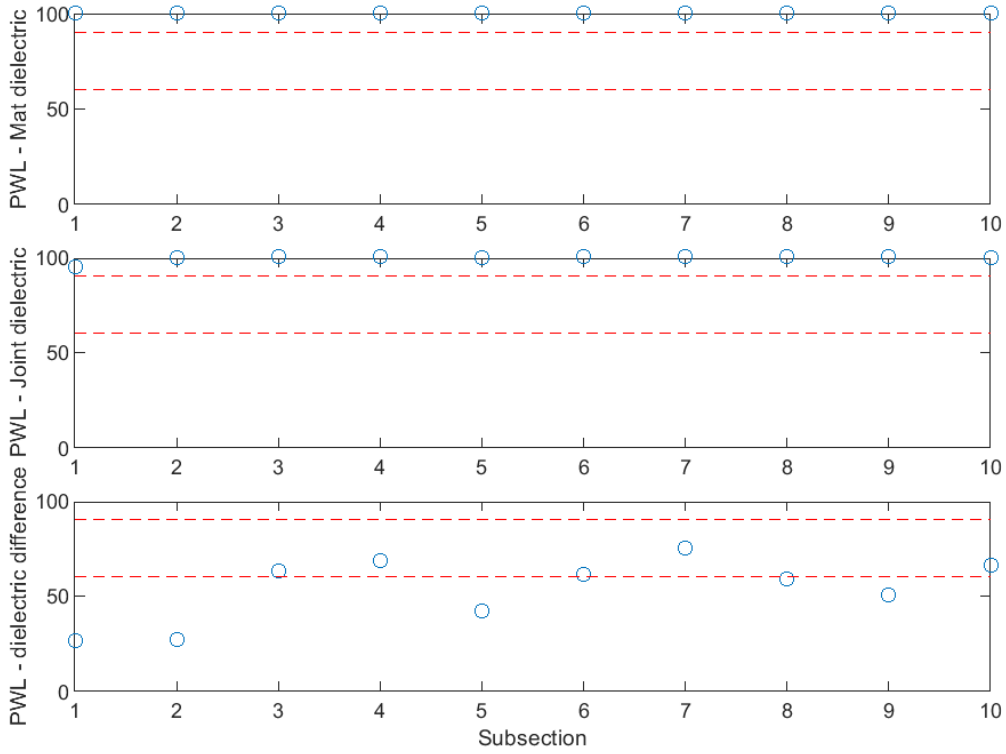

Figure B-136 PWL for dielectric values for echelon joint (100 ft subsections) – Manning Trail #2

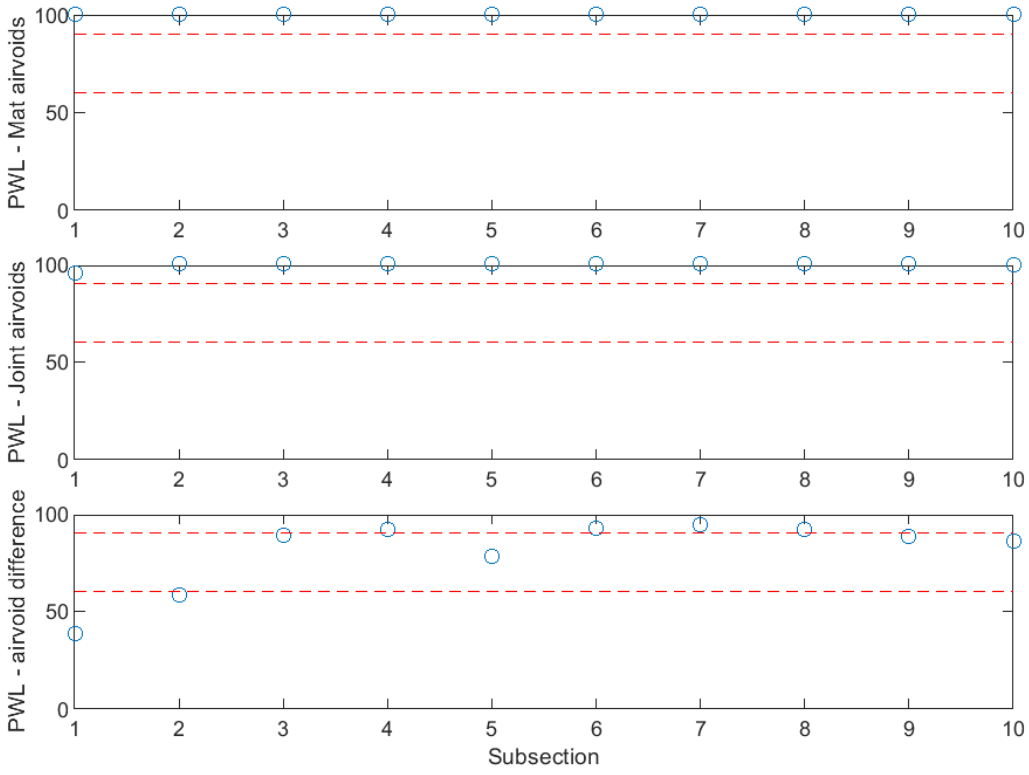

Figure B-137 PWL for air voids for echelon joint (100 ft subsections) – Manning Trail #2

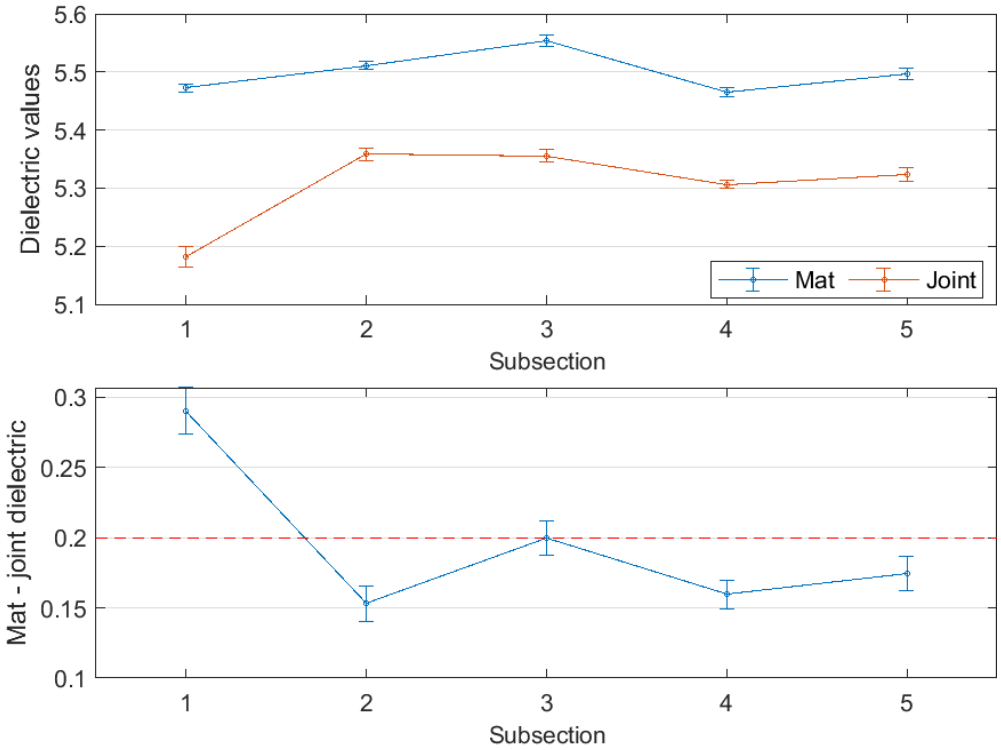

Figure B-138 Interval plot of dielectric values for echelon joint (200 ft subsections) – Manning Trail #2

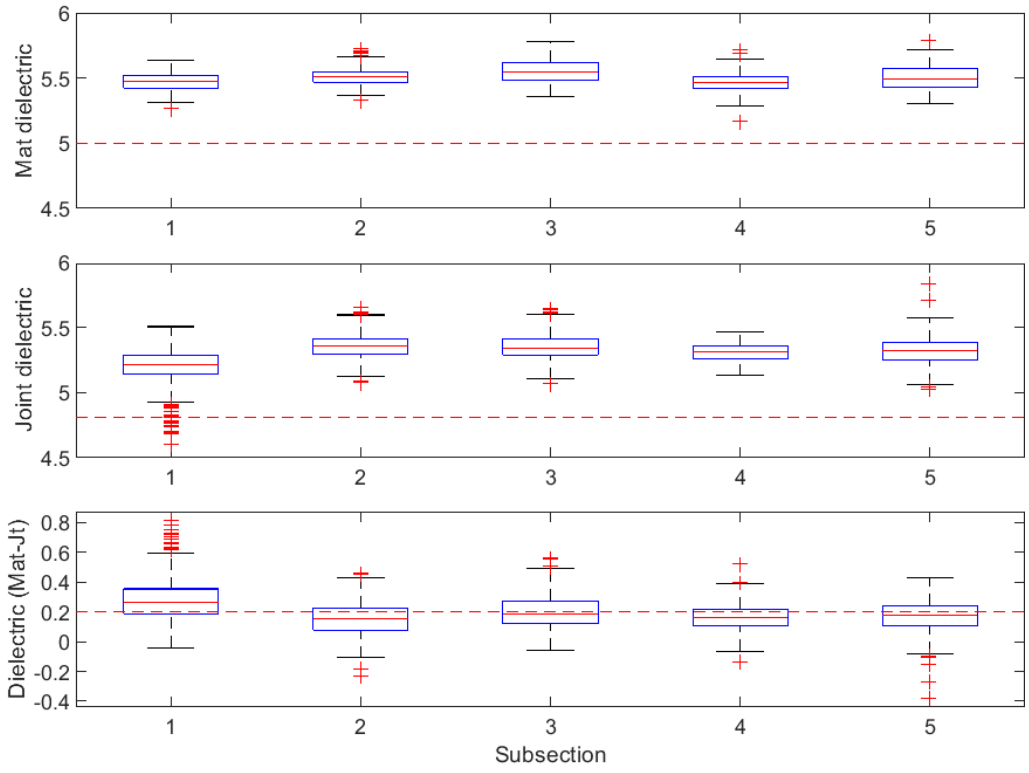

Figure B-139Box plot of dielectric values for echelon joint (200 ft subsections) – Manning Trail #1

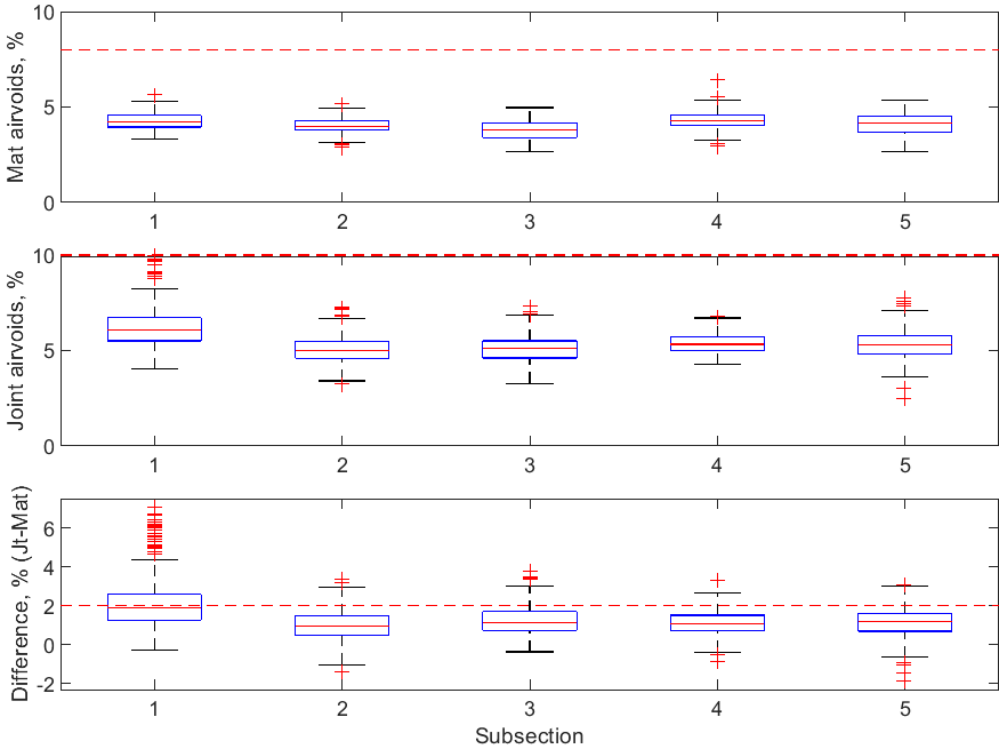

Figure B-140 Box plot of air voids for echelon joint (200 ft subsections) – Manning Trail #2

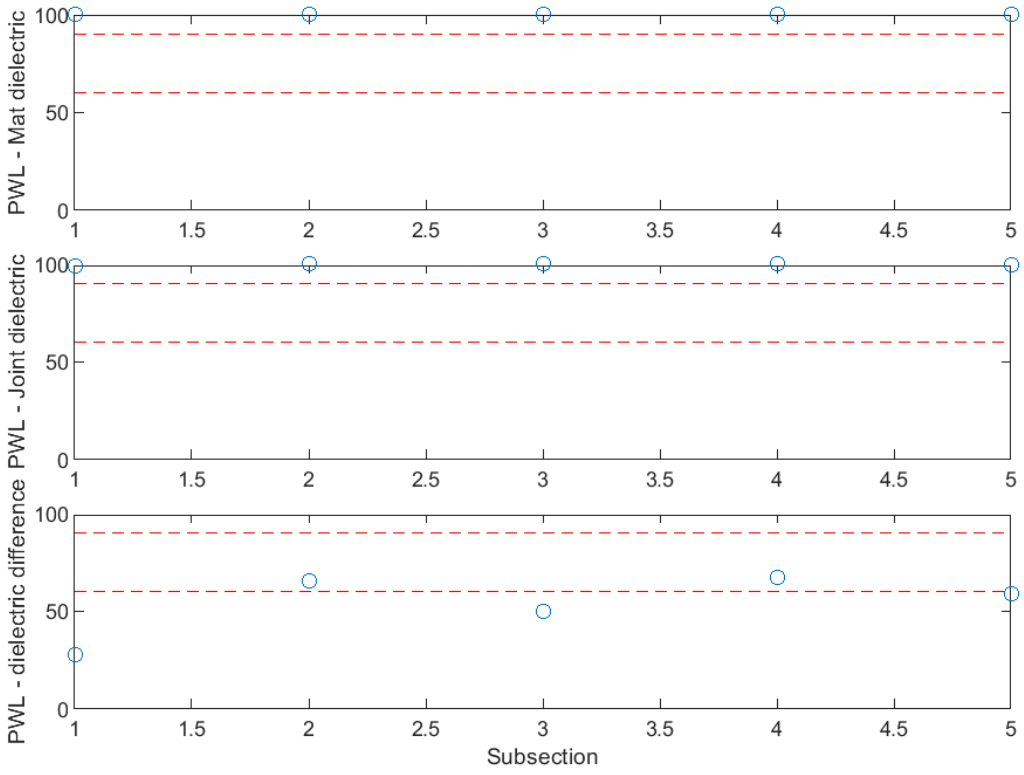

Figure B-141 PWL for dielectric values for echelon joint (200 ft subsections) – Manning Trail #2

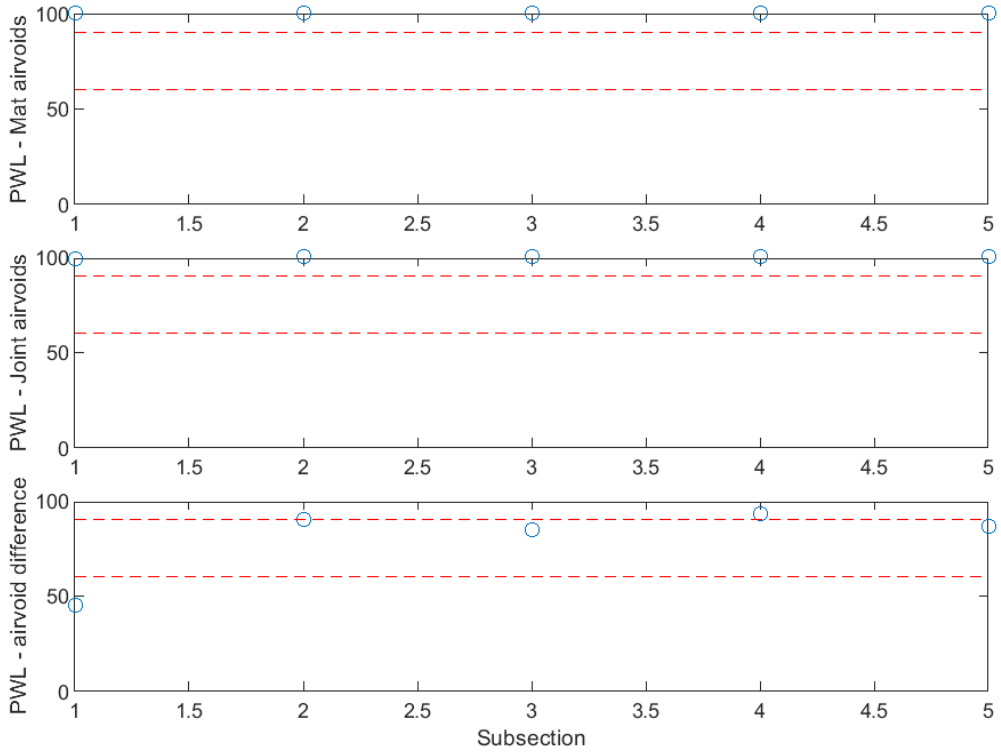

Figure B-142 PWL for air voids for echelon joint (200 ft subsections) – Manning Trail #2

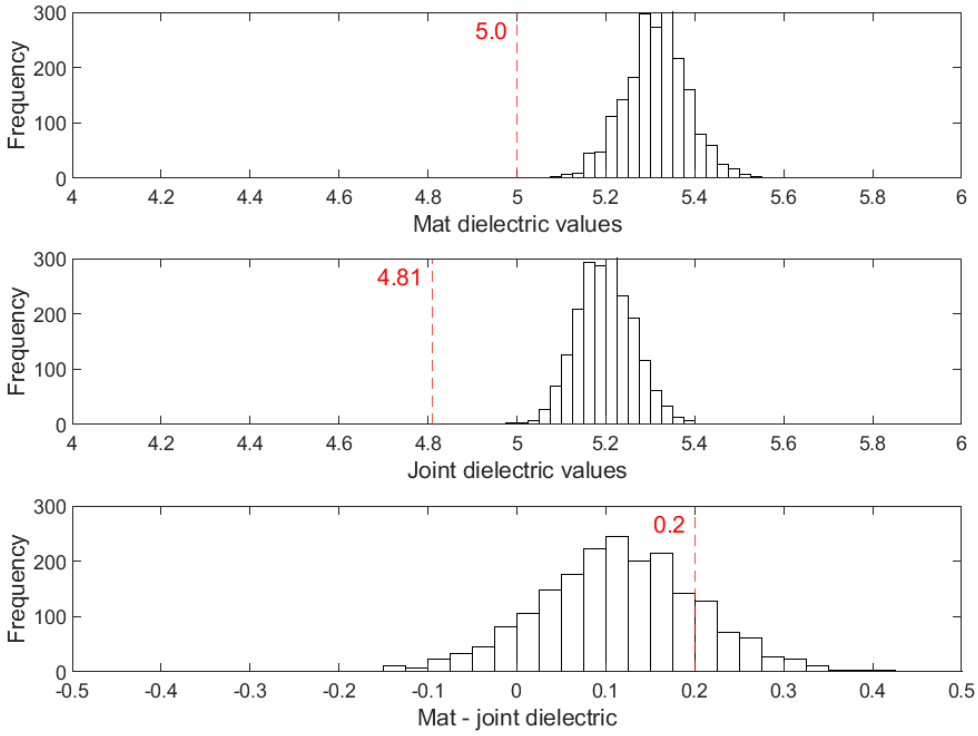

Figure B-143 Histogram of dielectric values for unconfined joint – I-496

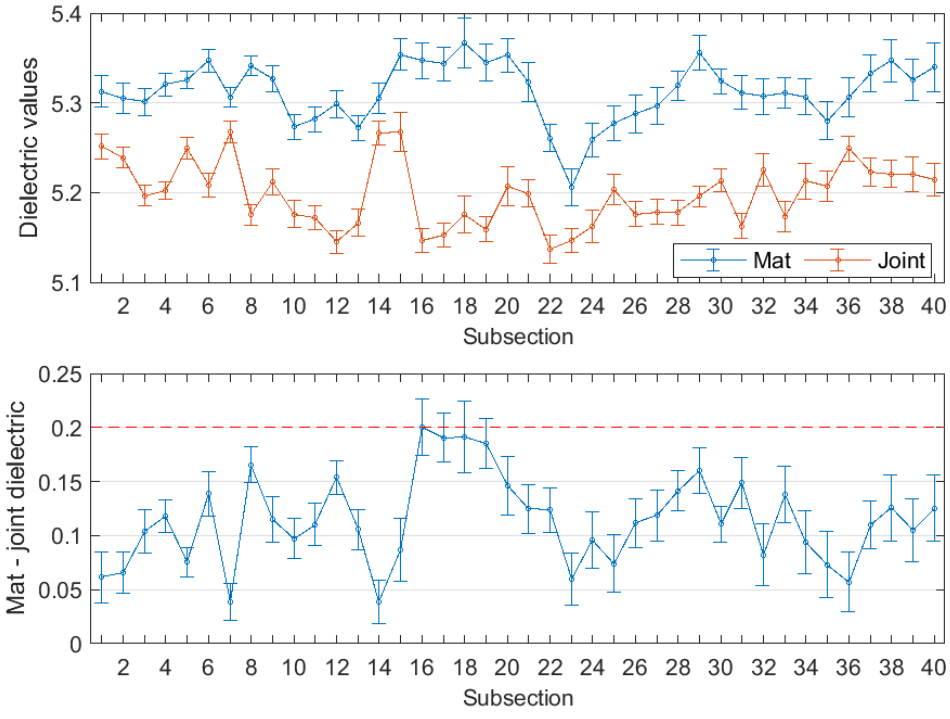

Figure B-144 Interval plot of dielectric values for unconfined joint (25 ft subsections) – I-496

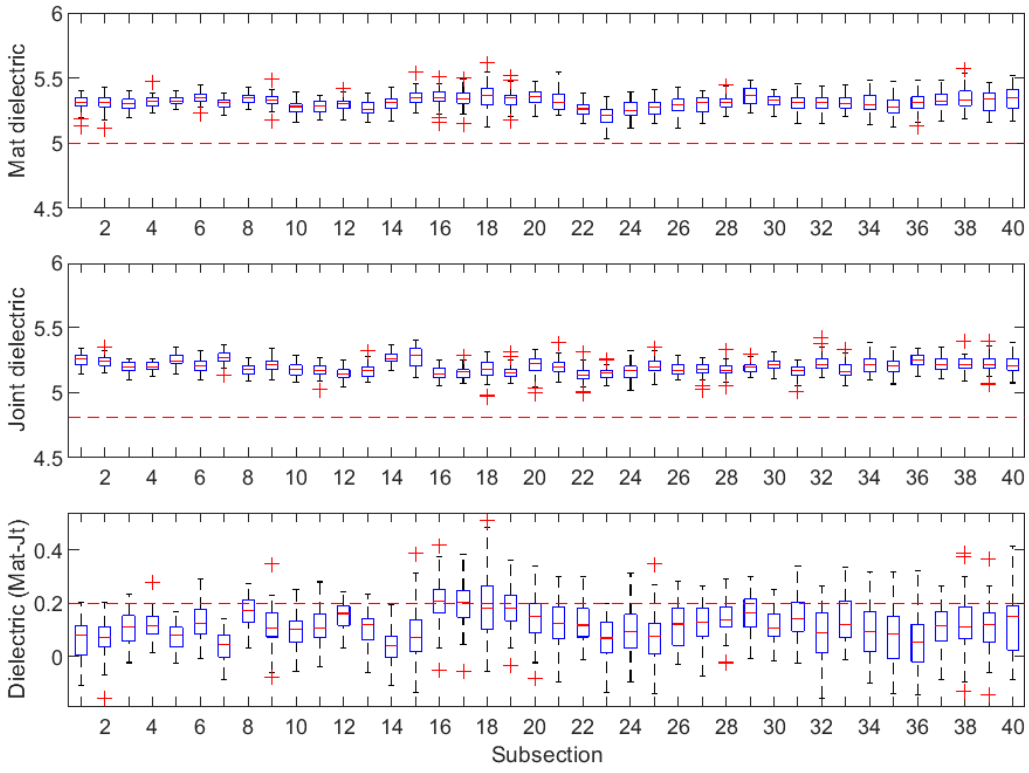

Figure B-145 Box plot of dielectric values for unconfined joint (25 ft subsections) – I-496

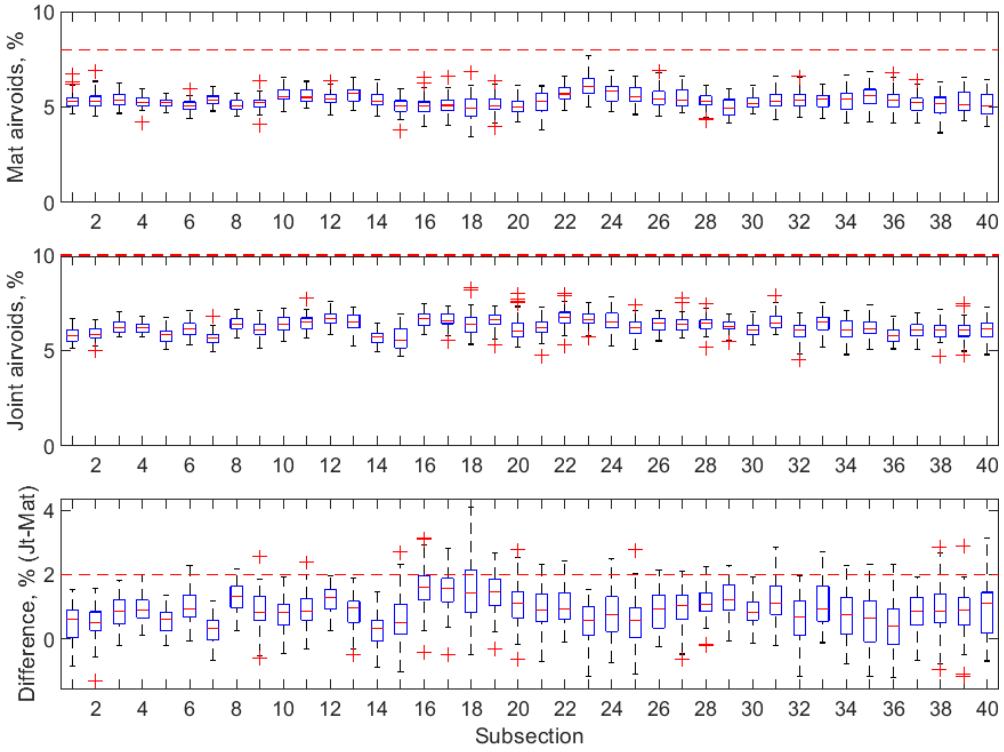

Figure B-146 Box plot of air voids for unconfined joint (25 ft subsections) – I-496

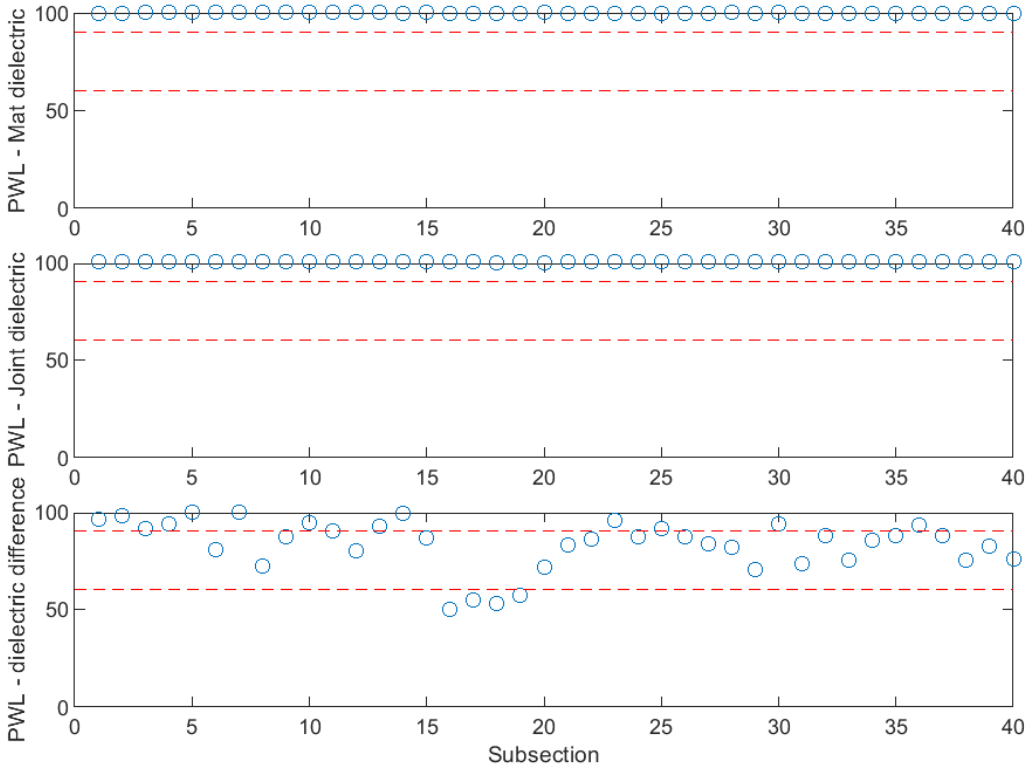

Figure B-147 PWL for dielectric values for unconfined joint (25 ft subsections) – I-496

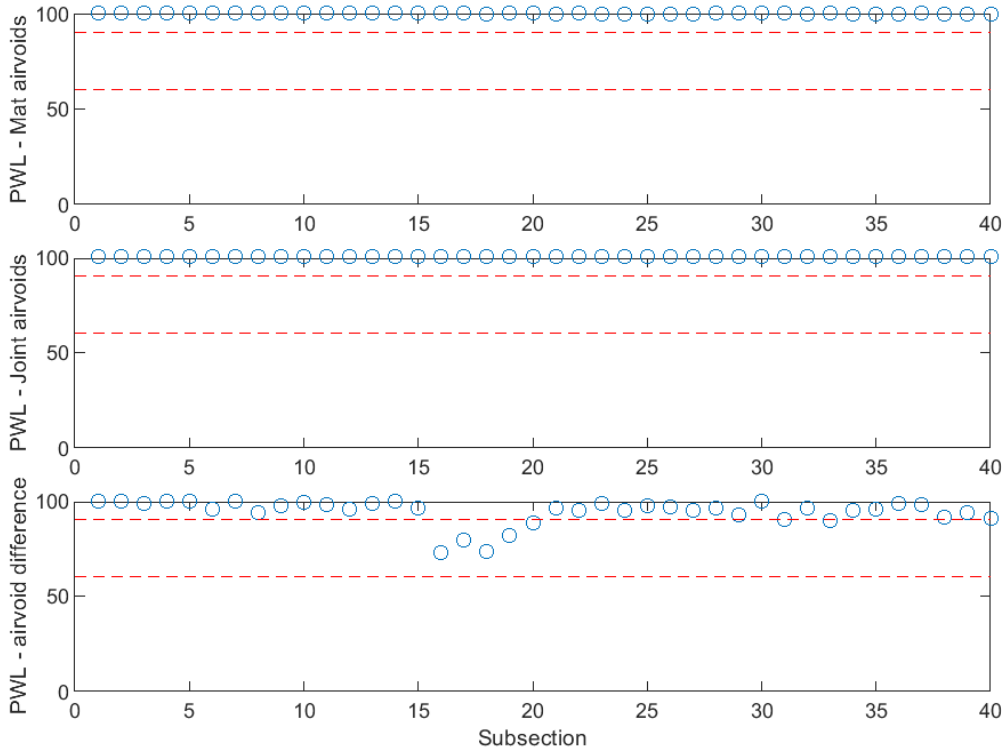

Figure B-148 PWL for air voids for unconfined joint (25 ft subsections) – I-496

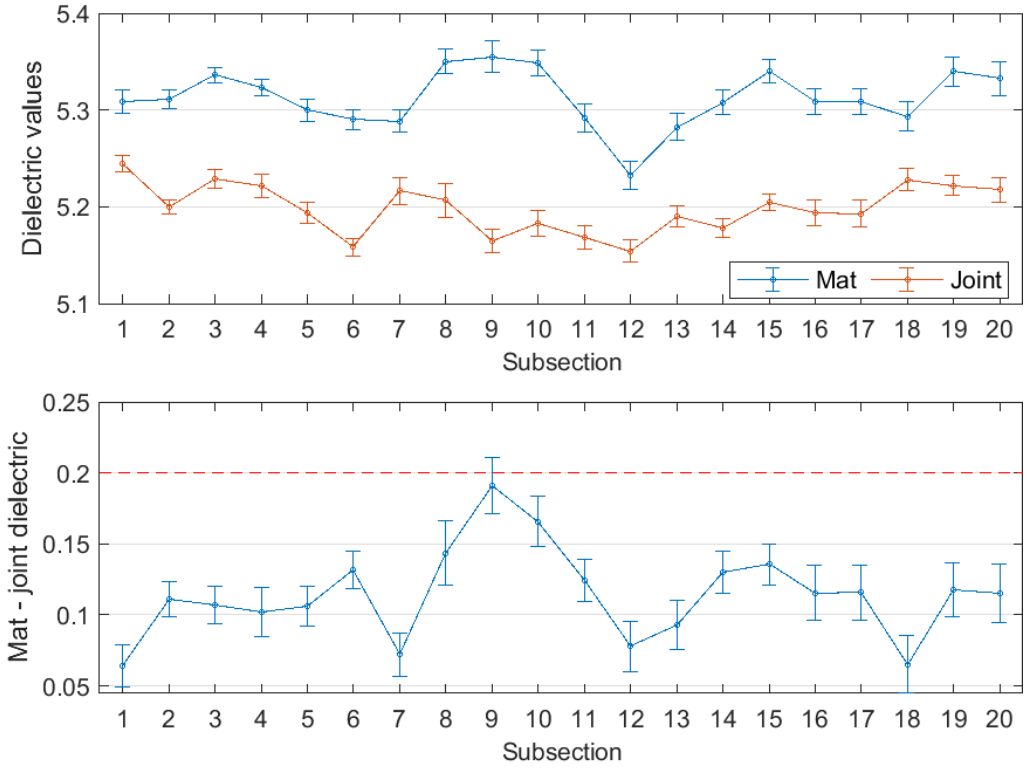

Figure B-149 Interval plot of dielectric values for unconfined joint (50 ft subsections) – I-496

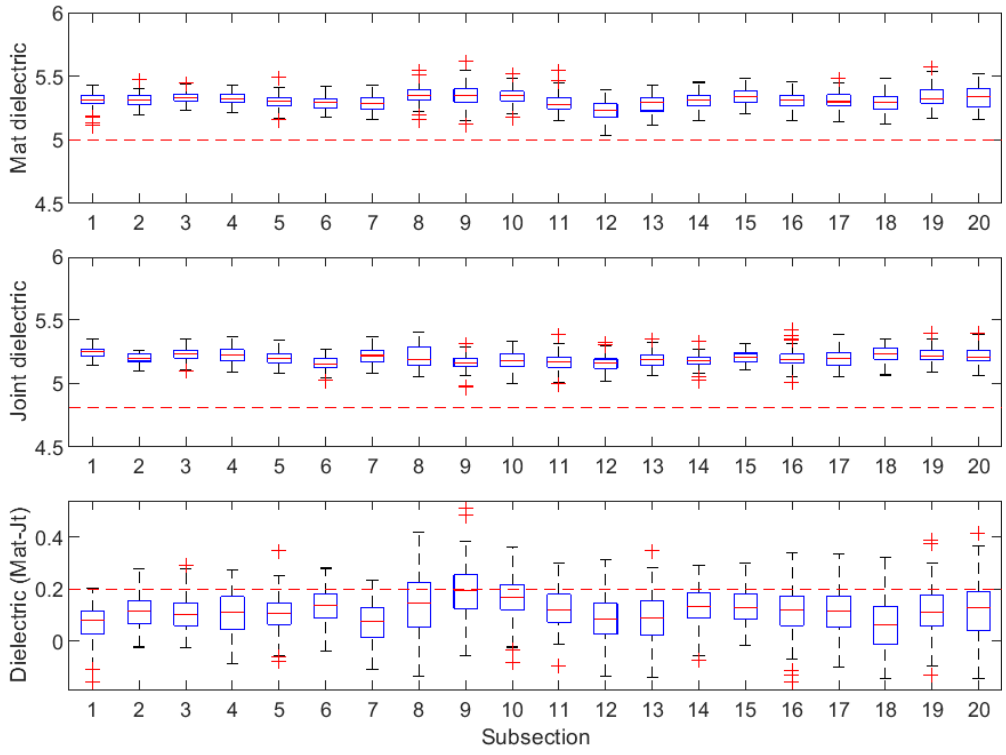

Figure B-150 Box plot of dielectric values for unconfined joint (50 ft subsections) – I-496

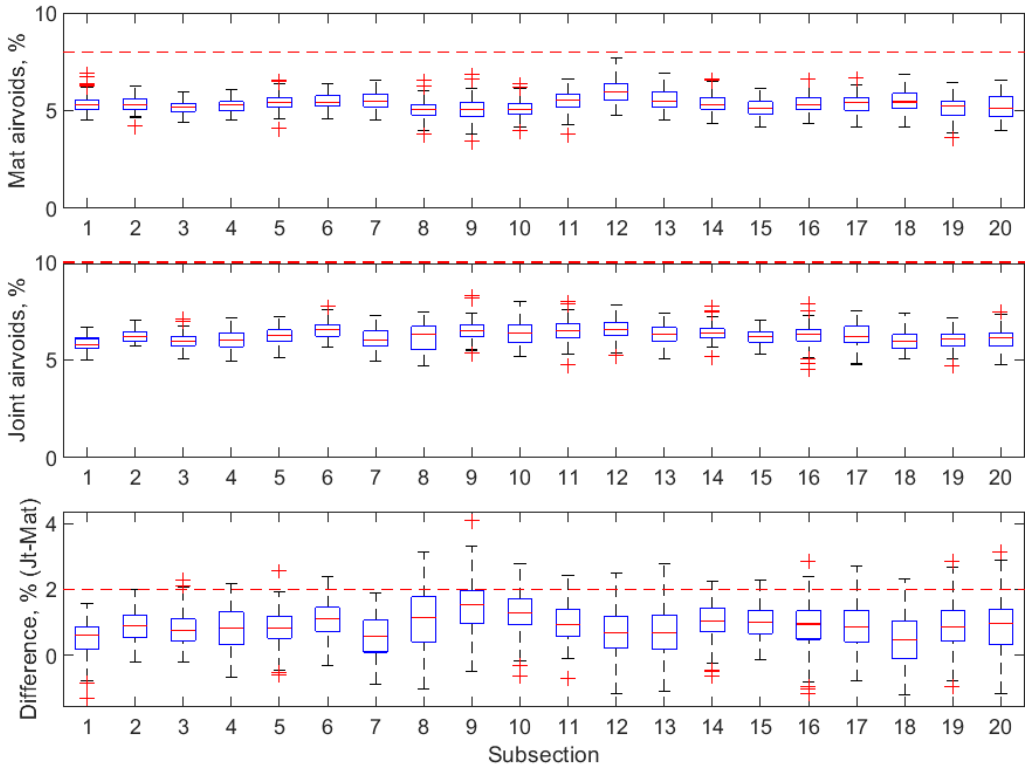

Figure B-151 Box plot of air voids for unconfined joint (50 ft subsections) – I-496

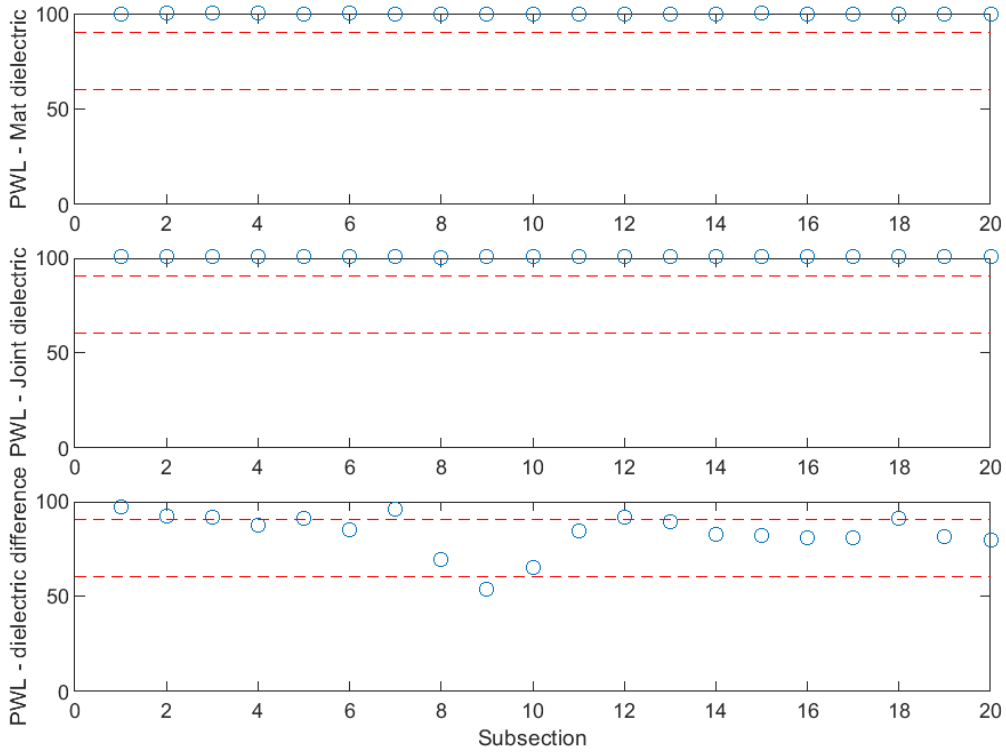

Figure B-152 PWL for dielectric values for unconfined joint (50 ft subsections) – I-496

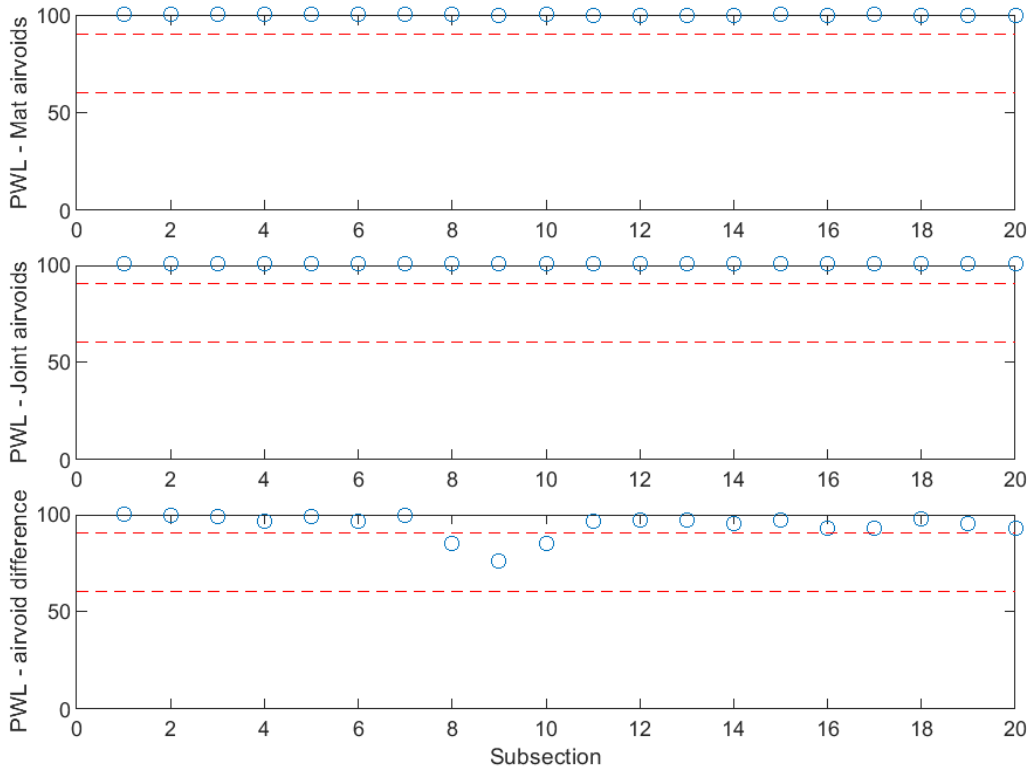

Figure B-153 PWL for air voids for unconfined joint (50 ft subsections) – I-496

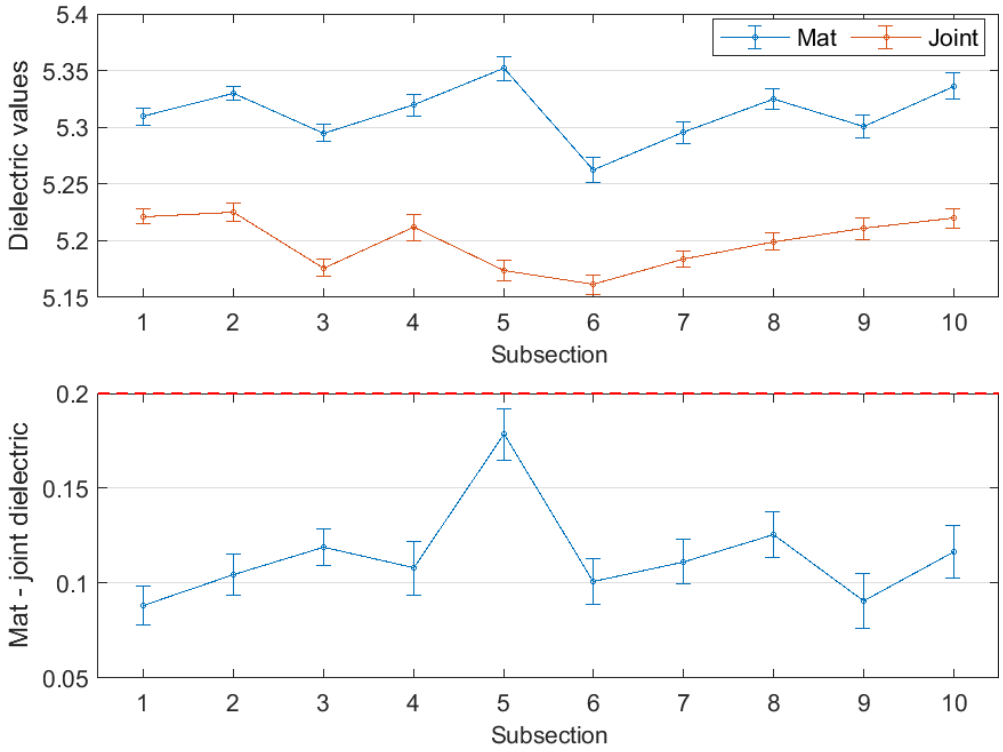

Figure B-154 Interval plot of dielectric values for unconfined joint (100 ft subsections) – I-496

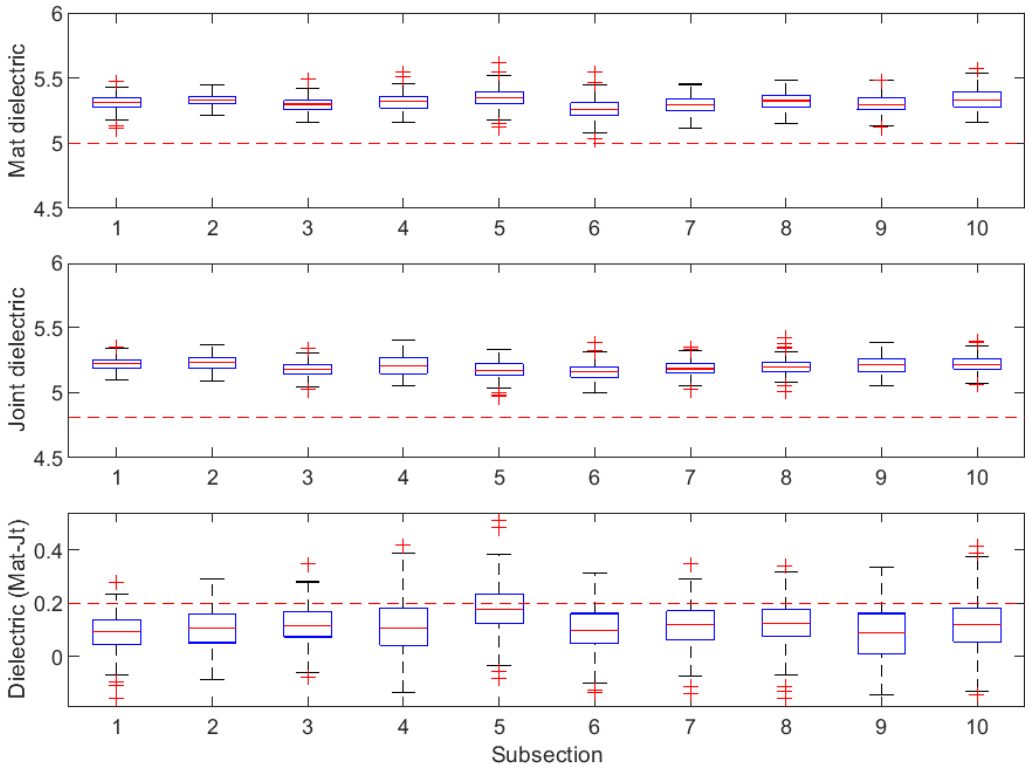

Figure B-155 Box plot of dielectric values for unconfined joint (100 ft subsections) – I-496

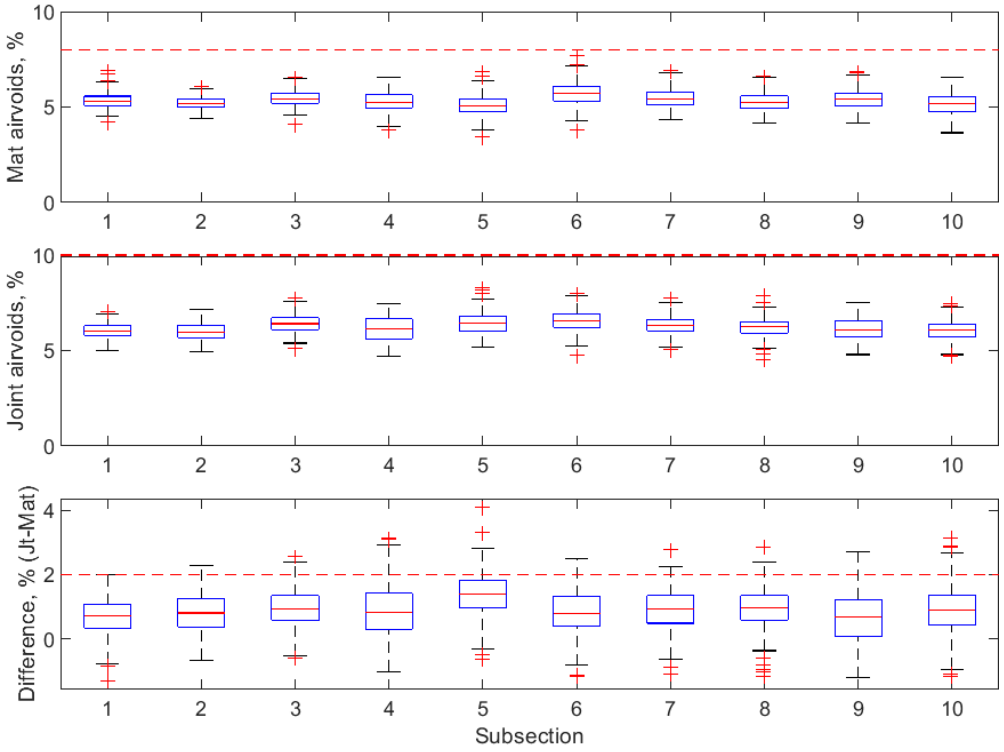

Figure B-156 Box plot of air voids for unconfined joint (100 ft subsections) – I-496

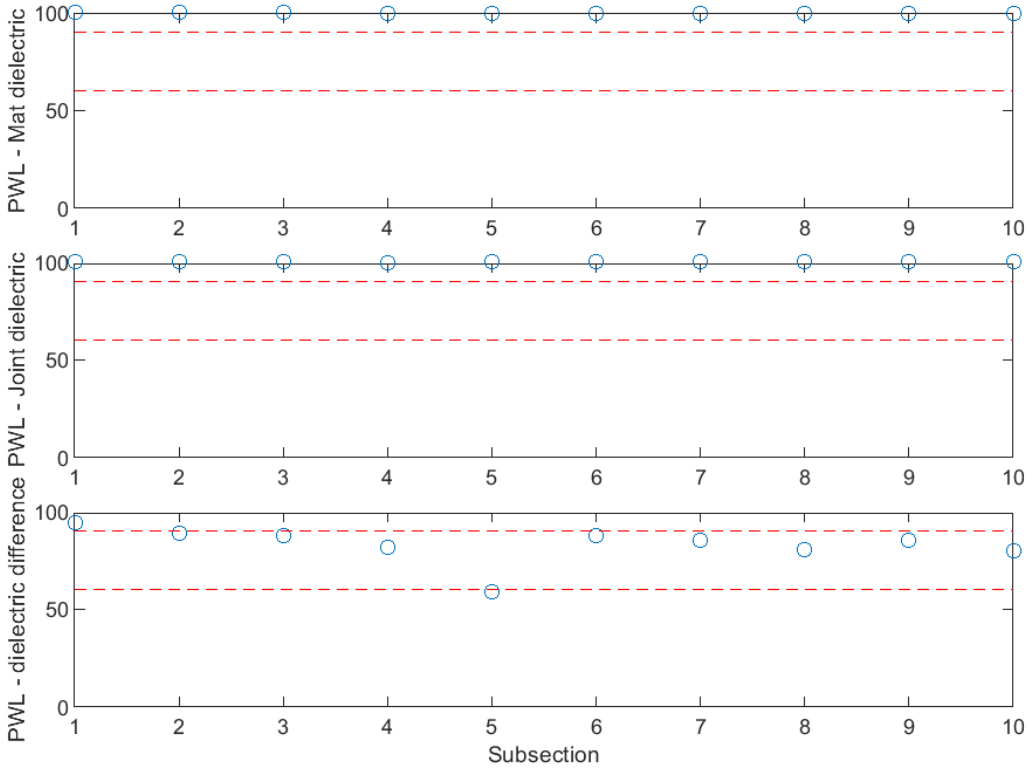

Figure B-157 PWL for dielectric values for unconfined joint (100 ft subsections) – I-496

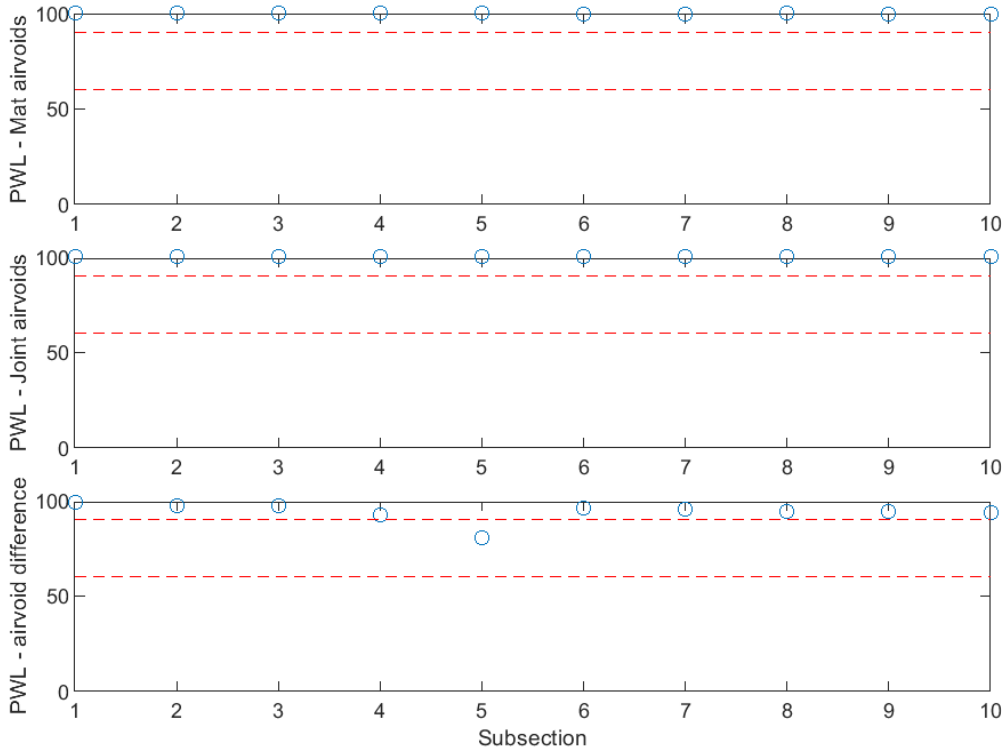

Figure B-158 PWL for air voids for unconfined joint (100 ft subsections) – I-496

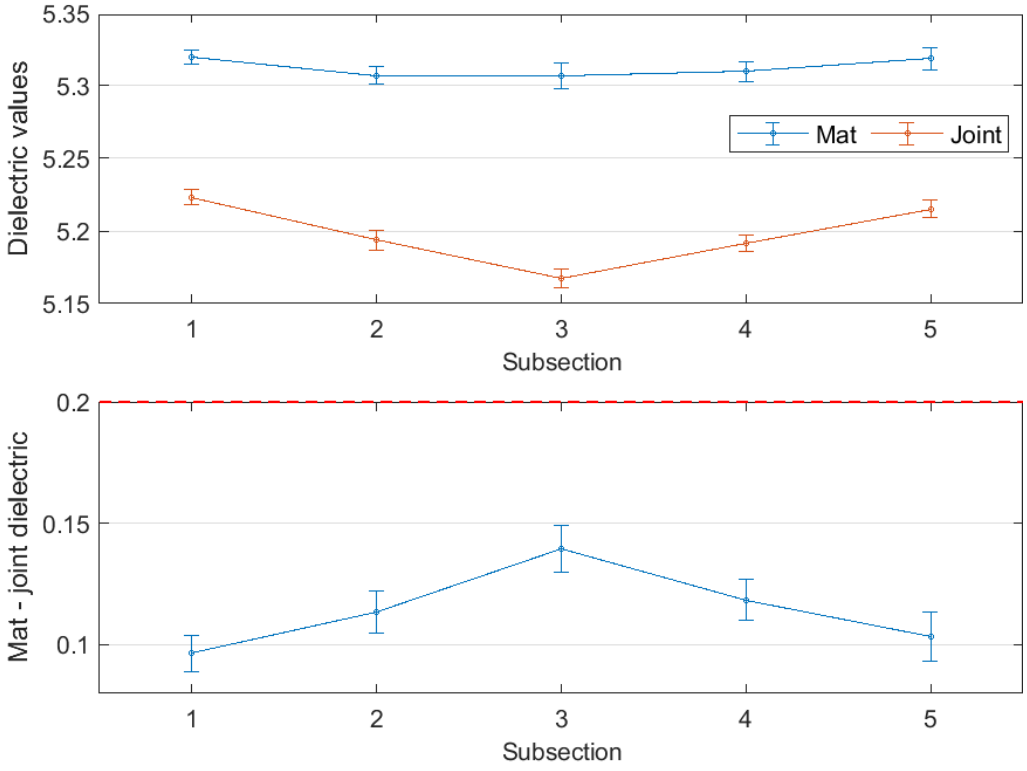

Figure B-159 Interval plot of dielectric values for unconfined joint (200 ft subsections) – I-496

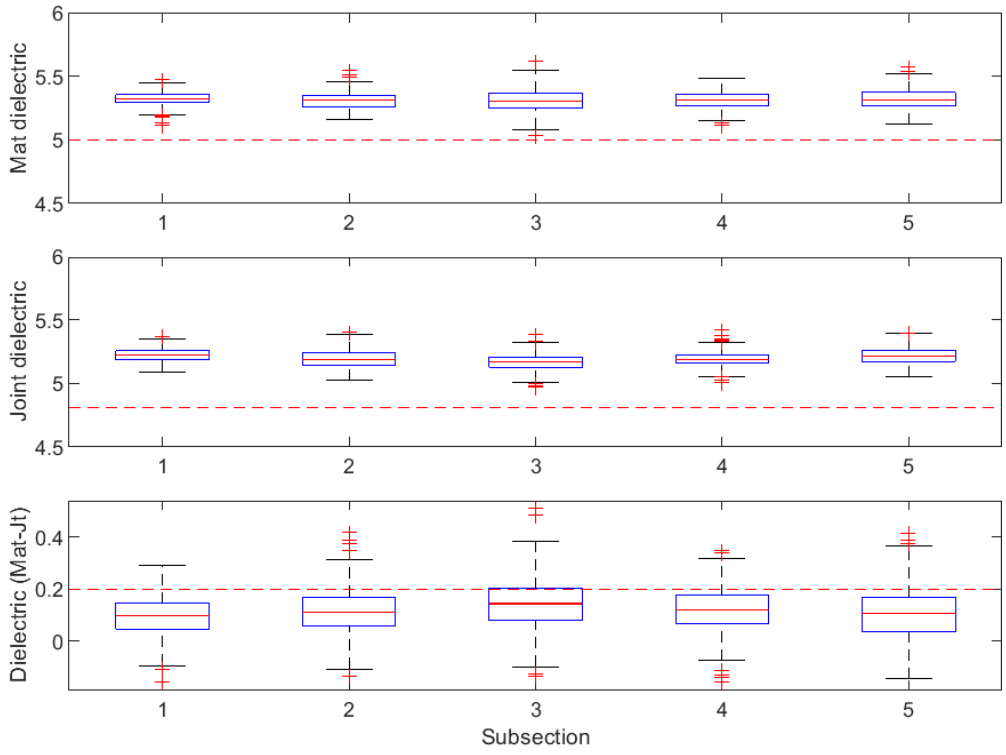

Figure B-160 Box plot of dielectric values for unconfined joint (200 ft subsections) – I-496

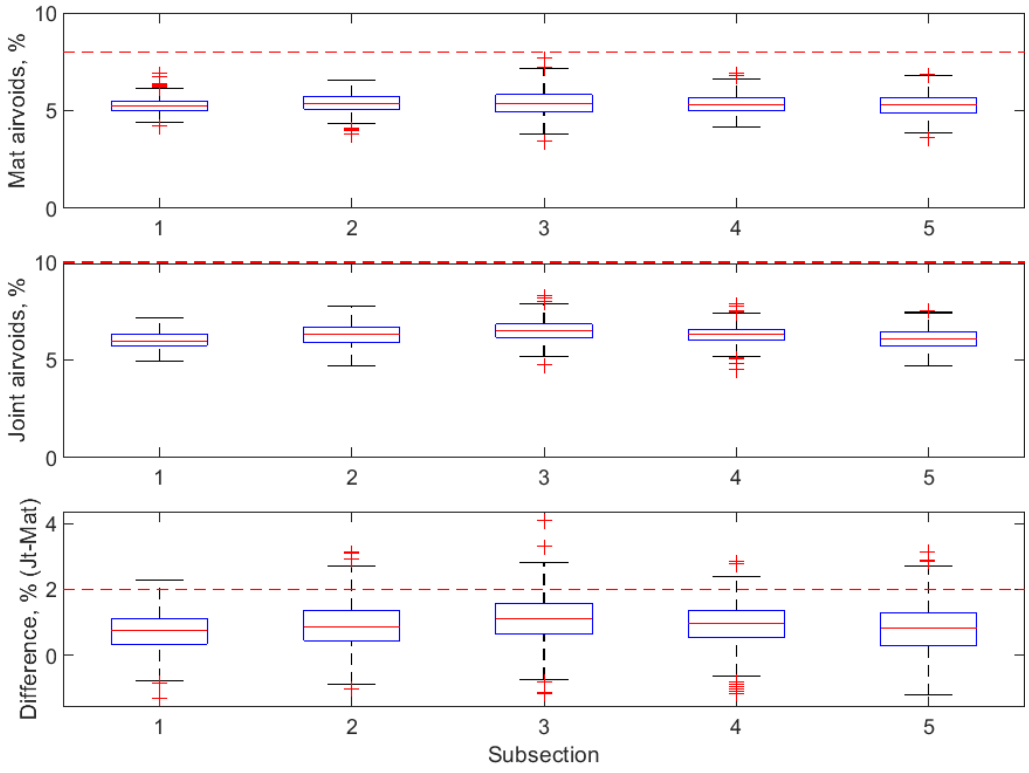

Figure B-161 Box plot of air voids for unconfined joint (200 ft subsections) – I-496

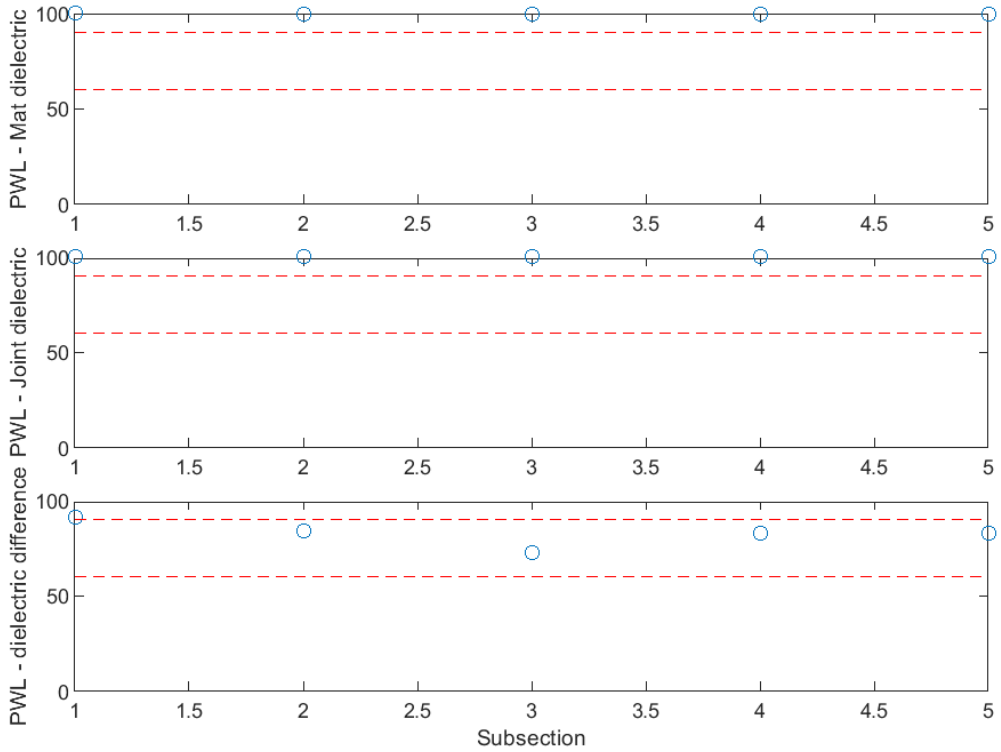

Figure B-162 PWL for dielectric values for unconfined joint (200 ft subsections) – I-496

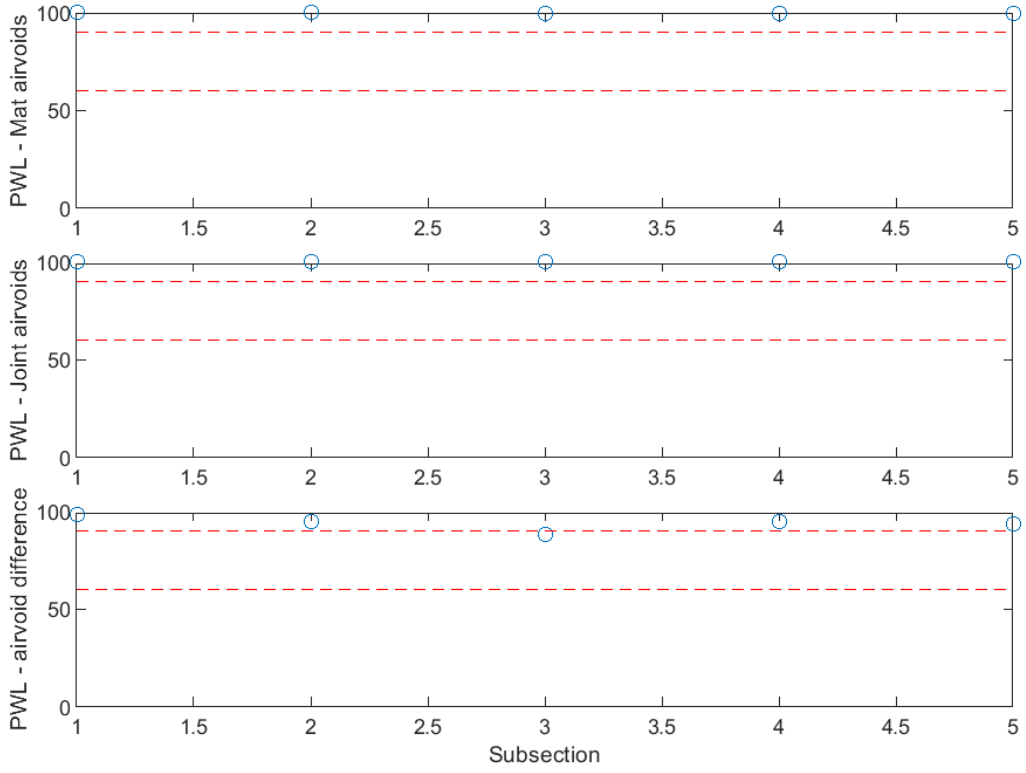

Figure B-163 PWL for air voids for unconfined joint (200 ft subsections) – I-496

US-31 Project

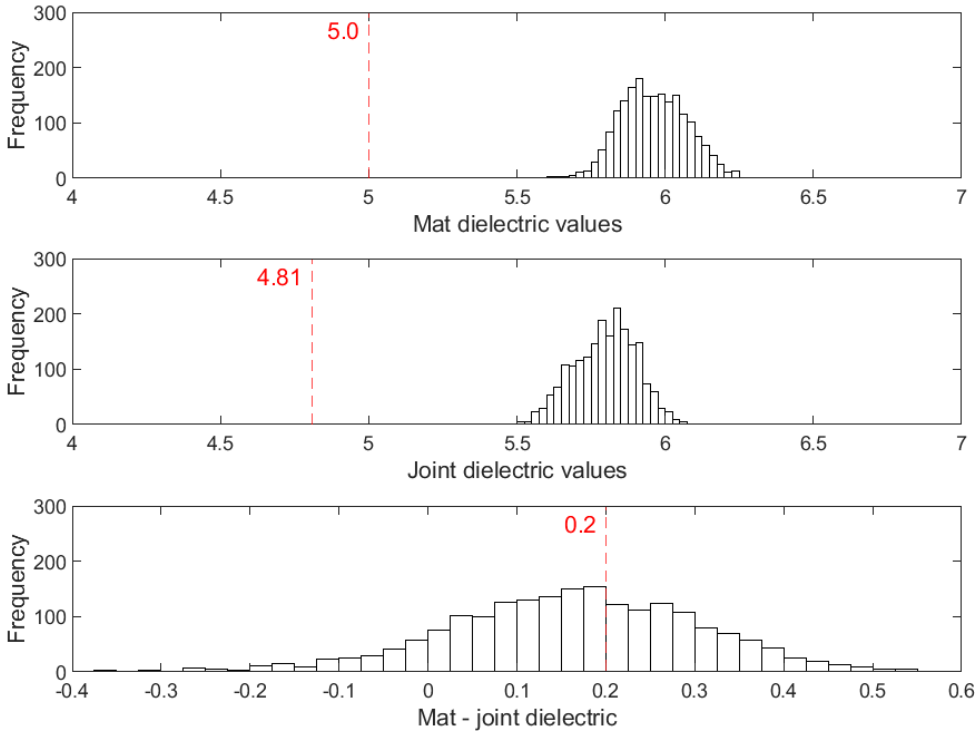

Figure B-164 Histogram of dielectric values for echelon joint – US-31

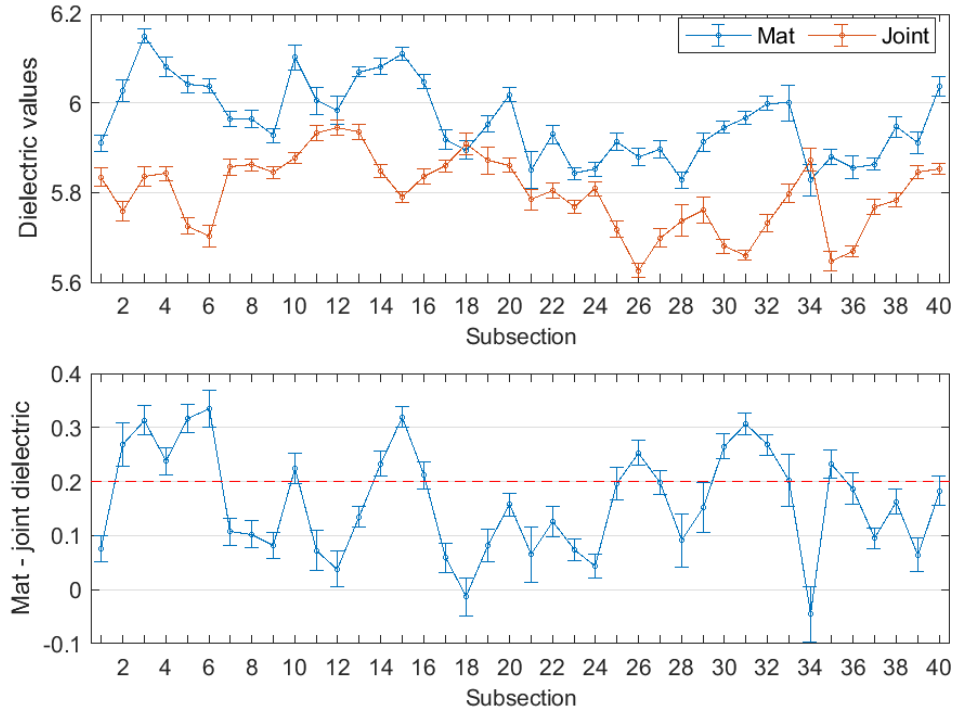

Figure B-165 Interval plot of dielectric values for echelon joint (25 ft subsections) – US-31

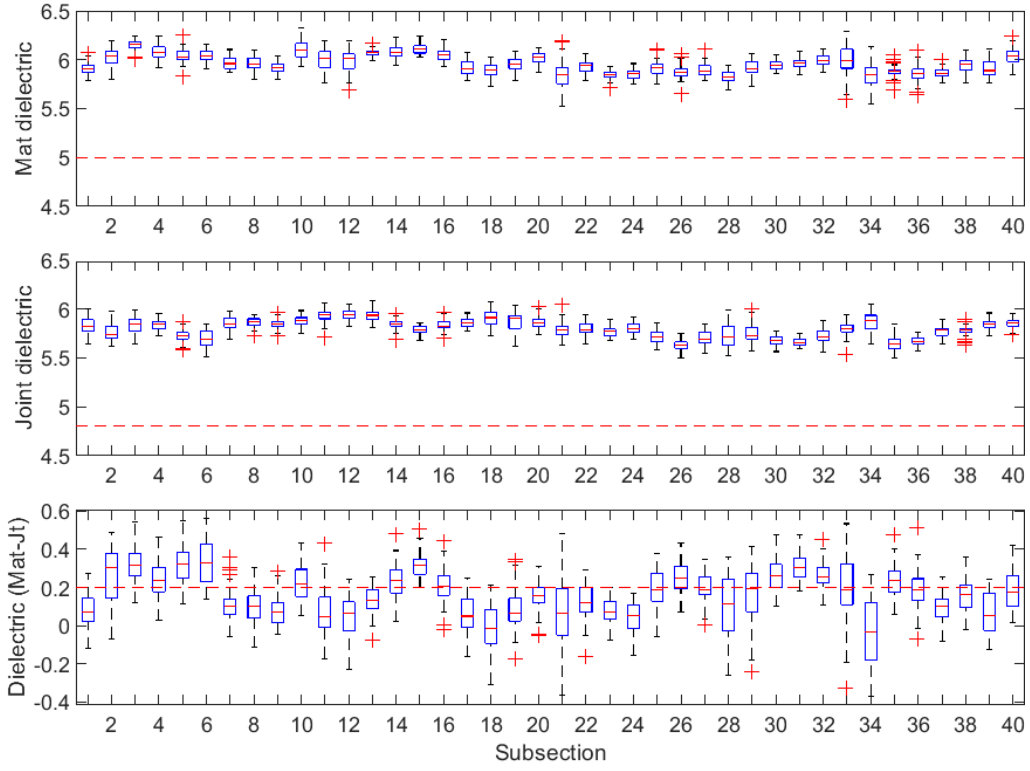

Figure B-166 Box plot of dielectric values for echelon joint (25 ft subsections) – US-31

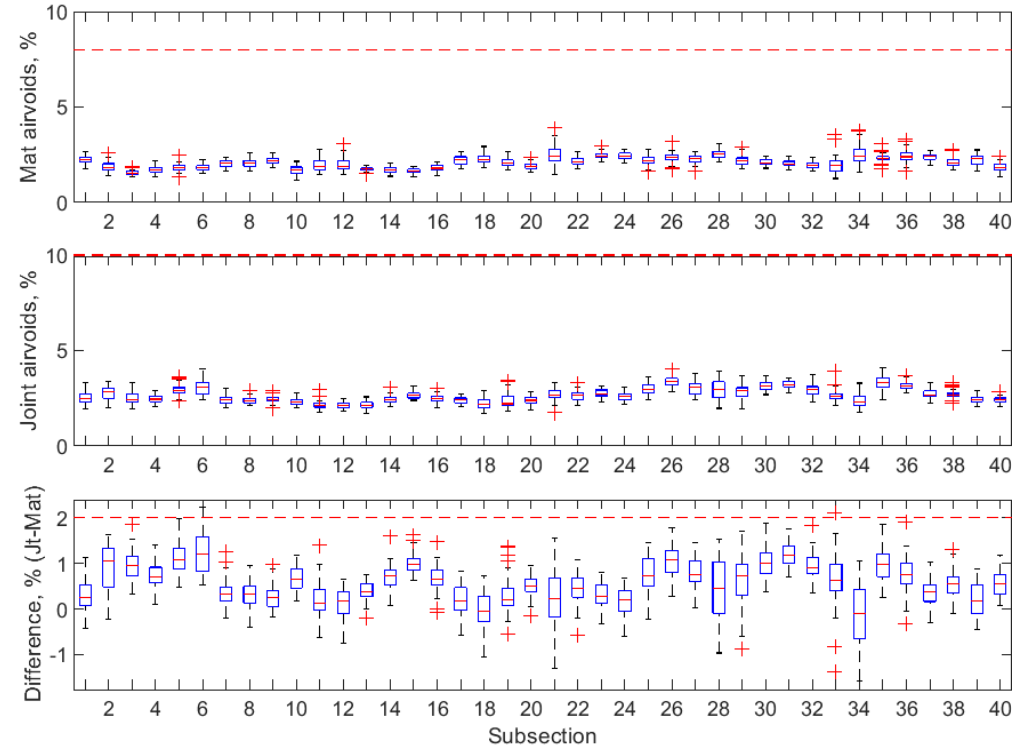

Figure B-167 Box plot of air voids for echelon joint (25 ft subsections) – US-31

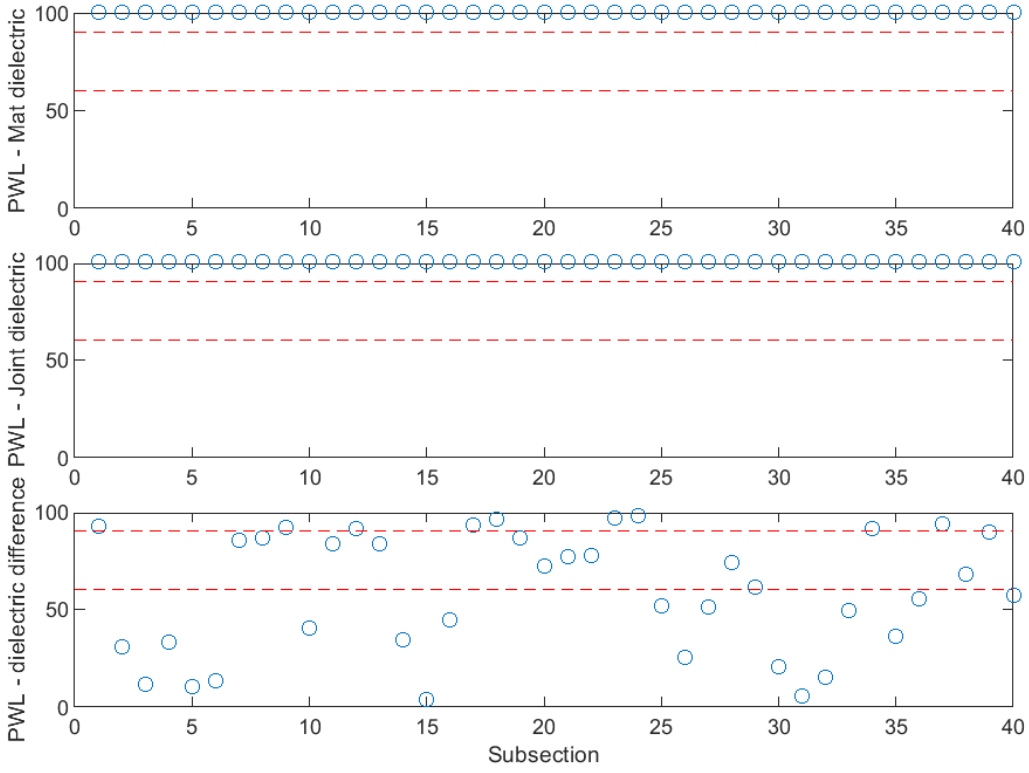

Figure B-168 PWL for dielectric values for echelon joint (25 ft subsections) – US-31

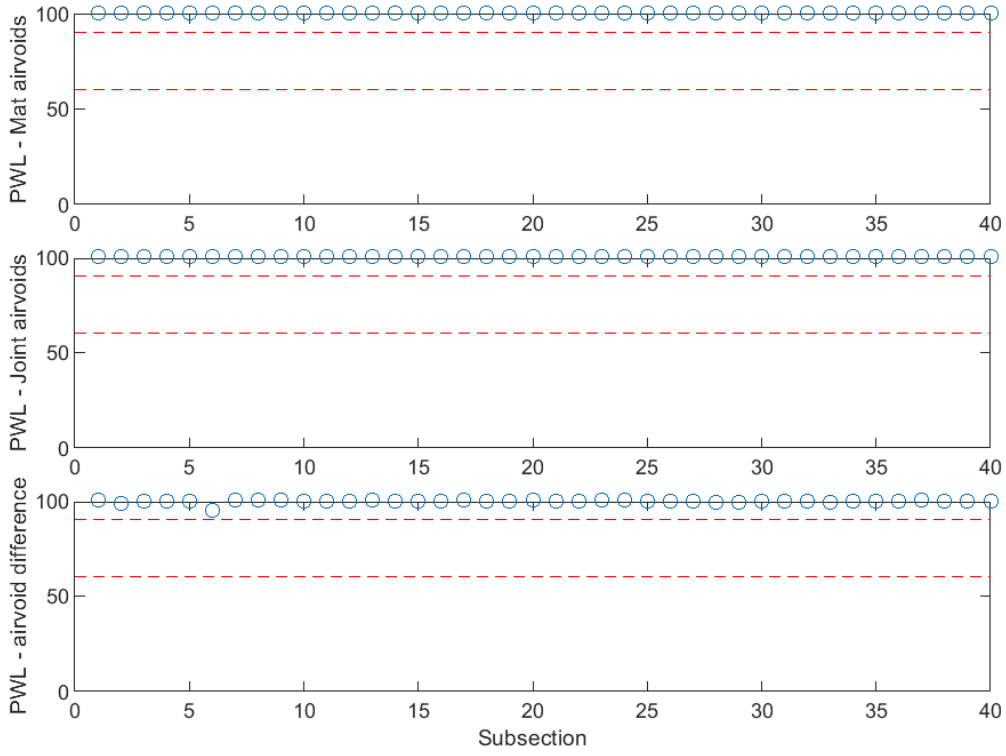

Figure B-169 PWL for air voids for echelon joint (25 ft subsections) – US-31

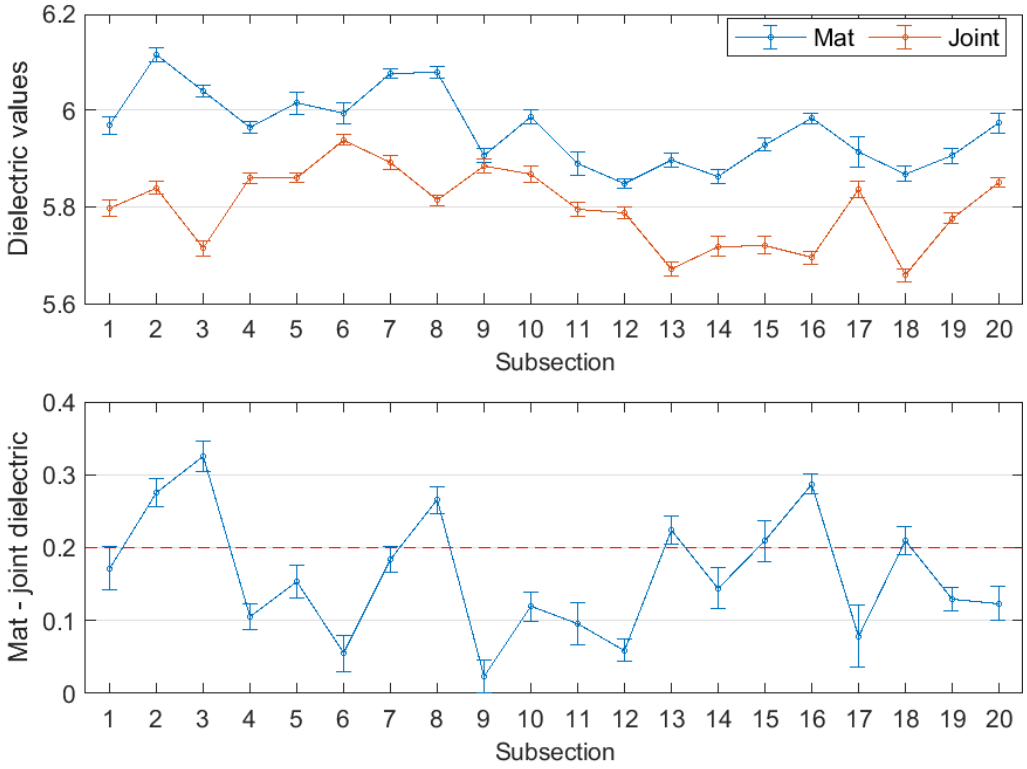

Figure B-170 Interval plot of dielectric values for echelon joint (50 ft subsections) – US-31

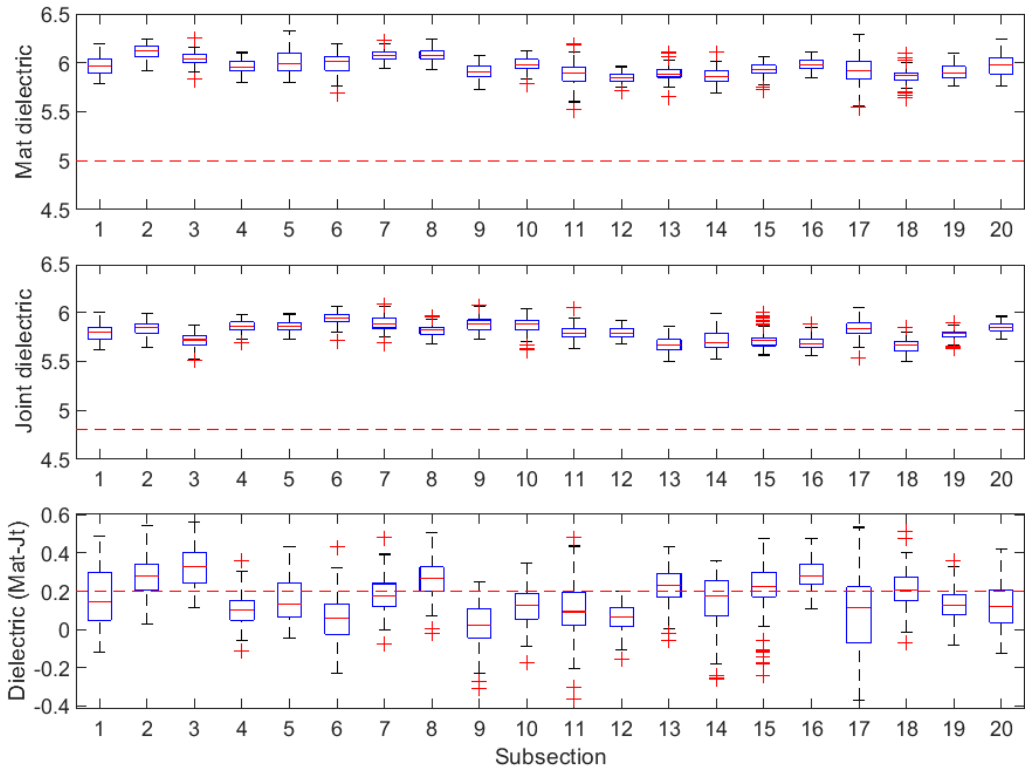

Figure B-171 Box plot of dielectric values for echelon joint (50 ft subsections) – US-31

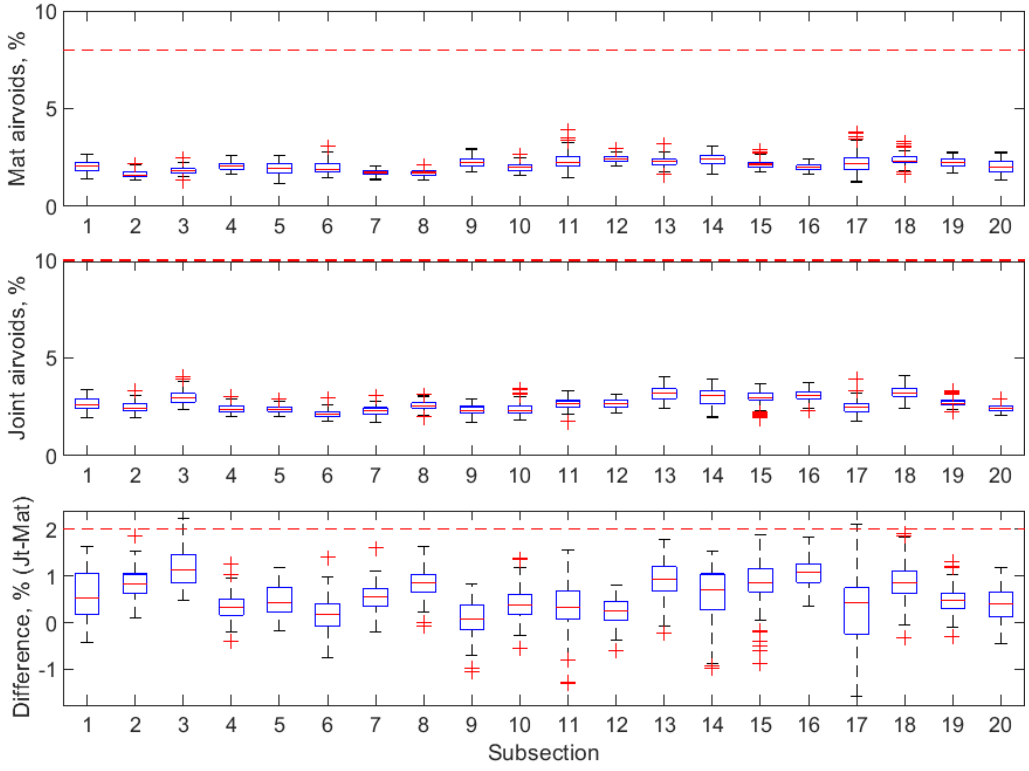

Figure B-172 Box plot of air voids for echelon joint (50 ft subsections) – US-31

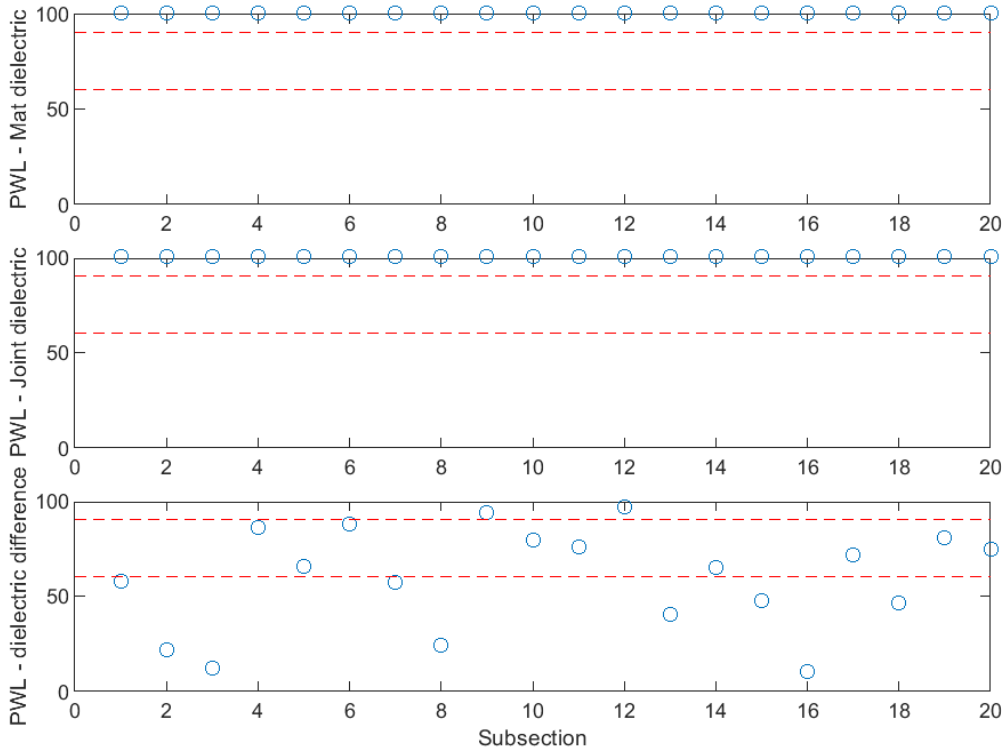

Figure B-173 PWL for dielectric values for echelon joint (50 ft subsections) – US-31

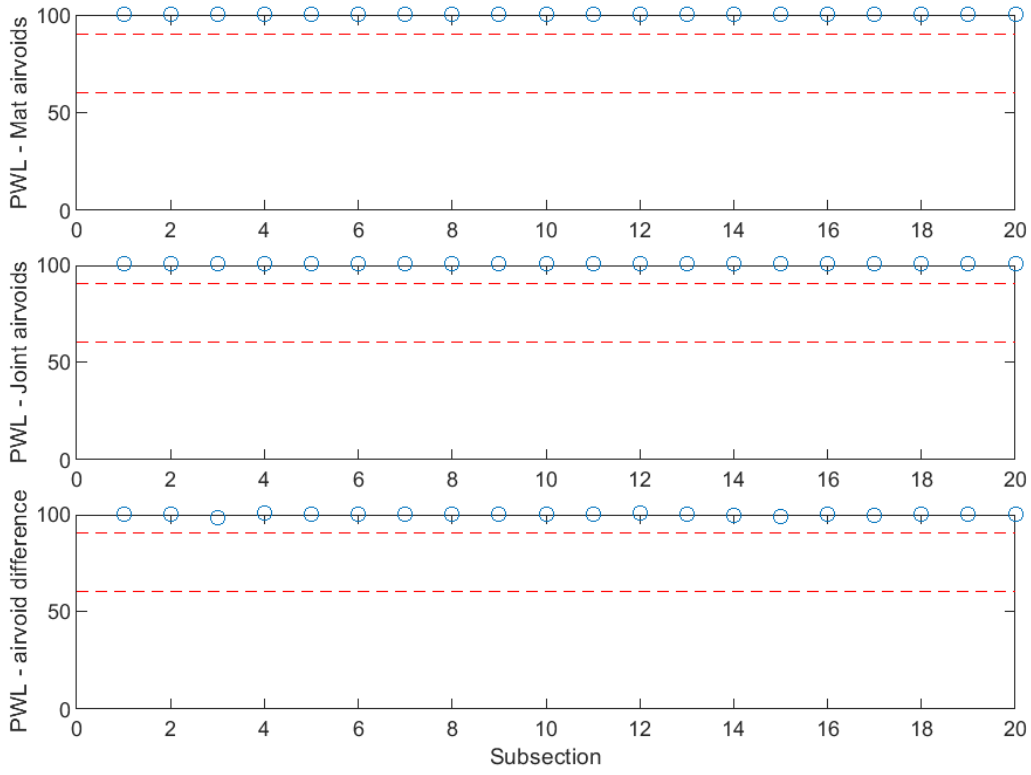

Figure B-174 PWL for air voids for echelon joint (50 ft subsections) – US-31

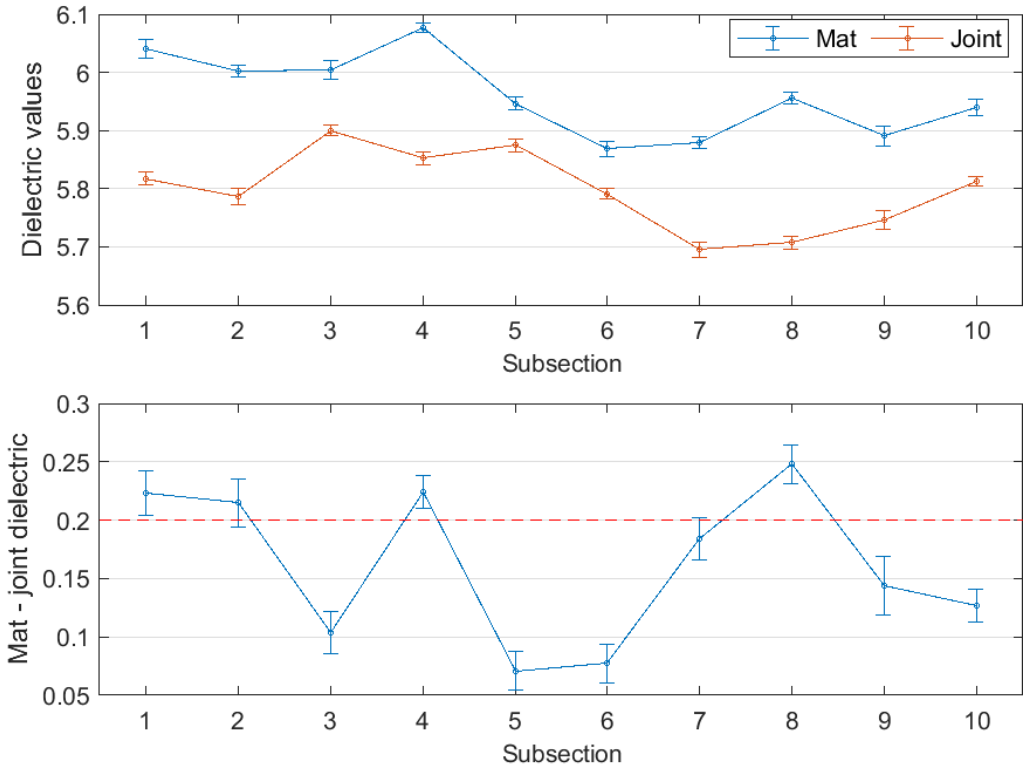

Figure B-175 Interval plot of dielectric values for echelon joint (100 ft subsections) – US-31

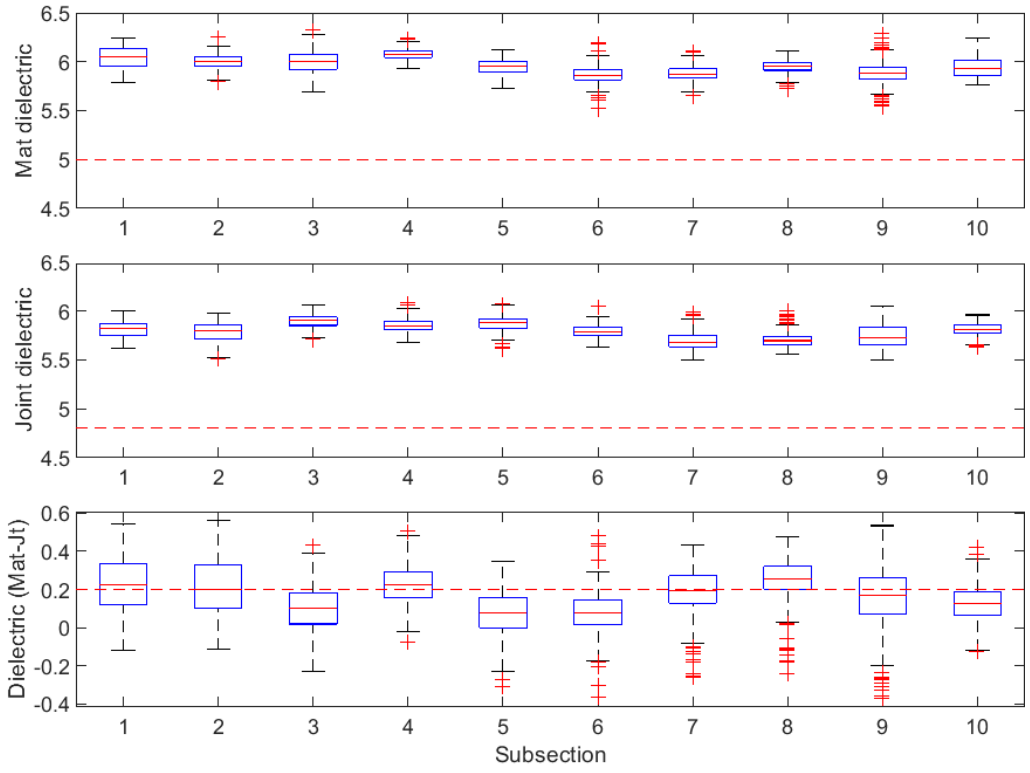

Figure B-176 Box plot of dielectric values for echelon joint (100 ft subsections) – US-31

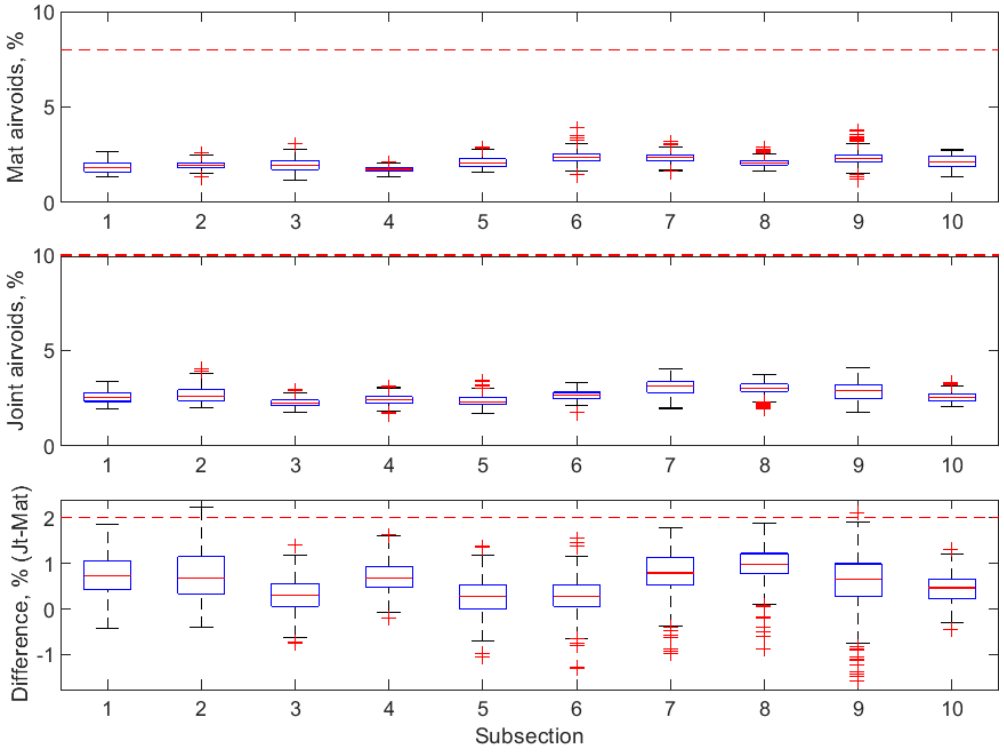

Figure B-177 Box plot of air voids for echelon joint (100 ft subsections) – US-31

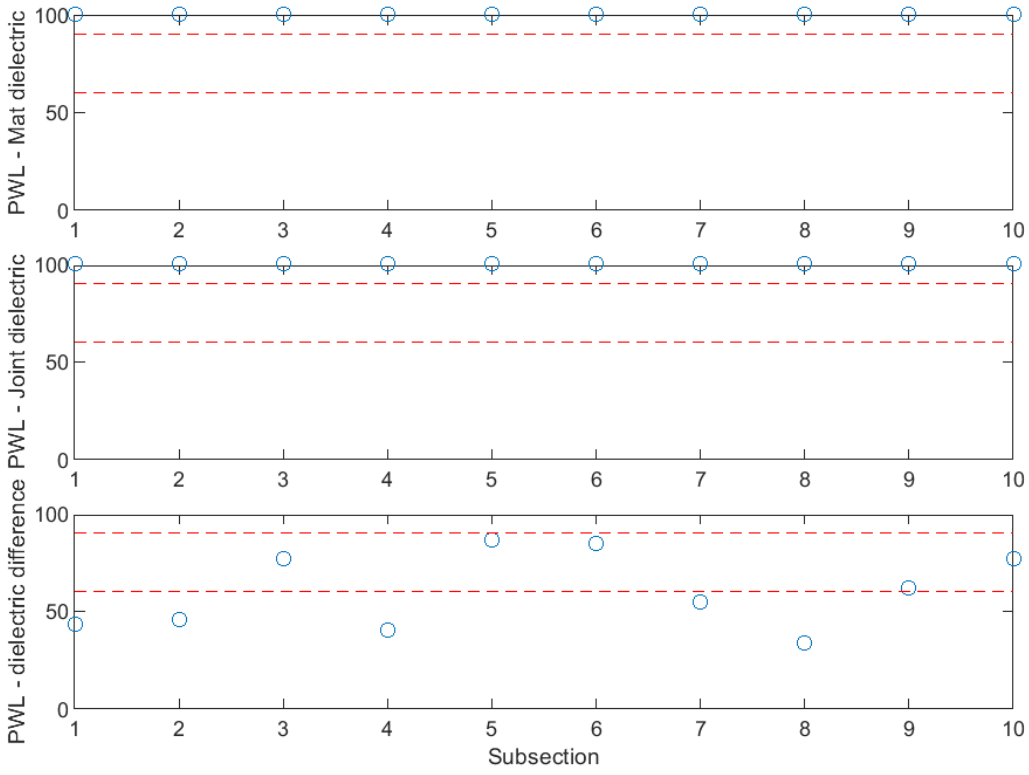

Figure B-178 PWL for dielectric values for echelon joint (100 ft subsections) – US-31

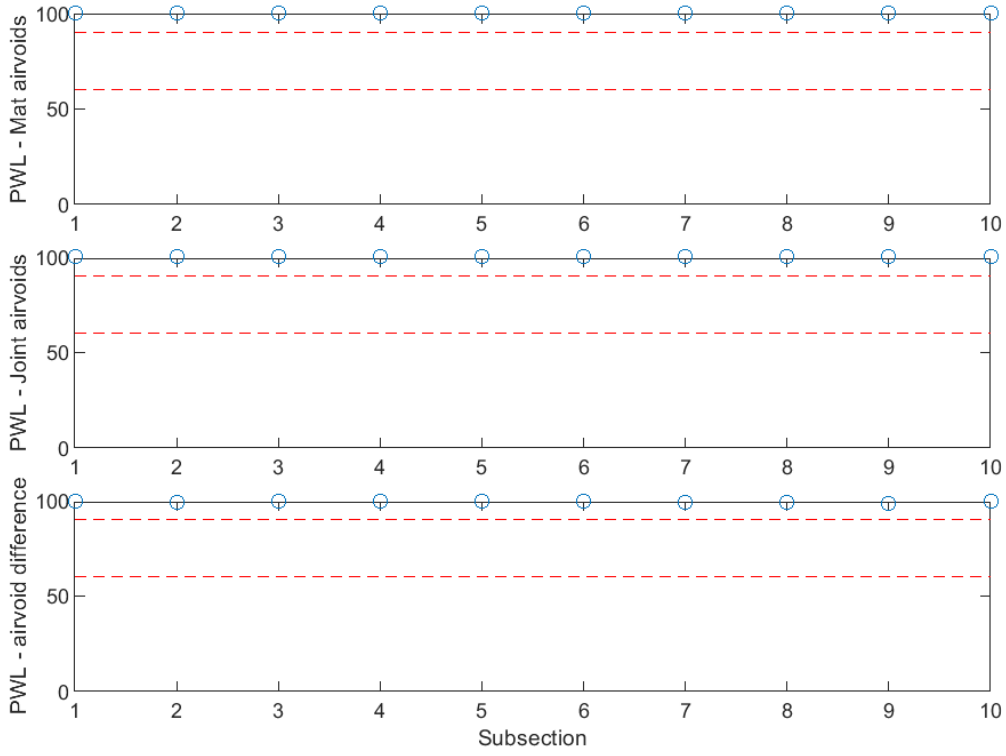

Figure B-179 PWL for air voids for echelon joint (100 ft subsections) – US-31

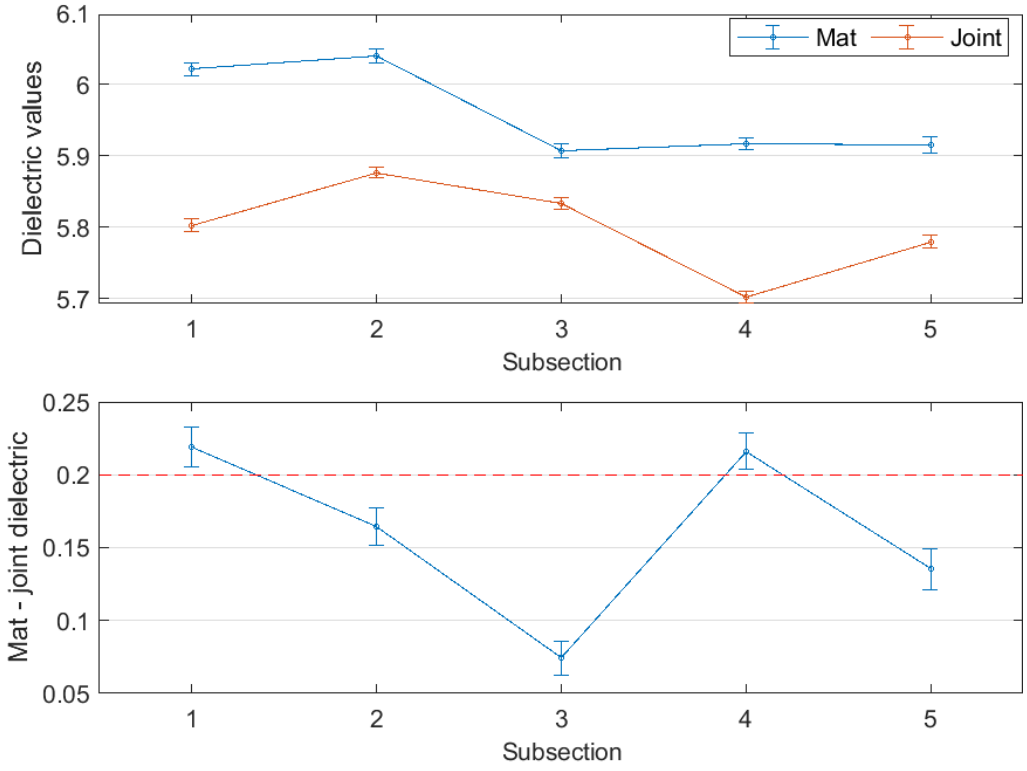

Figure B-180 Interval plot of dielectric values for echelon joint (200 ft subsections) – US-31

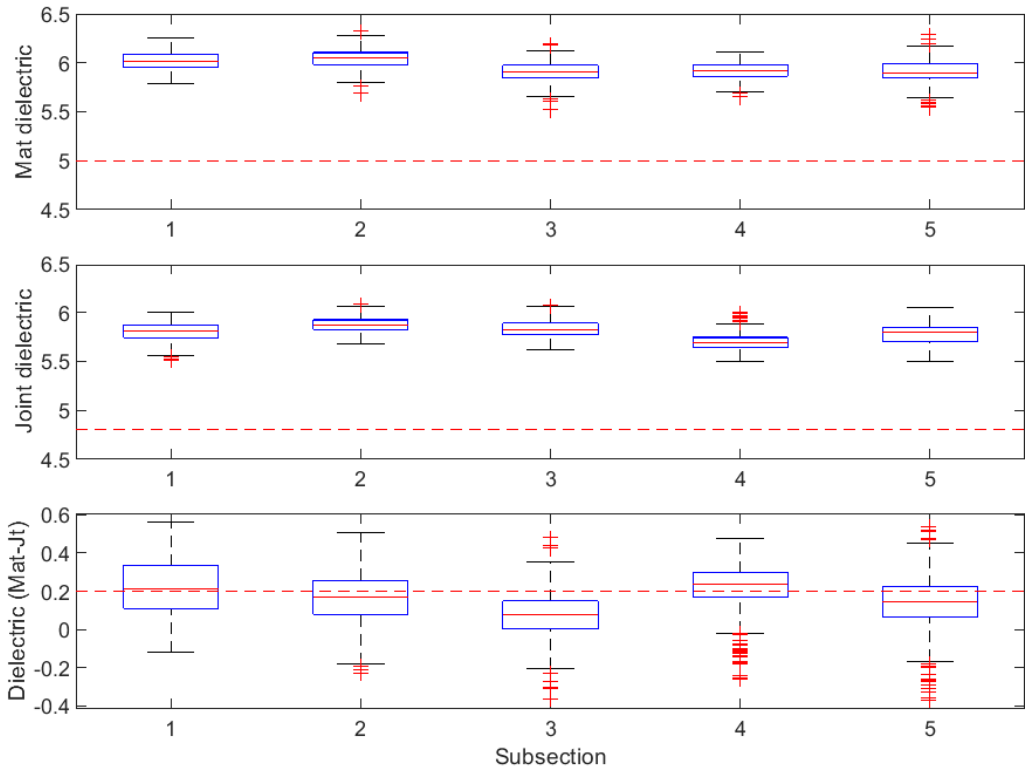

Figure B-181 Box plot of dielectric values for echelon joint (200 ft subsections) – US-31

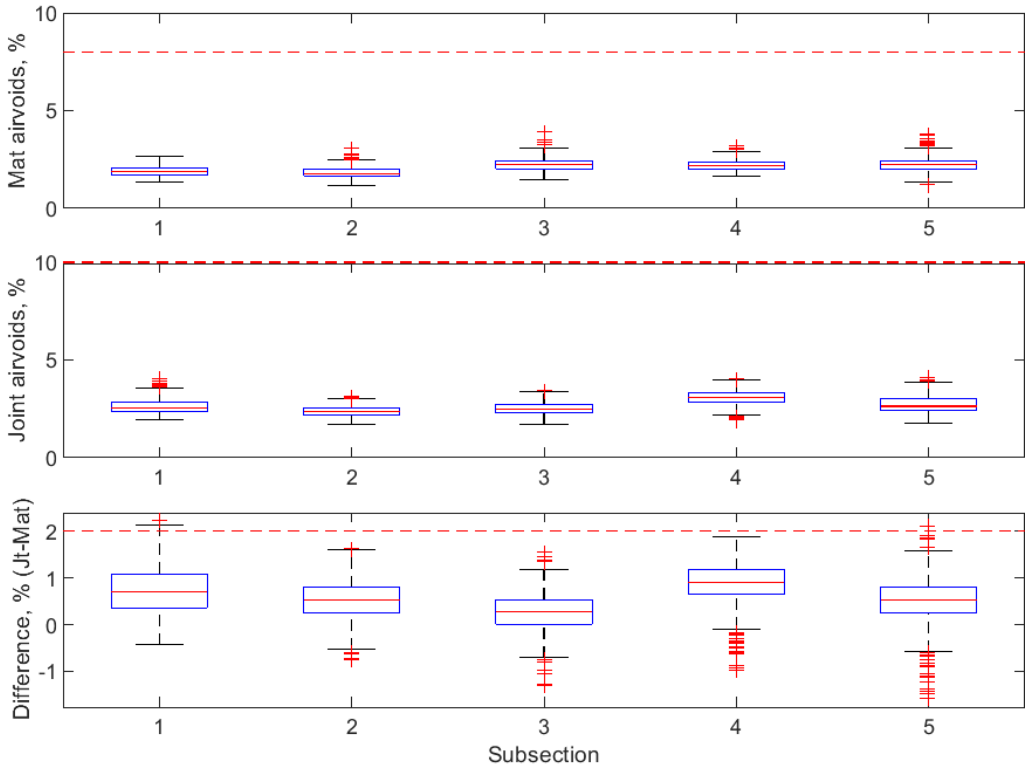

Figure B-182 Box plot of air voids for echelon joint (200 ft subsections) – US-31

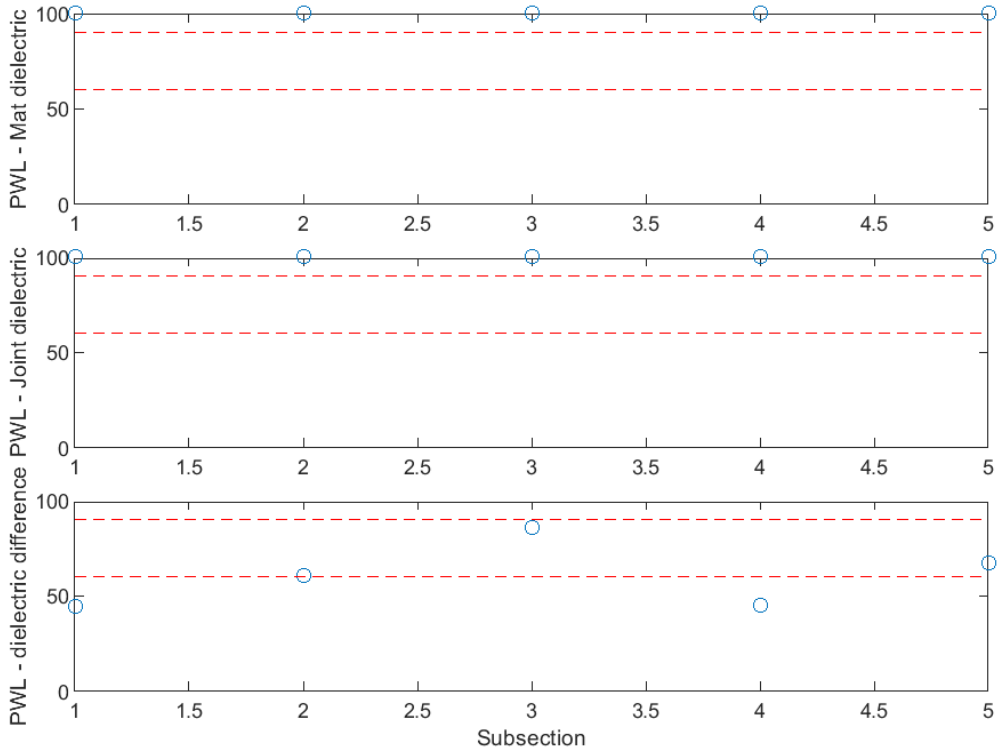

Figure B-183 PWL for dielectric values for echelon joint (200 ft subsections) – US-31

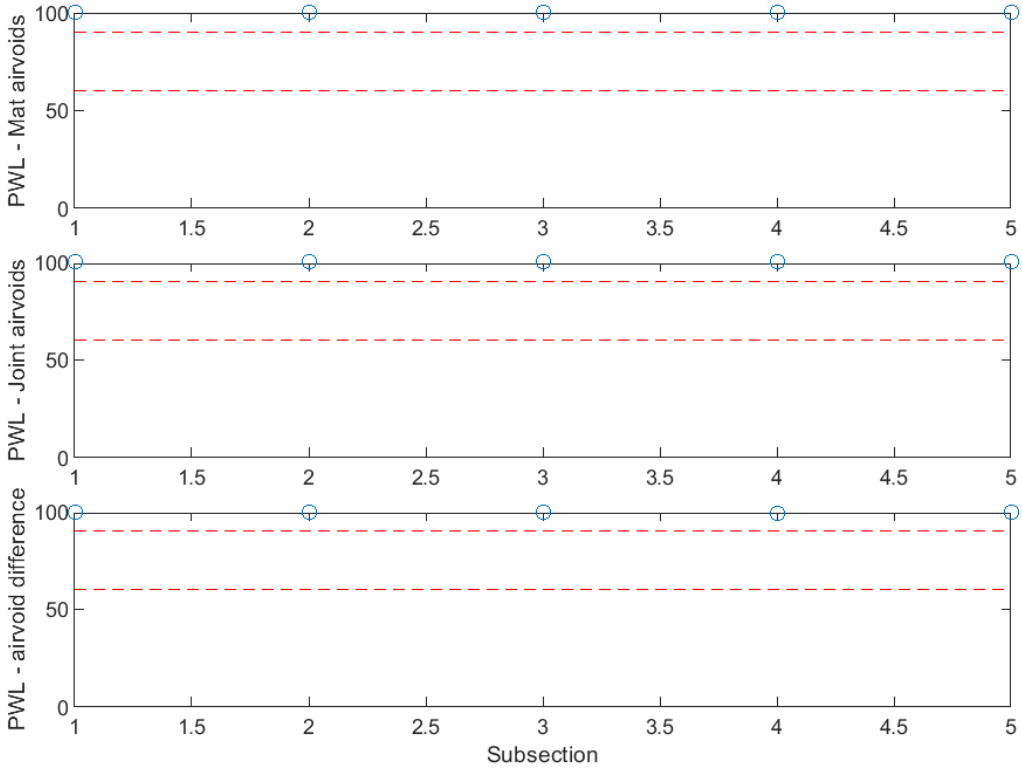

Figure B-184 PWL for air voids for echelon joint (200 ft subsections) – US-31

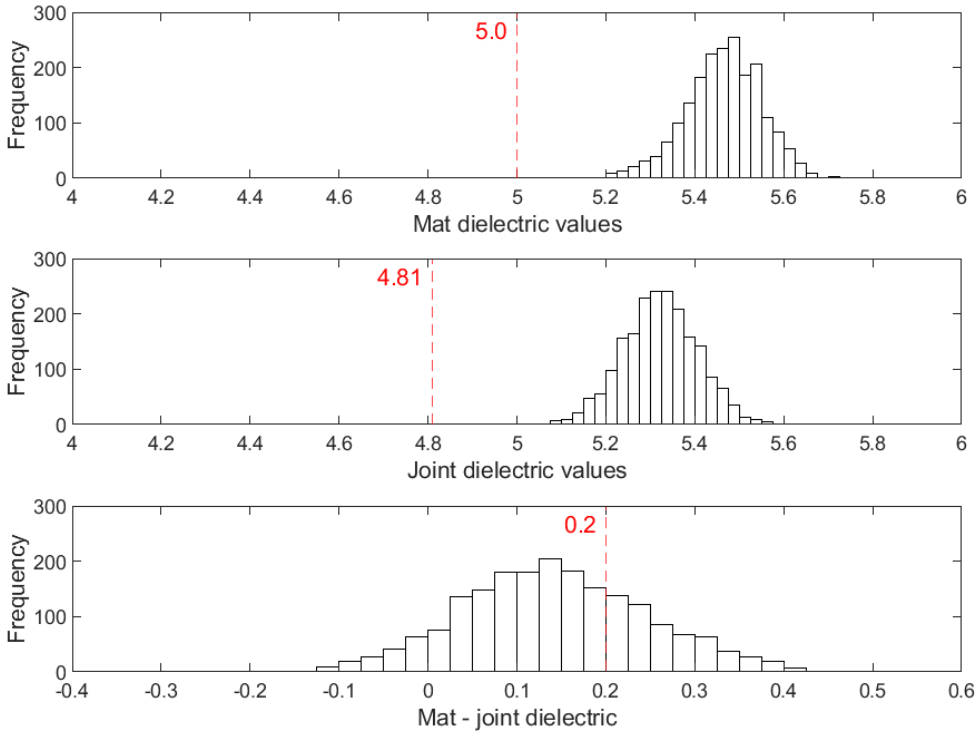

Figure B-185 Histogram of dielectric values for confined joint – M-25-1

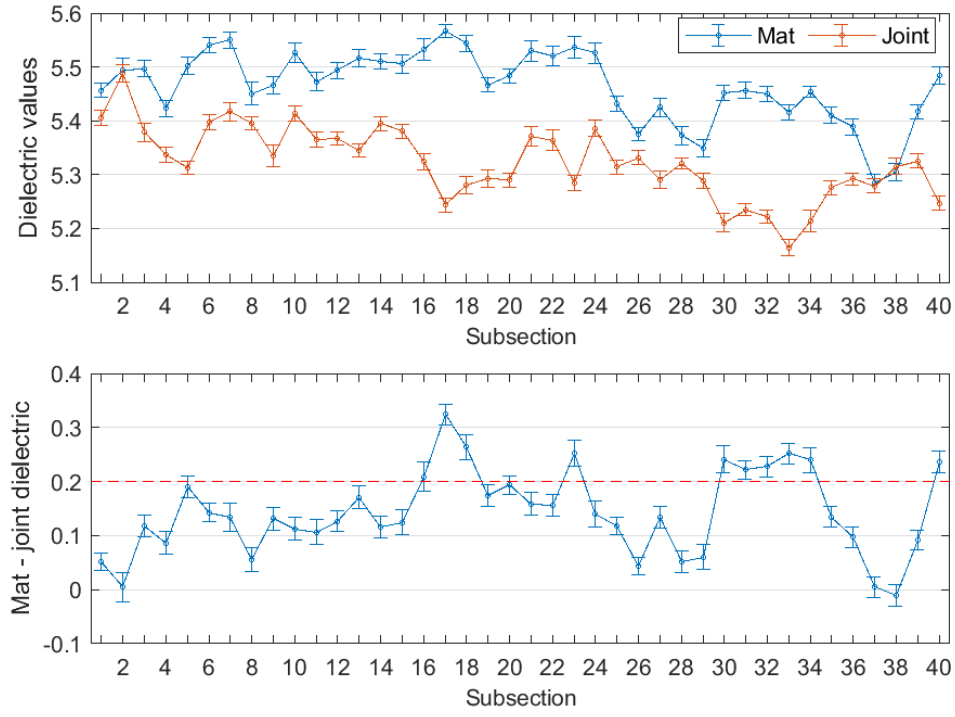

Figure B-186 Interval plot of dielectric values for confined joint (25 ft subsections) – M-25-1

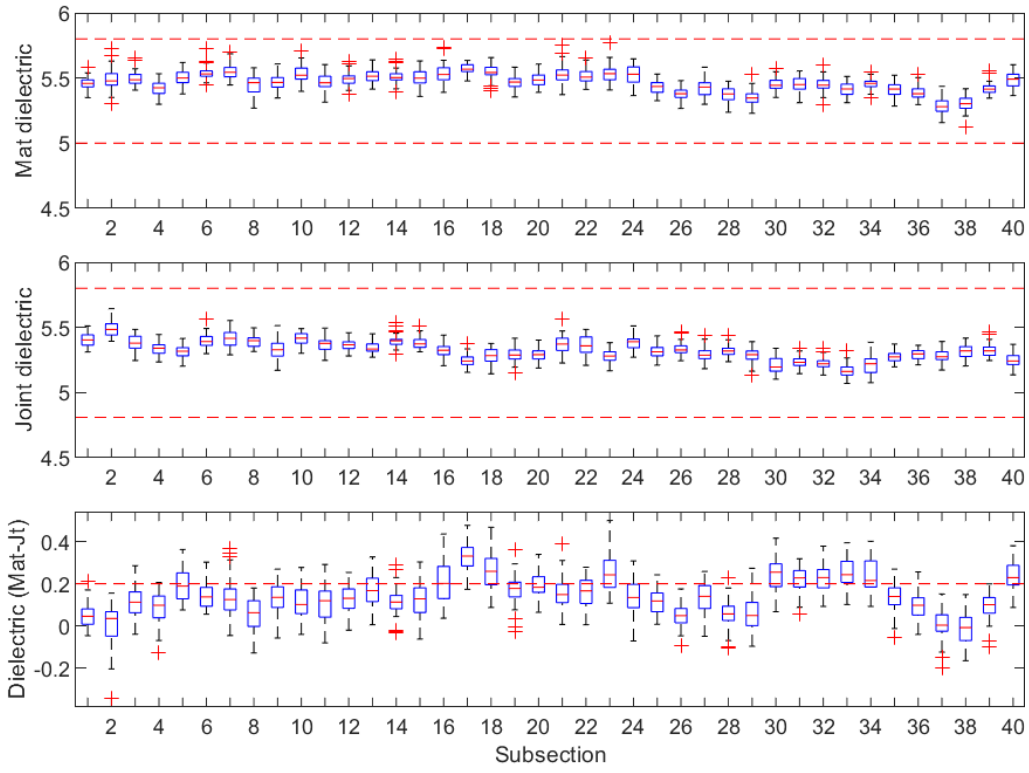

Figure B-187 Box plot of dielectric values for confined joint (25 ft subsections) – M-25-1

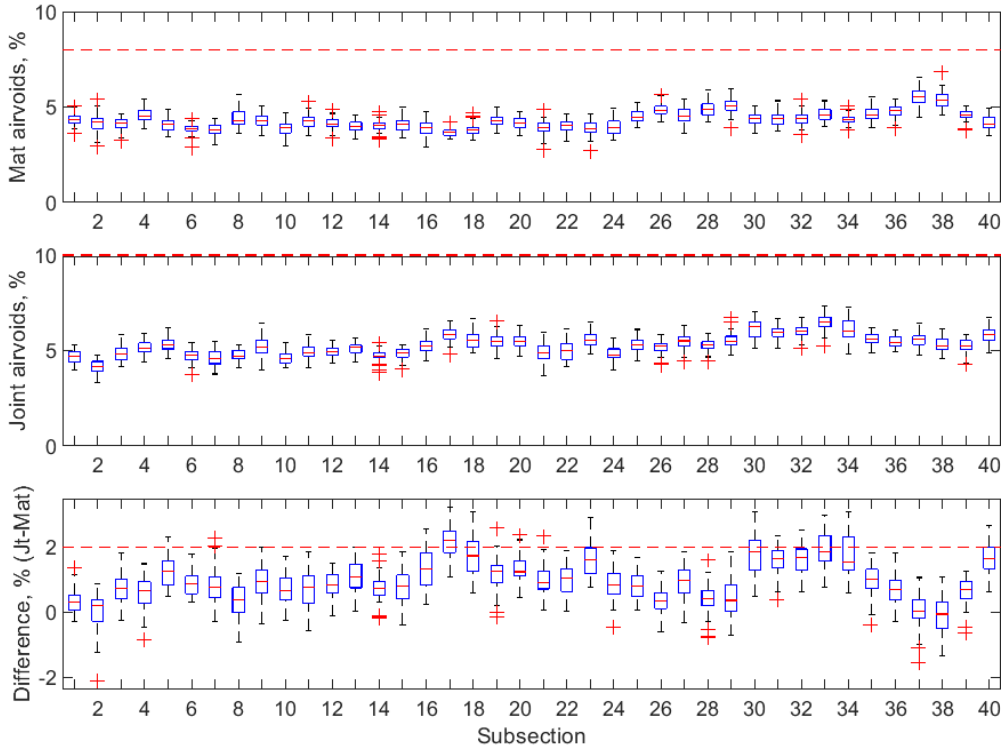

Figure B-188 Box plot of air voids for confined joint (25 ft subsections) – M-25-1

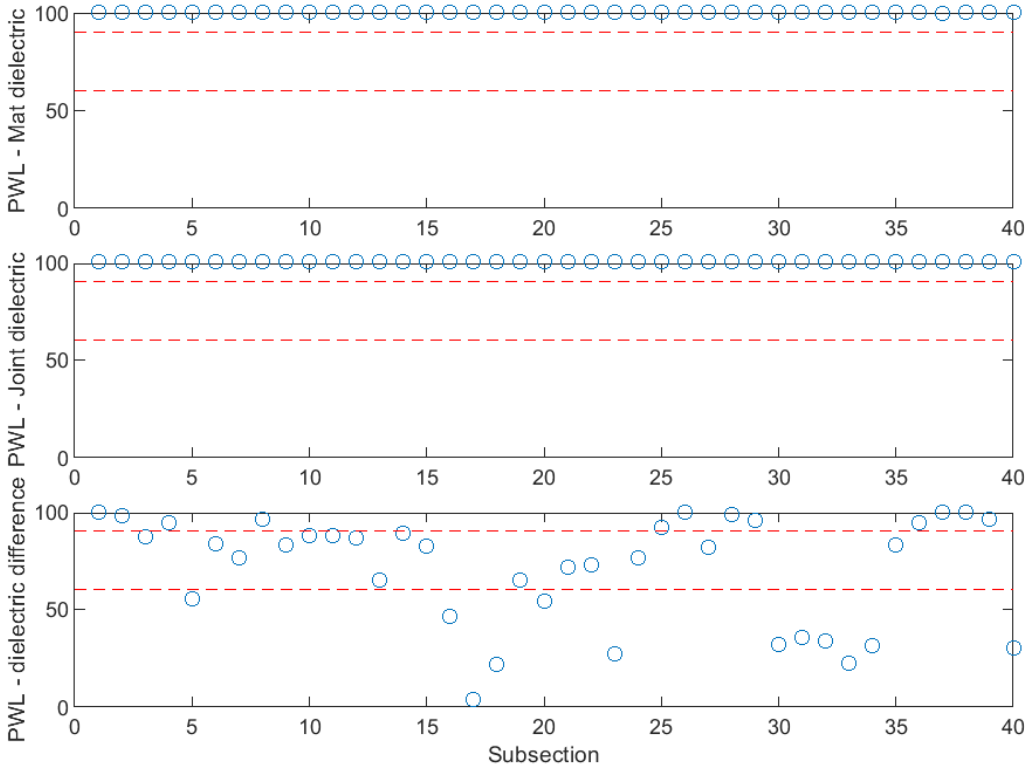

Figure B-189 PWL for dielectric values for confined joint (25 ft subsections) – M-25-1

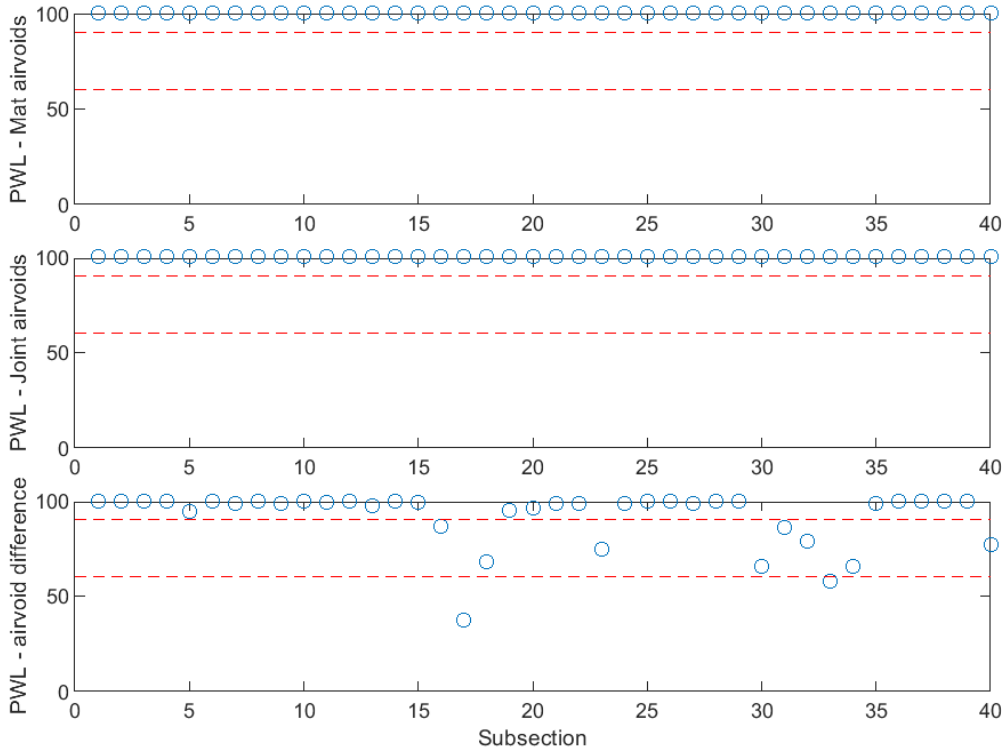

Figure B-190 PWL for air voids for confined joint (25 ft subsections) – M-25-1

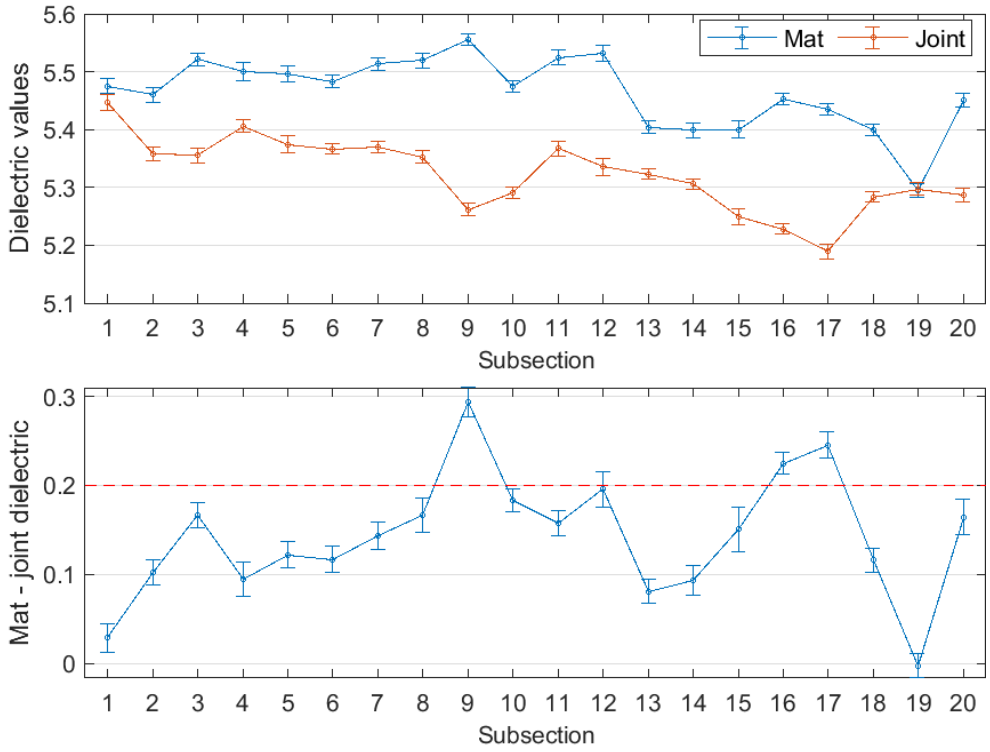

Figure B-191 Interval plot of dielectric values for confined joint (50 ft subsections) – M-25-1

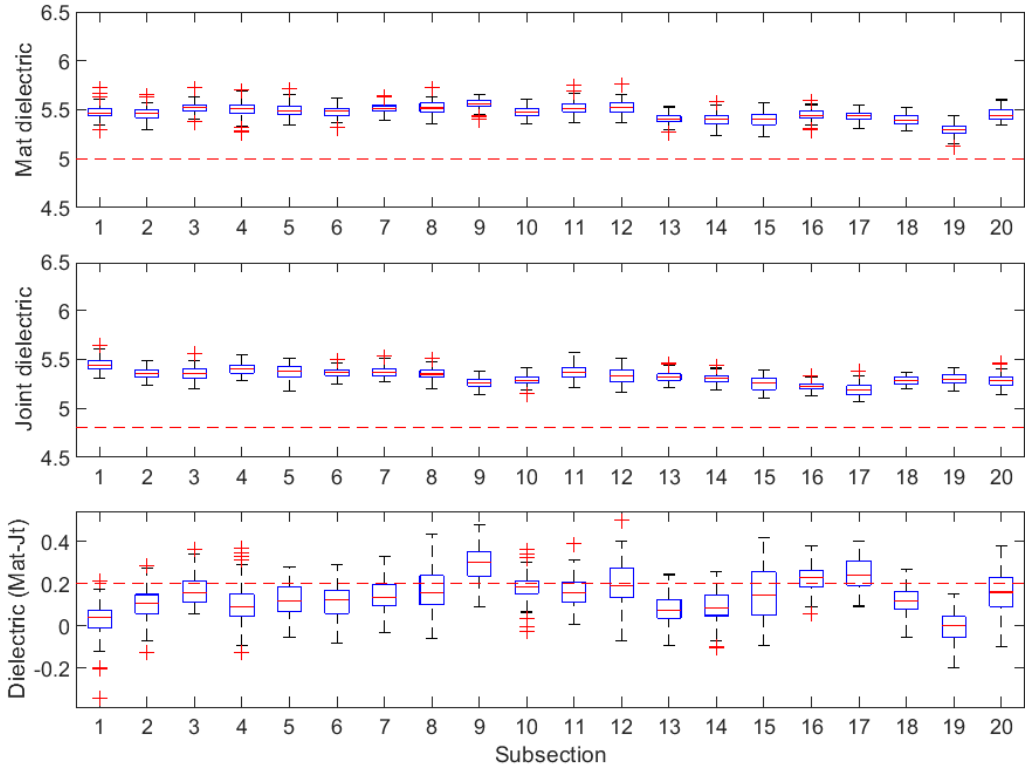

Figure B-192 Box plot of dielectric values for confined joint (50 ft subsections) – M-25-1

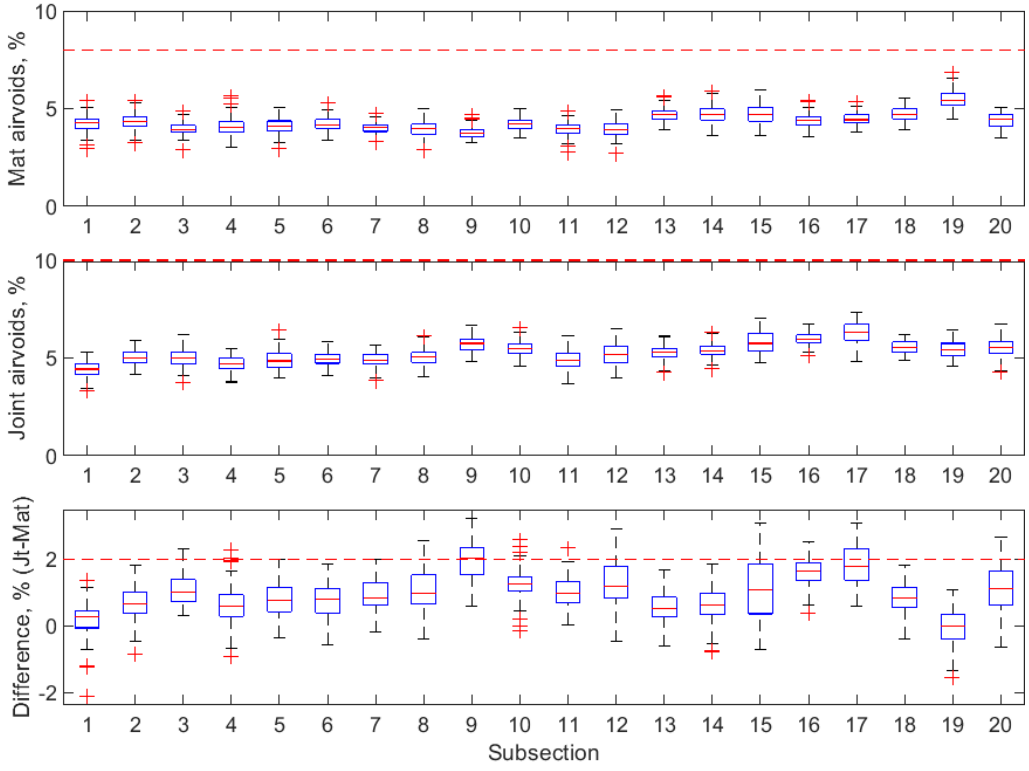

Figure B-193 Box plot of air voids for confined joint (50 ft subsections) – M-25-1

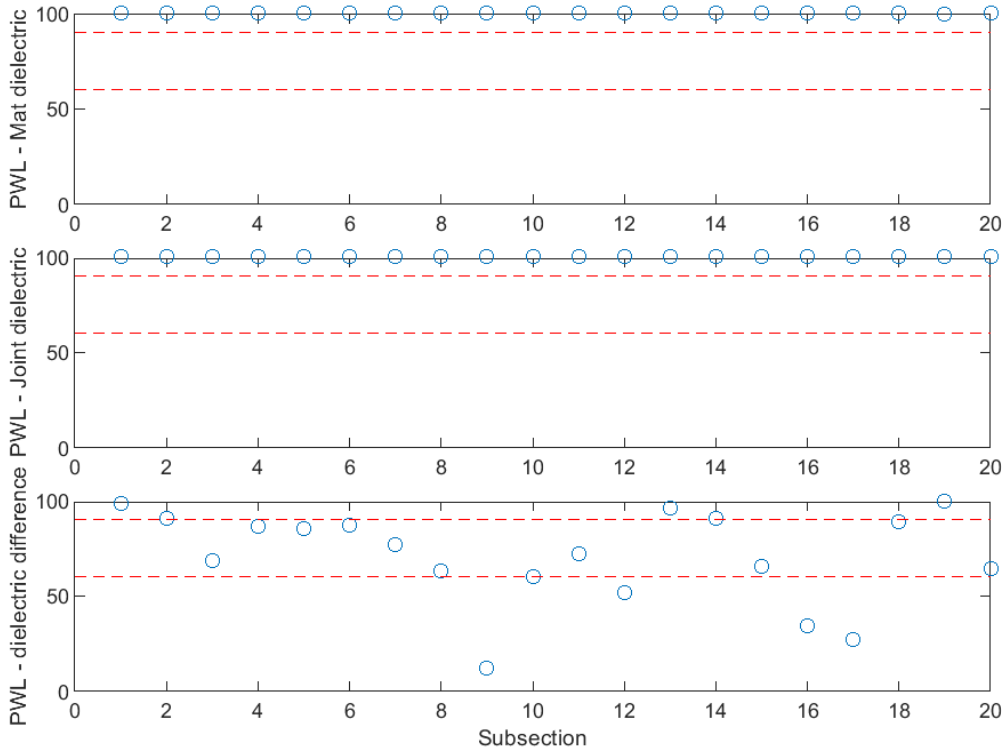

Figure B-194 PWL for dielectric values for confined joint (50 ft subsections) – M-25-1

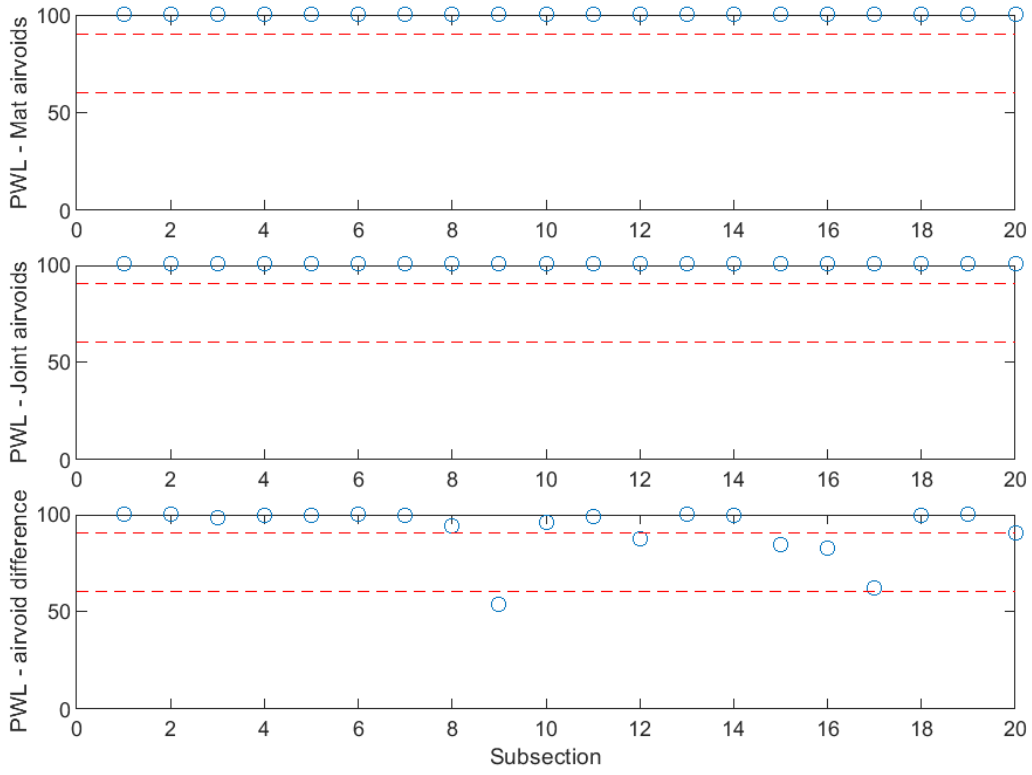

Figure B-195 PWL for air voids for confined joint (50 ft subsections) – M-25-1

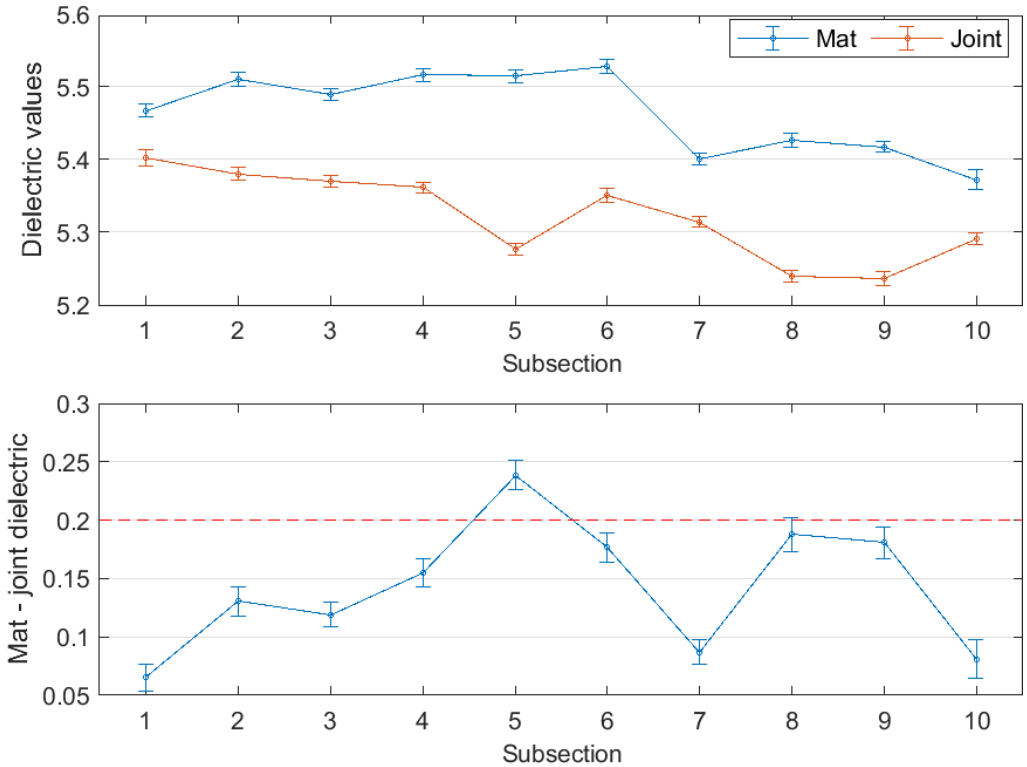

Figure B-196 Interval plot of dielectric values for confined joint (100 ft subsections) – M-25-1

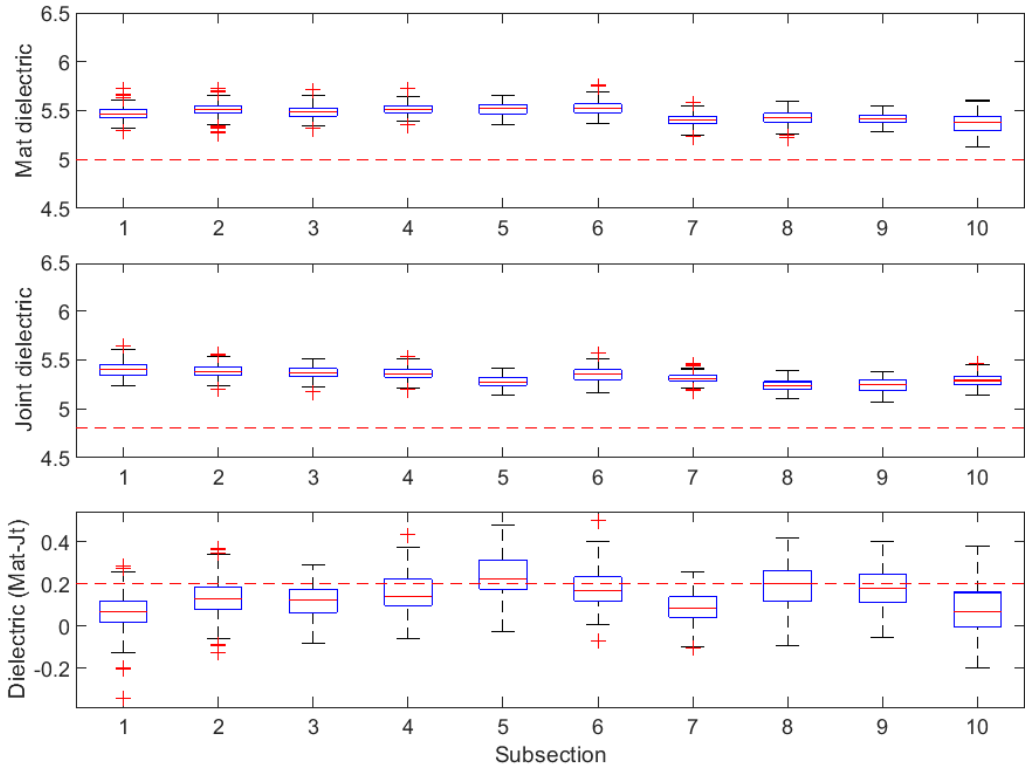

Figure B-197 Box plot of dielectric values for confined joint (100 ft subsections) – M-25-1

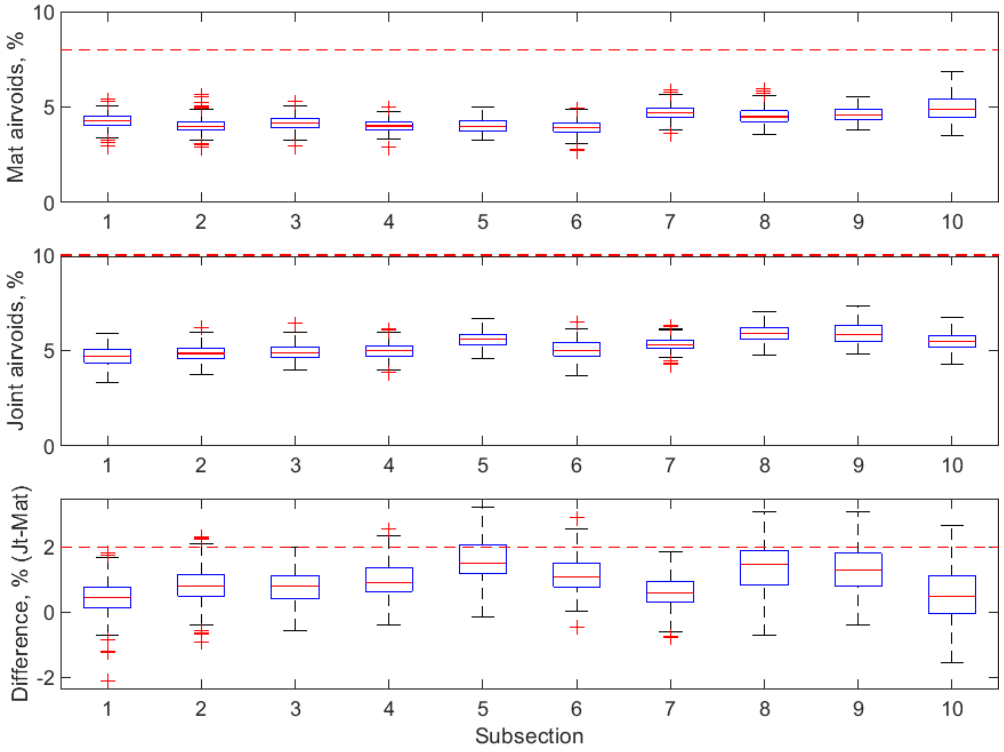

Figure B-198 Box plot of air voids for confined joint (100 ft subsections) – M-25-1

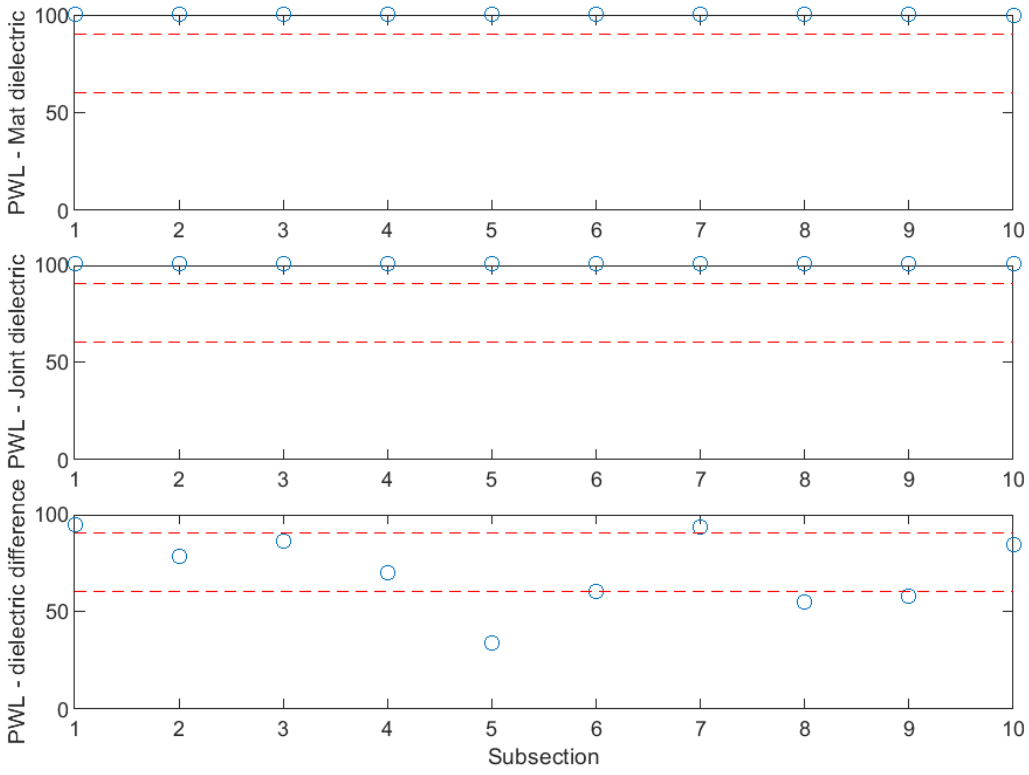

Figure B-199 PWL for dielectric values for confined joint (100 ft subsections) – M-25-1

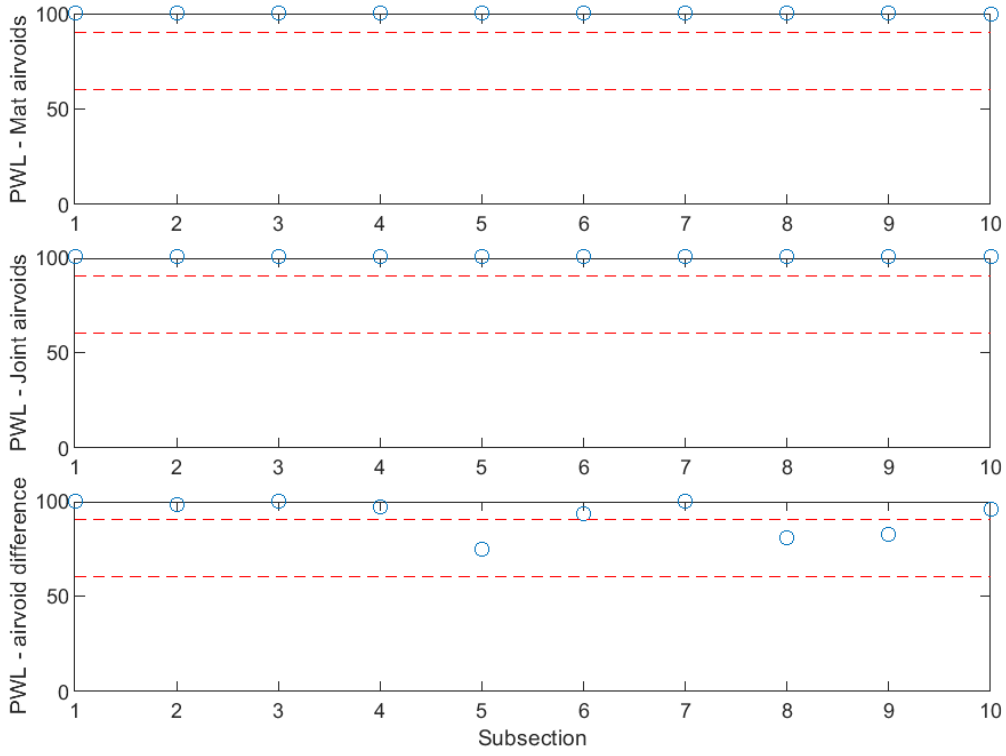

Figure B-200 PWL for air voids for confined joint (100 ft subsections) – M-25-1

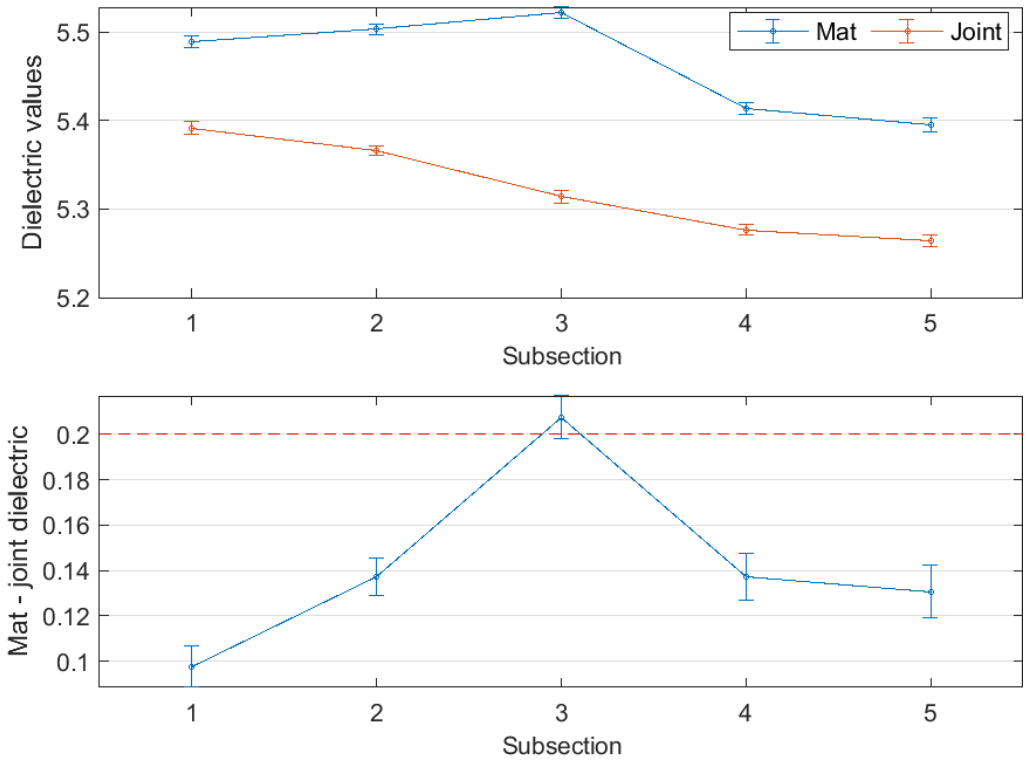

Figure B-201 Interval plot of dielectric values for confined joint (200 ft subsections) – M-25-1

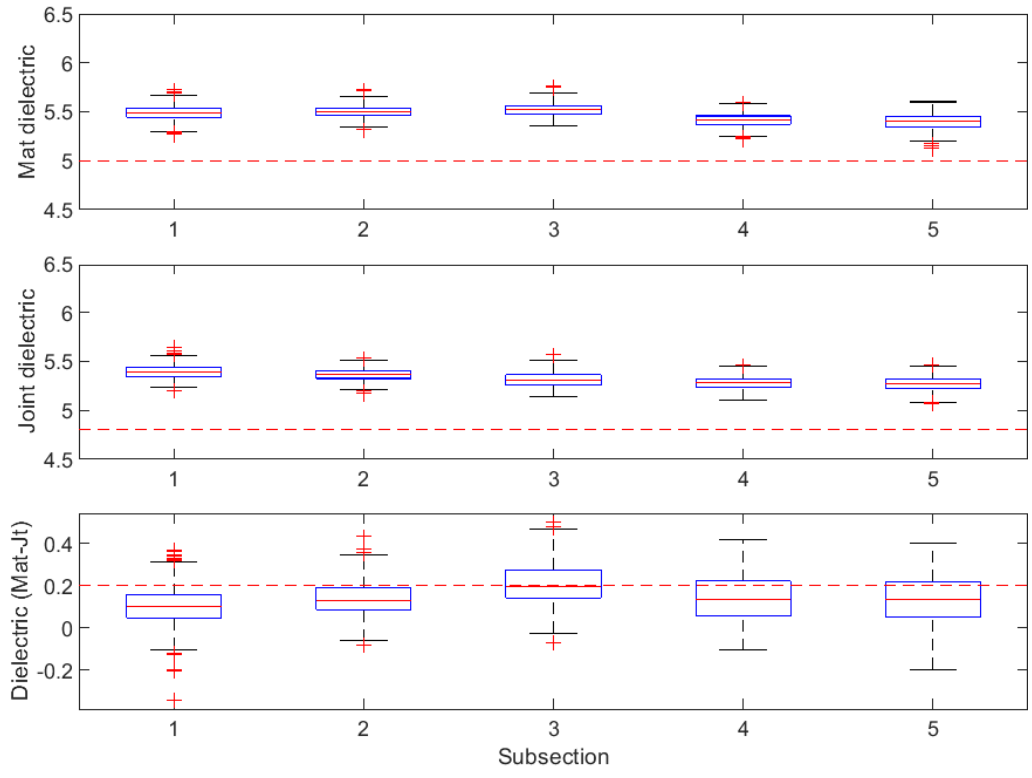

Figure B-202 Box plot of dielectric values for confined joint (200 ft subsections) – M-25-1

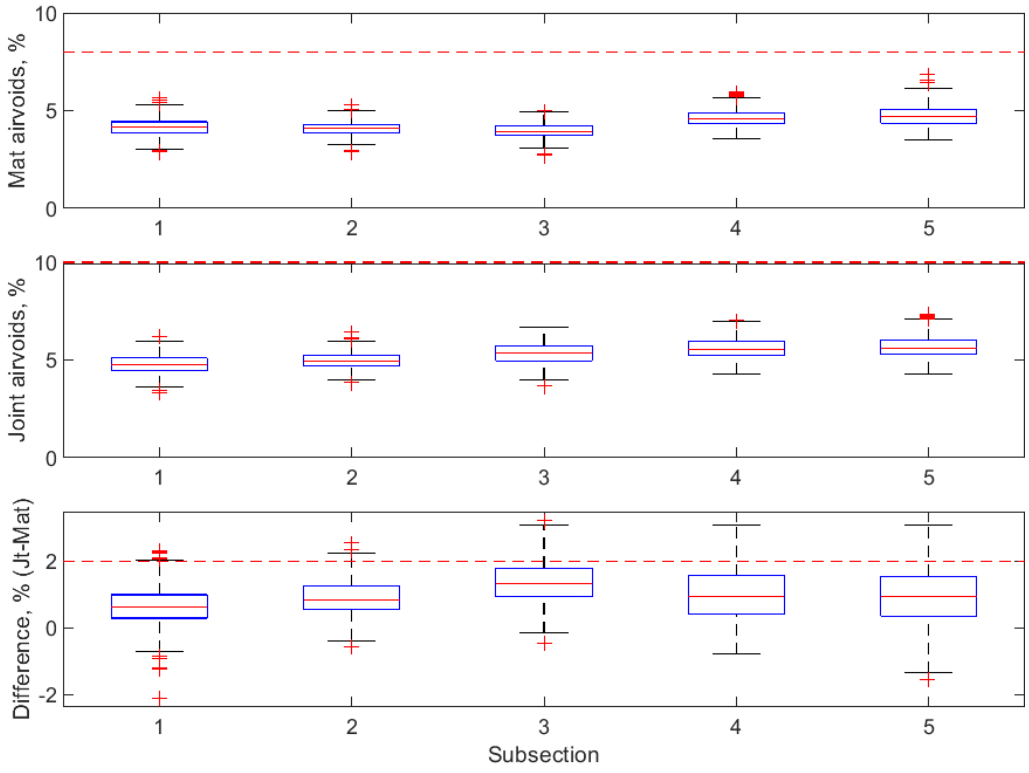

Figure B-203 Box plot of air voids for confined joint (200 ft subsections) – M-25-1

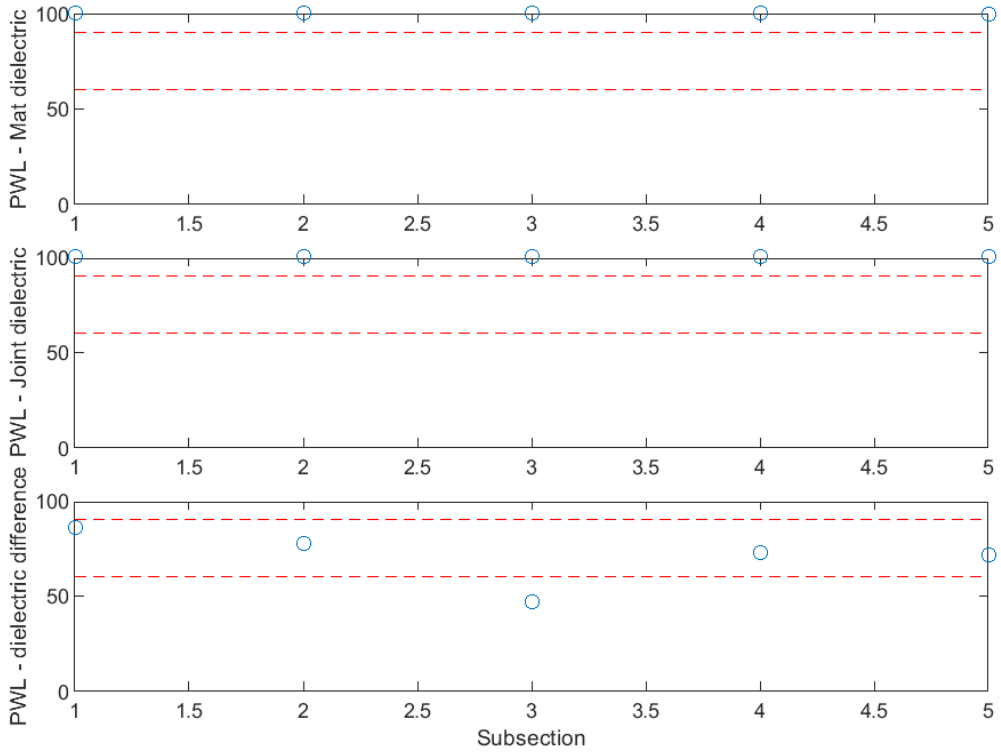

Figure B-204 PWL for dielectric values for confined joint (200 ft subsections) – M-25-1

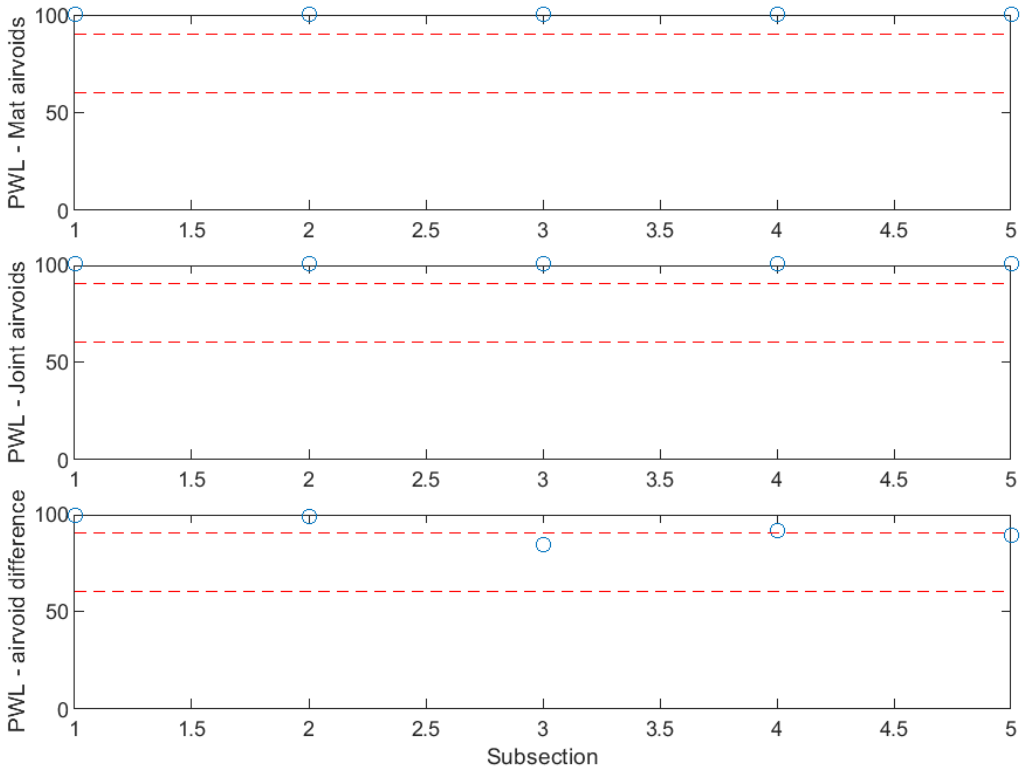

Figure B-205 PWL for air voids for confined joint (200 ft subsections) – M-25-1

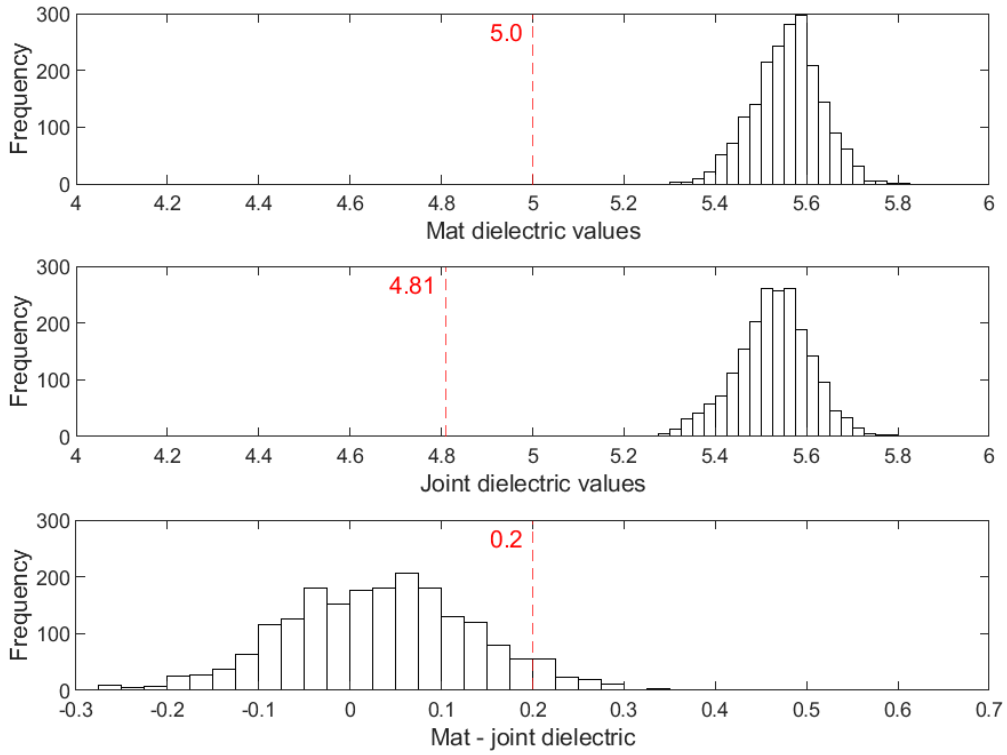

Figure B-206 Histogram of dielectric values for confined joint – M-25-2

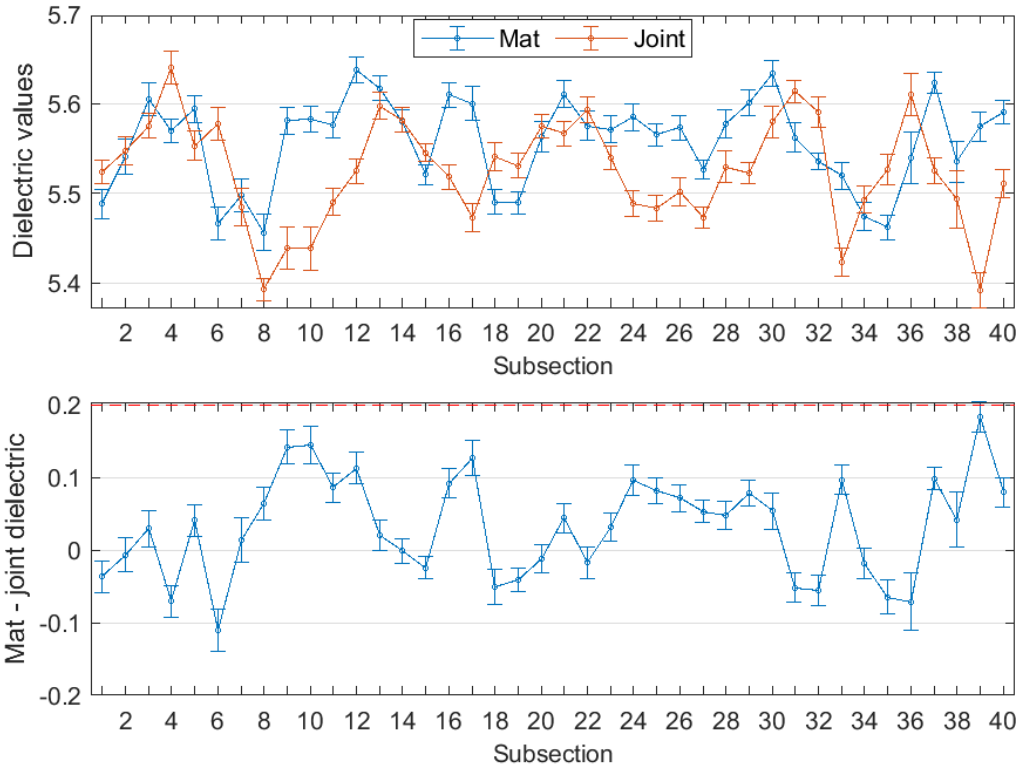

Figure B-207 Interval plot of dielectric values for confined joint (25 ft subsections) – M-25-2

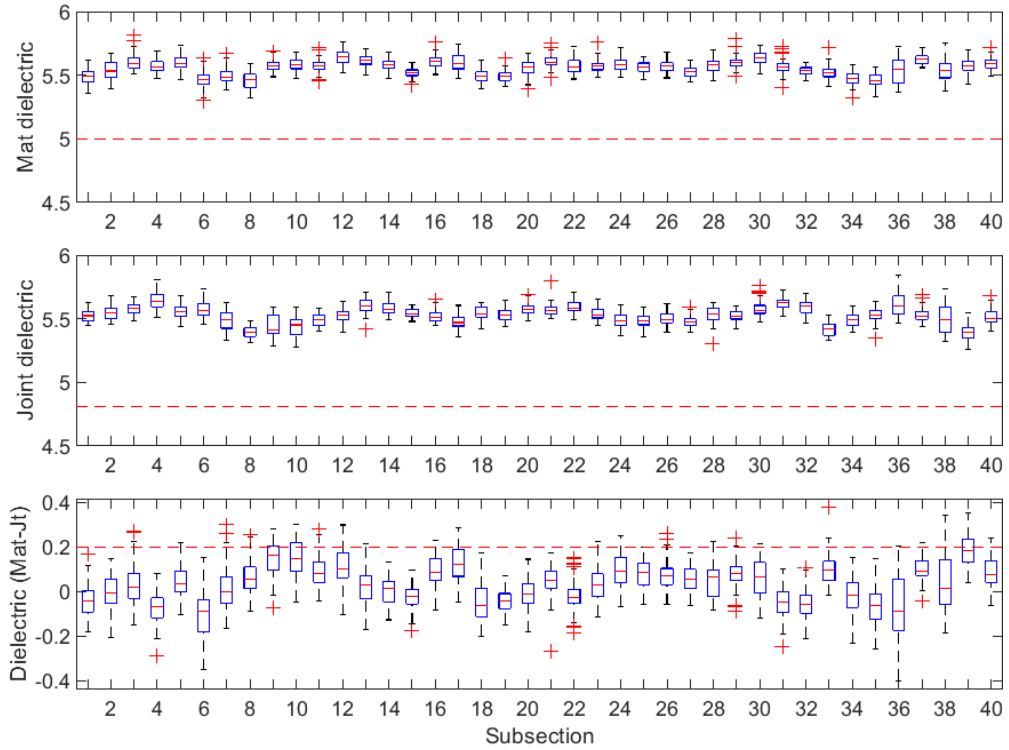

Figure B-208 Box plot of dielectric values for confined joint (25 ft subsections) – M-25-2

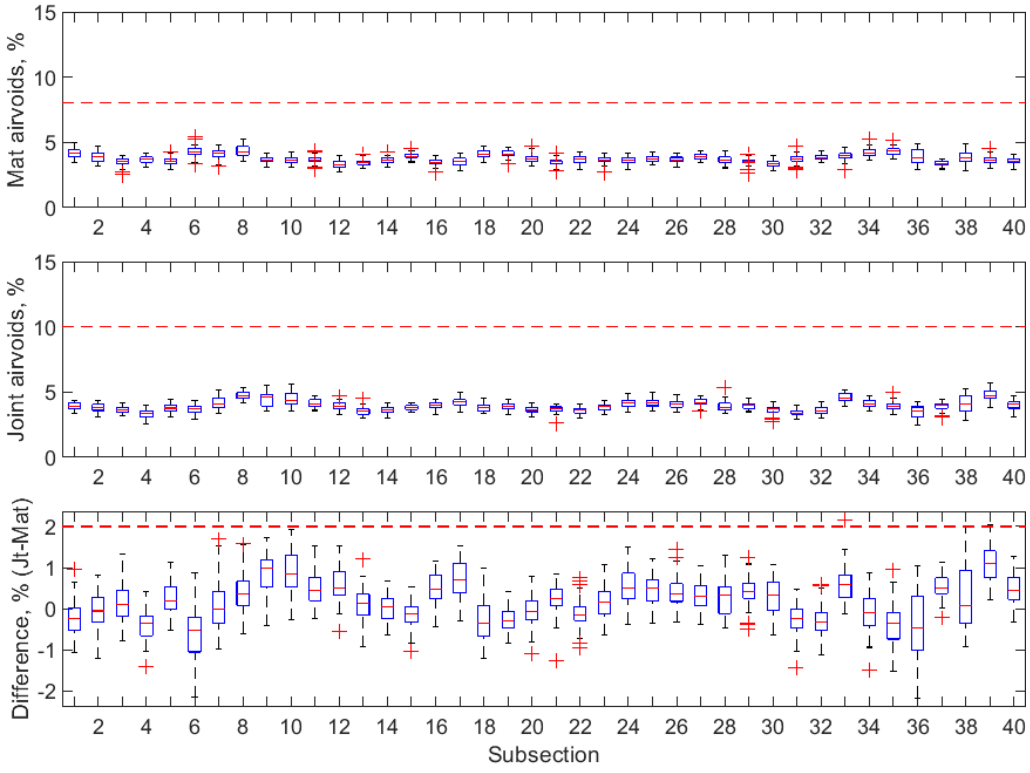

Figure B-209 Box plot of air voids for confined joint (25 ft subsections) – M-25-2

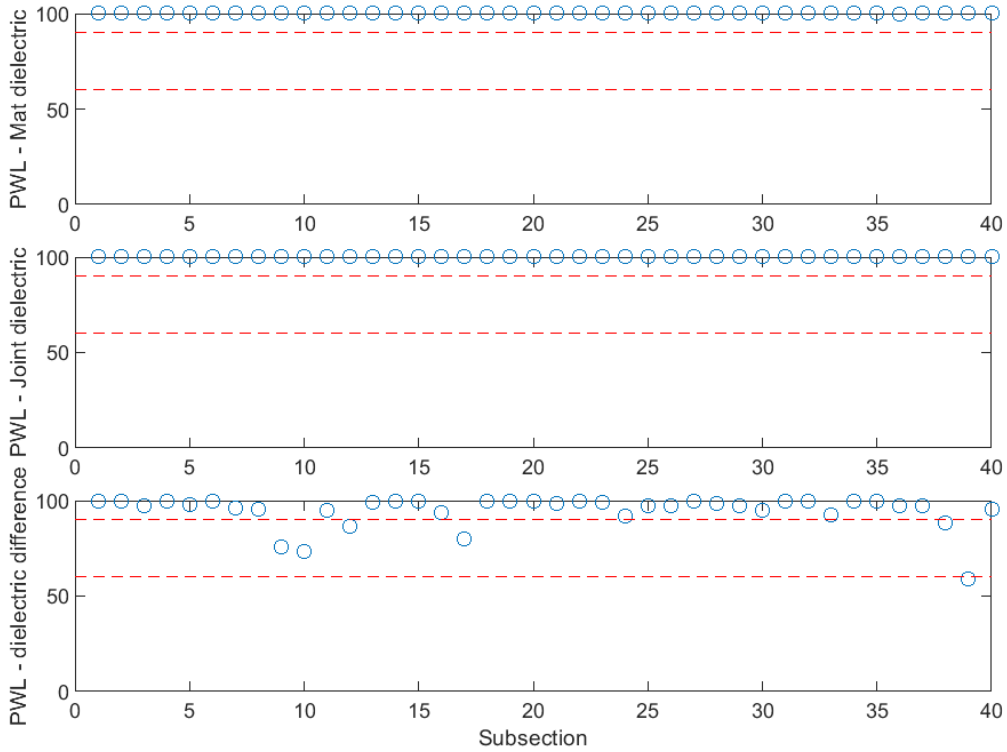

Figure B-210 PWL for dielectric values for confined joint (25 ft subsections) – M-25-2

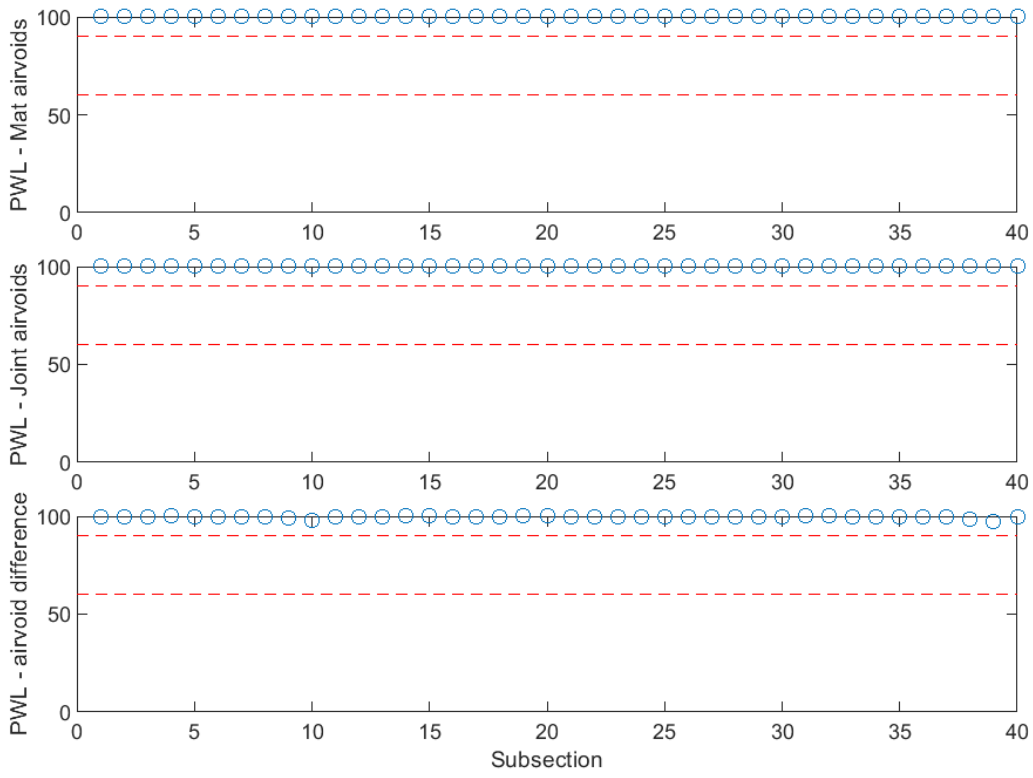

Figure B-211 PWL for air voids for confined joint (25 ft subsections) – M-25-2

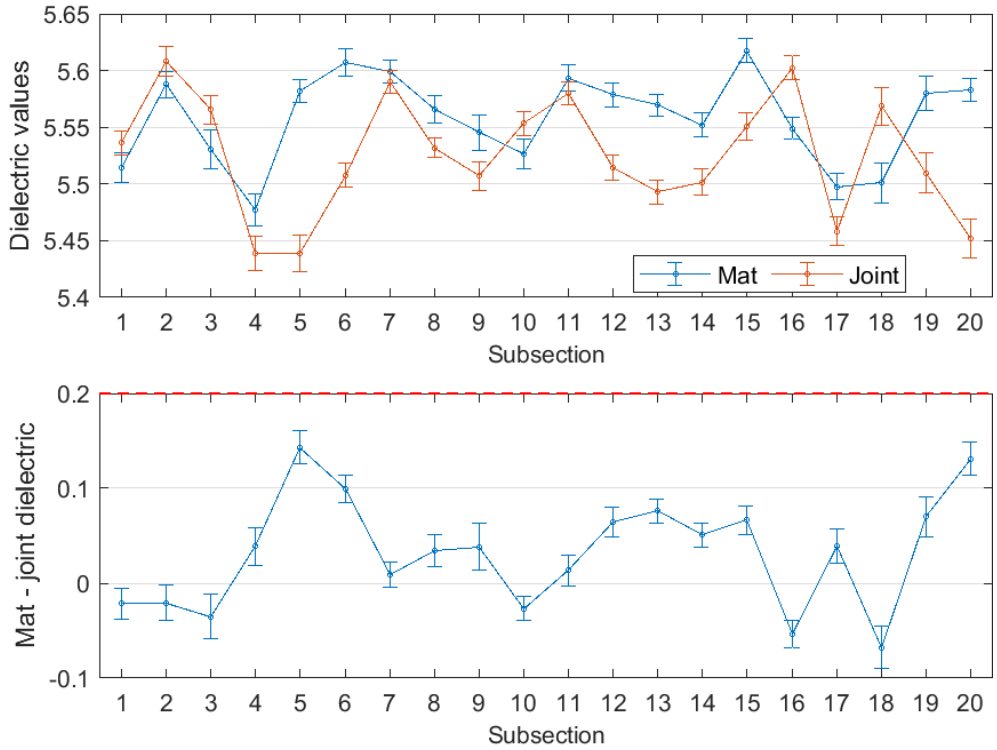

Figure B-212 Interval plot of dielectric values for confined joint (50 ft subsections) – M-25-2

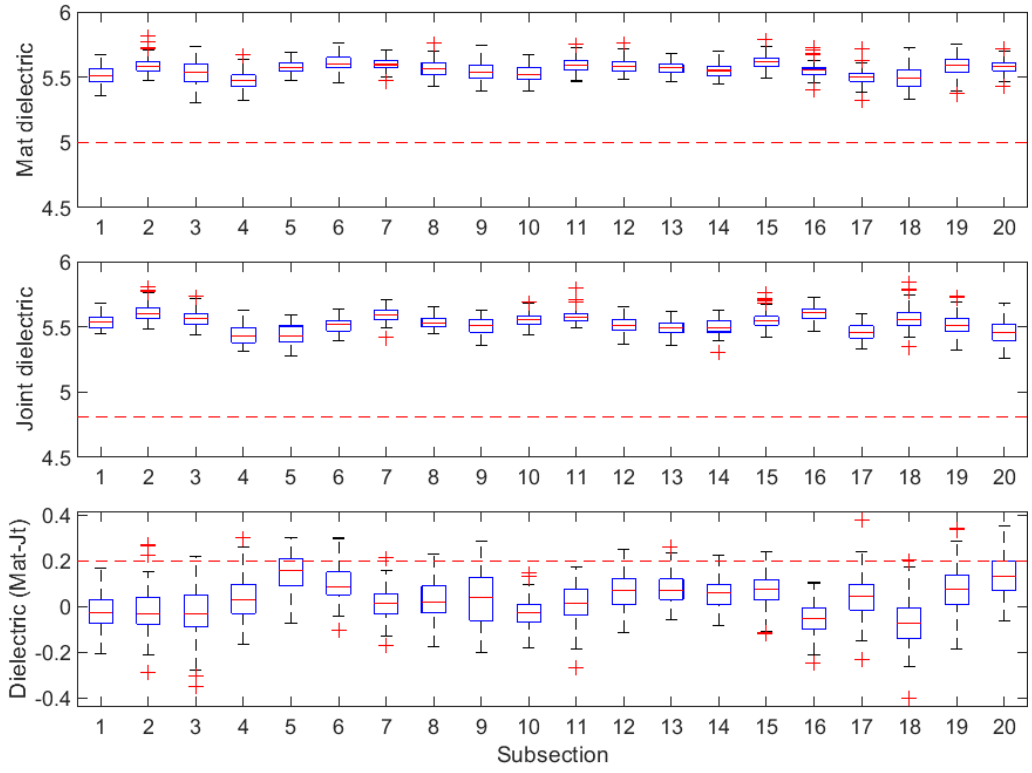

Figure B-213 Box plot of dielectric values for confined joint (50 ft subsections) – M-25-2

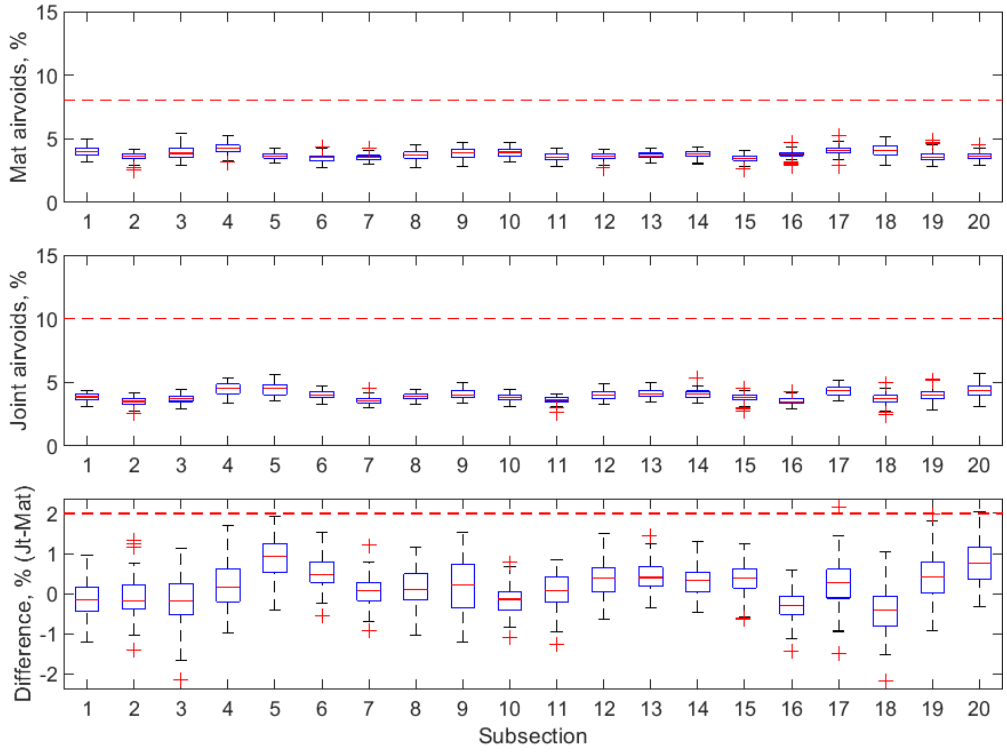

Figure B-214 Box plot of air voids for confined joint (50 ft subsections) – M-25-2

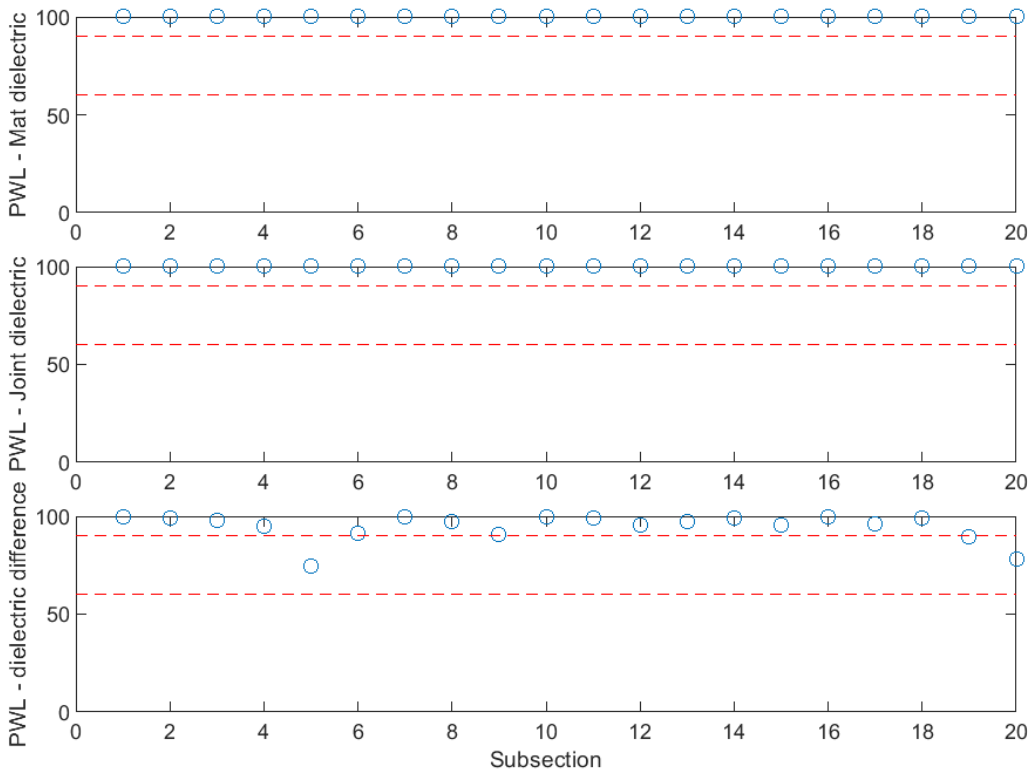

Figure B-215 PWL for dielectric values for confined joint (50 ft subsections) – M-25-2

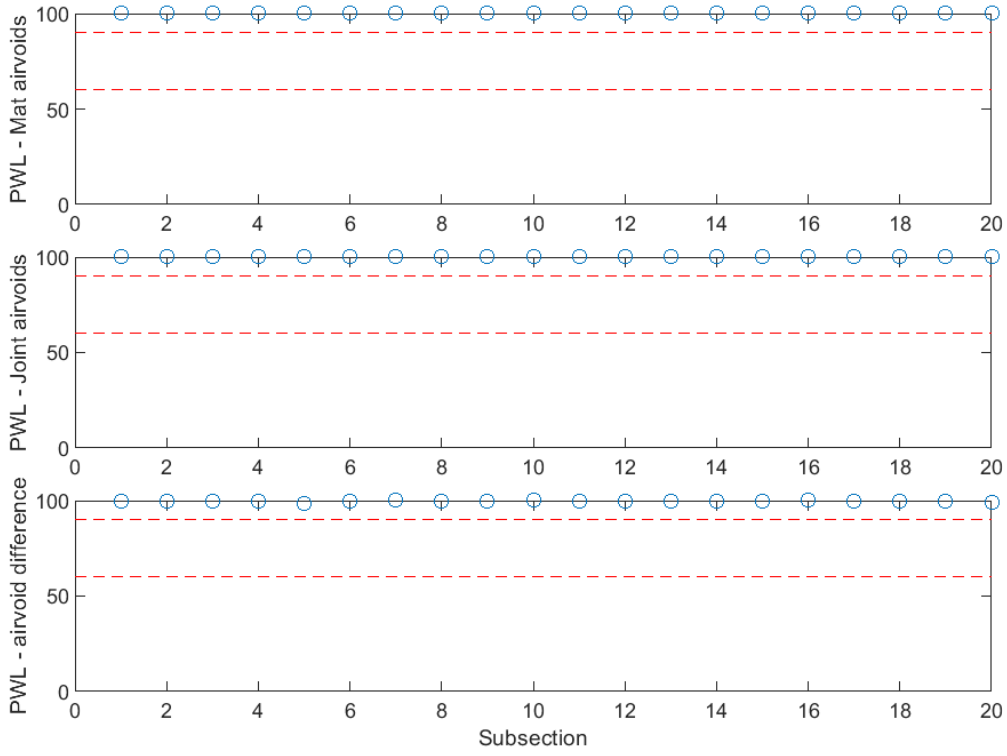

Figure B-216 PWL for air voids for confined joint (50 ft subsections) – M-25-2

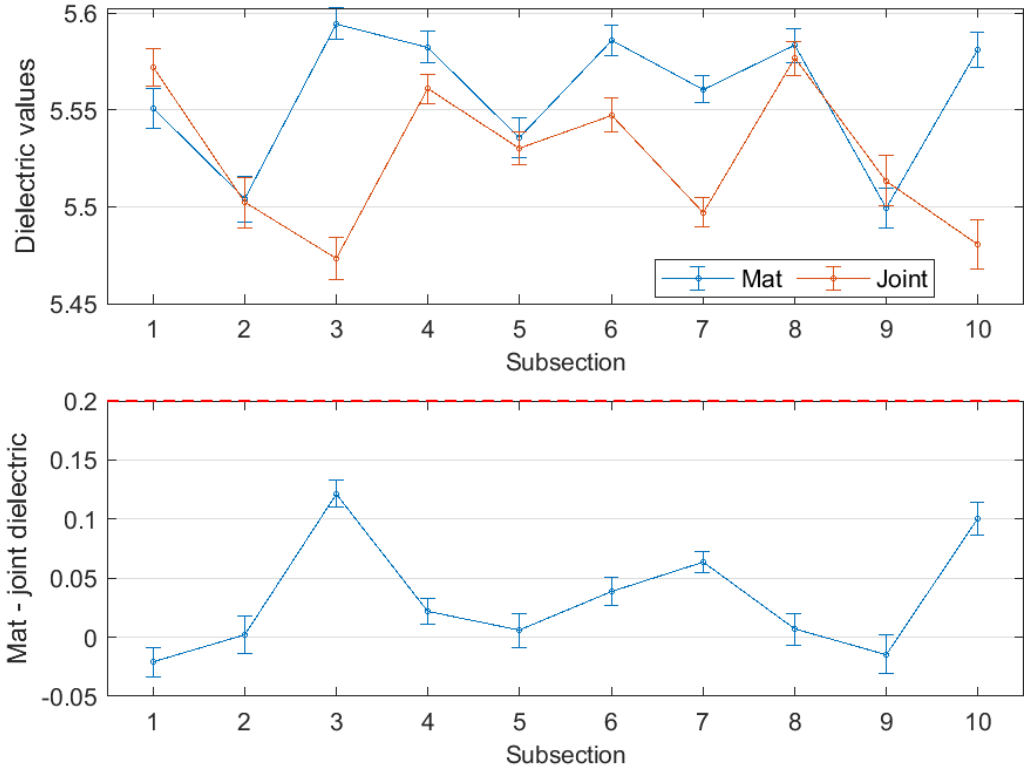

Figure B-217 Interval plot of dielectric values for confined joint (100 ft subsections) – M-25-2

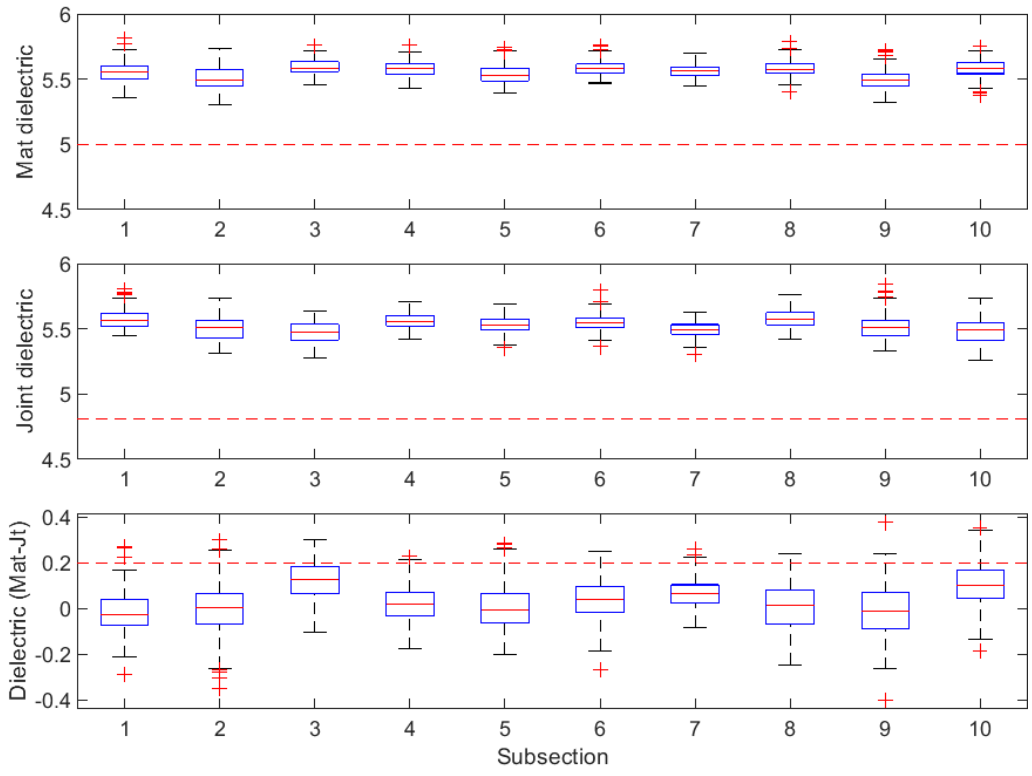

Figure B-218 Box plot of dielectric values for confined joint (100 ft subsections) – M-25-2

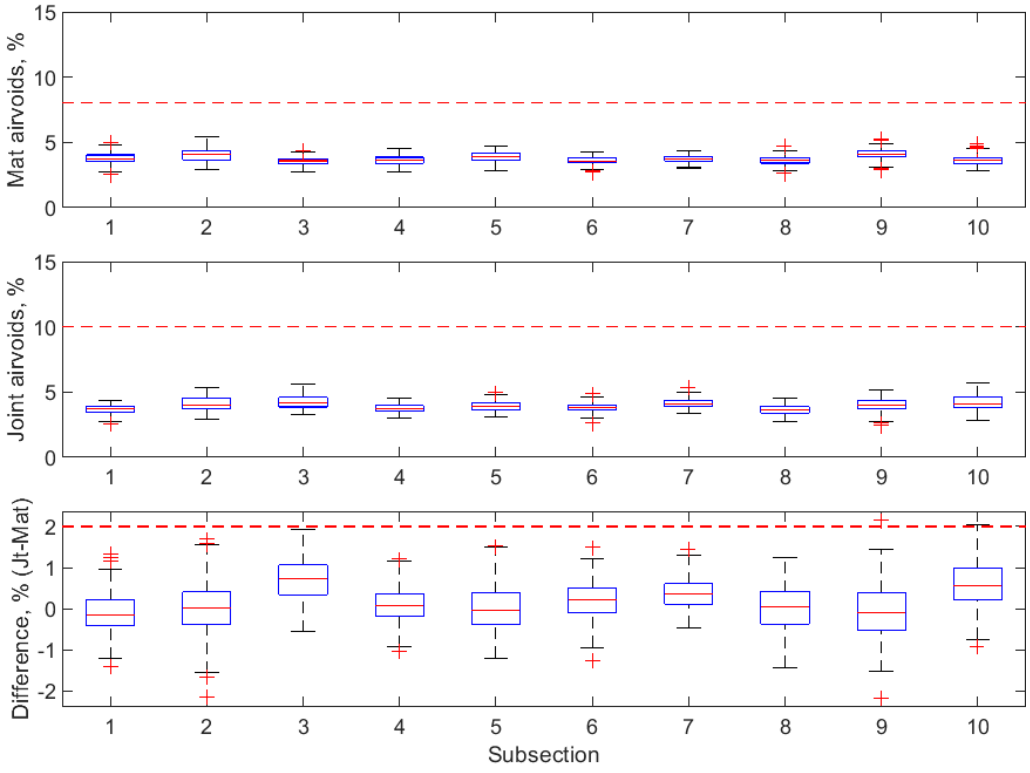

Figure B-219 Box plot of air voids for confined joint (100 ft subsections) – M-25-2

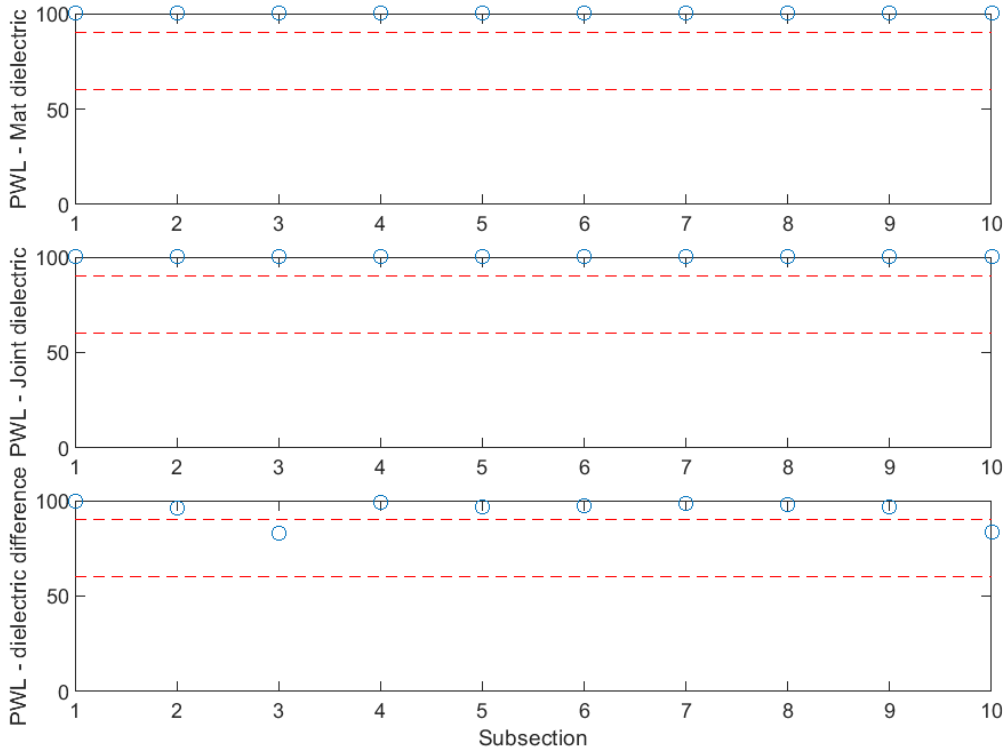

Figure B-220 PWL for dielectric values for confined joint (100 ft subsections) – M-25-2

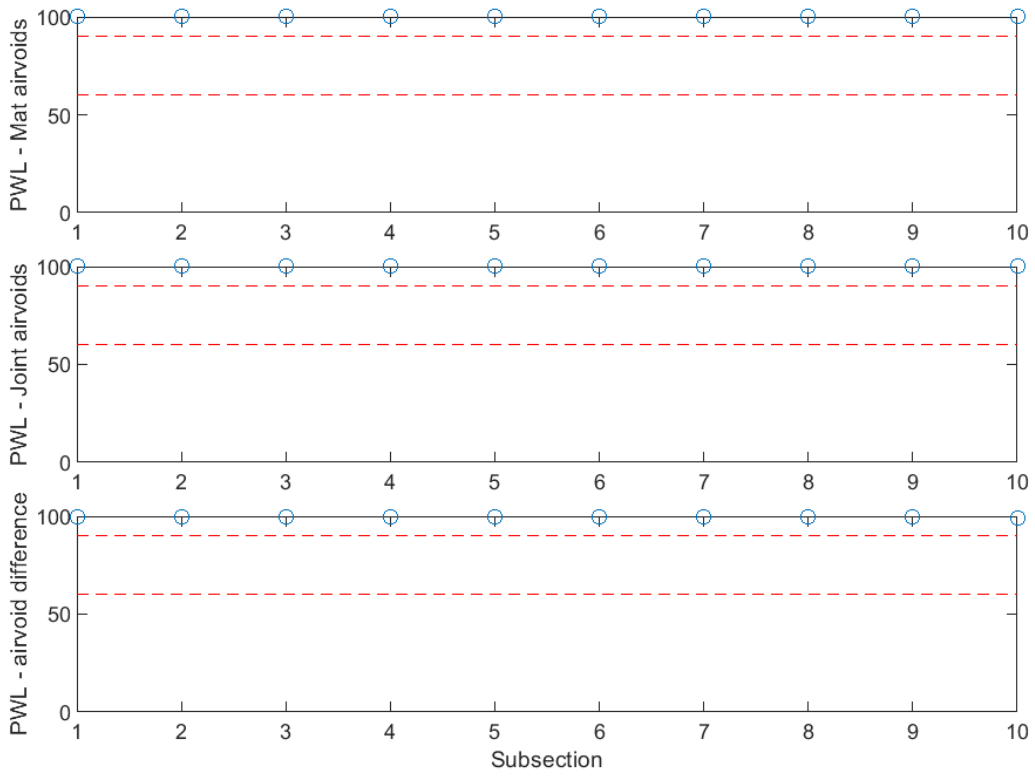

Figure B-221 PWL for air voids for confined joint (100 ft subsections) – M-25-2

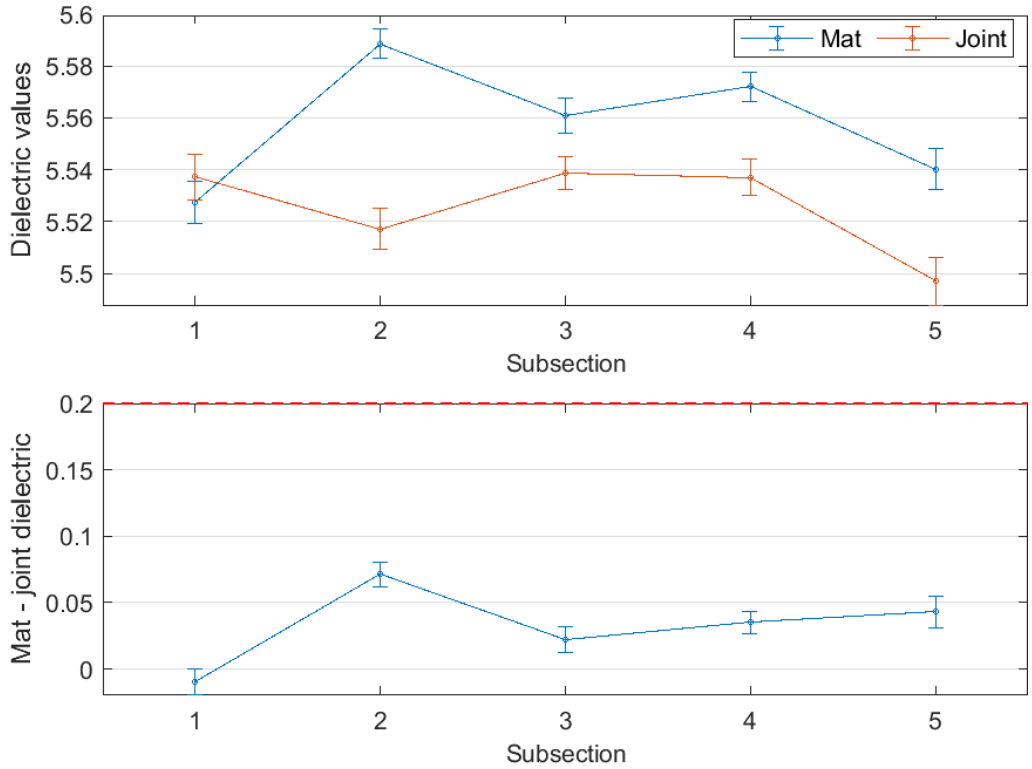

Figure B-222 Interval plot of dielectric values for confined joint (200 ft subsections) – M-25-2

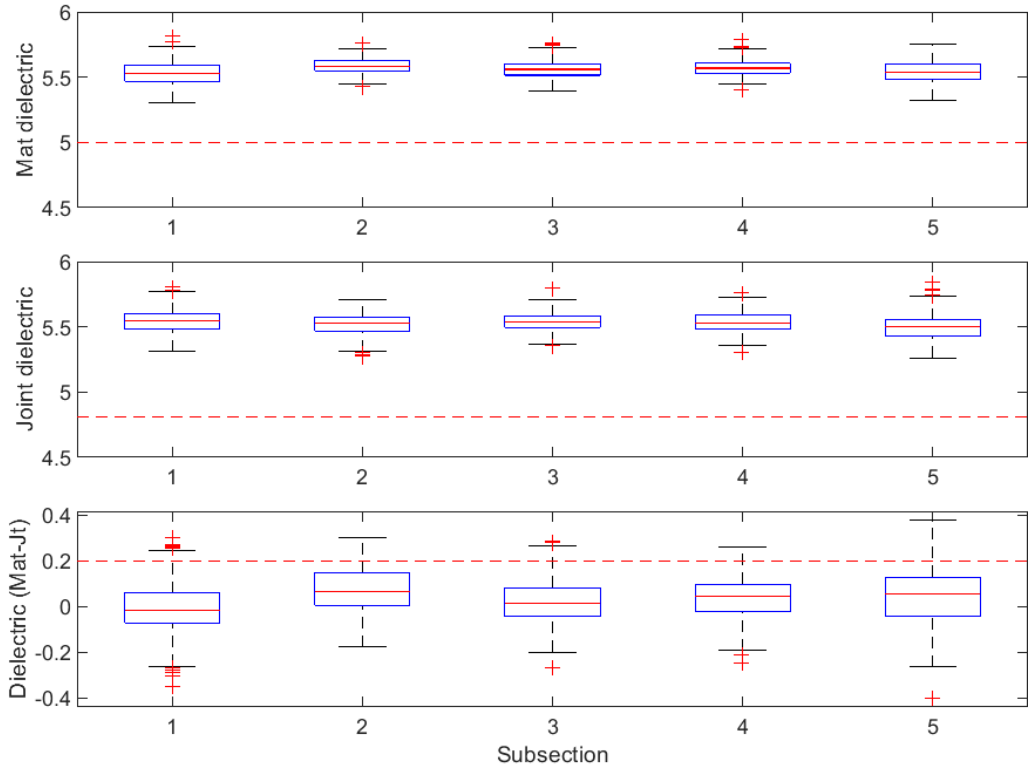

Figure B-223 Box plot of dielectric values for confined joint (200 ft subsections) – M-25-2

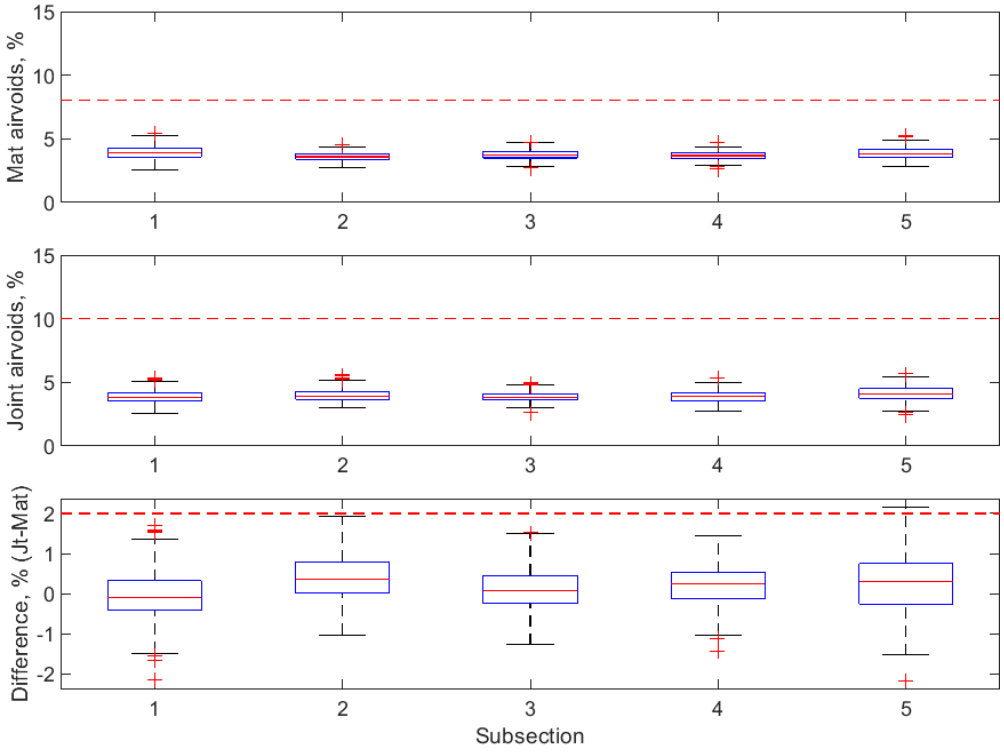

Figure B-224 Box plot of air voids for confined joint (200 ft subsections) – M-25-2

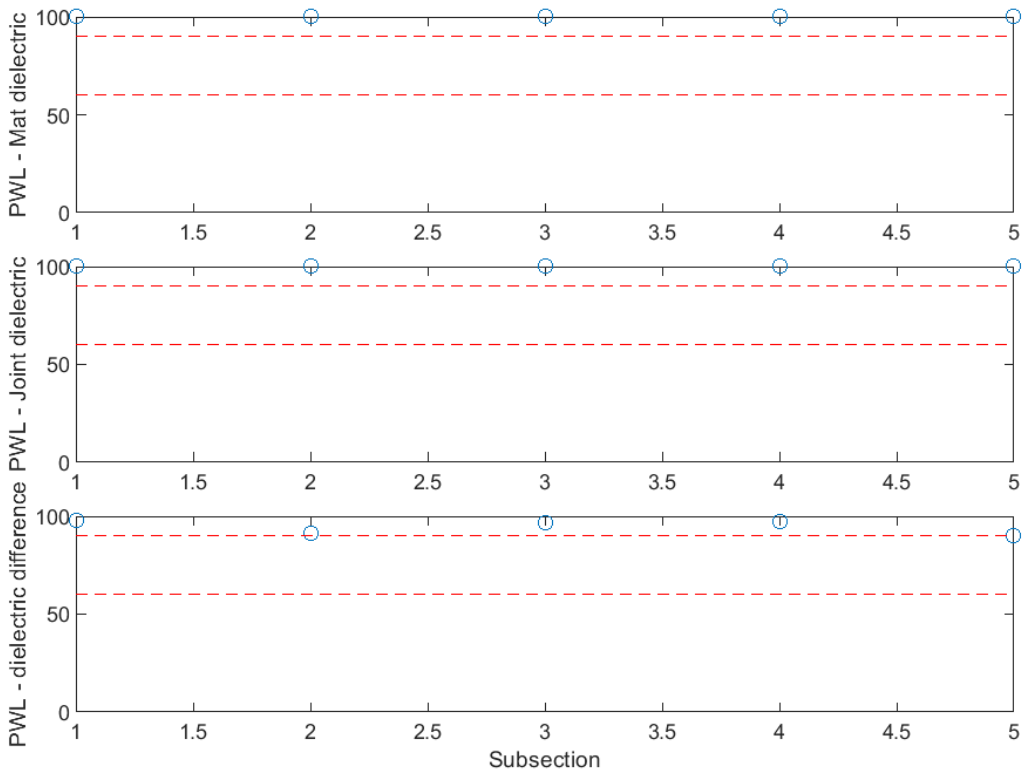

Figure B-225 PWL for dielectric values for confined joint (200 ft subsections) – M-25-2

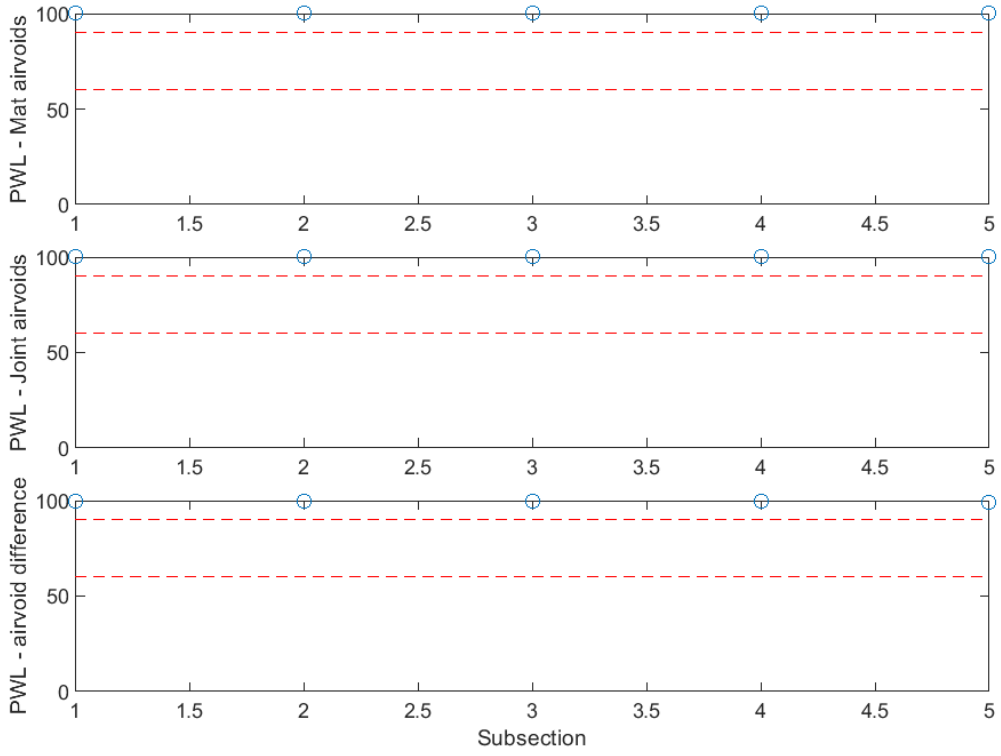

Figure B-226 PWL for air voids for confined joint (200 ft subsections) – M-25-2

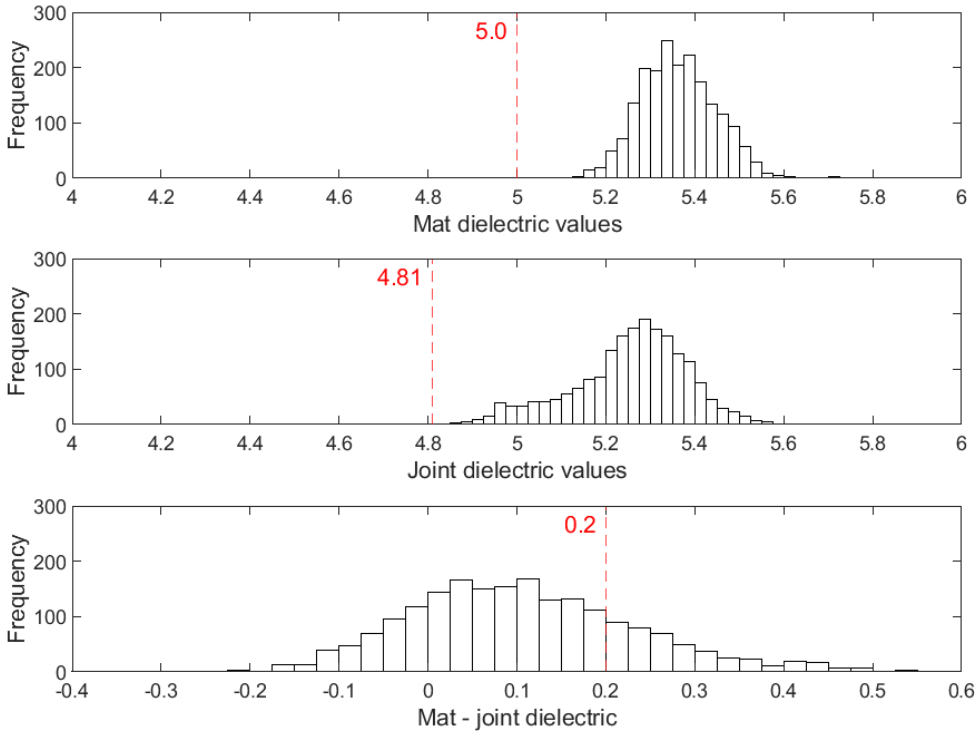

Figure B-227 Histogram of dielectric values for confined tapered joint – M-28-Day2-1

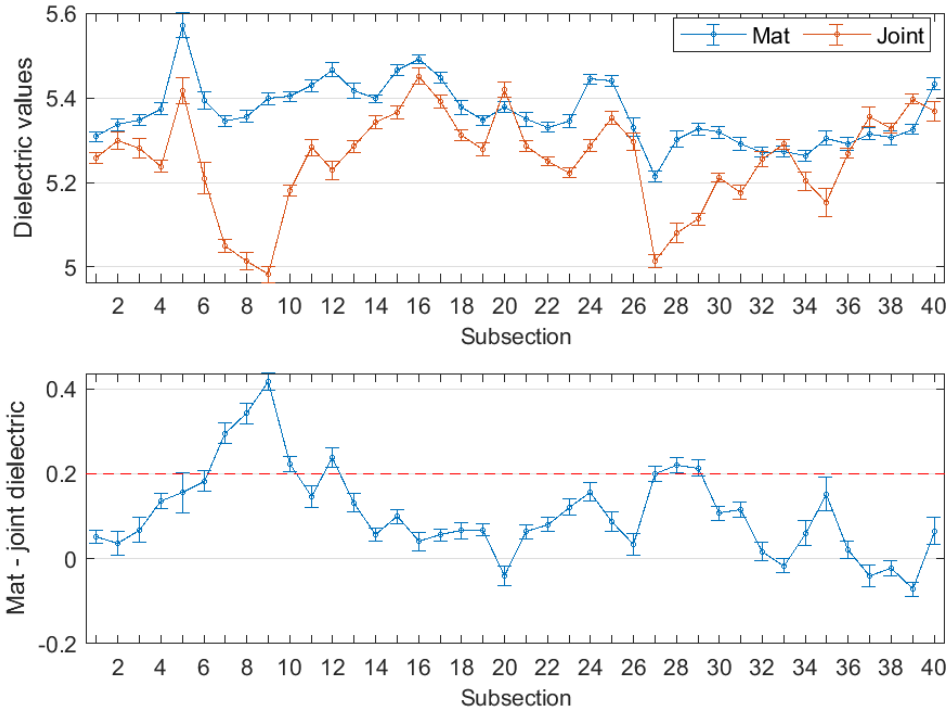

Figure B-228 Interval plot of dielectric values for confined tapered joint (25 ft subsections) – M-28-Day2-1

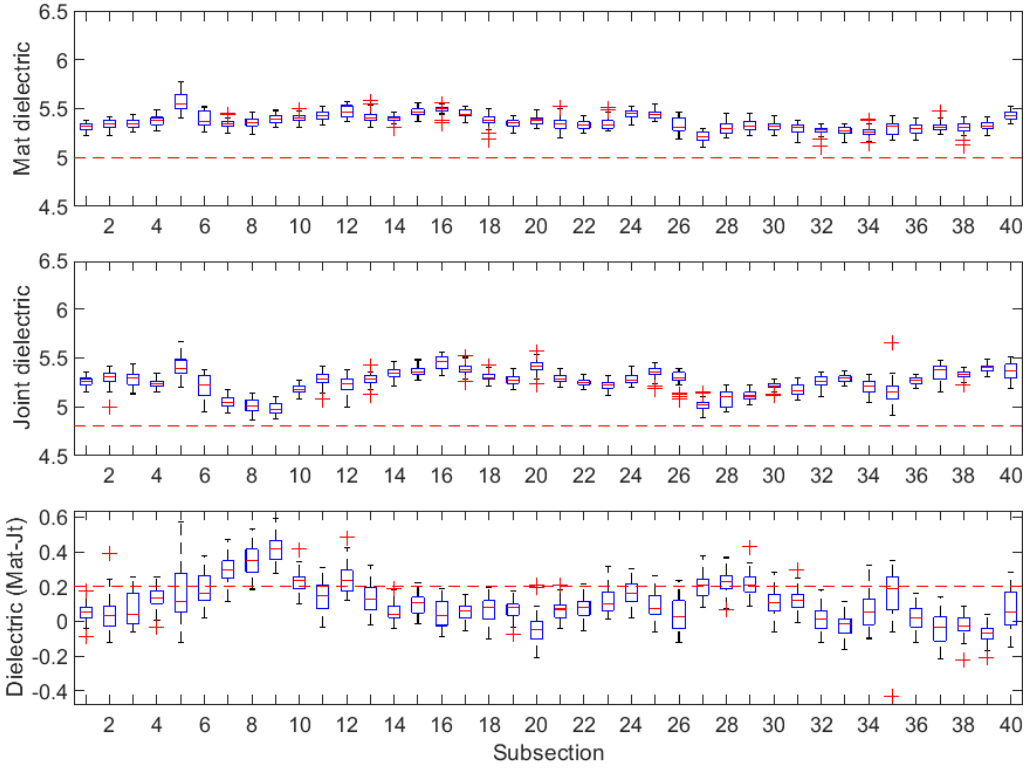

Figure B-229 Box plot of dielectric values for confined tapered joint (25 ft subsections) – M-28-Day2-1

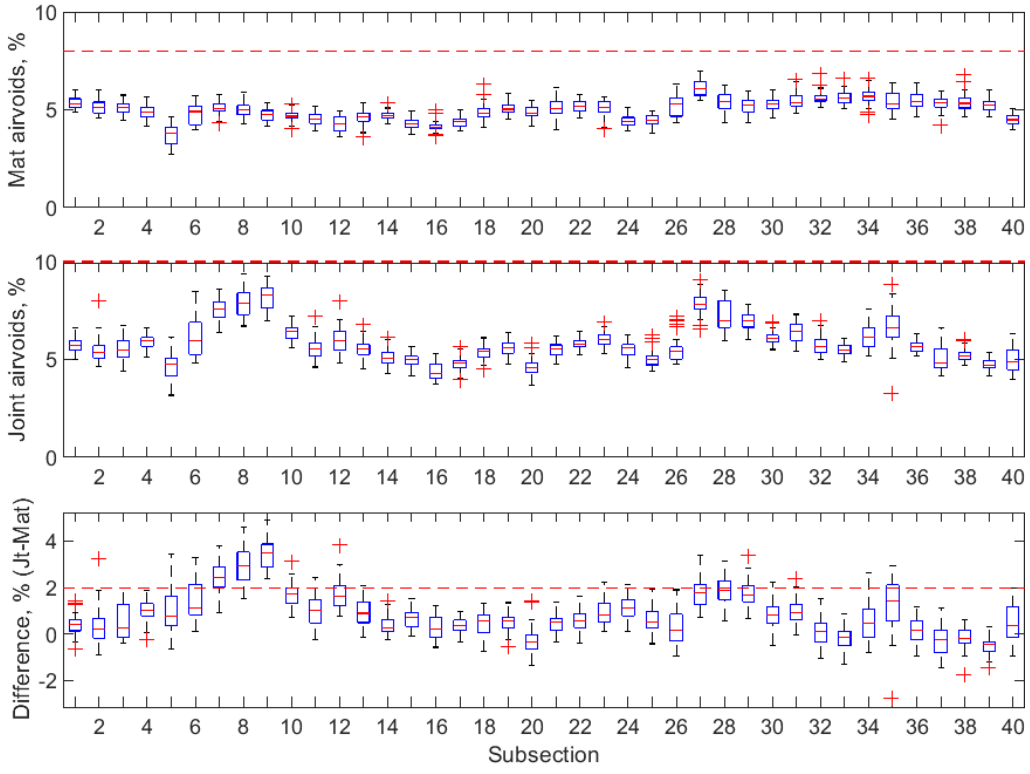

Figure B-230 Box plot of air voids for confined tapered joint (25 ft subsections) – M-28-Day2-1

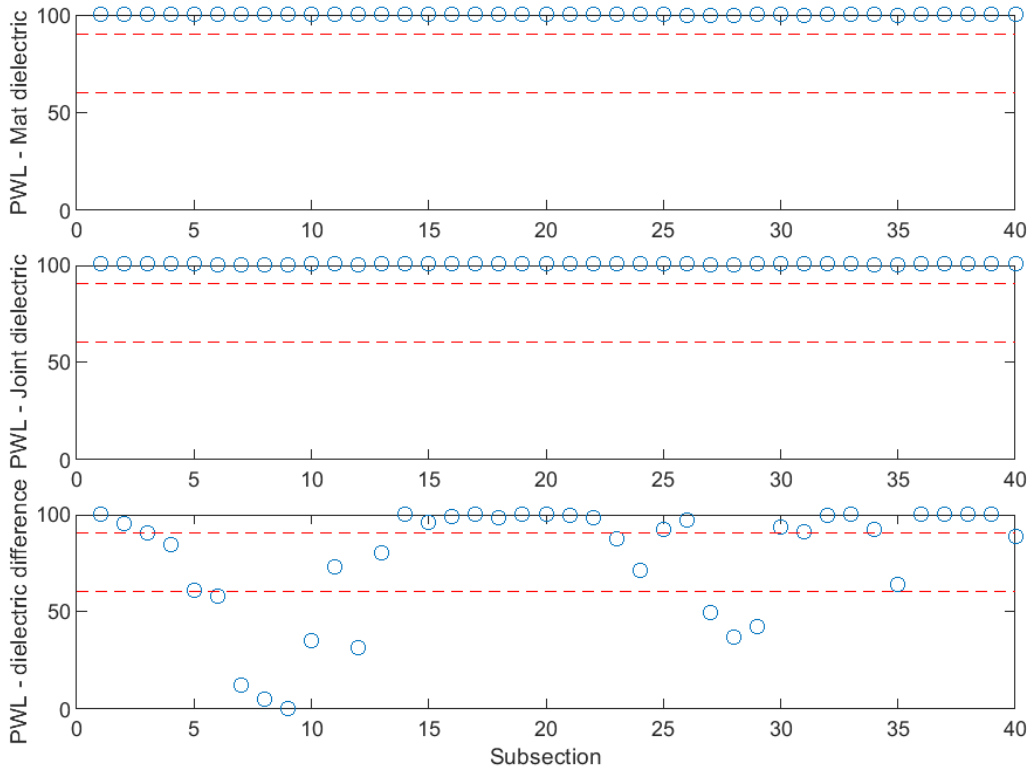

Figure B-231 PWL for dielectric values for confined tapered joint (25 ft subsections) – M-28-Day2-1

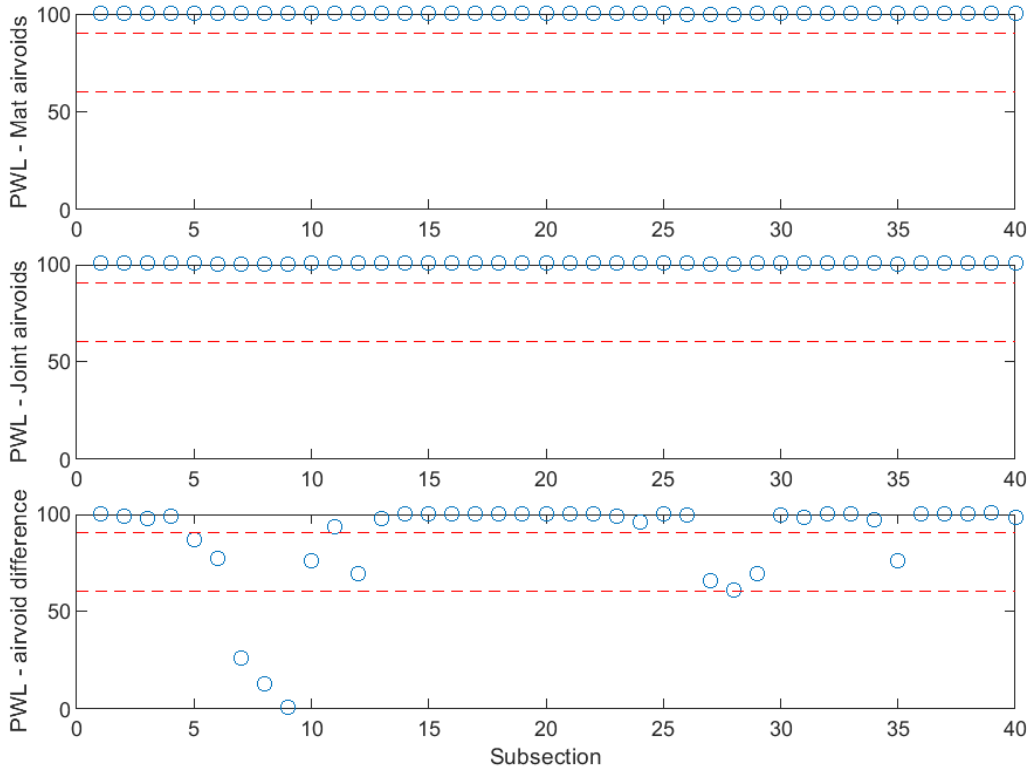

Figure B-232 PWL for air voids for confined tapered joint (25 ft subsections) – M-28-Day2-1

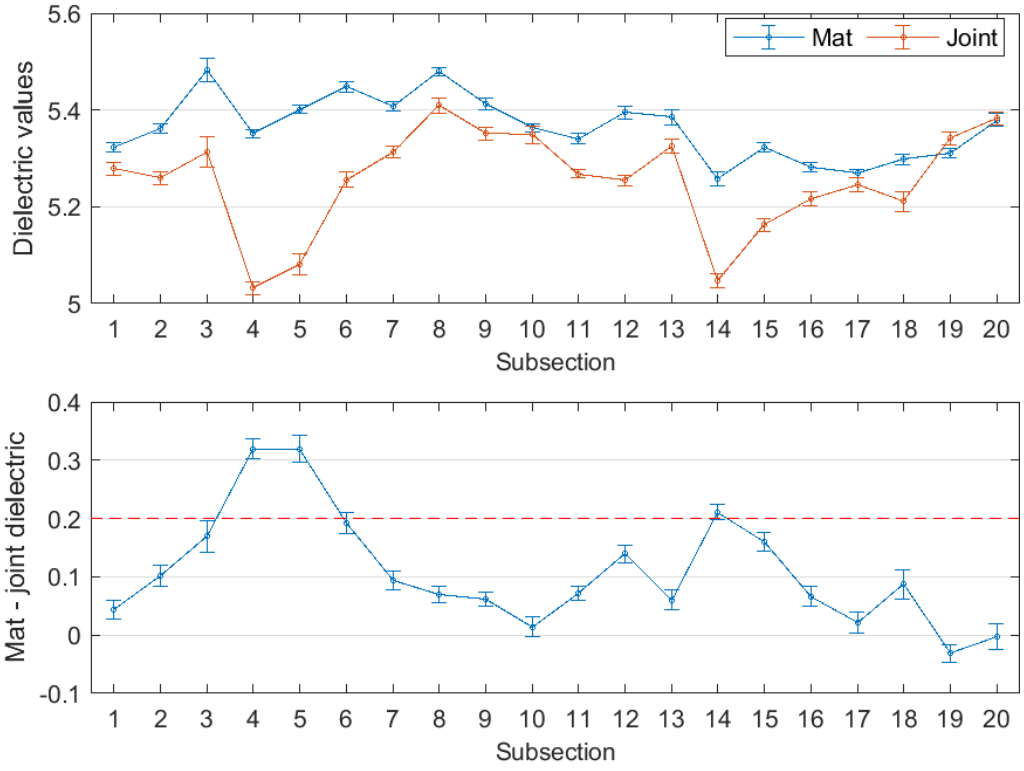

Figure B-233 Interval plot of dielectric values for confined tapered joint (50 ft subsections) – M-28-Day2-1

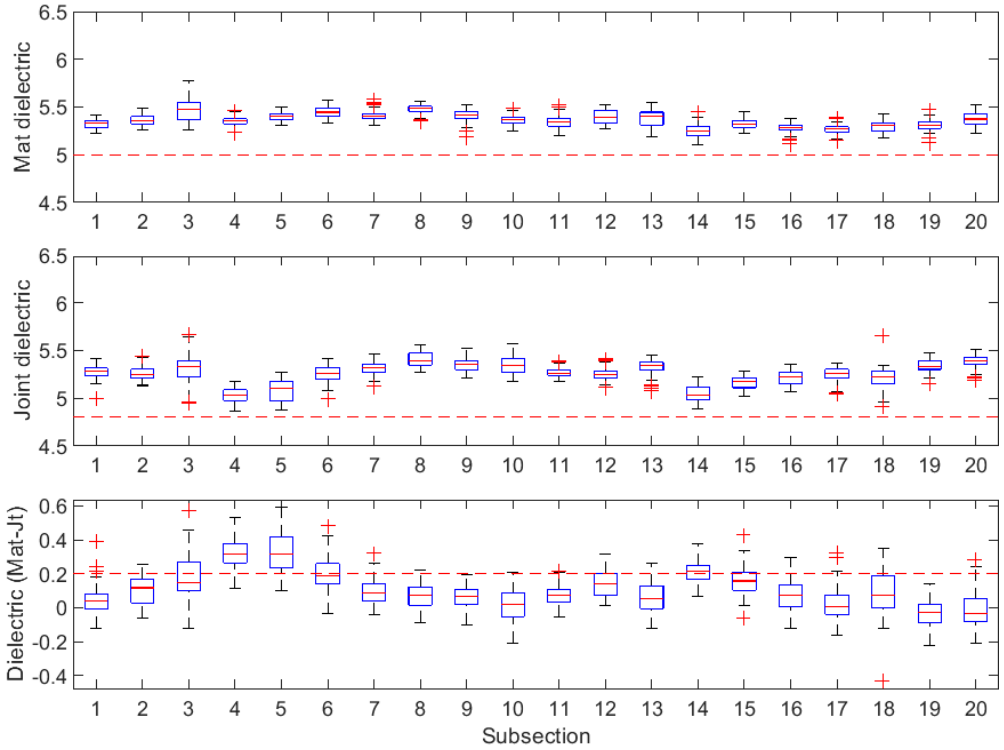

Figure B-234 Box plot of dielectric values for confined tapered joint (50 ft subsections) – M-28-Day2-1

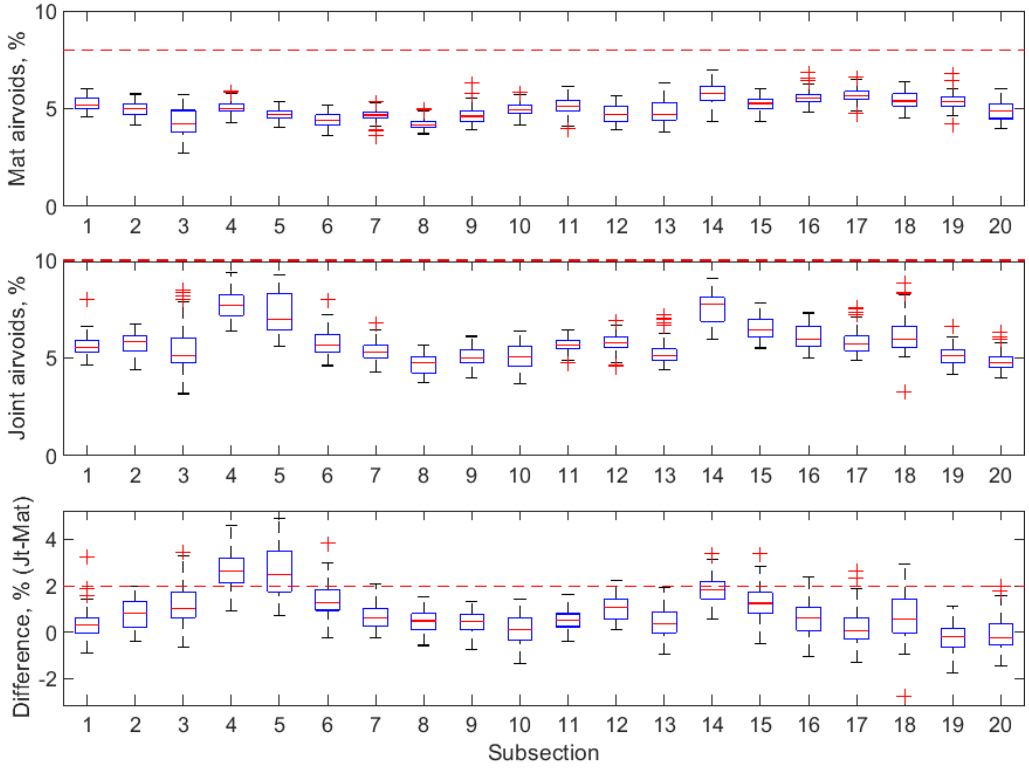

Figure B-235 Box plot of air voids for confined tapered joint (50 ft subsections) – M-28-Day2-1

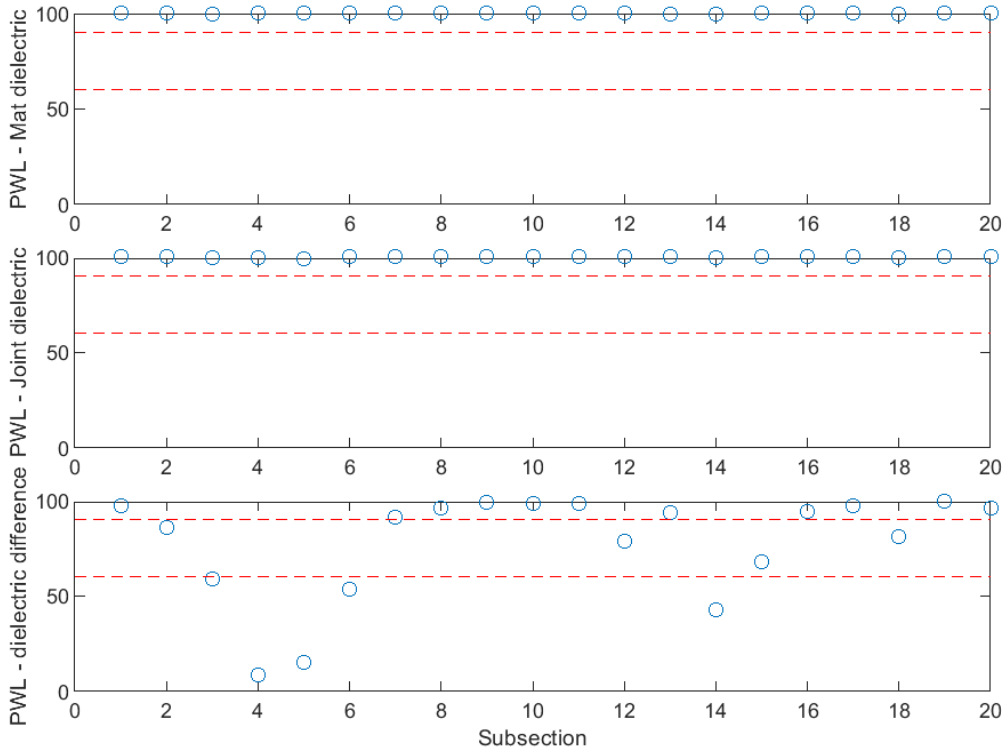

Figure B-236 PWL for dielectric values for confined tapered joint (50 ft subsections) – M-28-Day2-1

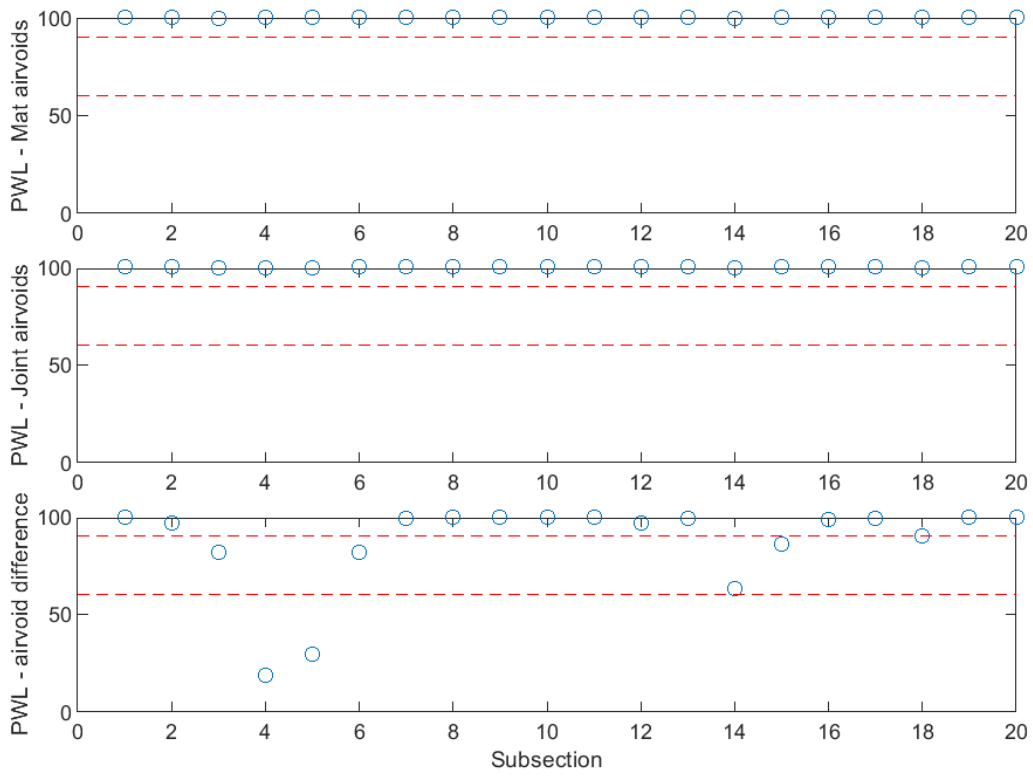

Figure B-237 PWL for air voids for confined tapered joint (50 ft subsections) – M-28-Day2-1

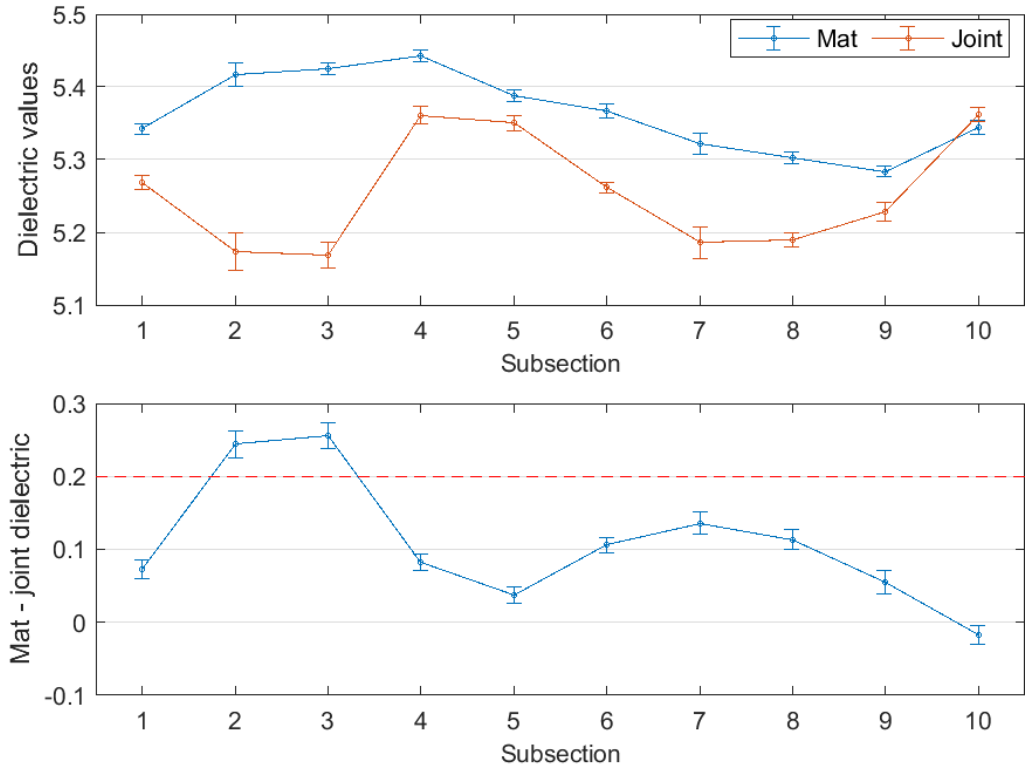

Figure B-238 Interval plot of dielectric values for confined tapered joint (100 ft subsections) – M-28-Day2-1

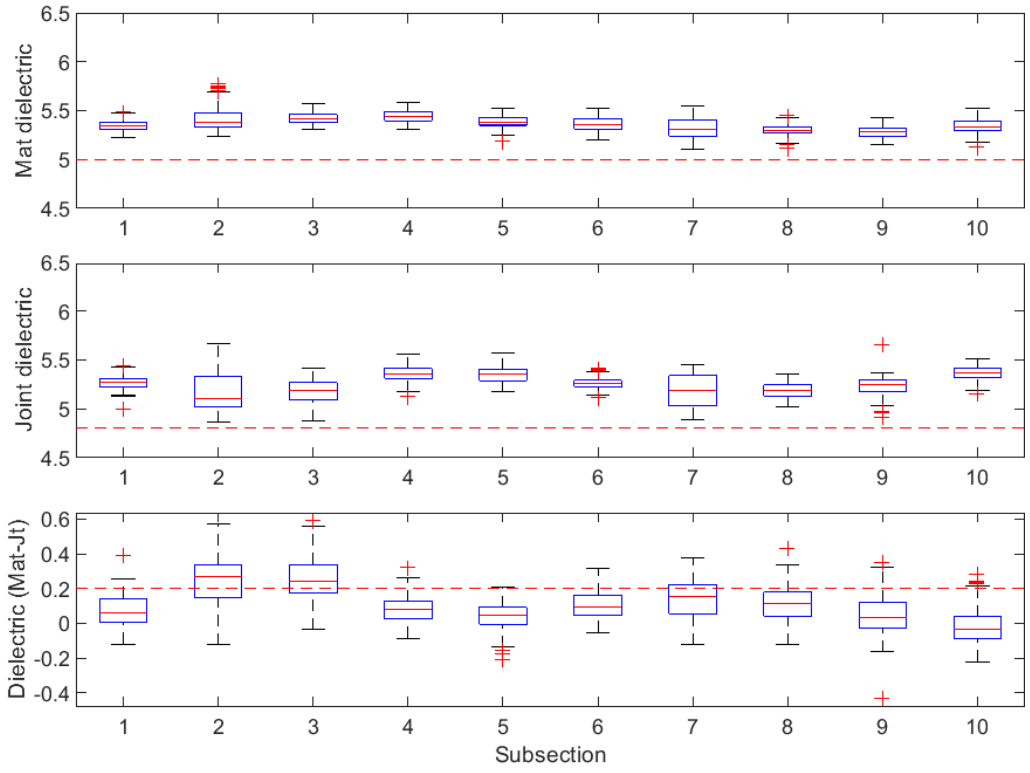

Figure B-239 Box plot of dielectric values for confined tapered joint (100 ft subsections) – M-28-Day2-1

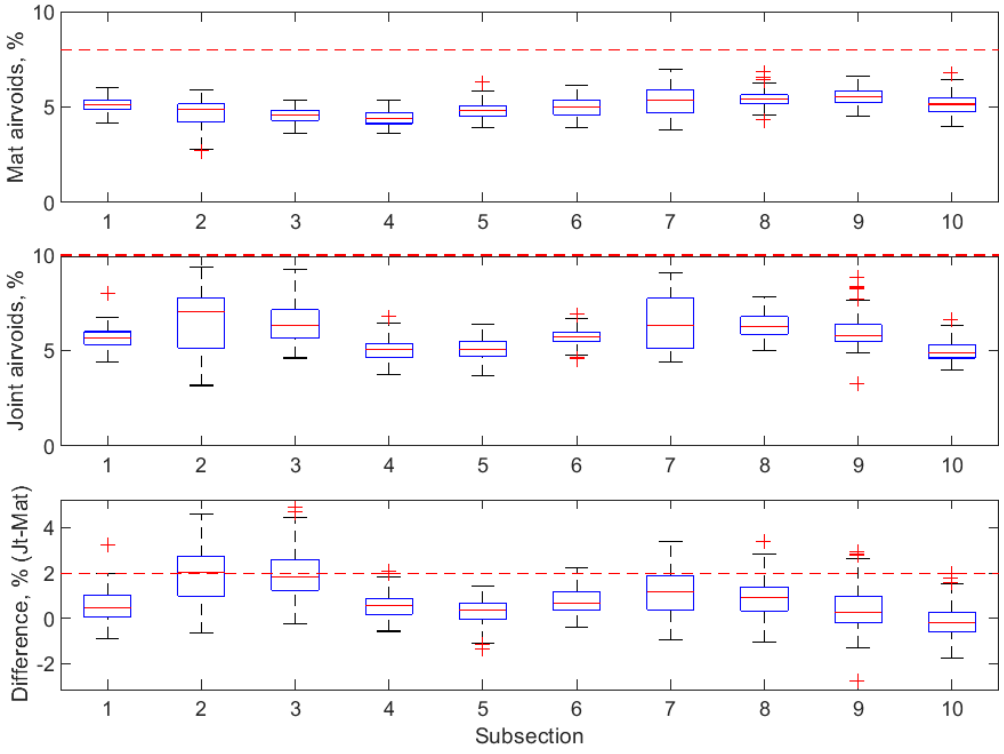

Figure B-240 Box plot of air voids for confined tapered joint (100 ft subsections) – M-28-Day2-1

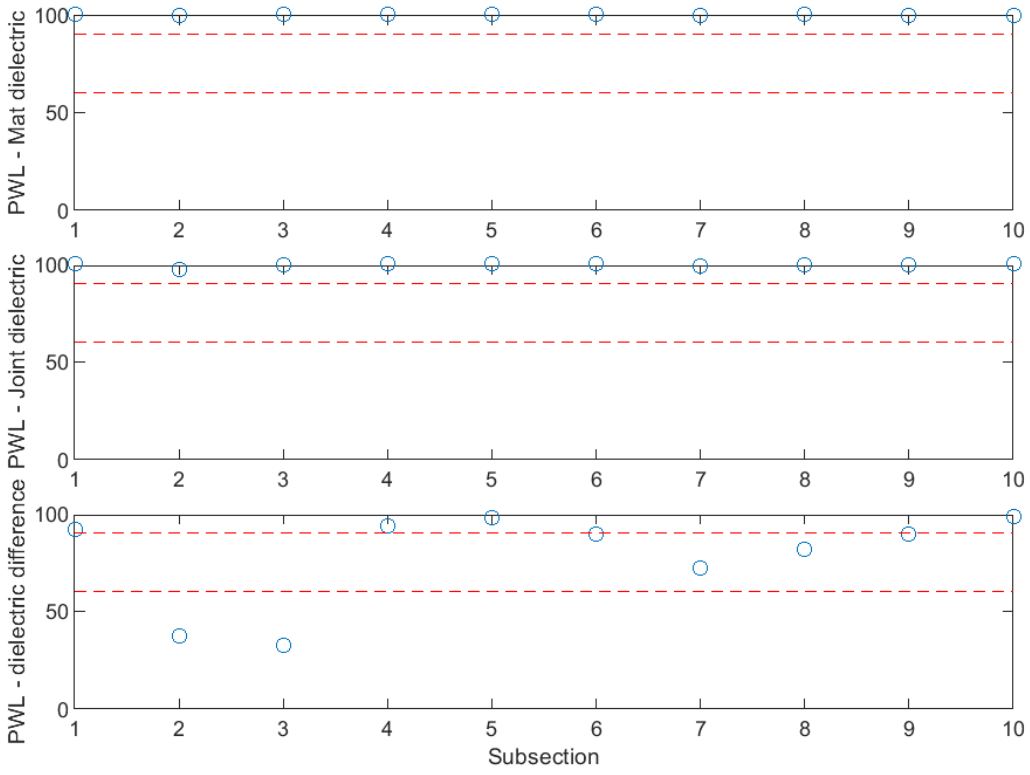

Figure B-241 PWL for dielectric values for confined tapered joint (100 ft subsections) – M-28-Day2-1

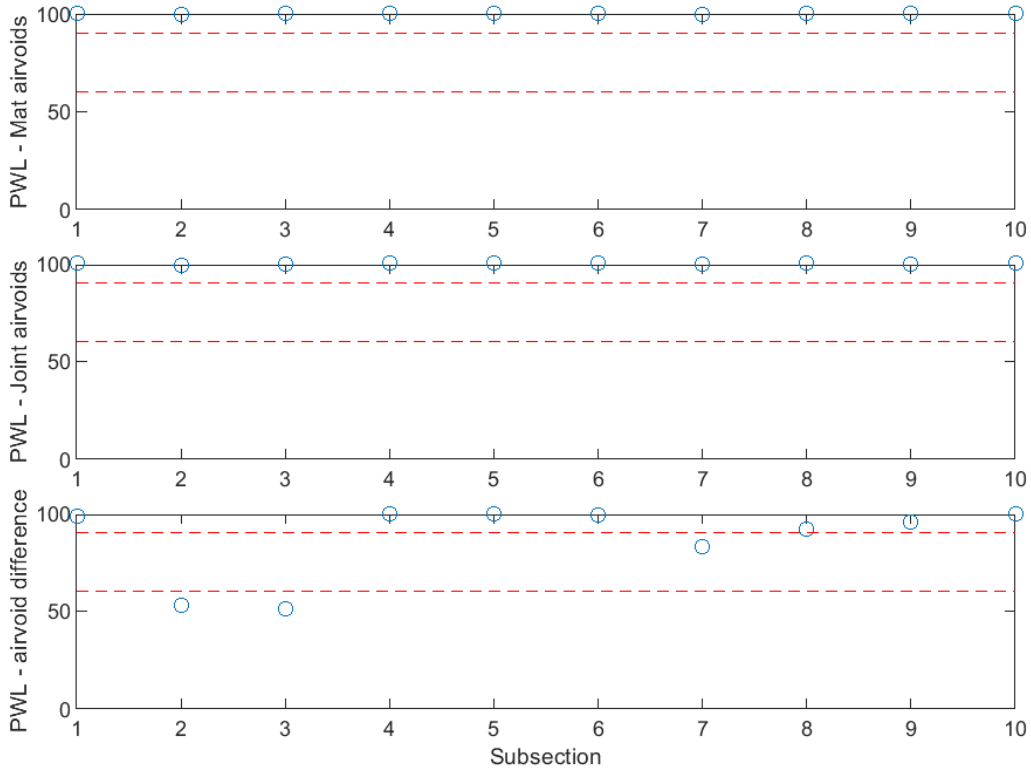

Figure B-242 PWL for air voids for confined tapered joint (100 ft subsections) – M-28-Day2-1

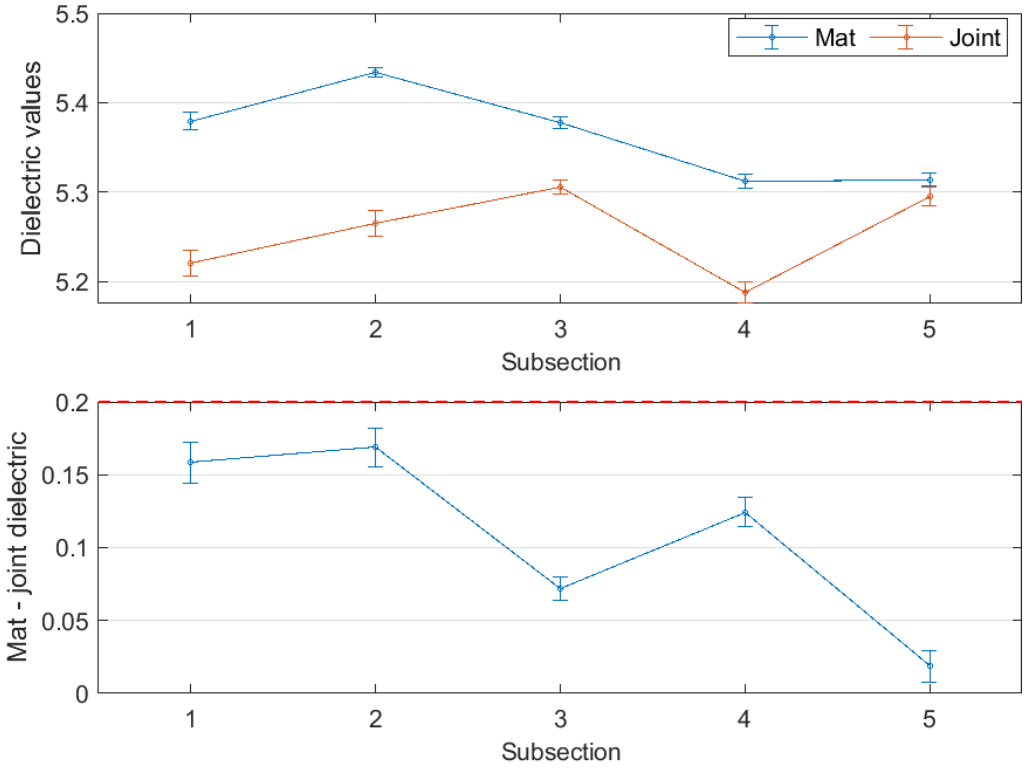

Figure B-243 Interval plot of dielectric values for confined tapered joint (200 ft subsections) – M-28-Day2-1

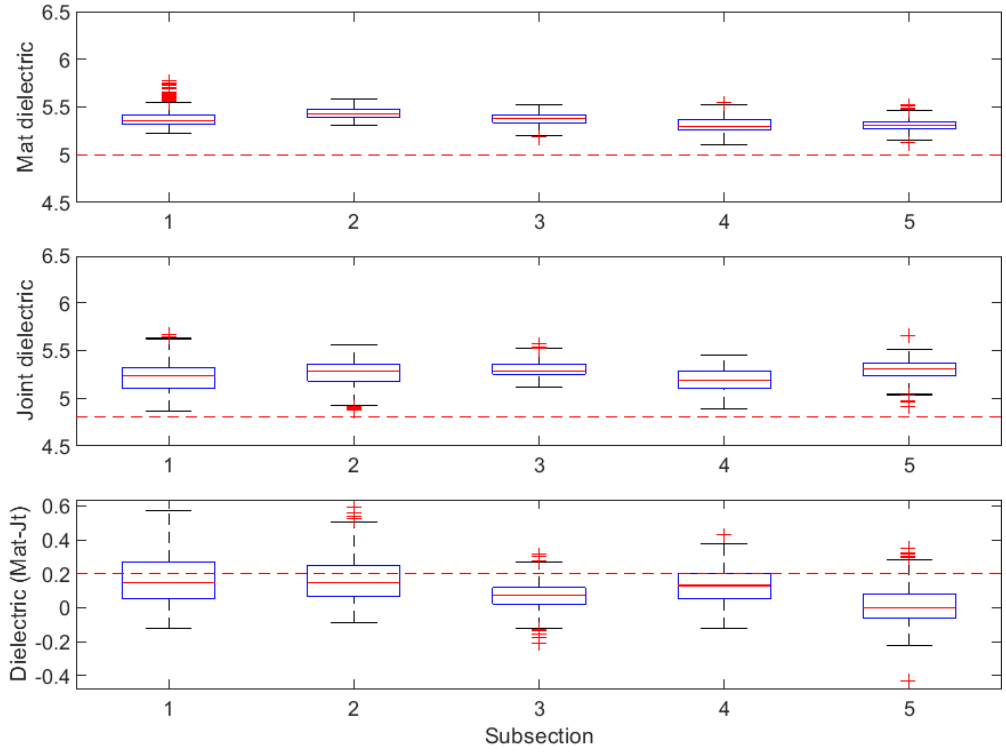

Figure B-244 Box plot of dielectric values for confined tapered joint (200 ft subsections) – M-28-Day2-1

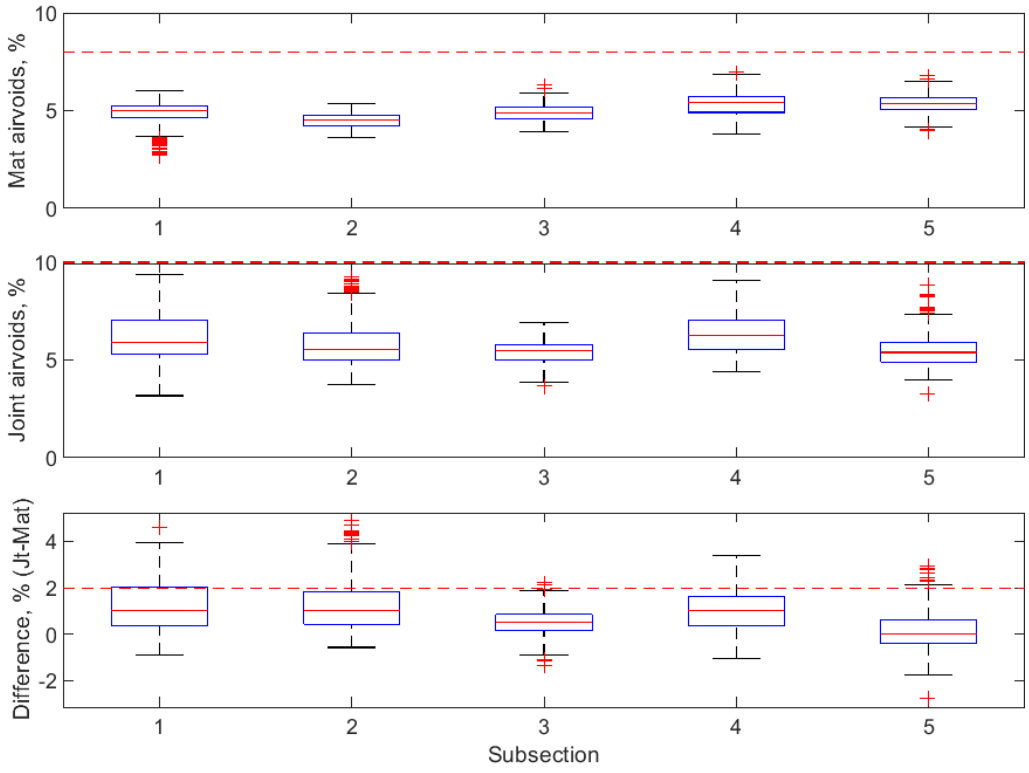

Figure B-245 Box plot of air voids for confined tapered joint (200 ft subsections) – M-28-Day2-1

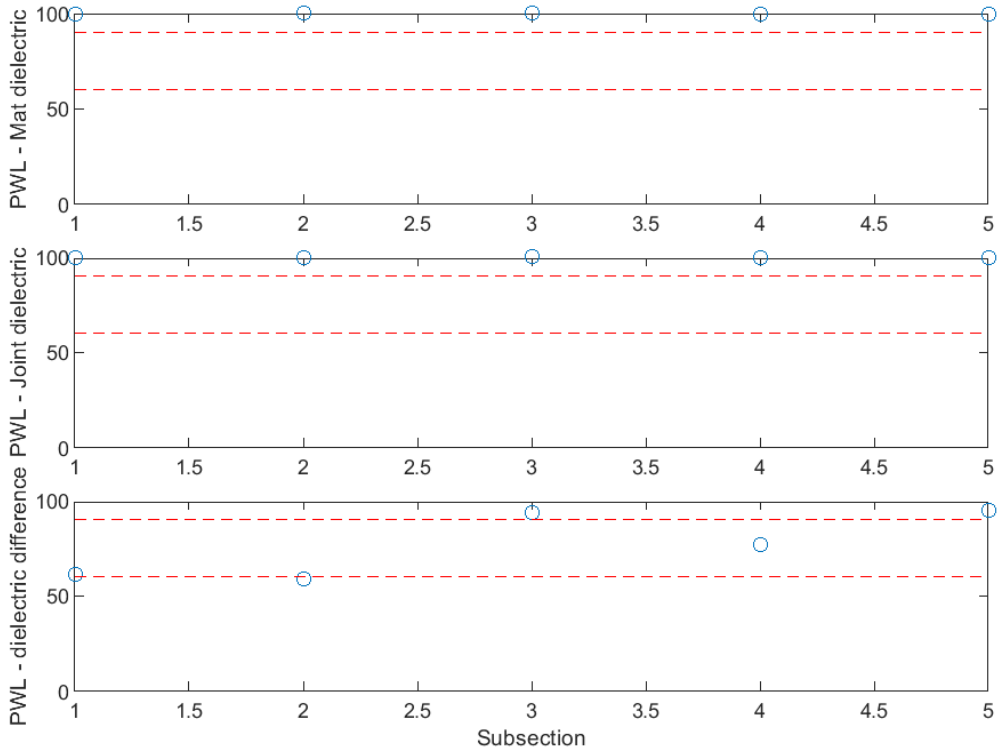

Figure B-246 PWL for dielectric values for confined tapered joint (200 ft subsections) – M-28-Day2-1

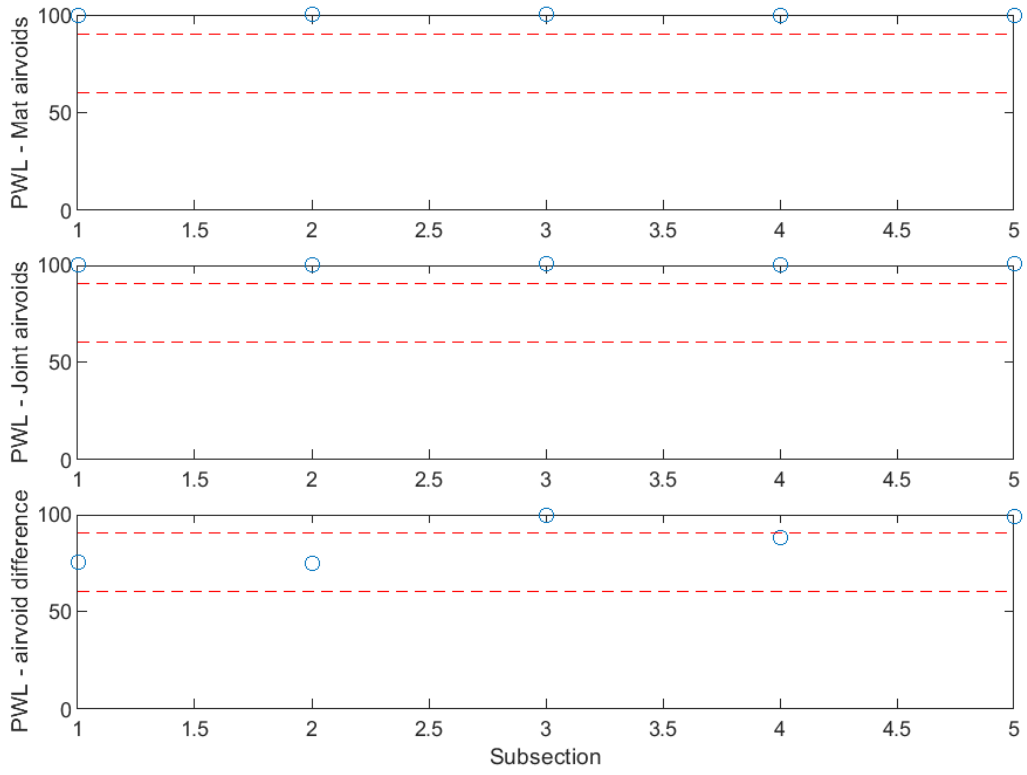

Figure B-247 PWL for air voids for confined tapered joint (200 ft subsections) – M-28-Day2-1

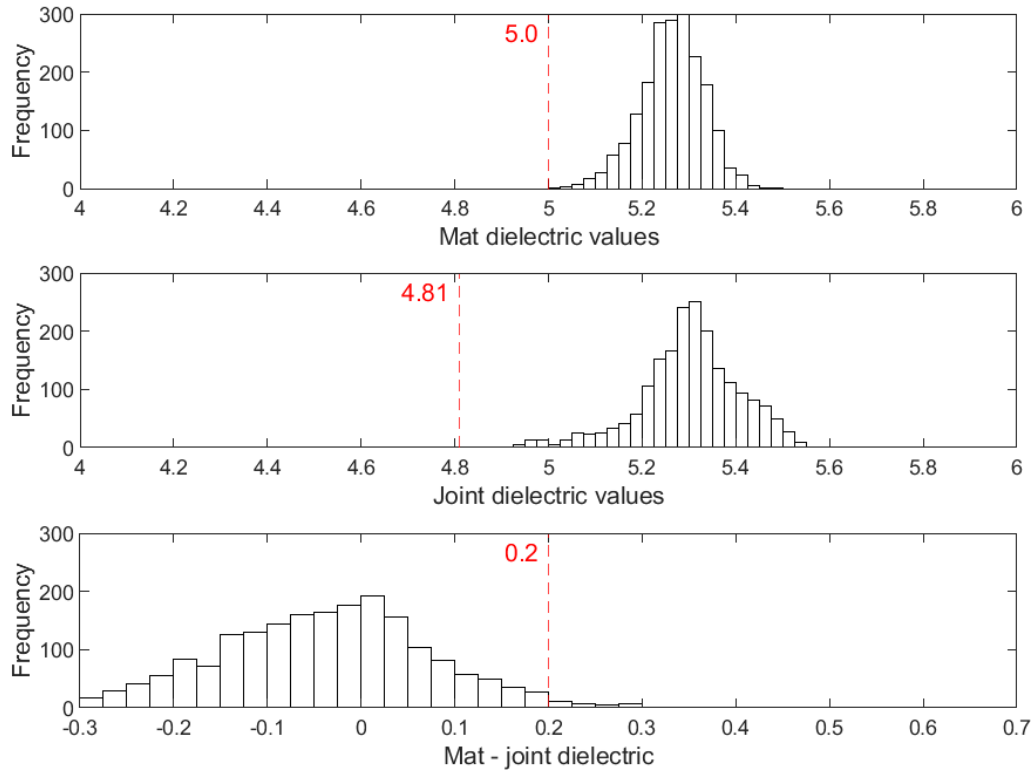

Figure B-248 Histogram of dielectric values for confined tapered joint – M-28-Day2-2

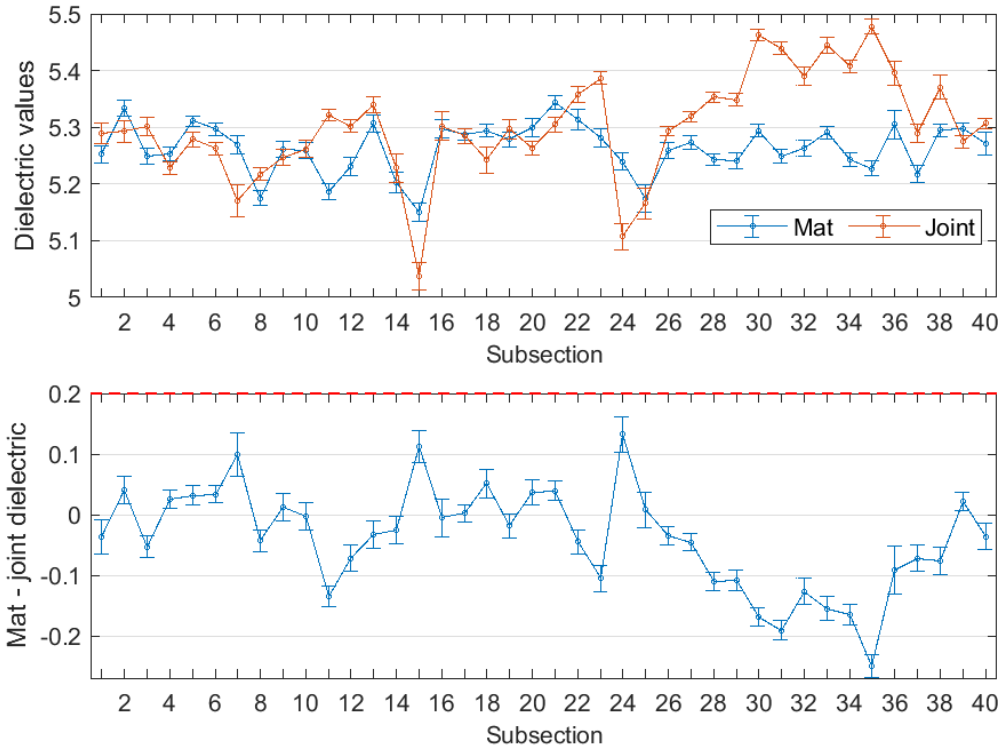

Figure B-249 Interval plot of dielectric values for confined tapered joint (25 ft subsections) – M-28- Day2-2

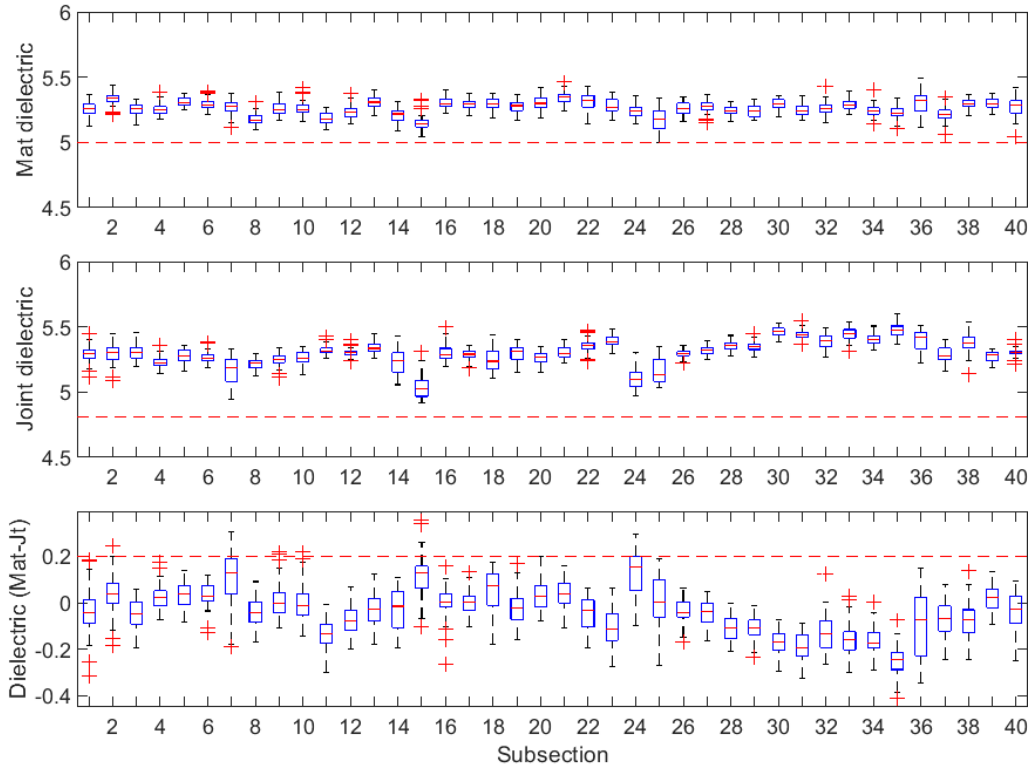

Figure B-250 Box plot of dielectric values for confined tapered joint (25 ft subsections) – M-28-Day2-2

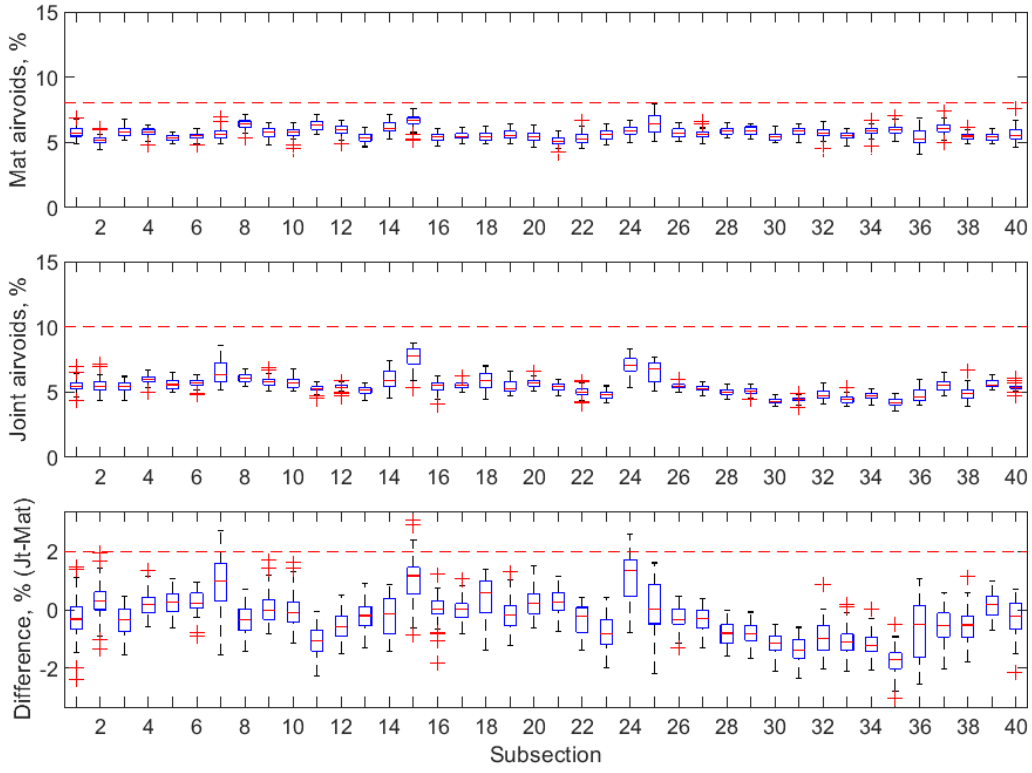

Figure B-251 Box plot of air voids for confined tapered joint (25 ft subsections) – M-28- Day2-2

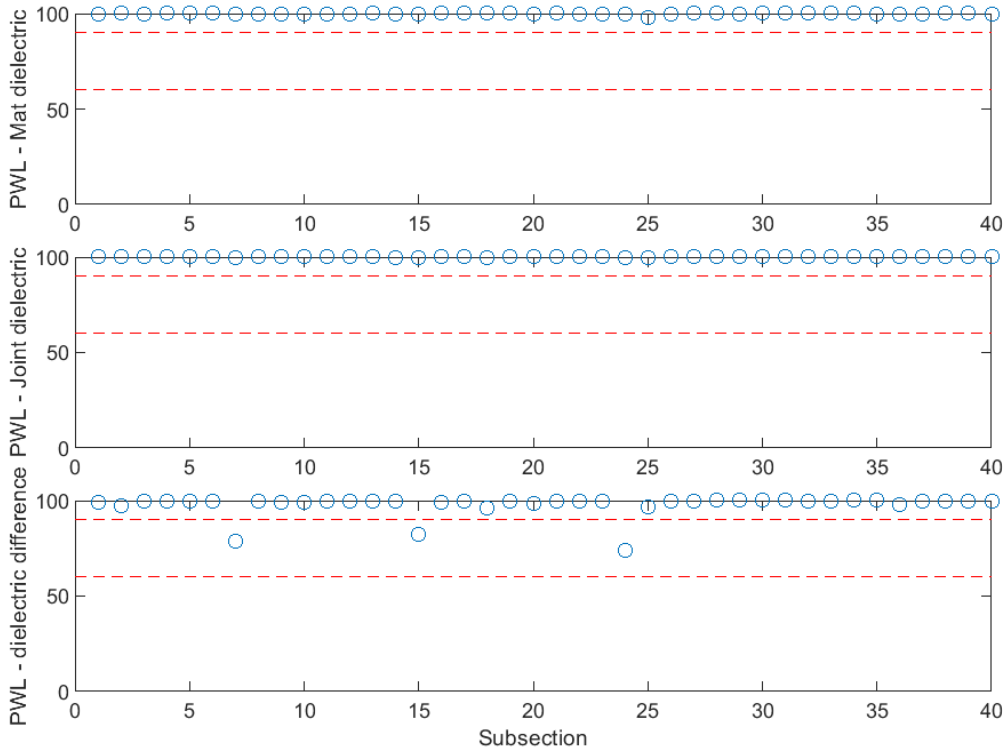

Figure B-252 PWL for dielectric values for confined tapered joint (25 ft subsections) – M-28- Day2-2

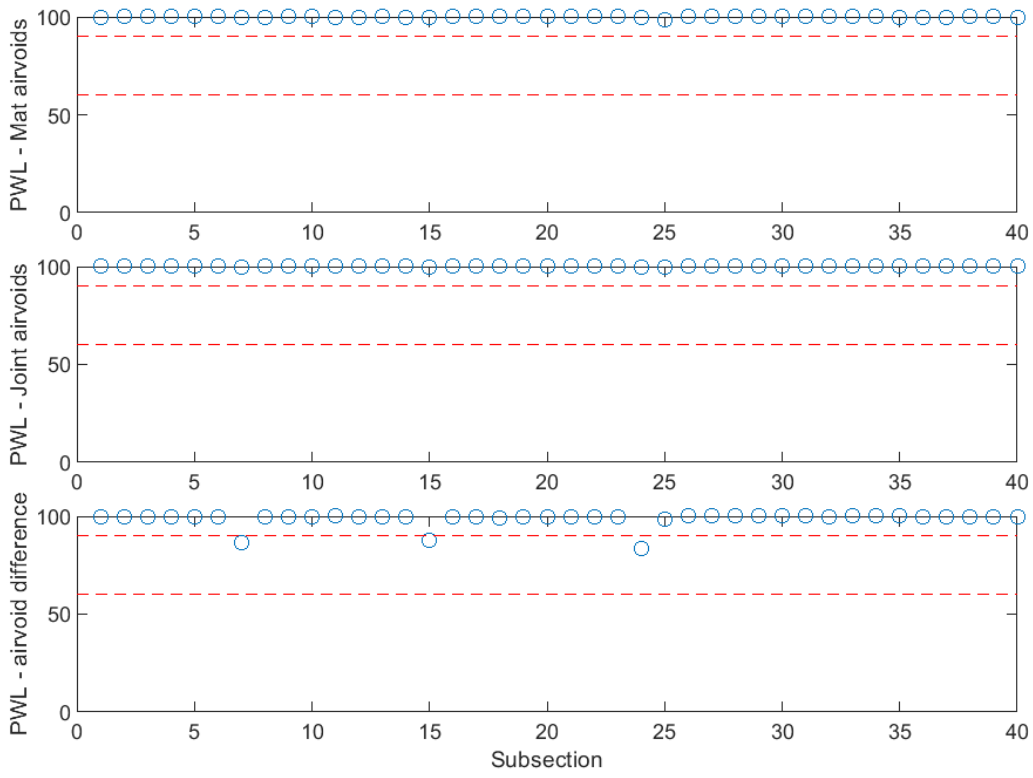

Figure B-253 PWL for air voids for confined tapered joint (25 ft subsections) – M-28- Day2-2

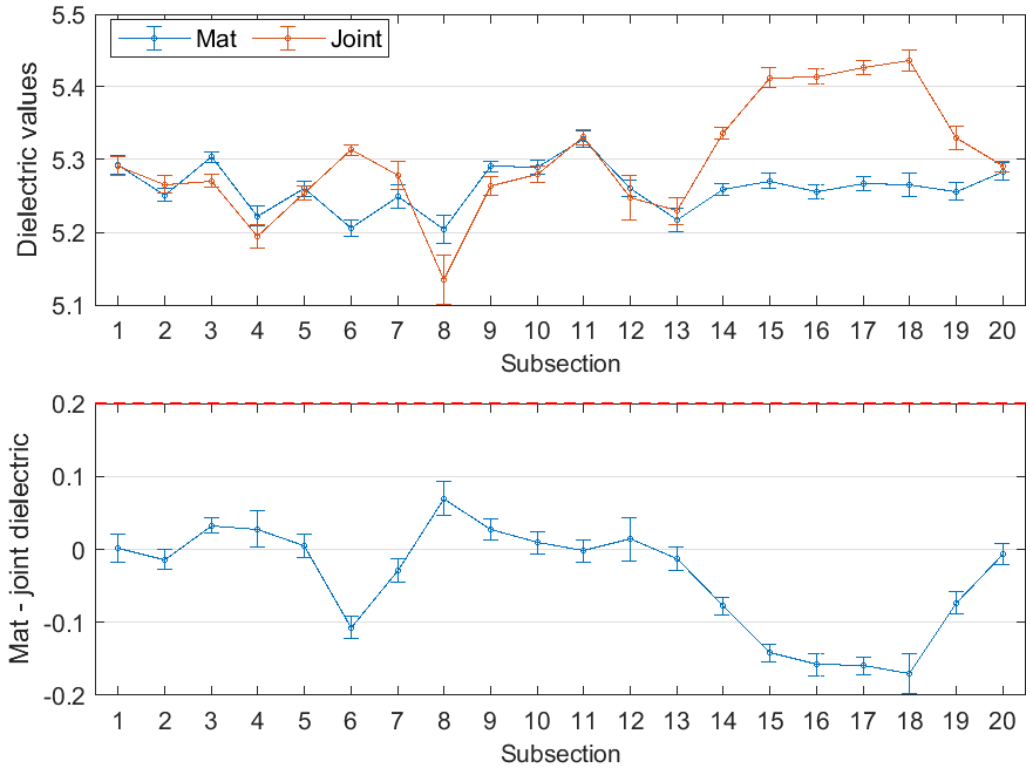

Figure B-254 Interval plot of dielectric values for confined tapered joint (50 ft subsections) – M-28- Day2-2

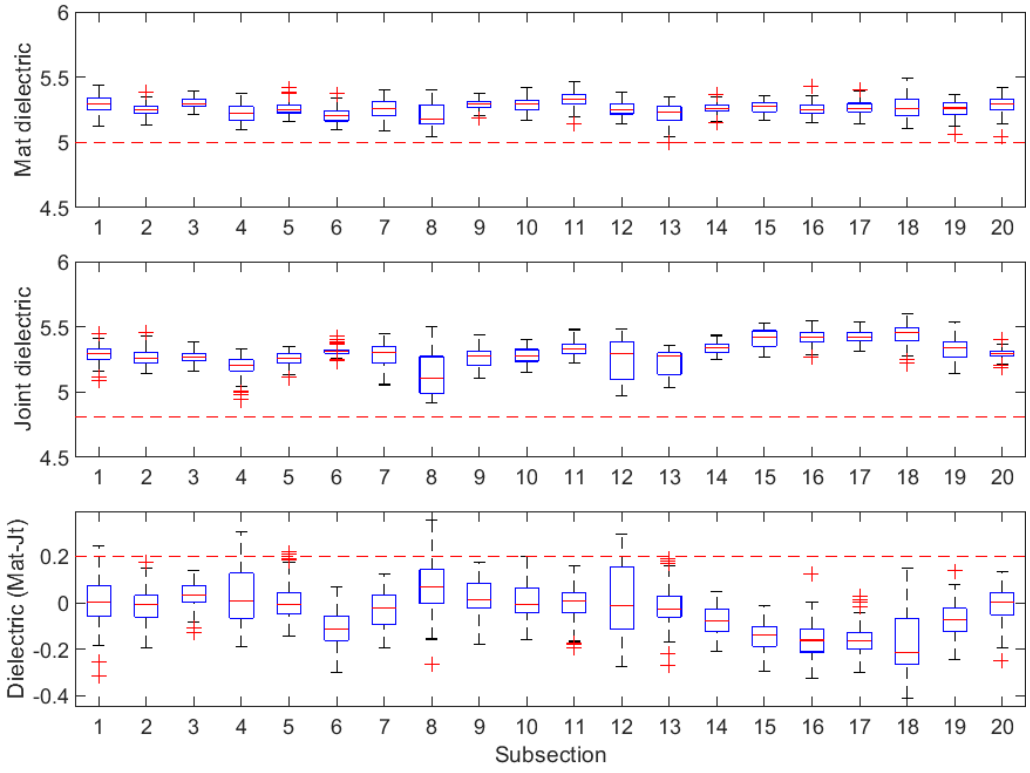

Figure B-255 Box plot of dielectric values for confined tapered joint (50 ft subsections) – M-28- Day2-2

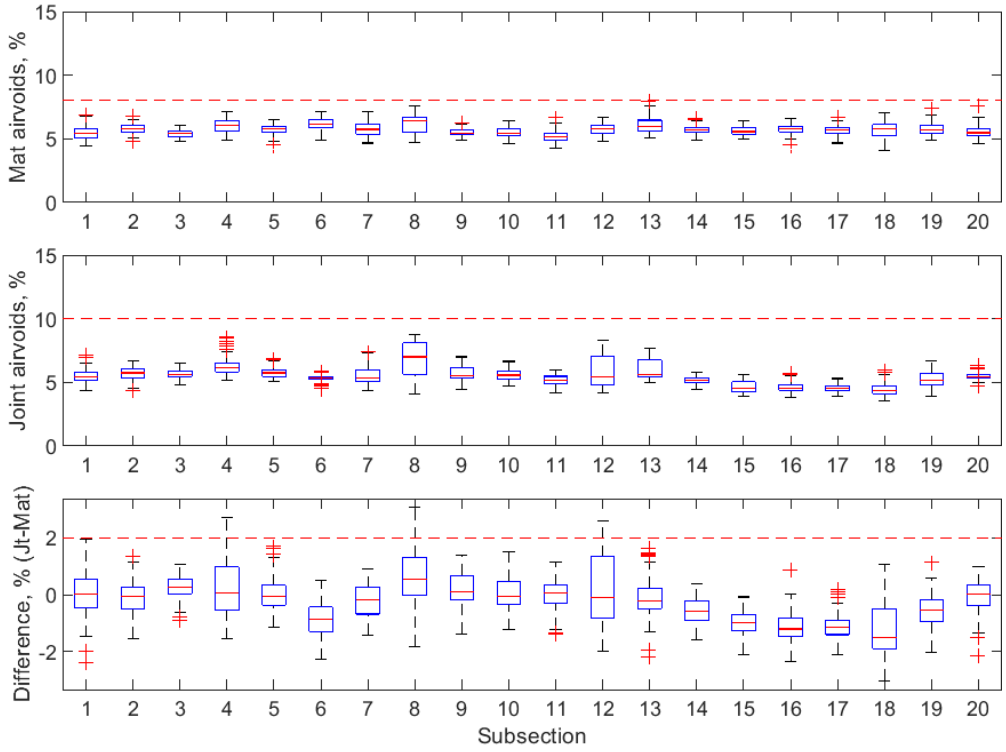

Figure B-256 Box plot of air voids for confined tapered joint (50 ft subsections) – M-28- Day2-2

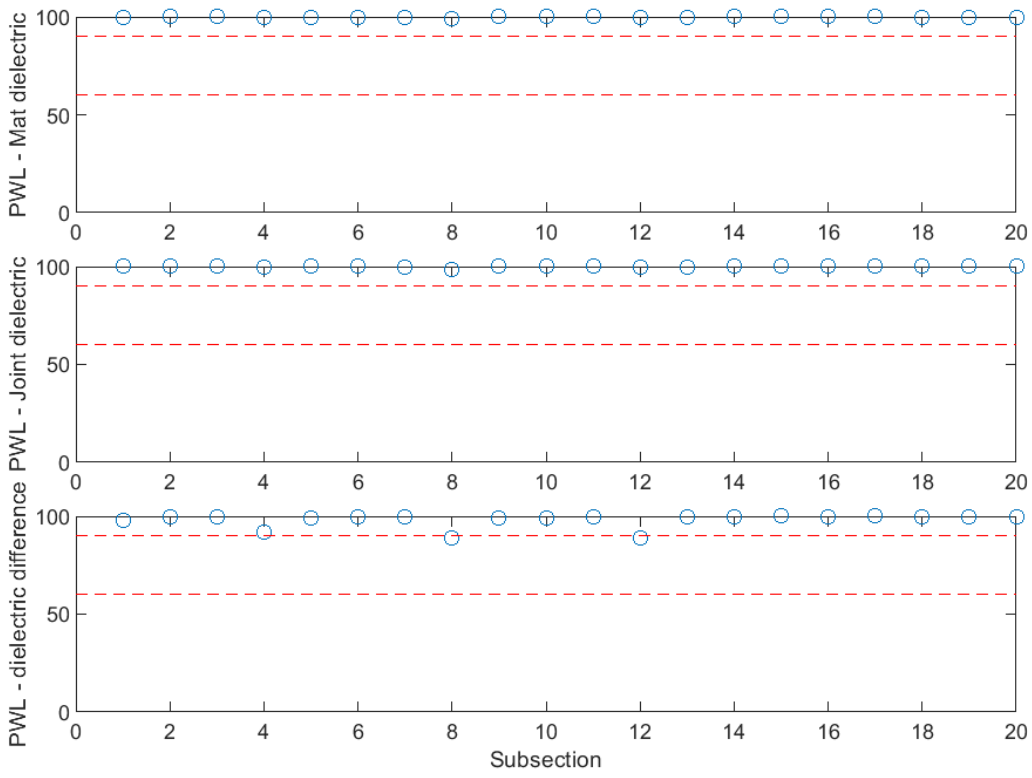

Figure B-257 PWL for dielectric values for confined tapered joint (50 ft subsections) – M-28- Day2-2

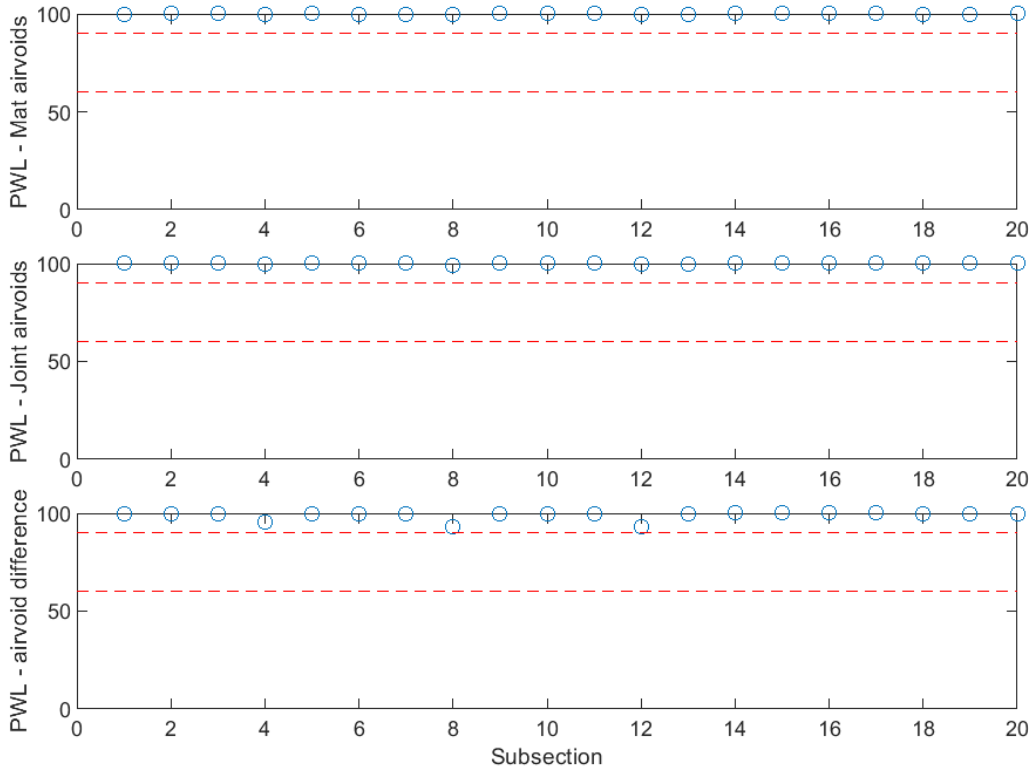

Figure B-258 PWL for air voids for confined tapered joint (50 ft subsections) – M-28- Day2-2

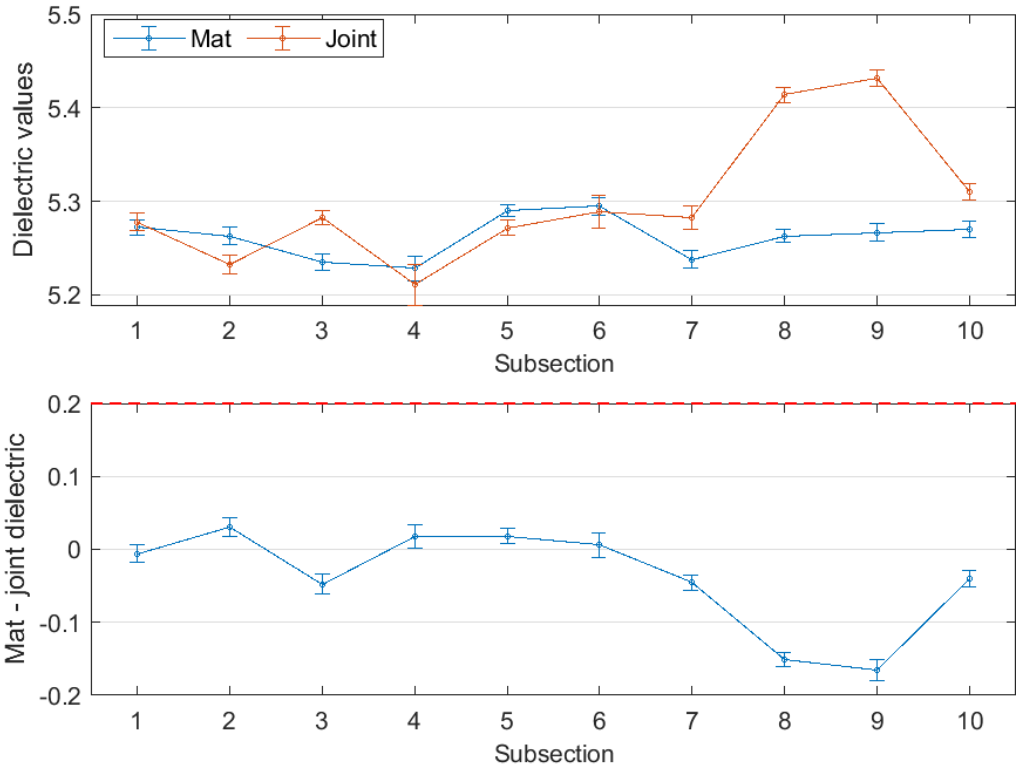

Figure B-259 Interval plot of dielectric values for confined tapered joint (100 ft subsections) – M-28- Day2-2

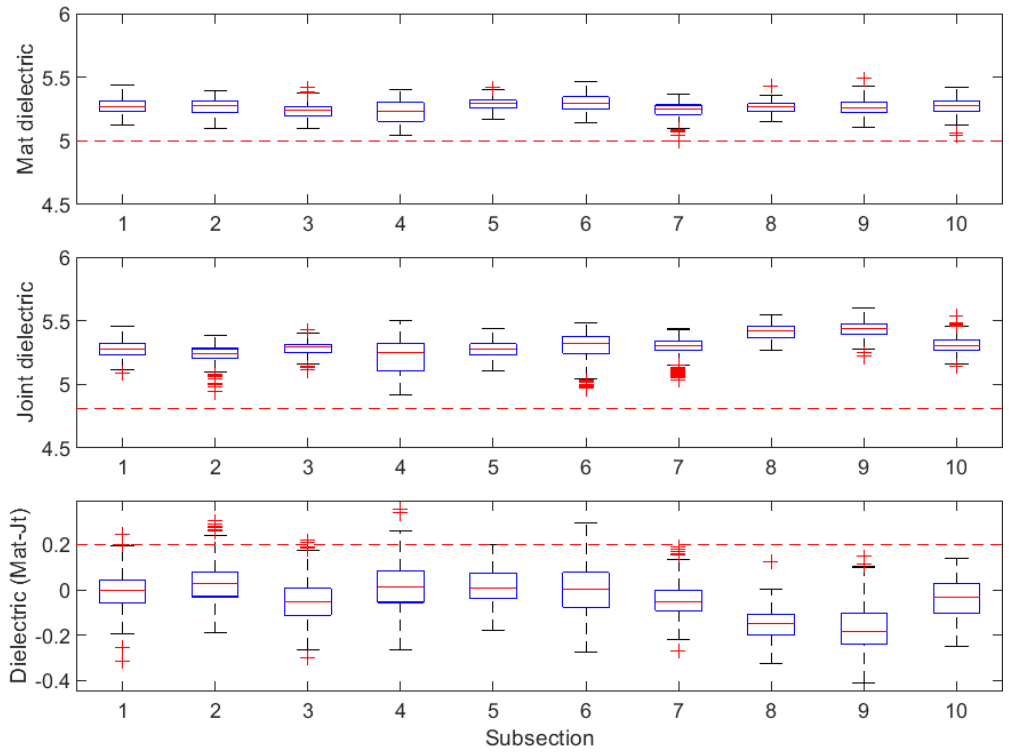

Figure B-260 Box plot of dielectric values for confined tapered joint (100 ft subsections) – M-28- Day2-2

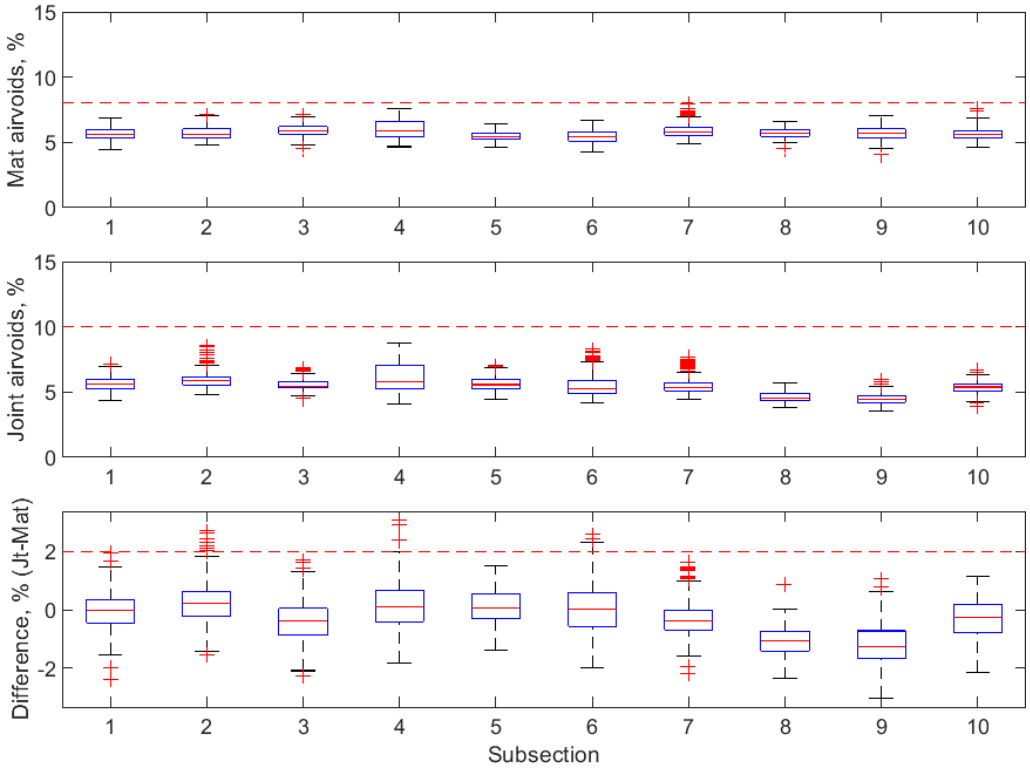

Figure B-261 Box plot of air voids for confined tapered joint (100 ft subsections) – M-28- Day2-2

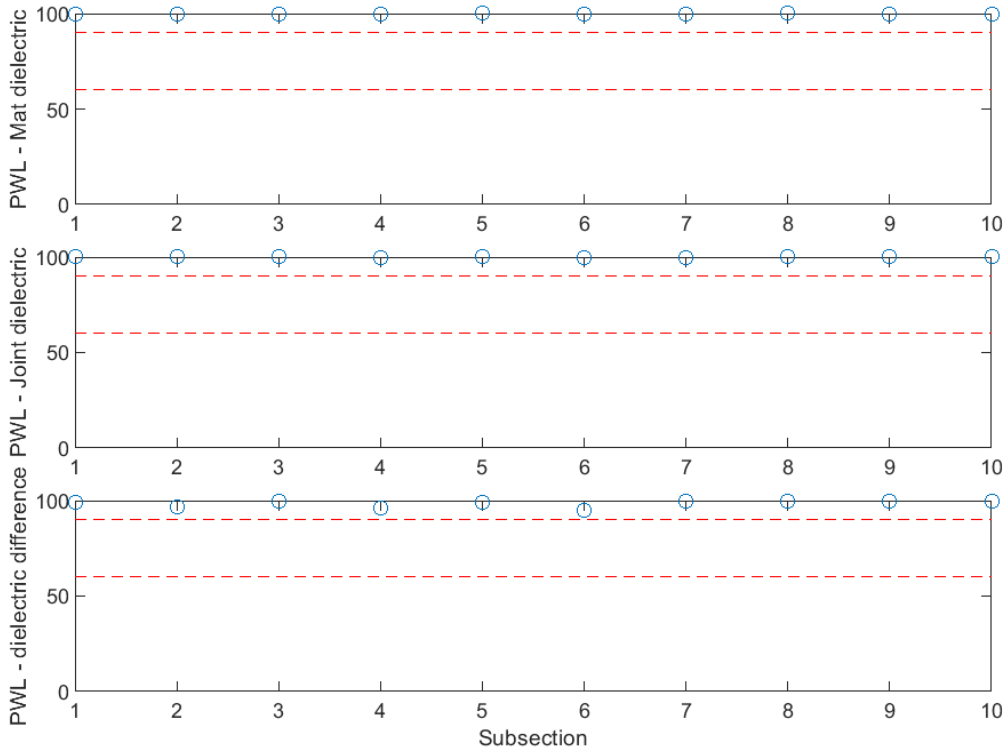

Figure B-262 PWL for dielectric values for confined tapered joint (100 ft subsections) – M-28- Day2-2

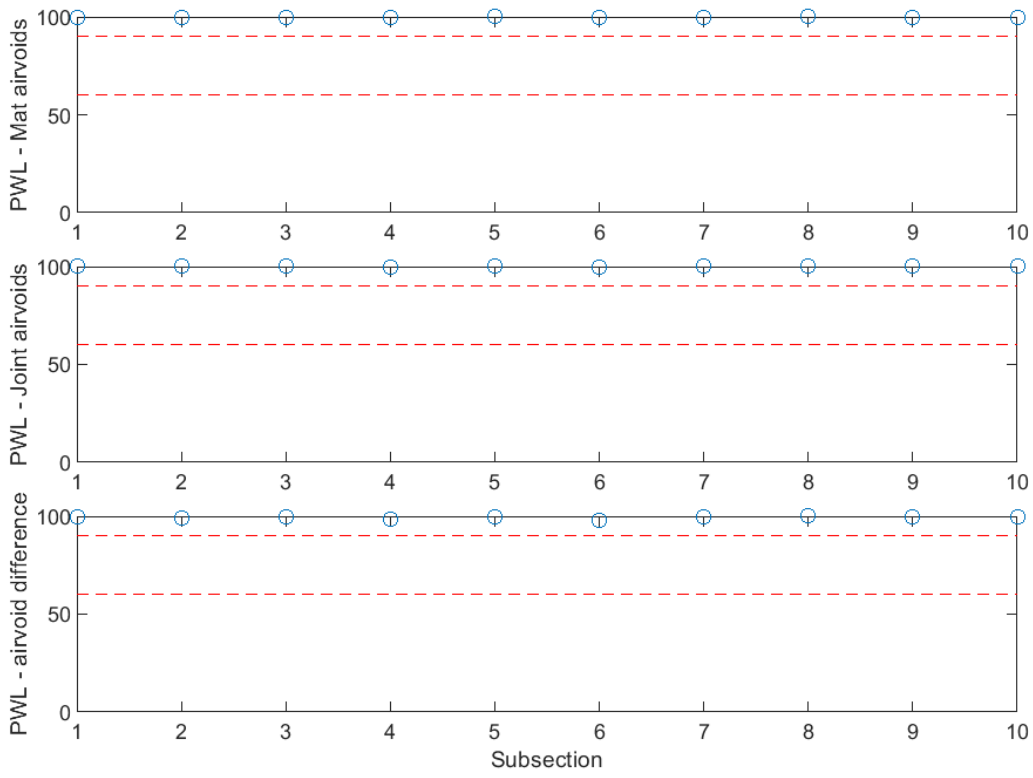

Figure B-263 PWL for air voids for confined tapered joint (100 ft subsections) – M-28- Day2-2

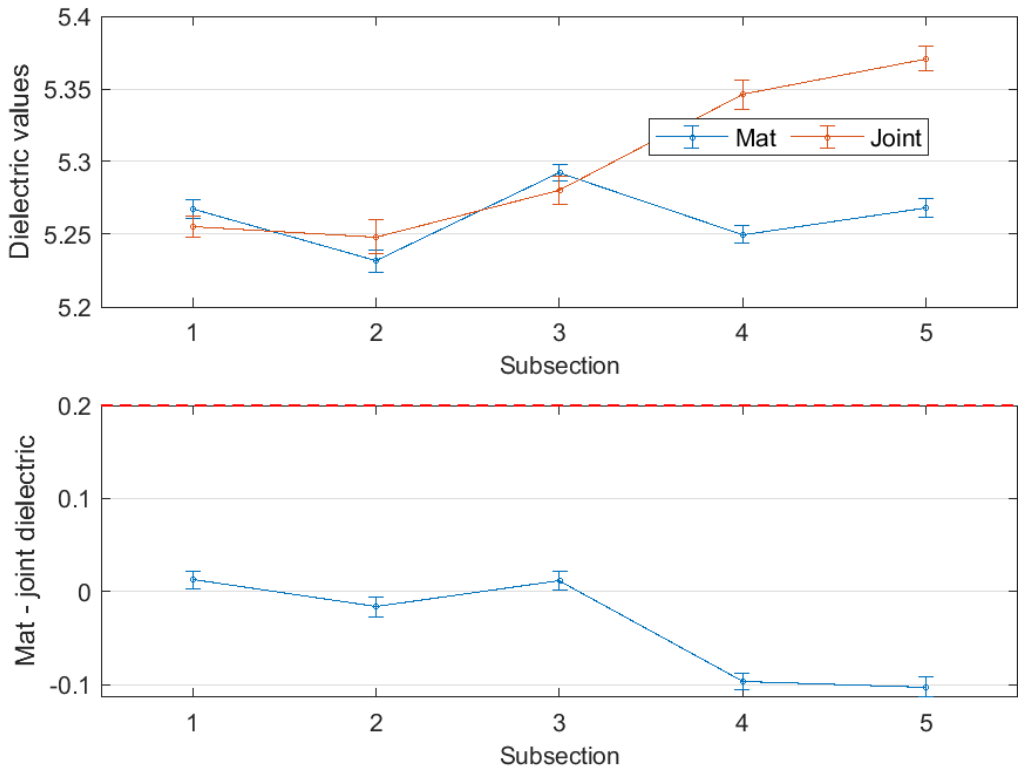

Figure B-264 Interval plot of dielectric values for confined tapered joint (200 ft subsections) – M-28- Day2-2

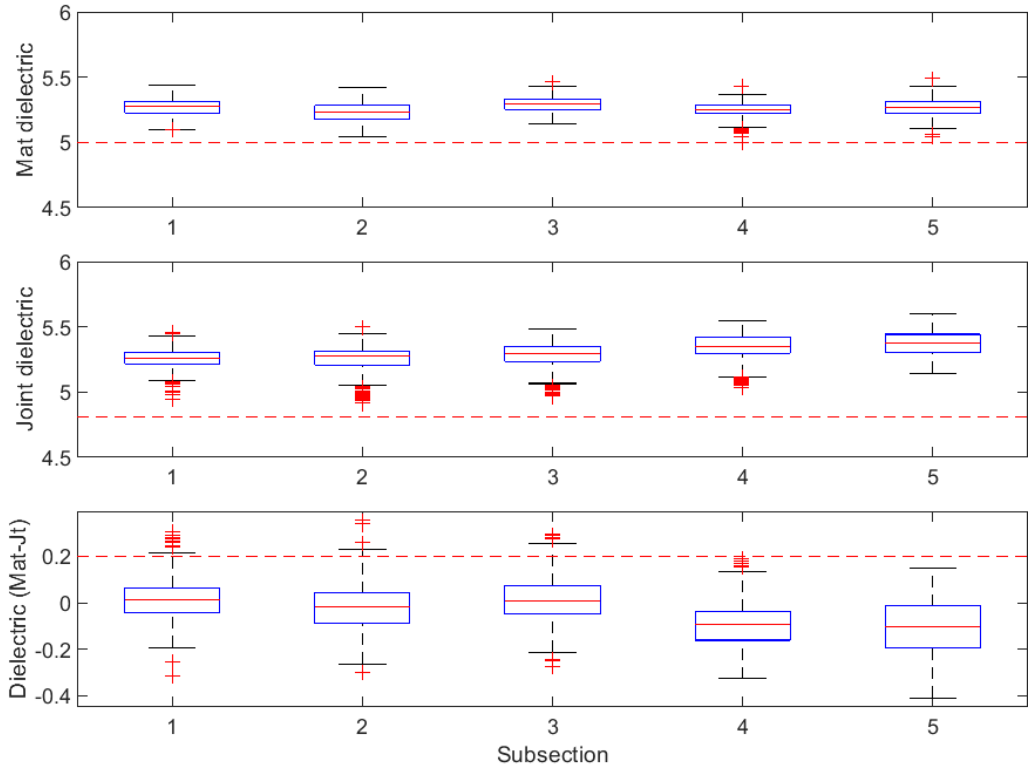

Figure B-265 Box plot of dielectric values for confined tapered joint (200 ft subsections) – M-28- Day2-2

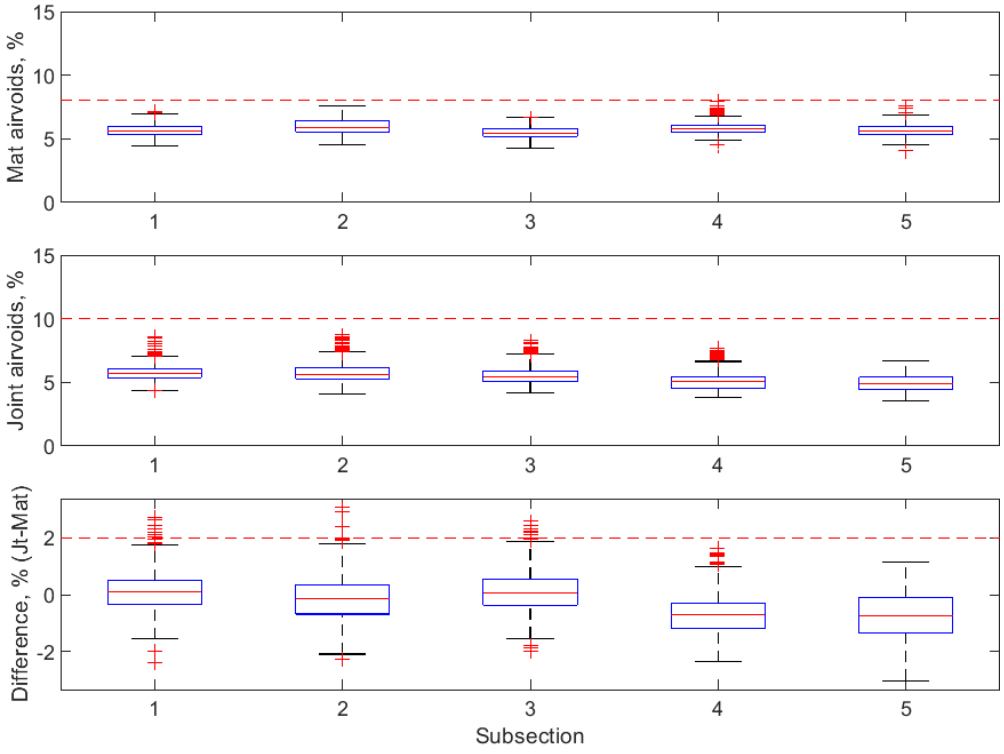

Figure B-266 Box plot of air voids for confined tapered joint (200 ft subsections) – M-28- Day2-2

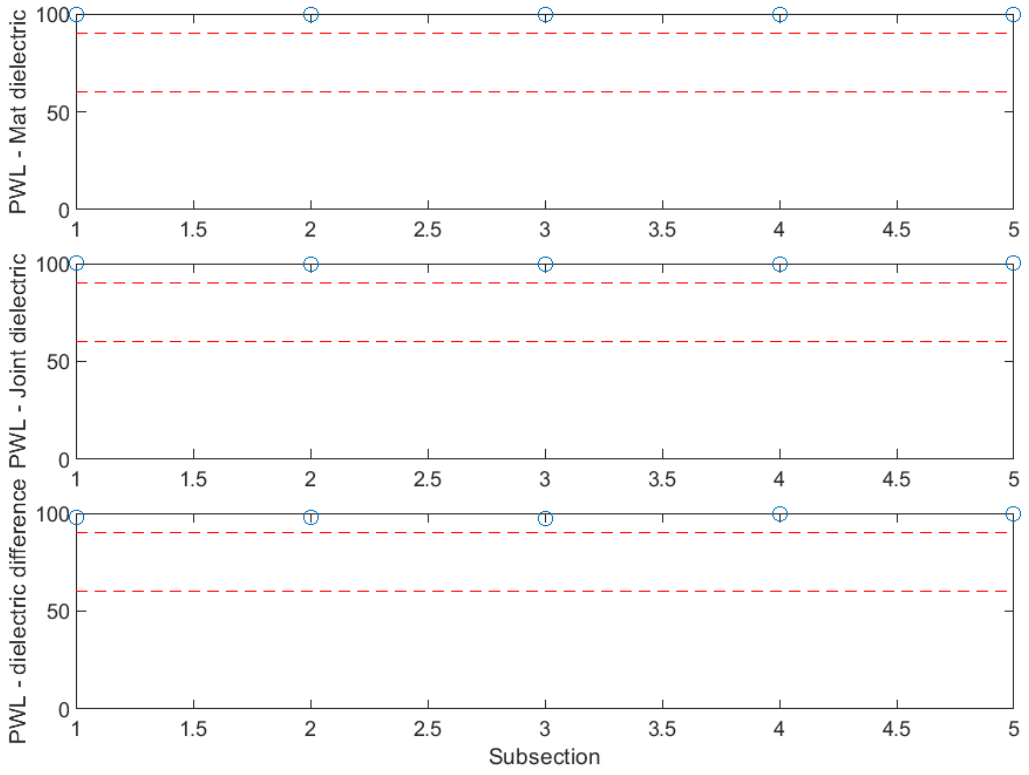

Figure B-267 PWL for dielectric values for confined tapered joint (200 ft subsections) – M-28- Day2-2

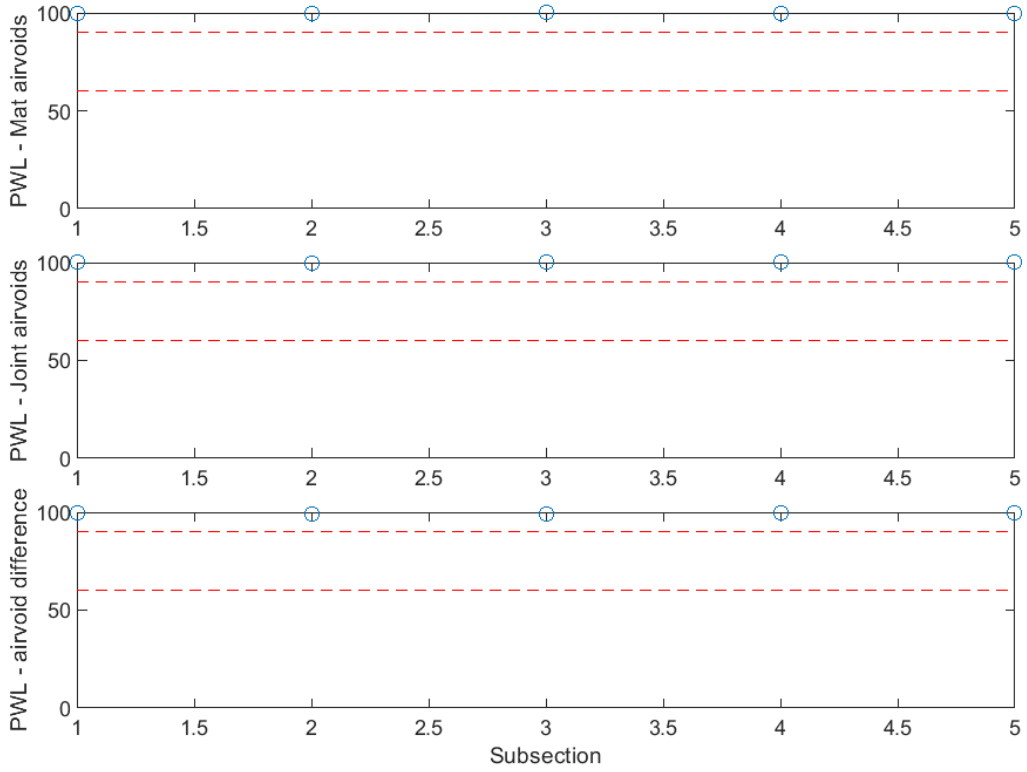

Figure B-268 PWL for air voids for confined tapered joint (200 ft subsections) – M-28- Day2-2

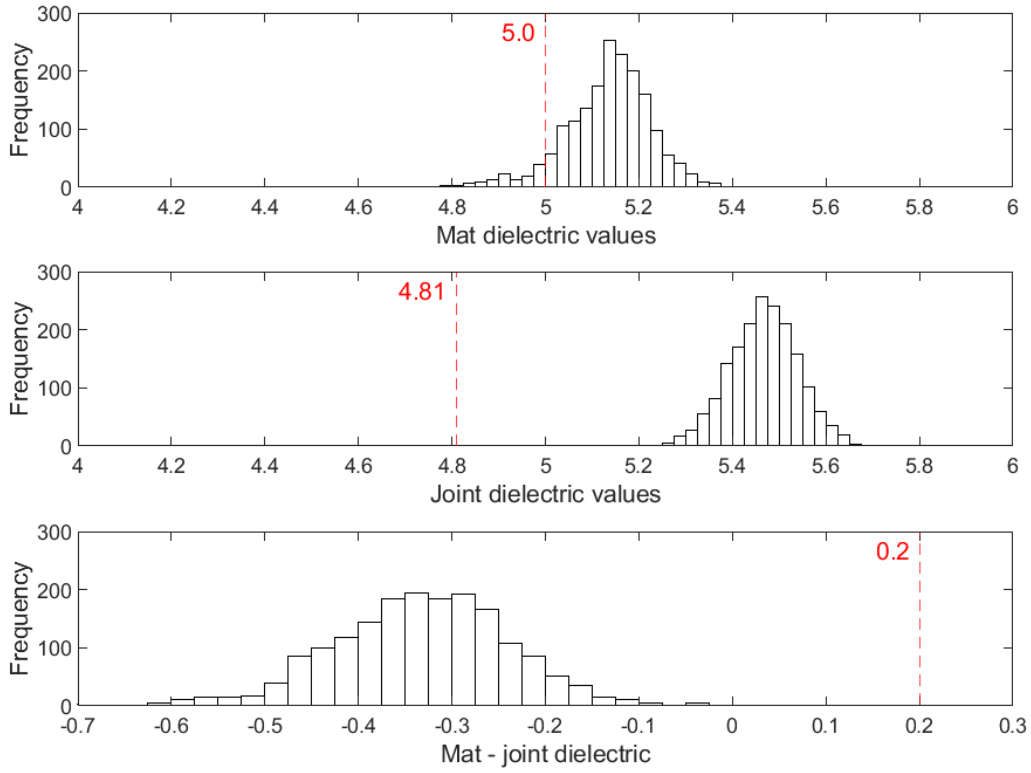

Figure B-269 Histogram of dielectric values for unconfined tapered joint – M-28-Day1-1

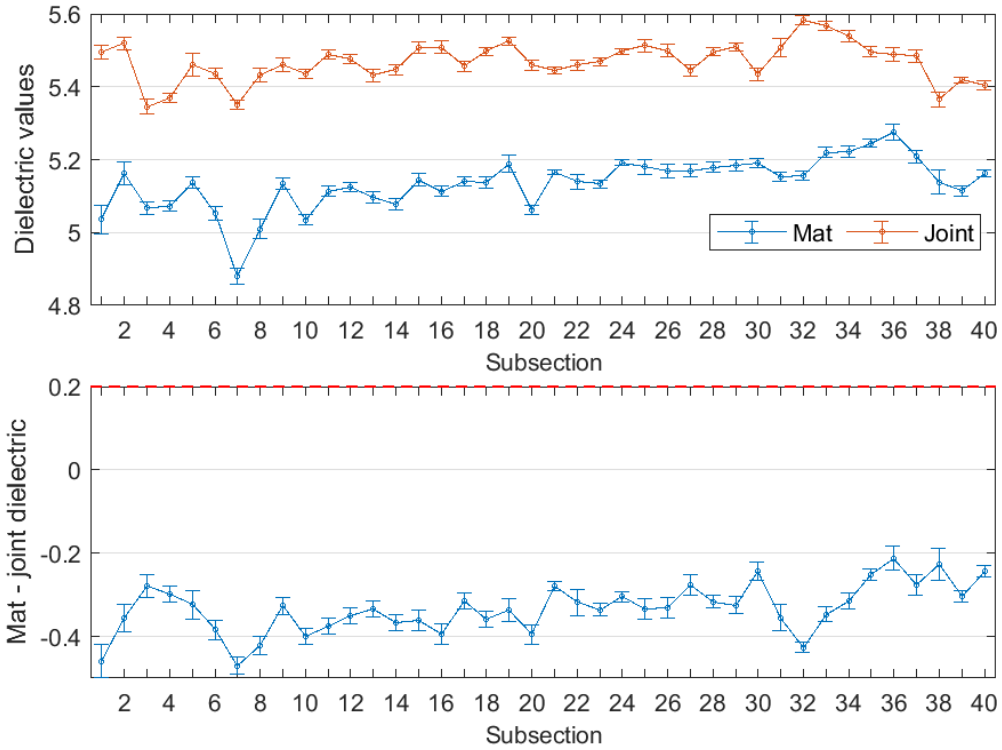

Figure B-270 Interval plot of dielectric values for unconfined tapered joint (25 ft subsections) – M-28-D1-1

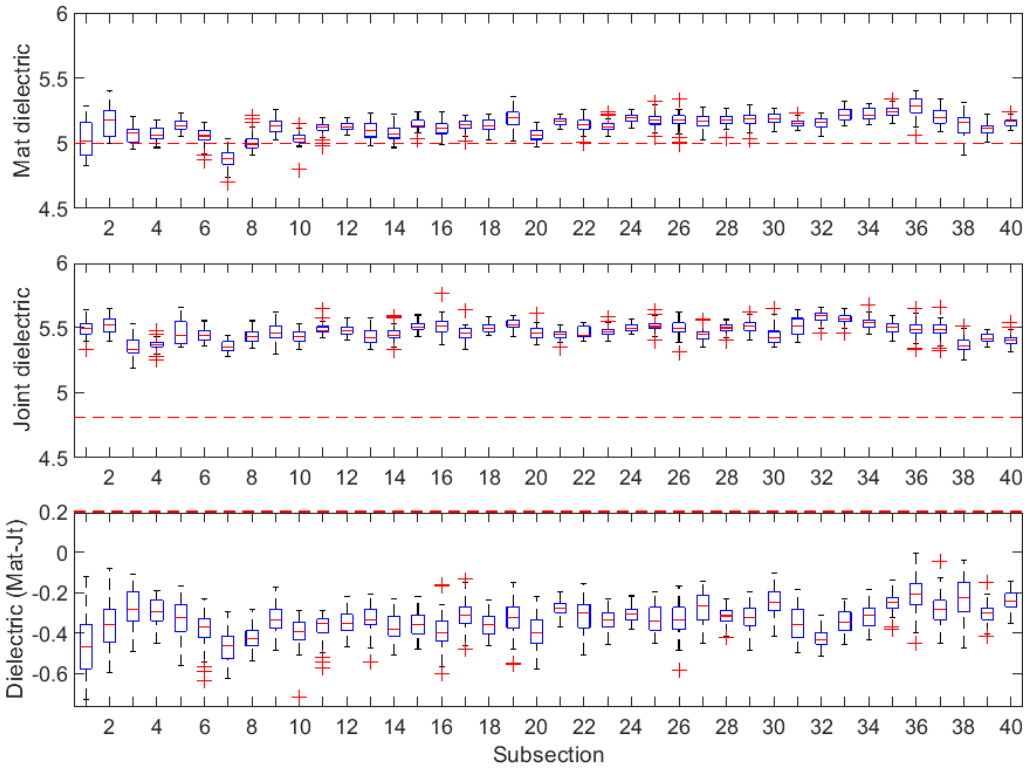

Figure B-271 Box plot of dielectric values for unconfined tapered joint (25 ft subsections) – M-28-D1-1

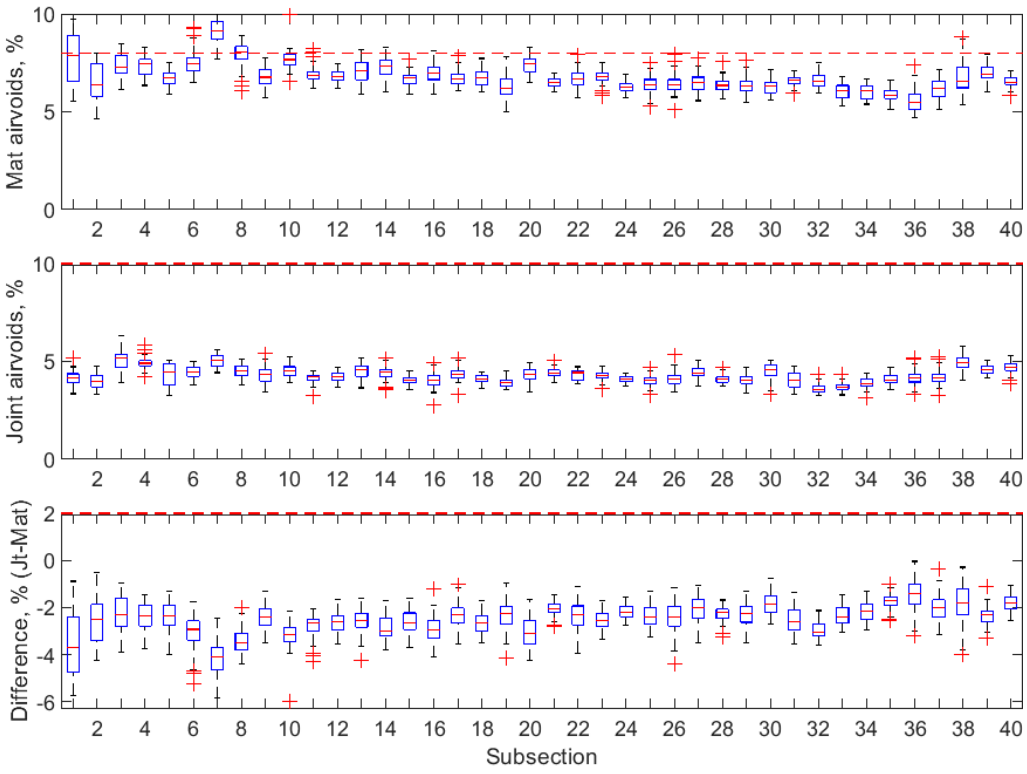

Figure B-272 Box plot of air voids for unconfined tapered joint (25 ft subsections) – M-28-D1-1

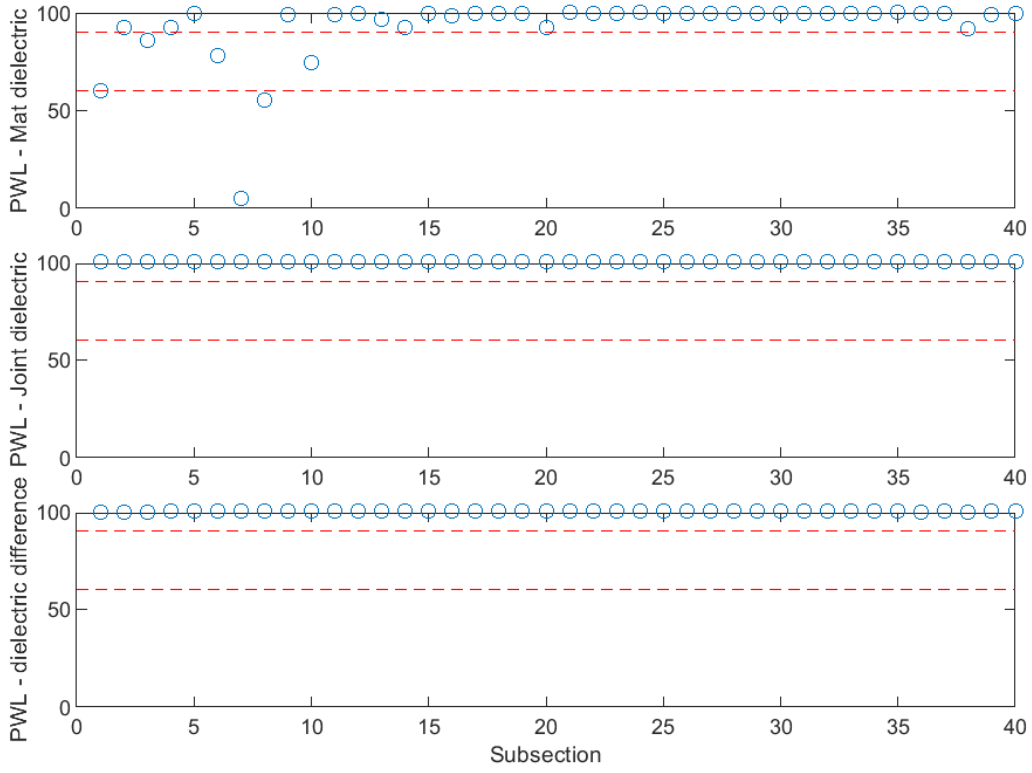

Figure B-273 PWL for dielectric values for unconfined tapered joint (25 ft subsections) – M-28-D1-1

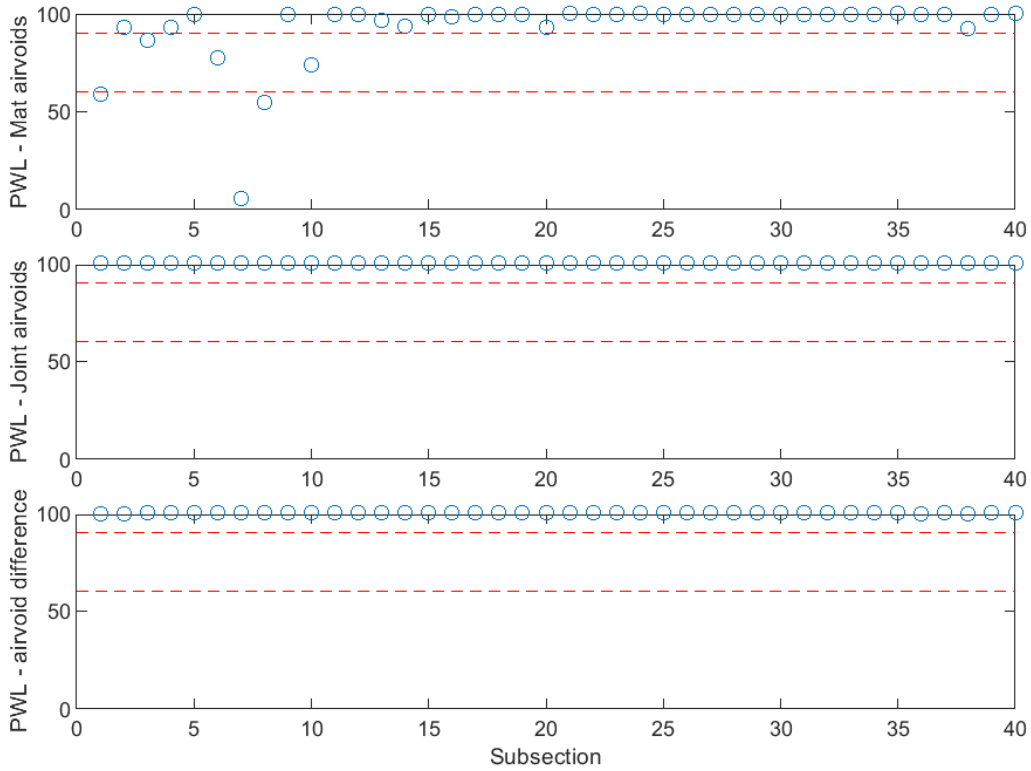

Figure B-274 PWL for air voids for unconfined tapered joint (25 ft subsections) – M-28-D1-1

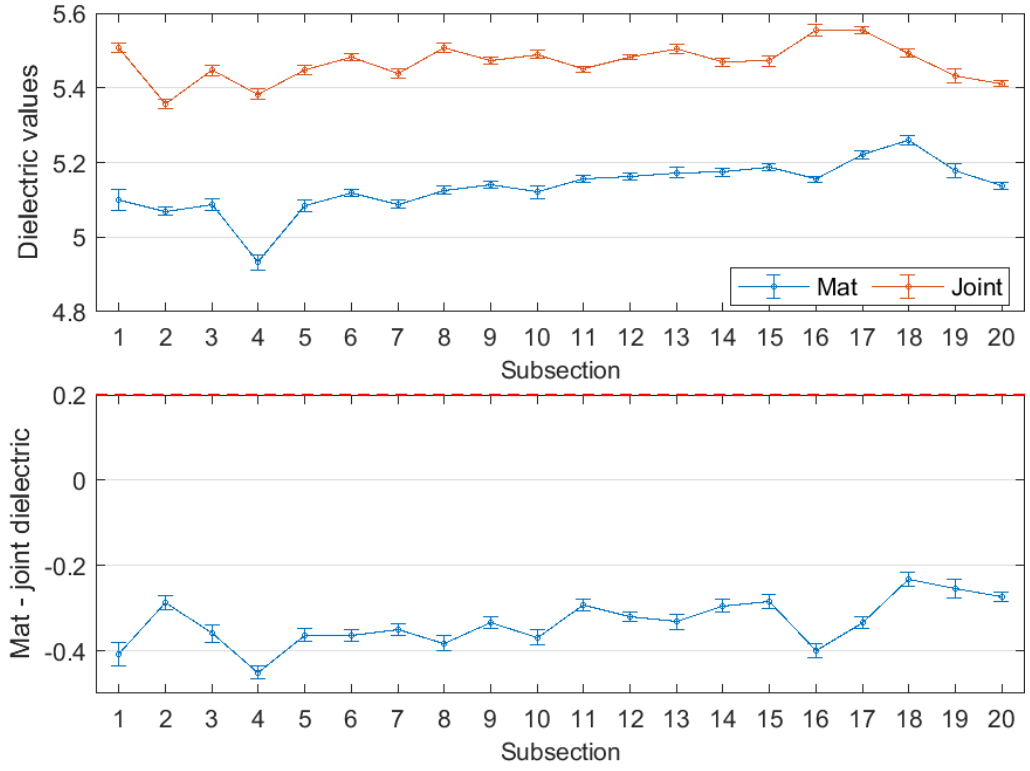

Figure B-275 Interval plot of dielectric values for unconfined tapered joint (50 ft subsections) – M-28-D1-1

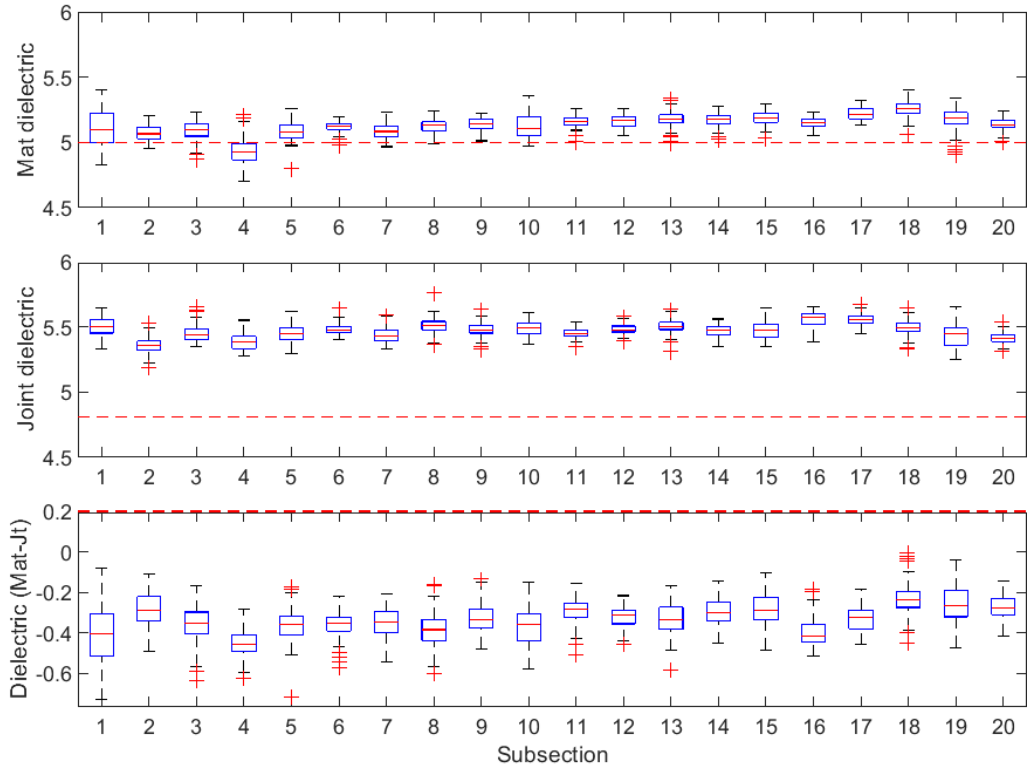

Figure B-276 Box plot of dielectric values for unconfined tapered joint (50 ft subsections) – M-28-D1-1

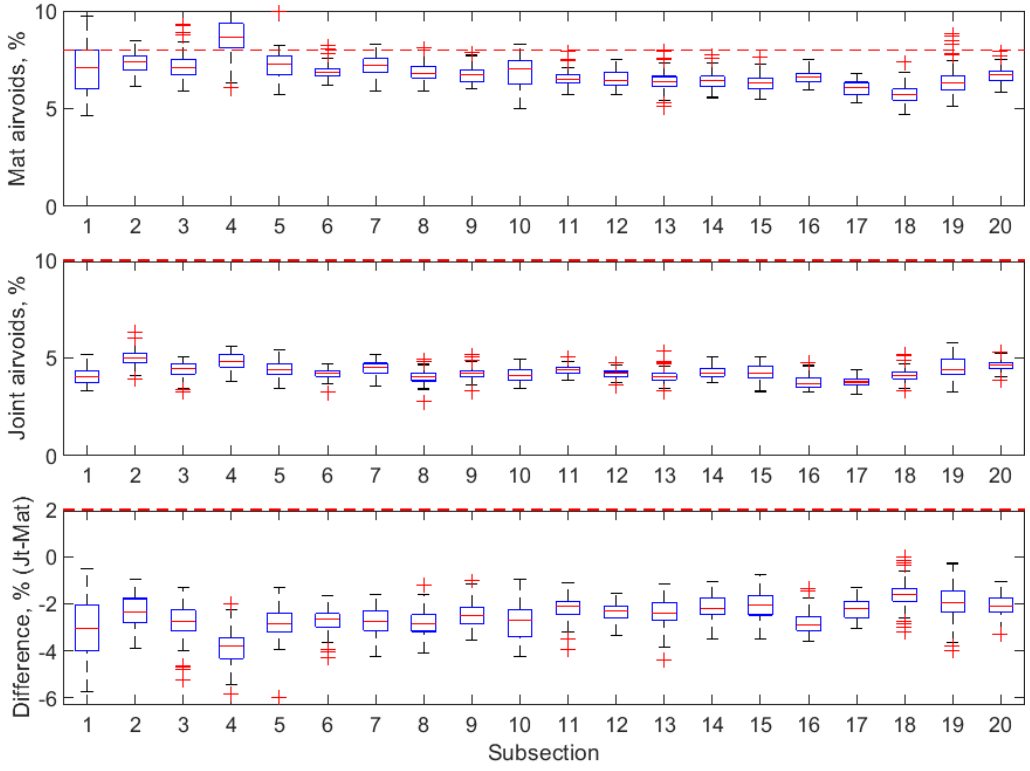

Figure B-277 Box plot of air voids for unconfined tapered joint (50 ft subsections) – M-28-D1-1

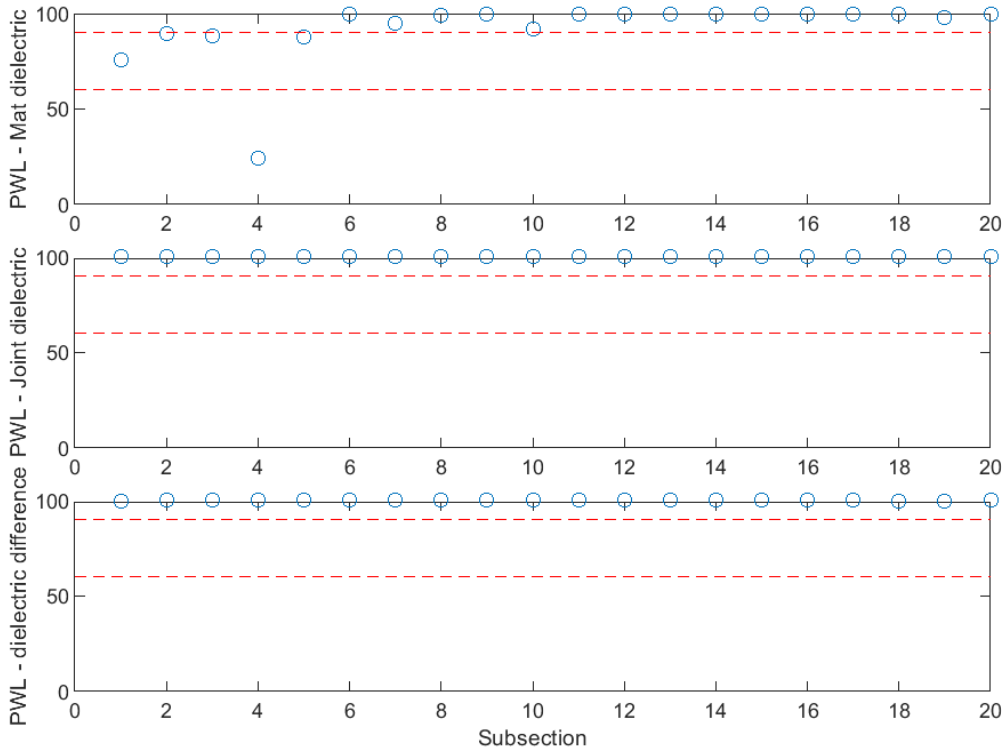

Figure B-278 PWL for dielectric values for unconfined tapered joint (50 ft subsections) – M-28-D1-1

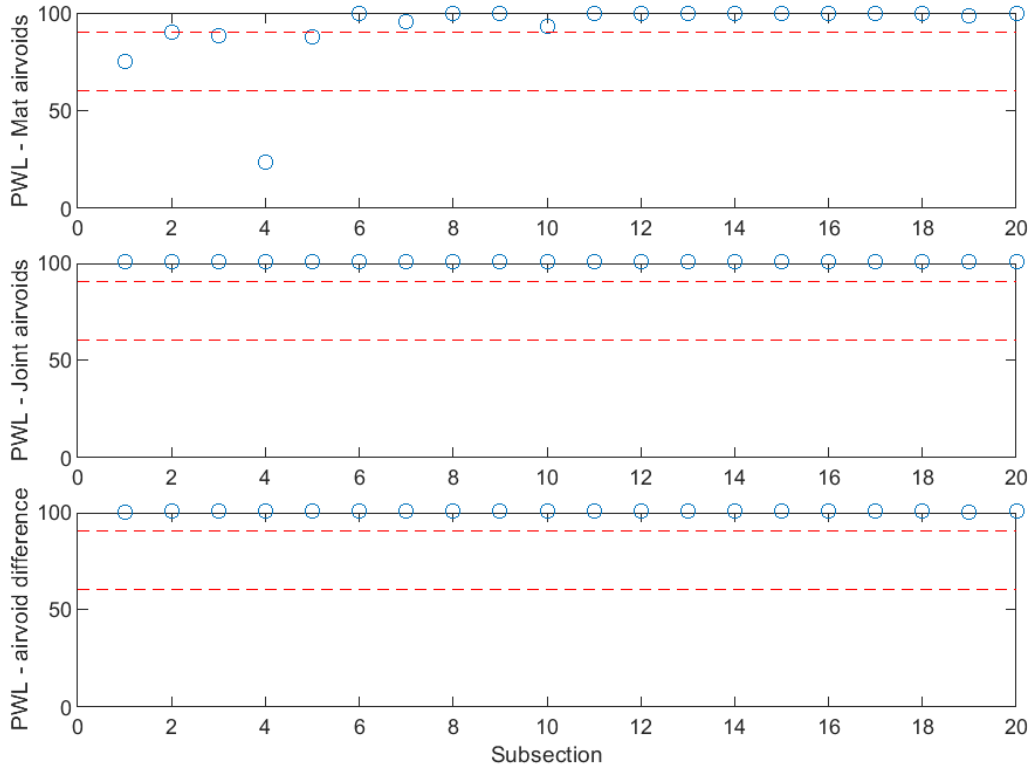

Figure B-279 PWL for air voids for unconfined tapered joint (50 ft subsections) – M-28-D1-1

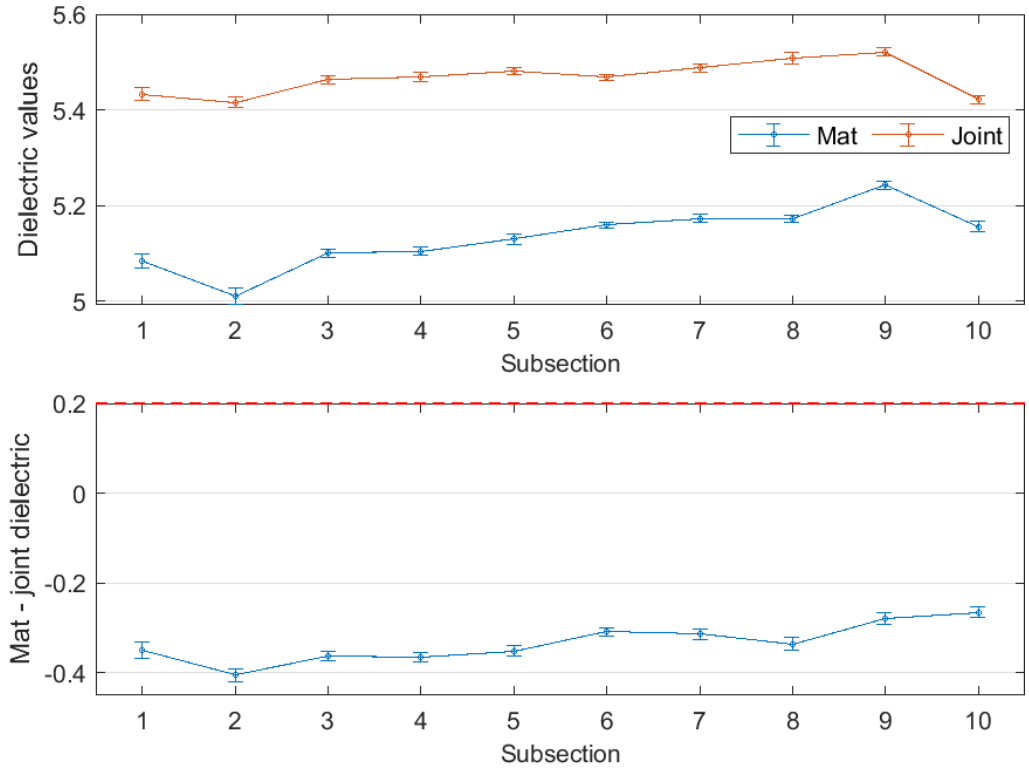

Figure B-280 Interval plot of dielectric values for unconfined tapered joint (100 ft subsections) – M-28-D1-1

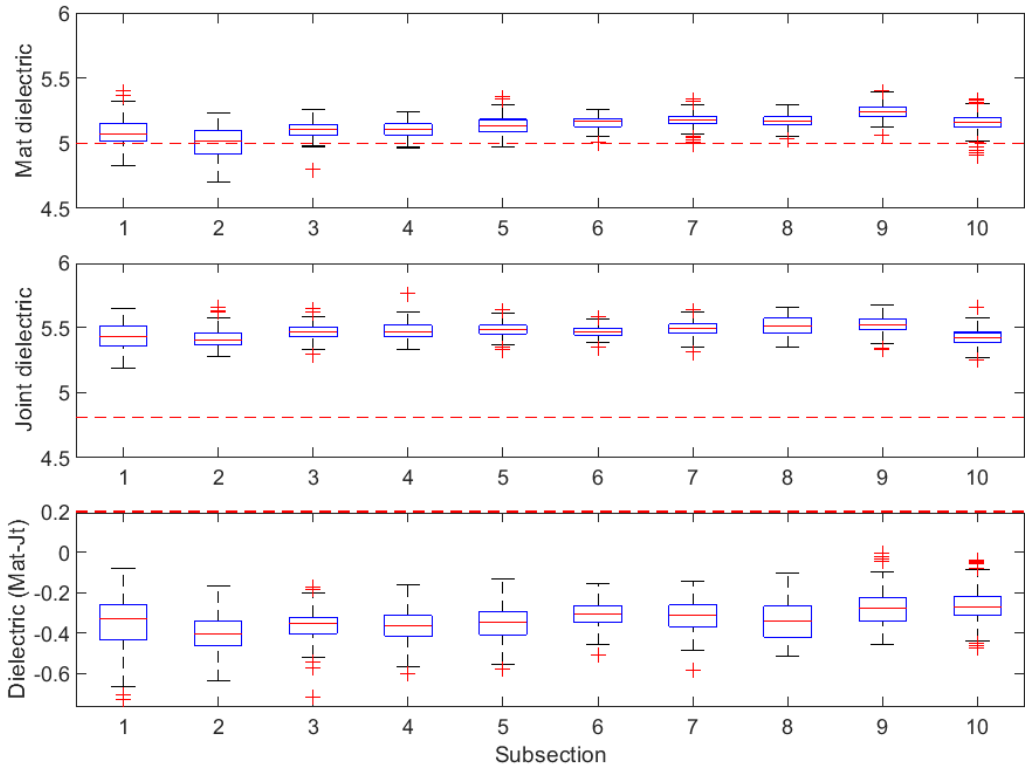

Figure B-281 Box plot of dielectric values for unconfined tapered joint (100 ft subsections) – M-28-D1-1

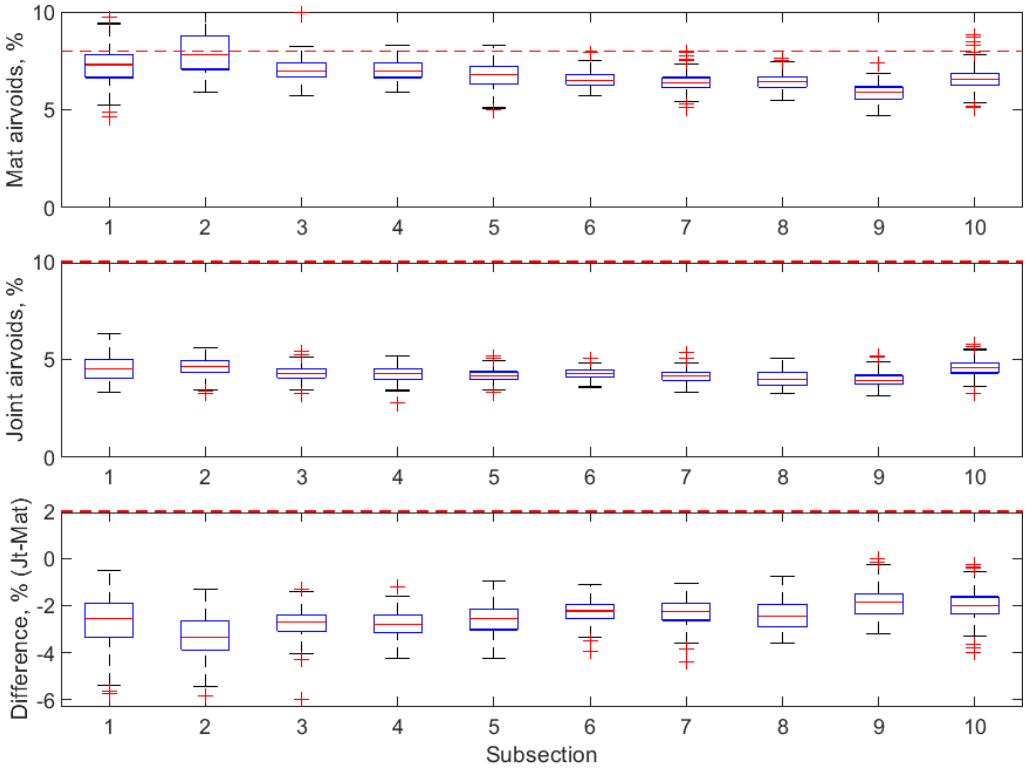

Figure B-282 Box plot of air voids for unconfined tapered joint (100 ft subsections) – M-28-D1-1

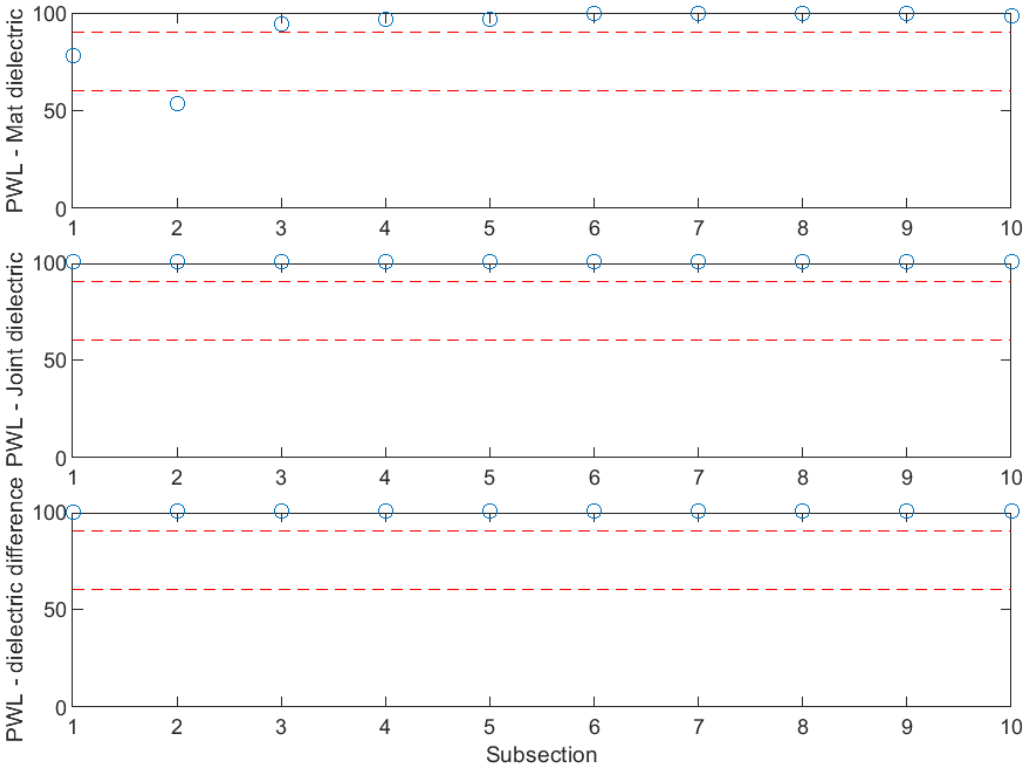

Figure B-283 PWL for dielectric values for unconfined tapered joint (100 ft subsections) – M-28-D1-1

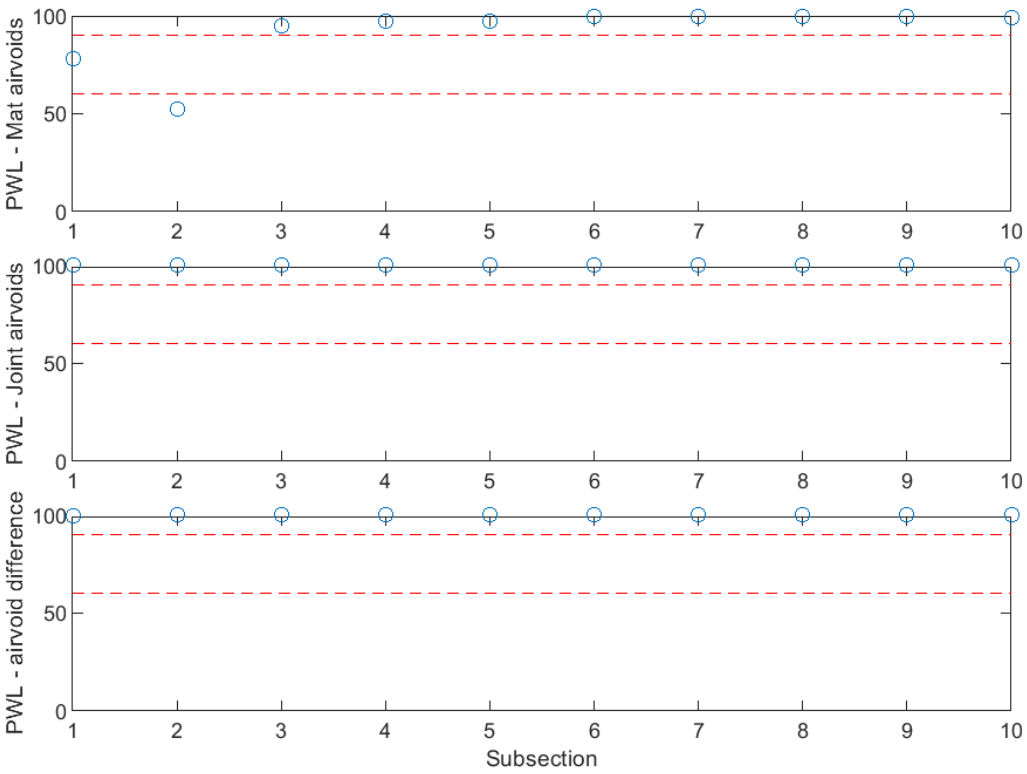

Figure B-284 PWL for air voids for unconfined tapered joint (100 ft subsections) – M-28-D1-1

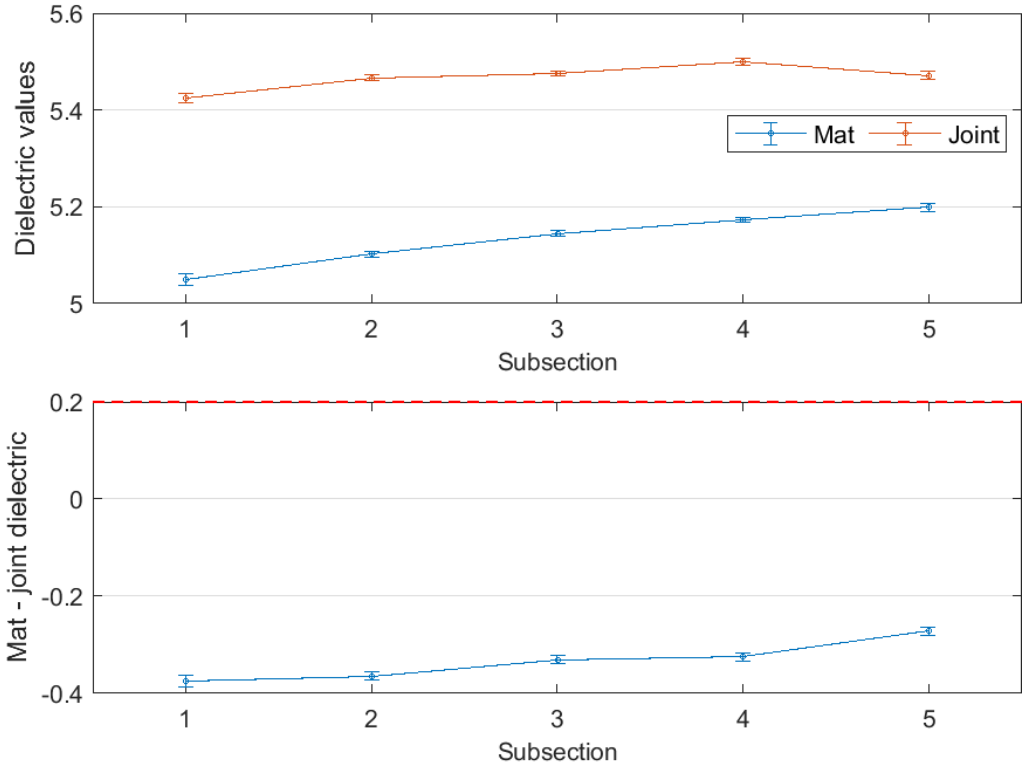

Figure B-285 Interval plot of dielectric values for unconfined tapered joint (200 ft subsections) – M-28-D1-1

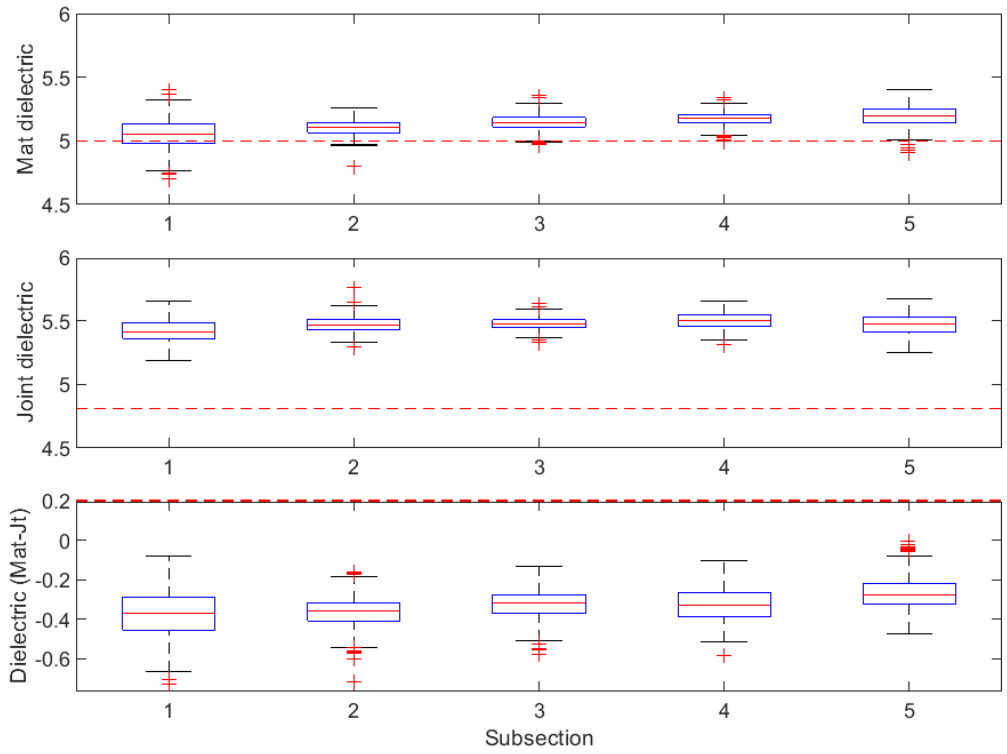

Figure B-286 Box plot of dielectric values for unconfined tapered joint (200 ft subsections) – M-28-D1-1

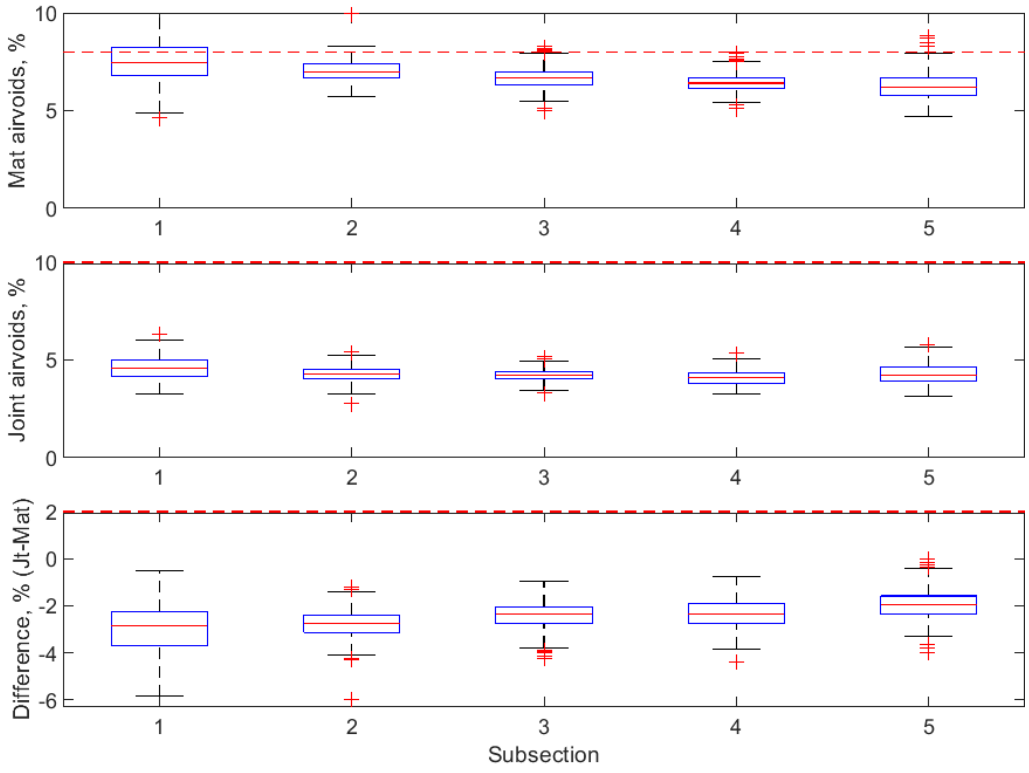

Figure B-287 Box plot of air voids for unconfined tapered joint (200 ft subsections) – M-28-D1-1

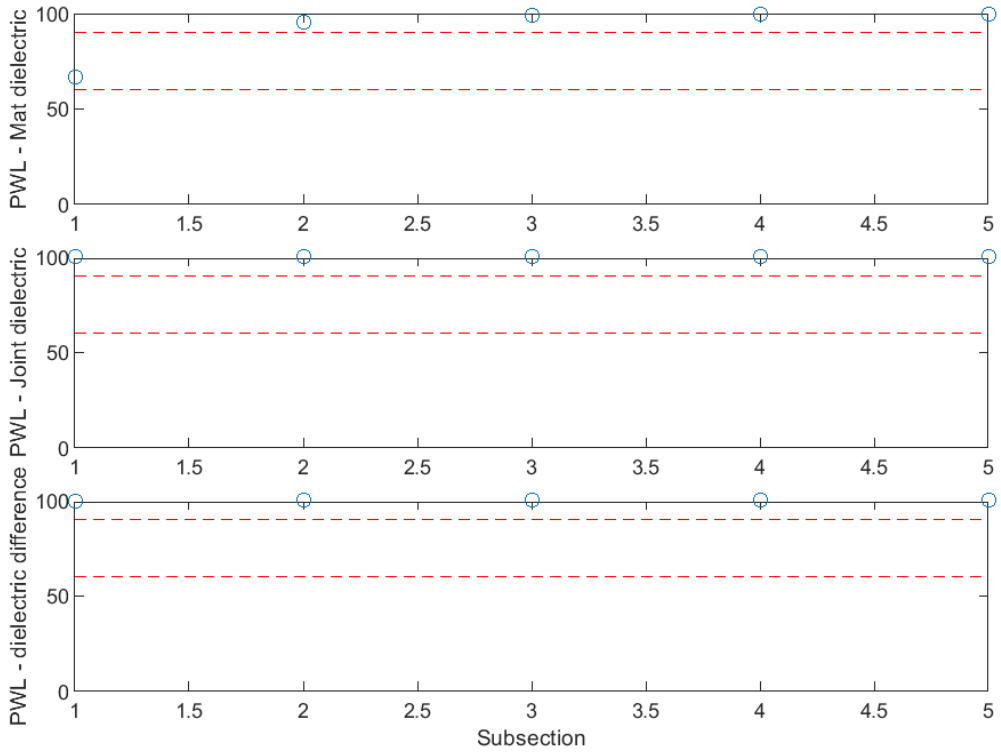

Figure B-288 PWL for dielectric values for unconfined tapered joint (200 ft subsections) – M-28-D1-1

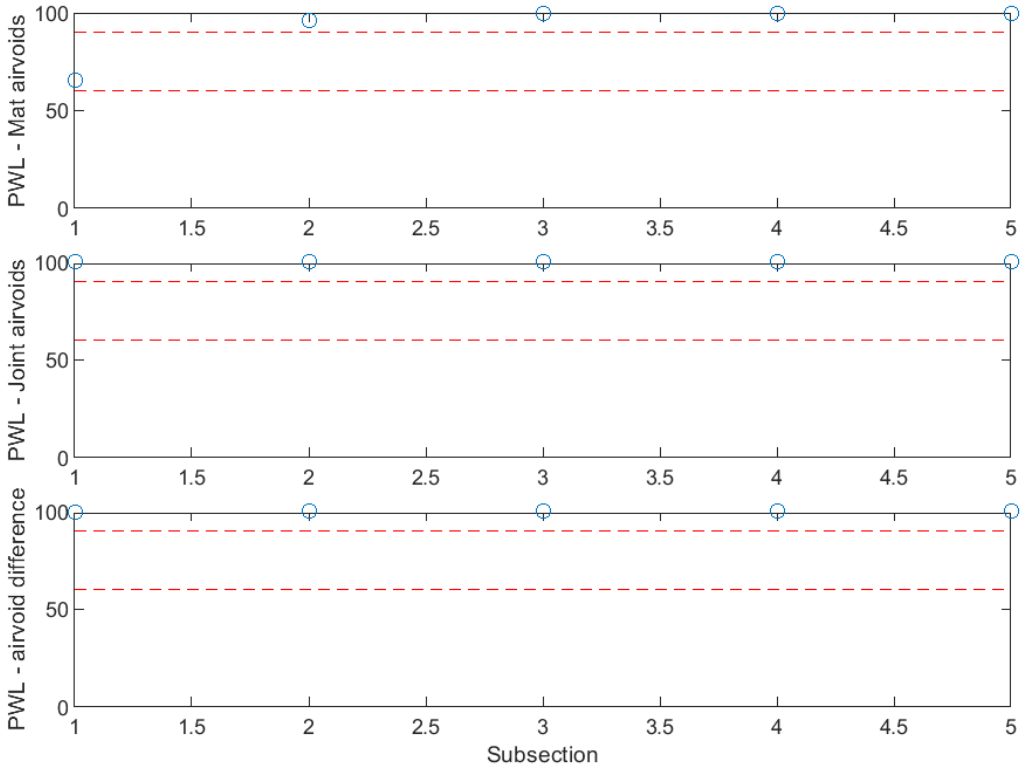

Figure B-289 PWL for air voids for unconfined tapered joint (200 ft subsections) – M-28-D1-1

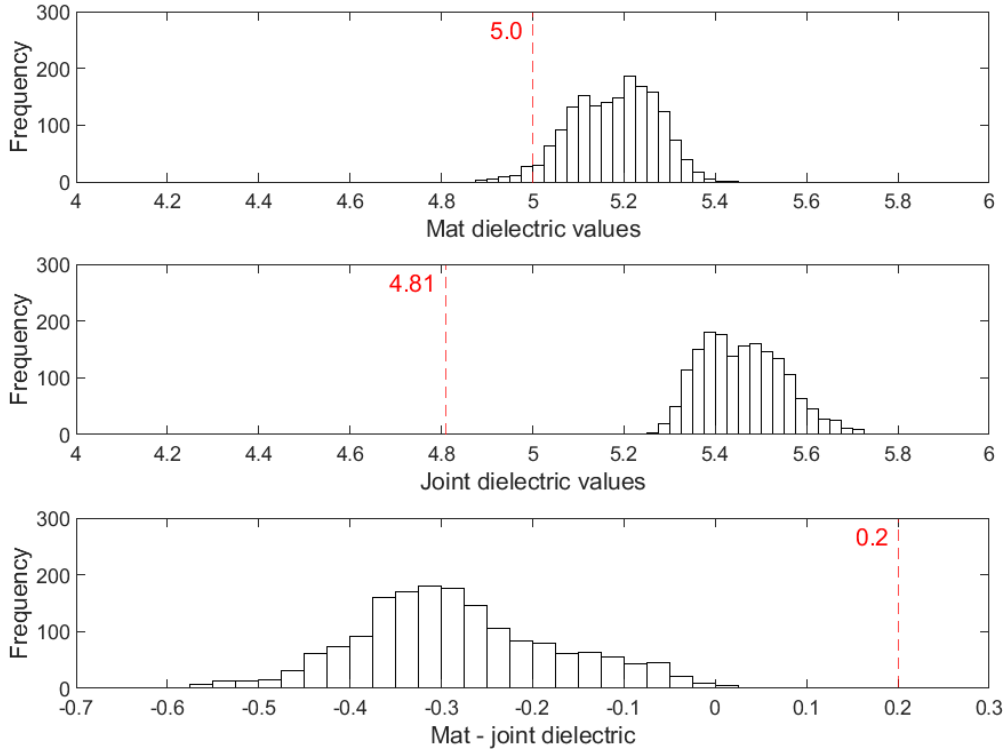

Figure B-290 Histogram of dielectric values for unconfined tapered joint – M-28-Day1-2

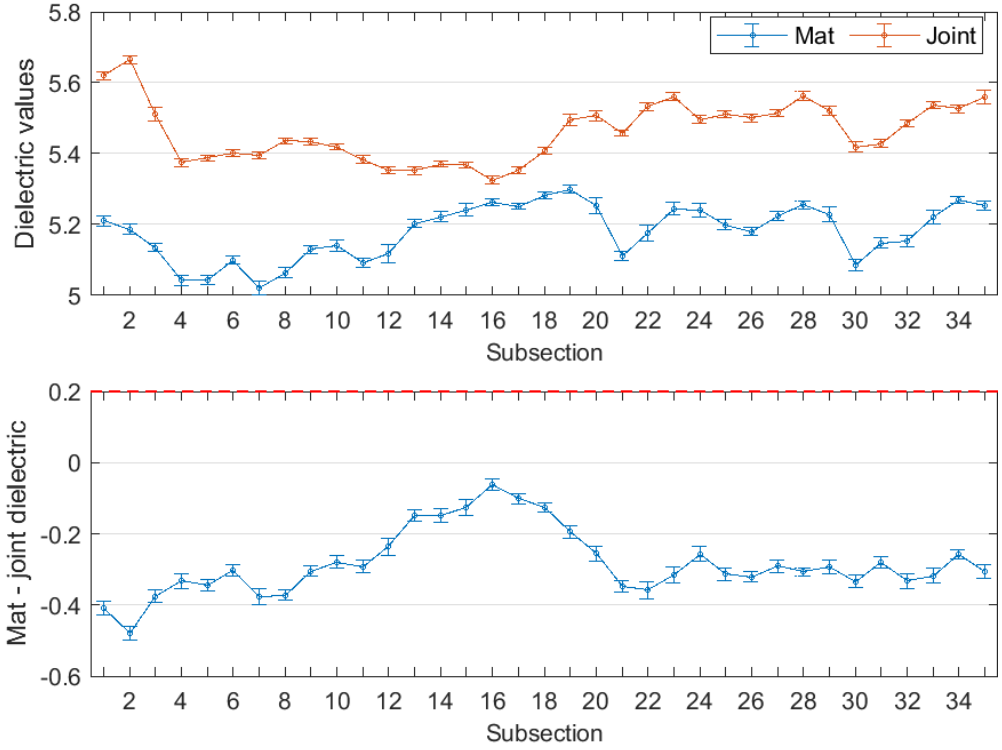

Figure B-291 Interval plot of dielectric values for unconfined tapered joint (25 ft subsections) – M-28-D1-2

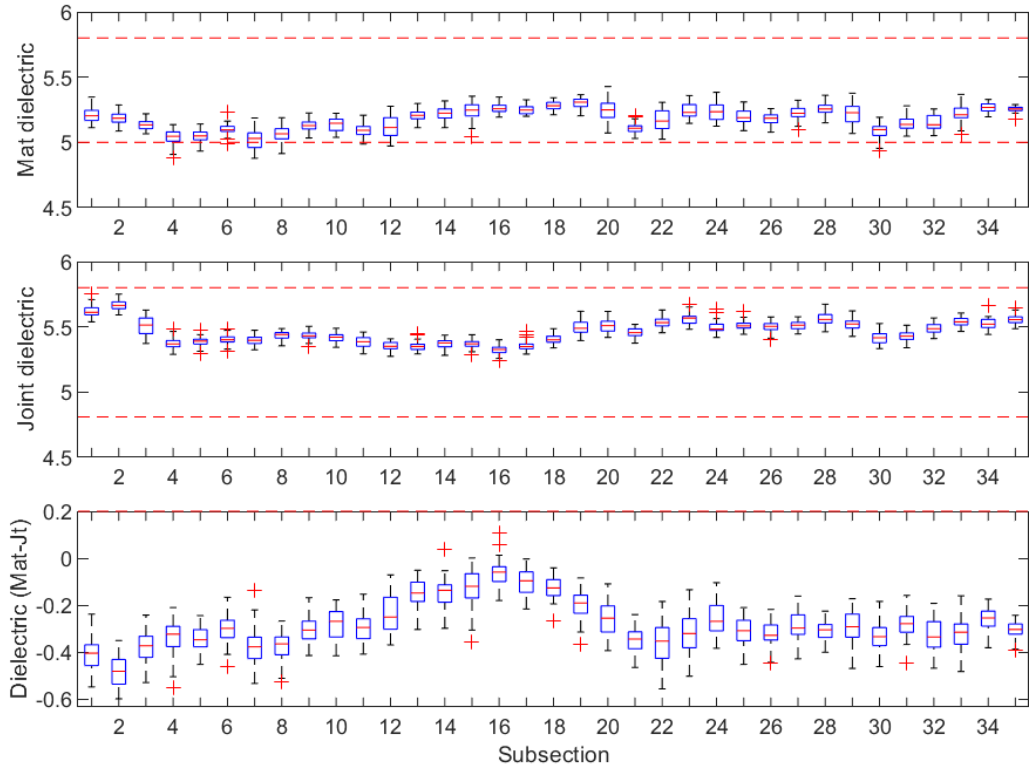

Figure B-292 Box plot of dielectric values for unconfined tapered joint (25 ft subsections) – M-28-D1-2

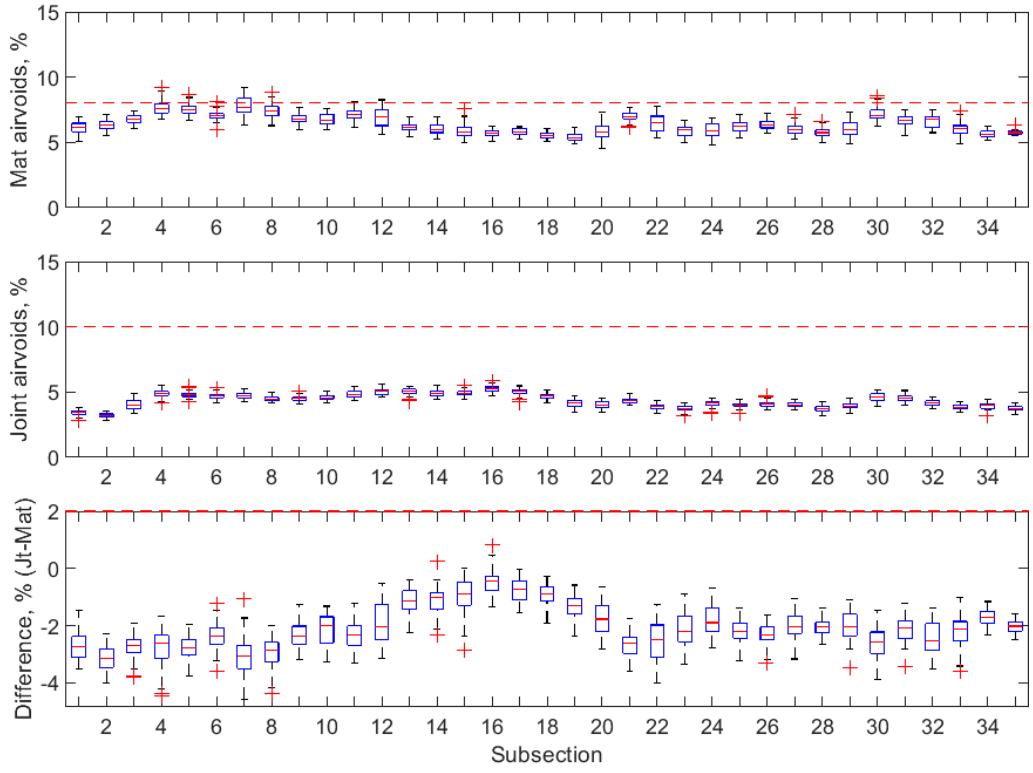

Figure B-293 Box plot of air voids for unconfined tapered joint (25 ft subsections) – M-28-D1-2

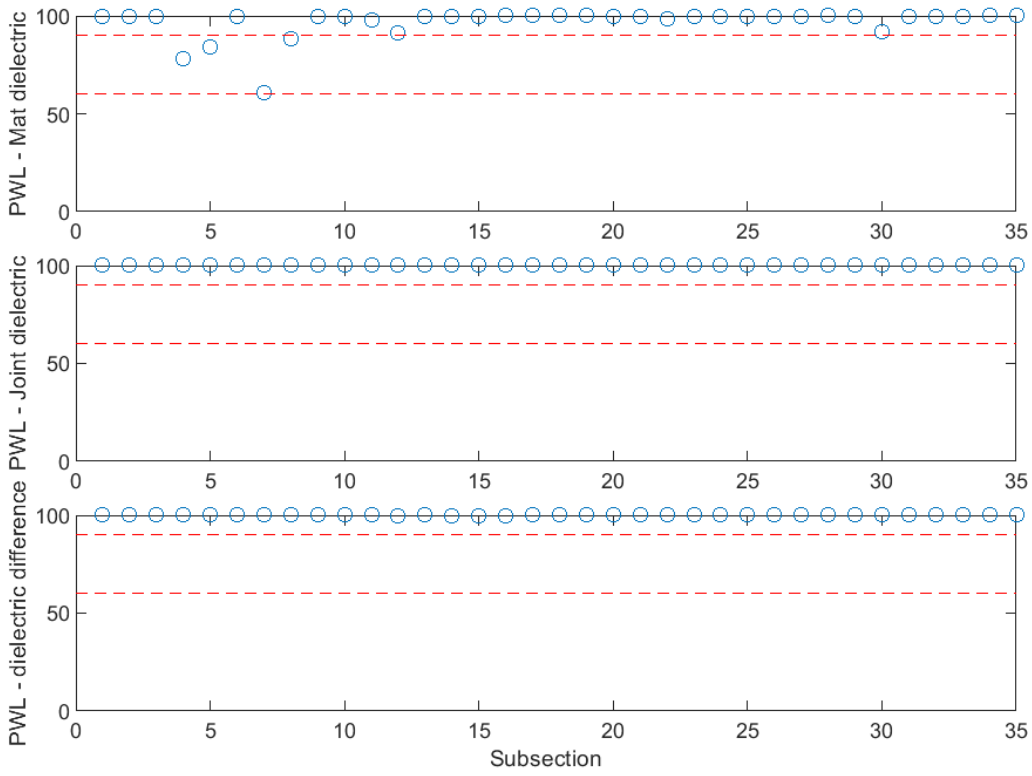

Figure B-294 PWL for dielectric values for unconfined tapered joint (25 ft subsections) – M-28-D1-2

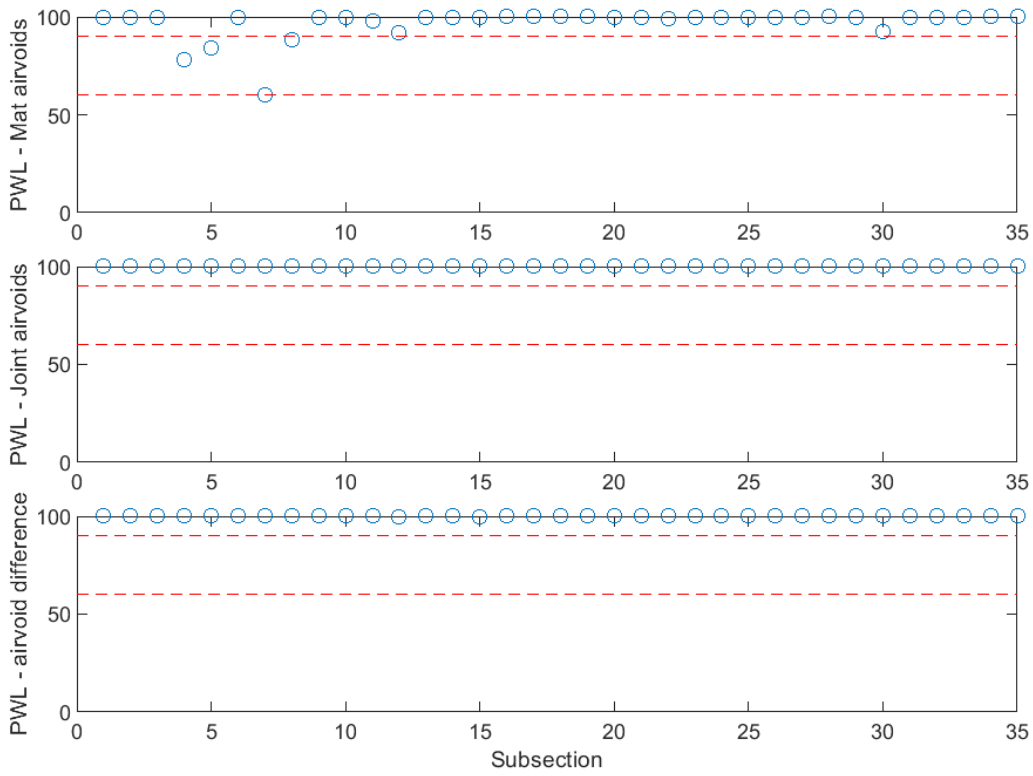

Figure B-295 PWL for air voids for unconfined tapered joint (25 ft subsections) – M-28-D1-2

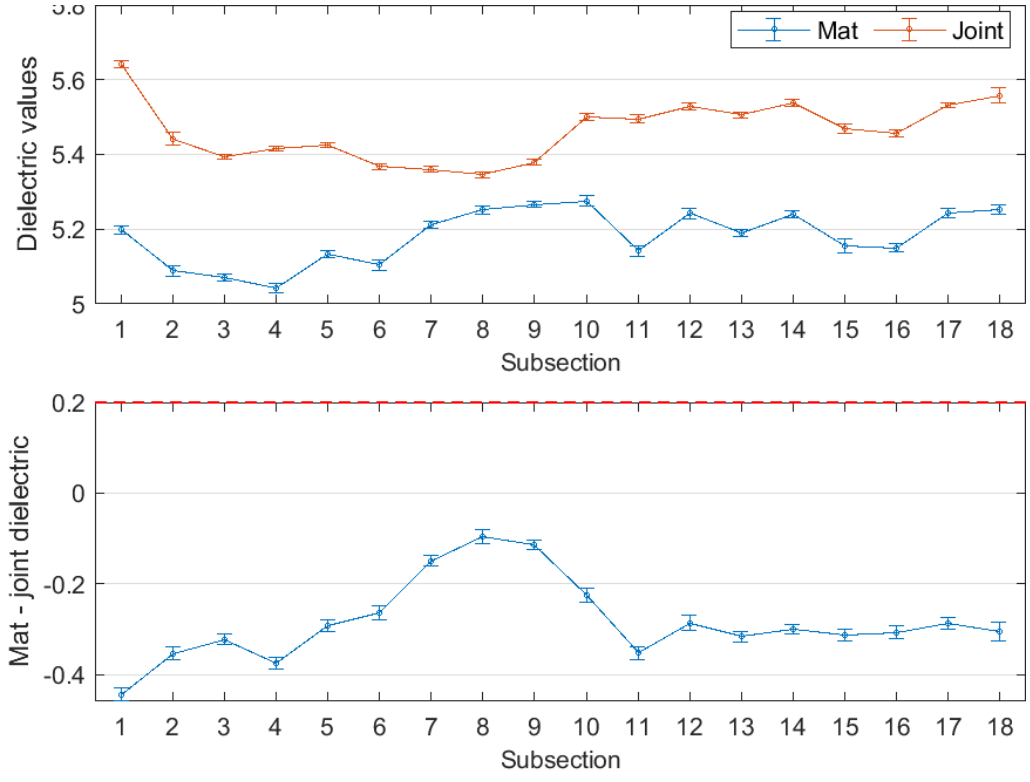

Figure B-296 Interval plot of dielectric values for unconfined tapered joint (50 ft subsections) – M-28-D1-2

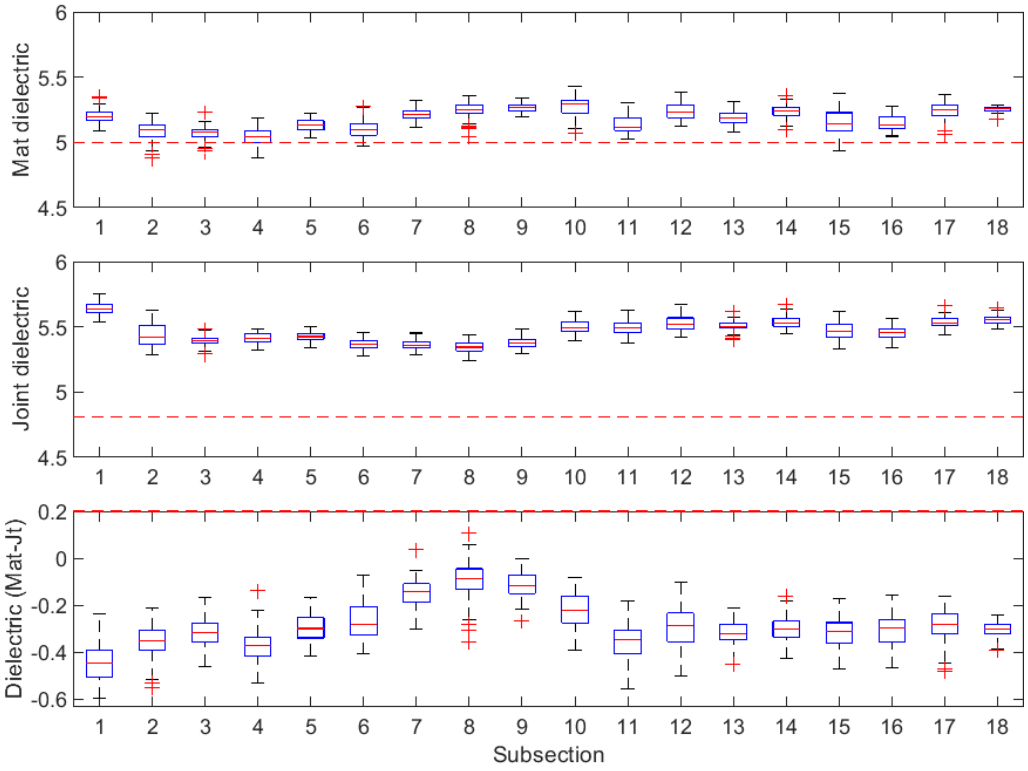

Figure B-297 Box plot of dielectric values for unconfined tapered joint (50 ft subsections) – M-28-D1-2

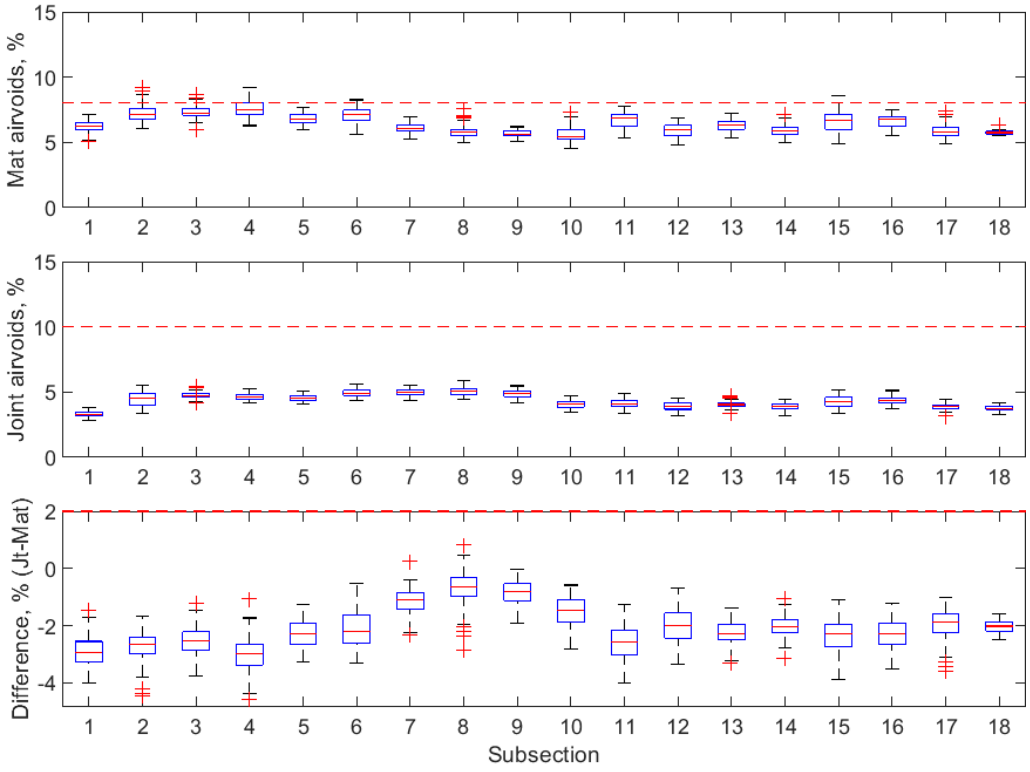

Figure B-298 Box plot of air voids for unconfined tapered joint (50 ft subsections) – M-28-D1-2

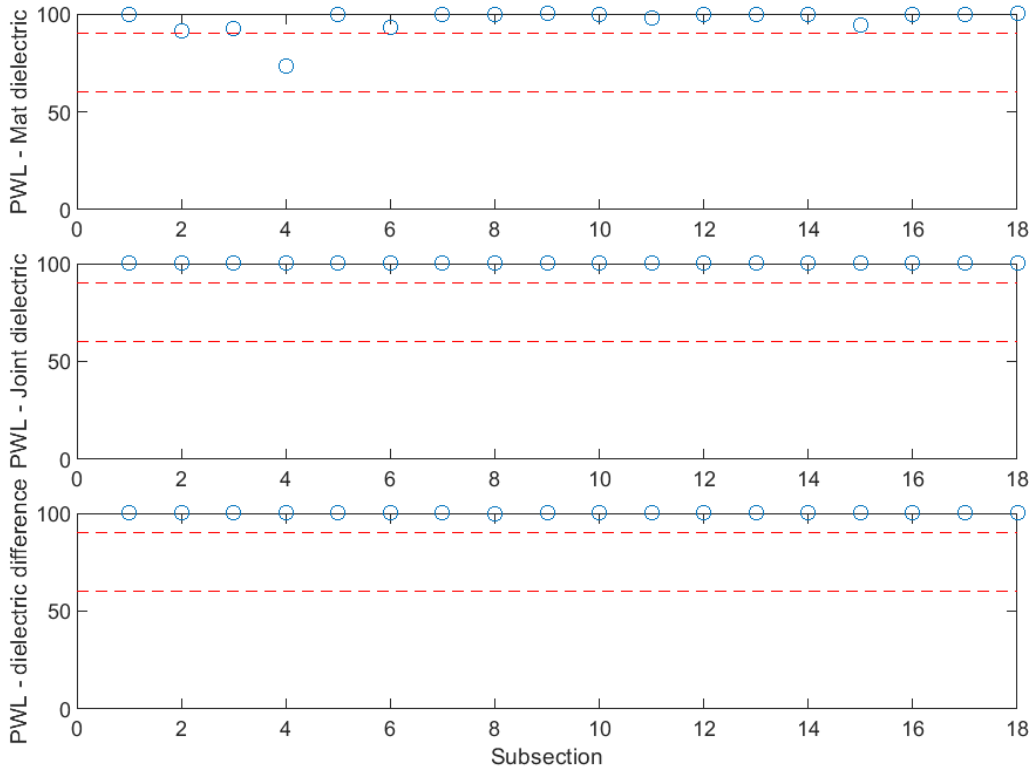

Figure B-299 PWL for dielectric values for unconfined tapered joint (50 ft subsections) – M-28-D1-2

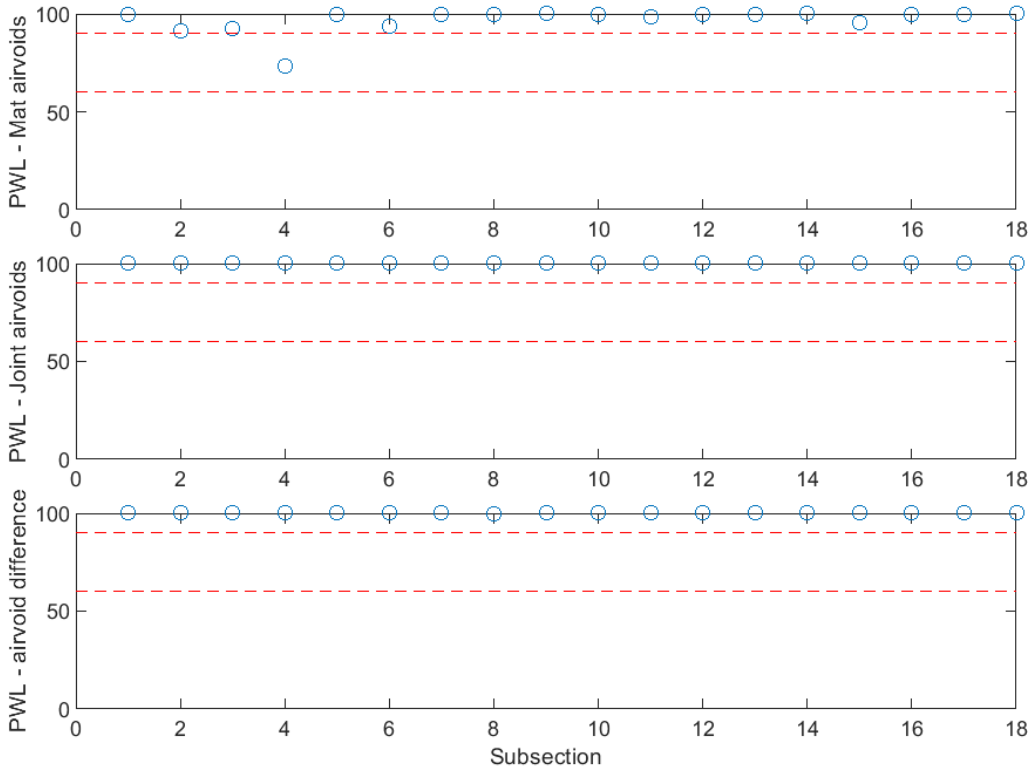

Figure B-300 PWL for air voids for unconfined tapered joint (50 ft subsections) – M-28-D1-2

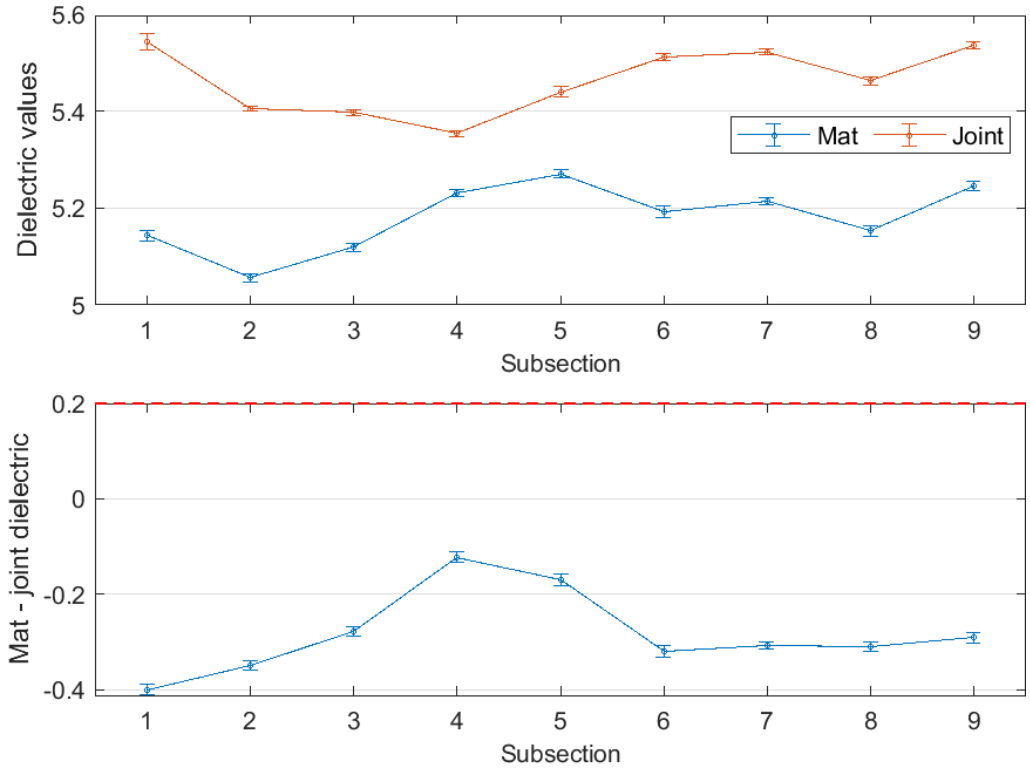

Figure B-301 Interval plot of dielectric values for unconfined tapered joint (100 ft subsections) – M-28-D1-2

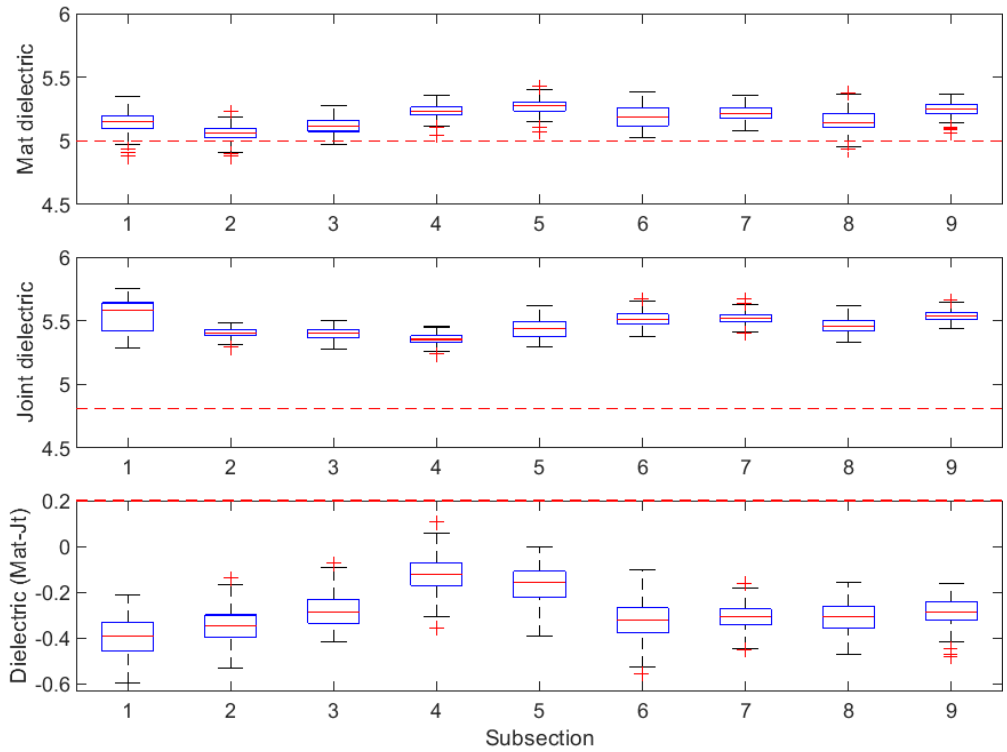

Figure B-302 Box plot of dielectric values for unconfined tapered joint (100 ft subsections) – M-28-D1-2

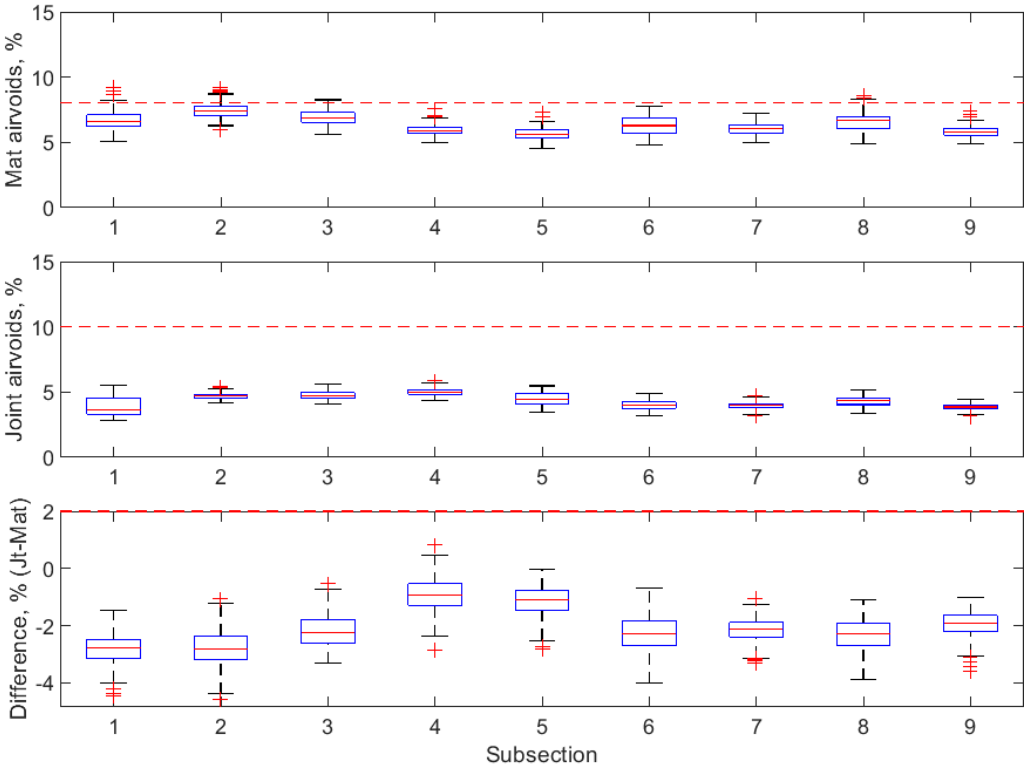

Figure B-303 Box plot of air voids for unconfined tapered joint (100 ft subsections) – M-28-D1-2

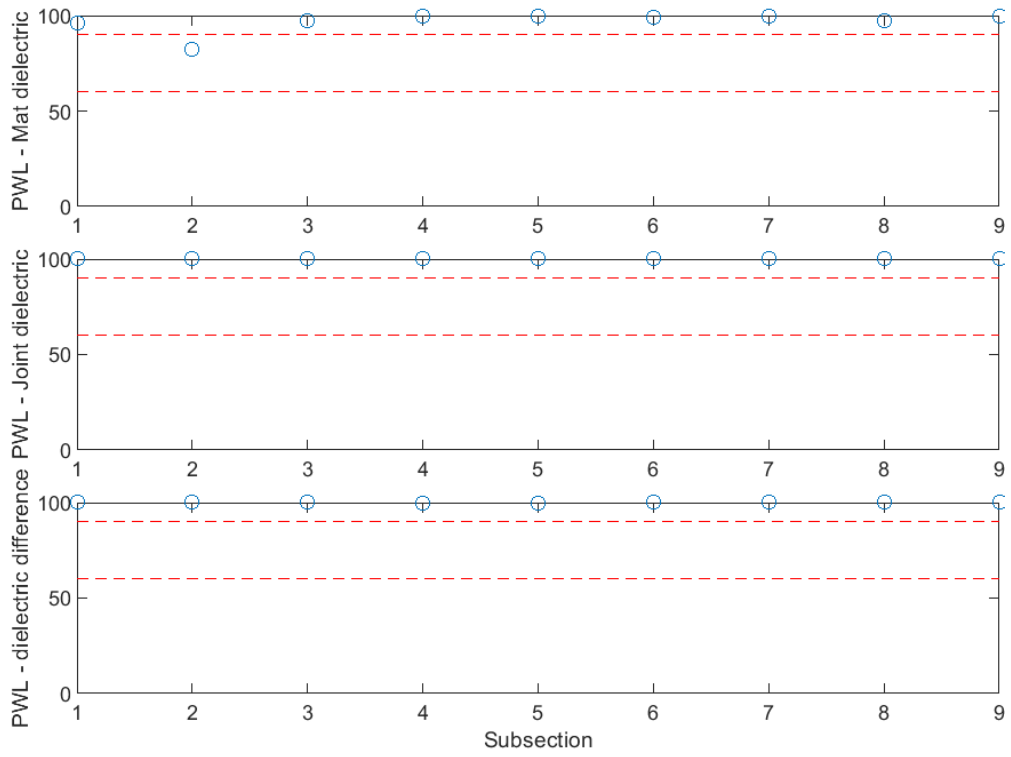

Figure B-304 PWL for dielectric values for unconfined tapered joint (100 ft subsections) – M-28-D1-2

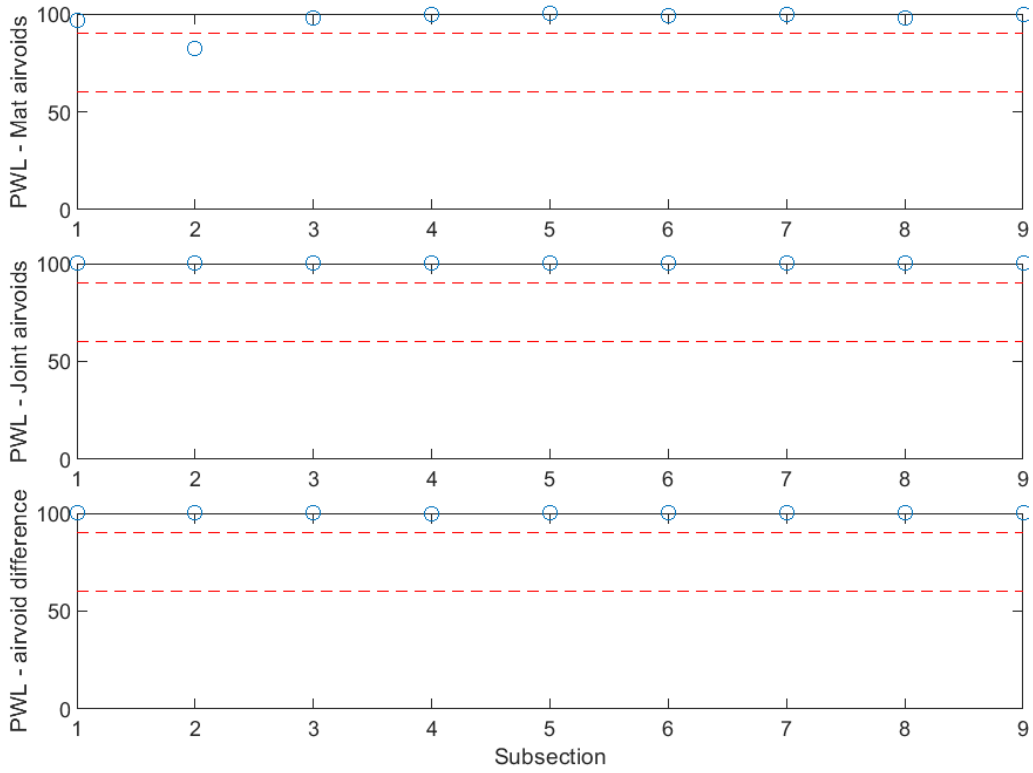

Figure B-305 PWL for air voids for unconfined tapered joint (100 ft subsections) – M-28-D1-2

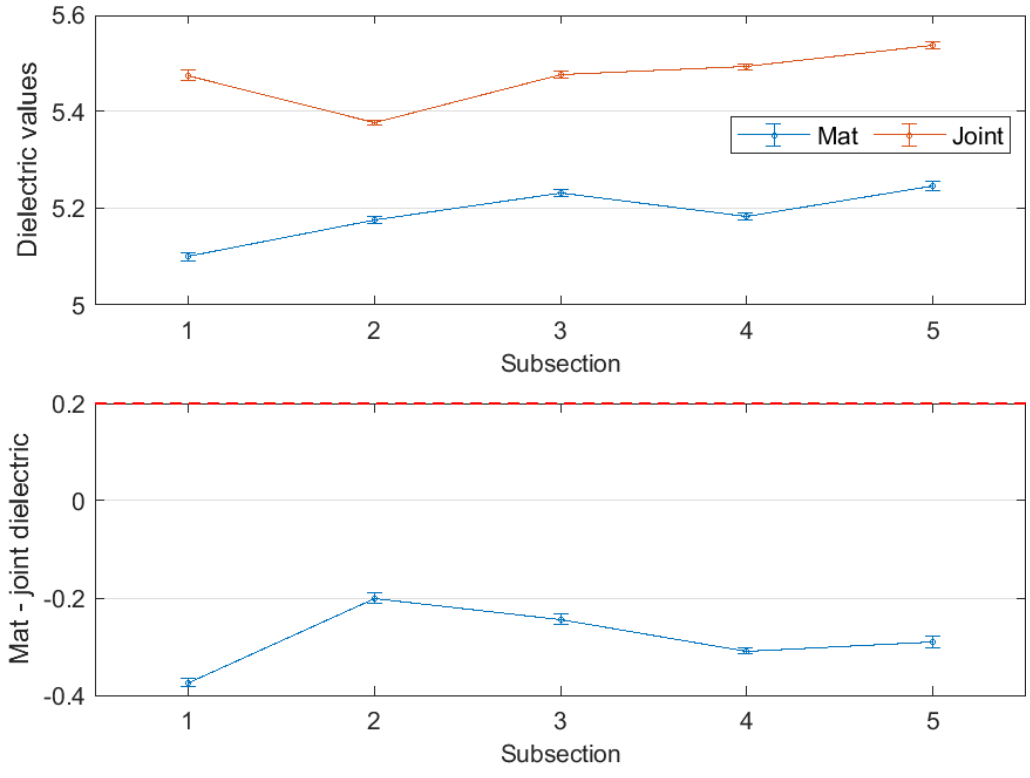

Figure B-306 Interval plot of dielectric values for unconfined tapered joint (200 ft subsections) – M-28-D1-2

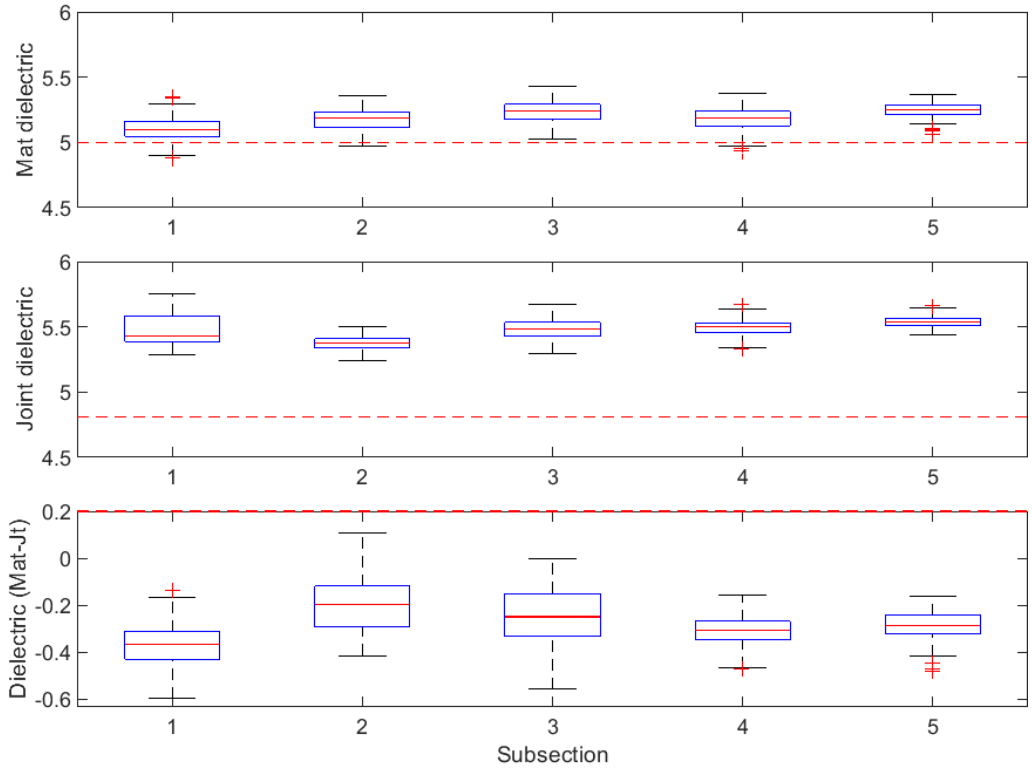

Figure B-307 Box plot of dielectric values for unconfined tapered joint (200 ft subsections) – M-28-D1-2

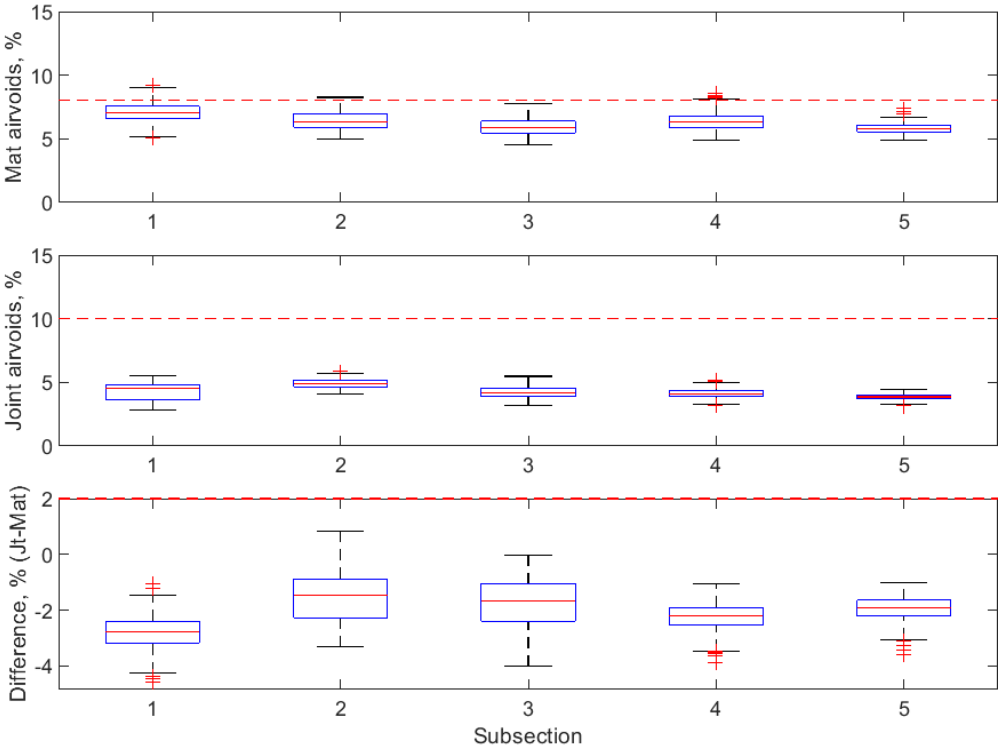

Figure B-308 Box plot of air voids for unconfined tapered joint (200 ft subsections) – M-28-D1-2

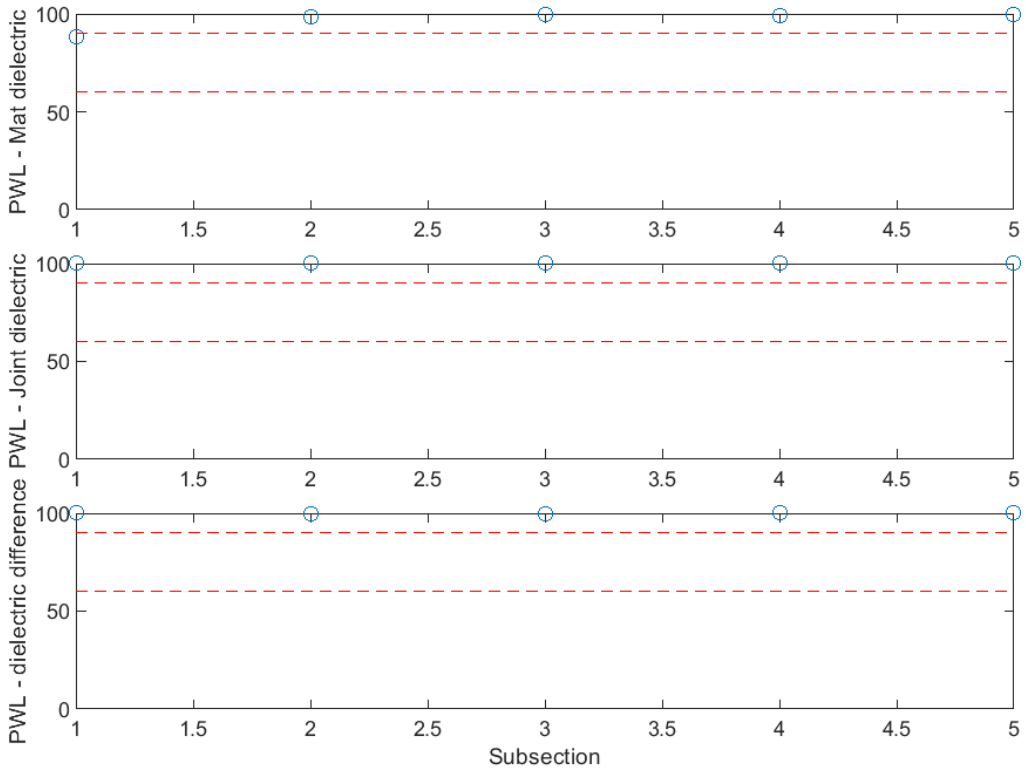

Figure B-309 PWL for dielectric values for unconfined tapered joint (200 ft subsections) – M-28-D1-2

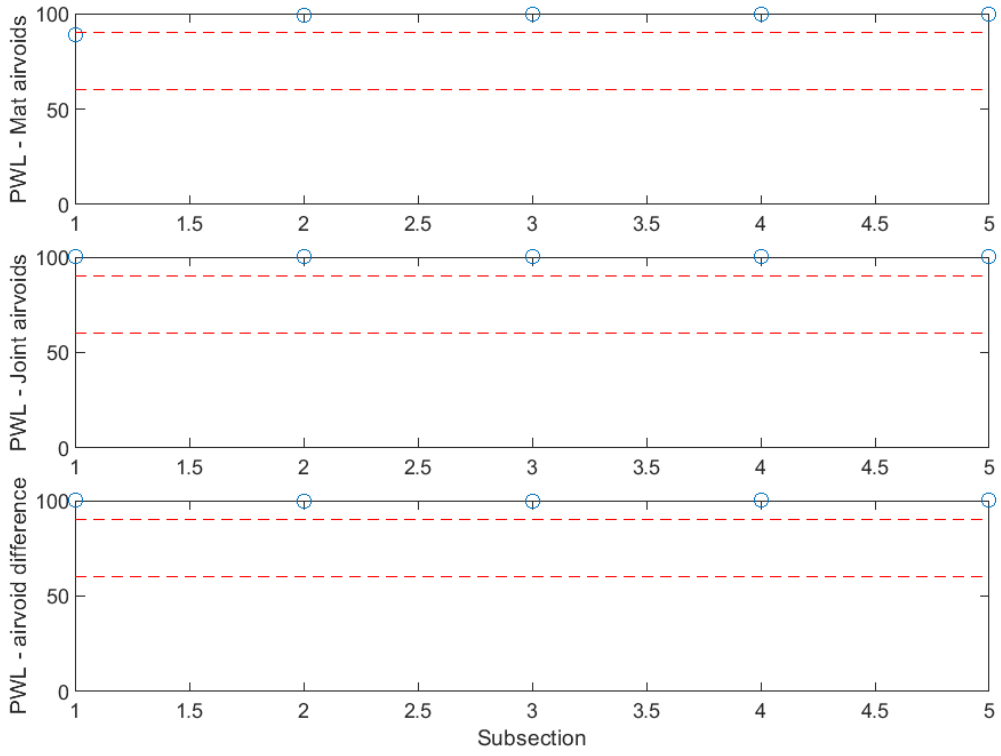

Figure B-310 PWL for air voids for unconfined tapered joint (200 ft subsections) – M-28-D1-2

M-89 Project

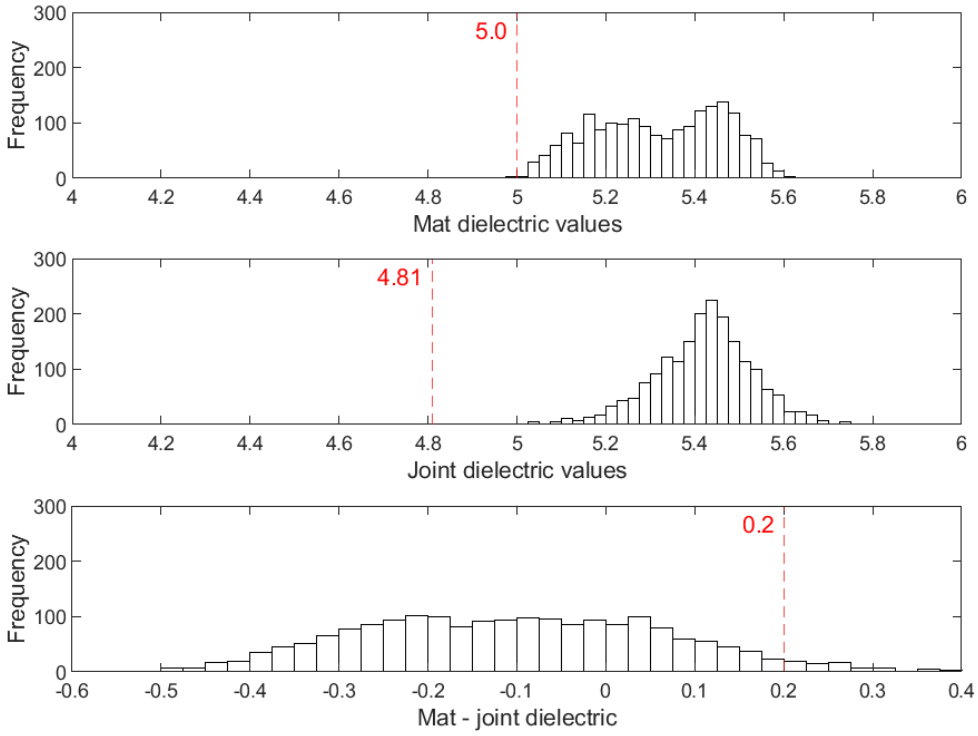

Figure B-311 Histogram of dielectric values for confined joint – M-89

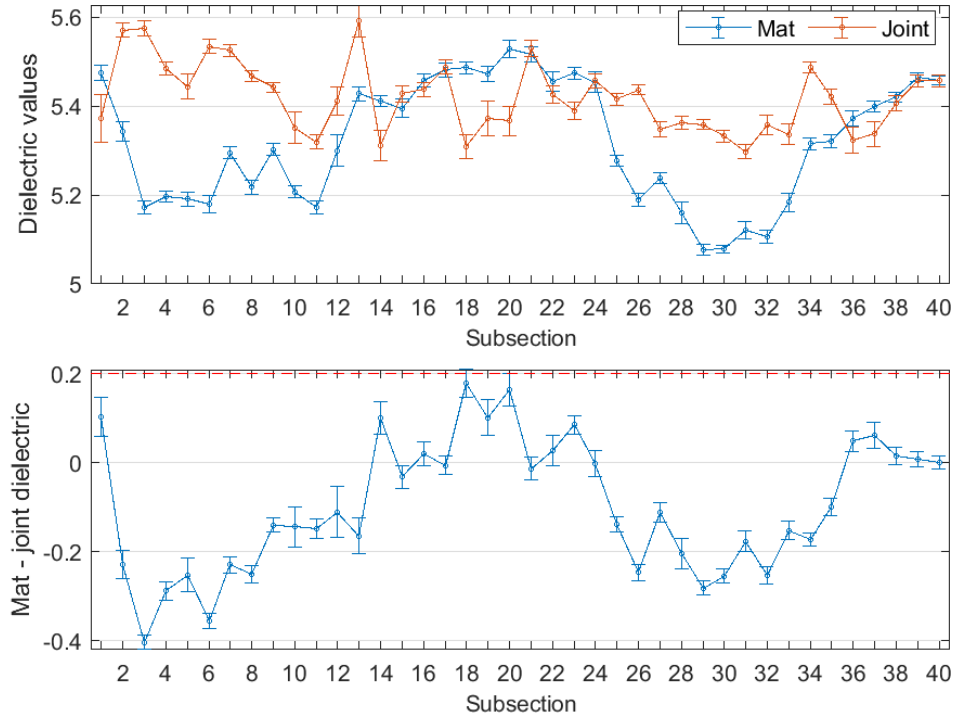

Figure B-312 Interval plot of dielectric values for confined joint (25 ft subsections) – M-89

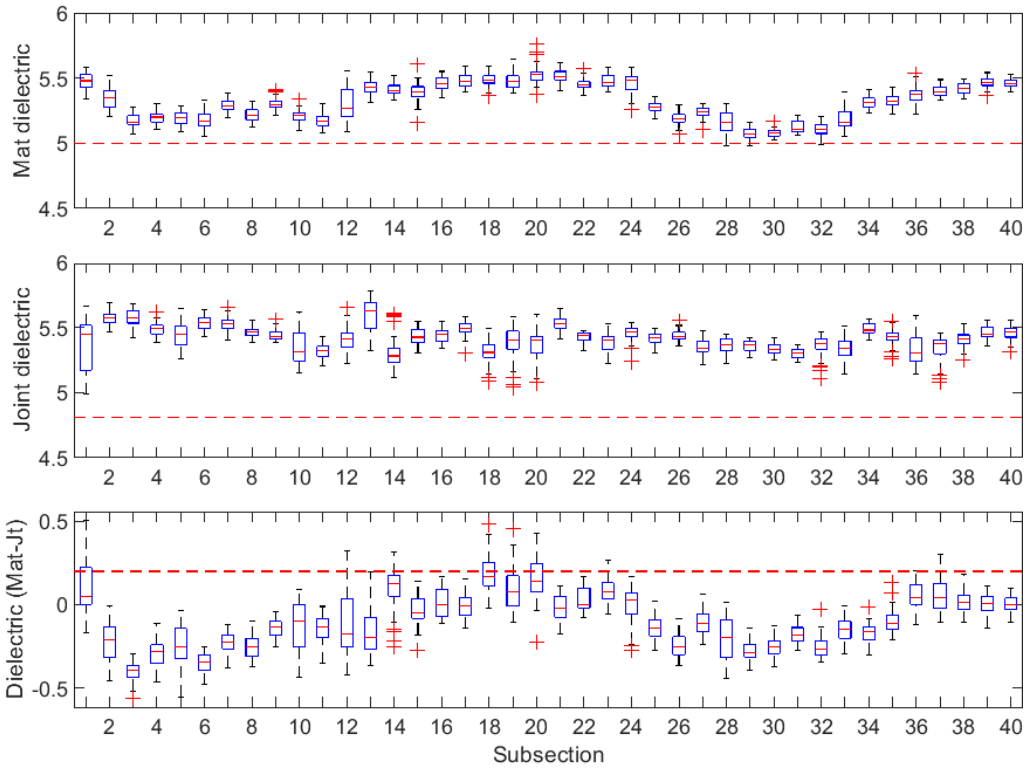

Figure B-313 Box plot of dielectric values for confined joint (25 ft subsections) – M-89

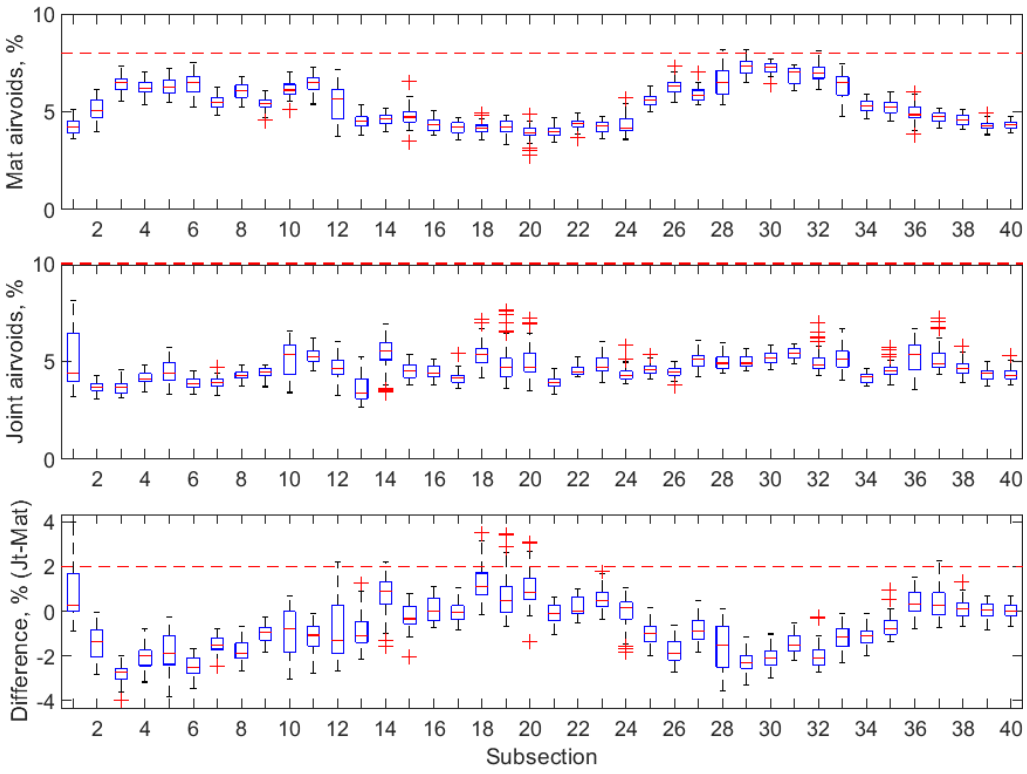

Figure B-314 Box plot of air voids for confined joint (25 ft subsections) – M-89

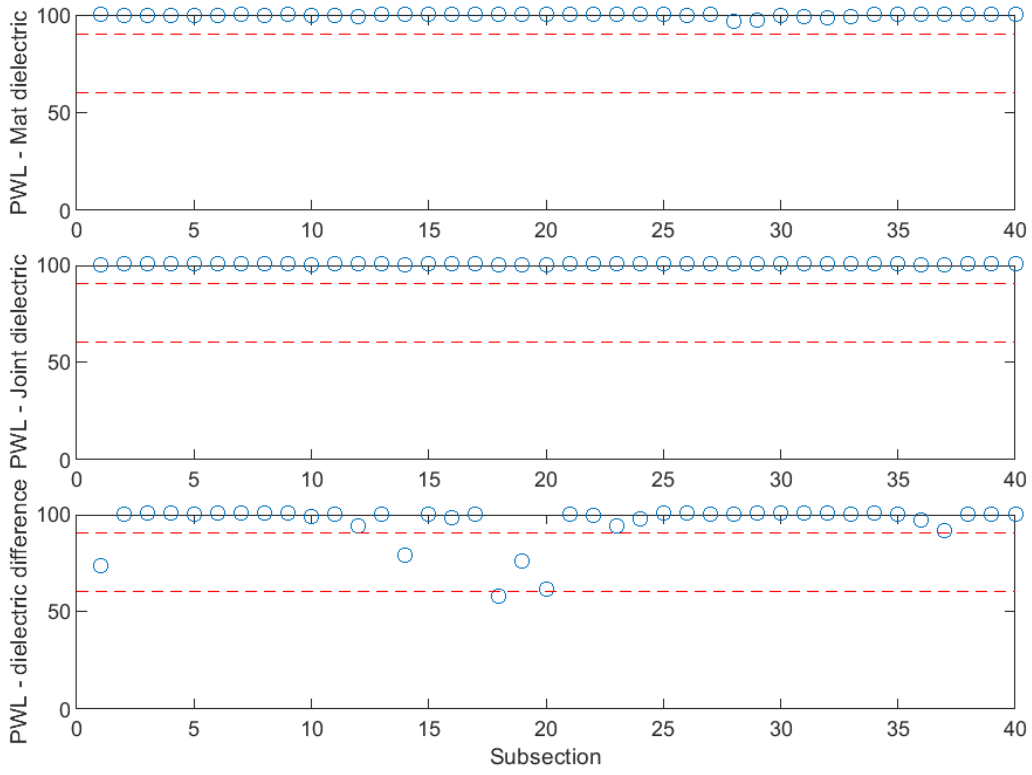

Figure B-315 PWL for dielectric values for confined joint (25 ft subsections) – M-89

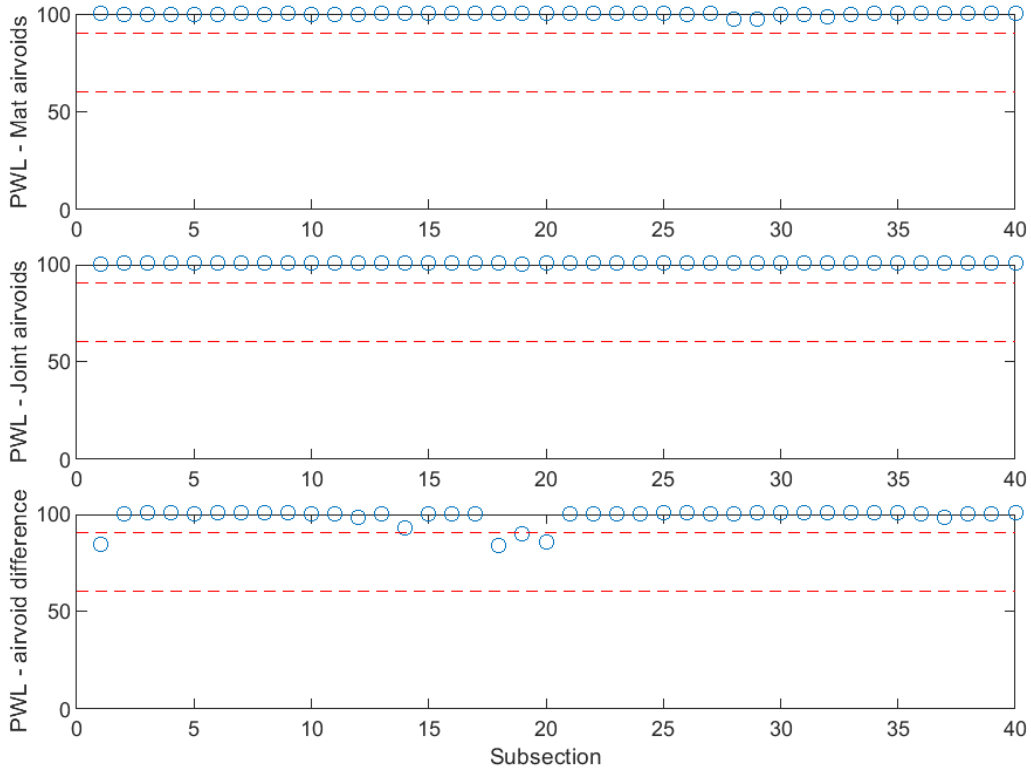

Figure B-316 PWL for air voids for confined joint (25 ft subsections) – M-89

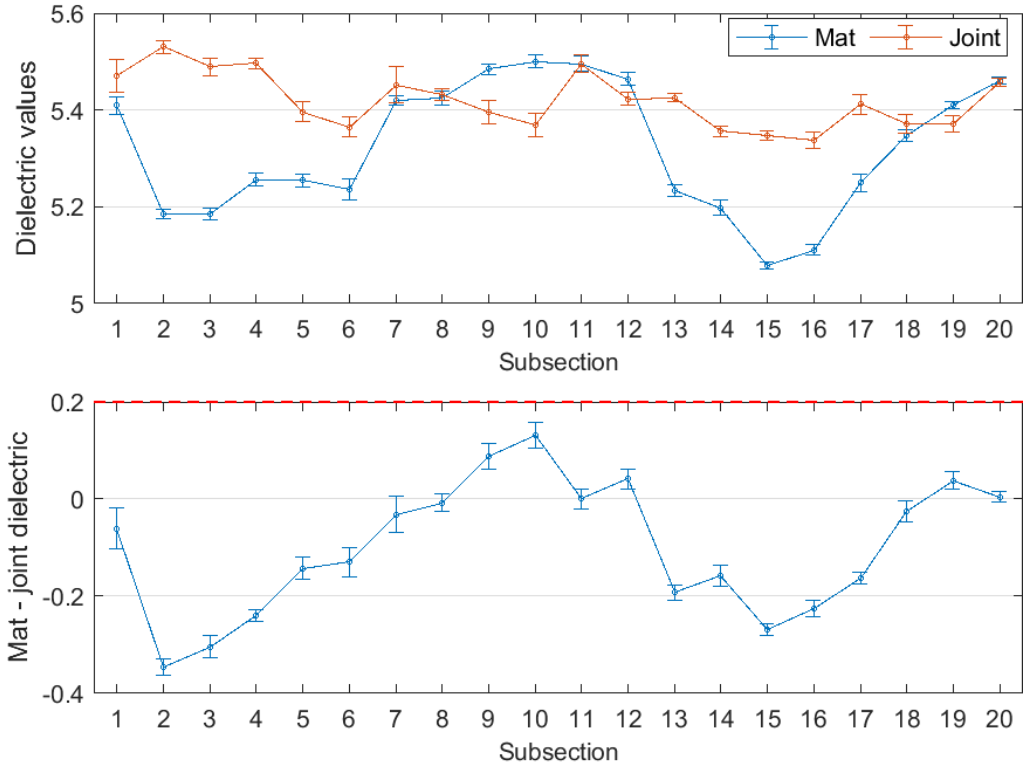

Figure B-317 Interval plot of dielectric values for confined joint (50 ft subsections) – M-89

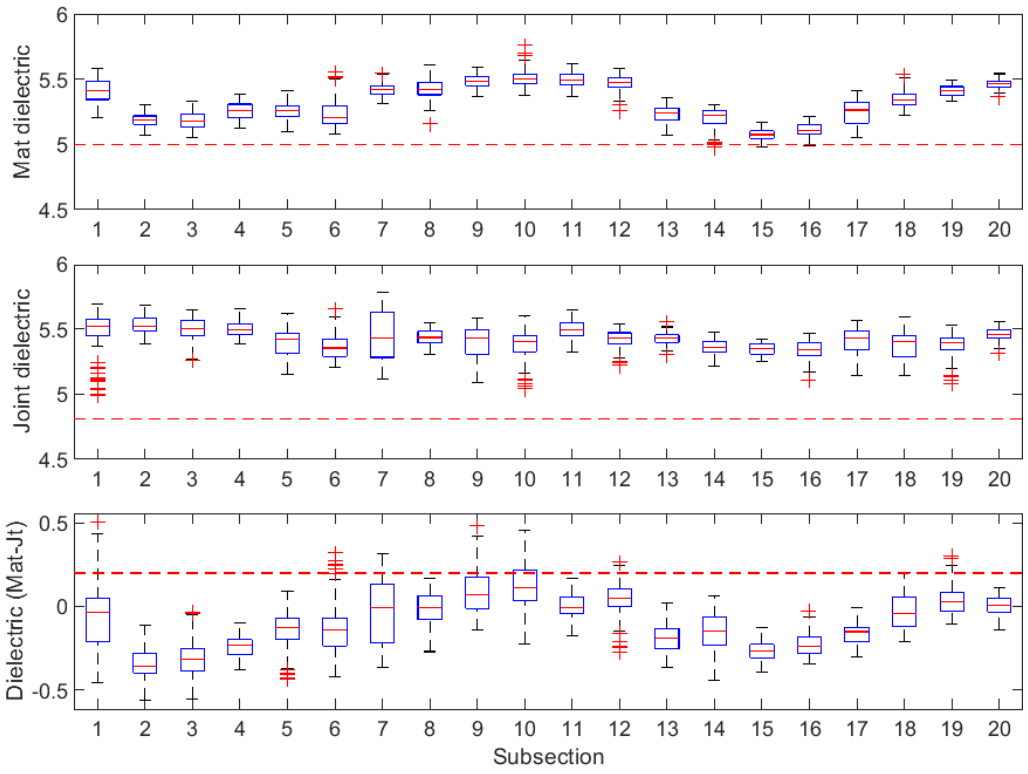

Figure B-318 Box plot of dielectric values for confined joint (50 ft subsections) – M-89

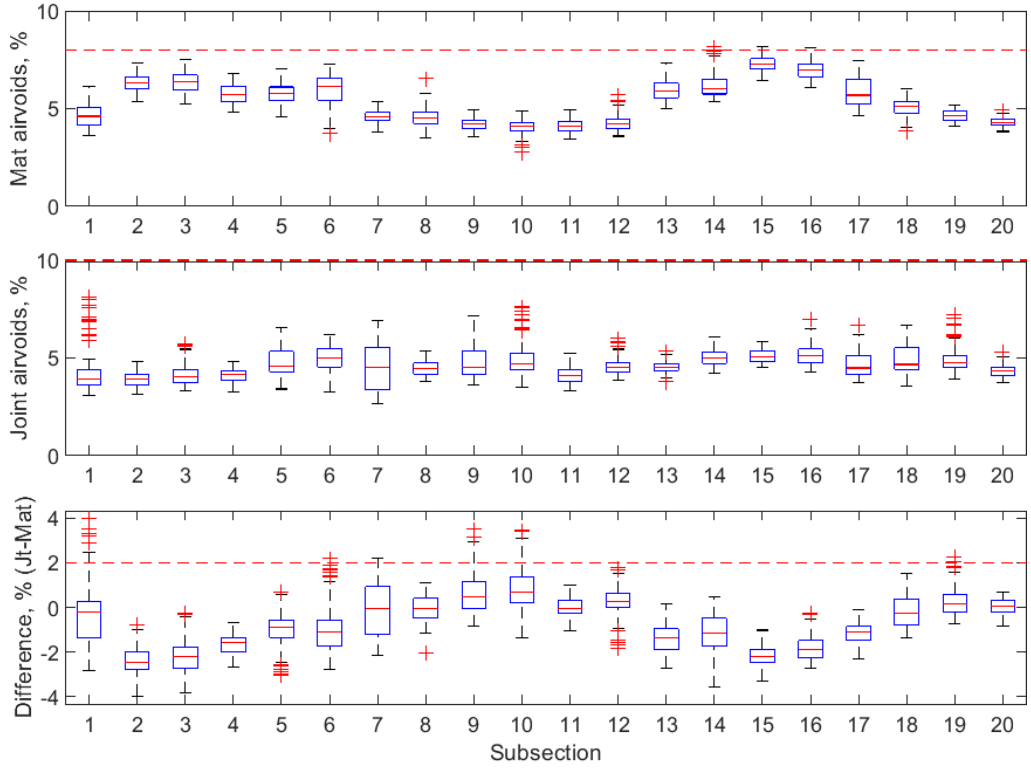

Figure B-319 Box plot of air voids for confined joint (50 ft subsections) – M-89

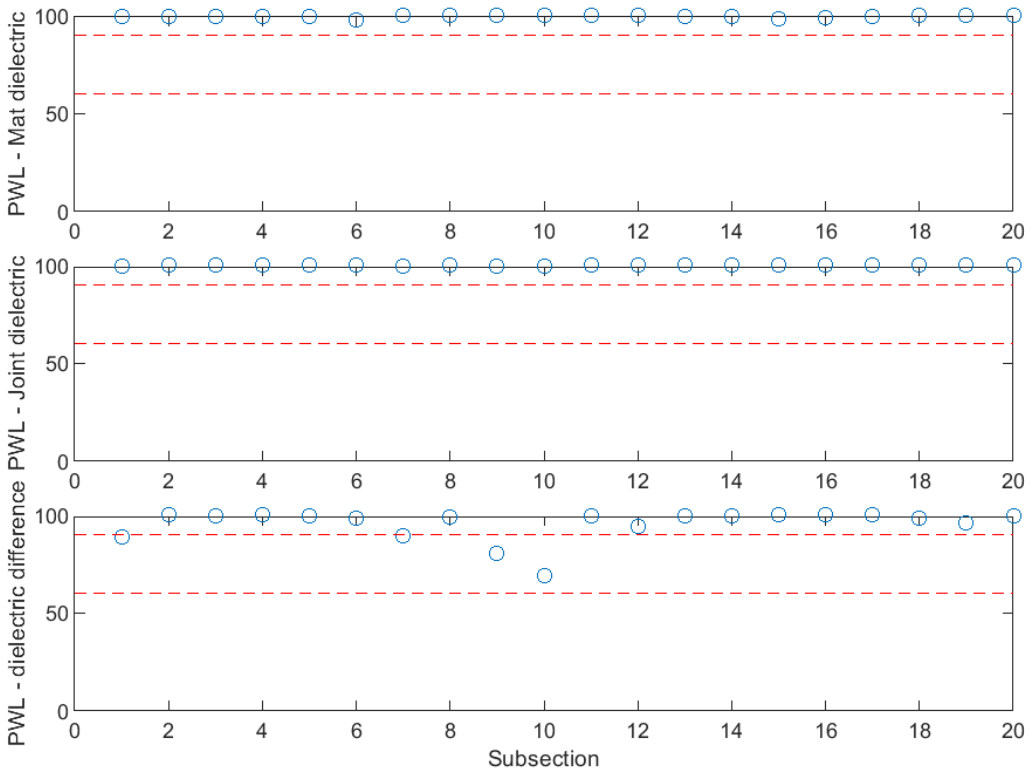

Figure B-320 PWL for dielectric values for confined joint (50 ft subsections) – M-89

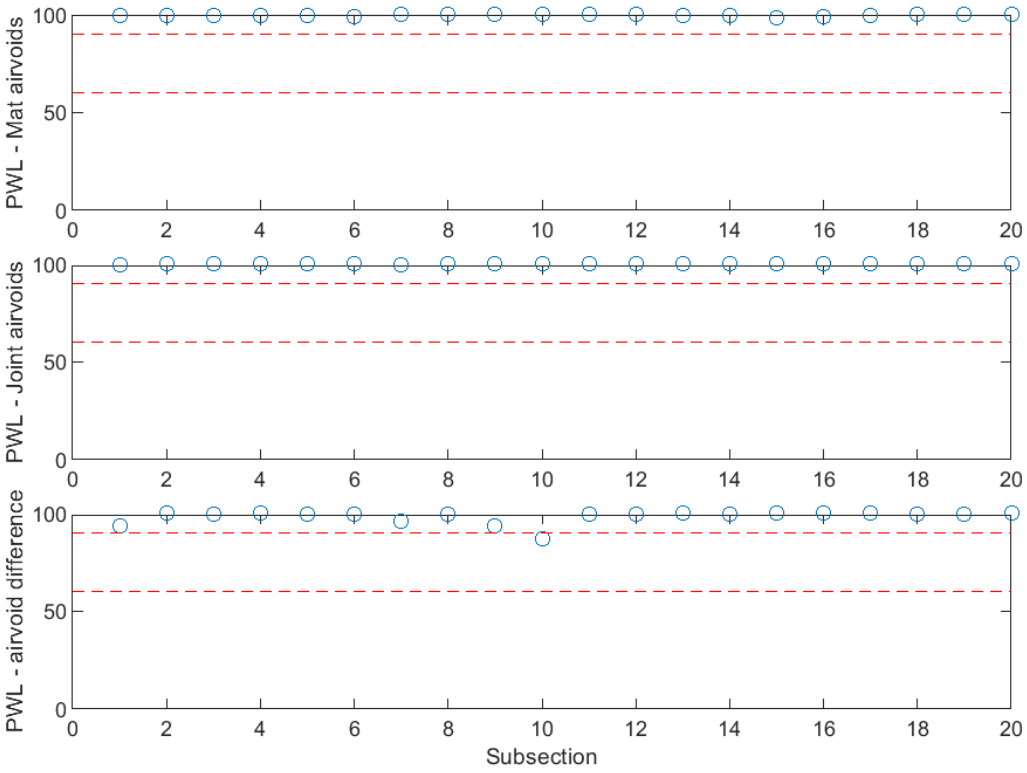

Figure B-321 PWL for air voids for confined joint (50 ft subsections) – M-89

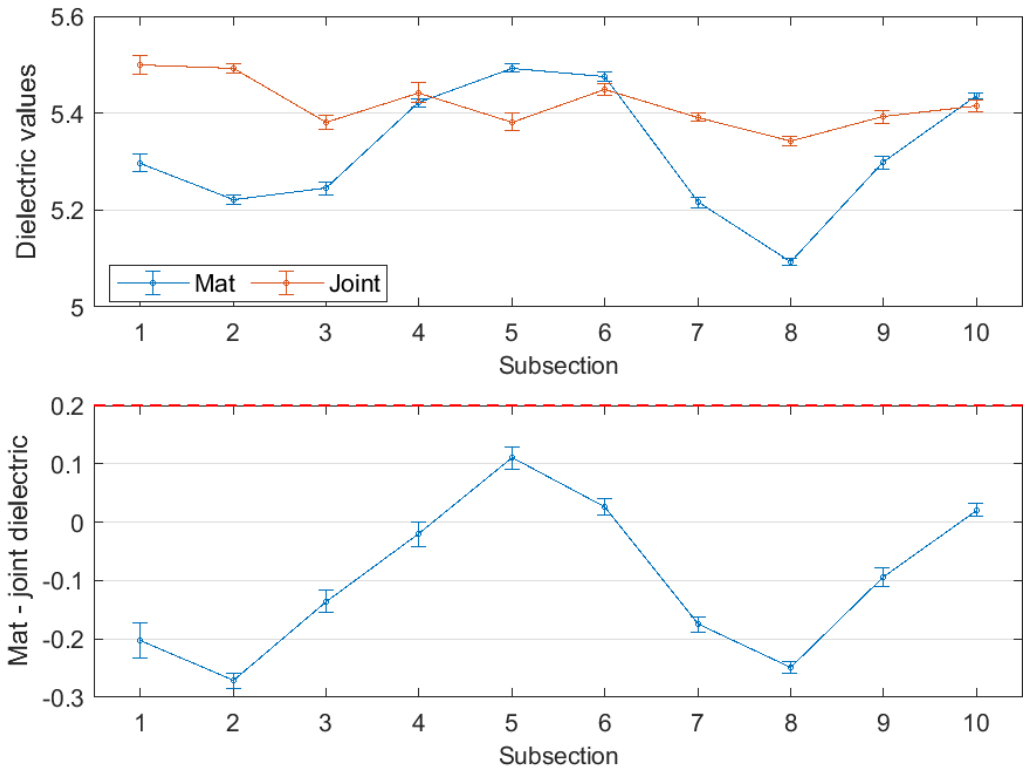

Figure B-322 Interval plot of dielectric values for confined joint (100 ft subsections) – M-89

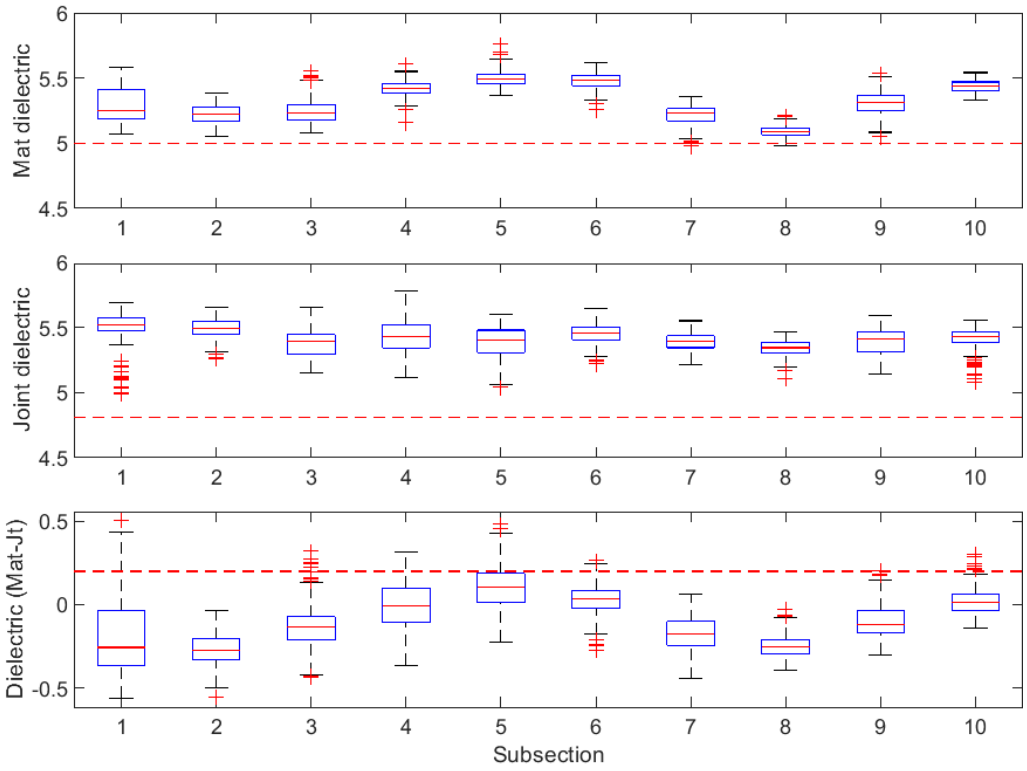

Figure B-323 Box plot of dielectric values for confined joint (100 ft subsections) – M-89

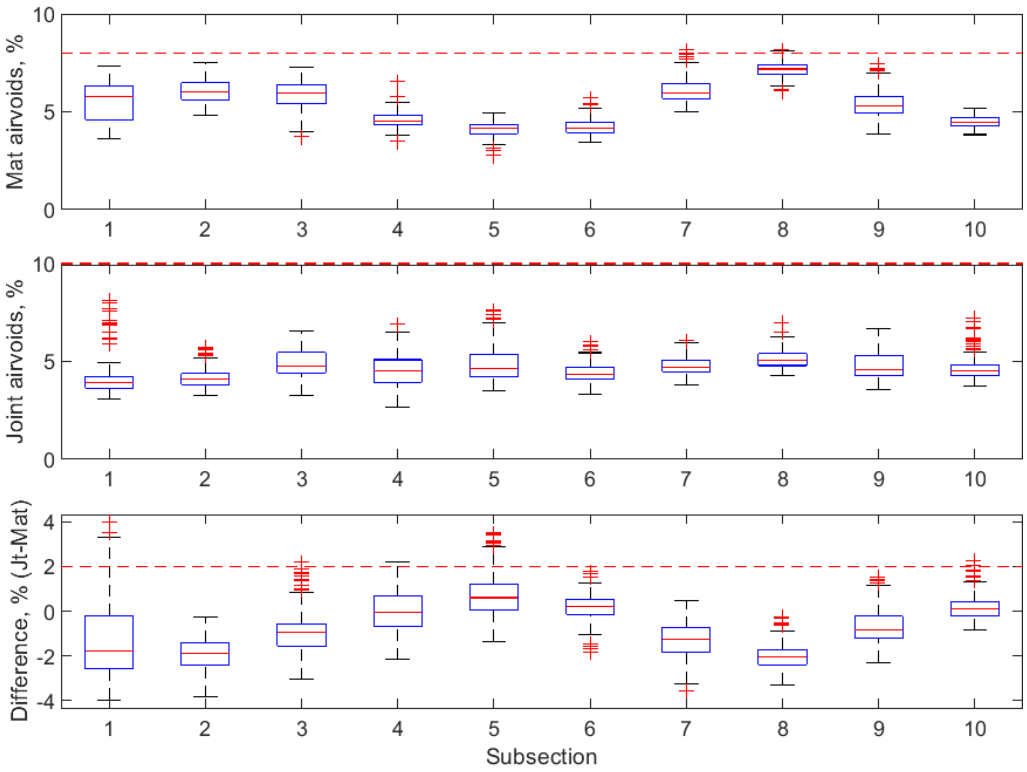

Figure B-324 Box plot of air voids for confined joint (100 ft subsections) – M-89

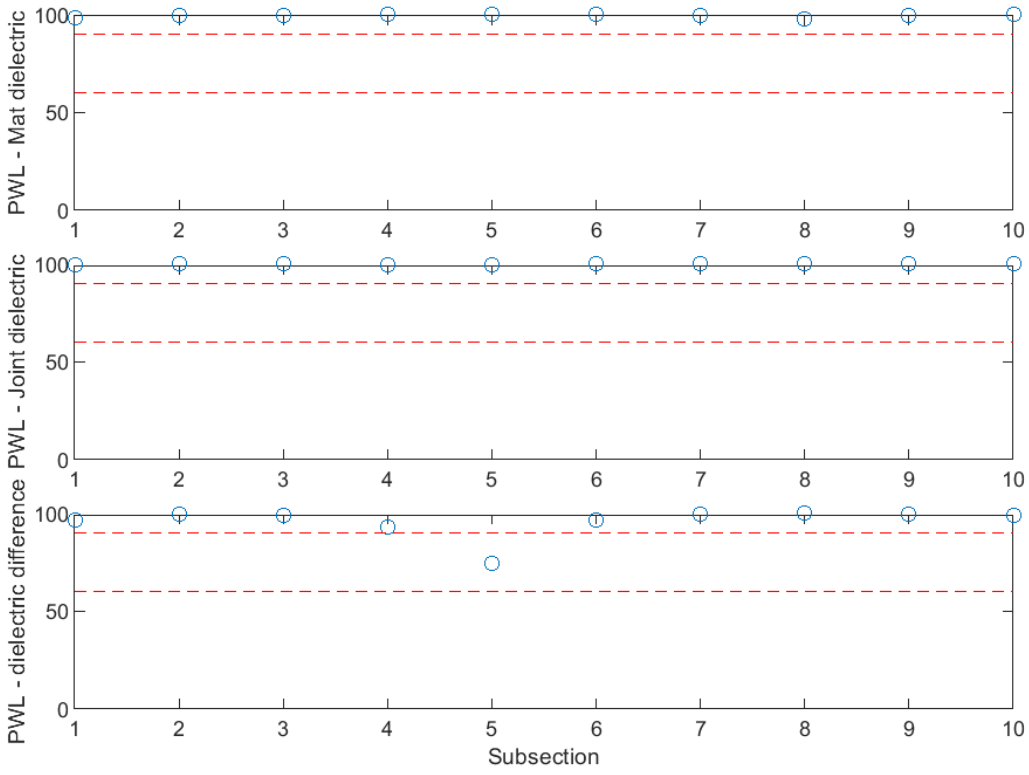

Figure B-325 PWL for dielectric values for confined joint (100 ft subsections) – M-89

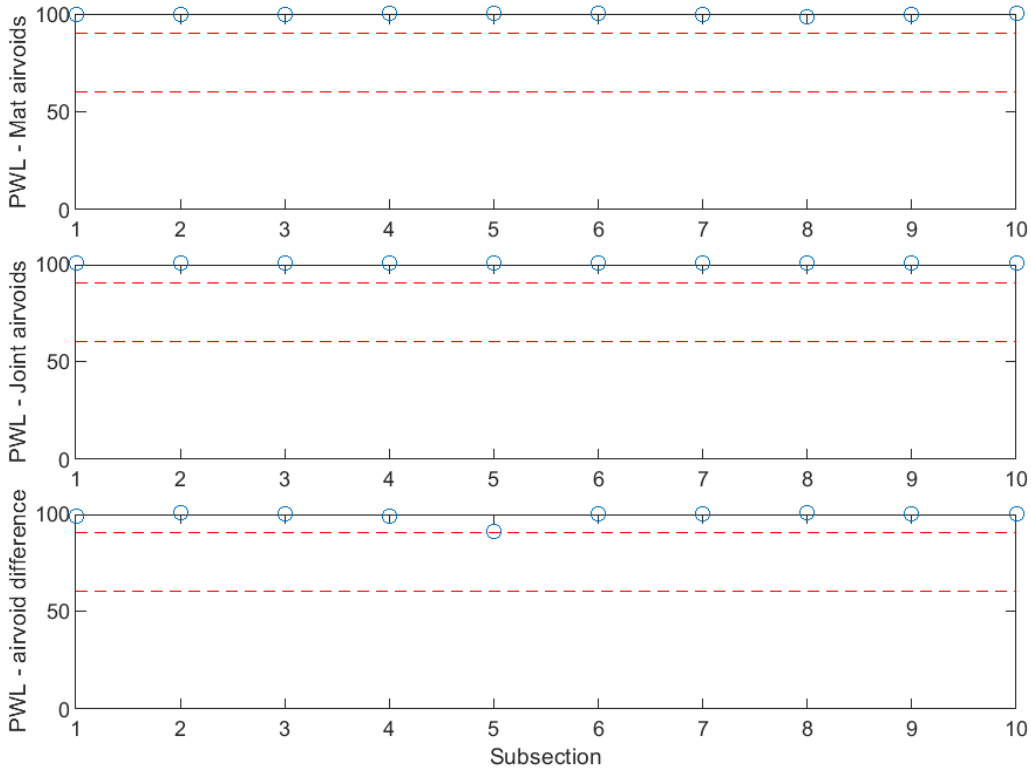

Figure B-326 PWL for air voids for confined joint (100 ft subsections) – M-89

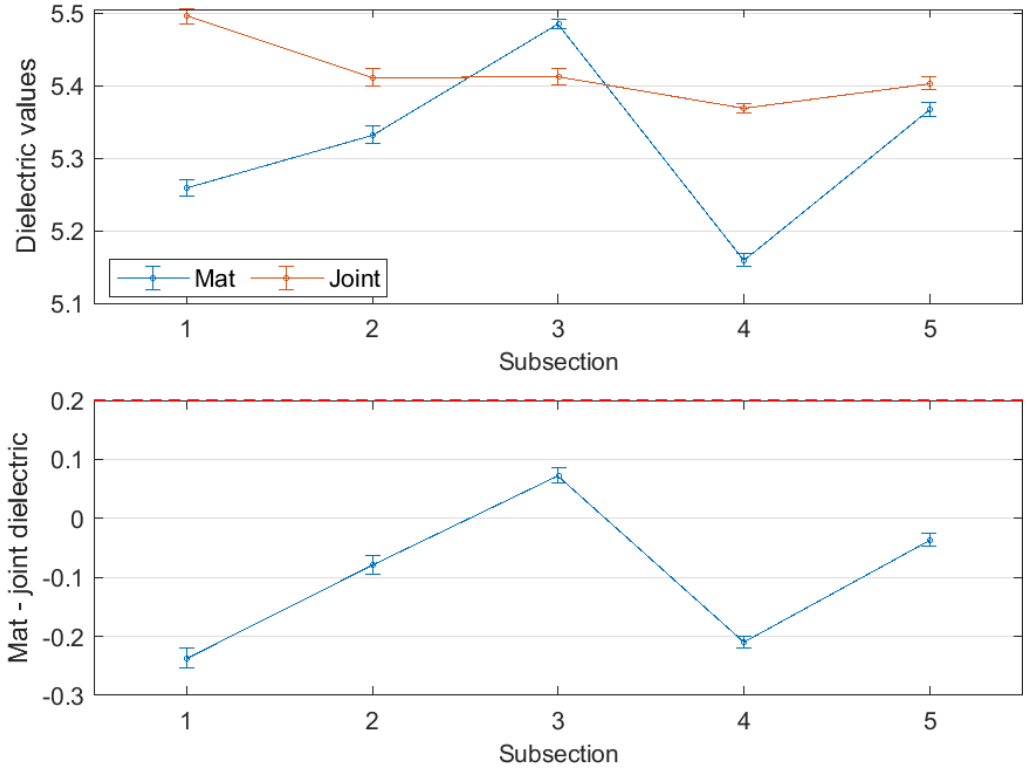

Figure B-327 Interval plot of dielectric values for confined joint (200 ft subsections) – M-89

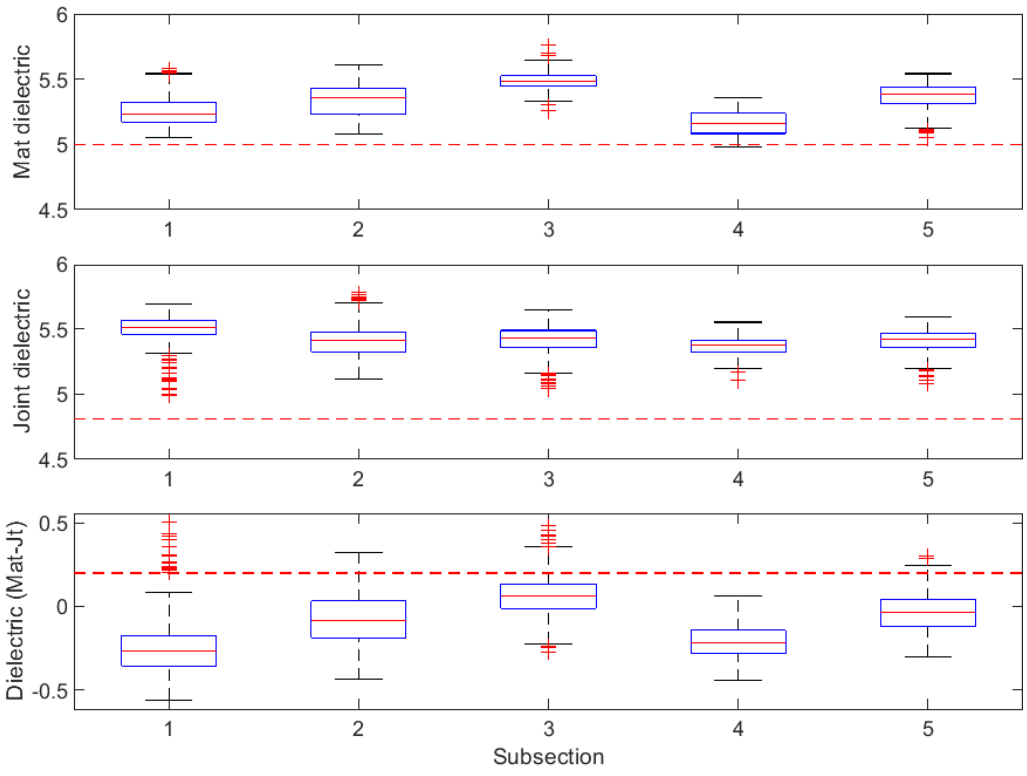

Figure B-328 Box plot of dielectric values for confined joint (200 ft subsections) – M-89

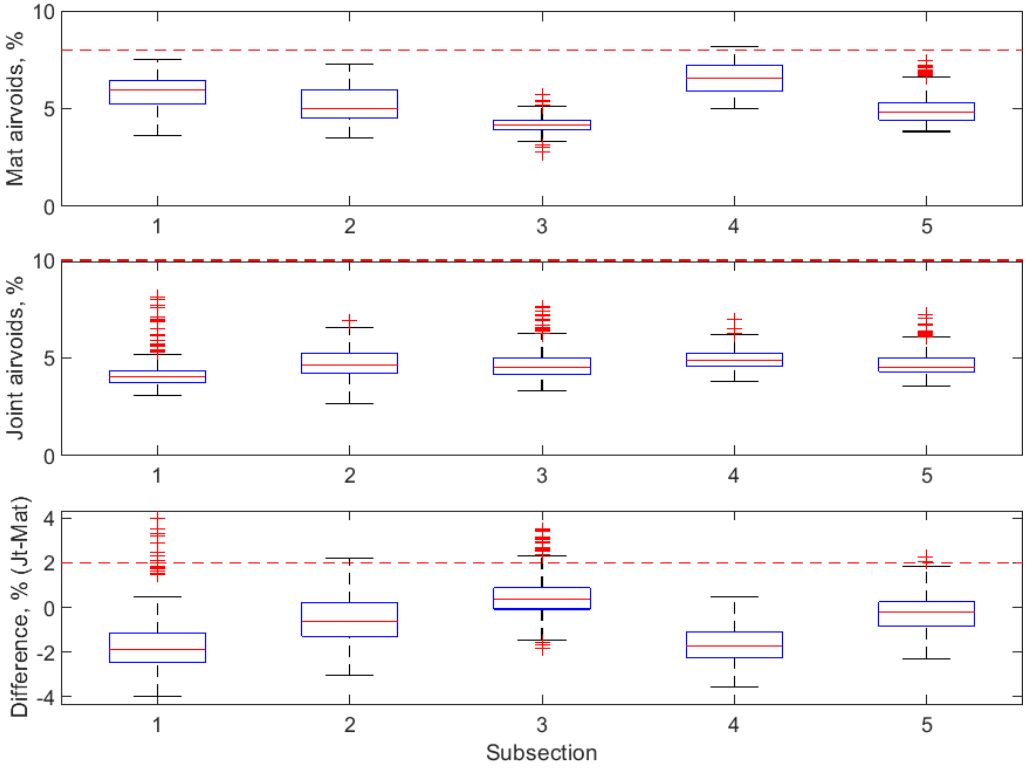

Figure B-329 Box plot of air voids for confined joint (200 ft subsections) – M-89

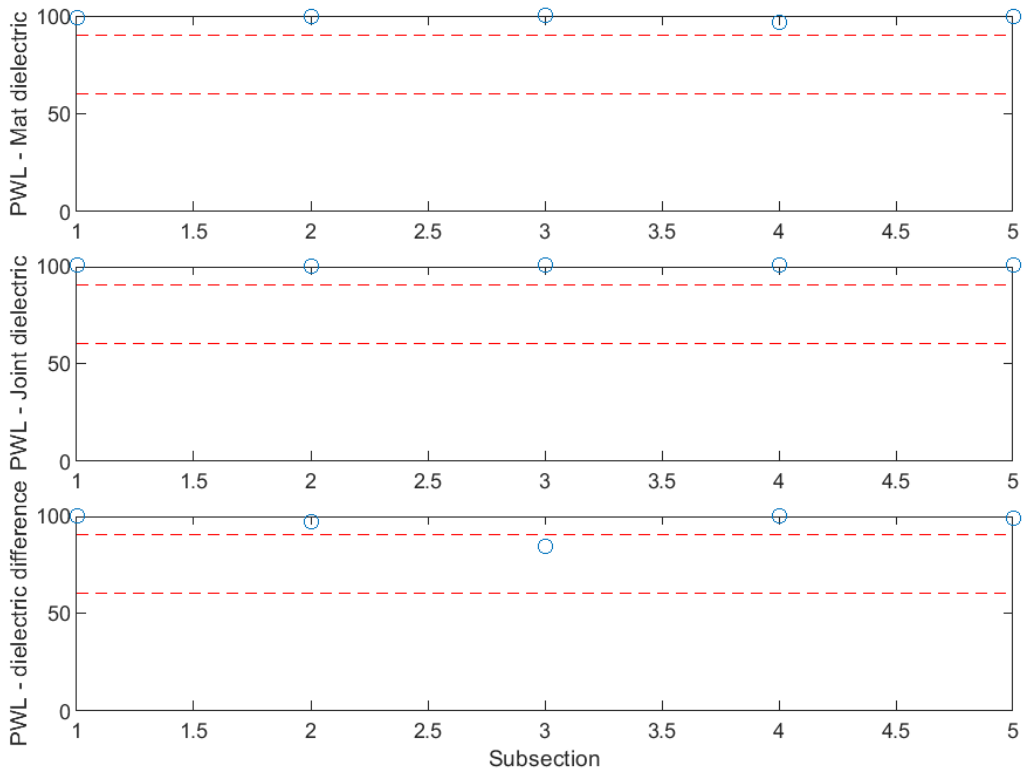

Figure B-330 PWL for dielectric values for confined joint (200 ft subsections) – M-89

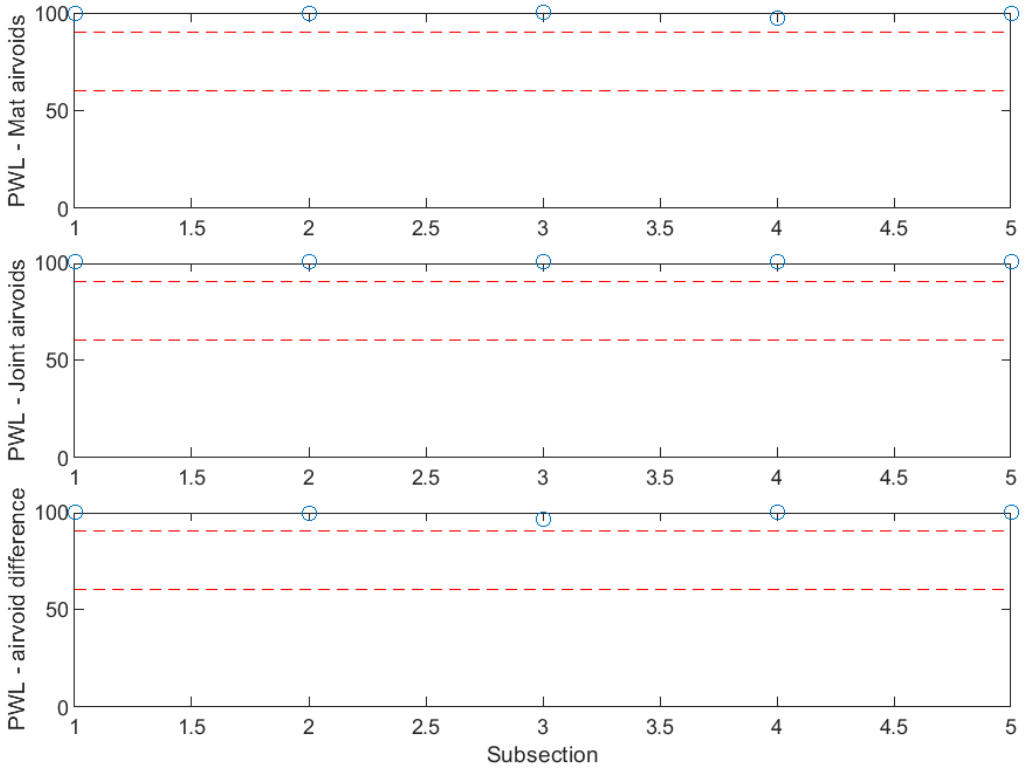

Figure B-331 PWL for air voids for confined joint (200 ft subsections) – M-89

US-23 Project

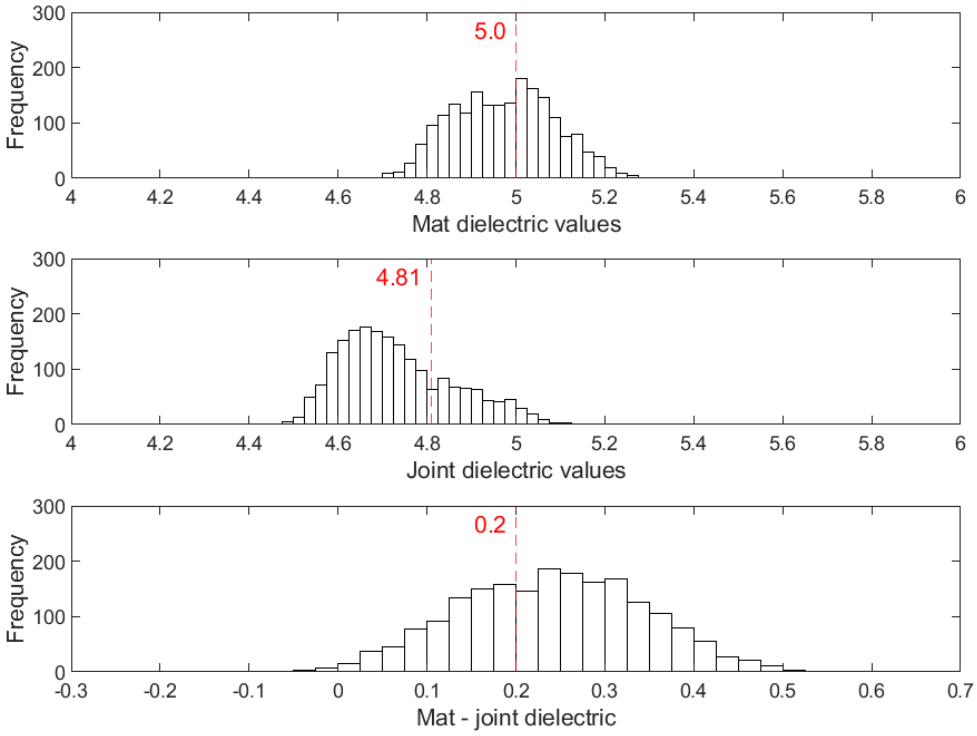

Figure B-332 Histogram of dielectric values for unconfined joint – US-23

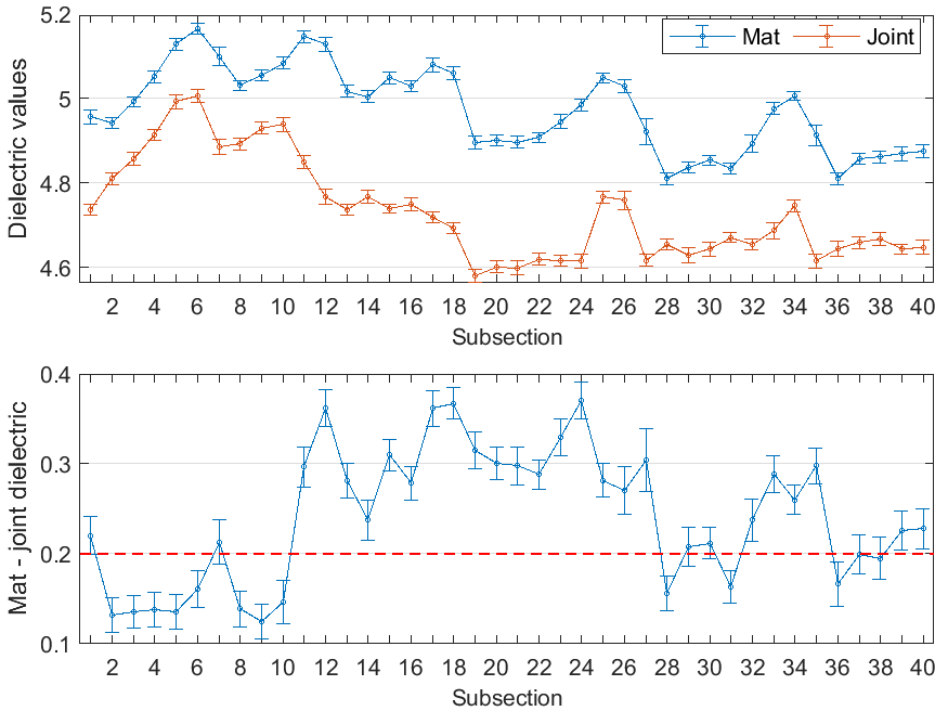

Figure B-333 Interval plot of dielectric values for unconfined joint (25 ft subsections) – US-23

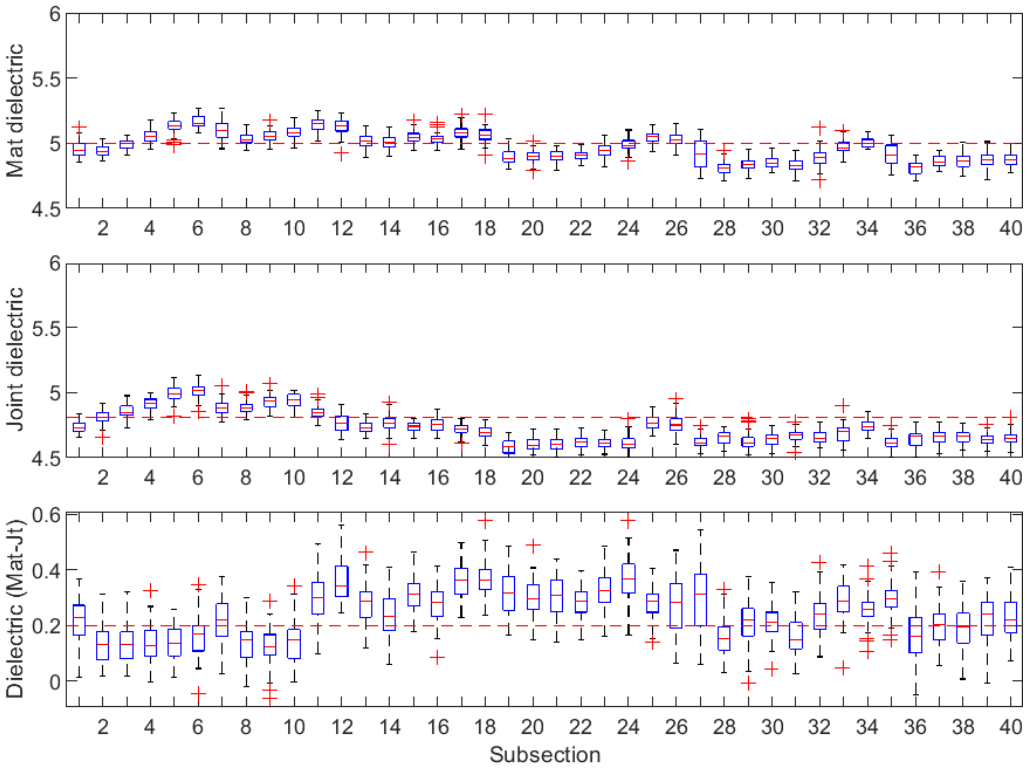

Figure B-334 Box plot of dielectric values for unconfined joint (25 ft subsections) – US-23

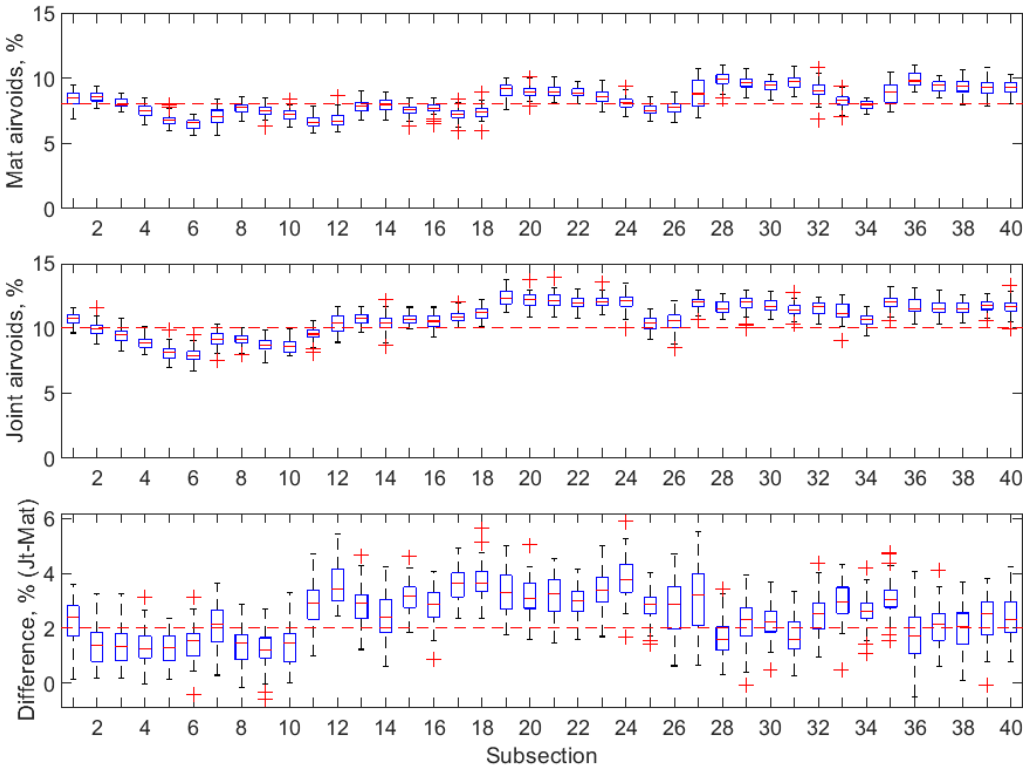

Figure B-335 Box plot of air voids for unconfined joint (25 ft subsections) – US-23

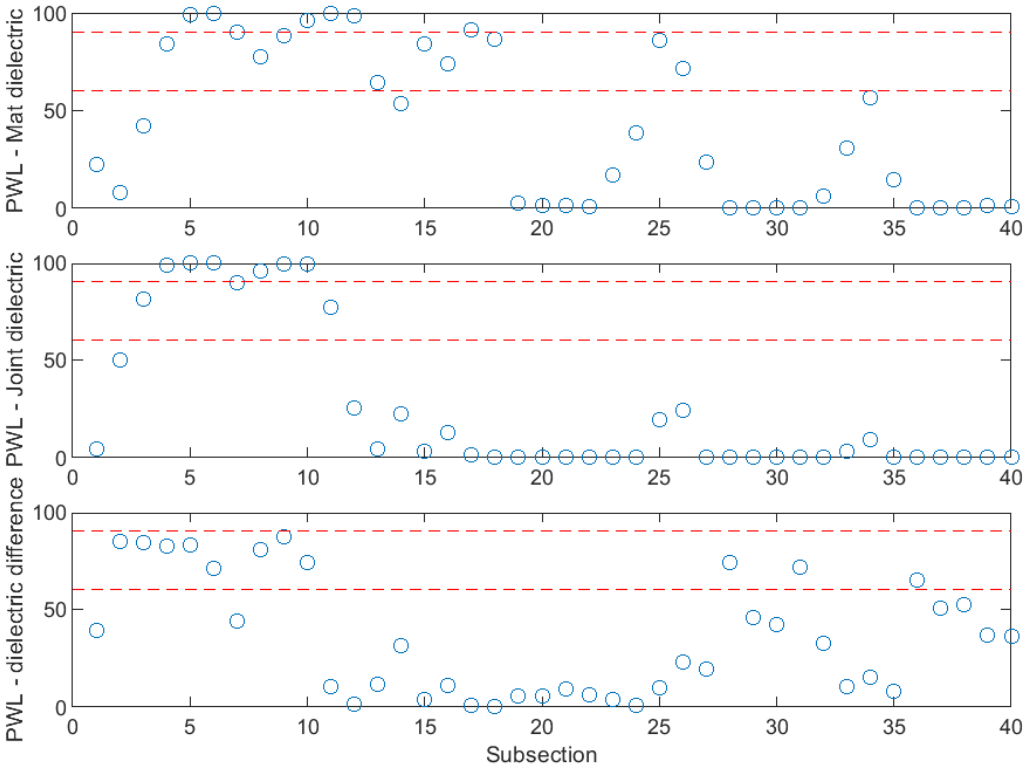

Figure B-336 PWL for dielectric values for unconfined joint (25 ft subsections) – US-23

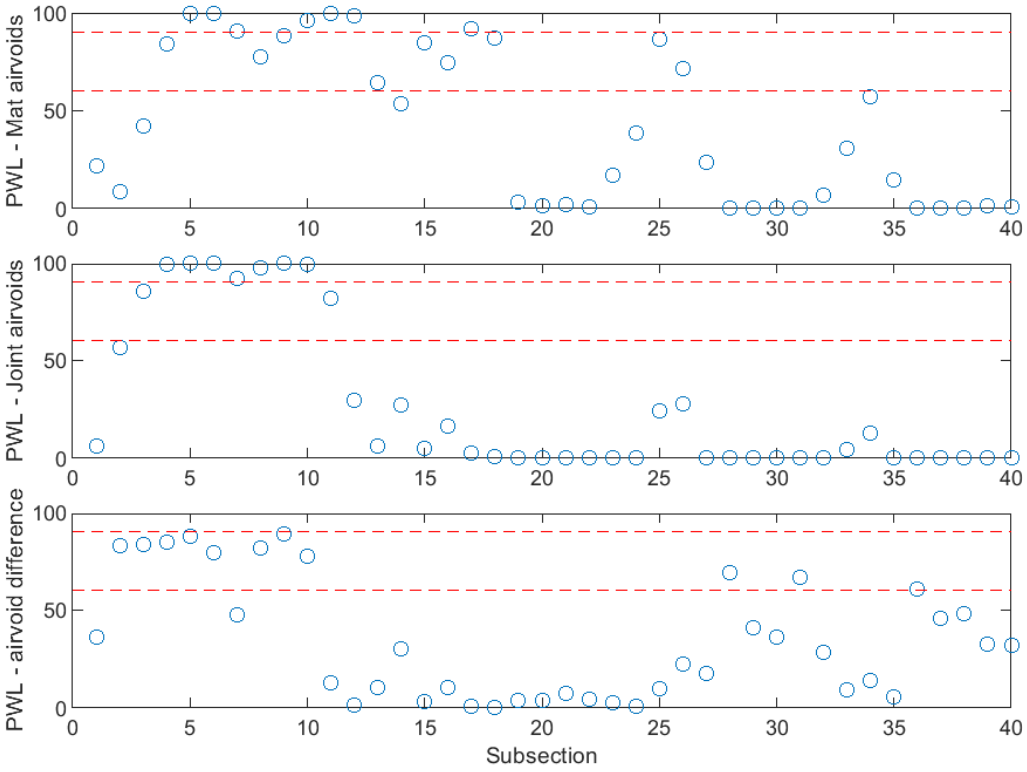

Figure B-337 PWL for air voids for unconfined joint (25 ft subsections) – US-23

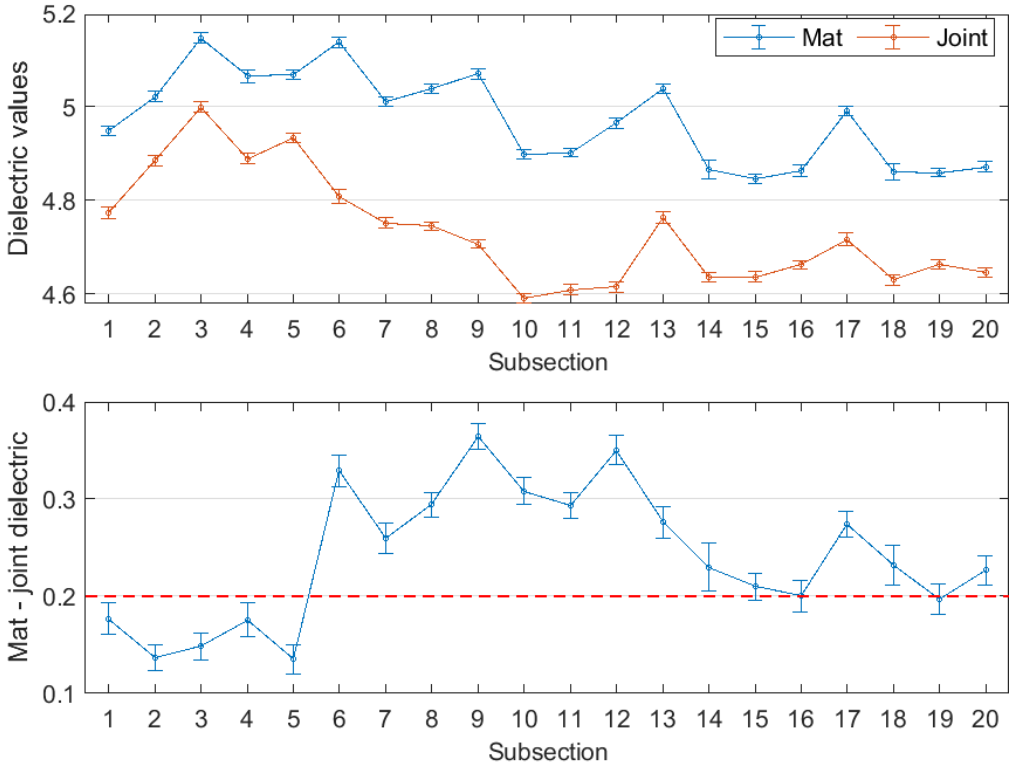

Figure B-338 Interval plot of dielectric values for unconfined joint (50 ft subsections) – US-23

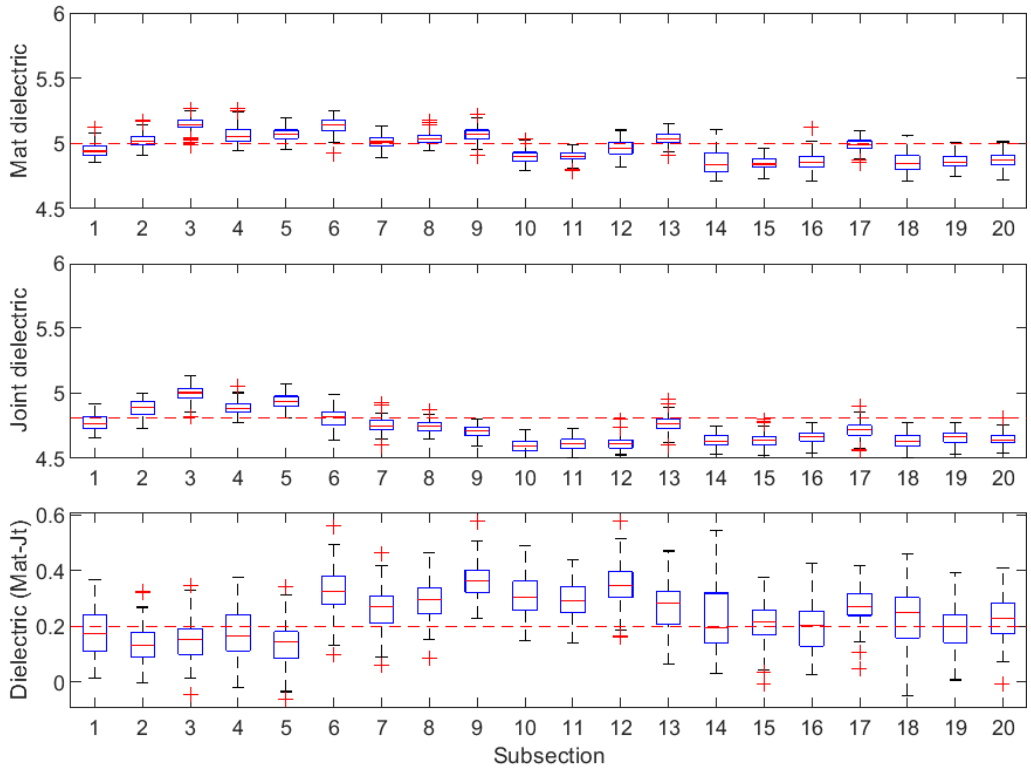

Figure B-339 Box plot of dielectric values for unconfined joint (50 ft subsections) – US-23

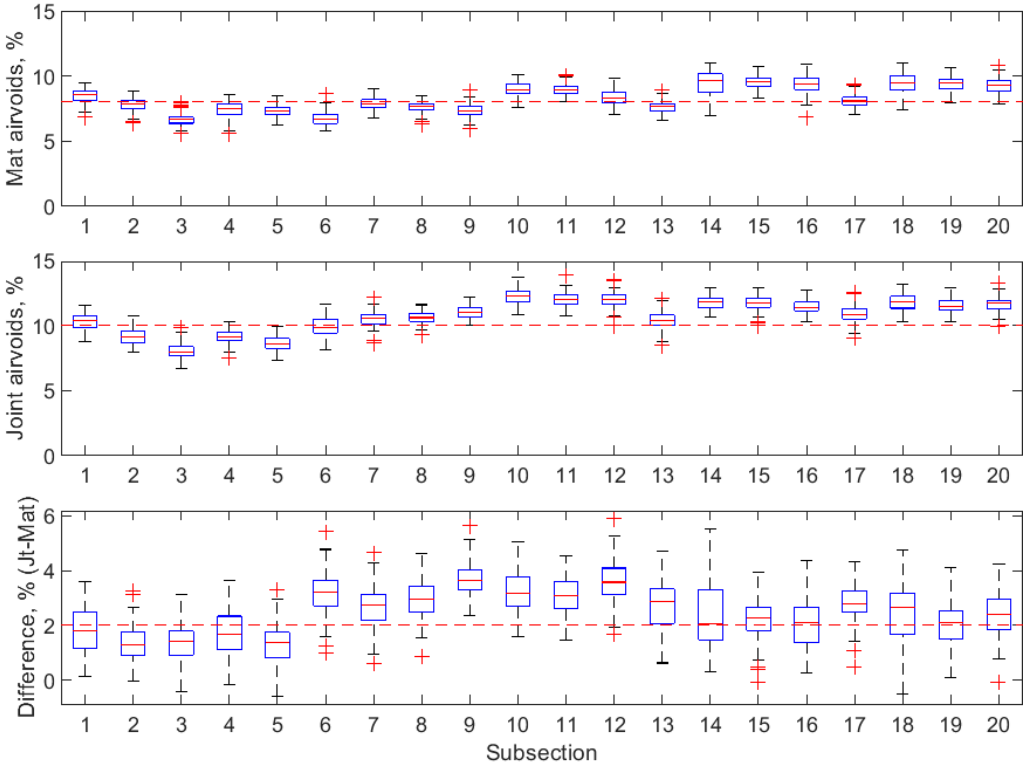

Figure B-340 Box plot of air voids for unconfined joint (50 ft subsections) – US-23

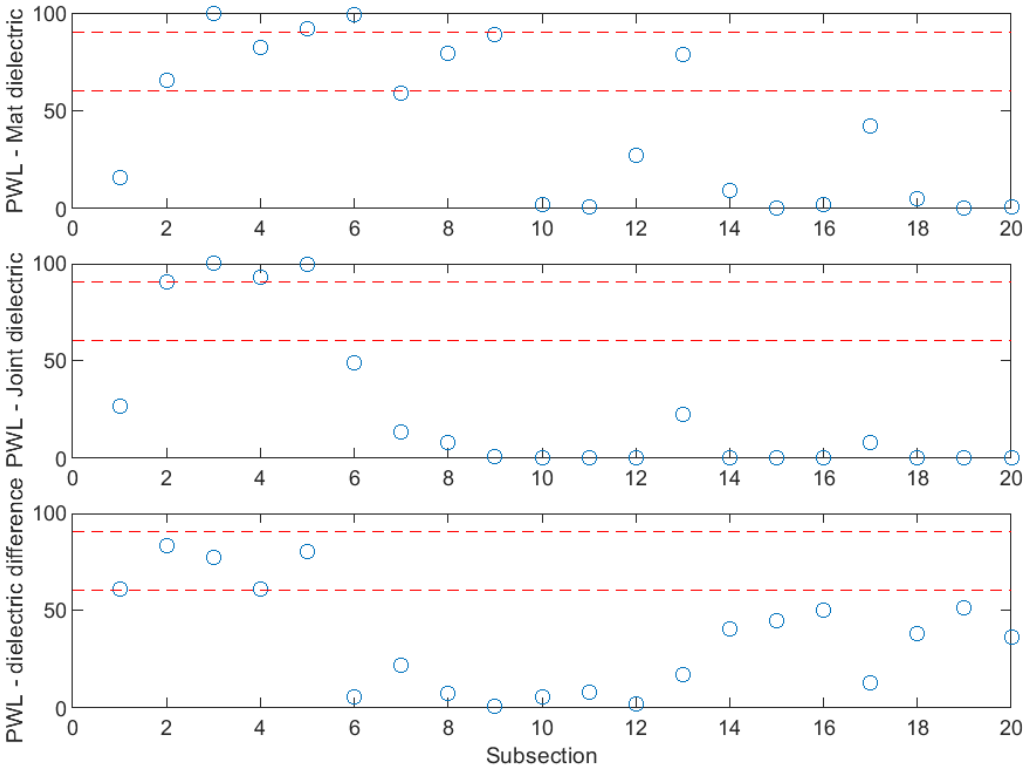

Figure B-341 PWL for dielectric values for unconfined joint (50 ft subsections) – US-23

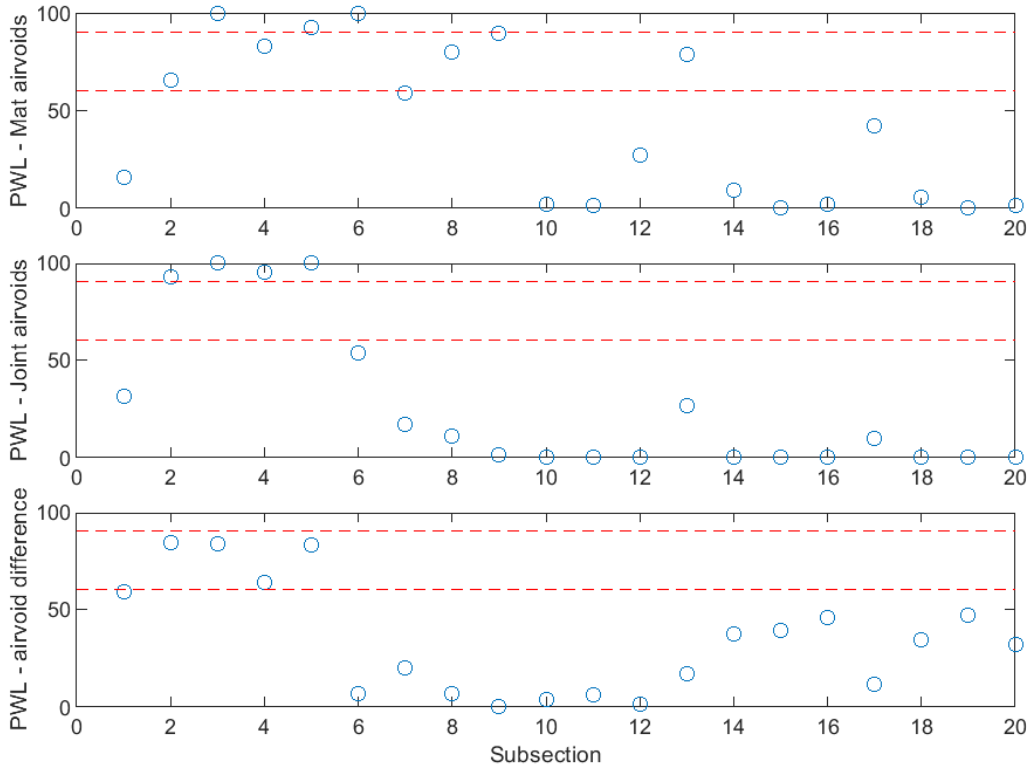

Figure B-342 PWL for air voids for unconfined joint (50 ft subsections) – US-23

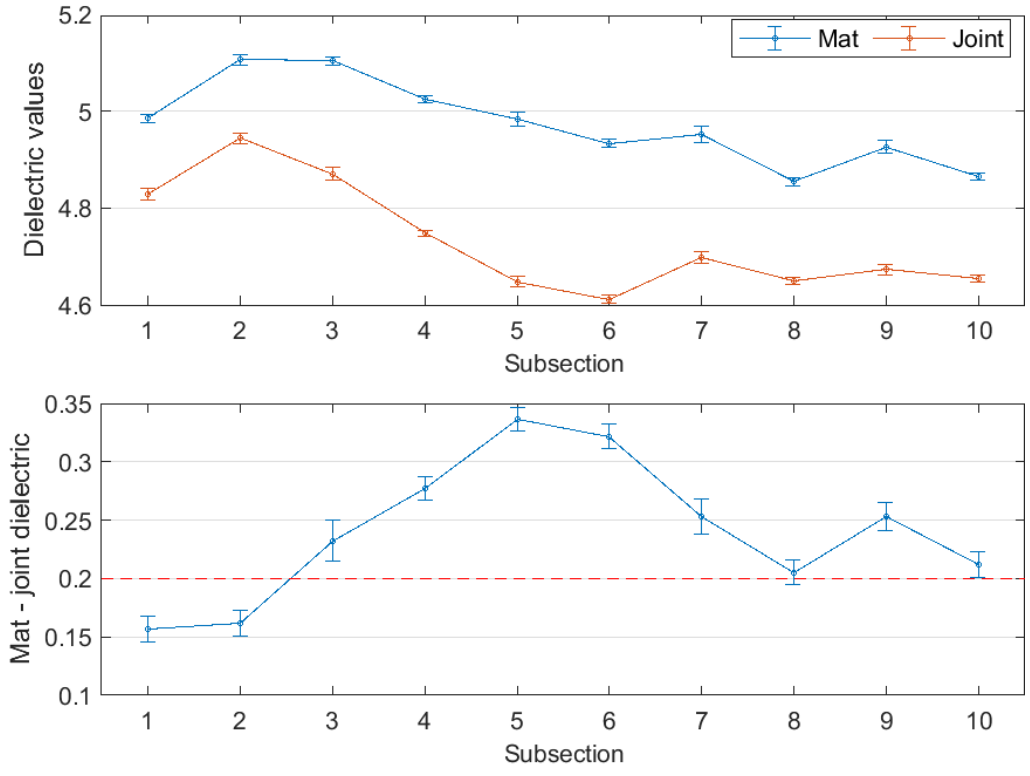

Figure B-343 Interval plot of dielectric values for unconfined joint (100 ft subsections) – US-23

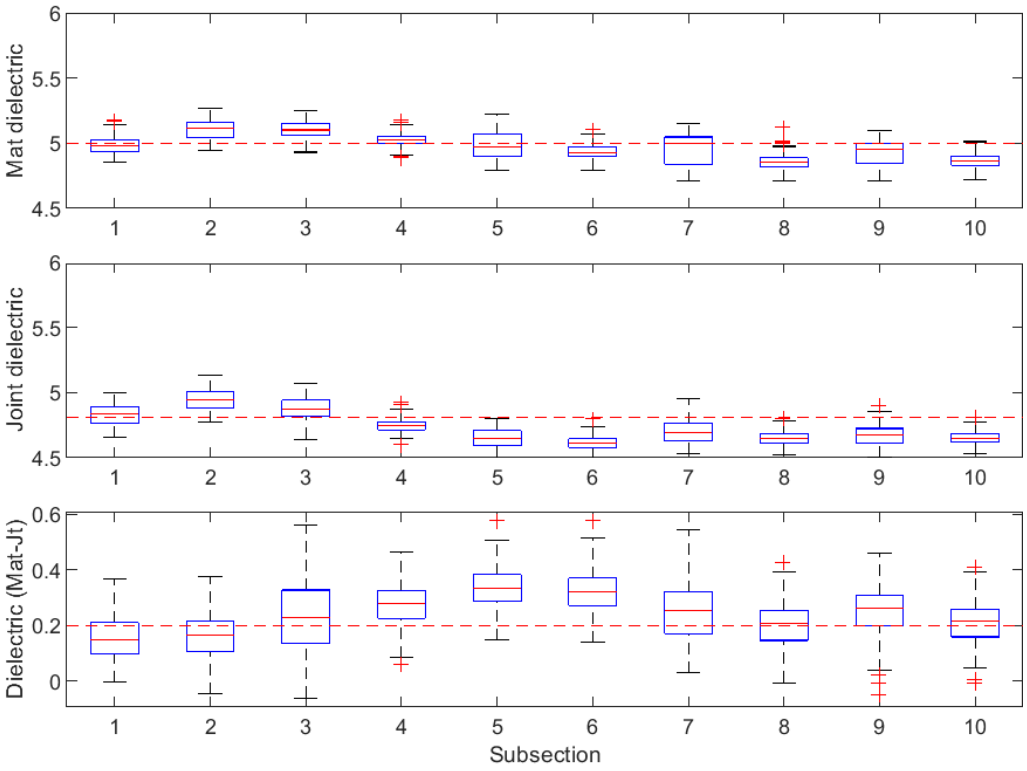

Figure B-344 Box plot of dielectric values for unconfined joint (100 ft subsections) – US-23

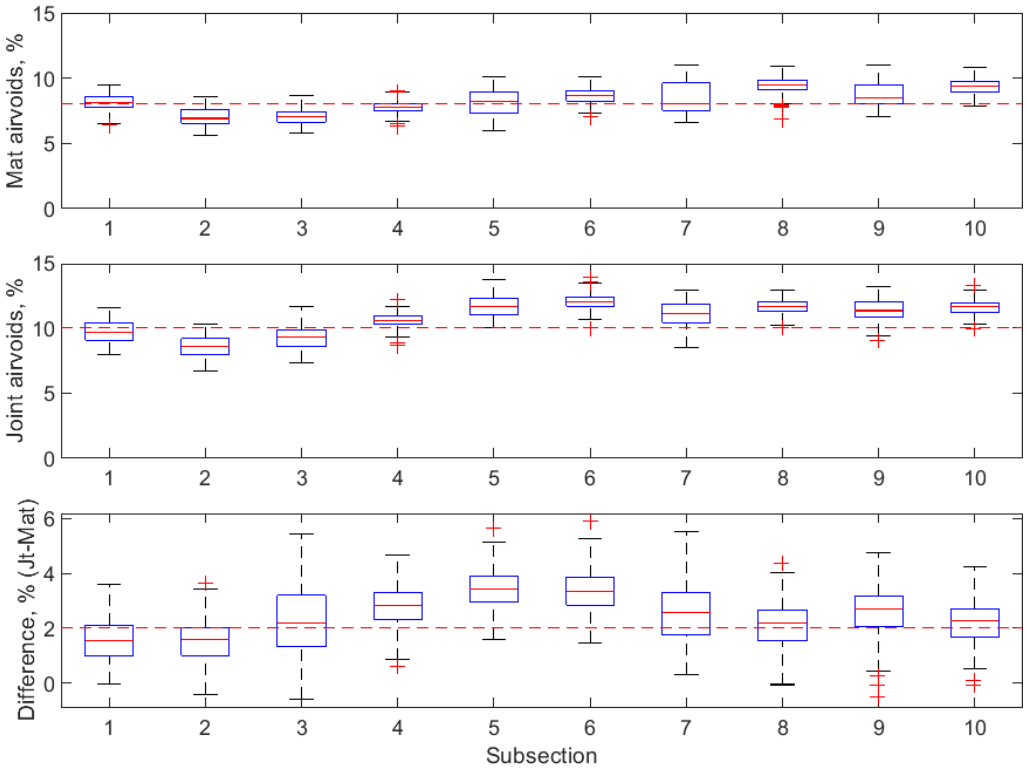

Figure B-345 Box plot of air voids for unconfined joint (100 ft subsections) – US-23

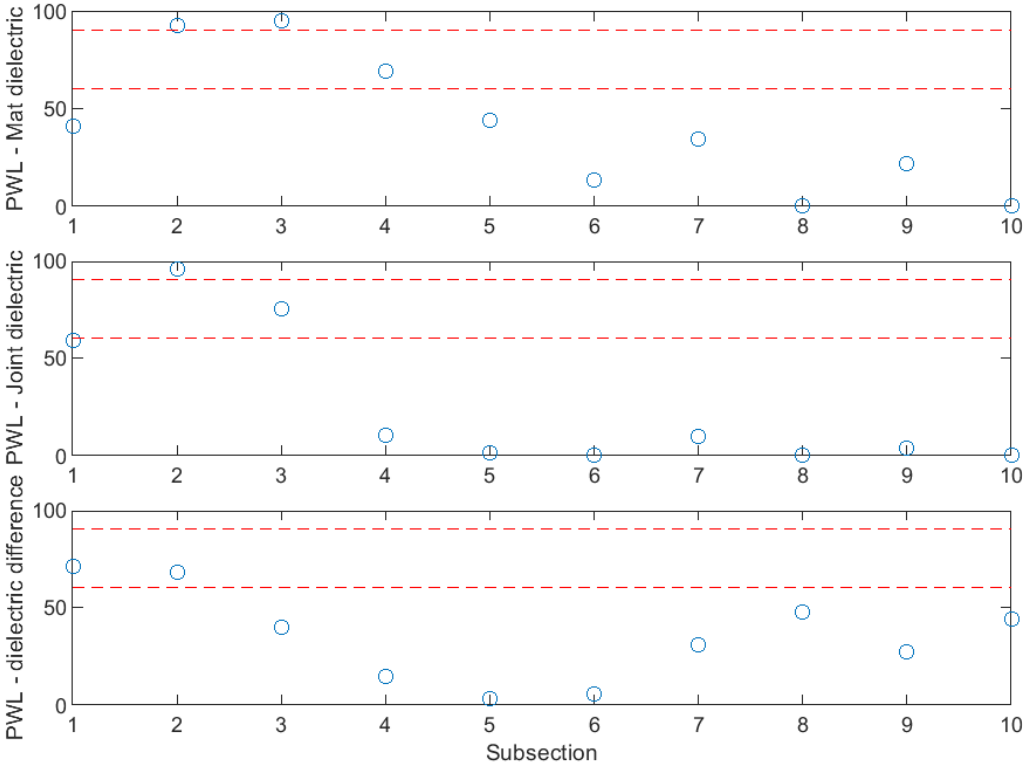

Figure B-346 PWL for dielectric values for unconfined joint (100 ft subsections) – US-23

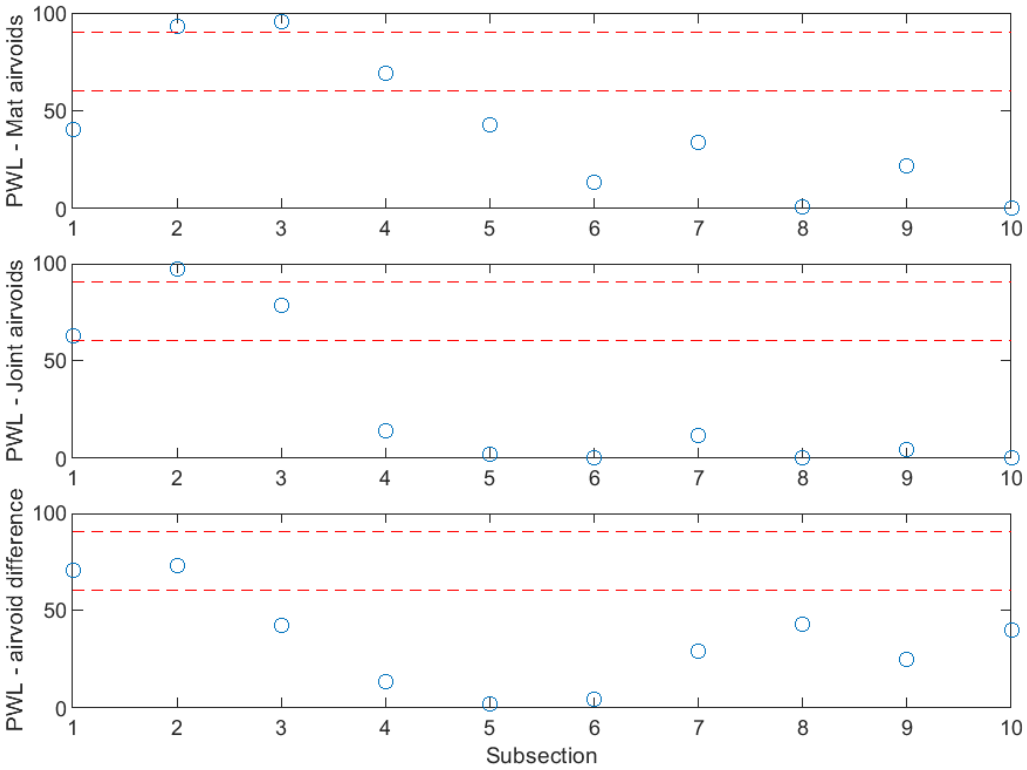

Figure B-347 PWL for air voids for unconfined joint (100 ft subsections) – US-23

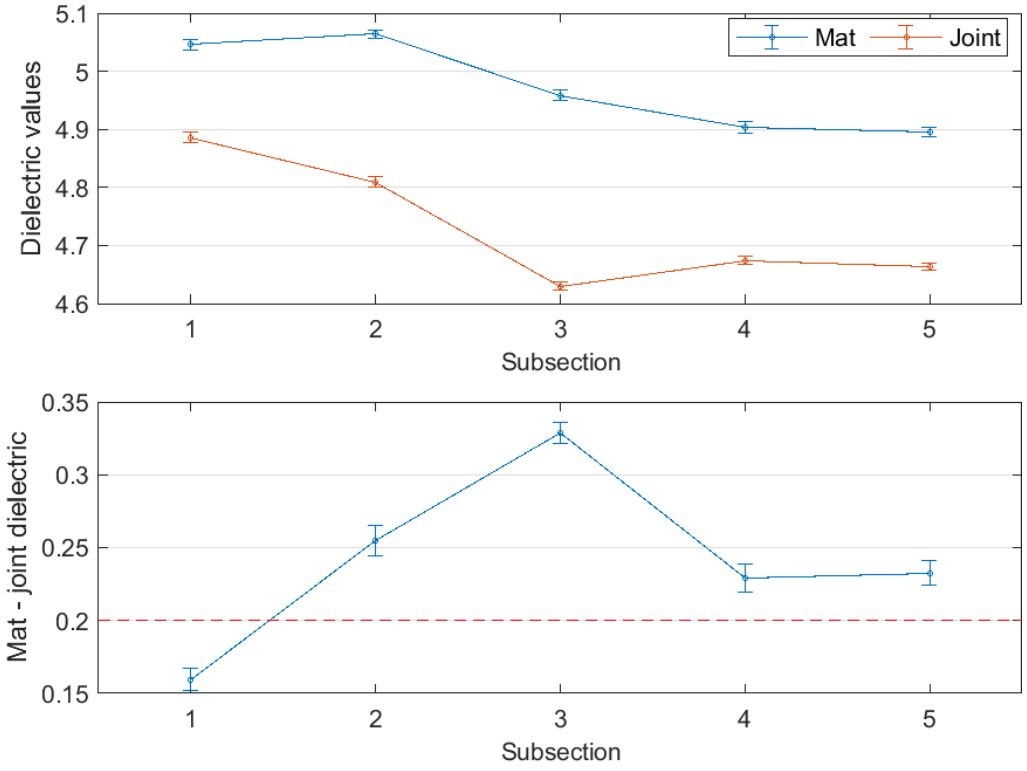

Figure B-348 Interval plot of dielectric values for unconfined joint (200 ft subsections) – US-23

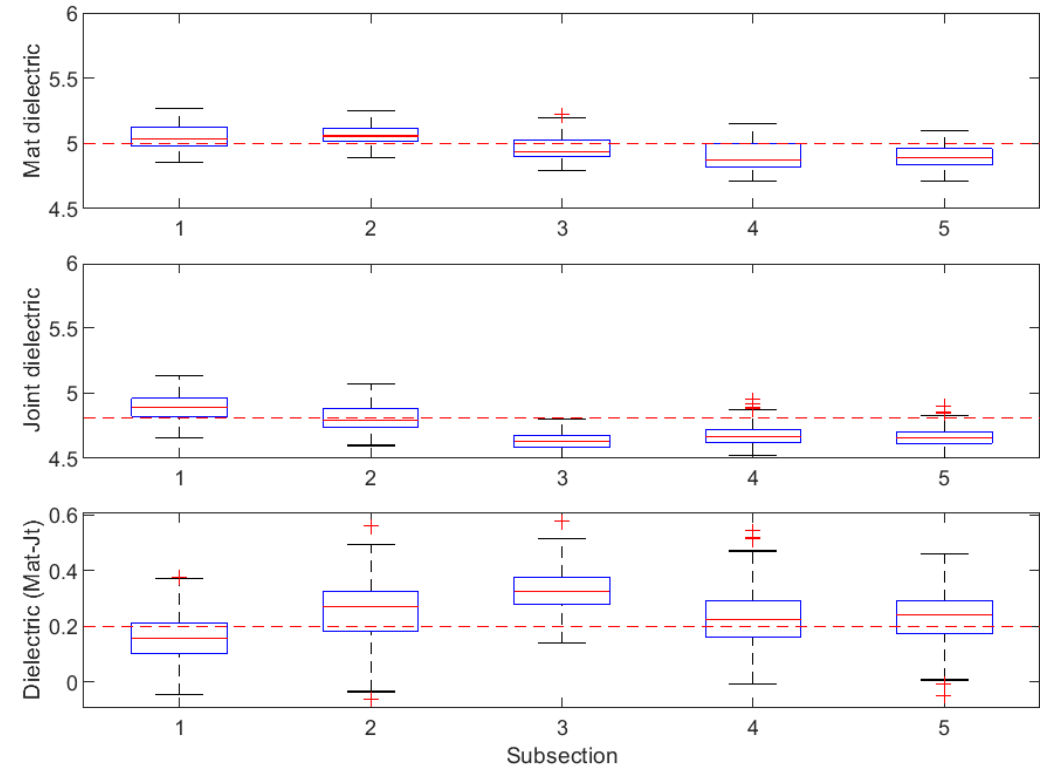

Figure B-349 Box plot of dielectric values for unconfined joint (200 ft subsections) – US-23

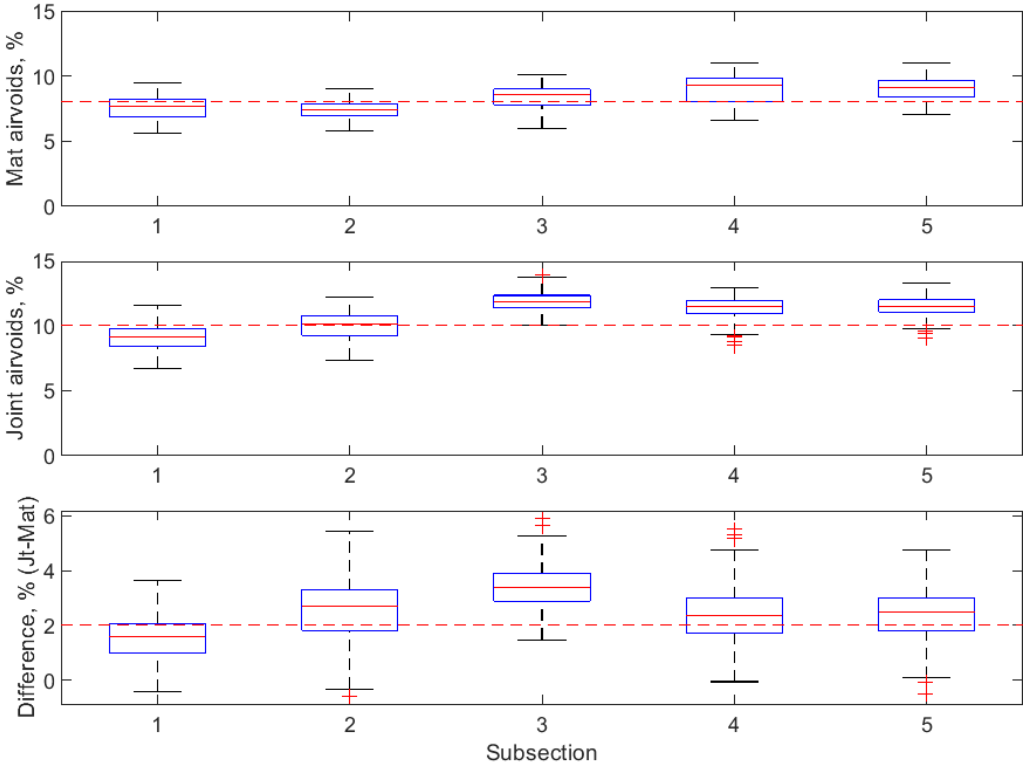

Figure B-350 Box plot of air voids for unconfined joint (200 ft subsections) – US-23

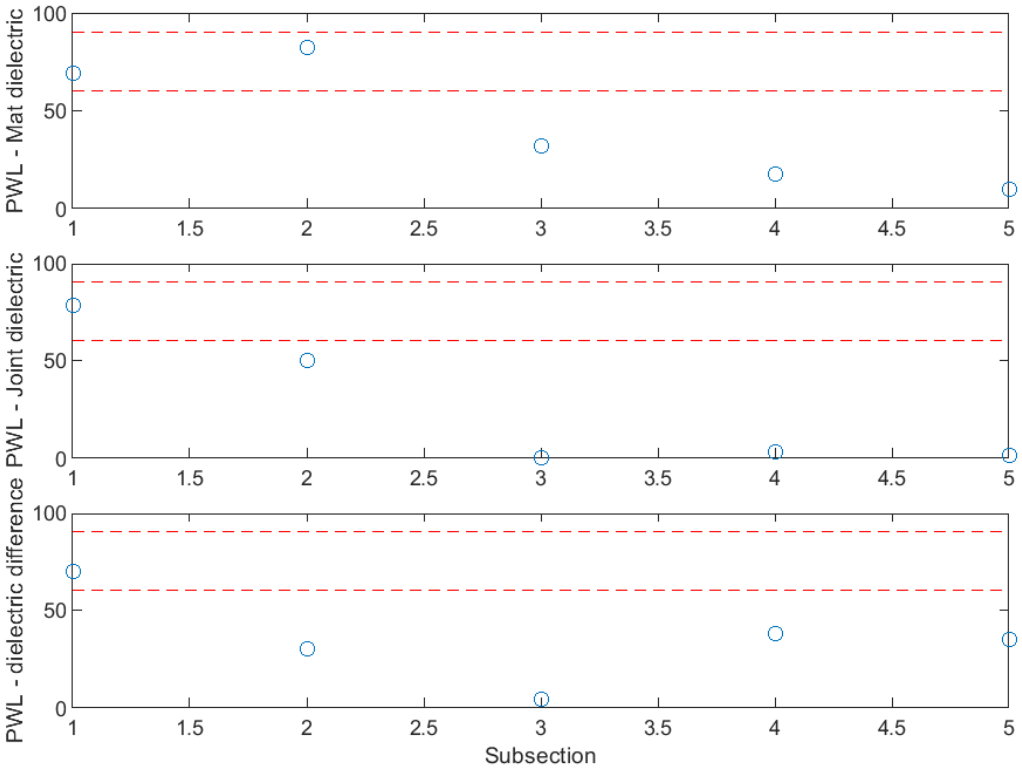

Figure B-351 PWL for dielectric values for unconfined joint (200 ft subsections) – US-23

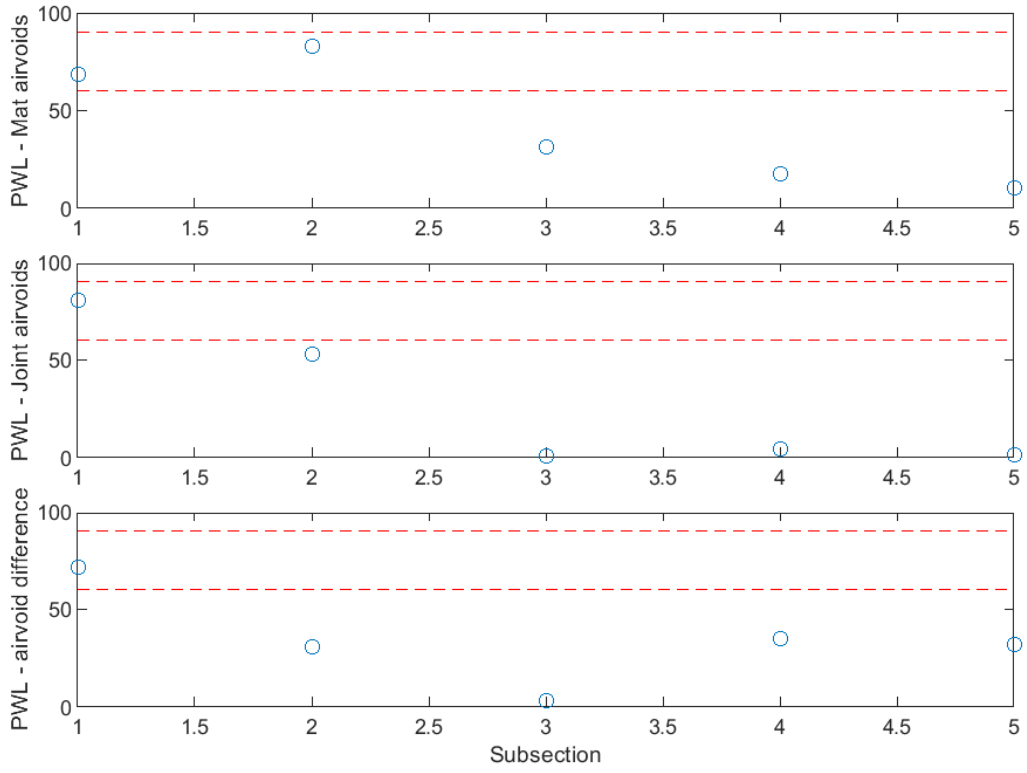

Figure B-352 PWL for air voids for unconfined joint (200 ft subsections) – US-23

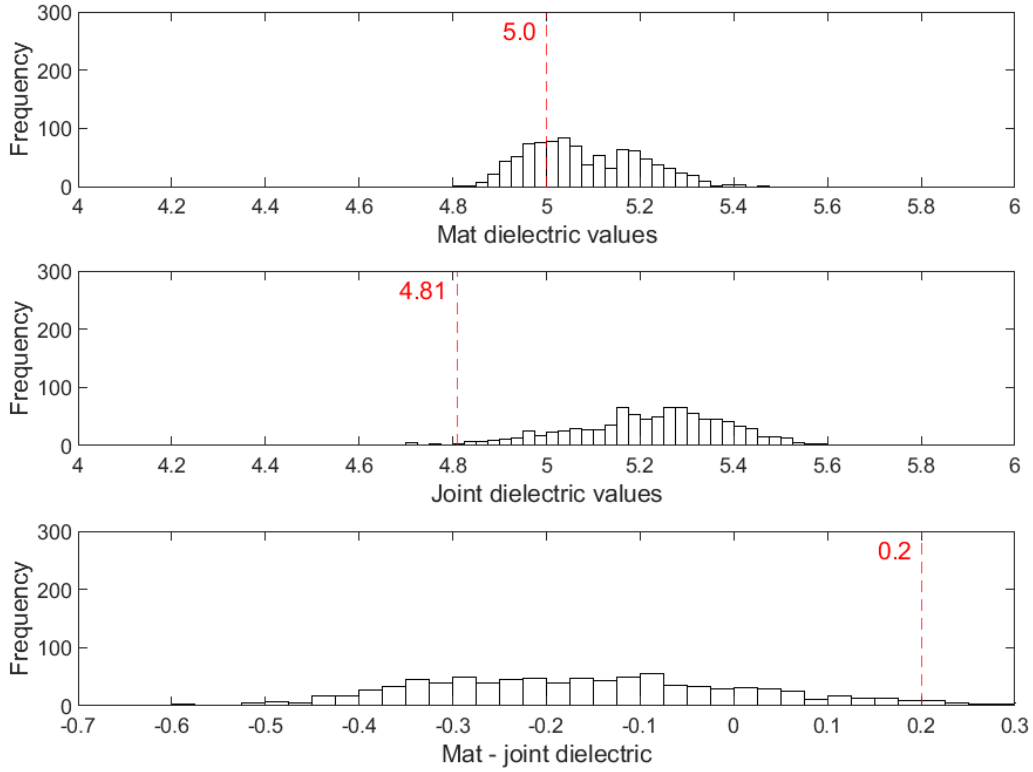

Figure B-353 Histogram of dielectric values for confined joint – US-23

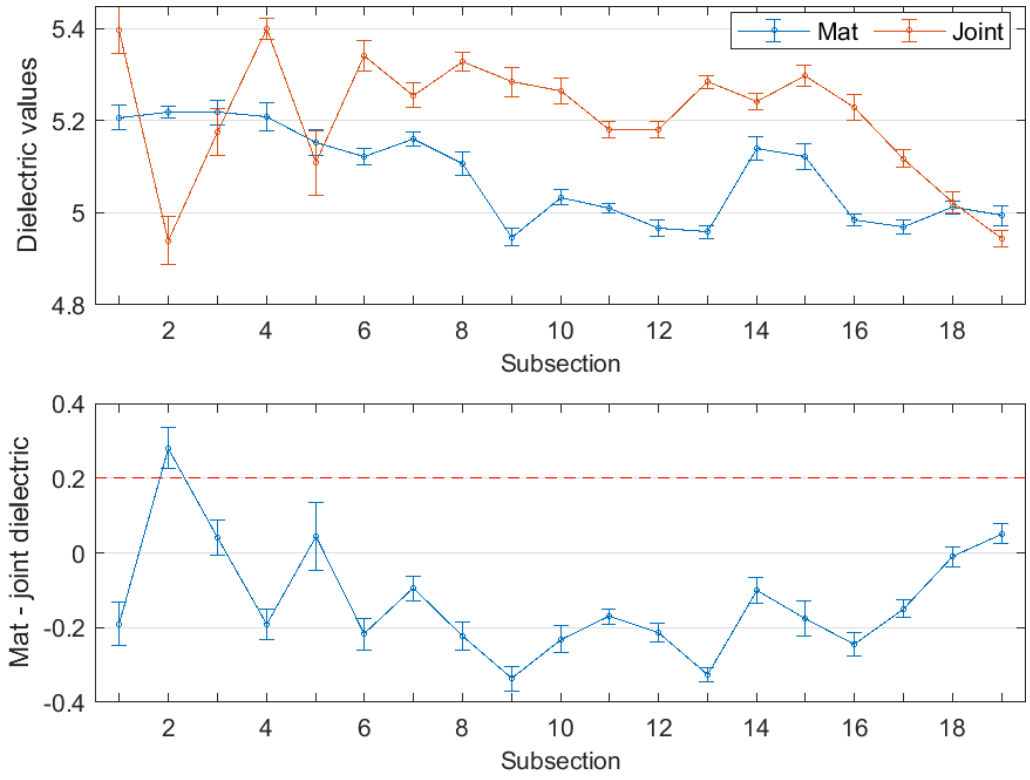

Figure B-354 Interval plot of dielectric values for confined joint (25 ft subsections) – US-23

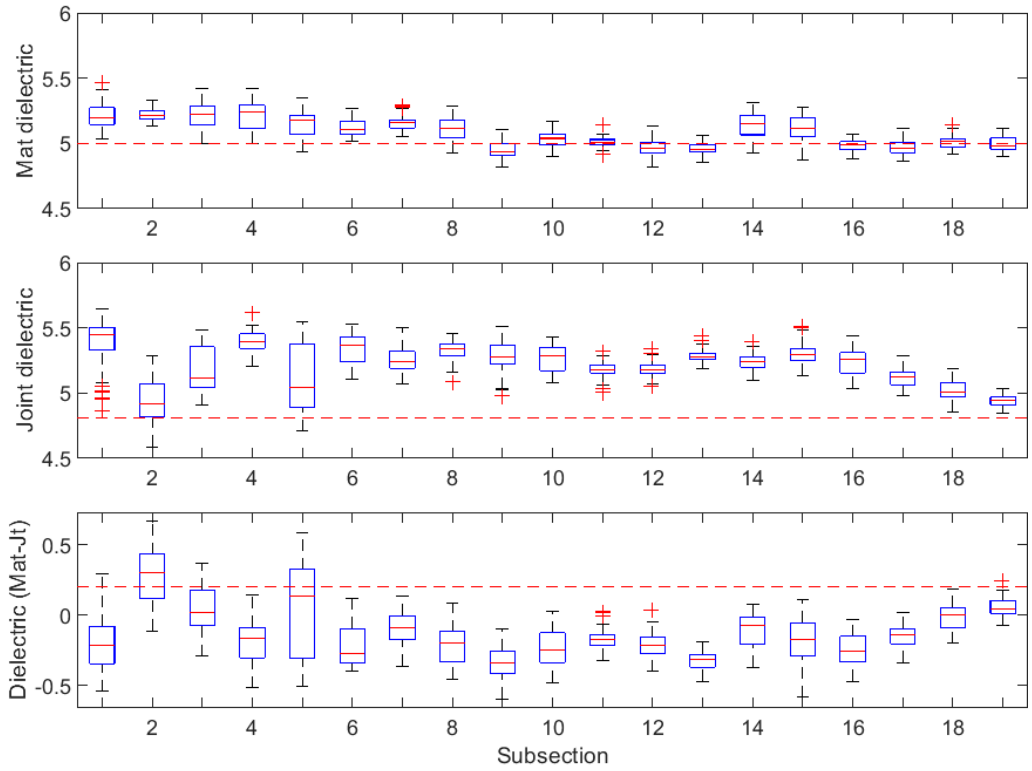

Figure B-355 Box plot of dielectric values for confined joint (25 ft subsections) – US-23

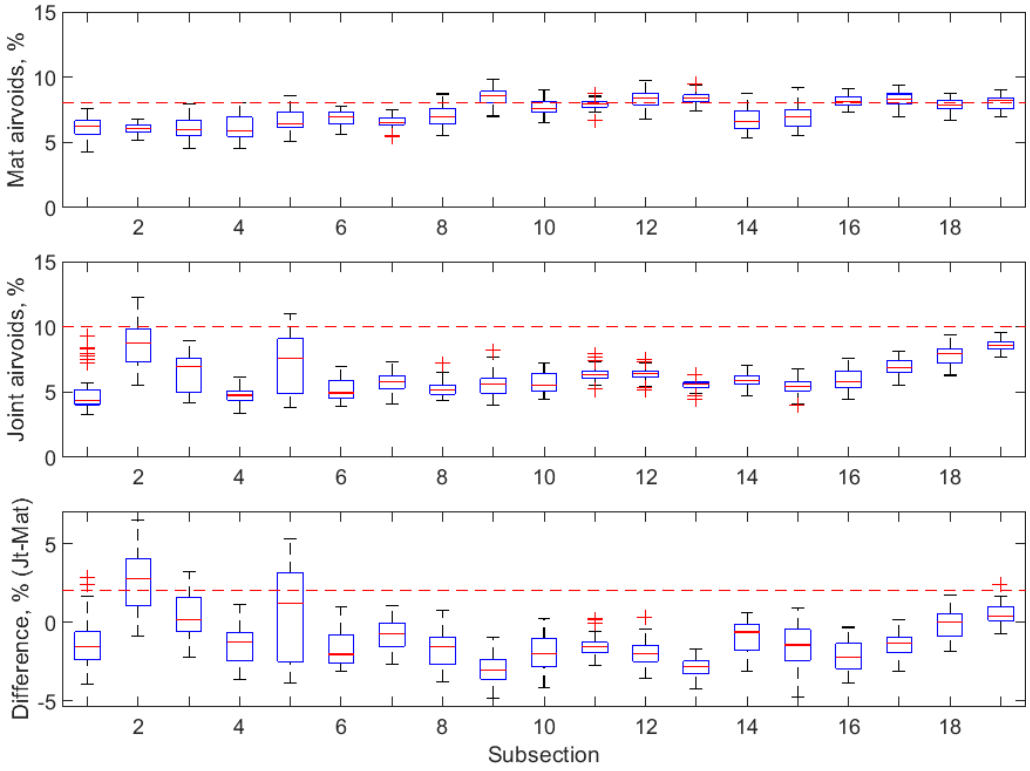

Figure B-356 Box plot of air voids for confined joint (25 ft subsections) – US-23

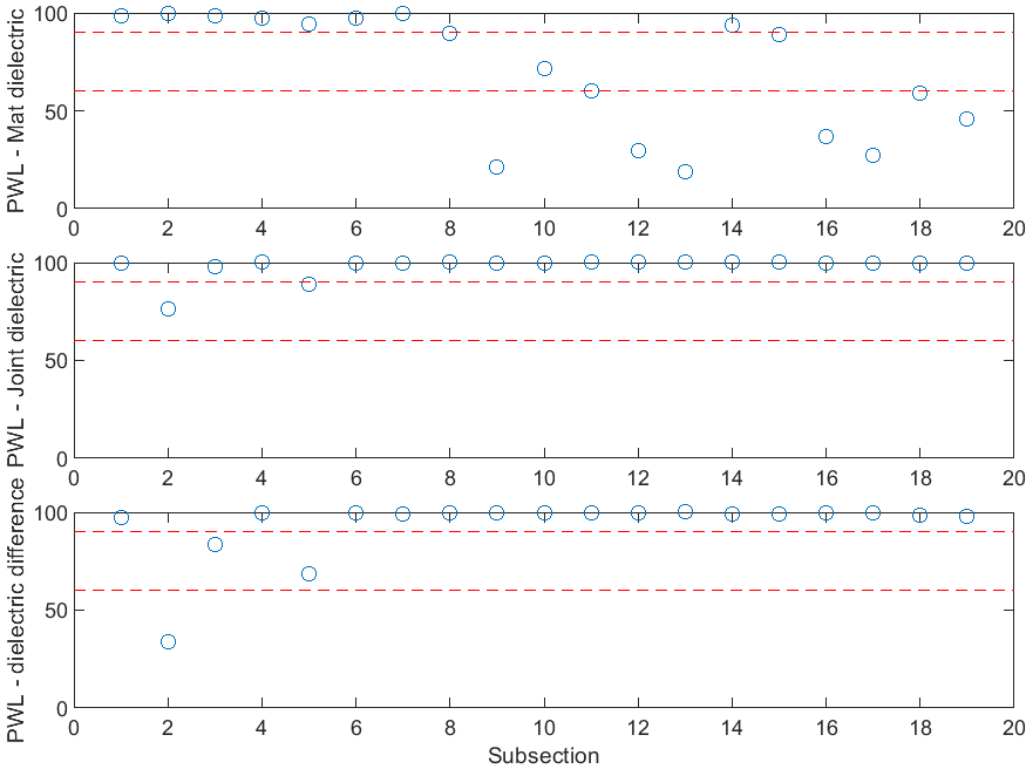

Figure B-357 PWL for dielectric values for confined joint (25 ft subsections) – US-23

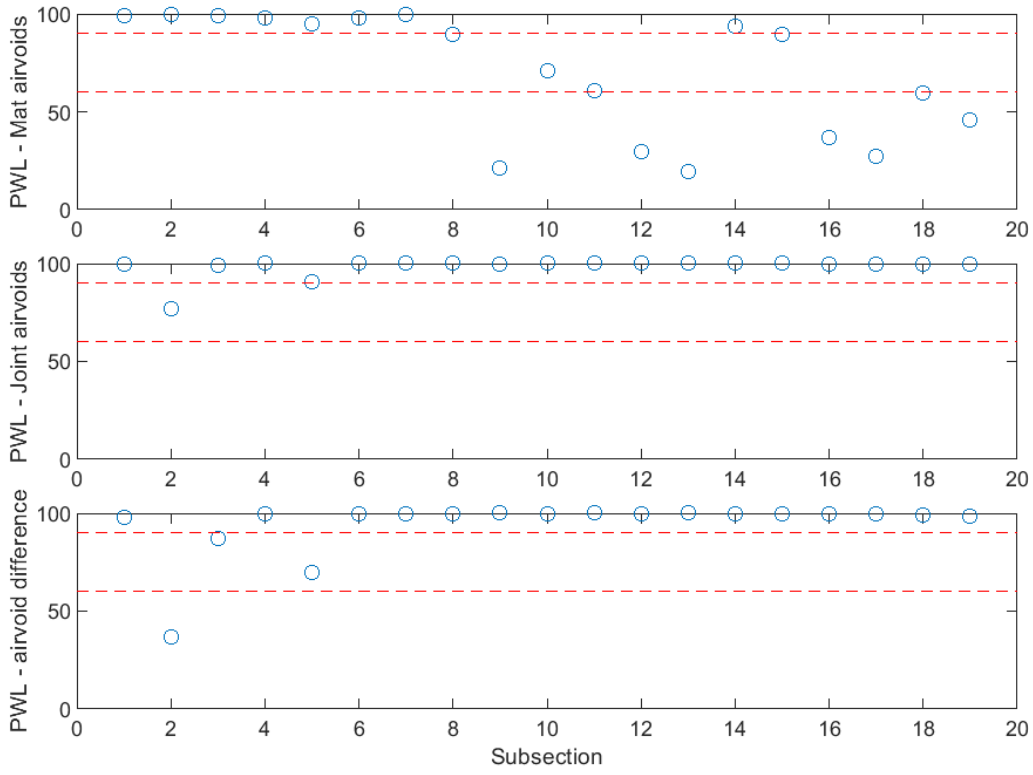

Figure B-358 PWL for air voids for confined joint (25 ft subsections) – US-23

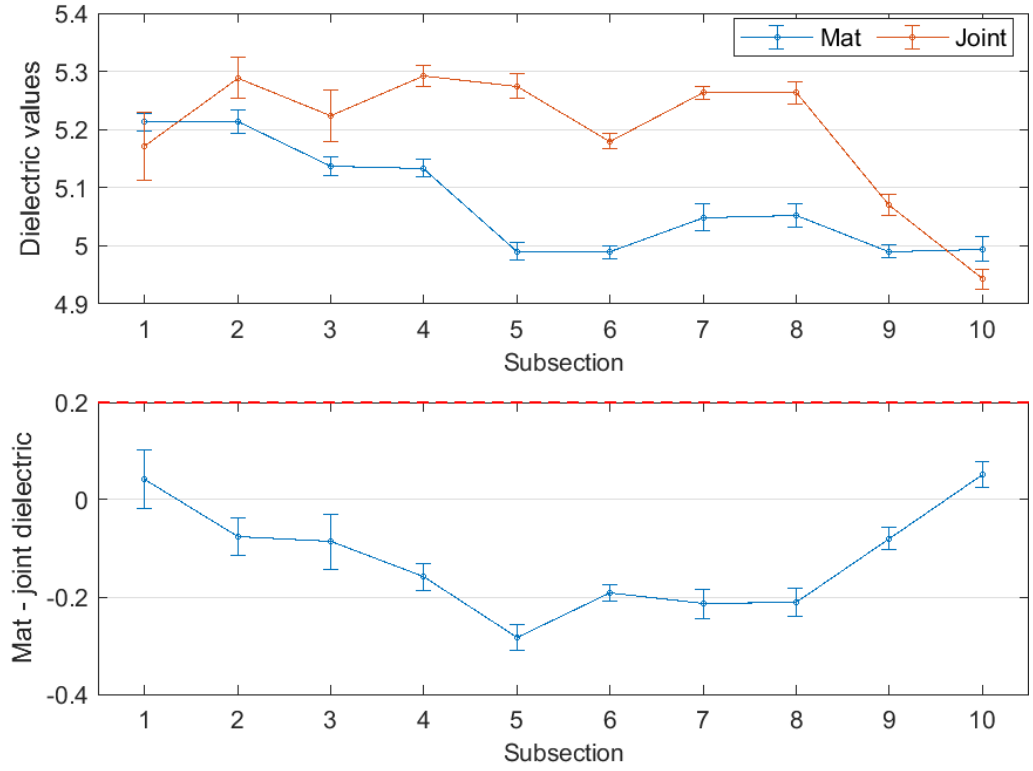

Figure B-359 Interval plot of dielectric values for confined joint (50 ft subsections) – US-23

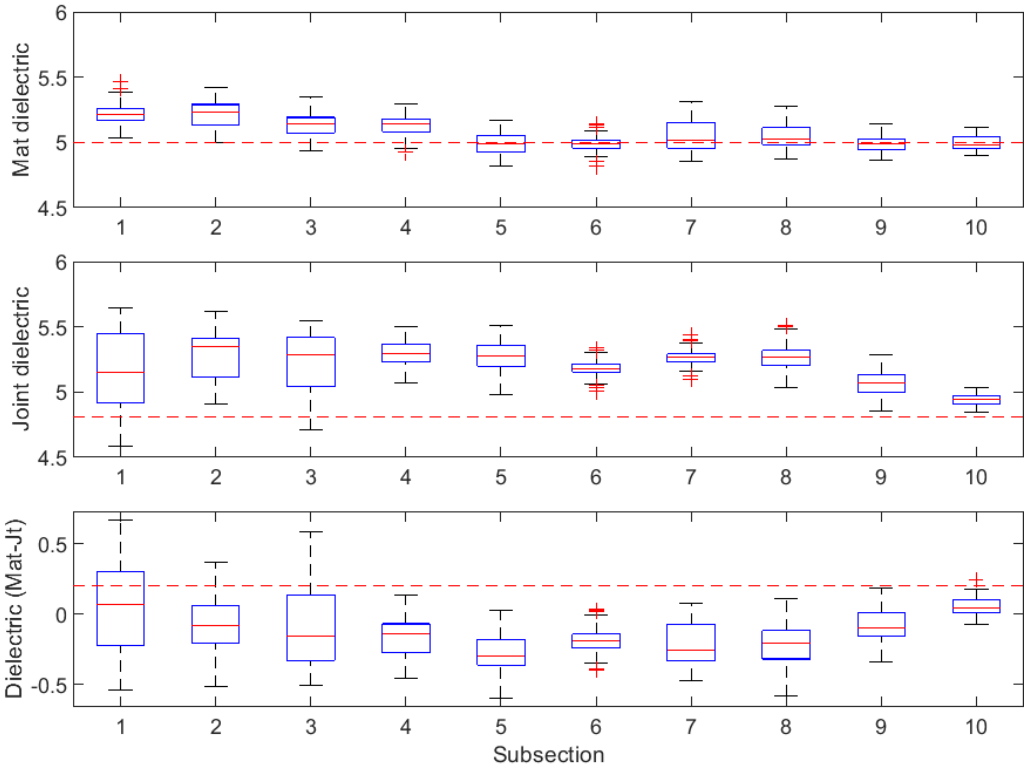

Figure B-360 Box plot of dielectric values for confined joint (50 ft subsections) – US-23

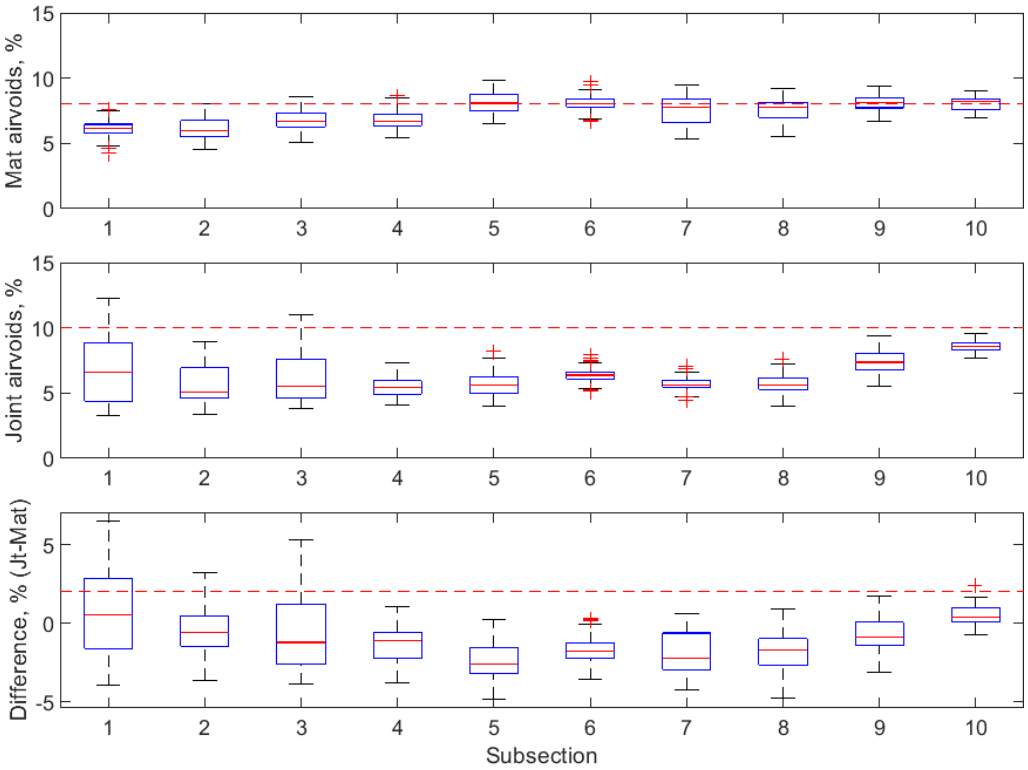

Figure B-361 Box plot of air voids for confined joint (50 ft subsections) – US-23

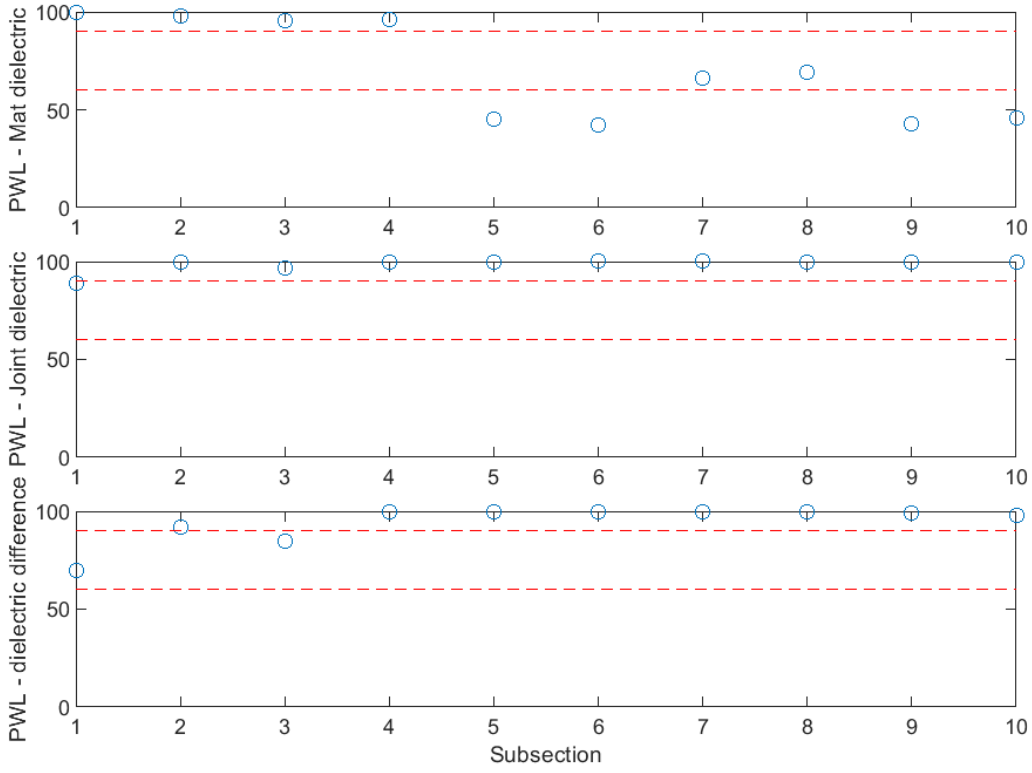

Figure B-362 PWL for dielectric values for confined joint (50 ft subsections) – US-23

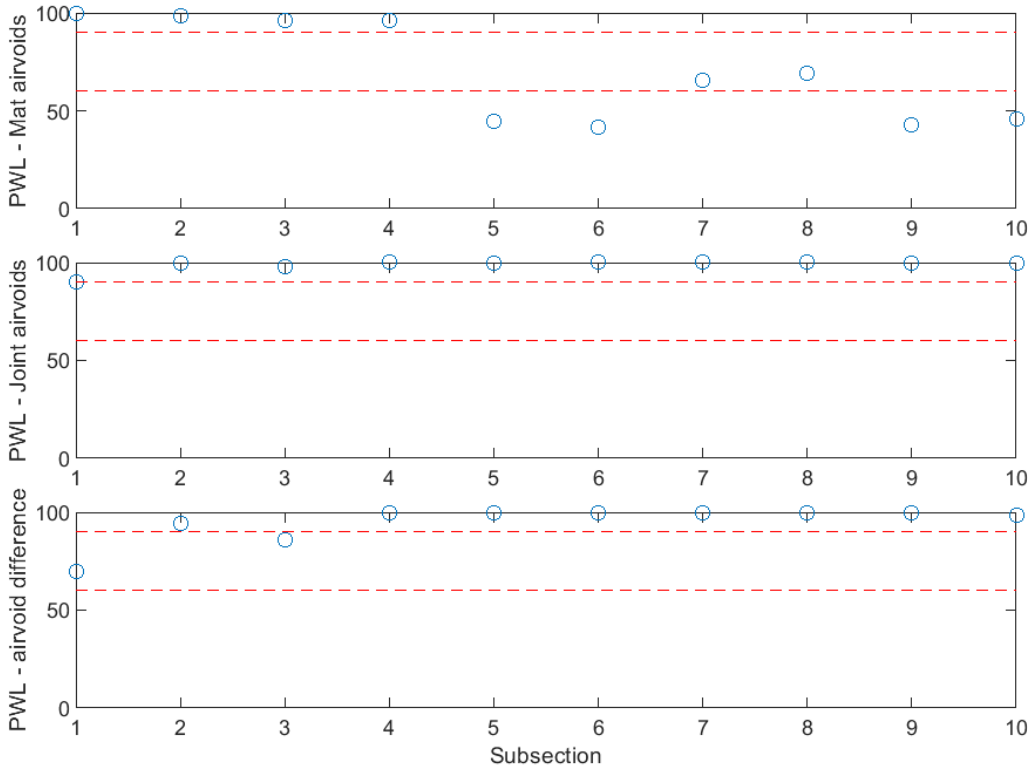

Figure B-363 PWL for air voids for confined joint (50 ft subsections) – US-23

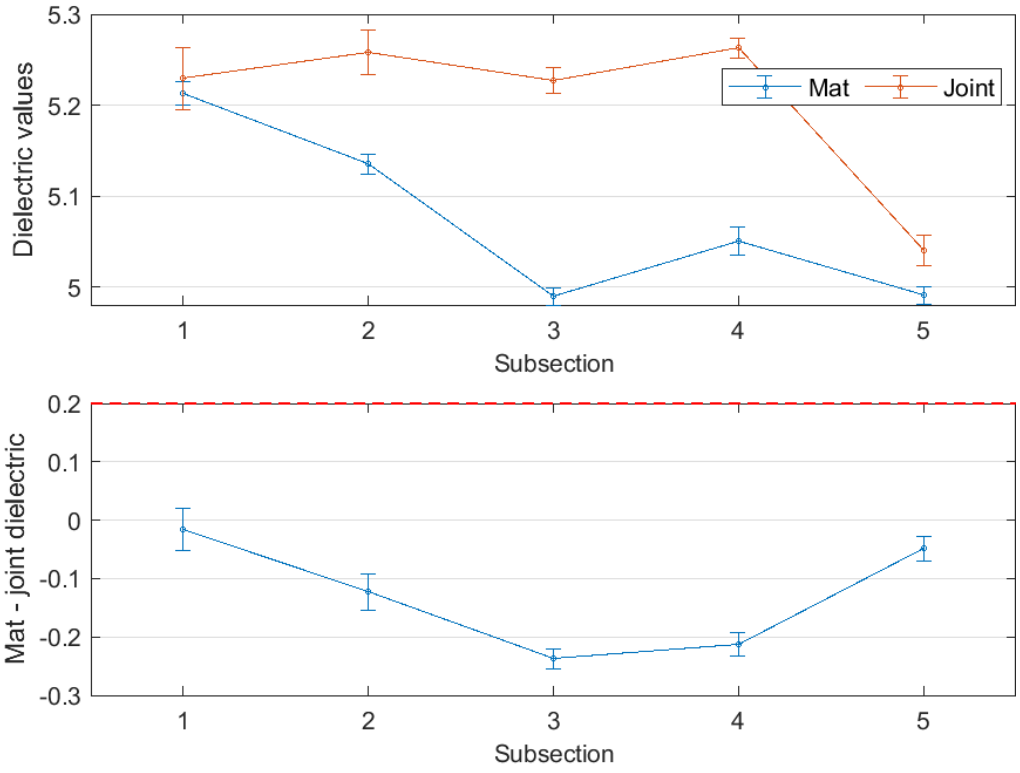

Figure B-364 Interval plot of dielectric values for confined joint (100 ft subsections) – US-23

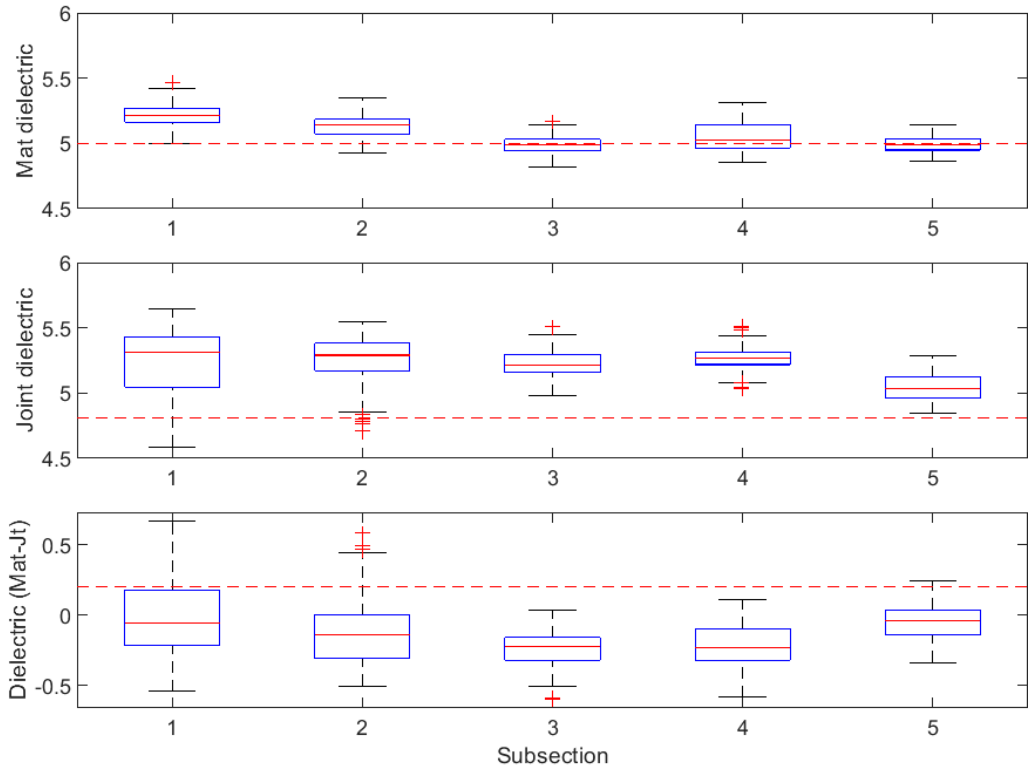

Figure B-365 Box plot of dielectric values for confined joint (100 ft subsections) – US-23

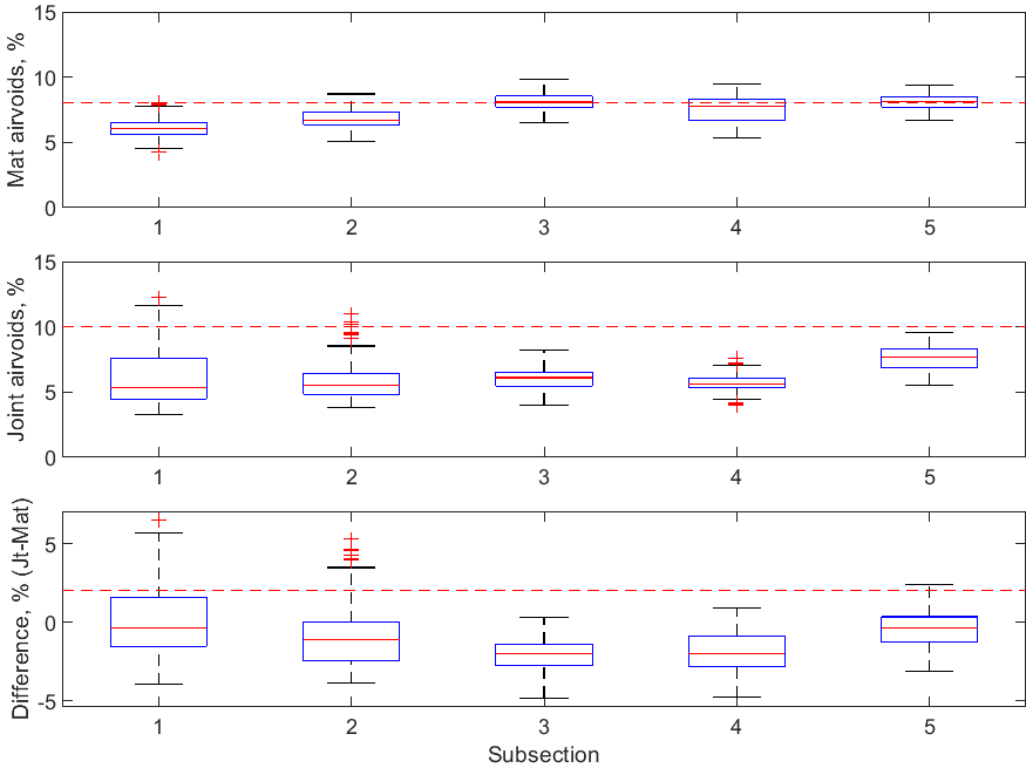

Figure B-366 Box plot of air voids for confined joint (100 ft subsections) – US-23

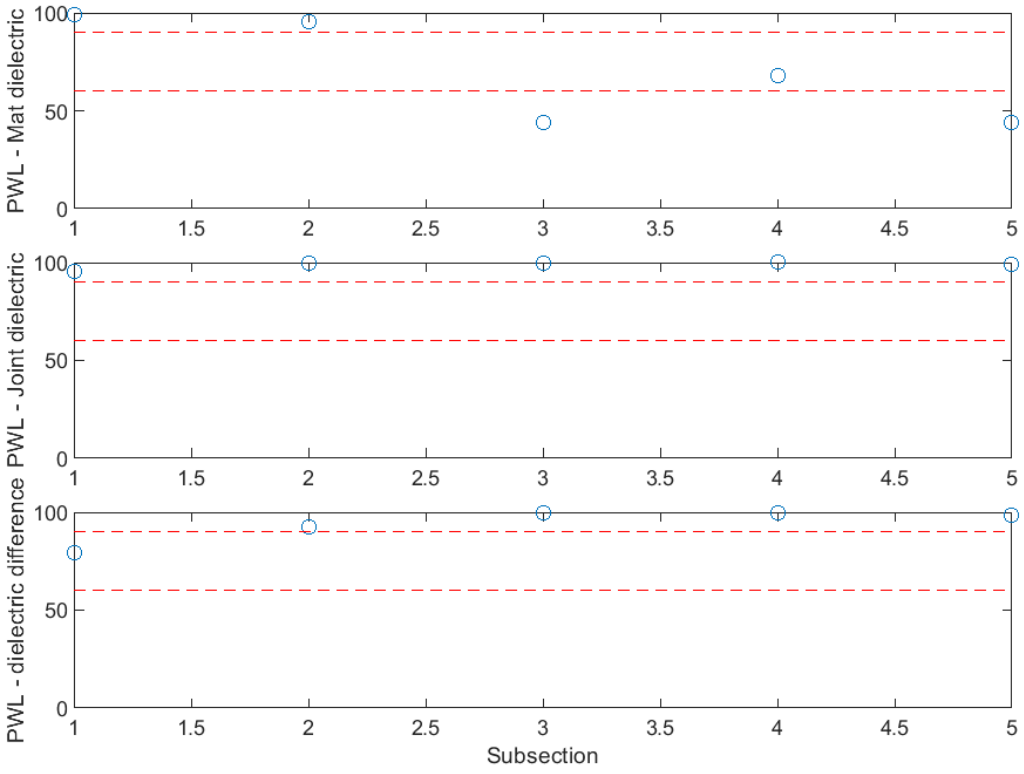

Figure B-367 PWL for dielectric values for confined joint (100 ft subsections) – US-23

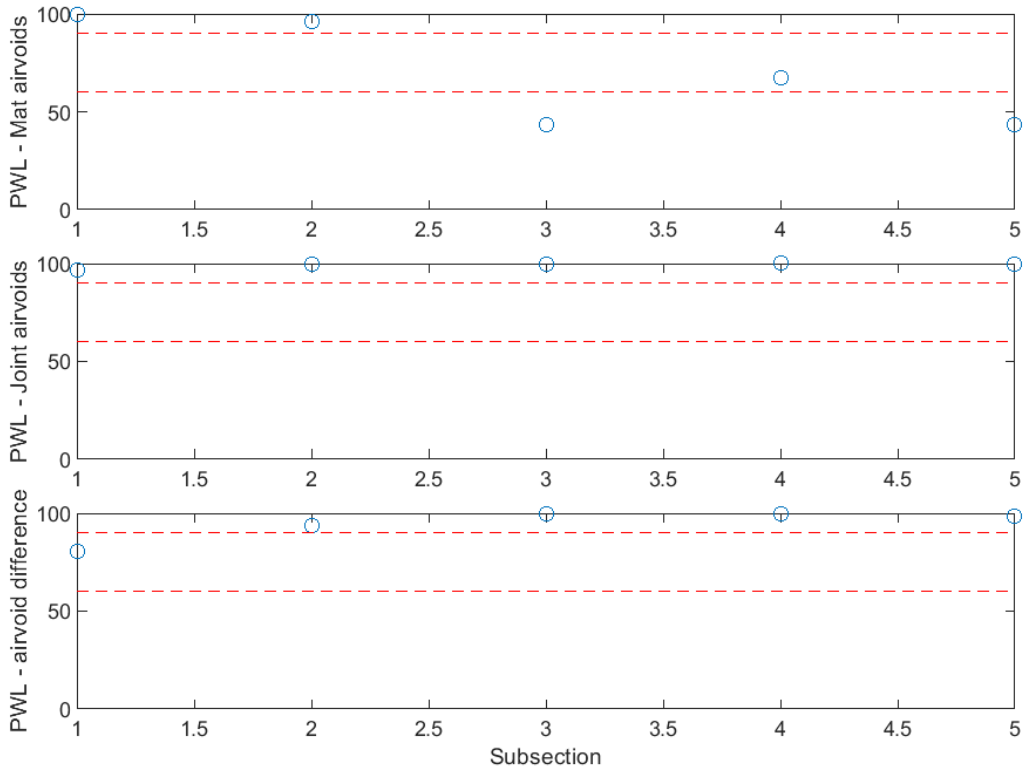

Figure B-368 PWL for air voids for confined joint (100 ft subsections) – US-23

Conditional probability plot for air voids

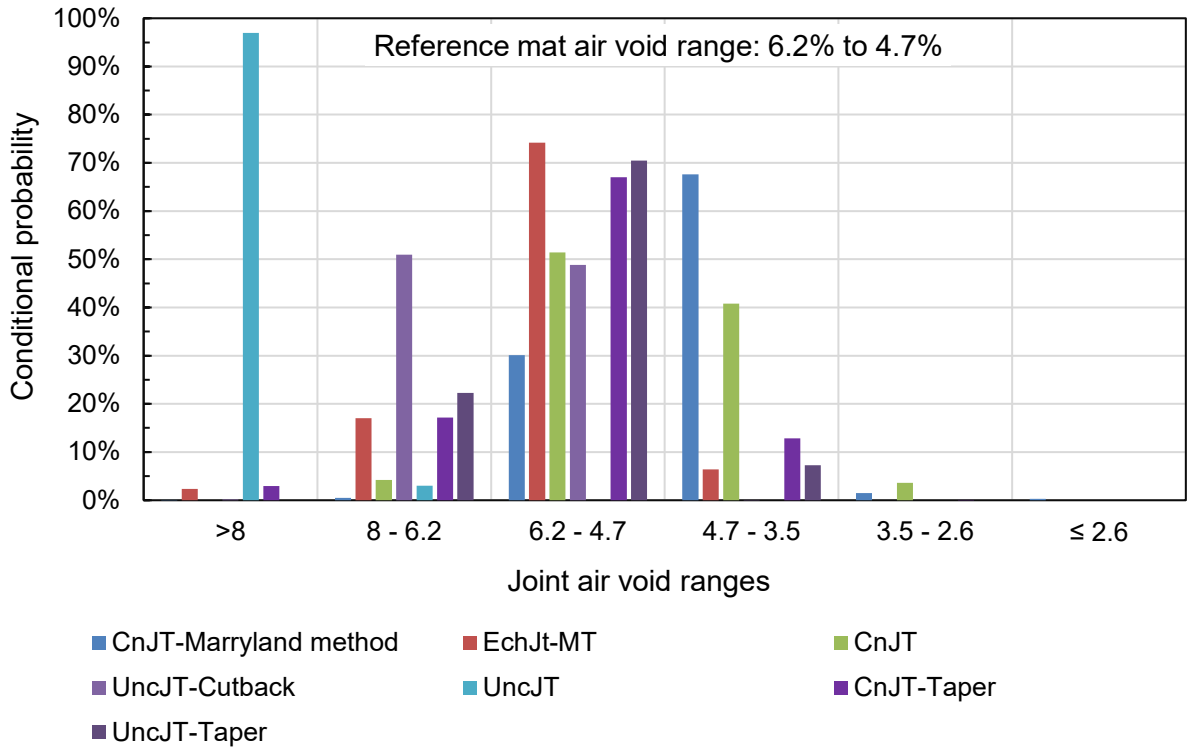

Figure B-369 Conditional probability-based comparison of air voids between different joint types